Nuclear Science ISBN 92-64-02084-5

CRISSUE-S – WP2

Neutronics/Thermal-hydraulics Coupling in LWR Technology: State-of-the-art Report (REAC-SOAR)

With the contributions of

ANAV-UPC, Spain
Studsvik Eco & Safety AB (later Studsvik Nuclear AB), Sweden
SKI, Sweden
University of Madrid, Spain
University of Valencia, Spain
NRI, Czech Republic
Pennsylvania State University, USA
University of Illinois at Urbana-Champaign, USA
OECD/NEA, Paris, France
FZR (VALCO Project Co-ordinator), Germany
Royal Institute of Technology in Stockholm, Sweden
Westinghouse Electric Sweden AB, Sweden, Sweden

NEA No. 5436

NUCLEAR ENERGY AGENCY
ORGANISATION FOR ECONOMIC CO-OPERATION AND DEVELOPMENT

ORGANISATION FOR ECONOMIC CO-OPERATION AND DEVELOPMENT

Pursuant to Article 1 of the Convention signed in Paris on 14th December 1960, and which came into force on 30th September 1961, the Organisation for Economic Co-operation and Development (OECD) shall promote policies designed:

- to achieve the highest sustainable economic growth and employment and a rising standard of living in member countries, while maintaining financial stability, and thus to contribute to the development of the world economy;
- to contribute to sound economic expansion in member as well as non-member countries in the process of economic development; and
- to contribute to the expansion of world trade on a multilateral, non-discriminatory basis in accordance with international obligations.

The original member countries of the OECD are Austria, Belgium, Canada, Denmark, France, Germany, Greece, Iceland, Ireland, Italy, Luxembourg, the Netherlands, Norway, Portugal, Spain, Sweden, Switzerland, Turkey, the United Kingdom and the United States. The following countries became members subsequently through accession at the dates indicated hereafter: Japan (28th April 1964), Finland (28th January 1969), Australia (7th June 1971), New Zealand (29th May 1973), Mexico (18th May 1994), the Czech Republic (21st December 1995), Hungary (7th May 1996), Poland (22nd November 1996), Korea (12th December 1996) and the Slovak Republic (14th December 2000). The Commission of the European Communities takes part in the work of the OECD (Article 13 of the OECD Convention).

NUCLEAR ENERGY AGENCY

The OECD Nuclear Energy Agency (NEA) was established on 1st February 1958 under the name of the OEEC European Nuclear Energy Agency. It received its present designation on 20th April 1972, when Japan became its first non-European full member. NEA membership today consists of 28 OECD member countries: Australia, Austria, Belgium, Canada, the Czech Republic, Denmark, Finland, France, Germany, Greece, Hungary, Iceland, Ireland, Italy, Japan, Luxembourg, Mexico, the Netherlands, Norway, Portugal, Republic of Korea, the Slovak Republic, Spain, Sweden, Switzerland, Turkey, the United Kingdom and the United States. The Commission of the European Communities also takes part in the work of the Agency.

The mission of the NEA is:

- to assist its member countries in maintaining and further developing, through international co-operation, the scientific, technological and legal bases required for a safe, environmentally friendly and economical use of nuclear energy for peaceful purposes, as well as
- to provide authoritative assessments and to forge common understandings on key issues, as input to government decisions on nuclear energy policy and to broader OECD policy analyses in areas such as energy and sustainable development.

Specific areas of competence of the NEA include safety and regulation of nuclear activities, radioactive waste management, radiological protection, nuclear science, economic and technical analyses of the nuclear fuel cycle, nuclear law and liability, and public information. The NEA Data Bank provides nuclear data and computer program services for participating countries.

In these and related tasks, the NEA works in close collaboration with the International Atomic Energy Agency in Vienna, with which it has a Co-operation Agreement, as well as with other international organisations in the nuclear field.

FOREWORD

Controlled fission power has been utilised for electricity production worldwide in nuclear power plants (NPPs) based on light water reactor (LWR) technology for several decades. It has proven its efficiency and safety during these years and has manifested itself as a reliable and durable energy source. The foundation pillar in the peaceful utilisation of fission nuclear power has always been the strong emphasis on safety. Safety has been accomplished by continuously pursuing in-depth reviews and re-evaluation of safety-related issues incorporating findings from ongoing nuclear safety research activities worldwide. Specific requirements have been deployed at the design and in the permissible operation conditions of the NPPs in order to always ensure adequate margins against critical system conditions, thus preventing the occurrence of accidents. It is realised that as new findings and analysis capabilities become available safety will be increased, and it is further possible that the safety margins presently employed will eventually be relieved (decreased) without compromising the actual safety. Prevention and mitigation measures, however, must be properly balanced with cost-reduction needs. A thorough knowledge of fundamental issues – in the present case the interaction between neutronics and thermal-hydraulics – allows pursuing the goal of ensuring safety at reasonable costs.

Consistent with this goal, the CRISSUE-S project was created with the aim of re-evaluating fundamental technical issues for LWR technology. Specifically, the project seeks to address the interactions between neutron kinetics and thermal-hydraulics that affect neutron moderation and influence the accident performance of the NPPs. This is undertaken in the light of the advanced computational tools that are readily available to the scientific community today.

The CRISSUE-S activity deals with the control of fission power and the use of high burn-up fuel; these topics are part of the EC Work Programme as well as that of other international organisations such as the OECD/NEA and the IAEA. The problems of evaluating reactivity-induced accident (RIA) consequences and eventually deciding the possibility of NPP prolongation must be addressed and resolved. RIAs constitute one of the most important of the “less-resolved” safety issues, and treating this problem may have significantly positive financial, social and environmental impacts. Public acceptance of nuclear technology implies that problems such as these be satisfactorily resolved.

Cross-disciplinary interaction (regulators, industry, utilities and research bodies) and co-operation within CRISSUE-S provides results which can directly and immediately be beneficial to EU industry. Concerning co-operation at an international level, the participation of the EU, former Eastern European countries, the USA, and observers from Japan testify to the wide interest these problems engender. Competencies in broad areas such as thermal-hydraulics, neutronics and fuel, overall system design and reactor surveillance are needed to address the problems that are posed here. Excellent expertise is available in specific areas, while limited knowledge exists in the interface zones of those areas, *e.g.* in the coupling between thermal-hydraulics and neutronics. In general terms, the activities carried out and described here aim at exploiting available expertise and findings and gathering together expert scientists from various areas relevant to the issues addressed.

Added value for the CRISSUE-S activity consists of proposing and making available a list of transients to be analysed by coupled neutron kinetics/thermal-hydraulic techniques and of defining “acceptability” (or required precision) thresholds for the results of the analyses. The list of transients is specific to the different NPP types such as PWR, BWR and VVER. The acceptability thresholds for calculation precision are general in nature and are applicable to all LWRs. The creation of a database

including the main results from coupled 3-D neutron kinetics/thermal-hydraulic calculations and their analysis should also be noted.

The CRISSUE-S project is organised into three work packages (WPs). The first WP includes activities related to obtaining and documenting relevant data. The second WP is responsible for the state-of-the-art report (SOAR), while the third WP concerns the evaluation of the findings from the SOAR and includes outcomes of the entire project formulated as recommendations, mainly to the nuclear power industry and to regulatory authorities. The present state-of-the-art report is the result of the second WP. It discusses such aspects as: thermal-hydraulics, neutron kinetics, fuel, coupled analyses, operator training, regulatory position and a database of results. It also summarises findings from recent international projects and activities.

A comprehensive report such as the present one, composed of contributions from the different CRISSUE-S participating organisations, unavoidably implies non-homogeneous treatment of the various topics, although an effort was made to provide consistency between the various sections. However, it is realised that the adopted level of detail is not commensurate with the safety relevance or the technological importance of the issues discussed.

The report has been written to accomplish the objectives established in the contract between the EU and its partners. Expected beneficiaries include institutions and organisations involved with nuclear technology (*e.g.* utilities, regulators, research, fuel industry). In addition, specific expected beneficiaries are junior- or senior-level researchers and technologists working in the considered field of research and development and application of coupled neutron kinetics/thermal-hydraulics.

Six plenary CRISSUE-S meetings took place over the course of the project implementation period. The meetings were held at:

- University of Pisa, Pisa, Italy, 25-26 February 2002 (kick-off meeting).
- OECD/NEA, Issy-les-Moulineaux, Paris, France, 5-6 September 2002.
- Technical University of Catalonia (UPC), Barcelona, Spain, 23-24 January 2003.
- SKI, Stockholm, Sweden, 26-27 June 2003.
- European Commission, Luxembourg, 12 November 2003 (status information meeting).
- University of Pisa, Pisa, Italy, 11-12 December 2003 (final meeting).

An Internet site has been established at the University of Pisa and has been kept alive during the project lifetime (2001-2003). The address is www.ing.unipi.it/crissue_s. The site also contains the discussion records of the six meetings.

The importance of the CRISSUE-S project has been expressed by the OECD/NEA Nuclear Science Committee. This interest has also been emphasised by the OECD/NEA Committee on the Safety of Nuclear Installations, as the project discusses many of their activities. It was agreed that the CRISSUE-S reports be published by the OECD/NEA as its contribution to the project.

This report was produced by the members of the CRISSUE-S project for use within their organisations. The present version is being made widely available for the greater benefit of organisations and experts working in the nuclear power area. Several of the graphics in the report are in colour; interested readers can request a colour version of the report on CD-ROM from the NEA.

Acknowledgements

Many thanks to Nicola D'Amico (ITER Consult, Rome) for his review of the report, and to Amanda Costa for contributing to the final editing.

This report is dedicated to the memory of Gianni Frescura, who as Head of the Nuclear Safety Division of the Nuclear Energy Agency provided strong support for this activity and arranged for the co-operation between the OECD/NEA and this EC Project to be an effective one.

TABLE OF CONTENTS

List of figures

List of tables

LIST OF CONTRIBUTORS

University of Pisa, Italy – Project Co-ordinator
F. D'Auria, A. Bousbia Salah, G.M. Galassi, J. Vedovi
ANAV-UPC, Spain
F. Reventós, A. Cuadra, J.L. Gago
Studsvik Eco & Safety AB (later Studsvik Nuclear AB), Sweden
A. Sjöberg, M. Yitbarek
SKI, Sweden
O. Sandervåg, N. Garis
University of Madrid, Spain
C. Anhert, J.M. Aragonés
University of Valencia, Spain
G. Verdù, R. Mirò, D. Ginestar, A.M. Sánchez, F. Maggini
NRI, Czech Republic
J. Hadek, J. Macek
Pennsylvania State University, USA
K. Ivanov
University of Illinois at Urbana-Champaign, USA
R. Uddin
OECD/NEA, Paris, France
E. Sartori
VALCO Project Co-ordinator at FZR, Germany
U. Rindelhardt, U. Rohde
Royal Institute of Technology in Stockholm, Sweden
W. Frid
Westinghouse Electric Sweden AB, Sweden
D. Panayotov

EXECUTIVE SUMMARY

The CRISSUE-S project

The CRISSUE-S project aims at re-evaluating fundamental technical issues in the technology of light water nuclear reactors that are connected with the interactions between neutron kinetics and thermal-hydraulics modelling aspects that deal with the neutron moderation and cause concerns for the accident performance of the NPP. All of this is undertaken in light of the advanced computational tools that are currently available to the scientific community.

The objectives of the CRISSUE-S project can be summarised as follows:

- To establish a state-of-the-art report (SOAR).
- To provide results of best-estimate analyses of complex transients in existing reactors.
- To provide recommendations to interested organisations.
- To identify areas of the NPP design where the design/safety requirements can be relaxed.

The current SOAR (also mentioned below as REAC-SOAR) summarises among other things the findings from recent international projects or activities (*e.g.* OECD/CSNI SOAR on BWR, IAEA workshops and TECDOCs, recent OECD/NEA/NSC benchmarks including the PWR-MSLB and the BWR-TT benchmarks, boiling stability activities in the EU IV Framework, etc.). Within this context, the results of a co-operation established with the EU VALCO project are discussed, as are ongoing activities within the EU NACUSP project. The SOAR also addresses reactivity accidents (REAC) with regard to the selection of relevant transients from proper PSA studies, consideration of the needed tools and databases including computer codes, NPP nodalisations (input decks) and realistic boundary and initial conditions, consideration of criteria for using the mentioned tools and databases including the qualification process and the uncertainty evaluation.

The establishment of a SOAR on REAC implies the availability of information about the system performance should relevant selected accident occur. Therefore, NPP transients have been analysed and relevant results have been considered in the SOAR together with qualified results available from different sources. The accident scenarios are typically identified as MSLB, ATWS, LOFW, CR ejection, DW stability, MSIV closure and TT. The relevance of 3-D neutronics/thermal-hydraulics coupling upon the prediction of a LBLOCA scenario is also evaluated. In relation to the mentioned transients, a CRISSUE-S database has been created.

A response is provided for the question, “Will the assigned NPP core survive the assigned transient whatever the fuel type and the burn-up are?” If yes, what are the available safety margins?” Parameters linked to rod surface temperature and fission power are considered for the evaluation of safety margins. The maximum tolerable fuel burn-up is evaluated in reference cases. The validity of the emergency operating procedures (EOP) implemented is challenged and recommendations are made

as concerns accident management, possibly outside the scope of current designs. In fact, the potential benefits of the activity performed concern the two last items listed above. Two examples give an idea of the results achieved:

- In the case of LBLOCA-DBA, the "physical" scram occurrence (due to voiding) has been demonstrated to take place well before (in terms of time since the break opening) control rod insertion. In practical terms, this constitutes one of the green lights necessary for raising the rated power of the NPP.

- The conservatism of results from the current calculation approach using 0-D neutron kinetics has been demonstrated. Again, this constitutes one of the green lights to relax the current requirements, *e.g.* for the boron concentration in various tanks installed in the NPP.

The present report (REAC-SOAR)

The present report is the second in a series of three issued within the CRISSUE-S framework. The first report deals with the required input database for the analyses and includes the identification of NPP transients useful for the qualification of the coupled techniques. The third report deals with recommendations, mainly directed toward the industry and its regulators, which constitute the final result of the project.

The description of the modelling and of the related capabilities in the areas of thermal-hydraulics, 3-D neutron kinetics and nuclear fuel is the main topic of the present report, together with the needed numerical techniques. Emphasis has also been placed upon transient measured data in nuclear power plants, to connected aspects of the technology (*e.g.* the simulator) and to the presentation of the licensing/regulatory point of view. Finally, a database of results has been created and is described in Annex I of this report.

Thermal-hydraulics

System thermal-hydraulics codes based upon six partial differential balance equations, mass momentum and energy per each of the two phases, solved in 1-D geometry constitute the state of the art. Specific techniques are available to construct equivalent (fictitious) 3-D nodalisations for the core or the vessel regions as needed. Errors in the predictions mostly originated in the incomplete knowledge of the constitutive relationships that determine the evolution of the two-phase mixture, *e.g.* the prediction of transient flow regimes in complex geometries like those characterising the reactor pressure vessels. Approximate numerical solution methods aggravate such a problem but do not become the main cause of uncertainty in the predictions.

The acceptability of the results is intrinsically linked to the quality assurance process and with the rigor in developing and qualifying input decks or nodalisations.

Models belonging to the structure of existing codes, the quality of which are critical as concerns the acceptability of the code prediction, are identified. An example is constituted by the dynamic subcooled void formation, *e.g.* void formation following fast neutron power excursions. Models that cannot be considered within the capabilities of current computational tools that are relevant to the 3-D neutron kinetics/thermal-hydraulic coupled analyses, are highlighted. One example is the modelling of the pressure wave propagation phenomena inside vessels, where reflections and attenuations in crossing

through geometric discontinuities occur. In a two-phase environment (occurring in both PWR and BWR), pressure wave propagation largely affects void formation and collapse and therefore neutron moderation as well.

With regard to codes that allow the 3-D porous media modelling approach (*i.e*. those codes that do not have the capability to predict the local turbulence-associated phenomena like the velocity or temperature profile inside a cross-section), the conclusion is that these codes are available and ready to be used, but their level of qualification is not acceptable.

Neutron kinetics

In the case of neutron kinetics the fundamental structure of the models is consistent with the physics of the phenomena involved. Even though approximate diffusion equations are typically adopted in the available industrial computational tools, reference solutions exist that are obtained with more sophisticated techniques, including Monte Carlo and deterministic neutron transport methods. These solutions are used to benchmark the results from diffusion equations.

Consequently, the problem of uncertainty evaluation is more manageable and the numerical solution methods play a greater role in the accuracy of results than in the case of thermal-hydraulics.

History and instantaneous modelling together with the correct definition of the assembly discontinuity factors (ADF) constitute the main challenges in neutron kinetics. The greatest limitation comes from the approximations embedded into the neutron cross-sections, this being connected with the need to isolate few energy ranges. This last imperative is principally the consequence of the available computer power.

Fuel

In physical terms nuclear fuel constitutes the subject of investigation of coupled neutron kinetics/ thermal-hydraulic calculation. Actually, fuel is considered as a sort of boundary condition for these calculations. This aspect is further discussed in Chapter 7, Section 7.3.

A wide range of phenomena connected with nuclear fuel burning in nuclear reactors has been reviewed, ranging from matrix restructuring to fission gas diffusion to corrosion, to the various chemical and physical aspects of the interaction between clad and pellet. Mechanisms for fuel failure have been considered in this context. The potential influence of crud formation upon RIA has been pointed out.

Emphasis has been placed upon high burn-up and uranium-plutonium fuel (MOX). In both cases a number of aspects that play an insignificant role with fresh UO_2 fuel may become important as concerns predicting phenomena of interest.

The major role of the fuel within the coupled neutron kinetics/thermal-hydraulic environment was noted and constitutes a main finding of the study. It was determined that transient modelling of fuel performance must become the third ring of an (ideal) un-broken chain which includes the two other disciplines. Changes of fuel geometric and physical properties are expected during RIA and must be properly accounted for in the modelling. In case of local power increase, for example, fuel fragmentation and release of fission gases may have an effect on neutron kinetic cross-sections as well as on the thermal properties of the gap and of the fuel itself. The feedback in terms of neutron power and of power transmitted to the coolant might be non-negligible. At present, there is no global approach to deal with this phenomenon.

Coupled analyses

The prediction of NPP transient scenarios constitutes the final goal of coupled neutron kinetics/ thermal-hydraulics techniques. However, the full exploitation of those techniques implies streamlining their use and developing recommendations to do so. Therefore transients have been selected within the present framework whose analysis is recommended by coupled techniques. The distinction is made between BWR, PWR and VVER and only the PWR-related list of transients is proposed hereafter. This includes:

- MSLB.
- LOFW-ATWS.
- CR ejection.
- LBLOCA-DBA.
- Incorrect connection (start-up) of an inactive (idle) loop.
- MSLB-ATWS.
- SBLOCA-ATWS.

Responding to the question “How good is good enough?” is a task that cannot be undertaken once for all time. The progress of science always moves faster than the acceptability of any technological product, and this applies to the results of code applications to nuclear reactor safety. However, an attempt has been made to establish acceptable targets for calculation precision, distinguishing between (acceptable) quantity and time errors. The values considered provide a notion of the current capabilities of computational tools, provided that qualification methods are adopted. Four examples of acceptability thresholds are reported below:

- For pressure pulses characterised by FWHM < 0.1 s the acceptable error is 10% nominal pressure.
- For core power pulses characterised by FWHM < 0.1 s the acceptable error is 100% nominal power or 300% initial power, which ever is smaller.
- For core power pulses characterised by FWHM ≥ 0.1 s, the acceptable threshold error is 20% nominal power or 100% initial power, which ever is smaller.
- The acceptable time error that can be associated with the prediction of occurrence in time of pressure or core pulse is 100% of the best-estimate value.

The acceptability of neutron kinetics calculations shall be consistent with discrepancies in the application of state-of-the-art codes to reference problems. Errors in predicting k_{eff} (or k_{∞}) of the order of 3-4% appear acceptable.

Due to various reasons (discussed in the report), the results from coupled 3-D neutron kinetics/ thermal-hydraulic calculations are imperfect (or affected by uncertainties). Therefore, uncertainty must be linked to any prediction. Two main findings are the outcome of the performed activity. The first one is connected with the demonstration that the Internal Assessment of Uncertainty method, based

upon the interpolation of the detected accuracy, is applicable for coupled techniques, though relevant resources are necessary to develop a suitable error database. The second finding is connected with the identification of the main sources of uncertainty or inadequacies of the current approach. These can be summarised as follows:

- Subcooled HTC, namely in transient conditions with "high" time derivative for the produced power.

- Pressure wave propagation inside the complex vessel geometry when a single phase of two-phase fluid is present.

- Effect of (prompt) radiolysis upon neutron cross-section following fast transients.

- Effect of direct energy release to the coolant following a fast transient.

- Detailed specifications about mechanical components such as valves and control rods. The function valve net cross-sectional flow area versus time during opening or closure events is irrelevant for the majority of thermal-hydraulic transients, but may become important when neutron kinetics feedback is computed. Analogously, the velocity as a function of time during a control rod ejection transient is relevant (*i.e.* not only the total ejection time).

- Parameters associated with fuel must be calculated during RIA transient to allow proper feedback. For instance, neutron kinetic cross-section and thermal parameters such as gap thickness and conductivity should be calculated as a function of time and should provide suitable feedback to the thermal-hydraulics and the neutron kinetics for the power evaluation.

Uncertainty sources related to the selected neutron kinetics parameters are discussed. Rod worth, fraction of delayed neutron and Doppler coefficients are typically defined with uncertainties given by ±10%, ±5% and ±20%, respectively.

Operator training

The operator role may be relevant in the event of a reactivity accident in a NPP. It is worthwhile to note again that potential operator action, if needed, may be beneficial in the direction opposite to that requested in cases when loss of flow or loss of coolant accidents occur. For instance, stopping recirculation pumps and preventing cold water from reaching the core are typical actions required following RIA-ATWS. Within the present project it was not possible to assess whether adequate qualification of the operator for dealing with such situations is currently available from the industry.

Here, the attention is focused toward simulator, control room and especially emergency operating procedures. The interaction of these subjects with the coupled 3-D neutron kinetics/thermal-hydraulic calculations is mentioned. The subject has not been treated as deeply as would seem necessary because it does not appear to be part of the current technological practice.

Regulatory position

Attention is focused toward the regulatory approach pursued by various countries as concerns NPP accidents where neutron physics is relevant. Specifically, a non-systematic review of regulations in force and of performed licensing calculations is presented. Acceptance criteria and guidelines for

conducting the analyses are discussed. The overall picture shows that a lot of attention is devoted to transients involving neutron physics (*i.e.* control rod ejection, ultimate fuel resistance), but little or no importance is given to the capabilities of the coupled 3-D neutron kinetic/thermal-hydraulic techniques.

Making reference to the ATWS issue, the survey of the regulatory position in eight countries, brings to light the following additional main findings:

- ATWS analyses are mandatory (*i.e.* foreseen in the licensing process) in only a small number of countries in relation to the number of countries that were taken into consideration. However, generic safety analyses are performed in almost all countries to address the issue.

- The attention devoted to coupled 3-D neutron kinetics/thermal-hydraulic techniques from the regulatory bodies is insignificant in almost all cases.

Database of results

A database of results has been gathered within the framework of the CRISSUE-S project. This complements the input database that constitutes the main content of the first CRISSUE-S report [170]. The database of results constitutes Annex I to the present report and includes results of transient coupled 3-D neutron kinetics/thermal-hydraulic calculations performed to predict transient scenarios in BWR, PWR, VVER-440 and VVER-1000 NPPs. Those considered are part of the ensemble of transients recommended for safety analyses (see also above).

The database of results presented in Annex I provides a notion of the transient behaviour of the selected NPP in cases when neutron kinetics/thermal-hydraulic coupling is relevant and constitutes a reference for those code users engaged in similar analyses.

New frontiers for research and recommendations emerging from the activities undertaken are summarised as follows:

- Systematic qualification of the various steps in the application of coupled neutron kinetics/ thermal-hydraulic techniques is needed, including the adoption of available tools and procedures.

- Full consideration shall be given to the identified sources of uncertainties (see above).

- It must be clear that results obtained by 0-D neutron kinetics coupled with thermal-hydraulics are not necessarily conservative. This observation must provide the impulse for wider application of coupled 3-D neutron kinetics/thermal-hydraulic techniques in the nuclear safety domain.

- The integration of nuclear fuel-related models into neutron kinetics thermal-hydraulics coupling is necessary. This also includes the chemistry, with main reference to the processes of crud formation and release.

- The industry and the regulatory bodies should become fully aware of the capabilities (and of the limitations) of the techniques concerned. It is expected that regulatory bodies consider the list of transients in LWR whose analysis is recommended by coupled techniques: BWR stability, ATWS and those transients characterised by asymmetric core behaviour are the most important. On the industry side, operators should be made aware of transients that are calculated by 3-D coupled neutron/thermal-hydraulic techniques and simulators, control rooms and EOP should benefit from the experience gained from the application of such techniques.

The project meetings

Six plenary CRISSUE-S meetings were held over the course of the project. The WP2 report was an important issue of discussion during each meeting. CRISSUE-S meetings were held at:

- University of Pisa (Pisa, Italy), 25-26 February 2002 (kick-off meeting).
- OECD/NEA (Issy-les-Moulineaux, France), 5-6 September 2002.
- Technical University of Catalonia (UPC, Barcelona, Spain), 23-24 January 2003.
- SKI (Stockholm, Sweden), 26-27 June 2003.
- European Commission, Luxembourg, 12 November 2003 (status information meeting).
- University of Pisa (Pisa, Italy), 11-12 December 2003 (final meeting).

INTRODUCTION

CRISSUE-S is an acronym for *Critical Issues in Nuclear Reactor Technology: A State-of-the-art Report*. The project was conceived with the realisation that there exist areas within the technology of LWR for which a limited comprehension imposed the necessity of wide safety margins, this at the time when the current generation of NPPs was designed. Such safety margins placed limits on the operation of the plants, thus increasing the cost of electricity production, and also continue to leave islands in the sea of knowledge that must be flooded. The relatively recent availability of powerful computers and computational techniques together with a continuing increase in operational experience are the incentives for revisiting the areas of limited understanding with the aim of reducing operational costs, improving the common perception of safety and design/operating conditions and, finally, expanding the basis for advancing the technology.

The main subject of the CRISSUE-S activity is the interaction between 3-D neutron kinetics and system thermal-hydraulics. This is relevant for both the safety and the design/operation of existing reactors. Therefore, regulatory authorities and industry may benefit from the main findings. A direct impact is expected upon the design of innovative water-cooled reactors.

Bases of the subject and motivation for CRISSUE-S

The main impetus behind the proposed activity stems from the availability of advanced coupled neutronics/thermal-hydraulics computer tools and of powerful computers. It is now possible to perform realistic best-estimate analyses of very complex transients and thus potentially to optimise emergency operating procedures (EOP) for existing nuclear power plants. These capabilities have not yet been fully exploited due to a lack of funding. They may allow the solution of what may be termed “old fashioned” problems (critical issues) in nuclear reactor technology. Issues related to the interaction between thermal-hydraulics and neutronics that continue to challenge the design and operation of light water reactors, with particular reference to reactivity-initiated accidents (RIA), constitute the subject of the proposal. Such obstacles can be definitely addressed as a follow-up of the present activity. Recent events occurring in Swedish nuclear power plants underscore the importance of the issue.

Additional motivations for the activity include:

- A spread of results calculated in comparison exercises has appeared over the past few years. There seemed to be no clear, agreed-upon common view within the technical community as concerns the safety relevance of the issues considered here, rendering clarification necessary.

- There are many initiatives in progress, not only within the EU, to produce state-of-the-art and/or status reports concerning a number of topics. Due to lack of funding, however, these are not based upon a thorough analysis of existing information. Consequently, related planning is not very coherent.

- The wide interest generated within the technical community by two benchmarks proposed by the OECD/NEA/NSC, the PWR MSLB (TMI-1 NPP) and the BWR-TT (Peach Bottom NPP). The former scenario concerns a main steam line break in one of the two steam generators of the TMI-1 NPP: asymmetric core cooling gives rise to a fission power peak localised in one part of the core. The latter is the BWR turbine trip: closure of the turbine inlet valve causes a pressure wave propagation into the vessel that leads to void collapse and, again, to a fission power peak. Both of these involve tight neutronics/thermal-hydraulic interaction and require 3-D neutron kinetics tools coupled with thermal-hydraulic codes.

Objectives for the activity and of the present report

The general and strategic objective of the activity is the improvement of the safety and design quality of nuclear power plants, these two goals aiming to increase public acceptance of nuclear technology, as can also be derived from the statements above.

The main objectives for the CRISSUE-S activity have been established as:

a) State of the art on the subject covering thermal-hydraulics including steam line dynamics, neutronics, core and primary circuit surveillance and monitoring techniques, feedback in the areas of accident management, operator training and control room optimisation, present and envisaged regulatory requirements/criteria. The importance of uncertainty in the best-estimate calculations considered is evaluated.

b) Providing results of best-estimate analyses of complex transients in existing reactors. These are subsequently called RIA (reactivity-initiated or induced accidents) or REAC (reactivity accidents). Reference is made to main steam isolation valve (MSIV) closure and instability events in BWR and MSLB (main steam line break) in PWR and VVER. Relevant transients involving close interaction between thermal-hydraulics and neutronics, *e.g.* start-up of an idle de-borated loop in VVER-440 and anticipated transients without scram (ATWS) are of interest in the framework considered. These transients challenge the safety of the NPP and may require improved engineered safety features and emergency operating procedures.

c) Providing recommendations to interested organisations, utilities and regulators about:

   c1) Possible safety margins of existing reactors.

   c2) Optimised management of the events considered.

d) Identifying areas of the NPP design where the design/safety requirements can be relaxed due to improved knowledge in the area of neutronics/thermal-hydraulics coupling; a rough estimate of cost savings will be provided.

Structure and content of the report

The structure of the report can be derived from Table 1. Six main topics have been identified. Each of these has been divided into subtopics which are addressed in the text.

Table 1. List of topics and contributors to the REAC-SOAR

		UPISA	ANAV-UPC	STUD	SKI	UMAD	UVAL	NRI	PSU	UIUC	NEA	VALCO	RIT
Topic 1	**PSA***		C	R				C					C
1.1	BWR (including ATWS and extreme transients)												
1.2	PWR (as above)												
1.3	VVER (as above)												
1.4	Methods												
1.5	Results												
1.6	Interactions with other topics												
Topic 2	**3-D neutronics and system thermal-hydraulics**	C					C	C	R			C	
2.1	Transients of interest and available database**		R		C								
2.2	Suitable codes					C							
2.3	Coupling												
2.4	Nodalisation requirements												
2.5	Needed precision, including level of detail of coupled calculation					C							
2.6	Uncertainty												
2.7	Cross-section derivation												
2.8	BWR stability*												
2.9	Heat transfer modelling inside pin					C		C					
2.10	Neutron transport and diffusion								C	C			
2.11	Numerical methods (time, spatial discretisations, etc.)					C			C	C			
2.12	Interactions with other topics	C											
Topic 3	**Fuel****					R				C	C		
3.1	Fuel failure												
3.2	Design limits												
3.3	Needed modelling capabilities												
3.4	Material properties												
3.5	Innovation												
3.6	Interaction: chemistry, HTC, boron, bending and other topics												
3.7	NEA database												
3.8	Differences PWR/VVER: pin-hole, & lattice												
3.9	Reloading/misalignment												
Topic 4	**Advanced fuel**					R					C		
4.1	High BU and Pu (weapons & reactor grade)												
4.2	Kinetics parameters & spectra												
4.3	Epithermal core												
4.4	Issues as item 3.												
Topic 5	**Operator training**												
5.1	Simulator		R					C					C
5.2	Control room												
5.3	EOP												
5.4	Interaction with other topics												
Topic 6	**Regulatory requirements**				R		C		C,+				
6.1	ATWS												
6.2	Low power (hot, cold)												
6.3	High power												
6.4	Acceptance criteria												
6.5	BWR stability												
6.6	Interaction with other topics												

* The subtopics listed constitute reference subjects for the REAC-SOAR, but do not necessarily correspond to subsections in the report.

** A subtask has been created.

R = Responsible, C = Contributor, + = PSU to contact US NRC about this topic.

State of the art and limitations

Limitations characterising the state of the art in the concerned area, already emphasised in the proposal of the present activity, are synthesised below and give an idea of the subjects discussed and of the drawbacks addressed in the report.

- *Identification of transients that have the potential to originate reactivity accident events*. No systematic/comprehensive study exists. Results are plant specific. Basically, the interaction between the results of the PSA study and a coupled neutronics/thermal-hydraulics evaluation to confirm the importance of the selected transients was lacking.

- *Thermal-hydraulics characterisation of the transients*. Qualified system thermal-hydraulics codes, coupled with 0-D or point neutron kinetics, are available and are suitable for calculating system behaviour. Problems exist in the areas of: a) coupling with 3-D neutronics codes, b) accepting nodalisation qualification criteria, and therefore c) predicting global NPP transient behaviour. Making reference to the BWR stability issue, not fully characterised inadequacies exist in the area of density waves instabilities. It is also unclear what happens when the amplitudes of the oscillations escalate into the non-linear domain.

- *3-D neutronics*. Computer tools suitable for calculating core performance once fuel and thermal-hydraulic parameters are available do exist and are reliable. Problems occur due to coupling with thermal-hydraulics (item above) and the availability and proper averaging of fuel data (item below).

- *Fuel simulation*. Fuel data are necessary in different areas of nuclear technology ranging from thermal-hydraulics to radiation protection to structural mechanics (design of resistant cladding), to neutronics to core life management. Uncertainties in related parameters can be quite important depending upon the application. In the present framework, uncertainties may affect the thermal-hydraulics and neutronics calculation separately and, to a greater extent, the coupled neutronics/thermal-hydraulics evaluations. Cross-sections that are also a function of burn-up, pellet-clad gap and fuel conductivity constitute typical major sources of uncertainties in the neutronics and thermal-hydraulics areas, respectively. The averaging procedures accounting non-homogeneous fuel bundle geometric configuration, coolant/moderator distribution and presence in the core of structural (*e.g.* fuel box in BWR, spacer grids, etc.) and absorbing (*e.g*. different types of control rods) materials constitute additional sources of uncertainties. The consideration of reflector material and/or, in thermal-hydraulics terms, of bypass flow paths at the outer core boundaries (mainly in the radial direction) also introduces uncertainties in the analysis.

- *System effects*. Modelling of balance of the plant (BOP) and NPP control systems play an important role when predicting reactivity accidents that involve neutronics/thermal-hydraulics feedback. Typical BOP and control systems are constituted by feed water pre-heater, level and pressure control (steam generator in PWR plants and RPV in BWR plants), pressuriser heaters and chemical and volume control system (CVCS) in PWR as well as recirculation loop flow rate control and flows from control rod drive system in BWR.

A detailed solution to the problems outlined here and the quantification of all the uncertainties mentioned are well beyond the resources available even if the case a single NPP type is considered. Nevertheless, within the present framework, all relevant sources of uncertainty are identified and responses are provided to the concerns raised.

Chapter 1

PROBABILISTIC SAFETY ASSESSMENT (PSA)

It is not practical to envision simulating all the transient situations that can be expected in a typical NPP. However, a hierarchy of transients can be achieved through the use of suitable probabilistic techniques. The importance of the transient is established on the basis of its probability to occur and the consequences of the potential accident in terms of radioactive releases. In this way, a number of transient scenarios can be analysed through conservative or deterministic approaches [1].

The main focus of PSA is to provide realistic answers, thus best-estimate codes and realistic input data are used. However, the results of the deterministic analyses may be "bounded" by results of conservative analyses to show that equipment performance is satisfactory. The bounding analysis approach shall not be pursued in any situation, like for designing or optimising the EOP.

The main purpose for this chapter is to derive a suitable list of transients for PWR, BWR and VVER in relation to which the application of deterministic coupled 3-D neutronics/thermal-hydraulic techniques is recommended. This is done in Sections 1.2 (PWR), 1.3 (BWR) and 1.4 (VVER). A consistent derivation of those transients would imply a comprehensive use of PSA techniques.

The application of probabilistic techniques is not included among the main objectives of the CRISSUE-S activities and thus of the current report. Nevertheless, a few statements are provided in Section 1.2 in relation to the use of probabilistic techniques within the general framework of accident analysis. More details connected with PSA can be found on the first deliverable from the CRISSUE-S project [2].

1.1 Available tools and performed activity

The PSA traditionally concentrates on events that can lead to core damage. The PSA for core damage comprises three levels, each successive level incorporating a more comprehensive analysis than the previous level [2]. The first level, PSA Level 1, focuses on the estimation of core damage frequency, expressed as a probability of core damage per year of reactor operation. The second level, PSA Level 2, includes Level 1 analysis and a further study of the physical processes during the core melt so as to quantify the amount of various radioactive compounds that can be released from the core (source term). PSA Level 3 include Level 2 analysis and investigates the dispersion of radioactive substances in the environment and of associated possible consequences to life, health and property.

In principle, a "PSA methodology" could be applicable to any end condition, not only to core damage. The end condition could for instance be the situation of having the fuel exposed to excessive power escalation as a result of a RIA. The specification of this type of end condition could be in accordance with the RIA fuel failure limit based on the definition in Section 4.2 of the US Standard Review Plan [3], which is used in most countries. This provides a limit on maximum radially averaged fuel enthalpy of 170 cal/g for BWR and a limit defined as a DNB criterion for PWR. The trend of using fuel with high burn-up (approximately 50 MWd/kg and higher) can possibly alter these limits [4,5].

In order to classify and find a probability for a certain sequence leading to a RIA it is sufficient to undertake an associated PSA Level 1 analysis. This analysis is comparable to a Level 1 analysis for core damage, and is based on a systematic reliability analysis of systems and components whose level of operational functionality will have an essential impact on the transient response during the course of events leading to the RIA. As is emphasised by an OECD/NEA report [6], this analysis includes several prerequisites such as acquiring an in-depth understanding of the NPP system and collecting pertinent information, identifying initiating events and states of the RIA, setting-up fault tree models of the system to reveal performance and system interactions, and develop databases of component reliability data. It is clear that PSA studies are concerned only with specific sequences in a given plant and are therefore plant specific.

It is obviously not feasible to analyse all conceivable types of events in a plant. Instead, the events may be classified according to the expected probability of their occurrences, expressed as an occurrence frequency per year of reactor operation, and associated consequences on the plant overall safety features. The event classification is usually based on recommendations given in ANS 51.1 and 52.1, and is made considering probability ranges as detailed in Ref. [2].

Considering the above framework, but without any application of PSA techniques, recommendations for coupled 3-D neutron kinetics/thermal-hydraulic analysis are provided in the following three sections.

1.2 Relevant PWR transients for coupled 3-D neutronics/thermal-hydraulic analyses

PWRs exist with varying configurations, *i.e*. UTSG and OTSG. The UTSG PWR is different as concerns the number of loops and the core nominal power, these two parameters not necessarily being interconnected. Two to four SG characterise UTSG plants, though one NPP operates with one SG. The OTSG are all equipped with two SG and differentiate with regard to the core power level.

Accordingly, a request for transient analysis should be plant specific. An attempt is made below, however, to identify transients (characterised by an acronym or by key words) that are of general interest. The reasons for their selection are outlined together with a short phenomenological description of the expected events. When selecting transient scenarios, consideration has been given to the recently issued IAEA guidelines [1,7].

- *MSLB.* Accident originated by the double-ended guillotine break of one SL. Positive reactivity is caused by the cooling of the primary water following depressurisation of the SG. The “plug” of cold water typically reaches the core a few seconds after the break occurs in the steam line. A regional core power increase may occur due to partial mixing in the RPV downcomer of cold water from the affected SG with hot water from the intact SG. The potential regional nature of the transient and the amount of positive reactivity introduced justify the coupled analysis. HZP and FP initial conditions can be investigated at BOC and EOC conditions.

- *LOFW-ATWS.* Blockage of FW pumps also originated by partial station blackout causes LOFW. Primary loop temperature increase and moderator and Doppler neutron feedbacks contribute to power decrease. The ATWS analysis is deemed necessary considering the (relatively high) accident frequency. The accident scenario originated by the MSIV closure, again with the ATWS condition (*i.e.* MSIV closure-ATWS) could be studied with similar assumptions (apart from the initiating event) as the LOFW-ATWS.

- *CR ejection.* Regional reactivity increase is expected following CR ejection. This justifies the application of the 3-D coupled techniques. The highest worth CR should be considered. HZP and FP initial conditions can be investigated at BOC and EOC conditions. Ejection of CR

banks or of a group of CR can be of interest. The CR ejection is connected with an SBLOCA due to the damage of the holding mechanism for the ejected rod (this is mostly not considered in the current analyses).

- *LBLOCA-DBA.* The accident is originated by the double-ended guillotine break of one CL at a location between the RPV and the MCP. The accident constitutes a pillar in the safety demonstration and in the licensing of any LWR, with main reference to the evaluation of the ECCS design and thus is part of the official NPP FSAR. The proposal for 3-D neutron kinetics/thermal-hydraulic analysis is mainly linked to the need to quantify the conservatism introduced by the highly conservative peak factors (PF) for linear power that cause high values for PCT. The use of advanced coupled neutron kinetics/thermal-hydraulic techniques engenders the removal of that conservatism and emphasises the industrial relevance of the same techniques. A specific LBLOCA-RIA occurs in the case of positive moderator temperature coefficient, which is possible in principle at BOC with a high boron concentration.

- *Incorrect connection (start-up) of an inactive (idle) loop*. The inactive loop is assumed to have de-borated water in the loop seal having a volume consistent with the system geometry. This transient is representative of transients originated by the presence of boron in the primary loop (see also the SBLOCA-ATWS, below).

- *MSLB-ATWS*. The MSLB constitutes a DBA transient (see description above). The ATWS feature is not justified by any PSA study. Rather, the recommendation for the 3-D coupled analysis derives from the bounding nature that this transient might have (*i.e*. in terms of input reactivity for the core) and from the consideration that core integrity can be predicted for such an extreme situation.

- *SBLOCA-ATWS*. This is a TMI-type accident originated by a small loss of integrity in the primary loop. The relatively high frequency of occurrence justifies the ATWS condition. Positive reactivity insertion can be assumed to come from de-borated water coming from any ECCS, *i.e*. HPIS and ACC (or SIT) and LPIS. The amount of fresh (un-borated) water injection should be in accordance with the individual plant's features and maintenance programmes.

1.3 Relevant BWR transients for coupled 3-D neutronics/thermal-hydraulic analyses

As for PWRs, various BWRs exist that differentiate mostly with regard to the configuration of the recirculation loop. IP, JP and EP BWRs can be distinguished. The internal pump (IP) reactor constitutes the latest accepted advancement in the technology (ABWR, jointly realised by US and Japanese firms, though the solution was proposed and realised decades ago by EU companies). The jet pump (JP) reactor is the most widely diffused BWR and a few earlier-designed external pump (EP) reactors are still in operation.

Accordingly, a request for transient analysis should be plant specific. Nevertheless, an attempt is made below to identify transients (characterised by an acronym or by key words) that are of general interest. The reasons for their selection are outlined together with a short phenomenological description of the expected events. When selecting transient scenarios, consideration has been given to the recently issued IAEA guidelines [8]. In all BWR transient scenarios the use of coupled 3-D techniques is justified by the broad variation in the axial linear power distribution as a function of time. This cannot be predicted by any 0-D neutron kinetics model.

- *TT without condenser bypass available*. TT constitutes a (relatively) frequent event in BWR operation. A positive pressure wave propagates from the turbine isolation valve to the RPV and reaches the core from the top (*e.g*. across the steam separator and dryer) and from the bottom (*e.g*. across the downcomer and the lower plenum). Void collapse causes positive reactivity insertion and power excursion typically stopped by scram occurrence. Opening the condenser bypass valves makes the effect of the pressure wave propagation milder, but this effect is neglected in the proposed scenario.

- *LBLOCA-DBA*. The rupture of one recirculation line (if present) originates the accident. The regulatory framework and the reasons for the analysis are the same as those discussed in relation to PWR (see above).

- *CR ejection*. The same considerations made for PWR apply here.

- *FW temperature decrease (ATWS)*. Malfunction of FW pre-heaters (*e.g*. sudden depressurisation in one pre-heater on the heating side) and of FW pumps (*e.g*. DC level control system) may cause FW temperature decrease that reflects in colder water at the core inlet. This creates a potential for reduction of the steam occupied volume into the core and a consequent increase in moderation and in fission power. This partly covers the *FW flow rate increase* event (see also below).

- *MCP flow rate increase*. The flow rate increase may be caused by a malfunction of valves installed in the MCP lines or by a spurious signal controlling the pump speed (whatever is realistic for the NPP concerned). This partly covers the *FW flow rate increase* event.

- *MSIV closure (ATWS)*. The closure of the main isolation valves creates a pressure pulse (same situation as TT) that causes void collapse in the core and reactivity excursion. The ATWS condition must be considered as a bounding condition in safety analysis. The application of the 3-D neutron kinetics/thermal-hydraulic technique has the potential to show that even in such extreme and unrealistic (low probability) conditions the safety margins embedded in the system design allow recovery of the core.

- *Stability analysis*. Stability performance of BWR has been thoroughly investigated during the entire nuclear era. Synthesis reports have been issued [9], and recently published analyses show the applicability of the 3-D coupled techniques [10,11]. The use of different fuel types in the same core renders the proposed investigation all the more potentially valuable and necessary. Recommended transient can be originated at nominal power and include MCP trip that brings the plant into the exclusion region of the BWR flow map [9]. Transient analysis should go on until NC steady state is established, at roughly 50% nominal core power and 30% nominal core flow. The FW and the SL flow rates should be varied according to the core power and the RPV pressure should be kept (nearly) constant during the simulation. Control systems for RPV pressure and DC level (and various BOP components) can be simulated: their role in determining the stability performance of the system should be evaluated.

- *Stability analysis (ATWS)*. The same analysis as discussed in the previous paragraph should be performed, further assuming failure of the scram system. Though this condition is beyond the DBA boundaries due to its low probability of occurrence, results can be useful to designers and to safety analysts to optimise EOP and to better understand NPP safety margins.

1.4 Relevant VVER transients for coupled 3-D neutronics/thermal-hydraulic analyses

VVER is the Russian-type PWR that differentiates from the Western PWR mostly with regard to the presence of horizontal tubes SG (HOSG), the design of the primary circuits loop (loop seal on hot leg –VVER-440), ECCS injections to UP and in the hexagonal geometry of the core. These differences are relevant to the activity of interest here. Other system features also distinguish PWR from VVER, though they are not addressed here. The VVER-440 and the VVER-1000 NPP classes must be distinguished. The core power (about 440 MWe and 1 000 MWe, respectively), the number of SG (six and four, respectively), the core configuration (presence of closed hexagonal fuel assemblies and follow up control rods, fuel elements in the case of VVER-440 and open core with cluster CR in the case of VVER-1000) and the containment design (confinement with various features and a pressure suppression system for VVER-440/213 and full containment for VVER-1000) are different in the two NPP classes. Between the two classes further differences among individual NPP are can be observed, which are not relevant to the present investigation.

Once again, a request for transient analysis should be plant specific. In addition, general statements applicable to PWR can also be applied to VVER. The same list of transients is valid. Hereafter, reasons for transient selection are not repeated; only information relevant to VVER is added. When selecting transient scenarios, consideration has been given to the recently issued IAEA guidelines [7].

- *MSLB*. The accident (namely in VVER-440) is expected to be less severe than in PWR due to the large amount of water in the primary and secondary circuits of the SG (namely, ratios between initial SG fluid mass and system power and break area over SG fluid volume are larger than in PWRs). This is from the point of view of coolability of the core, though from the point of overcooling of the core (very low core input temperature) the large amount of water in the secondary circuits is undesirable.

- *LOFW-ATWS*. No special remark in addition to the PWR description. The amount of water in the secondary circuit plays a large role. This accident is less severe in VVER-440 than in PWR.

- *CR ejection*. The accident would be a valid proposition only for the VVER-1000. Whole absorber assemblies could be ejected in the case of VVER-440. Practically, the transients are the same in VVER-440. No discrepancy between VVER-440 and VVER-1000.

- *LBLOCA-DBA*. Making reference to the VVER-440, current DBA is originated by a 32 mm break in CL. The proposed analysis may contribute to demonstrate that current ECCS are suitable for coping with the 200 mm break and the 500 mm break. Therefore those two events can be added to the DBA list. Here is the difference between VVER-440/230 and their modifications and VVER 440/213. For VVER 440/213 the double-ended guillotine break (500 mm) constitutes the maximum DBA.

- *Incorrect connection (start-up) of an inactive (idle) loop*. It should be noted that VVER-440 are equipped with main isolation valves installed in HL and CL. The probability of such an accident occurring can be larger than is the case for PWRs.

- *MSLB-ATWS*. No special remark in addition to the PWR description. Over-cooling from the secondary side is probably larger.

- *SBLOCA-ATWS*. No special remark in addition to the PWR description.

- *Isolation of one loop (ATWS)*. This accident may occur only in VVER-440 NPP equipped with main isolation valves. The transient shall be considered complementary to the transient *Incorrect connection (start-up) of an inactive (idle) loop* listed previously. The ATWS condition is added, notwithstanding the low probability of occurrence, so as to test the intrinsic safety margin of the system.

1.5 Reference transient scenarios

Comprehensive, best-estimate calculations and the resulting data evaluation for the transients specified in the last three sections constitute an enormous task, which (among other things) is plant and plant-cycle specific. Therefore, no information obtained for a specific application may be generalised to different plants or to different situations within the same plant.

Notwithstanding the above an effort has been made within the CRISSUE-S framework to produce reference data for the largest number of transients specified above. The main purpose of the effort is to constitute a database of results that can be used by analysts as well as by decision makers to obtain a quantitative idea about expected transient scenarios and, equally, to support decisions about the need to perform coupled calculations related to a generic NPP.

Calculations have been performed utilising computational tools and input decks developed and already employed for different purposes. The level of qualification of those tools and of the related results *does not* comply with the requirements and the recommendations proposed in Chapter 2.

The computational tools adopted include the CASMO code for neutron cross-section derivation, the RELAP5/mod3.2, RELAP5/mod3.3 and RELAP5 3-D © codes for thermal-hydraulics, and the PARCS and the NESTLE codes for 3-D neutronics (see Section 2.2 for more detail). The Penn State University (PSU) has made all sets of cross-sections needed for the various analyses available [12-14] related to PWR, BWR and VVER-1000, respectively. The RELAP5 input decks were developed at the University of Pisa (UPISA) [15-17]. The PARCS and the NESTLE input decks were developed within the framework of co-operation between PSU, UPISA and Texas A&M University (TAMU) [18-20]. BWR stability analyses were partly performed within a co-operation between UPISA and the University of Valencia (UVA) [21].

The resulting databases (*i.e*. results of coupled 3-D neutronics/thermal-hydraulic calculations) are outlined in Annex I, following the transient identification given in Sections 1.2, 1.3 and 1.4. Each calculation is documented by a one-page description and two pages of significant system-related time trends or 3-D snapshots of core-related quantities. The last section of Annex I is devoted to the calculation of the enthalpy release to the fuel for some of the most significant calculations (*i.e*. for calculations that produced the highest local power excursion) documented in the previous sections of the same Annex.

The following main limitations apply to the performed calculations that are documented in Annex I:

- The cross-section sets have been derived for a specific NPP status that does not coincide with the worst or the most critical status expected for the considered transient. As a consequence, the range of validity of the derived cross-sections may be over-passed when different transient are analysed (by adopting the same set of cross sections).

- Although an effort has been made to achieve qualified results, a comprehensive check of the various qualification requirements has not been made, as mentioned earlier. Therefore, the reported results should be considered qualified as-far-as-possible. This is true for stand-alone RELAP5or PARCS or NESTLE input decks as well as for the coupled input decks.

- Actuation logics of all NPP systems that may have a role during the assigned transients have not necessarily been simulated.

Chapter 2

THREE-DIMENSIONAL NEUTRONICS AND SYSTEM THERMAL-HYDRAULICS

2.1 Transients of interest and available database

LWR transients that have been analysed by coupled 3-D neutron kinetics/thermal-hydraulics techniques are outlined hereafter. Associated available databases, not necessarily open to the scientific community, are mentioned. The objective is to provide an impression of the current trends from the industry side. The transients considered are not necessarily related to the transients discussed in Sections 1.2 to 1.4, in relation to which analyses by coupled techniques are recommended.

A list of representative transients is given in Table 2, which gives an idea of the current interest in the world toward 3-D neutronics/thermal-hydraulics coupled calculations. Along with the authors of the paper or document, the information listed in the table includes the adopted codes, the NPP type under investigation and the considered transient scenario. In the last column of the table references are indicated (*i.e.* from [22a] to [22n]).

2.2 Suitable codes

Complex codes are required for the following three steps in the application of 3-D coupled techniques:

- Code for deriving suitable neutron kinetics cross-sections (CSC = cross-section code).
- Thermal-hydraulic system code (THSC).
- Neutron kinetics codes (NKC).

The codes described here are internationally known and suitably qualified. The list is by no means exhaustive but can serve as an indication of the type of codes available today within the area of coupled THSC/NKC. Features and capabilities of those codes are mentioned in the following sections. Details can be found in the references. Other, simpler codes used within the licensing process are described in Chapter 6 (*e.g.* Section 6.4.1.5).

The consistent application of CSC, THSC and NKC is required to perform a full 3-D coupled neutron kinetics/thermal-hydraulic calculation. However, the CSC can be used independently and THSC and NKC must be coupled and should interact at each time step.

Table 2. Overview of 3-D coupled neutronics/ thermal-hydraulics calculations available from the literature

No.	Title and authors	Coupled codes	NPP	Transient type	Ref.
1	*Coupling of the Thermal-hydraulic Code TRAC with 3-D Neutron Kinetics Code SKETCH-N* H. Asaka, V.G. Zimin, T. Iguchi, Y. Anoda	J-TRAC TRAC-BF1 Sketch-N	PWR	RIA	[22]
			BWR (Ringhals-1)	Stability benchmark cases	
			BWR	Instabilities	
2	*Core-wide DNBR Calculation for NPP Krško MSLB* I-A. Jurković, D. Grgić, N. Debrecin	RELAP5/MOD3.2 COBRA III C QUABOX/CUBBOX	PWR (NPP Krško)	MSLB	[22b]
3	*MSLB Coupled 3-D Neutronics/Thermal-hydraulic Analysis of a Large PWR Using RELAP5-3-D* F. D'Auria, A. Lo Nigro, G. Saiu, A. Spadoni	RELAP5/MOD.3.2.2 NESTLE	PWR B&W TMI-1	MSLB	[22c]
			AP-1000		
4	*TMI-1 MSLB Coupled 3-D Neutronics/ Thermal-hydraulics Analysis: Application of RELAP5-3-D and Comparison with Different Codes* R. Bovalini, F. D'Auria, G.M. Galassi, A. Spadoni, Y. Hassan	RELAP5/MOD3.2.2 PARCS	PWR (B&W TMI-1)	MSLB	[22d]
		RELAP5/MOD3.2.2 QUABBOX			
		RELAP5/3-D NESTLE			
5	*PWR REA Sensitivity Analysis of TRAC-PF1/NEM Coupling Schemes* N. Todorova, K. Ivanov	TRAC-PF1 NEM	PWR (B&W) TM-1	REA	[22e]
6	*Coupled 3-D Neutronic/Thermal-hydraulic Codes Applied toPeach Bottom Unit 2* A. Mª Sánchez, G. Verdú , A. Gómez		BWR (Peach Bottom Unit 2)	TT	[22f]
7	*Study of the Asymmetric Steam Line Break Problem by the Coupled Code System KIKO3D/ATHLET* Gy. Hegyi, A. Keresztúri, I. Trosztel	ATHLET KIKO3D	VVER 440	MSLB	[22g]
8	*Development of Coupled Systems of 3-D Neutronics and Fluid-dynamic System Codes and their Application for Safety Analysis* S. Langenbuch, K. Velkov, S. Kliem U. Rohde, M. Lizorkin, G. Hegyi, A. Kereszturi	ATHLET DYN3D BIPR-8	VVER-1000	LOFW	[22h]
				Station black out	
				MCP stop	
9	*VIPRE-02 Subchannel Validation Against NUPEC BWR Void Fraction Data* Y. Aounallah, P. Coddington	VIPRE-02 ARROTTA	BWR	Void fraction validation study	[22i]
10	*High Local Power Densities Permissible at Siemens Pressurised Water Reactors* K. Kuehnel, K.D. Richter, G Drescher, I. Endrizzi	PANBOX	PWR	Maximum local heat flux investigation	[22j]
11	*Analysis of a Boron Dilution Accident for VVER-440 Combining the Use of the Codes DYN3D and SiTap* U. Rohde, I. Elkin, V. Kalinenko	SiTap DYN3D	VVER 440	RIA	[22k]
12	*RELAP5-PANTHER Coupled Code Transient Analysis* B.J. Holmes, G.R. Kimber, J.N. Lillington, M.R. Parkes	RELAP5 PANTHER	PWR (Sizewell-B)	Grid frequency error injection test	[22l]
				Single turbine trip event	
13	*TACIS R2.30/94 Project Transient Analysis for RBMK Reactors* H. Schoels, Yu.M. Nikitin Nikiet	FLICA GIDRA SADCO DINA CRONOS QUABOX/CUBOX	RBMK (Smolensk 3)	RIA	[22m]
14	*PWR Anticipated Transients Without SCRAM Analyses Using PVM Coupled RETRAN and STAR 3-D Kinetics Codes* M. Feltus, K. Labowski	RETRAN STAR 3-D	PWR	ATWS	[22n]
15	*Development and First Results of Coupled Neutronic and Thermal-hydraulic Calculations for the High-performance LWR* C.H.M. Broeders, V. Sanchez-Espinoza, A. Travleev	RELAP5 KAPROS	HPLWR	FA tests	[22o]
16	*Analysis and Calculation of an Accident with Delayed Scram on NPP Greifswald using the Coupled Code DYN3D-ATHLET* S. Kliem	ATHLET DYN3D	VVER-440 (Greifswald)	Delayed scram	[22p]
17	*Multi-dimensional TMI-1 Main Steam Line Break Analysis Methodology using TRAC-PF/NEM* K. Ivanov, T. Beam, A. Baratta, A. Irani, N. Trikouros	TRAC-PF NEM	PWR (B&W TMI-1)	MSLB	[22q]
18	*Realistic and Conservative Rod Ejection Simulation in a PWR Core at HZP, EOC with Coupled PARCS and RELAP Codes* J. Riverola, T. Núñez, J. Vicente	RELAP PARCS	Three-loop PWR	Peripheral rod ejection	[22r]

Table 2. Overview of 3-D coupled neutronics/ thermal-hydraulics calculations available from the literature (*cont.*)

No.	Title and authors	Coupled codes	NPP	Transient type	Ref.
19	*OECD/NRC BWR Benchmark 3rd Workshop*	ATHLET QUABOX/CUBBOX	BWR (Peach Bottom)	TT	[22s]
		TRAC-BF1COS3D			
		TRAC-BF1 SKETCH-INS			
		TRAC-BF1/ENTRÉE			
		RELAP5/PARCS			
20	*Calculation of the Drop of One Turbine to House Load Level Experiment on Loviisa-1 NPP with Coupled Codes DYN3D/ATHLET – Final Results* J. Hadek, J. Macek	ATHLET-DYN3D	VVER 440 (Loviisa-1)	Load drop of one turbo-generator	[22t]
21	*Final Results of the Fifth Three-dimensional Dynamic AER Benchmark Problem Calculation* J. Hadek	ATHLET-DYN3D	VVER 440	Symmetrical MSH break	[22u]
22	*Interim Results of the Sixth Three-dimensional AER Dynamic Benchmark Problem Calculation. Solution of Problem with DYN3D and RELAP5-3-D© Codes.* J. Hadek, P. Kral, J. Macek	RELAP-3-D©	VVER 440	Asymmetrical MSLB	[22v]
23	*Thermal-hydraulic Analyses of 2 MSL Break for Safety Case 28 m, Temelin NPP* J. Macek, R. Meca, J. Hadek	ATHLET-DYN3D	VVER 1000 (Temelin)	MSLB	[22w]
24	*Methods and Results for MSLB NEA Benchmark Using SIMTRAN and RELAP5*	SIMTRAN-RELAP5	PWR	MSLB	[22x]

2.2.1 Cross-section generation codes

CASMO-3 [23]

The modern lattice physics codes such as CASMO-3, -4, PHOENIX, HELIOS, CPM-3, APOLLO2 and TransLAT are used for cross-section generation in both core design and transient analysis. These codes utilise integral transport methods such as collision probabilities and/or the method of characteristics in 2-D single assembly geometry using, in general, reflective boundary conditions. The cross-section dependencies on history and instantaneous feedback parameters, including burn-up, thermal-hydraulic conditions, control parameters and core environment can be treated through a number of alternative approaches with varying degrees of sophistication.

The widely used cross-section parameterisation model available in CASMO-3 attempts to model the cross-section cross-term dependence involving an approximate type of cross-section representation. Each cross-section can be evaluated as a summation of base and partial values. The base cross-sections represent the burn-up dependence (exposure, spectral history and control history) while the partial cross-section represents the instantaneous dependence on local feedback parameters.

Performing branch calculations generates the partial cross-sections, where one feedback parameter is changed only for a given perturbation. The model tries to account for the cross-term dependence by using separate partial cross-sections for different feedback effects. While the model is an improvement over the polynomial fitting procedure it is, again, limited to small perturbations.

2.2.2 Thermal-hydraulic system codes

ATHLET [49]

The thermal-hydraulic computer code ATHLET (*A*nalysis of *TH*ermal-hydraulics of *LE*aks and *T*ransients) is being developed by the Gesellschaft für Anlagen- und Reaktorsicherheit (GRS) for the

analysis of anticipated and abnormal plant transients, small and intermediate leaks, and large breaks in light water reactors.

The structure of ATHLET is highly modular, allowing simple implementation of different physical models. The code is composed of several basic modules for the calculation of the different phenomena involved in the operation of a light water reactor, including thermo-fluid dynamics (TFD), heat transfer and heat conduction (HECU), neutron kinetics (NEUKIN), general control simulation module (GCSM), and the numerical integration method (FEBE).

Other independent modules (*e.g.* large models with their own time advancement procedure) can be coupled without structural changes in ATHLET by means of a general interface. ATHLET provides a modular network approach for the representation of a thermal-hydraulic system. A given system configuration can be simulated simply by connecting basic fluid-dynamic elements, called objects.

ATHLET offers the possibility to choose between various models to simulate fluid-dynamics. In the current code version, the basic fluid-dynamic option is a five-equation model with separate conservation equations for liquid and vapour mass and energy, a mixture momentum equation that accounts for thermal and mechanical non-equilibrium, and including a mixture level tracking capacity.

The time integration of the thermo-fluid-dynamics is performed with the general purpose ordinary differential equation solver called FEBE (Forward-Euler, Backward-Euler). It provides the solution of a general non-linear system of differential equations of first order, splitting it into two subsystems, the first being integrated explicitly, the second implicitly. Generally, the fully implicit option is used.

The simulation of heat conduction in structures, fuel rods and electrical heaters is performed within the basic HECU module. The one-dimensional heat conductor HECU provides the simulation of the temperature profile and the energy transport in solid materials. The heat transfer package covers a wide range of single-phase and two-phase flow conditions. Correlations for critical heat flux and minimum film boiling temperature are included.

Nuclear heat generation is generally modelled by means of the neutron kinetics model NEUKIN. The nuclear reactor power generated consists of two parts: the prompt power from fission and decay of short-lived fission products, and the decay heat power from the long-lived fission products. The steady state part of the decay and its time-dependent reduction after a reactor scram are provided in the form of a GCSM signal. The time-dependent behaviour of the prompt power generation is calculated either by a point-kinetics model or by a one-dimensional neutron dynamics model. The point-kinetics model is based on the application of the kinetics equations for one group of prompt neutrons and for six groups of delayed neutrons. The reactivity changes due to control rod movement or reactor scram are given by a GCSM signal. The reactivity feedback effects for fuel temperature, moderator density and moderator temperature are calculated by means of either dependencies given by input tables or with reference reactivity coefficients. The one-dimensional model solves the time-dependent neutron diffusion equations with two energy groups of prompt neutrons and six groups of delayed neutrons. The active zone can be subdivided into zones with different materials. A reflector zone is also considered.

In general, major plant components (*e.g*. pressuriser, steam generator) can be modelled by connecting thermo-fluid-dynamic objects (TFO) and heat conduction objects (HCO) via input data. Simplified, compact models for those components are also available as special objects. The simulation of balance-of-plant systems within ATHLET is performed by the basic module GCSM. This contains a block-oriented simulation language for the description of control, protection and auxiliary systems [50].

RELAP5 – US NRC version [24]

This is a thermal-hydraulic system code extensively used for the analysis of any kind of transient in LWRs. The code is based upon the solution of six partial differential equations that are coupled (or that are required for their solution) with:

- A wide range heat transfer surface for the determination of the HTC.
- The equations for the conduction heat transfer into the solid.
- A variety of constitutive equations (*e.g*. interfacial drag).
- A variety of external models (*e.g*. two-phase critical flow, pump, separator).
- The equations for tracking various non-condensable gases.
- The equation for tracking boron in the system.
- Zero-dimensional (0-D) neutron kinetics equations.

Material properties are embedded into the code, but can also be supplied by the user. The numerical solution method has been specifically adapted for the code and is based upon the use of a semi-implicit finite-difference technique. The thermal-hydraulic model can be classified as a porous media type, so as to distinguish it from the open media that is typical of CFD models. The code is capable of modelling the primary and secondary circuits (where applicable) of NPP as well as all the components belonging to the BOP, including the related actuation logic.

The code is classified as a one-dimensional (1-D) code, though fictitious 3-D nodalisations (input decks) can be set up to simulate three-dimensional flow configurations in open zones. For instance, the core of a NPP can be simulated by several (actually, up to a few hundred) parallel nodes interconnected at different axial elevations by cross-junctions. The code is capable of handling all the transients of interest in the present framework (Sections 1.2 to 1.4 and 2.1). Provided suitable procedures for code applications (Section 2.4) are used, the achieved uncertainty in the results (Section 2.6) can comply with the needed requirements (Section 2.5).

RELAP-3-D © – DOE version [25]

The discussion in the previous paragraph related to RELAP5 NRC applies here. It can be further added that RELAP-3-D © has the capability to apply the 3-D thermal-hydraulic general model and porous media type in selected zones of the NPP. The NESTLE 3-D neutron kinetics code is embedded in this computer code version of RELAP.

CATHARE-2 – CEA code [26]

The discussion in earlier paragraphs related to RELAP5 NRC applies here. It can be added that CATHARE was directly developed for PWR plants, though it has recently been applied to the analysis of transients in VVER and BWR NPP. Related to RELAP5, a different numerical solution method is adopted and a different structure of the input deck must be set up by the user. The code has the design capability of simulating the containment.

CATHARE is modular; several basic modules may be assembled to model the primary and the secondary circuits of any pressurised water reactor or of any analytical test rig (separated effects) or integral test rig (system effects). Zero-dimensional (0-D), 1-D and 3-D modules are available. All of the modules can be connected to walls, exchangers and fuel rods (radial conduction, thermo mechanics). A 2-D conduction calculation is generally made to cope with the quenching of a hot reactor core during a reflooding process. Other submodules are used to compute point-kinetic neutronics, pump speeds, accumulators, sources and sinks. All the modules listed above use the *Two-fluid Model* to transport steam-water flows mixed to four non-condensable gases. Thermal and mechanical non-equilibrium are described through mass, energy and momentum balance equations written for each phase.

All kinds of two-phase flow patterns – stratified, bubbly, slug, churn, annular, dispersed – may be treated. Co-current and counter-current flows are computed with the prediction of the Counter-Current Flow Limitation. Heat transfers with wall structures or fuel rods are calculated taking into account all possible heat transfer processes such as natural and forced convection with liquid or gas phases, subcooled to saturated nucleate boiling, critical heat flux, film boiling and film condensation. The interfacial heat and mass transfers describe stable mechanisms like condensation due to subcooled liquid and vaporisation due to superheated steam. Metastable mechanisms can also be represented, *i.e.* flashing of superheated liquid and condensation of subcooled steam. The effects of non-condensable gases such as hydrogen, nitrogen and air are taken into account during the modelling of the previously described phenomena.

The range of physical parameters in CATHARE is rather large and is devoted to the study of many nuclear power plant accidents: pressure from 0.1 to 16 MPa, liquid temperature from 20°C to 350°C, gas temperature from 20°C to 1 800°C, fluid velocities up to supersonic conditions, duct hydraulic diameters from 0.01 to 0.75 m. An important and rather extensive experimental programme has been carried out to support the validation of the code.

All the CATHARE modules – except the 3-D module which is semi-implicit in time – use a fully implicit time discretisation. Inter-phase exchanges, pressure propagation and advective terms are thus totally implicitly evaluated. This numerical choice was made as CATHARE was being developed in 1979 and was confirmed by a market research stage before the development of the more recent versions of the code. The purpose of such a choice was to reach the largest time step possible without time step limitation, especially for transients of long duration. Concerning space nodalisation, 1-D and 3-D modules use finite volumes discretisation methods for mass and energy equations and finite differences discretisation methods for momentum balance equations. The meshes are staggered according to the ICE method: scalar points are bounded by vector points, mass and energy balances are assessed on scalar points and momentum balances are assessed on vector points. Finally, at each time step and for every type of CATHARE module, one has to find the solution of a set of non-linear equations; a full Newton iterative method is then used

TRAC-PF1 [27]

Los Alamos National Laboratory (LANL) developed the original TRAC thermal-hydraulic code in the mid 70s for analysis of PWRs. TRAC-PF1 is considered as probably one of the most advanced thermal-hydraulic code because of its full six-equation, two-fluid model of the vessel component, such that accurate modelling of the transient can be accomplished. The code can treat a non-condensable gas in a vapour field as well as a dissolved solute in the liquid field. TRAC-PF1 is a best-estimate system transient analysis code, which has a 3-D thermal-hydraulic analysis capability. A modified version of TRAC-PF1/MOD2 version 5.4 [1] is currently being used at the Pennsylvania State University (PSU). Version 5.4 incorporates a one-dimensional decay heat model that dynamically computes the decay heat

axial shape during the transient. The code solves the general transient two-phase coolant conditions in one, two or three dimensions using a realistic six-equation, two-fluid, finite-difference model combining 3-D vessel hydrodynamics and 1-D balance-of-plant modelling. Two-dimensional treatment of fluid-wall heat transfer is incorporated through the ROD and SLAB components. The ROD component provides the treatment of power generation and its transfer to the coolant. The six-equation representation of the two-phase flow conditions, in conjunction with specialised empirical modes for a variety of PWR primary and secondary-loop components and control systems, allows TRAC-PF1/MOD2 version 5.4 to accurately model both mild and severe T-H transients.

TRAC-M (TRACE) [28]

The United States Nuclear Regulatory Commission (US NRC) is currently in the process of consolidating the capabilities of its four T-H codes (TRAC-P, TRAC-B, RELAP, and RAMONA) into a single code. The goal of the efforts is to combine the capabilities of the current suite of codes while reducing the maintenance and development burden. The user community will then be able to focus on one code instead of four, thereby enhancing the knowledge base. A modernised and modularised TRAC-P code, now called TRAC-M, serves as a basis for the consolidation. The architecture has been revamped and the language migrated to FORTRAN90 to produce a more modular, readable, extendable and developer-friendly code. A neutronics package has been coupled to TRAC-M using parallel virtual machine (PVM) to provide 1-D and 3-D kinetics models without having to add this functionality to the code itself, thus permitting to independently improve the neutronics or T-H models in TRAC-M.

TRAC-BF1 [29]

TRAC-BF1 is a best-estimate, full-system thermal-hydraulics code for a boiling water reactor [3]. The two-fluid flow models are solved in one and three dimensions. The code is modular in nature and is based on component models.

POLCA-T [113-116]

This coupled 3-D core neutron kinetics and system thermal-hydraulics computer code is able to perform steady-state and transient analysis of BWR [113]. It is based, to varying extents, on models and tools for BWR and PWR analysis used in the POLCA7 [114], BISON and RIGEL codes [115]. The code uses new, advanced methods and models in neutron kinetics, thermal-hydraulics and numerics. The main features of the code can be summarised as follows:

- Full 3-D model of the reactor core: The neutronics models in the code are the same as those in the well-known static core analyser POLCA7 with addition of proper 3-D kinetics model.

- Advanced five-equation thermal-hydraulic model with thermal non-equilibrium description of the steam-water mixture and its coupling to the heat structures. Separate mass- and energy balances of the phases. Drift flux model that can handle all flow regimes.

- Heat transfer model that works also in post-dry-out.

- The gas phase can consist of steam and non-condensable gases. The liquid phase can contain dissolved non-condensable gas.

- Boron transport model.

- Use of the same thermal-hydraulics model for core and plant systems.

- Two-dimensional (2-D) fuel rod heat transfer model, gas gap model consistent with design code, and a complete range of heat transfer regimes. The code is also able to model all plant heat structures.

- Dry-out and DNB correlations (using pin power distributions model).

- Full geometrical flexibility of the code: volume cells, flow paths, heat structures, materials, pumps, measurements, controls, etc., are all input data. The code is able to analyse different power plants and test facilities.

- Balance-of-plant, control and safety systems: The reactor pressure vessel, external pump loops, steam and feed water system, ECC systems and steam relief system are modelled to desired details. Large and valuable set of input models that already exists can be used.

- Stable numerical method allowing long time steps, which is also used for steady-state solution. Low dependence on the size of the time step, as the implicit numerical integration is close to second order by means of θ-weighting.

Such features allow the POLCA-T code to undertake a comprehensive approach to plant analysis with full consistency in steady-state and transient calculations. Consistency in BWR core and system modelling, when transient analyses are performed, is also achieved using the same basic model and the same design database for core data (cross-section data, burn-up, xenon and other 3-D distributions obtained from depletion calculations), fuel thermal-mechanical behaviour (properties) and system data. Thus consistency is also possible between predicted core and system parameters and their behaviour over a wide range of phenomena and processes important for both design and safety analyses. The application areas of the POLCA-T code consist include the following three domains: BWR steady-state core design, BWR stability, transients and accident analyses, and the modelling of experimental test facilities.

Applications for BWR steady-state core design are covered by POLCA7 wide-ranging capabilities as concerns:

- Evaluation of reactivity and power distribution at cold and hot core conditions.

- Detailed thermal-hydraulic analysis.

- Control operations (reactivity search modes: boron, power, flow, control rod, axial offset and minimum boron control).

- Detector simulation.

- Evaluation of fuel pin, pellet powers and burn-up.

- Evaluation of peaking factors based on pin results.

- Dry-out and DNB margin calculations (based on pin-power distributions).

- Fission heat load parameter (margin) calculations.
- Pellet-cladding interaction calculations.
- Depletion calculation with tracking of the most important fissile isotopes and fission products.
- Fuel bundle, control rod, fuel channel and fixed in-core detector depletion.
- Shutdown margin evaluation.
- Shutdown cooling.
- Xenon transients.
- Reactivity coefficients (void, burn-up, moderator temperature).

Applications for BWR safety analysis include operational transient, stability, RIA, ATWS, ATWC and LOCA as follows:

- Feed water flow increase/feed water temperature decrease transients.
- Loss of feed water flow transients.
- Pressure increase transients – analysis with regard to the cladding.
- Pressure increase transients – analysis with regard to the reactor coolant pressure boundary.
- Pressure decrease transients.
- Recirculation flow increase transients.
- Recirculation flow decrease transients.
- Control rod withdrawal error.
- Inadvertent loading transients.
- Control rod drop accident.
- Stability analysis.
- Anticipated transient without scram (ATWS).
- Anticipated transient without control rods (ATWC).

The POLCA-T code is well adapted to analyse scenarios that include a number of failing control rods. The boron transport model also makes it possible to analyse different types of boron shutdown scenarios. Applications for the modelling of separate test facilities (such as FRIGG) are foreseen not only for code validation but also for pre-test analysis and the planning and optimisation of experiments.

2.2.3 Neutron kinetics codes

DYN3D [51,52]

DYN3D was developed at FZ Rossendorf and is used to investigate reactivity transients in the cores of thermal power reactors with hexagonal or quadratic fuel assemblies. The three-dimensional neutron kinetics model HEXDYN3D of the code is based on the nodal expansion method for solving the two-group neutron diffusion equation. If it is supposed that the reactor core consists of hexagonal fuel assemblies divided into a number of slices, than the nodes are the parts of the fuel assemblies in each slice. The neutron group constants are assumed to be spatially constant in each node. The solving of the time-dependent neutron diffusion equations, including the equations for delayed neutrons for all nodes, is used for transient processes calculation. The thermal-hydraulic component, FLOCAL, consists of a two-phase flow model describing coolant behaviour and a fuel rod model. The fuel elements are simulated by separate coolant channels. Additionally, some hot channels with power-peaking factors belonging to chosen fuel elements can be considered. The flow model (one- and two-phase flow) is based on four differential balance equations for mass, energy and momentum of the mixture and mass balance of the vapour phase. Several safety parameters such as temperature, DNBR and fuel enthalpy are evaluated. Macroscopic cross-sections depending on thermal-hydraulic parameters and boron concentration are the input data of the code. The stationary state and transient behaviour can be analysed. The transient processes in the core can be investigated as long as the core geometry is maintained.

For the analysis of a static state, there are several possibilities to make the reactor critical: a) division of multiplication cross-sections by k_{eff}, b) variation of boron acid concentration and c) variation of reactor power. If a transient calculation should be undertaken, the following perturbations can be treated: 1) movements of single control rods or a control rod bank, 2) variation of core coolant inlet temperature, 3) variation of boron acid concentration, 4) changes of core pressure drop or total mass flow rate and 5) changes of pressure. If a transient starts from the subcritical state, two possibilities exist, *i.e*. prompt jump from a critical state with a given subcriticality at start of transient, and calculation with a time-independent source of fast neutrons.

The present version of the code DYN3D-2000/M1 has the following main features:

- Implementation of burn-up calculation.
- Unification of the stand-alone version of DYN3D with the option of external coupling with the thermal-hydraulic system code ATHLET (see below).
- Input and output of fission product poison distributions.
- Better handling of input data for fuel distribution (input of core load maps).
- Simpler definition of control rods and control rod motion.
- Improved control rod model for VVER-440 (control assemblies).
- Damping of cusping effects during slower control rod motion through an improved flux weighting procedure.
- Arrays used are defined on separate commons in BLOCKDATA program units.

- The connection with the user's cross-section libraries is simplified by the new structure of the code to connect one's own subroutines for cross-section handling with DYN3D/H1.1.

- Possibilities for adjusting the feedback coefficients.

- Coupling with an improved mixing model in the lower plenum of VVER-440.

A deterministic model of fuel rod failure during accidents is not included in DYN3D2000/M1, but some parameters for diagnostics of possible fuel rod failure are given, such as fuel enthalpy for each axial node of the rod, cladding oxide thickness, signalisation of possible cladding rupture when the cladding stress is positive (inner pressure is larger than outer pressure) and exceeds the yield point.

The core reactor DYN3D model is coupled with the ATHLET code through two different methods [53,54]. The first uses only the neutron kinetics component of DYN3D and integrates it into the heat transfer and heat conduction model of ATHLET. The power distribution is transferred from the neutron kinetics of DYN3D to ATHLET and the fuel temperature, moderator temperature, moderator density and boron acid concentration are provided by ATHLET as feedback parameters for DYN3D. This is a very close coupling; the data must be exchanged between all core nodes of the single models (internal coupling), engendering the transfer of a great number of data. In the second method of coupling the whole core is cut out of the ATHLET plant model (external coupling) and the reactor core is completely substituted by the DYN3D code model.

The thermal-hydraulics of the whole NPP system is split into two parts, the first part describing the thermal-hydraulics of the reactor core model and the second describing the thermal-hydraulics of the rest of the NPP coolant system. The interfaces between them are located at the bottom and the top of the reactor core. The pressures, mass flow rates, enthalpies and boron acid concentrations are transferred at the interfaces. The exchange of these parameters is performed by the GCSM of the ATHLET system code [49,50]. All thermal-hydraulic models included in the code DYN3D can be used in this external coupling manner. The use of larger time steps can cause the oscillation of the pressure drop over the core and mass flow rates in this type of coupling. These phenomena are damped through the use of a low pass filter of first order. According to the recommendation, a low pass filter time constant of 1 s or higher should be used [54].

NEM [30a,30b]

NEM is a 3-D multi-group nodal code developed and used at The Pennsylvania State University (PSU) for modelling both steady-state and transient core conditions. The code has options for modelling 3-D Cartesian, cylindrical and hexagonal geometry. Its source is the nodal expansion method for solving the nodal equations in three dimensions. It utilises a transverse integration procedure and is based on the partial current formulation of the nodal balance equations. The leakage term in the one-dimensional transverse integrated equations is approximated with a standard parabolic expansion using the transverse leakages in three neighbour nodes. The nodal coupling relationships are expressed in partial current formulation and the time dependence of the neutron flux is approximated by a first order, fully explicit, finite difference scheme. This method has been shown to be very efficient, although it lacks the precision of the advanced nodal codes. An upgrade of the method has recently been completed, replacing the fourth-order polynomial expansion with a semi-analytical expression which contains a more accurate approximation of the transverse leakage.

This code has been benchmarked for Cartesian, cylindrical and hexagonal geometry. NEM is coupled with the Penn State versions of TRAC-PF1 and TRAC-BF1.

NESTLE [31]

NESTLE is a multi-dimensional neutron kinetics code developed at North Carolina State University which solves the two- or four-group neutron diffusion equations in either Cartesian or hexagonal geometry using the Nodal Expansion Method (NEM) and the non-linear iteration technique. Three-, two-, or one-dimensional models may be used. Several different core symmetry options are available including quarter, half and full core options for Cartesian geometry and 1/6, 1/3 and full core options for hexagonal geometry. Zero flux, non-re-entrant current, reflective and cyclic boundary conditions are available. The steady-state eigenvalue and time-dependent neutron flux problems can be solved by the NESTLE code. The new Border Profiled Lower Upper (BPLU) matrix solver is used to efficiently solve sparse linear systems of the form AX = B. BPLU is designed to take advantage of pipelines, vector hardware and shared-memory parallel architecture to run fast. BPLU is most efficient for solving systems that correspond to networks, such as pipes, but is efficient for any system that it can permute into border-banded form. Speed-ups over the default solver are achieved in RELAP5-3-D© running with BPLU on multi-dimensional problems, for which it was intended.

PARCS – US NRC version [32a,32b]

PARCS is a three-dimensional reactor core simulator developed at Purdue University that solves the steady-state and time-dependent neutron diffusion equation to predict the dynamic response of the reactor to reactivity perturbations such as control rod movements or changes in the temperature/fluid conditions in the reactor core. The code is applicable to both PWR and BWR cores loaded with either rectangular or hexagonal fuel assemblies.

The neutron diffusion equation is solved with two energy groups for the rectangular geometry option, while any number of energy groups can be used for the hexagonal geometry option. PARCS is coupled directly to the thermal-hydraulics systems codes TRAC-M and RELAP5, which provide the temperature and flow field information to PARCS during the transient. The thermal-hydraulic solution is incorporated into PARCS as feedback into the few-group cross-sections. The Coarse Mesh Finite Difference (CMFD) formulation is employed in PARCS to solve for the neutron fluxes in the homogenised nodes. In rectangular geometry, the Analytic Nodal Method (ANM) is used to solve the two-node problems for accurate resolution of coupling between nodes in the core, and the Triangle-based Polynomial Expansion Nodal (TPEN) method is used for the same purpose in hexagonal geometry. Since the initial release of the NRC version of PARCS (V1.01) in November 1998, there have been numerous functional improvements and code feature extensions, including the addition of a pin power reconstruction feature, input/output system renovation, modification of TRAC-M coupling routines, 1-D kinetics capability addition, dynamic memory allocation, automatic thermal-hydraulic to neutronics mapping, a Windows user interface, UNIX on-line graphics, and, finally, the hexagonal geometry option was initially implemented with only two-group solutions and was then extended to cover multi-group solutions. Major calculation features in PARCS include the ability to perform eigenvalue calculations, transient (kinetics) calculations, xenon transient calculations, decay heat calculations, pin power calculations and adjoint calculations. The primary use of PARCS involves a 3-D calculation model for the realistic representation of the physical reactor. However, various one-dimensional modelling features are available in PARCS to support faster simulations for a group of transients in which the dominant variation of the flux is in the axial direction, as for example in several BWR applications.

Numerous sophisticated spatial kinetics calculation methods have been incorporated into PARCS so as to achieve the various tasks with high accuracy and efficiency. The CMFD formulation, for example, provides a means of performing a fast transient calculation while avoiding expensive nodal calculations at times in the transient when there is no strong variation in the neutron flux spatial

distribution. Specifically, a conditional update scheme is employed so that the higher-order nodal update is performed only when there are substantial changes in the core condition to require such an update. The temporal discretisation is performed using the theta method with an exponential transformation of the group fluxes. A transient fixed-source problem is formed and solved at each time point in the transient. For spatial discretisation, the stabilised ANM two-node kernel or the multi-group TPEN kernel is used to obtain the nodal coupling relation that represents the interface current as a linear combination of the node average fluxes of the two nodes contacting the interface. The solution of the CMFD linear system is obtained using a Krylov subspace method that employs the BILU3D pre-conditioner in rectangular geometry and a point pre-conditioner in hexagonal geometry.

The eigenvalue calculation to establish the initial steady state is performed using the Wielandt eigenvalue shift method. The pin power calculation method employs a reconstruction scheme in which pre-defined heterogeneous power form functions are combined with a homogeneous intranodal flux distribution. The homogeneous flux shape is obtained by analytically solving a two-dimensional boundary fixed-source problem consisting of the surface average currents specified at the four boundaries. For 1-D calculations, two modes are available in PARCS: normal 1-D and quasi-static 1-D. The normal 1-D mode uses a 1-D geometry and pre-collapsed 1-D group constants, while the quasi-static 1-D maintains the 3-D geometry and cross-sections, but performs the neutronics calculation in the 1-D mode using group constants which are collapsed during the transient. The group constants to be used in the PARCS 1-D calculation can be generated through a set of 3-D PARCS calculations. During the 1-D group constant generation, “current conservation” factors are employed in the PARCS 1-D calculations to preserve the 3-D planar averaged currents in the subsequent 1-D calculations.

PARCS was written in FORTRAN90 and its portability has been tested on various platforms and operating systems, which include SUN Solaris UNIX, DEC Alpha UNIX, SGI UNIX, HP UNIX, LINUX and various Windows OS (*i.e*. 95, 98, NT and 2000). During the testing it was determined that there are minor platform dependencies that need to be treated with compiler directives.

QUABOX [33]

QUABOX is a neutron kinetics code developed in the 70s at Gesellshaft für Anlagen und Reaktorsicherheit (GRS) in Germany for 3-D core neutron flux and power calculations in steady-state and transient conditions. It solves the two-group neutron energy diffusion equation through local polynomial approximation of the neutron flux.

2.2.4 Examples of coupled 3-D neutron kinetics and thermal-hydraulics codes

2.2.4.1 Description and validation of SIMTRAN

An extended description of the SIMTRAN code is given below that includes the key issues for neutron kinetics/thermal-hydraulics coupling. SIMTRAN was developed by a team led by Professors J.M. Aragones and C. Ahnert of the Polytechnic University of Madrid [141,144].

In the early 70s Aragonés and Ahnert introduced and demonstrated a key paradigm for accurate and fast nodal or coarse-mesh 3-D reactor core calculations, which they called “a linear-discontinuous scheme for synthetic coarse-mesh finite-difference (CMFD) multi-group diffusion”, implemented and successfully validated for a wide range of applications, including [145,152]:

- The one-group synthetic acceleration of multi-group fine-mesh finite-difference diffusion calculations in 1-D and 2-D.

- The two-group 2-D diffusion calculations by local (fine-mesh) and global (nodal or coarse mesh) alternating dissections of core planes (COBAYA code).

- The one-group synthetic CMFD 3-D nodal code SIMULA for fast, accurate LWR core neutronics, because the synthetic nodal cross-sections and discontinuity factors are obtained through detailed 2-D fine-mesh diffusion calculations (with consistent transport corrections for absorber cells) of the core mid-plane along the cycle burn-up and at several rodded planes, performed with the COBAYA code.

Later on, in the early 90s, Aragonés, Ahnert and co-workers developed the SIMTRAN code for 3-D LWR core dynamics in two neutron groups, with six families of delayed neutron precursors [153, 154]. SIMTRAN has been undergoing development and validation for over 10 years, including applications for core surveillance and manoeuvres [155-157], transient analysis [160,161] and best-estimate safety analysis [164]. The process has been one of integral and continuous development and validation employing actual plant design and operational data [157] and international benchmarks.

Characteristics of SIMTRAN and the coupling of neutronics and T-H

SIMTRAN was developed as a single code merge, with data sharing through standard FORTRAN commons, of the 3-D neutronics nodal code SIMULA and the multi-channel (with cross-flows) thermal-hydraulics code COBRA-IIIC/MIT-2 [142]. Both codes solve the 3-D neutronics and T-H fields with maximum implicitness, using direct and iterative methods for the inversion of the linearised systems.

SIMULA solves the neutron diffusion equations in one or two groups, on 3-D coarse-mesh nodes (quarter or full fuel assemblies) using a linear-discontinuous finite-difference scheme where the interface net currents are given in terms of the actual node average and the corrected interface averaged fluxes, using synthetic interface flux discontinuity factors for each group and node interface. SIMULA uses these synthetic coarse-mesh discontinuity factors in the XY directions, pre-calculated using 2-D pin-by-pin two-group diffusion calculations of whole-core planes. In the axial direction it performs embedded iterative 1-D fine-mesh two-group diffusion solutions for each node stack, with the radial leakage terms interpolated from the nodal two-group solution.

To solve the neutron kinetics equations with six groups of delayed neutron precursors, a forward linear time differencing is used for each precursor concentration equation. These are implicitly substituted in the fission source nodal equations. The exponential expansion in time of the fission source, with nodal frequencies from the previous time step, and its linear time differencing results in a non-diagonal linear system. The extra diagonal terms are small and positive, except for large negative frequencies (during rod trips) that are moved to the source term in the RHS.

COBRA-III-C/MIT-2 [142] is a public code for thermal-hydraulics calculations with implicit cross-flows and homogeneous two-phase fluids. It is used world-wide for DNBR analysis in LWR subchannels, as well as for 3-D whole PWR core simulation with one or more channels per fuel assembly. COBRA uses direct inversion at each plane of the axial flow equations, with cross-flows updated over an outer iteration loop, for the homogenous model single-phase coolant; and finite-element direct solution of the fuel rod radial temperatures.

SIMTRAN is our coupled code for 3-D dynamic analysis of LWR cores, integrating SIMULA and COBRA in the coupling scheme depicted in Figure 1, where the main variables exchanged by both codes are summarised, as is the arbitrary correspondence among the meshes used in both codes.

Figure 1. Variables for the 3-D neutronics/thermal-hydraulics coupling in SIMTRAN

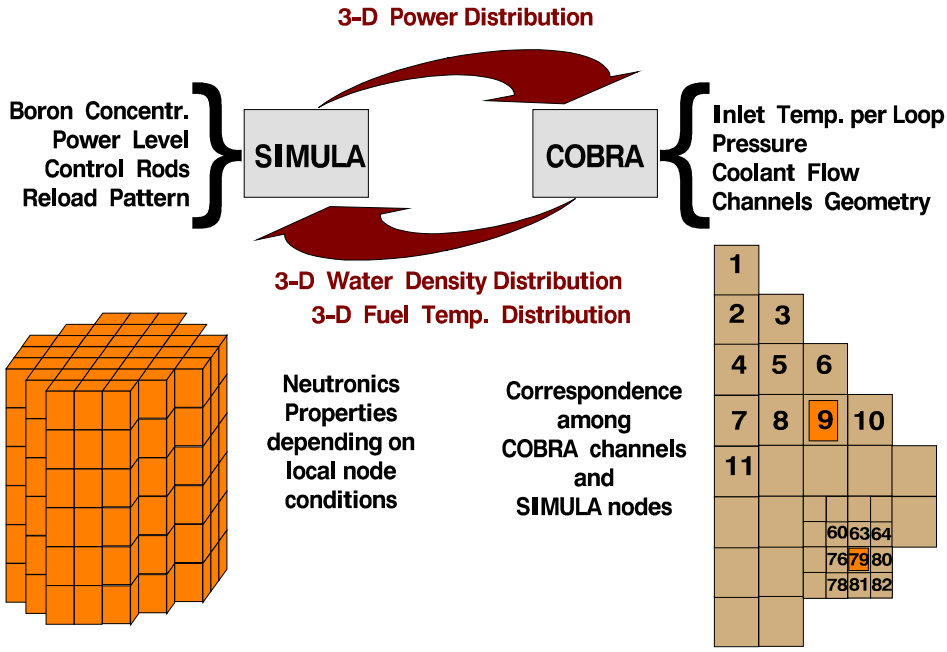

The 3-D core N/T-H coupling is achieved internally in SIMTRAN through a semi-implicit scheme, which uses a staggered alternate time mesh, as shown in Figure 2.

Figure 2. Temporal coupling of NK and T-H for fast transients in SIMTRAN

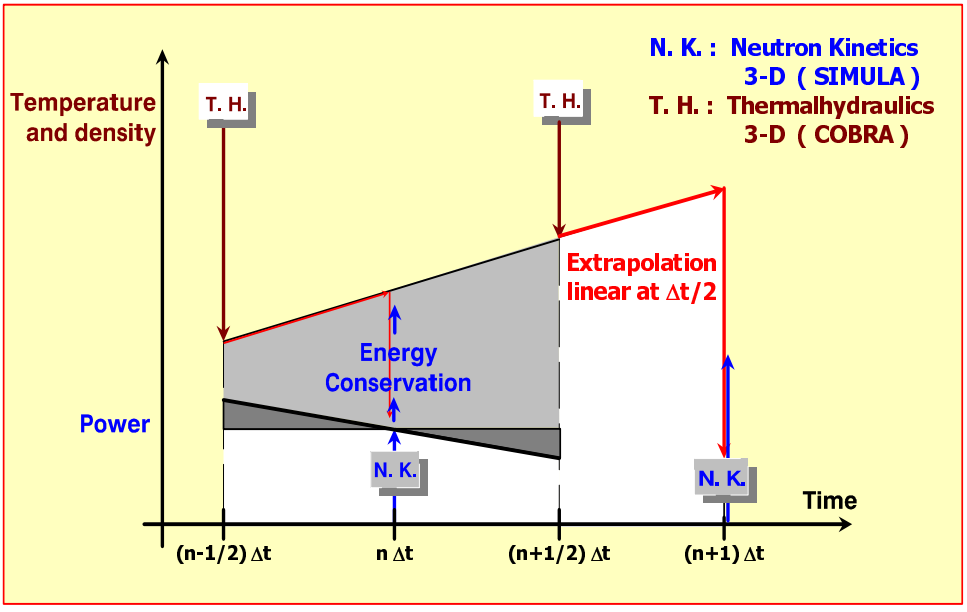

The T-H solution is advanced over one-half of the neutronic time step, thus conserving energy by taking the neutronic nodal power centred in the time step. Then, the implicitly calculated 3-D T-H variables (water density, water and fuel temperatures) are extrapolated over another half of the time step. The neutronic constants are thus nearly implicitly calculated in the next time step as a function of the extrapolated T-H variables, where the limited half-step extrapolation prevents significant oscillations, allowing for larger time steps.

For the NEA/NSC benchmarks, the SIMTRAN code was extended to address the axial subdivision of cross-section sets, including varying and moving boundaries, to allow for continuous control rod movement in axially subdivided zones/compositions. The synthetic two-group nodal discontinuity factors were generated by 2-D fine-mesh diffusion calculations of the different (15) core planes. This included un-rodded and rodded configurations for the initial, mid-transient and final quasi-steady-state conditions, with axial bucklings and local T-H conditions per node (quarter of assembly) obtained by iterating the 3-D and 2-D solutions that converged in two or three iterations.

Special models: Mixing of flow from loops in the vessel and subchannel analysis

In reactors with multiple loops it is of particular interest to model the water flow and enthalpy mixing from the cold legs inside the reactor vessel (downcomer and bypass) up to the inlet of the core channels (Figure 3), as well as the mixing from the outlet of the core channels in the upper plenum up to the hot leg nozzles. The effect of enthalpy mixing is quite important in the transients with cooling of a single cold loop or with boron dilution also in a single loop.

Figure 3. Mixing of flow-enthalpy from loops and effect in the ex-core detectors

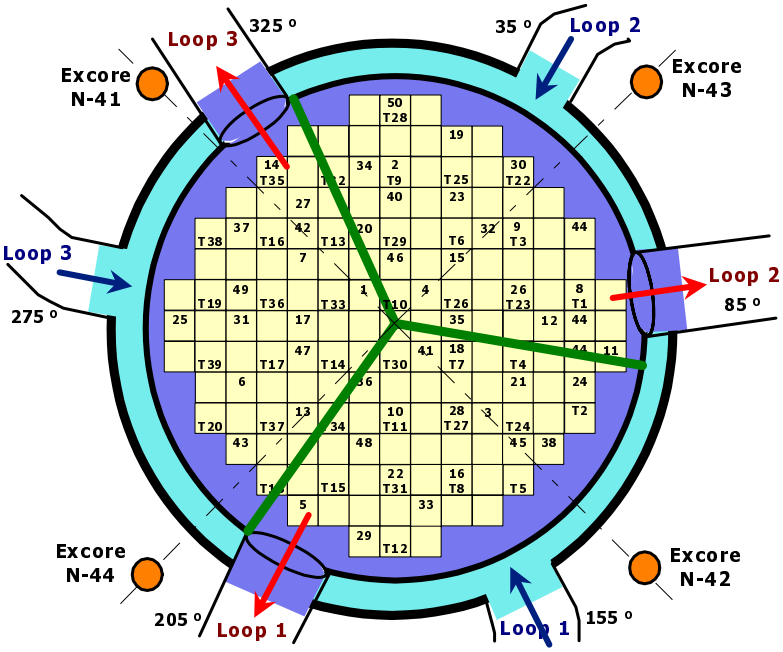

SIMTRAN incorporates an empirical model of the mixing among the cold leg inlets to the vessel to yield the enthalpies at the inlets of the core channels. The model uses Fermi functions for the inlet channel enthalpies in terms of the products enthalpy-mass flow-distance between the vessel inlets of each loop to the core channel inlet, with a single parameter to be fitted to the measurements. The model allows for extreme mass flow and enthalpy variations per loop, as well as for rotational mixing. The

same functional model is also used for the mixing from the outlets of the core channels to the vessel outlet nozzles of the hot legs; a different mixing (exponential) parameter is employed, with larger mixing in the hot upper plenum.

Another special effect to model is that due to the changes in the loop inlet temperatures (cold legs), that cause changes in the water density of the core reflector (downcomer and bypass) and hence in the exponential attenuation of the neutrons that leak from the core through the vessel internals and wall, thus causing the variation of the currents at the ex-core detectors. SIMTRAN uses general response matrices, with exponential attenuation in the reflectors proportional to the water density changes, with each detector affected by the different inlet cold legs, to account for this effect.

Another capability developed in SIMTRAN is detailed DNBR analysis in the hottest core subchannels using 3-D and pin-by-pin powers. This is achieved using off-line COBRA calculations in one or more subdomains, with a detailed adaptive mesh, as sketched in Figure 4.

Figure 4. Analysis of the DNBR per subchannels in subdomains with adaptive mesh

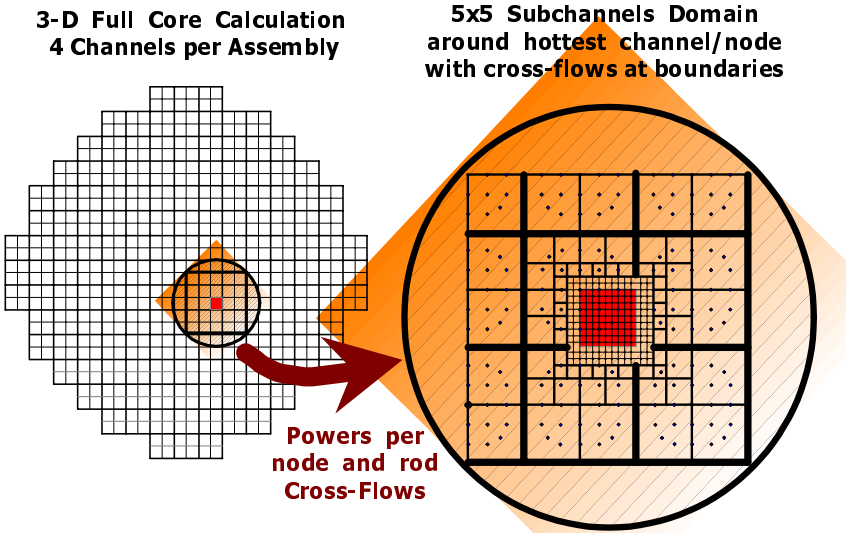

Coupling of SIMTRAN to RELAP5 and TRAC-M

In the framework of the project for a consolidated US NRC T-H code, Professor T. Downar and his group at Purdue University have developed and distributed a “General Interface” (GI) to couple the 3-D neutronics code PARCS with the T-H system codes RELAP5 and TRAC-M [145,146].

Sets of similar routines have been implemented in these codes to perform the data transformations between the different meshes (“*Data Mapping*”) of the respective codes, with their own dispositions in memory. This is done by using “vectors” that group all the data to be exchanged; these are then transmitted among the codes via a standard PVM (Parallel Virtual Machine) library, developed at ORNL by J. Dongarra. An intermediate program (GI) “gets” these vectors, as well as the semaphores of communication and error, multiplies them using the permutation matrices for the mesh transformation, and sends the product vectors to the other code, also via calls to PVM routines. Figure 5 displays this coupling scheme.

Figure 5. Scheme of the coupling between PARCS or SIMTRAN and RELAP5 or TRAC-M

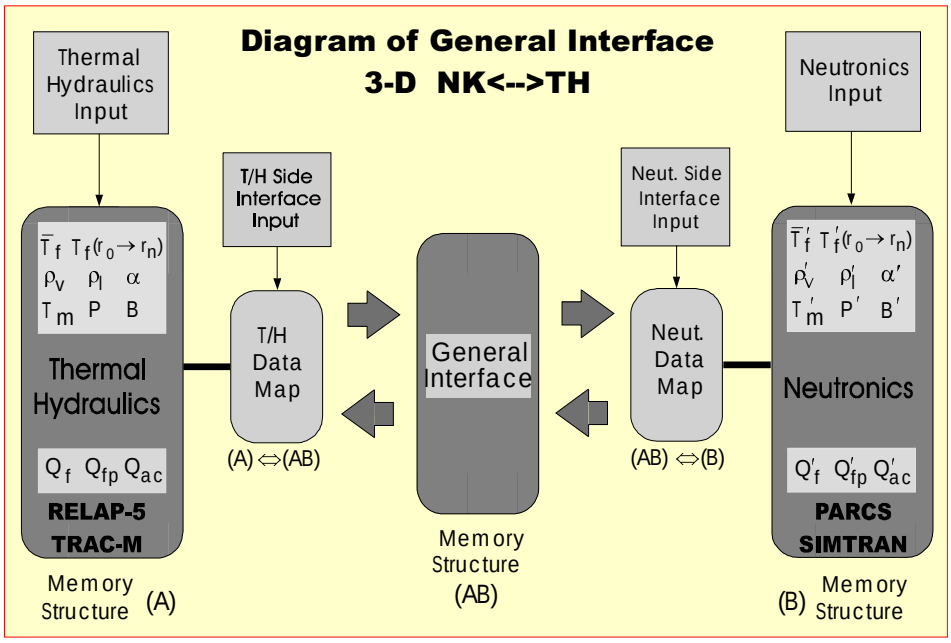

This coupling scheme was designed and implemented with emphasis on maximum flexibility and minimum modifications to the existing codes, so as to facilitate their maintenance and portability to other neutronics and thermal-hydraulics codes.

For its implementation in the SIMTRAN code, the set of routines PDMR that perform the mapping of the data to transmit and acquire to or from the memory layout of PARCS or SIMTRAN and the exchange vectors, and the calls to PVM routines, have been adapted. This has been done by replacing the data in the PARCS memory layout (commons) by the corresponding data in the SIMTRAN commons, employing a direct mesh transform among both 3-D nodal meshes. In this way the permutation matrices for the general interface (GI) are the same as those generated to couple PARCS with RELAP5 or TRAC-M, simplifying the management of the databases for validation and application [164].

In the implementation in SIMTRAN we have used a semi-implicit scheme for time coupling in a staggered mesh, as described above. In the present version, named SIMREL, all the COBRA routines have been suppressed. All the T-H variables are thus acquired from the system code.

In the present versions of RELAP5 and TRAC-M the number of hydraulic channels parallel or coupled in the core and reflectors is limited, to 18 and 1 respectively in the practical nodalisations, while the number of heat structures that can practically be used is much larger, with one mean fuel rod for each fuel assembly. In ongoing work we are reinserting the COBRA cod, in the US NRC COBRA-TF version, for a more detailed T-H core nodalisation, with one mean channel and fuel rod per assembly or quarter of assembly, using the T-H variables consistently at core inlet and outlet.

Developments in SIMTRAN for 3-D best-estimate transient analysis

Advanced features and models being developed in SIMTRAN for improved accuracy and efficiency in 3-D best-estimate transient analysis have already been implemented and validated at least at the proof-of-principle level and 2-D full implementation (readily extendible to 3-D), including:

- Extended dependence in full parameter space of node or assembly averaged cross-sections in two groups as a function of local instantaneous variables (water density and temperature, fuel temperature, boron, Xe and Sm, control), generalised spectral history and heterogeneous burn-up (including effects of voids, control and fuel temperature) and non-linear effects (flux gradients due to neighbour perturbations) [162,163]. This XS representation per fuel assembly type is even more general than that used in the SIMULATE code such that the conversion of the last libraries is guaranteed, maintaining their accuracy or improving it.

- Generalised non-linear analytical coarse-mesh finite-difference (ACMFD) nodal method, which uses the Chao method for homogeneous large nodes with transverse leakage, extended to include non-linear 3-D heterogeneity effects coupled in two groups, using interface flux discontinuity factors (DF) per node face with very effective (fast) implementation and successful demonstration in 2-D [164].This technique avoids the expensive two-node 1-D solutions required for every node-to-node interface and space direction in every time step using the state-of-the-art nodal codes.

- Efficient and robust mathematical solvers for the sparse non-symmetric linear systems of the external source transient problems, using tuned Krilov space solvers (GMRES and BiLU) and pre-conditioners for once-thru convergence of the two-group 3-D nodal fluxes; and the eigenvalue initial steady-state problem, using the Wielandt Iteration method.

- Multi-grid modelling with synthetic non-linear iteration in full two groups from the nodal detailed solution (one node per fuel assembly in BWR cores, with 24 axial nodes) to a super-nodal grid (with four fuel assemblies around each control rod and 12 axial nodes for BWR cores), where the super-nodes XS and DF retain full non-linear dependence on local (instantaneous, history and heterogeneity) variables and neighbourhood non-linear effects.

As the high-order (nodal) solution requires about 4-5 times more time than the low-order (super-nodal), yet equally accurate, solution this scheme is well suited for real-time performance in any fast transient, where the system-wide T-H and related modules will require as much as that 4-5 time factor as the NK module. This means that the NK SIMTRAN module can return a super-nodal 3-D solution for the next half time step, sufficient and consistent with the T-H core nodalisation, in a quite short time period after receiving the updated NK variables, and then updating the high-order (nodal) solution and the synthesis of the consistent super-nodal XS and DF, working in parallel with the system T-H and related modules.

2.2.4.2 Coupling of BIPR8KN with ATHLET

The 3-D neutron kinetics computer code BIPR8KN [179] was developed by the Department of Physics of the Kurchatov Institute in Moscow. A two-group 3-D hexagonal coarse mesh nodal approximation for neutron flux is used. The static branch of this code allows the simulation of VVER core burn-up and refuelling, including the calculation of the eigenvalue and other parameters of criticality and reactivity coefficients for different core states. The adopted nuclear data libraries include dependence of properties for fuel assemblies of different types from burn-up, coolant parameters, fuel and coolant temperature and Xe and Sm poisoning. The kinetic branch of BIPR8KN calculated the core power and the 3-D neutron flux deformation as a function of time, caused by reactivity perturbations of different natures taking into account prompt neutrons and six delayed neutron groups and feedback effects.

The code has been coupled with ATHLET [180]. The innovation lies in the number of hydraulic nodes adopted for modelling the vessel of a VVER-440. The presently available nodalisation amounts about 10 000 elements for the vessel and 2 000 elements for the other parts of the system. The nodalisation has been adopted to describe coolant flow mixing processes in the vessel with a high level of resolution.

2.2.4.3 The SAPHYR code system

The CEA/DEN has developed the SAPHYR code system for reactor analysis. This package is composed of the CEA modular codes APOLLO, CRONOS and FLICA4 [181-183].

APOLLO is a 2-D neutronic code used for assembly calculations. It solves the multi-group transport equation in space and energy. CRONOS2 is a 3-D neutronic code used for core calculation and based on the resolution of the equation of the dynamic or static diffusion or transport of neutrons. FLICA4 is a 3-D thermal-hydraulic code for compressible two-phase flow for static and dynamic configuration. A thermal module is included into the core. A zoom tool has also been developed to locally (one or several assemblies) reach the neutronic mesh size. The FLICA4 zooming feature is aimed at refining the spatial description in a limited area of the computational domain. The zoom is based on coupling two FLICA4 calculations, one on the full domain with a coarse mesh and one in the area of interest with a fine mesh. Results from the coarse mesh are used as boundary conditions on the external faces of the fine mesh. These boundary conditions are consistent with the numerical method (Riemann solver at cell interfaces). Zooming can also be performed by a single FLICA4 computation with a non-conform mesh.

The cross-section databases used for the neutronic core description are computed by APOLLO2. During the transient, CRONOS2 calculates power distribution in the core. Each time, this information is transmitted to FLICA4 to determine fuel temperature and moderator density for the actualisation of cross-sections (Doppler and moderator feedback effects) in CRONOS2. The ISAS software based on the PVM manages this coupling.

2.3 Coupling

Certain requirements with regard to the coupling of thermal-hydraulic system codes and neutron kinetics codes should be considered [34-37]. The objective of these requirements is to provide accurate solutions in a reasonable amount of CPU time in coupled simulations of detailed operational transient and accident scenarios. These requirements are met by the development and implementation of six basic components of the coupling methodologies:

1) Coupling approach – integration algorithm or parallel processing.

2) Ways of coupling – internal or external coupling.

3) Spatial mesh overlays.

4) Coupled time-step algorithms.

5) Coupling numerics – explicit, semi-implicit and implicit schemes.

6) Coupled convergence schemes.

More details related to the first three items are given in Sections 2.3.1 to 2.3.3, respectively. The consideration of the coupling involving CFD codes is discussed in the Section 2.11 and the following sections (*i.e.* Sections 2.3.1 to 2.3.3) are limited to coupling between THSC and NKC.

2.3.1 Coupling approach – integration algorithm or parallel processing

Two different approaches are generally utilised to couple 3-D kinetics models with system codes: serial integration coupling and parallel processing coupling. Serial integration requires modifications of the codes usually performed by implementing a neutronics subroutine into the T-H system code. Parallel processing allows the codes to be run separately and exchange data during the calculation. The data exchange is usually performed using a PVM environment or MPI. PVM is a powerful tool for the coupling of large, stand-alone codes and performs calculations on multiple processors. The PVM environment requires development of an interface routine and modification of the stand-alone codes and inputs for use with PVM.

When the thermal-hydraulic model is built using parallel T-H channels there is also a possibility that the different channels are processed on different processors. In this way the calculation time could be significantly reduced, especially when modelling large BWR cores.

2.3.2 Ways of coupling – internal or external coupling

The core models in T-H system codes generally consist of point kinetics models or 1-D neutron kinetics models, which are coupled to an average fluid-dynamic channel of the core region and to a corresponding average channel/fuel rod model. In most codes the point kinetics can be related to several parallel coolant channels and corresponding fuel rod models describing parts of the reactor core. The 3-D neutron kinetics models for core analysis have been expanded to full reactor core models, which comprise complete models of the T-H in the core region. The coupling can be achieved in two ways – internal and external (Figure 6).

Figure 6. Exchange of parameters for different ways of coupling

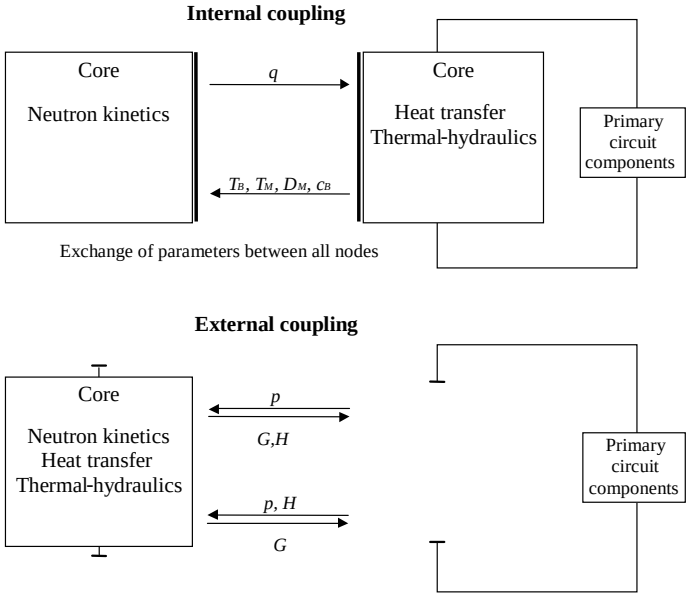

With internal coupling, the 3-D nodal neutron kinetics model is integrated into the core T-H model of the system code. Each neutron kinetic node is coupled directly to a core thermal-hydraulic cell in the system code and is solved with each T-H iteration. Though this method requires the exchange of a significant amount of information between the two codes, it also allows for detailed and direct system calculations. One major disadvantage of this method is that it involves significant modifications in both codes.

In external coupling the neutron kinetics code is combined with a separate core T-H model. It is then coupled to the full T-H system code by passing boundary conditions at the top and bottom of the core. Only a few parameters need to be exchanged between the two codes. This method facilitates the coupling procedure because it requires little or no modification of the T-H or neutron kinetics codes to be performed. However, there are certain problems with the external coupling method associated with the different T-H models for core and system modelling, which can lead to numerical instabilities and slow convergence.

2.3.3 Spatial mesh overlays

Choosing proper spatial mesh overlays for a given transient to provide accurate solutions over a reasonable period of time is a challenging task. Exact, detailed mapping provides better spatial resolution in coupled calculations. However, this refinement requires significant computational resources even when taking advantage of recent progress in computer resources. The computer requirements become enormous when these models are used to simulate transients with coupled core/system interactions. In the case of spatially asymmetric transients it is expected that detailing in the 3-D T-H model plays a large role in determining the local parameters and hence the power distribution during the simulated transient.

Three-dimensional asymmetric transients in which the spatial power distribution is significantly affected constitute a basis for verifying the performance of coupled-code systems. The main objective in such calculations is to predict the 3-D power distribution and local boiling transition as accurately as possible. The verification procedure involves testing the functionality, the data exchange between different modules and the neutronics/T-H coupling, which is designed to model the combined effects determined by the interaction of neutronics and thermal-hydraulics.

For a PWR licensing, the required design basis bounding analyses are usually REA and MSLB. As PWRs have an open lattice with existing radial cross-flows, the use of 3-D core thermal-hydraulic models is desirable. Each of these models can be built using different spatial meshing structure. The manner in which the coupling is performed is of utmost importance, such as to obtain sufficient accuracy over a reasonable time period. Usually the system thermal-hydraulic codes as TRAC-PF1 and TRAC-M have two options for 3-D T-H vessel modelling – cylindrical and Cartesian geometry. The Cartesian option is a better geometrical match with the neutronics core model, especially when each neutronics assembly is directly coupled to a thermal-hydraulic cell and heat structure in both the radial and axial direction. The exact, detailed mapping provides better spatial resolution in coupled calculations. Such detailing, however, requires significant computational effort.

The sensitivity studies performed on spatial mesh overlays for PWR REA analysis [38] suggested that the local refinement of the Doppler feedback model does not necessarily improve accuracy of the results. It is shown that the REA simulations are sensitive to the spatial coupling schemes, especially in the radial plane. While the impact of neutronics mesh refinement is well known, it has recently been that the local predictions (and the global predictions) are very sensitive to thermal-hydraulic refinement. The obtained results indicate that the T-H feedback phenomenon is non-linear and cannot be separated even in REA analysis, where the Doppler feedback plays a dominant role.

These conclusions have been reinforced through the comparative analysis of the MSLB results with the 3-D core thermal-hydraulic models. The results obtained indicated that the detail and geometry approximation of the core thermal-hydraulics can be an important source of deviations for local parameters, especially for the relative power and fuel temperature distribution in the vicinity of the stuck rod. During the course of the MSLB transient, a power spike is seen at the position of the stuck rod. However, in the coarse-mesh model this assembly is averaged with several of the surrounding assemblies while mapping the neutronics model to the thermal-hydraulics model. This has a significant effect: that of underestimating the feedback in this part of the core. On the other hand, the detailed model more accurately predicts the feedback (as a result of a better spatial feedback resolution) – and therefore the relative power shape and local safety parameters – near the stuck rod. Refinement in the neutronic or heat structure model does not have an impact on the total power transient evolution during the MSLB simulation.

A boiling water reactor core contains a large number of fuel assemblies (usually about 800). The exact, detailed T-H and kinetics modelling of such core requires significant computational resources. Thus the optimisation of coupled neutronics/thermal-hydraulic calculations generates a great amount of interest. Calculation costs could be reduced when collapsing similar assemblies into a single T-H channel while maintaining the detailed neutronics modelling. Furthermore, collapsing the number of T-H channels smoothes the power distribution and the resultant reactivity feedback. Finding an optimised number of T-H channels helps to improve the accuracy and duration of calculation.

When mapping neutronics assemblies to thermal-hydraulic channels, different rules usually must be respected. Similar (in terms of design) neutronic assemblies, for example, are generally mapped in one channel. This average channel is built based on neutronics and thermal-hydraulic information obtained from a core simulator code that accounts for steady-state core thermal-hydraulic conditions. Some of the characteristics used to lump together several neutronics assemblies to a thermal-hydraulic channel are the relative power, coolant flow, void distribution, type of bundle throttling (orificing), type of fuel (enrichment), etc. Another rule that should be followed when performing such mapping is to maintain core symmetry. The usual approach is to rank the fuel assemblies according to their initial steady-state power level (which is obtained from a licensed core diffusion simulator, *i.e*. SIMULATE-3) and classify them into groups, keeping power range as narrow as possible. This approach is known as “power flattering” mapping. Sensitivity studies have shown that the steady-state analysis is sufficient to design a suitable T-H model for BWR transients. Mapping non-identical (in terms of initial power level) assemblies to a single T-H channel smoothes the power distribution and the resultant reactivity feedback. Decreasing the number of channels leads to overestimation of local parameters demonstrated by the comparison of normalised radial power distribution. A specific discussion related to the BWR stability issue can be found in Section 2.7.

2.4 Neutron kinetics and thermal-hydraulic nodalisation requirements

Computer codes require the preparation of a mathematical model that can adequately simulate all or part of a nuclear power plant or processes occurring therein. This mathematical model consists of the computer code itself, and a set of input data grouped in a file (or files) that substantially describe the plant (or facility) within the boundaries and assumptions of the code models. Preparation of such a model is not only the source of the largest number of errors, but also of uncertainties that affect the use of best-estimate codes. Comprehensive knowledge of the computer code models is not sufficient for the error-free preparation of the nodalisation [72].

A major issue in the use of mathematical models or codes is the model’s actual capability to reproduce plant (or facility) behaviour under steady-state and transient conditions. Model verification and qualification are concerned by this question. The related fundaments are discussed in Refs. [73-75].

The availability of a proper nodalisation constitutes a prerequisite for a consistent code assessment process including both the verification and the validation (or qualification) steps. Proper nodalisation is also necessary for a satisfactory application of the codes.

It is well beyond the purposes of the present document to discuss code assessment requirements and their related present status in detail. However, considering the relevance of nodalisation in code applications, including the analysis of the complex phenomena object of coupled 3-D neutronics/ thermal-hydraulics calculations some details are given hereafter in relation to the development of a nodalisation and the achievement of a suitable level of quality. The attention is focused toward thermal-hydraulic nodalisation.

2.4.1 Thermal-hydraulic nodalisation (input deck) development

Four fundamental pre-conditions should be met to enable a complex thermal-hydraulics system code to be properly applied to the prediction of transient scenarios expected in a NPP:

1) The code should be frozen.

2) The code should be properly qualified through a comprehensive (preferably international) assessment programme, as mentioned earlier.

3) The developer of the nodalisation should be a qualified code user of the selected code [76,77].

4) The nodalisation (of the plant), once developed, should be properly qualified [191,192].

Each portion of the plant that is of interest for the analyses is divided into discrete components (nodes). The model is developed though the process of dividing the real plant component volumes into a set of control volumes that are essentially stream tubes with inlet and outlet flow path connections. Obviously, the subdivision of a complex system such as a LWR plant can be undertaken in a number of ways. The simplest subdivision of a plant model would be into a set of control volumes or nodes that are equally sized, but for a successful analysis solution a number of factors must be addressed: numerical stability, run time and spatial convergence. Modelling LWR systems requires not only the simulation of the fluid stream tubes, but also the modelling of solid structures (slabs) that store heat or contain heat sources. Thus, discretisation of the structures is also necessary.

To a great extent, engineering judgment is used to develop an input deck. The importance of establishing a procedure for the nodalisation set-up and qualification is a consequence of employing such judgement. The procedure can be split into the following steps: a) gathering of a verified set of NPP data, b) set-up of the plant nodalisation (input deck for nominal steady-state conditions) and c) qualification of the nodalisation.

A verified database related to the plant should be developed according to the following criteria: a) only qualified plant documents should be used, b) the traceability of each reference should be maintained in accordance with the plant documentation database, c) QC and QA procedures for nodalisation development should be considered, and d) the quality of reference data should be independently checked.

Plant nodalisation should be developed according to a predefined list of qualitative criteria [78]. For instance, geometrical fidelity with the real modelled system should be maintained, all fluid flow

paths should be modelled, logics for normal and off-normal operating conditions should be included, and the sliced (or sandwich-type) nodalisation concept should be followed, as far as possible.

A nodalisation can be considered "qualified" when 1) it is geometrically faithful to the involved plant, 2) it reproduces the nominal measured steady-state condition of the plant and 3) it demonstrates a satisfactory behaviour under time-dependent conditions; that is, according with the time-dependent data of any test performed or (if available) of any actual transient occurring in the nuclear power plant. Therefore, qualification of the nodalisation has been divided in two separate processes: steady state and on-transient.

A schematic of the overall process of nodalisation qualification (at steady state and on-transient levels) and improvement can be found in Figure 7. An outline of the two main processes is provided in below and more details can be found in Ref. [78].

2.4.1.1 Acceptability of the nodalisation at the steady-state level

A number of questions arise for the analyst during the development of an input deck. All the items described above (user qualification including detailed knowledge from the user side of the code characteristics, code qualification, availability of suitable system data, etc.), must be systematically considered before beginning the process of developing a nodalisation. Once the nodalisation is ready, *i.e*. the input deck is running, a number of additional questions arise, generally connected with the question of how to prove that the nodalisation results are satisfactory (at the steady-state level).

In order to address the last question, the University of Pisa proposed a number of acceptability conditions that are summarised in Table 3 [76]. These conditions were adopted over ten years ago at the time the present report was issued [79,80].

Two sets of conditions can be distinguished: the former (rows 1 to 11 in Table 3) deals with the values of the quantities that are part of the input deck, the latter (rows 12 to 25) deals with the results predicted by the code at the end of the steady-state calculation.

The data in the table are self explanatory. It should be noted that items 7 and 19 require the preparation of diagrams, system volume vs. height and system pressure vs. length along the flow path, respectively, and the demonstration that the acceptable error condition is locally achieved. In addition, care must be taken when demonstrating the acceptability of the condition at the second footnote of the table. These may depend upon the features of the adopted code and, in some cases, upon the user selected modalities for achieving a stationary solution.

All values derived from any qualified database are affected by their own errors which, in the majority of the cases, are not declared nor known to the code user who is adopting those data. This error must be considered when applying the definition at the first footnote of the table.

2.4.1.2 Acceptability of the nodalisation at the transient level

The demonstration of the nodalisation quality at the steady-state level does not ensure that the prediction of a transient scenario is phenomenologically correct or even that the nodalisation (input deck) error-free; errors can be part of an input deck that has been qualified at the steady-state level. In order to achieve full qualification the newly-developed NPP input deck, already qualified at the steady-state level (see Section 2.4.1.1), must undergo the on-transient nodalisation qualification process.

Figure 7. Thermal-hydraulic nodalisation qualification process

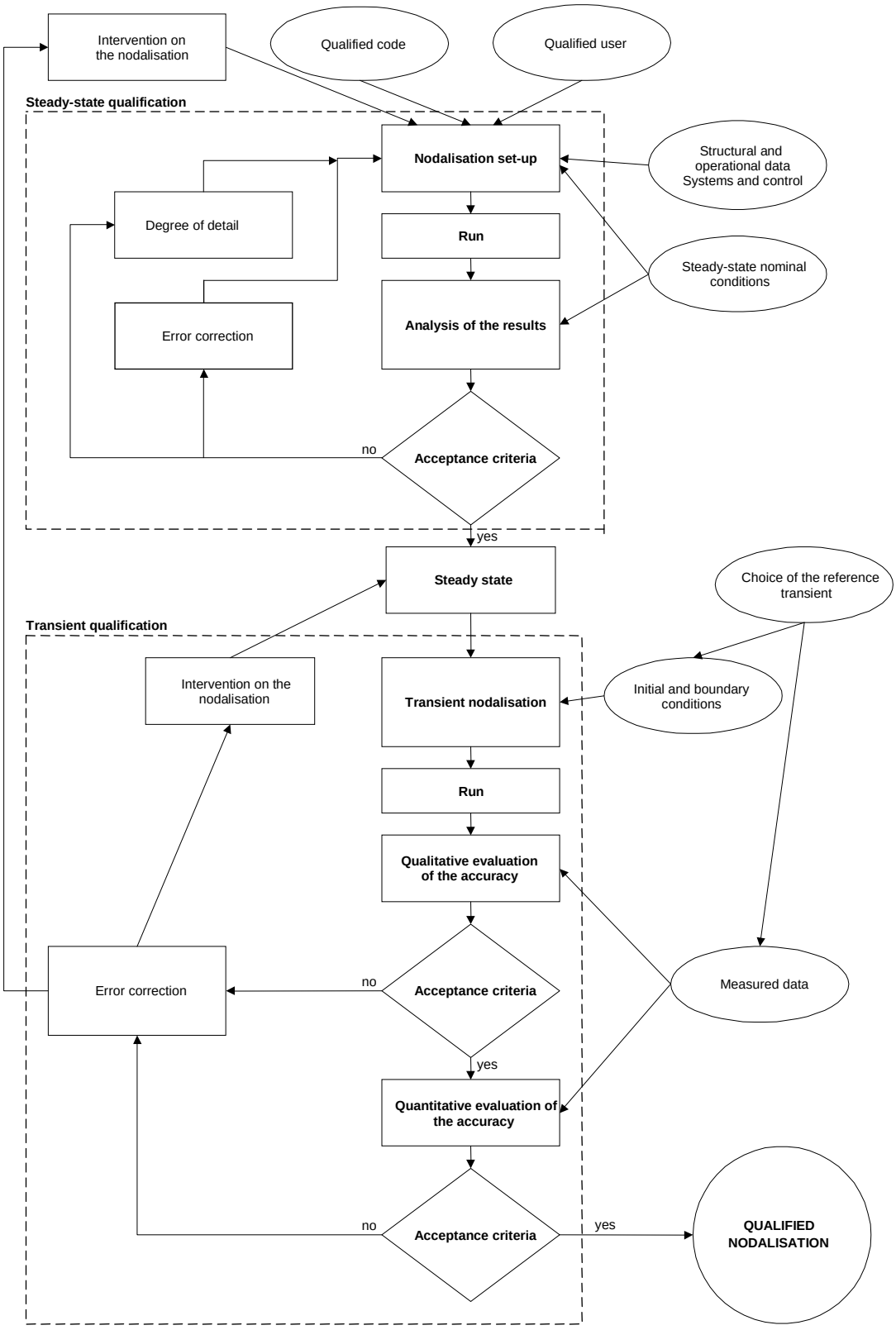

Table 3. Acceptability criteria for thermal-hydraulic nodalisation qualification at steady-state level [78]

	Quantity	Acceptable error (°)
1	Primary circuit volume	1%
2	Secondary circuit volume	2%
3	Non-active structures heat transfer area (overall)	10%
4	Active structures heat transfer area (overall)	0.1%
5	Non-active structures heat transfer volume (overall)	14%
6	Active structures heat transfer volume (overall)	0.2%
7	Volume vs. height curve (*i.e.* "local" primary and secondary circuit volume)	10%
8	Component relative elevation	0.01 m
9	Axial and radial power distribution	1%
10	Flow area of components like valves, pumps and orifices	1%
11	Generic flow areas	10%
(*)		
12	Primary circuit power balance	2%
13	Secondary circuit power balance	2%
14	Absolute pressure (PRZ, SG, ACC)	0.1%
15	Fluid temperature	0.5% (**)
16	Rod surface temperature	10 K
17	Pump velocity	1%
18	Heat losses	10%
19	Local pressure drops	10% (^)
20	Mass inventory in primary circuit	2% (^^)
21	Mass inventory in secondary circuit	5% (^^)
22	Flow rates (primary and secondary circuit)	2%
23	Bypass flow rates	10%
24	Pressuriser level (collapsed)	0.05 m
25	Secondary side or downcomer level	0.1 m

(°) The % error is defined as the ratio |reference value – calculated value|/|reference value|. The dimensional error is the numerator in the above expression.
(*) With reference to each of the quantities below, following a 100 s transient steady-state calculation, the solution must be stable with an inherent drift < 1%/100 s.
(**) And consistent with power error.
(^) Of the difference between maximum and minimum pressure in the loop.
(^^) And consistent with other errors.

This is aimed at reproducing (or simulating) one or more transient scenarios in Integral Test Facilities (ITF) that have characteristics similar to those in the scenarios that constitute the objective for the NPP related application. In other words, the NPP nodalisation must be used to predict an experimental scenario. This is achieved through the so-called Kv-scaled procedure suitable to derive input boundary conditions for the NPP nodalisation [76] and to evaluate the comparison between NPP predictions and ITF data [81].

A quality demonstration of the output of the Kv-scaled calculation is obtained using a qualitative and quantitative accuracy evaluation [82-84], adopting suitable analytical tools.

The Kv-scaled calculation may be substituted by a proper benchmark activity, where NPP calculation results are compared with results of other qualified nodalisations and by the evaluation of suitable operational transients in relation to which data from the concerned NPP are available.

2.4.2 Neutron kinetics nodalisation (input deck) development and qualification

In order to achieve a neutron kinetics nodalisation a much smaller number of code-user decisions and choices is needed in comparison with thermal-hydraulic nodalisation. This can easily be understood by considering that only the core is concerned and makes the process of developing a 3-D neutron kinetics nodalisation more straightforward.

Nevertheless, the generic recommendations given in Section 2.4 and the acceptability criteria discussed in relation to thermal-hydraulic nodalisation (Section 2.4.1), can be translated into a number of preliminary requirements. A first group of requirements (nodalisation development) includes the identification of:

- The core array matrix (square, triangular, plate, etc.).
- The variety of fuel elements or fuel assemblies (FA) that constitute the core.
- The variety of fuel rods that constitute each FA (burnable poisons, etc.).
- The relative position of control rods (CR), FA and of fuel rods, as needed.
- The role of the fluid-dynamic core bypass and of the neutronic reflector including massive structures in radial and axial positions (barrel, fuel boxes, core support plates, etc.).

The ranges of validity of the parameters, namely of cross-sections, should be compared with the ranges of variations expected during the transient calculation. Thermal-hydraulic input parameters (required by the stand-alone 3-D neutron kinetics codes) should be properly identified and consistently fixed. User choices, including ADF, xenon consideration, etc., shall be properly justified, along with the selected value of the time step. Reproduction of reference code runs is recommended before any use of the code.

2.5 Needed precision, including level of detail of coupled calculation

The precision or target precision from any analytical derivation can be viewed as synonymous of an uncertainty or accuracy level. The precision necessary for any code calculation must derive from the specific application. However, the capabilities of the computational tools, including the computer power, may play an important role in assigning a target precision. For this reason, and due to the continuous (over the last 30-50 years) fast growth of both computer power and of capabilities of numerical techniques, target precision is seldom requested in complex code applications for nuclear technology.

Notwithstanding the above, an attempt is made hereafter to formulate criteria and to define thresholds of acceptability for the results of coupled 3-D neutron kinetics/thermal-hydraulics calculation. A straightforward process is pursued: a minimum reasonable number of quantities of interest is first identified and requested error is assigned based on engineering judgment that takes into account the current state of the art. A short description of the suitable level of detail requested for coupled calculation is given before the selection of quantities of interest and the related acceptability thresholds.

Suitable level of detail of input deck

As already discussed, nodalisations that allow the evaluation of neutron kinetics cross-sections, 3-D neutron kinetics and thermal-hydraulic nodalisations should be distinguished. Various degrees of freedom are left to the user when setting up nodalisations to perform the simulation of a requested transient in an assigned system. The recommendations listed here consider the capability of current computers (year 2003) and aim at reducing the user effect (or the degrees of freedom):

- Nodalisations for CSC, THSC and NKC must be consistent: the same elementary cell must be considered in each application.

- Individual fuel elements (minimum level of detail) should be considered in each of the codes concerned. They typically differ among one other for burn-up and initial enrichment, presence of burnable poison and of control rod, position in the core and (in some cases) for the number of rods.

- Lumping together similar fuel elements, typically in the THSC nodalisations, should be avoided as much as possible.

- Symmetry assumptions must be justified and applied in similar manner for the various codes.

- Axial node subdivisions of the order of 20 (or greater) must be adopted: *i.e*. each fuel assembly must be divided into 20 or more parts, typically equal in terms of axial length.

- In THSC nodalisation, the level of detail of the different parts of the RPV should be consistent with the level of detail of the core region.

- Energy ranges for neutrons must be the same for CSC and NKC nodalisations.

- Care must be taken in identifying the range of cross-section variation (validity) from the CSC calculation. It must be ensured that those limits are not exceeded in the THSC/NKC coupled calculation.

- The core bypass (typical THSC nomenclature) and the reflector (typical NKC nomenclature) nodalisation must be consistent in the various steps of the coupled calculation (*e.g*. volume of the core bypass, input parameter for THSC, must be consistent with the reflector thickness utilised in the NKC input deck).

Quantities of interest

A variety of quantities of interest for the design and safety evaluation of LWR are the output of coupled 3-D neutron kinetics/thermal-hydraulics calculation. These range from the k_{eff}, to the boron concentration to reach criticality, to the worth of CR, to the transient pressure, the fuel temperature, the flow rate, the level (*e.g*. in the PRZ), the amount of radioactive liquid discharged from a relief valve (SRV or PORV). The identification of these quantities is connected with the transient type (*e.g*. ATWS or LBLOCA), with the application type, notably licensing or design analysis and is related to the duration of the transient. Each application is definitely associated with a set of quantities of interest. A minimum reasonable set of quantities of interest is defined below, making reference to a transient duration of the order of 100 s. The following quantities are selected and related point values are considered:

- [Quantity 1 and 2]. Peak pressure in RPV (UP location) and in PRZ (if applicable), related FWHM (if applicable) and time of occurrence.

- [Quantity 3]. Peak total core power, related FWHM (if applicable) and time of occurrence.

- [Quantity 4]. CHF (or DNB) occurrence time.

- [Quantity 5]. PCT and time of occurrence.

- [Quantity 6]. Maximum fuel temperature (MFT) and time of occurrence.

- [Quantity 7]. Total thermal energy released to the fluid (TTEF) during the transient.

- [Quantity 8]. Maximum % of core, in terms of heat transfer area (HTA) of the active region where, at any time, rod surface temperature > 1 000 K occurs (CRHST = core region at high surface temperature).

- [Quantity 9]. Maximum % of core in terms of volume occupied by fuel pins in the active region where, at any time, fuel temperature > 3 000 K occurs (CRHFT = core region at high fuel temperature).

Acceptability thresholds for the quantities of interest

The definition of acceptability thresholds encounters the same difficulties mentioned earlier as concerns the quantities of interest. The dimension of the core, including the nominal power, the power generated per unit volume and various other nominal operating conditions (*e.g*. nominal pressure, set point for valves opening) may also affect the identification of thresholds of acceptance.

However, the errors that are acceptable (acceptability thresholds) for the identified quantities are defined here. In the present approach it is assumed that the overall error for a point-value quantity is the combination of two independent contributions: the quantity errors and the time error. Therefore, the predicted point-value quantity stays in a rectangle whose geometric centre is the BE prediction and whose edges are given by the "quantity" and the "time" error values [7].

- [Quantity error, situation 'a']. For pressure pulses characterised by FWHM < 0.1 s in the reference BE evaluation, the acceptable threshold error is 10% nominal pressure of the considered system.

- [Quantity error, situation 'b']. For pressure pulses characterised by FWHM ≥ 0.1 s in the reference BE evaluation, the acceptable threshold error is 2% nominal pressure of the considered system.

- [Quantity error, situation 'a']. For core power pulses characterised by FWHM < 0.1 s in the reference BE evaluation, the acceptable threshold error is 100% nominal power or 300% initial power of the considered system, which ever is smaller.

- [Quantity error, situation 'b']. For core power pulses characterised by FWHM ≥ 0.1 s in the reference BE evaluation, the acceptable threshold error is 20% nominal power or 100% initial power of the considered system, which ever is smaller.

- [Quantity error, situation ‘b’]. For PCT, the acceptable threshold error is 150 K (larger errors can be tolerated for BE prediction of PCT below 1 000 K).

- [Quantity error, situation ‘b’]. For MFT, the acceptable threshold error is 200 K.

- [Quantity error]. For TTEF the acceptable threshold error is 10% of energy released to the fluid in nominal conditions or 100% of energy released to the fluid at the actual initial power, during the considered transient duration, which ever is smaller.

- [Quantity error]. For CRHST the acceptable threshold error is 10% of core HTA.

- [Quantity error]. For CRHFT the acceptable threshold error is 10% of core pin volume.

- [Time error, situation ‘a’]. The acceptable time error that can be associated to the prediction of time of occurrence of Quantities 1 to 3 is 100% of the BE value.

- [Time error, situation ‘b’]. The acceptable time error that can be associated to the prediction of time of occurrence of Quantities 1 to 6 is 20% of the BE value.

- [Time error, situations ‘a’ and ‘b’]. The acceptable time error that can be associated to the prediction of FWHM for Quantities 1 to 3 is 20% of the BE value.

The proposed acceptable threshold errors are consistent with the expected capabilities of current computational tools assuming the best practice in their application.

2.6 Best-estimate versus conservative approach and need for uncertainty evaluation

Uncertainty and the need for uncertainty evaluation are linked to the use of best-estimate (BE) codes as opposed to conservative codes or assumptions in the code application. The application of coupled 3-D neutron kinetics/thermal-hydraulic codes implies the choice of the BE approach. A short discussion is provided in relation to the need for BE, the difference between the BE and conservative approaches, the origin of uncertainties and the current status of uncertainty evaluation. Additional details can be found in Refs. [3,8].

The selection of a best-estimate analysis in place of a conservative one depends upon a number of conditions that are independent of the analysis itself. These include the available computational tools, the expertise inside the organisation, the availability of suitable NPP data (*e.g.* the amount of data and the related details can be very different depending on the type of analyses), or the requests from the national regulatory body. In addition, conservative analyses are still widely used to avoid the need for developing realistic models based on experimental data, a task that may reveal to be unrealistic in the case of BDBA, or simply to avoid the burden of changing an approved code and/or the approaches or procedures to obtain the licensing.

The conservative approach does not provide any indication of the real margins between the actual plant response and the conservatively estimated response. In contrast, the uncertainty estimate provided in the best-estimate approach is a direct measure of such margins. As a result the best-estimate approach may allow for the elimination of unnecessary conservatism in the analysis and could permit the regulatory body and plant operating organisation to establish a more consistent balance for a wide

range of acceptance criteria. A conservative approach does not give any indication about actual plant behaviour, including the time scale for preparation of emergency operating procedures, or for use in accident management and preparation of operation manuals for abnormal operating conditions.

Although the acceptability of the approach to be used for an accident analysis needs to be defined by the regulatory body, the use of totally conservative approaches (conservative models, input data and plant conditions) is unwarranted nowadays, given the broad acceptance of best-estimate methods (*e.g.* mature best-estimate codes are widely available around the world, an extensive database exists for nearly all power reactor designs and best-estimate plant calculations are well documented). The use of an exclusive best-estimate approach implies the difficulty of quantifying code uncertainties for every phenomenon and for every accident sequence.

Uncertainty analyses include the estimation of uncertainties in individual modelling or of the overall code, uncertainties in representation and uncertainties in plant data for the analysis of an individual event. Scaling studies to quantify the influence of scaling variations between experiments and the actual plant environment are included in this definition. In some references, code scaling and uncertainty analysis are identified separately. These concepts are applicable to any of the CSC, NKC and THSC. The derivation of a comprehensive picture about uncertainty methods currently developed and in use for supporting thermal-hydraulic best-estimate code prediction is beyond the purpose of the present report. A few observations provide an idea of the current status [8]:

- The approaches pursued for uncertainty evaluation can be placed into two main categories, *i.e.* propagation of code-input uncertainties and of code-output uncertainties. Methods fully based upon statistics can also be distinguished from fully deterministic methods where the expertise of uncertainty-methodology-user is needed at different steps to achieve meaningful results.

- The different levels of maturity achieved by various methods and the eventual qualification process through which these methods have undergone (or not), must be noted. The pioneering effort constituted by the CSAU methodology is now recognised. In addition, various methods have been occasionally proposed, applied or qualified. The uncertainty methodologies proposed by GRS and by the University of Pisa (UMAE) appear to have achieved a reasonable level of maturity [85].

- In relation to the actual application method, the support of uncertainty estimate to the evaluation of the large break LOCA, within the licensing process of Angra-2 NPP, constitutes the most significant example. The Siemens method applied combines features of the GRS and of the UMAE methods.

- The idea of Internal Assessment of Uncertainty was developed in 1996 (see below) and was realised through the CIAU method that utilises the basic approach of the UMAE at the University of Pisa [86]. The CIAU (Code with capability of Internal Assessment of Uncertainty) allows the achievement of continuous uncertainty bands simultaneously with the BE calculation, thus avoiding the uncertainty-methodology-user effect and the need of resources for uncertainty prediction. However, a suitable error database must be made available to pursue the CIAU approach. In a joint effort between University of Pisa and PSU the CIAU method has recently been extended to the evaluation of uncertainty from coupled 3-D neutronics/thermal-hydraulics calculations as discussed in the following section.

2.6.1 The CIAU method and its extension

All of the uncertainty methodologies suffer from two main limitations:

- The resources needed for their application may prove to be prohibitive, ranging to up to several man-years.

- The achieved results may be strongly methodology-user dependent.

The last item should be considered with the code-user effect [76], and may threaten the usefulness or the practical applicability of the results achieved by an uncertainty methodology. Therefore, the Internal Assessment of Uncertainty (IAU) was requested as the follow-up of an international US NRC and OECD/CSNI conference held in Annapolis in 1996. The CIAU approach considered here [86], has been developed keeping in mind the objective of removing the above limitations. In no uncertain terms, the internal assessment of uncertainty constitutes a desirable capability for thermal-hydraulic system codes allowing the automatic achievement of uncertainty bands associated with any code calculation result. A description of the CIAU method is provided in Ref. [86].

The concept at the origin of the CIAU can be summarised by three items:

1) *Build-up of NPP status*. Each status is characterised by the value of six relevant quantities (or phases) and by the value of the time since the transient start. Each of the relevant quantities is subdivided into a suitable number of intervals that may be seen as the edges of hypercubes in the phase-space. The transient time or duration of the transient scenario is also subdivided into intervals.

2) *Association of uncertainty with NPP status*. Accuracy values derived from the analysis of experimental data are associated with each NPP status.

3) *Use of the method*. Each time, the CIAU code calculation result is associated with a time interval and to a hypercube, *i.e*. a NPP status, from which the uncertainty values are taken and associated with the current value of the prediction.

The IAU concept can be applied with any uncertainty method. In other words, any existing uncertainty method (*e.g*. CSAU, GRS method, etc.) can be used to generate uncertainty values thus filling the hypercubes and the time intervals. The idea at the basis of the current CIAU is connected with the status approach.

First, quantities are selected to characterise space the thermal-hydraulic status of a LWR in a multi-dimensional space during any transient. In this way, hypercubes are defined and associated with time intervals accounting for the transient time duration. Then, the accuracy of each hypercube and time interval is calculated from the analysis of experimental data. The combination of accuracy values originating from hypercubes and time intervals allows the derivation of continuous uncertainty or error bands enveloping any time-dependent variables that are the output of a system code calculation.

Six driving quantities identify the hypercubes edges. In the case of PWR transients these quantities are: 1) primary system pressure, 2) steam generator system pressure, 3) mass inventory in primary system, 4) core power, 5) rod surface temperature at 2/3 of core height and 6) Steam generator downcomer level. A consistent ensemble of uncertainty values is included in any set constituted by a Quantity Uncertainty Matrix (QUM) and a Time Uncertainty Vector (TUV). The QUM is formed by hypercubes whose edges are the six selected variables above that are representative of a generic transient scenario.

The object quantities, *i.e.* the quantities in relation to which uncertainty is calculated are: 1) primary system pressure, b) rod surface temperature at 2/3 core height and c) primary mass inventory. Coincidence between the object quantities and the driving quantities is due to the relevance of such variables and is not mandatory in the structure of the method (*e.g.* mass flow rate at core inlet could be selected as an object quantity).

The RELAP5/mod3.2 system code and UMAE uncertainty methodology have been coupled to constitute the CIAU. Therefore, the uncertainty has been obtained from the extrapolation of the accuracy resulting from the comparison between code results and relevant experimental data; these may be obtained from integral test facilities as well as from separate effects test facilities.

Within the CRISSUE-S framework, the methodology has been extended to the prediction of the uncertainty of 3-D neutron kinetics/thermal-hydraulics calculations [172]. In order to achieve this undertaking, namely to predict uncertainty in core power and in its spatial distribution as a function of time, the number of driving and object quantities has been increased to eight and six, respectively. Reactivity and average burn-up constitute the additional driving quantities, and power peaking factors have been added as object quantities.

Basically, the demonstration of the feasibility of the approach has been achieved and sample results are shown in Figure 8, related to the BWR-TT transient in the Peach Bottom NPP [173] (see also Annex I). The full implementation and use of the procedure requires a database of errors not currently available. However, the data reported in Figure 8 give an idea of the errors expected from the application of present computational tools to problems of practical interest.

2.7 BWR stability

The issue of BWR stability dates to the inception of BWR technology [9] and can be summarised as follows: BWR plants are prone to instability due to the nature of the two-phase thermal-hydraulics further excited by the neutron kinetics feedback and by the control system of the NPP. The instability originates in the core and leads to oscillations in flow rate, pressure and void fraction. In a number of situations, scram and consequent reactor power shutdown are the only tools available to put a stop to uncontrolled power excursions.

Core oscillations are efficiently suppressed during nominal reactor operation through proper design choices. However, oscillations of local, regional or global nature may occur during accident/transient conditions. The core thermal-hydraulic configuration, corresponding to about 50% core nominal power and 30% core inlet flow rate, may be seen as the area in the core power-to-flow map where the highest probability for oscillations occurs. Specific exclusion zone procedures are mandatory in current BWRs to prevent operation in this zone.

Nevertheless, oscillations may occur and must be studied. The continued occurrence of such events suggests that system codes are not being efficiently utilised to avoid nuclear coupled thermal-hydraulics instabilities. One of the main reason why this is the case is that testing the large parameter space and operating scenarios of a BWR using the system codes is a time consuming task. Hence, if tools were available to *quasi-quantitatively but efficiently* test the large number of operating scenarios in BWR to identify conditions that *might* lead to instabilities, then high-fidelity system codes could be selectively used to *quantitatively* investigate the scenarios of interest.

The availability of coupled 3-D neutron kinetics/thermal-hydraulic techniques opens new horizons for such analysis.

Figure 8. Results from the sample application of the CIAU to the BWR-TT coupled 3-D neutron kinetics/thermal-hydraulics problem benchmark

Core power history with lower and upper uncertainty bands

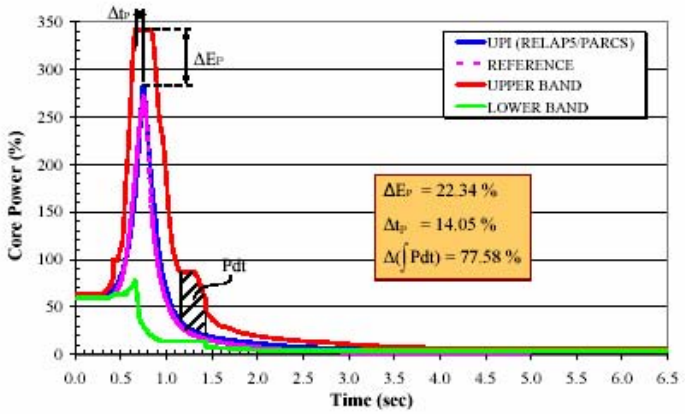

Axial peak factors' distribution when the core power peak occurs. Lower and upper uncertainty bands.

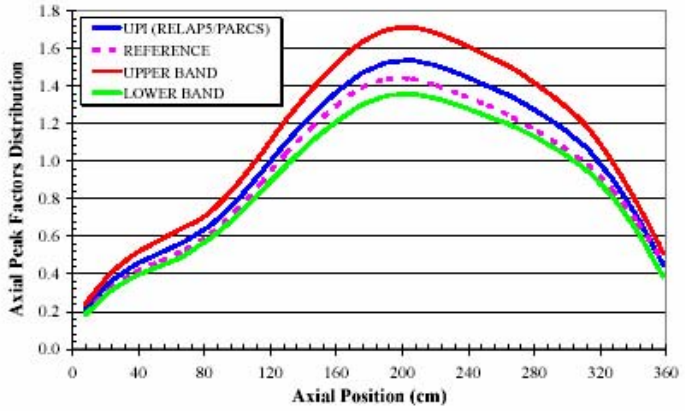

Radial peak factors' distribution when the core power peak occurs. Lower and upper uncertainty bands.

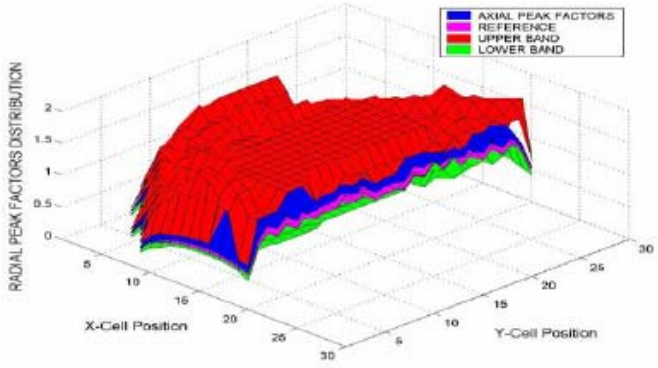

The development of the spatial mesh overlays for BWR stability analysis, especially in the case of regional instability analysis, requires a more sophisticated approach than that pursued for modelling a PWR core [36], which is based on a modal analysis method. The mapping of thermal-hydraulic channels is modelled considering not only the power peaks, orificing sizes and thermal-hydraulic characteristics but also the neutron flux fundamental and first azimuthal mode during the steady-state point.

The spatial coupling effect induced by the void feedback plays an important role in the regional instability events. In regional instability oscillations, the first azimuthal flux mode is deformed. The higher mode power shape and locations of hot bundles need to be properly reflected in the regional instability mapping. The out-of-phase flow oscillation has similarities with parallel channel instability and the identification of the neutral line is quite important to preserve a spatial coherence between thermal-hydraulic state variables and the first azimuthal mode flux. In order to accurately predict the initiation of oscillations, a sufficient number of hot bundles need to be isolated as individual regions. The hot bundles should be surrounded by regions that possess a larger flow area so that they would not constrain the oscillation in an unrealistic way.

During regional oscillations, the hot bundles' locations are determined assuming that the stationary fundamental mode is superposed by the oscillatory first azimuthal mode. The neutron spatial coupling helps the oscillation of the hottest region to spread over the entire core, therefore lowering the entire core threshold nearly to that of the hottest region threshold. When the number of channel components becomes sufficiently large, significant oscillations are observed in the individually modelled hot bundles and subsidiary small oscillations are observed in the surrounding regions. Without the neutron spatial coupling, oscillatory behaviours of the surrounding regions become somewhat random and they weakly constrain oscillations of the hot regions.

A more detailed review of the methods available to analyse nuclear coupled thermal-hydraulics stability in BWR is given in Appendix A. Also provided are the results of simulations using nuclear coupled thermal-hydraulics codes of specific instability incidents.

2.8 Cross-section derivation

The need for a more accurate method of modelling cross-section variations for off-nominal core conditions is becoming an important issue with the increased use of coupled three-dimensional (3-D) neutronics/thermal-hydraulic simulations. In traditional reactor core analysis for both steady-state and transient calculations of LWR conventional nuclear power plants, condensed few-group two-dimensional (2-D) cross-section sets are used as input data. These cross-section sets are generated by separate database calculations using characteristic weighting spectra and are parameterised in terms of burn-up and thermal-hydraulic feedback parameters. Under the real reactor conditions, especially in transient situations, these spectra change and the 2-D cross-section modelling based on a parameterisation model only approximately describes the effects of neutron flux distributions, which change in space, time and energy. This so-called 2-D off-line cross-section generation and modelling constitutes a basic input data uncertainty affecting the results of coupled 3-D neutronics/thermal-hydraulic calculations.

Historically, a two-step process is applied in traditional reactor core analysis for both steady-state and transient applications. The first step in the process is to calculate few-group cross-sections with different dependencies (*i.e.* as a function of burn-up and local feedback parameters) for various regions of a reactor core in 2-D geometry, employing lattice physics codes such as CASMO [23,39] and HELIOS [40]. The second step is to use this cross-section data in a 3-D nodal diffusion code for determination of different parameters throughout the reactor core. There are several shortcomings in this approach associated with both cross-section generation and cross-section modelling. In regard to the cross-section generation two shortcomings are addressed:

- The use of 2-D lattice physics codes for cross-section generation, based on the fact that the majority of current lattice physics codes use the collision probability method (CPM), becomes cumbersome and impractical in 3-D geometries.

- Current methodology homogenises representative assemblies assuming symmetry (reflective) boundary conditions. This approach introduces significant errors in the determination of neutron flow among assemblies in a real reactor core configuration. The errors are somewhat mitigated by the use of *ad hoc* assembly discontinuity factors for conventional reactor core analysis.

The amount of few-group cross-section data necessary for steady-state, depletion and transient analysis, is significant. Standard cross-section modelling for coupled 3-D steady state and transient simulations are based on the data generated in the so-called base and branch calculations using a lattice physics code. The cross-section history and instantaneous dependence models developed in this way are based on burn-up and local feedback parameters (*i.e.* fuel temperature, pressure, moderator temperature, void, boron concentration). The thermal-hydraulics model coupled with the neutronics simulator calculates these feedback parameters. Changing each of the parameters one at a time develops the instantaneous cross-section dependencies.

A typical dependence of a cross-section on a particular parameter is displayed in Figure 9. This shows that over a large range of values the cross-section does not behave linearly. More interesting cross-section behaviour is shown in Figure 10. The figure shows the interdependence of cross-sections when two parameters are varied at once. The cross-sections generated in this way are called cross-terms, since they are not dependent on just one parameter, but on all parameters. Such cross-term cross-sections have to be taken into account in transient analysis since they are actual points on the curved surface. However, standard methods (currently used in core steady-state, depletion and transient analysis) such as the polynomial fitting procedure (usually based on Taylor expansions) do not take these cross-terms into account. Since these methods utilise no cross-term dependencies on local feedback parameters they are especially inaccurate for transients in which large departures from nominal conditions exist.

Figure 9. Cross-section dependence on moderator temperature

Obtained at PSU with CASMO-3

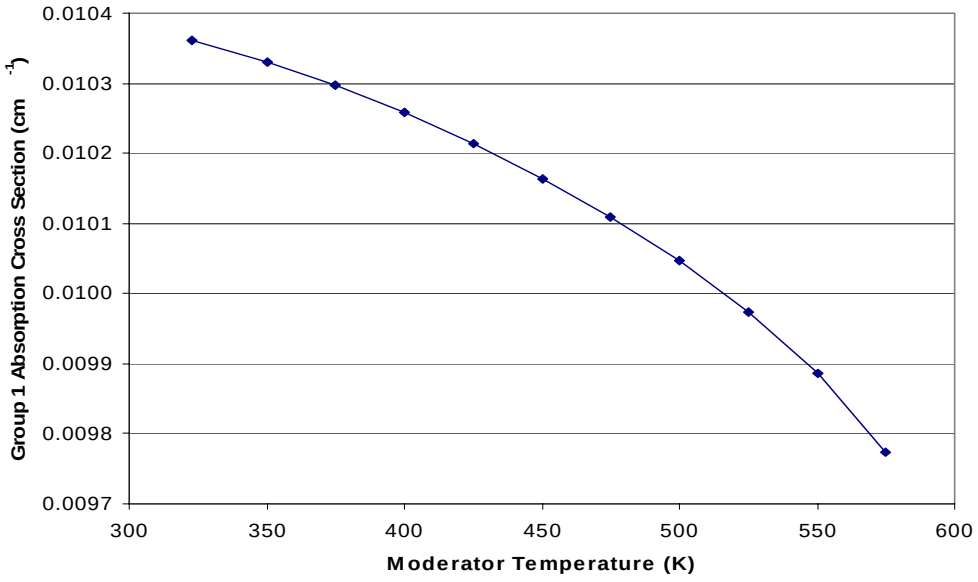

Figure 10. Cross-section interdependence between fuel temperature and moderator temperature

Obtained at PSU with CASMO-3

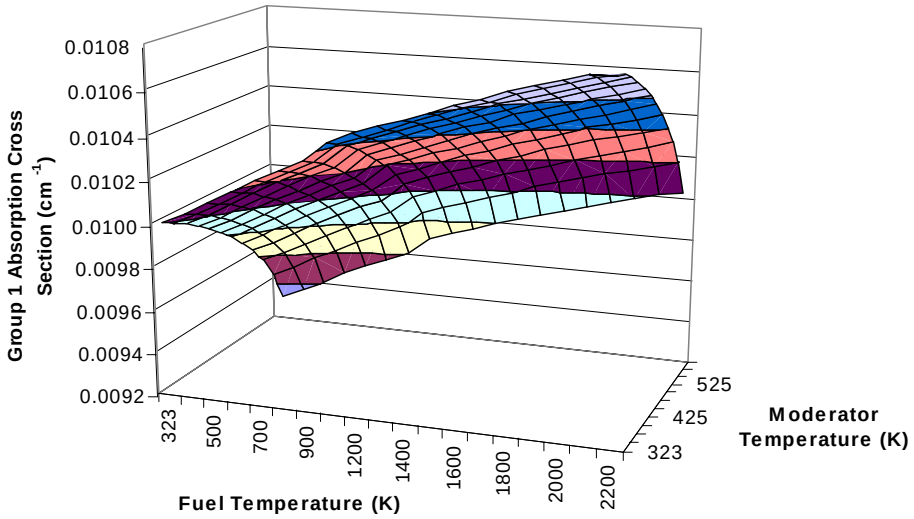

The typical calculation points necessary to develop the cross-section derivatives used in the polynomial fitting procedure can be seen from the schematic given in Figure 11. For simplicity only two parameters are shown, fuel temperature (T_F) and moderator temperature (T_M). This method uses a cross-section calculation at average conditions, shown as the black dot, as a reference value. From the reference value parameter perturbations are performed to develop cross-sections at different conditions, shown by the red dots. In this method only one parameter is varied at a time, all other parameters remain at average conditions. Once the new cross-section is established along with the magnitude of the individual parameter variation, a derivative can be constructed which is used directly in the polynomial equation. Using these derivatives along with the average cross-sections, a cross-section can be calculated at any reactor condition.

Figure 11. Cross-section calculation points for the polynomial fitting procedure

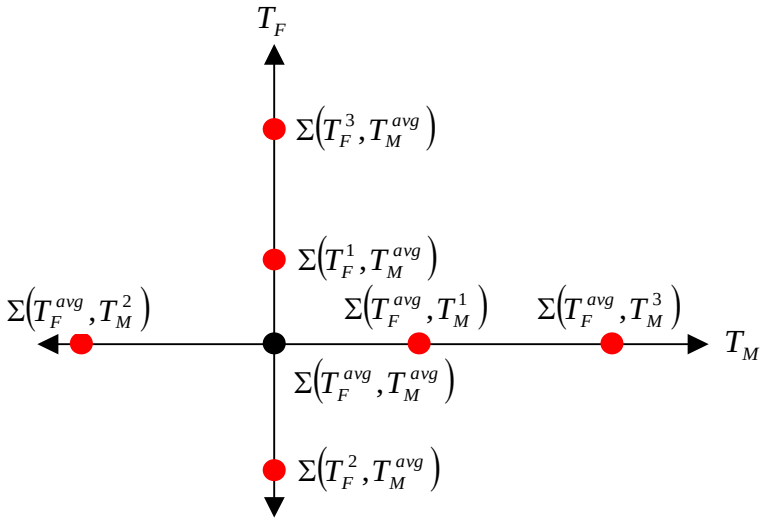

The most significant problem with this procedure is that it becomes more inaccurate as the parameter variations get farther away from average conditions. The areas where the polynomial fitting procedure becomes inaccurate are shown as the blue hashes in Figure 12. The increased inaccuracy of the cross-sections calculated in these regions is more important in transient analysis where parameter variations extend into this region during a typical transient calculation.

Figure 12. Areas of inaccurate cross-section calculation using the polynomial fitting procedure

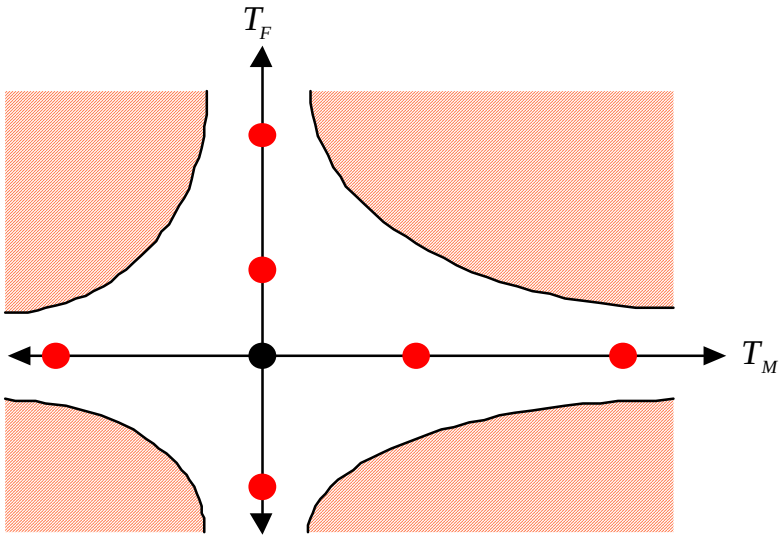

The widely used CASMO/SIMULATE cross-section parameterisation model attempts to model the cross-section cross-term dependence involving an approximate type of cross-section representation [23]. Each cross-section can be evaluated as a summation of base and partial values. The base cross-sections represent the burn-up dependence (exposure, spectral history and control history) while the partial cross-sections represent the instantaneous dependence on local feedback parameters. Performing branch calculations generates the partial cross-sections, where again as with the polynomial fitting procedure only one feedback parameter is changed for a given perturbation. The model tries to account for the cross-term dependence by using separate partial cross-sections for different feedback effects. While the model is an improvement over the polynomial fitting procedure it is limited to small perturbations.

To remedy the inaccuracies of the procedures described above, PSU has developed a sophisticated, unique cross-section representation methodology for 3-D coupled transient calculations [41]. The method developed at PSU employs not only the cross-section at average conditions, but also the cross-term cross-sections, as can be seen in Figure 13. Cross-term cross-sections are cross-sections calculated by varying two or more parameters at the same time. The cross-sections are then tabulated in N-dimensional tables. The N-dimensional tables are then interpolated for the appropriate cross-section value. The tabulated cross-sections completely encompass the full range of conditions that may be present during the initial steady state and the transient. This method is called the Adaptive High-order Table Look-up Method (AHTLM) [42]. In the AHTLM the user develops an operating condition box-envelope. This box bounds the expected range of change of the feedback parameters during both steady-state and transient operation. The cross-sections are then calculated for the bounding box edges and within the box. These reference cross-section values are placed in multi-dimensional tables that are used in a sophisticated table interpolation method that is employed to calculate the cross-sections.

The advantage of this method is that there is no chance that the calculation of the cross-section can be outside the bounds set by the user and to involve extrapolation procedure. In addition, this approach

Figure 13. The PSU transient cross-section representation

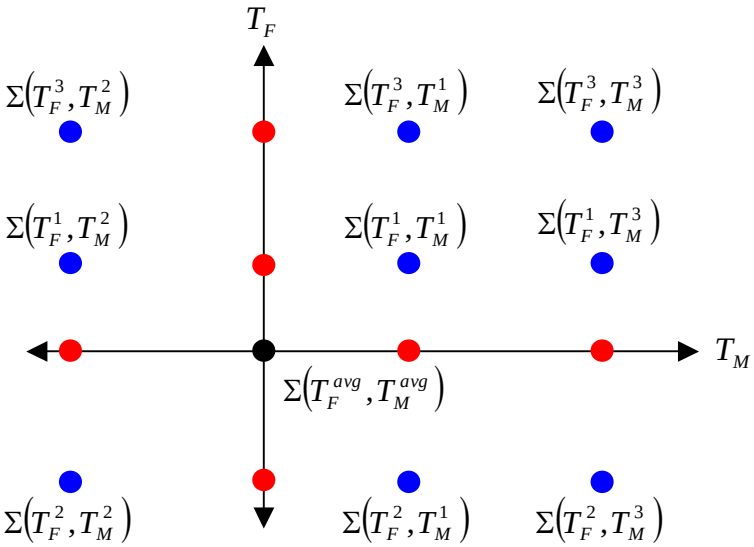

helps to improve the accuracy of modelling the cross-section variations by avoiding user-calculated coefficients that could contain errors. This method takes into account the non-linear thermal-hydraulic feedback parameter phenomena that are critical for the accurate prediction of cross-section behaviour.

2.8.1 Depletion and spectral effects

The long-term time-dependent modelling of the core behaviour is a complicated and tedious task. Many parameters have to be taken into account to properly predict the changing fuel properties. When a depletion model is used, it is very important to include as many of the known properties of the fuel as possible, as well as the operating conditions at which the node of interest depletes during the particular part of time. When performing a depletion calculation to a particular exposure, one has to take into account the changes in power that a reactor undergoes, the insertion or removal of control rods, the shuffling of fuel, and the local thermal-hydraulic changes. All of these variables contribute to the particular properties of fuel in a node at some point in the future. To obtain accurate cross-sections at a particular exposure point all of these effects have to be considered. This is done through developing accurate input decks for the spectral code, which include as many of these effects as possible. In order to include all of these effects to a very accurate degree, a cross-section modelling algorithm based on the core analysis is performed with a three-dimensional simulator code. Within an integrated core analysis package a more detailed method for developing accurate cross-sections, exactly for modelled initial steady-state conditions for each calculation node has to be implemented.

Cross-sections are dependent on burn-up, control variables and thermal-hydraulic properties. The burn-up dependence of cross-sections is a three-dimensional vector of exposure, spectral history and burnable poison history (for PWR) or control rod history (for BWR). It is based on isotopic depletion. As fuel is burnt the isotopic content is changed in the fuel and, therefore the cross-section behaviour changes. For example, with the production of Pu isotopes there is a hardening of the cross-section spectrum due to the increase of Pu in the fuel. Other changes occur due to the decay and production of fission products. This means that even if all other thermal-hydraulic properties are constant (*i.e.* steady-state conditions) there is still a change in the cross-section behaviour due to the long-term change in isotopes in the fuel while it is being depleted or (as it is usually called) changes in nodal isotopics. Another parameter that affects the cross-section behaviour is control history, which in PWRs is

consists of burnable poisons (BP). The burnable poisons cause the fuel to deplete differently with respect to time and space, changing the radial power distribution at each depletion step. When the burnable poisons are removed or depleted the behaviour of the fuel changes. In the case where burnable poisons are present during one period of time in a reactor cycle and then are removed from the reactor during a second time period the effect of the burnable poison in the first time period is still present. This is called a history effect. The knowledge that the burnable poison was there has to be considered since the fuel in this location has different properties than other fuel without burnable poisons. The effect of control rod (CR) movement during a BWR cycle is similar.

2.8.2 Importance of the spectral history modelling

As fuel is depleted in a reactor, the fission process and the consequent decay of nuclide fragments change many of the fuel properties. The production of nuclides and the decay of others affect the neutron spectrum. These effects depend on the node conditions at which depletion takes place. When the fuel, moderator and structural materials are smeared together in the homogenisation process, any change in the properties greatly affects the cross-sections through shifting the neutron spectrum. It can easily be seen that under non-static conditions, the modelling of all of the properties of the reactor can be very difficult. The spectral code calculates the shift in the neutron spectrum based on the enrichment of the fissile material, type of fissile material and the other materials present in the fuel. The code's knowledge of the different decay and production chains allows this. The only control the user has over this process is determining the fuel type and enrichment. The spectral code takes care of the rest. Since the spectral code has no knowledge of the change in the other properties, with time it is more important for the user to inform the spectral code of as many of these changes as possible. The change in control variables or in thermal-hydraulic conditions during the depletion process will change the local properties of the fuel in the future. The first changes are called control (BP or CR) history effects, while the second are called spectral history effects.

A strong history effect can be seen if the depletion calculation is performed at core average thermal-hydraulic conditions. This is called a density history effect. The density of the coolant at the core outlet is smaller than the density of the core inlet ($T_{out} > T_{ave} > T_{in}$), meaning that if a calculation is performed at core average conditions the neutron behaviour will be modelled inaccurately. At the core inlet, the actual cross-sections contain more moderation than the values calculated at average conditions and less moderation at the top of the core. Further, if the approximate values are used by the nodal code the calculated power is shifted by the density of the water when thermal-hydraulic feedback is considered in the calculation. The density history has a direct effect on the axial power shape and produces a power shape that is skewed towards the bottom of the core. The cross-sections at the bottom of the core are generated based on under-moderated conditions and on over-moderated conditions at the top of the core. The modelling of the cross-sections for the axial temperature distribution in a reactor core is very important to accurately predict the axial power distribution.

2.8.3 Importance of the assembly discontinuity factors (ADF)

It is well known that the diffusion approximation is not accurate in areas where the flux changes rapidly (*i.e.* there is a steep flux gradient). In a typical core calculation these areas are at the core boundary, near strongly absorbing media such as a node where a control rod is inserted, and when two very different assemblies are placed next to each other (UO_2 and MOX(UO_2/PuO_2) assemblies).

Assembly discontinuity factors (ADF) are also calculated by the spectral code. When single 2-D assembly calculations are performed there is no knowledge of the neighbouring nodes/fuel assemblies. The homogenisation process preserves the reaction rates in infinite single assembly geometry. When the

node/assembly of interest is put in a real reactor core it is exposed to a different environment than during the homogenisation process. This means that the homogenised flux solutions will not be continuous at the radial node/assembly boundary [the actual physical (heterogeneous) flux between the assemblies is continuous]. When material properties vary greatly this approximation leads to a large error since the real core environment is very different from the infinite geometry with reflective boundary conditions. Such places are near nodes with control rods inserted, at the reflector region and areas where unlike fuel assemblies are in proximity (*i.e*. uranium fuel next to MOX fuel). ADF quantify the relative difference between the homogenised flux solution at the boundary and the actual heterogeneous transport solution at the boundary of the node/assembly. Using these, one can construct a correction to the flux at the node boundaries, which accounts for the real core environmental effects. It assumes a discontinuous homogeneous flux shape at the boundaries. In our methodology the ADF are treated as the rest of the cross-sections and are based on history and instantaneous dependencies. This consistent modelling is especially important during a transient, during which the thermal-hydraulic and control variables are changing. It is most important to note that the greatest improvement is at the interface between the outer nodes and the reflector. There are steep flux gradients at the fuel/reflector boundary and large errors are produced when cross-sections are generated using single assembly calculations. The implementation of ADF improves the leakage description between nodes/assemblies of different types and the error is significantly reduced.

ADF are primarily used for the radial boundaries of each node. In the axial direction there are fewer discontinuities since the fuel is uniform in the axial direction. As discussed earlier, axial changes in the properties are observed based on the history of the reactor, but this change is a continuous change in the fuel and can be accurately represented by the nodal decomposition. In the radial direction the inherent dislocations are caused by different types of fuel placed next to each other. In the axial direction, ADF are most important at the interface between the top and bottom reflectors. As in the radial model this is the location where the highest errors can occur in the axial direction.

2.8.4 Dependencies on instantaneous parameters

The linear interpolation in multi-dimensional tables is widely used to obtain accurate reproducible results. This is dependent on the linearity of the cross-section with respect to the different dimensions (chosen principal feedback parameters) and the distance between the data points. Several studies have been completed showing that the cross-section dependence on fuel temperature, moderator temperature and pressure is not linear. This indicates that the number of points necessary for accurate results will have to be developed so that the behaviour of the cross-section is accurately modelled. The more points used in the development of the transient cross-section library, the more the overall size of the library will increase, as do the total number of spectral calculations.

The linear surface interpolation has been used for the last several years. The model used is a standard linear interpolation model. Eq. (1) shows the equation used to determine the dependent parameter based on the selected independent parameters:

$$y = y_1\left(1-\frac{x-x_1}{x_2-x_1}\right)+y_2\left(\frac{x-x_1}{x_2-x_1}\right) \tag{1}$$

In this equation, x is the independent parameter where the interpolation should be made. It lies between x_1 and x_2, and y is the new function value. This equation is evaluated for each of the independent parameters up to a maximum of four parameters. Recent modifications extended the capabilities of this subroutine to include extrapolation. If the values lie below the first table entry, the dependent values are derived from:

$$y = y_1\left(\frac{x_2 - x}{x_2 - x_1}\right) + y_2\left(1 - \frac{x_2 - x}{x_2 - x_1}\right) \tag{2}$$

If the independent value is beyond the last table entry, the linear extrapolation is performed via Eq. (3):

$$y = y_1\left(1 - \frac{x - x_1}{x_2 - x_1}\right) + y_2\left(\frac{x - x_1}{x_2 - x_1}\right) \tag{3}$$

In the case of entries that lie within the bounds of the cross-section table, the same interpolation is performed as described in the original method.

The advantages of using a linear interpolation scheme are that it is fast and extrapolation can be done if it is necessary. The disadvantage is that there is a loss in accuracy when this method is used due to the non-linearity of the cross-sections. This means that more points have to be used to obtain an acceptable accuracy, as can be derived from Figure 12. In order to achieve an acceptable precision, more spectral branch calculations have to be performed and the size of the library files becomes very large.

It is possible to develop incorrect cross-sections by using density alone as a feedback parameter. Density as a parameter depends on void fraction, moderator temperature and pressure, and accounts for all the effects on number density due to changes in these parameters. It does not, however account for the effect of moderator temperature on microscopic cross-sections. One solution to this problem is to remedy the thermal-hydraulic state by adding another thermal-hydraulic parameter (*i.e*. moderator temperature or pressure). In so doing, the exact cross-section for this state can be determined. The second problem with this representation is embedded in the method used to determine the range of density values that the cross-sections should be based on. For PWR the density range is based on the variation of moderator temperature and pressure for both steady-state and transient conditions.

The first iteration for the improved methodology involved adding moderator temperature as an independent parameter to the tables to remove the uncertainty in the thermal-hydraulic state. The second iteration involved developing the tables based on varying both density and temperature at the same time. This turned out to be impossible for two reasons. First, the density is a function of the temperature, thus introducing non-linear cross-section dependence. Second, it is not possible to create a space that will completely cover all ranges of density and temperature during both steady state and transients.

The third iteration solves all of these problems and creates a more flexible methodology. This is done by using pressure and temperature as the tabulated independent parameters for single-phase simulations (mostly for PWR applications). Also, this method can be easily extended. For example, when void is present (as in BWR calculations) the existing methodology proved to be very difficult to develop based on the wide range of densities, compounding the error in calculation of the cross-sections. In the new methodology this can be overcome simply by creating a second library containing void as an independent parameter. This is done by replacing the pressure dependence with void dependence. The pressure is replaced due to the fact that when void is present the location is by definition in the steam dome (saturated conditions), and pressure and temperature are no longer independent parameters. When one changes the other will change in the appropriate corresponding manner. This means that the thermal-hydraulic state cannot be accurately described by pressure and temperature alone. The inclusion of void fraction as an independent parameter will “fix” the thermal-hydraulic state. In these situations, pressure and temperature are dependent on each other, so only one of the two is needed in the tables. It was determined that, temperature having the greatest effect on cross-section behaviour, it should be the independent parameter used. Moderator temperature has a large effect on the behaviour of

cross-sections during the slowing-down process. It is generally assumed that a neutron in the moderator has the same temperature as the moderator. This means that changes in the moderator temperature will cause changes in the neutron temperature and shift the spectrum accordingly.

2.8.5 Linear versus higher-order interpolation

One of the drawbacks of the multi-dimensional table methodology is that it involves *n* times more calculations than were previously necessary. A sufficient number of points must be tabulated to achieve the degree of accuracy that is desired. When linear interpolation is used and the behaviour of the cross-sections is not linear with respect to a particular parameter (*i.e.* fuel temperature), more points are necessary. When more points are added the table size increases by a factor of *n*. This is because every combination of each parameter that is tabulated must be used to represent each point in space. If the number of independent parameters is increased slightly the total amount of data to be tabulated is significantly affected, as is the total number of lattice physics branch calculations.

To keep the amount of data and the number of lattice physics calculations to a minimum while maintaining a particular degree of accuracy, a higher-order interpolation scheme must be used to interpolate the tables. The use of a higher-order interpolation over linear interpolation has the advantage of being able to obtain the same degree of accuracy with fewer points. Several types of interpolation schemes can be considered. The research performed at PSU has indicated that the quintic spline routine has shown the greatest accuracy and has been found to be stable [43]. This routine uses a fifth-order polynomial to fit the data. The routine calculates the coefficients at a set of knots (independent points at which dependent points are known) and these coefficients are then used for the interpolation.

A front-end routine is needed to supply the routine with the required data and a back-end routine is needed to perform the interpolation using the coefficients. The curve-fitting subroutine calculates the coefficients of a piece-wise natural quintic spline with knots and uses the method of least resistance. The term “spline” was adopted from a tool that draftsmen used to create a smooth curve through a set of points. The method of least resistance ensures that the curve passes through each point with the least amount of tension on the curve. This is important to prevent the formation of oscillations between the points defining the curve (knots.) This curve-fitting method can only be used for a strictly increasing or decreasing sequence of knots. The knots must be formed such that the fifth power of $X(I+1) - X(I)$ can be formed without overflow or underflow of the exponents. This does not create a problem with the parameters used in this application. The equations used are:

$$S(x) = ((((F(I)\times P + E(I))\times P + D(I))\times P + C(I))\times P + B(I))\times P + Y(I) \text{ or} \tag{4}$$

$$S(x) = ((((-F(I+1)\times Q + E(I+1))\times Q - D(I+1))\times Q + C(I+1))\times Q - B(I+1))\times Q + Y(I+1)$$

where $S(x)$ is the interpolated spline value at point x, $F(I)$, $E(I)$, $D(I)$, $C(I)$ and $B(I)$ are the calculated spline coefficients at point I, $P = x - x(I)$ and $Q = x(I + 1) - x$.

The PSU methodology works well at a given point in a reactor cycle depletion using up to five dimensions (feedback parameters) and modelling all the cross-term effects. This method showed the importance of the cross-term cross-section behaviour on transient analysis. However, it also has several shortcomings, *i.e.* the large amount of data needing to be tabulated and the sophisticated interpolation schemes needed to maintain accuracy, in turn leading to longer calculation times. Although the PSU methodology improves the cross-section feedback modelling, it still relies on standard 2-D cross-section generation using characteristics spectra and specified boundary conditions.

The above-mentioned major weaknesses of the coupled reactor analysis methodology, along with cross-section generation and modelling (especially for transient calculations), need to be appropriately addressed in future research and development activities. The objectives of such research are formulated as development, implementation and testing of innovative schemes and techniques for cross-section generation and modelling for coupled simulations. These goals can be met using a two-step approach. First, a more accurate and efficient method of modelling cross-section variations for off-nominal core conditions should be developed. Second, the feasibility of an improved calculation methodology in using on-line cross-section generation should be explored.

The first step is actually to develop a new type of cross-section library. This library will contain all of the data necessary for both the core depletion and transient calculations, including the cross-term cross-sections. It is necessary to tabulate the cross-term cross-sections at enough burn-up points to accurately capture the spectral shift in the cross-section due to the production and depletion of the different nuclides (see Figure 14).

Figure 14. Burn-up dependent cross-section representation with cross-term cross-sections at different intervals

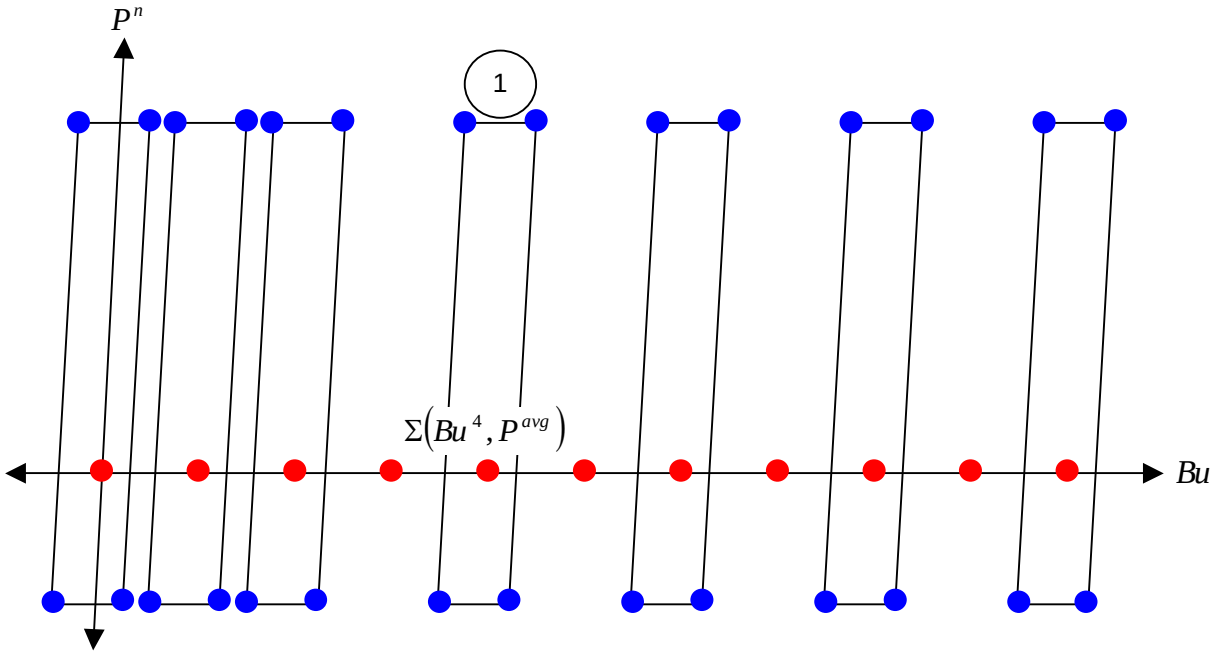

Appropriate methods for the interpolation of the cross-term cross-sections at intermediate burn-up points need to be developed. In our experience the current methods of interpolation are not adequate for many different reasons. Simple multi-dimensional interpolation schemes are fast but are not accurate enough to produce the results desired for non-linear data sets. Other higher-order interpolation schemes interpolate the data well but are too slow to be used efficiently. It is desirable to develop an innovative scheme based on a multi-level approximation of data, which is both accurate and efficient.

The cross-section data can be represented by a sum of functions changing on different scales. As such, a smooth data represents a quantity that changes globally throughout the domain of interest. On the contrary, rough oscillations in the data can be captured through a local procedure, because they are essentially local. This is, in fact, a basis for multi-level data approximation. It is thus possible to have a very coarse approximation in the libraries, which still well represents the smooth part of the data.

Further, if the difference between the coarse approximation and the true values of interest is determined, it should be oscillatory, and hence the coarse approximation can be recalculated and corrected locally, only using the samples near the point of interest.

In order to state the problem in more mathematical framework, the data approximation can be viewed as the fitting of a surface using uniform or non-uniform data samples. The goal to be achieved in solving this problem is to effectively and accurately represent the data by a function $f: \mathbb{R}d \rightarrow \mathbb{R}$. The spatial dimension d refers to the number of parameters on which the data depends. The graph of this function will be the surface needed, but a more important fact is that the function values at points, which are not sampled, will also be accessible. The latter property, namely the ability to interpolate the data, is very important in the approximations of the cross-sections used in the depletion computations. As has already been mentioned, such approximations have to be re-computed as accurately as possible for each time step in transient simulations. This increases the computational complexity and is not, in practice, acceptable. It is thus important to develop new interpolation techniques based on state-of-the-art mathematical techniques such as multi-level methods.

Many mathematical results have been established for the case of one parameter data sampling (*i.e.* $d = 1$). Stable approximations of uniform and non-uniform data in this case are usually based on B-splines or other piece-wise smooth curves. However, the extension to further dimensions is not straightforward. Different techniques have been proposed and tested in many branches of science and engineering. Some of the relevant algorithms can be found in applications arising from geosciences, image processing and quantum chemistry.

The main issue to be resolved in multivariate interpolation is in relation to the vast amount of computational time needed to construct the function f when the number of data samples is large. An easy – though impractical – solution would be to impose restrictions on the number of parameters and/or the allowed data distributions. Another approach would be to focus on the development and testing of an optimal multi-level algorithm for data representation. In two dimensions, such algorithms have been studied in image restoration, for example, but they can not be directly implemented for our problem, where the data usually depend on more than two parameters. As mentioned briefly above, the main idea behind a multi-level approximation method is to view the interpolating function f as a composition (sum) of functions on different scales.

The parts of the domain where the data is not smooth (*i.e.* changes rapidly over a short distance) will correspond to a fine scale, which means that an accurate approximation will require all sample points lying in this part of the domain to be used to construct an approximation. In the parts of the interpolation domain where the data is smooth and does not change much a coarse approximation will suffice to achieve the desired accuracy. The error (accuracy) between the interpolating function f and the given data is usually measured by some discrete norm. The problem, then, is reduced to seeking f, which will minimise the norm of the error (*i.e.* minimise a convex quadratic functional).

The relevant multi-level method to be used is thus the multi-grid method, of which a more detailed explanation follows. Let (X,Y) represent data containing n samples, $(X \in \mathbb{R}d \times n)$, $Y \in \mathbb{R}n$. We would like to minimise the error $E(f - Y)$, where f is a piece-wise polynomial function. We first construct $f0$ using a small subset $(x0,y0)$ of the data, minimising $E(f0 - y0)$. Having $f0$ in hand, we add more points to our initial set and obtain a new set $(x1,y1)$. Using *only the points we have added* to $(x0,y0)$, we construct $f1$ minimising $E(f1 + f0 - y1)$. Applied recursively this idea represents a multi-grid method.

Such a procedure can be quite effective from a computational point of view, if we add points *only* in the part of the domains where the data rapidly changes and oscillates. Oftentimes such a technique is called “local grid refinement” [44] and is commonly used in areas such as electricity, semiconductor

device modelling and other engineering fields. Local grid refinement provides the opportunity to use refined interpolation in the regions where more accuracy is needed in a non-conforming way. Evidently this non-conformity will complicate the error minimisation procedure, but there such difficulty can be overcome by tuning up the multi-level minimisation algorithm by using more levels in the refined domains [45].

A complete and practical implementation of the multi-level method would also require an optimal parallel implementation of the designed algorithms. Although the multi-grid method is among the most powerful strategies for the solution of minimisation problems, it is a product iterative method and unless special care is taken in its design, it will be sequential in nature. The technique used to parallelise this method is based on a suitable decomposition of the data samples in overlapping subsets, such that the load balancing is taken into account, each processor then separately minimising the interpolation error in each subdomain (using the block SOR or multi-grid method). The mathematical results for the algorithms mentioned show that there needs to be a certain amount of overlap between the subdomains in order to obtain an optimal error reduction [46-48].

Decreasing cost and increasing performance, especially through the development of parallel systems, have created conditions for exploring the feasibility of on-line cross-section generation and hence developing a transient methodology of improved accuracy. The integration of a cell/fuel assembly cross-section calculation methodology into the coupled transient code would be one way to achieve higher calculation accuracy for reactor transients. Alternatively, coupling two existing codes via a suitable interface in a parallel computing environment could prove to be more efficient. Research is needed to explore the feasibility of developing such a coupled cell/fuel assembly and transient code for core transient calculations. The application of parallel computing for such a new code system would also offer the advantage of short turn-around times in later production use. Thereby the feasibility of a new, markedly enhanced quality of coupled neutron physics and thermal-hydraulics safety analyses will be explored. This approach relates to long-term research goals, which (it is hoped) will serve to overcome present inaccuracies by providing more adequate time-dependent neutron physics cross-sections for 3-D reactor simulation.

The growing interest in LWRs with improved safety and economics characteristics is producing advanced fuel and reactor system designs of significant heterogeneity. These designs require innovative simulation methodologies that are capable of flexible and accurate 3-D modelling. The motivation behind the development of 3-D multi-group cross-sections for fuel lattice evaluations is to improve the accuracy of calculations in the core regions with a high degree of axial heterogeneity. Axial variations are caused by burn-up (exposure and spectral history), and these variations become more pronounced due to longer cycles and higher burn-up. The new fuel designs with axial variations of burnable poisons and partially inserted control rods during the reactor operation also introduce axial heterogeneity. Further, core transient simulations usually involve strong axial gradients of the feedback parameters, movement of control rods, etc.

With the continuing advancement of computer technology, it has become feasible to develop next-generation computer simulation programs to analyse next-generation nuclear power plants and their unique designs. It is now possible to develop coupled-core neutronics calculations with lattice physics calculations through parallel algorithms. With this capability accurate cross-sections can be calculated for each neutronic node under exact thermal-hydraulic feedback conditions and with exact boundary conditions and spectra. This method would significantly reduce uncertainty in cross-section predictions and therefore the overall core calculation uncertainty.

2.9 Physical phenomena involved and modelling capabilities

A variety of transients can be simulated by coupled 3-D neutron kinetics/thermal-hydraulic analyses. Transients involving widely different thermal-hydraulic scenarios are also recommended for analyses by coupled techniques (Sections 1.2 to 1.4). As a consequence a wide variety of physical phenomena are expected to occur and are relevant for the accuracy of the prediction, even making reference to the core region alone.

Thermal-hydraulic phenomena applicable to all expected DBA transient conditions have been classified by the CSNI [9,10], and it is not the purpose of the present report to summarise the content in the referenced documents. However, relevant phenomena in the area of thermal-hydraulics and neutron kinetics that can be the source of non-quantified uncertainties for the results of coupled calculations are mentioned.

2.9.1 Relevant thermal-hydraulic models

2.9.1.1 Critical models within the range of validation for existing codes

The following sections indicates some areas in the preparation of the T-H system models that can be of importance in relation to the T-H/neutronic analysis as derived from the WP1 of the present activity [2]. The list is by no mean intended to be exhaustive and will not repeat what can be found in the code manuals, but provides items that call for attention in certain situations and can be a contributing source to non-quantified uncertainties. The discussion has been divided in relation to T-H phenomena and process models that could have a specific influence on the kinetics responses, and to considerations at the NPP model set-up. In the latter case references are made related to PWR, BWR and VVER modelling aspects.

- *Dynamic subcooled boiling*. During the course of reactivity insertion and the associated fuel rod local power increase, the temperature difference between the rod surface and the adjacent boundary layer liquid will increase, eventually resulting in positive net void formation on the rod surface. The amount of void is determined by several factors, *e.g*. rod surface characteristics, temperature and flow velocity gradients across the boundary layer at the rod surface. As the two-fluid T-H system codes only have one liquid and one vapour temperature, the temperature gradient effects are not directly taken into account and instead these effects have to be included using specific models and correlations. For rapid transients the dynamics of these models can be questionable, resulting in unrealistic local reactivity responses.

- *Dynamic CHF*. The occurrence of CHF will result in a decrease of the fuel rod surface heat transfer coefficient with an associated increase in rod temperature, which in turn will influence the reactivity feedback through the Doppler effect. The CHF models are empirical in nature, and have been developed with data from static CHF tests (as the test procedures usually include a slow increase of rod power and/or of coolant flow characteristics a more accurate term might be “quasi-static” CHF tests) in tube or rod bundle geometries. The CHF models’ dynamic behaviour during power excursions as a result of core reactivity insertion requires more validation, though transient CHF data from well-defined SET are very few if any. The indirect validation against IET data provides some insight, but as the T-H conditions for the simulated core in those tests are not systematically varied an in-depth interpretation of the CHF conditions is difficult.

- *Volume void weighting on HT surface for two-fluid models*. In the two-fluid two-phase T-H system codes some method to partition the total rod surface heat flux between the two phases is necessary. Usually this is based on the void fraction in the attached T-H node and the partition of the heat transfer surface is directly void fraction weighted. The partition is executed in a similar way on all boiling heat transfer surfaces in connection with the node and includes no allowances for the void distribution within the node. Thus the HTC variation between the surfaces due to "near surface conditions" has been neglected, as has the associated discarding of corresponding variation of the fuel rod temperatures. Recent computational tools may follow the near-wall voiding approach when partitioning the wall heat between the phases. Even in such cases, some arbitrariness is necessary that cannot be fully resolved with the current availability of experimental data.

- *Spacers with mixing vanes*. This type of spacer is usually located in the upper part of the fuel assemblies to promote turbulence and mixing and also to increase the margins against CHF. Due to design characteristics these spacers will also increase the detachment of the vapour bubble layer on the rod surface into the bulk of the fluid flow, which in case of subcooled conditions will enhance the void condensation. Thus there will be a change in the void fraction and, as a result, in the reactivity and fuel rod power. The spacers are simulated in the T-H system codes through their pressure loss coefficients and area contractions, but no allowances are included to simulate the increased mixing effects on void distribution although some provisions do exist to include the mixing effects on CHF. Thus there are currently no means in the codes to simulate influences on reactivity from these types of devices.

- *Valve characteristics*. Valve characteristics, *i.e*. valve area changes such as function of time with associated pressure losses, must be provided as part of the valve component input. The exact characteristics of real valves are difficult to attain and thus the effects often have to be evaluated from sensitivity analyses. In relation to reactivity changes important influences from the valve operations can be the BWR core pressure variations at closure of the turbine stop valve and, especially, the associated pressure wave propagation through the steam line and into the RPV. The pressure wave will become more pronounced if the valve area change is incorporating a high valve area time derivative, *i.e*. from a pressure wave influence point of view the often-used linear area change will provide non-conservative results.

- *Frictional and discrete pressure losses*. Accurate pressure loss distribution in the T-H system is one essential prerequisite for the calculation of an accurate flow distribution, which in turn is necessary to obtain an adequate reactivity response. The frictional pressure losses are usually included by assigning the appropriate roughness to various surfaces in contact with the fluid. When it comes to the core, it is envisioned that the roughness is influenced by the time period during which the fuel assembly has been loaded into the core, *i.e*. by the burn-up, with an increased roughness with time due to the growth of the oxide layer. It is also realised that the detachment of a possible rod surface vapour layer, caused by spacers with mixing vanes as indicated above, can influence the resulting downstream frictional pressure loss. The T-H system codes rarely simulate this type of phenomenon.

  Usually the discrete loss coefficients are assigned a constant value, but for the fuel assembly spacers there are indications that a weak Reynolds number dependence is more adequate, as the loss coefficients decrease as the Reynolds number increases.

- *Phase separation at tees*. The phase separation phenomena at tee components can have a dominant influence on the course of the system depressurisation rate. So will, for a BWR steam line break, a perfect separation result in maximum depressurisation while the loss of

inventory is minimised. Reaching low pressure while maintaining a high liquid inventory may be non-conservative (*e.g.* by retaining the fuel temperature well below any critical levels). Activities are underway by the US NRC to review existing models and to evaluate and possibly improve their capabilities under an extended range of conditions.

2.9.1.2 Models outside the range of validation for existing codes

The list of thermal-hydraulic phenomena or system conditions that may require further investigation to validate the results of coupled neutron kinetics/thermal-hydraulic calculations, *i.e.* models outside the range of validation for current codes or a lack of standardised procedures in code application, includes the following:

- *High transient thermal flux*. As consequence of CR ejection, high local thermal flux occurs. Subcooled voids can be formed in a bulk of high-speed liquid. Void formation creates volume increase in an initially nearly incompressible fluid environment like the RPV of a PWR. Local thermal power exchange may reach values one order of magnitude larger than in nominal conditions and pressure may locally increase up to several MPa. DNB is expected. Validation of convection heat transfer correlations is questionable under these conditions.

- *Positive pressure pulse propagation in a BWR core causes void collapse and consequent positive reactivity excursion*. This creates the condition for sudden re-evaporation of the condensed liquid. Under these conditions the range of validity of convection heat transfer correlations is again questionable. Thus a careful consideration of the Courant limit, based on acoustic wave propagation, and of the calculation node length must be adopted [2]. The donor cell differential scheme has a strong tendency to attenuate pressure waves when using node lengths as usually applied in bulk flow transient scenarios; a careful evaluation of nodalisation and the use of time step sizes can possibly ameliorate the situation. The pressure wave propagation into the steam dome of the BWR through the dome outlet nozzle should be mentioned. This transmission, which is also accompanied by a reflection wave back into the steam line, is rarely simulated, and the resulting dome pressure response must be regarded as very uncertain [2].

- *Different stream flows occur in a typical LWR core*. Stream flow in contact with active fuel rods, stream flow passing through the CRGT, stream flow passing in the external part of the core in contact with the reflector assemblies (when present) or with the core barrel, stream flow passing through the instrumentation tubes, stream flow passing across the fuel box (BWR and VVER-440). Care must be taken in modelling the interaction among these streams and between the external core stream and the RPV DC region.

- *The CR movement creates local fluid displacements*. Such movement may be locally significant.

2.9.1.3 Critical aspects for nodalisations

When undertaking coupled T-H-neutronic analysis a limited model comprising only the NPP core with appropriate boundary conditions can be adequate in specific cases, but there is usually a need to include the actual influence from the reactor coolant loop system and even balance-of-plant components and control systems such as feed water pre-heater strings, level and pressure control systems and CVCS in PWR. Thus the complete model could be very complex, requiring a vast amount of plant

specific data not only of geometrical type but also, *e.g.* time dependent characteristics of various auxiliary systems. It is realised that some data are rarely available, an example being time constants of PWR hot and cold leg temperature gauges located in protective pockets in some NPPs, shielding them off from the direct coolant flow. Other data are proprietary, like the detailed performance of the steam separators for an extended range of operating conditions. To help reveal associated influences on system and reactivity responses in such cases, comprehensive sensitivity analyses must often be performed with reasonable variations of identified and thoroughly selected parameter ranges. In the following some areas are indicated which can call for specific attention during the preparation of T-H system code input and nodalisation.

Steam separator characteristics

In BWR the steam separator characteristics have a direct influence on the conditions in the downcomer through the amount of carry-under. Along with the feed water inflow into the downcomer and the mixing processes this will be a factor influencing the core inlet subcooling and thus the core reactivity. The amount of carry-under depends on the liquid level in the RPV (*i.e*. downcomer level), the core coolant mass flow rate and the core power. A low level results in higher carry-under and vice versa, although for modern steam separator designs the variation of carry-under for reasonable changes in liquid level is moderate. Also, the carry-under increases at lower coolant mass flow rate but decreases for decreasing core power. In some system codes, (*e.g.* RELAP5) the separator effects can be simulated using a basic model, with prescribed void fraction limits for determining ideal separation functionality, or by using a more mechanistic model simulating GE multi-staged centrifugal separator components. It is realised that the characteristics for an extended range of operating conditions can be difficult to acquire due to the proprietary nature of needed data. Usually inferred characteristics only for a single or very few operation points can be obtained, which naturally hampers a comprehensive modelling of the component. Additionally, the behaviour at pressure wave propagation passing through the separator model into the core is not very clear and caution is greatly advised when using this component to simulate this type of phenomenon.

FW distribution in BWR upper DC section

In BWR careful modelling of the feed water inlet sections that distribute the feed water into the downcomer and of the downcomer itself can be essential in order to adequately simulate effects from possible non-uniform feed water distributions. The feed water lines are connected to separate spargers and in some designs groups of the lines are fed by water pre-heated by separate feed water pre-heater strings. Dependent on the operating conditions for each pre-heater string, situations can be envisioned where different pre-heating can prevail thus resulting in different feed water temperature in the spargers or groups of spargers. Also the auxiliary feed water system, used for instance at start up and shutdown sequences, is only connected to some of the spargers, thus resulting in possible non-uniform conditions around the downcomer upper section when that very system is in operation. The associated non-uniform temperature distribution can, dependent on the downcomer flow conditions, remain at the core inlet and thus create local or regional reactivity heterogeneities. Therefore the utilisation of the T-H system codes' 3-D capability is necessary to at least to some extent be able to simulate at least to some extent the fluid flow temperature field development.

Cold leg flow distribution in PWR RPV upper DC section

In PWR the modelling of the cold leg inlet sections and the downcomer itself can be essential in order to adequately simulate effects from possible heterogeneities between the coolant flow from the different RCS cold legs. Dependent on the operating conditions in each steam generator and in auxiliary systems (CVCS), situations can be envisioned in which different cold leg temperatures and different cold leg boron concentration can prevail. The associated non-uniformities in temperature and boron concentration distributions can, depending on the downcomer flow conditions, also remain at the core inlet, thus creating local or regional reactivity heterogeneities. The utilisation of the T-H system codes' 3-D capability is therefore necessary (at least to some extent) to be able to simulate the fluid flow temperature and boron concentration field development. The use of UPTF experiments may reveal fundamental for improving the qualification of results when addressing this phenomenon.

Control systems (delays, etc.)

The control system can have profound influence on the T-H system responses and associated core reactivity behaviour. In some cases the control system can amplify disturbances originated elsewhere, for instance reactivity disturbances in BWR resulting in dome pressure increase, which in turn (through the pressure control system) influences the turbine valves with associated feedback on the dome pressure, although with some delay. In some plants (at least the Swedish BWRs) there is also a control system that monitors a pressure increase event in advance by allowing the turbine valves to be directly influenced by the measured core reactivity changes (APRM) and thus adjusting the valve before the resulting dome pressure change has occurred. Situations can be envisioned where an unfavourable combination of initial reactivity disturbance and control system characteristics can create – and also amplify – a resulting reactivity dynamic response.

It is necessary to model all relevant aspects of the control systems, not only the systems themselves but also influences from measurement gauges (*e.g.* the several-second delay in the measurement of PWR HL and CL temperatures as mentioned above, and similar delays of the FW temperature measurements in BWR), from possible sense lines and from the effects of using modern digital control systems, which can introduce delays due to different parts of the system using different operational frequencies. It can also be advantageous to model the dynamics of the actual level measurement systems in more detail, for instance including models of the differential pressure between the DC liquid column and the reference water column.

In some periods during a transient there could also be dynamic pressure contributions to flow velocity measurements due, for example, to non-symmetrical locations of pressure taps. When the same quantities are being measured, the signals from those types of equipments are usually calibrated to provide the same signals at a specific operating condition, *e.g.* at normal operation. Under deviating operating conditions the signals will consequently be different, thus resulting in erroneous indications of the flow velocities.

Core flow field 3-D effects including effects from BWR core inlet orifices

If heterogeneities of the RPV downcomer flow field are expected to prevail during some time windows of a transient scenario, the model used must be able to adequately handle those variations when the flow enters the lower plenum and is propagating upwards, into and through the core. It is necessary to set up a 3-D nodalisation of the lower plenum and the core so proper advantage is taken of the T-H system codes, 3-D flow simulation capabilities. The comparably more open space in the

lower plenum of PWRs lends itself to a fairly efficient mixing effects that smooth out gradients of the downcomer flow in contrast with the rather confined lower plenum space of BWRs, in which a large number of control rod guide tubes are present, thus decreasing the effective flow communication in the transverse direction. Regardless of the layout of the lower plenum, a nodalisation must be used which adequately preserves flow field heterogeneities from the downcomer throughout the progression of the lower plenum. The nodalisation in the transverse direction is expected to be more critical and must be made "more dense" in the BWR case compared to the PWR.

Important data when specifying the 3-D nodalisation include pure geometrical information as well as frictional and pressure loss data. Such data are rather readily found for the major flow direction (assumed to be the vertical direction) but require further elaboration with regard to the transverse directions. An example is the definition of the node flow area in the direction perpendicular to the control rod drives in the lower plenum of a BWR; this is not an easily determined characterisation, and usually a combination of some average node flow area and carefully selected junction flow areas has to be used. The friction influence in these directions can mostly be omitted and instead the discrete pressure drop coefficients related to the selected junction flow areas have to be specified (possibly also including Reynold number dependence) so that the momentum transport can be predicted as accurately as possible. The tendency of the 3-D numerics to strongly diffuse any gradients must also be taken into account, with the result that calculated gradients (after passing through the lower plenum) are less severe at the core inlet level. This can be non-conservative in relation to core reactivity responses and is of special importance when the intention is to simulate local reactivity events and out-of-phase BWR instability transients.

In PWRs the open core design provides for alleviating the effects of flow field heterogeneities at the core inlet and also of core local reactivity insertions along the core height. Consequently any core model intended to simulate the 3-D effects must be appropriately nodalised and the usually non-conservative influence from numerical diffusion also has to be evaluated. The core bypass flow (*i.e.* the amount of core coolant flow not directly involved in the heat transfer from the fuel rods) can in principle be related to the area around the core periphery close to the core baffle, but in some core designs the flow between the core baffle and the core barrel will be added – and therefore included – in the bypass flow. The bypass flow is usually included in the T-H system core model through properly defined parallel channels to the core main flow paths.

In BWRs each fuel assembly is operated, in principle, as an isolated channel between common headers and a balance of the flow rate will be reached through each assembly to achieve the common overall pressure drop. This overall pressure drop includes elevation, friction, acceleration and local pressure drops (from spacers, inlet orifices and outlet sections) with allowances for the two-phase characteristics in each assembly. In order to compensate for the radial power distribution of the core fuel assemblies different inlet orifices are used for assemblies located in different core regions. Two or three regions with different inlet orifice loss coefficients are usually used, with higher loss coefficients towards the core periphery. Thus the flow rate through the assemblies will differ somewhat, as will individual two-phase conditions and consequently the stability margins as well. In order to simulate the effects from these fuel assembly differences in a consistent and adequate way it is crucial to apply a well-founded strategy when defining the nodalisation and the coupling to the kinetics code. As the BWR core consists of 700-800 (and sometimes more) fuel assemblies, some sort of lumping of the T-H channels is necessary to develop a tractable, feasible model. This lumping process is even more demanding when preparing a model to be used for stability analysis, and especially for analysis of out-of-phase core power oscillations.

The core bypass flow in BWRs includes the flow paths outside the fuel assembly shrouds for which the associated flow is normally subcooled, although the conditions can approach saturation at

certain transient scenarios (*e.g.* depressurisation transients). Part of the same space between the fuel assemblies also contains the cruciform control rod blades (one control rod for each "supercell" consisting of four fuel assemblies) and a movement of the control rods in the core will reduce the available space to be occupied by the bypass flow, resulting in a somewhat reduced bypass flow. However, this effect is usually very small and is normally ignored in the T-H system BWR simulations. Standard practice is to simulate the core bypass by introducing simple core parallel flow paths that can be interconnected. It has been found that appropriate modelling of the bypass flow region can be important although no boiling occurs, and that the direct gamma heating to the bypass coolant (usually about 1.7%) has to be taken into account as well as the heat transfer from the interior of the fuel assemblies through the shrouds. The associated gradual density change of the bypass flow will have some influence on the reactivity and its spatial distribution.

BWR modern assembly with internal "water-crosses"

New designs of BWR fuel assemblies have developed advantageous features in relation to internal power factors and total power levels. This has been achieved basically by dividing the fuel assembly into four subassemblies separated by a double-wall structure forming an internal flow channel with a cruciform-shaped flow area. In some designs the fuel rods have also been made somewhat thinner and the number of fuel rods has been increased from 96 up to 100. This design results in a flatter internal power profile due to more favourable moderation effects from the internal water cross and an associated more uniform moderator distribution. Other characteristics include improved thermal margins (DO margins) and reduced fuel assembly pressure drop accomplished through the introduction of part-length rods and a modified design of the upper tie plate. Due to the thinner fuel rods a shorter time constant at power changes will result, as will different core responses at reactivity changes as compared to the old fuel assembly design. This faster response can have a destabilising effect under certain operating conditions (close to the upper left knee in the power-flow rate diagram) and can necessitate some modifications to the reactor control system (control and trip lines in the diagram). Modified reactivity characteristics (reactivity coefficients) also result from the design changes. At control rod movements it can be envisioned that the two-phase flow distribution amongst the four subassemblies can be changed comparably more than in the earlier assembly design with an "open" subchannel layout.

A limited amount of experience seems to be available on how to adequately model this type of fuel assembly in the T-H system codes with allowances for the four subassemblies and internal flow bypass through the water cross channel. It is obvious that validation against appropriate experimental data is needed in this respect, but it is also realised that those data are currently mostly proprietary to the fuel vendors. Accordingly, only tentative models can be prepared with the associated high uncertainty in transient behaviour.

2.9.2 Heat transfer modelling inside pin and fuel modelling

The heat transfer phenomena inside the fuel pins are comprised of heat conduction in the fuel pellets, heat transfer across the gap between fuel pellets and cladding inside surface, and heat conduction across the cladding thickness. The combination of these effects, along with the geometrical fuel pin design, will influence the fuel pin overall time constant at power variations, though the heat transfer across the gap (gap conductance) will have the greatest influence [2]. All the effects are dependent on the fuel pin burn-up and will consequently also have a variation in the axial direction. It is noted that with normal heat structure modelling practice these axial variations can not be taken into account. One possibility could be to axially use a stack of different heat structure geometry combinations, though this would impair the use of the moving mesh capability in case the reflood simulations are needed.

The list of pin heat conduction and fuel-related phenomena or related computational aspects that may require further investigation to validate the results of coupled neutron kinetics/thermal-hydraulic calculations includes the following:

1) Minimum number of concentric rings for the fuel rod that bring to the convergence of results for CSC, NKC and THSC (this number must be consistent in the three steps of the analysis). The suitable number of rings for the gap should be identified as well.

2) Pellet gap performance during the transient with main reference to variations in physical properties and geometry. The evaluation of such aspects is not within the typical current NKC and THSC capabilities.

3) Fuel deformation and change in physical properties during the transient (namely steep power rise). Coupling between THSC and fuel codes might be necessary.

2.9.3 Neutron transport and diffusion

The state of the art of currently used multi-dimensional neutron kinetics models for LWR calculations of core time-dependent spatial neutron flux distribution includes the utilisation of 3-D neutron diffusion equations based on two neutron energy groups and with six groups of delayed neutron precursors. This has found to be adequate for steady-state applications and for those transient applications where direct validation has been possible [87]. ADF has also proven to be sufficient for several applications. It is realised, however, that the utilisation of MOX fuels (with its higher contents of Pu) requires additional neutron energy groups to be included for accurate simulations [88]. The Pu isotopes have high absorption and fission resonance at around 1 eV (^{240}Pu absorption) and from 100 eV up to keV (^{239}Pu, ^{241}Pu absorption and fission).

Major calculation features of the neutron diffusion models include the ability to perform eigenvalue (k_{eff}), transient flux, xenon transient, decay heat, depleting (burn-up) and adjoint calculations. Pin power reconstruction capabilities are also available to obtain pin power and associated intranodal neutron flux distributions from the calculated nodal fluxes. The 3-D capability provides the basis for realistic representation of the complete reactor core, though provisions are included to use appropriate symmetry sections (such as half and quarter core parts) for computational efficiency. Carefully selected boundary conditions for the symmetry planes are paramount for adequate calculation results in those cases. One-dimensional capabilities are also usually available for simulation of transients with predominant axial neutron flux variations.

Important data for the neutron diffusion calculations – apart from pure geometrical descriptions of various core components – include tabulated macroscopic cross-sections as a function of T-H and fuel parameters, boron concentration, control rod positions (worth, used banks, etc.) and microscopic cross-sections for Xe and Sm, including corresponding dependencies. Other data are decay constants and the ADF for the four-sided fuel assemblies.

The list of neutron kinetics phenomena or related computational aspects that may require further investigation to validate the results of coupled neutron kinetics/thermal-hydraulic calculations includes:

- Identification of a suitable number of neutron energy groups.

- Influence of resonance absorption cross-section in individual layers of pellets (partly linked to the previous item).

- Systematic identification of the influence of material discontinuities (*e.g.* due to the presence of fuel box, CR, at the border between reflector and core active region, etc.).

2.10 Numerical methods (time and spatial discretisations)

Numerical methods are continuously improved and adapted to the latest capabilities of computers. Methods used in thermal-hydraulic and neutron kinetics applications are discussed in the following sections.

2.10.1 Methods used in thermal-hydraulic system codes

The two numerical methods for the hydrodynamic model use finite difference schemes having fixed, though staggered, spatial noding. The scalar properties (pressure, energies and void fraction) of the flow are defined at cell centres, and vector quantities (velocities) are defined on the cell boundaries. The term "cell" is used to mean increment in the spatial variable, *x*, corresponding to the mass and energy control volume.

- *Semi-implicit scheme*. The semi-implicit numerical solution scheme is based on replacing the system of differential equations with a system of finite-difference equations partially implicit in time. In numerical approximations several guidelines were used, the first of these being that mass and energy inventories are very important quantities in water reactor safety analysis. The numerical scheme should be consistent and conservative in these quantities. Second, to achieve fast execution speed, implicit evaluation is used only for those terms responsible for the sonic wave propagation time step limit and those phenomena known to have small time constants. Thus, implicit evaluation is used for the velocity in the mass and energy transport terms, the pressure gradient in the momentum equations, and the interface mass and momentum exchange terms. Next, to further increase computing speed, time-level evaluations are selected so the resulting implicit terms are linear in the new time variables. Where it is necessary to retain non-linearities, Taylor series expansions concerning old time values are used to obtain a formulation linear in the new time variables. (Higher-order terms are neglected.) Linearity results in high computing speed by eliminating the need to iteratively solve systems of linear equations.

- *Nearly-implicit scheme*. For the problems where the flow is expected to change very slowly with time, it is possible to obtain adequate information from an approximate solution based on very large time steps. The nearly-implicit scheme was developed for this purpose. It consists of two steps. The first step solves all seven conservation equations, treating all interface exchange processes, the pressure propagation process and the momentum convection process implicitly. These finite difference equations are exactly the expanded ones solved in the semi-implicit scheme with one major change. The convective terms in the momentum equations are evaluated implicitly (in a linearised form) instead of in an explicit donored fashion as is done in the semi-implicit scheme. The second step is used to stabilise the convective terms in the mass and energy balance equations. This step uses the final new time level velocities from the first step along with the interface exchange terms resulting from the provisional variables of the first step.

2.10.2 Neutronic diffusion equation and nodal methods

Under quite general assumptions the neutron flux distribution inside a nuclear reactor core is obtained by solving the neutron diffusion equation in the approximation of energy groups. To solve this equation numerically, the reactor core is discretised in nodes or cells where the nuclear properties are supposed to be constant. These nodes are associated with the fuel bundles or homogeneous groupings

of fuel bundles. Different kinds of methods, including finite difference methods, synthesis methods, finite elements methods and nodal methods have been used to numerically solve the neutron diffusion equation. Various types of nodal methods to solve the neutron diffusion equation exist, and many authors relate with each one of them. In this brief description it is impossible to discuss all the methods, but those presented here are some of the most popular. A possible classification of nodal methods is as follows:

- Transverse integrated nodal methods.
- Flux expansion methods.
- Other methods.

2.10.2.1 Transverse integrated nodal methods

The Transverse Integrated Nodal (TIN) methods include methods like the Analytical Coarse Mesh Finite Difference Methods (ACMFD) [117-118], the Nodal Expansion Methods (NEM) [119] and the Analytical Nodal Method (ANM) [120]. The latter two in particular have become the basis of popular production codes for spatial neutronics analysis [121-125].

A brief description of general guidelines that follow the TIN methods is presented. The numerical solution to the multi-group neutron diffusion equation is based on the neutron balance relation for the spatial node *m* in terms of the node average group flux $\bar{\phi}_g^m$ and the surface average net currents $J_{gus}^m \ (s=l,r)$:

$$\sum_{n=x,y,z} \frac{1}{a_u^m}\left(J_{gur}^m - J_{gul}^m\right) + \Sigma_{tg}^m \bar{\phi}_g^m = \frac{\chi^g}{K_{eff}} \sum_{g'=1}^{G} \upsilon\Sigma_{gg'} \bar{\phi}_{g'}^m + \sum_{g'=1}^{G} \Sigma_{sgg'} \bar{\phi}_{g'}^m \qquad (g=1,2,\cdots,G;\ m=1,2,\cdots,M) \tag{1}$$

where $a_u^m(u=x,y,z)$ denotes the node width of rectangular node *m* in the direction *u*, and the other notations are standard [126]. The TIN methods relate the surface average net currents to the node average fluxes from the solution of the transverse integrated 1-D equation in matrix form:

$$D\frac{d^2}{du^2}\phi_u(u) = A\phi_u(u) + L_u(u) \qquad u=(x,y,z) \tag{2}$$

The matrices *A* and *D* are the standard notation. Generally, the transverse leakage source, L_u, is assumed to be a quadratic polynomial:

$$L_{gu}(u) = \sum_{i=0}^{2} L_{igu} h_i(u/a_u) \tag{3}$$

where $h_0(\tau)=1;\ h_1(\tau)=2\tau;\ h_2(\tau)=6\tau^2-1/2$.

Different nodal methods are obtained using different methodologies to solve Eq. (2). In the Nodal Expansion Method (NEM) the solution to Eq. (2) is approximated by an expression of known functions:

$$\bar{\phi}_{gu}(u) = \sum_{i=0}^{4} C_{igu}^{NEM} h_i\left(\frac{u}{a_u}\right) \tag{4}$$

where $h_3(\tau)=2\tau(\tau-1/2)(2+1/2)$, $h_4(\tau)=(5\tau^2-4)(\tau-1/2)(\tau+1/2)$ and the expansion coefficients $C_{igu}^{NEM}(i=0,1,2,3,4)$ are determined by the node average flux, boundary fluxes of the node and two weighted residual method equations.

With the Analytical Nodal Methods (ANM), the analytic solution to Eq. (2) is obtained in terms of trigonometric and hyperbolic functions. Although these methods are very accurate, the ANM is slightly better than the NEM in computational accuracy, but the ANM has the drawback of having numerical instabilities near a critical node.

To improve the method, Joo, Jiang and Downar [125] proposed approximate stabilisation schemes such as the linear fundamental mode approximation and the hybrid ANM/NEM interface coupling technique. Also, Lee and Kim [127,128] demonstrated that the ANM solution can be reformulated in exactly the same way as the NEM solution, integrating the most popular transverse integrated modal method formulations into a unified nodal method. Some drawbacks of the TIN methods include:

- The equations involved in these methods are not solved directly; they always require the resolution of non-linear iterations.
- It is very difficult to obtain the eigenmodes associated with the static neutron diffusion equation (lambda modes).
- The extension of the existing methods for two groups of energy to take into account more energy groups ($G > 2$) is not easy, because of the complexity of the equations.

2.10.2.2 Flux expansion methods

In this family of methods are included:

- The Analytical Function Expansion Nodal Method (AFENM) developed by Cho and Noh [128-131].
- The higher-order Polynomial Expansion Nodal (PEN) method [131,132].
- The Nodal Collocation Method (NCM) [133-135].
- The Cubbox and Quabox approach [136].

These methods differ from the TIN methods in that they make use of an approximate but direct solution to the multi-dimensional diffusion equations such as the intranodal flux for each computational node. They have more unknowns, and do not rely on transverse integration techniques. Although they are superior in performance compared to TIN methods in terms of computational accuracy, the main drawback of these methods is the computational cost associated with the solution of systems of linear equations with big and sparse matrices of coefficients.

An important feature of AFEN methods is that the intranodal flux distributions can be directly used. Also, the AFEN methods, unlike conventional nodal methods, do not suffer from the singularity problem resulting from the transverse integration in hexagonal geometry. Lee and Kim have developed a unified nodal formulation for the analytic function expansion nodal method applied to the two-energy-group neutron diffusion equation [127,128].

In spite of its successful applications to two-group neutron diffusion problems, this methods has a shortcoming. In the AFEN method, the intranodal flux is expanded in terms of analytic eigenfunctions of a Helmoltz equation. Consequently, in multi-group problems, complex eigenmodes must be used as basic functions. To overcome this problem an AFEN polynomial expansion nodal (PEN) hybrid method has developed [131]. A pure PEN method has also been developed, much faster than the AFN method and readily applicable to multi-group diffusion.

The Nodal Collocation Method is an elegant Legendre Polynomial Method but has the drawback of requiring mapping transformation to allow the extension to hexagonal geometry, spoiling the simplicity of the method in Cartesian geometry.

In the Quadratic Approximation (QUABOX) [136], the neutron flux, $\phi(x)$, is approximated within the node by the sum of one-dimensional Taylor polynomials. In the Cubic Approximation (CUBBOX) the authors use higher-order approximations, but the set of admissible functions requires additional conditions. In consequence, suitable variational principles are necessary. Some variational methods have been proposed using spline functions and Galerkin weighting.

A hybrid TIN method/Flux Expansion Method has recently been developed for hexagonal geometry [137]. The main advantage of the Flux Expansion Method is the accuracy of the solutions; and that they do not present numerical instabilities. It is also possible to obtain the eigenmodes as a solution of an algebraic eigenvalue problem. This kind of problem is efficiently solved using methods based on Krylov's subspaces [138], in turn implying the resolution of large systems of equations and a large computing time. As new computing capabilities become available, however, this disadvantage becomes less relevant.

Possible sources of errors in the nodal methods are the intranodal heterogeneities. To overcome this difficulty, a new methodology has been developed which accounts for the dependence of the nodal homogenised two-group cross-sections and nodal coupling factors with interface flux discontinuity factors that account for heterogeneities on the flux-spectrum and burn-up intranodal distribution, as well as the neighbour effects [118].

2.10.2.3 Other methods

As others methods, we include finite difference methods and nodal finite elements methods, see Hennart, *et al*. [139]. Finite difference methods are easy to implement, but to obtain a reasonable accuracy it is necessary to use a spatial mesh with small nodes, leading to huge problems that cannot be treated with current computational tools. Finite element methods are based on functional and a space of base functions [140]. They are complex methods and present some technical drawbacks when compared with nodal expansion methods. On the other hand, these methods are general and they can be used in problems with both rectangular and non-rectangular geometry.

2.11 Consideration of CFD and subchannel codes

Some thermal-hydraulic codes comprise 3-D fluid dynamics modules, mostly of porous media type. Due to coarse nodalisation, these modules require volume-averaged coefficients for turbulent exchange of mass, energy and momentum. Such coefficients are not well known. Generic CFD codes including basic turbulence models do not require these coefficients, but can not be integrated into coupled codes anytime in the near future because of huge computation resource requirements. Generic CFD should be used, however, to validate exchange coefficients in the porous media models.

Experimental and numerical investigations of cross-flow in rod bundles have been performed at FZR. Detailed measured velocity fields in a Plexiglas facility containing a rod bundle with plane inlet and asymmetric outlet have been compared with calculations in the porous body approach and with standard turbulence models in detailed geometry resolution. Published material can be provided, if of interest.

In some cases interface modules are integrated into the coupled codes, which provide unfolding of the parameters calculated by 1-D thermal-hydraulic codes to 2-D distributions as boundary conditions for the components to be modelled in 3-D, *e.g.* to unfold cold leg temperatures to a distribution at the core inlet considering mixing in the downcomer and lower plenum. In these interfaces, information is used from detailed mixing investigations.

At FZR a Semi-analytical Perturbation Reconstruction (SAPR) module has been developed providing time-dependent 2-D coolant temperature and boron concentration distributions at the core inlet derived from the parameters in the cold legs by superposition of response functions, obtained experimentally or by CFD calculations.

Coupling activities involving subchannel codes should also be considered within the present context. Some information can be inferred from Section 2.4.1.

2.12 Uncertainties connected with neutron kinetics calculations

In complement to the discussion about uncertainties expected or embedded into thermal-hydraulic system code calculations (Section 2.6.1), and about needed precision (Section 2.5), exemplificative uncertainties connected with the neutron kinetics calculations are outlined hereafter, as derived from Refs. [174-178].

Uncertainty in input neutron kinetics parameters

A number of input parameters are uncertain. Typical input uncertainties can be derived from Refs. [174] and [177] as indicated below:

- Rod worth ±10% [177], ±15% (individual banks) [174].
- Fraction of delayed neutrons (β) ±5% [177].
- Doppler coefficient ±20% [177].
- Moderator coefficient ±30% [174].
- Fuel heat capacity ±10% (this is also a relevant thermal parameter) [177].
- Boron reactivity coefficient ±15% [174].
- Change in the reactivity per unit change in the fuel and moderator temperature when fuel and moderator are at the same temperature $\pm 0.36 \times 10^{-4}$ $\Delta\rho/°C$ [174].
- Critical boron concentration at 100% core power ±50 ppm [174].
- Power distribution (at intermediate level and at 100% power) ±0.1 * relative power density for each measured assembly power [174].

Uncertainty in output neutron kinetics parameters

In a static calculation, the main output parameter is constituted by the k_∞. The variations Δk_∞ related to the value calculated by the ENDF/B-VI.8 library can be found in Figures 15 and 16, derived from Ref. [176]. The reported values can be interpreted as minimum acceptable values for the error in calculating k_∞. The contribution to the error from individual cross-section values can be deduced from Figure 17, taken from the same source.

Figure 15. The library-based differences in k_∞ as a function of the fuel-to-moderator ratio [176]. The error bars show 95% confidence intervals.

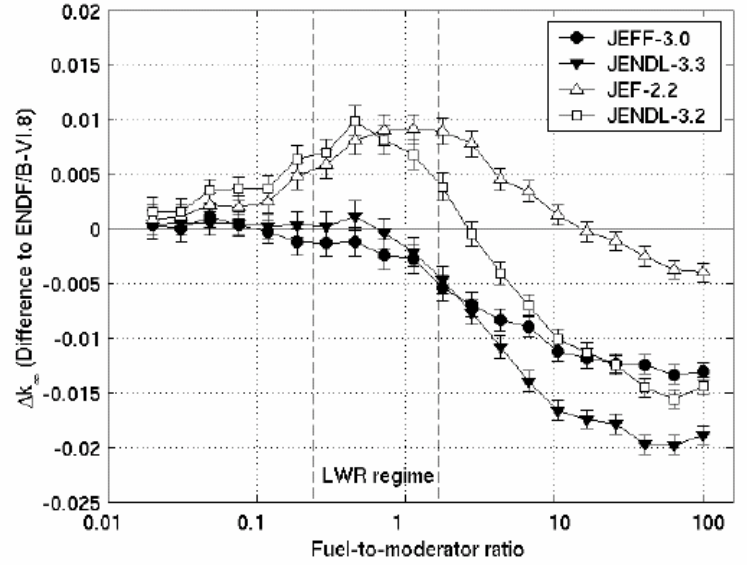

Figure 16. The library-based differences in k_∞ as a function of the fuel-to-moderator ratio, when only the cross-sections of ^{235}U are taken from the library under study [176]. The error bars show 95% confidence intervals.

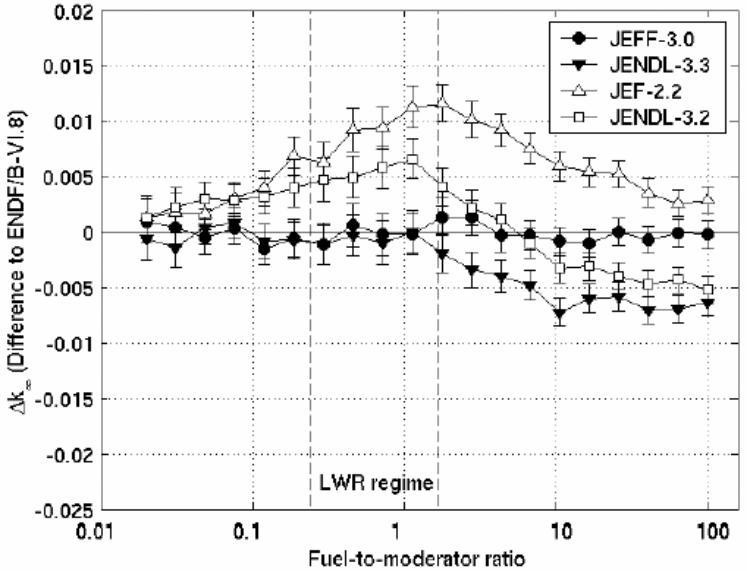

Figure 17. The contribution of individual groups of cross-sections to discrepancies in calculating k_∞ as a function of the fuel-to-moderator ratio [176]. Comparison between JEF-2.2 and ENDF/B-VI.8.The error bars show 95% confidence intervals.

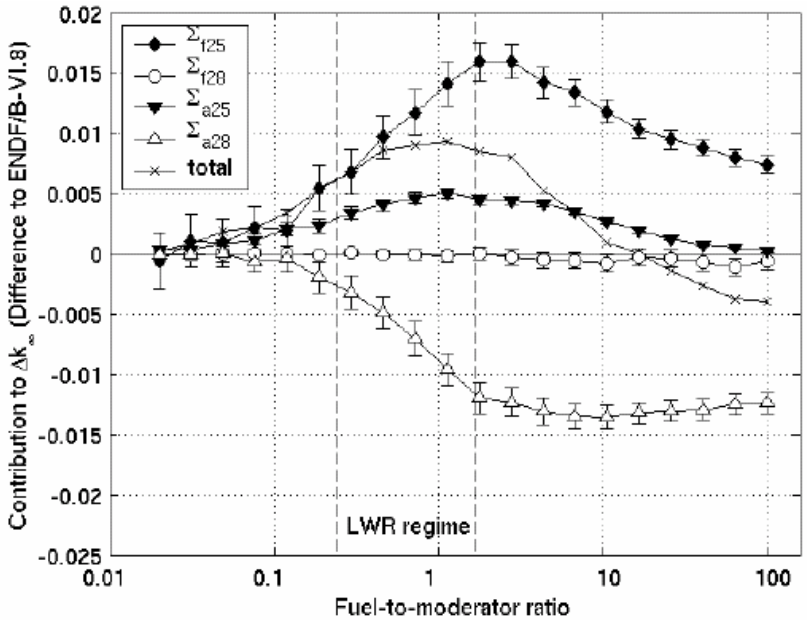

A further example of uncertainty in relevant neutron kinetics output parameters is taken from Ref. [205]. Two recently developed deterministic codes, DOORS and DANTSYS [184,185], that use multi-group discrete ordinate methods to perform the transport calculation, have been applied to the VENUS OECD/NEA/NSC benchmark [186].

The results are given in Table 4. In the same paper [205], discrepancies between the two codes (2-D calculations with buckling correction) have been analysed as a function of the spatial co-ordinates. It was found that major discrepancies appear outside the core where the meshes become coarser and the flux falls more than an order of magnitude.

Table 4. Influence of the buckling and of the solution method (2-D or 3-D) upon the calculated value of k_{eff} when two transport codes (DOORS and DANTSYS) are used [178]

Code	Buckling correction	k_{eff}
DOORS 2D(DORT)	Yes	0.962549
DANTSYS 2D(TWODANT)	Yes	0.99791
DOORS 2D(DORT)	No	1.04260
DANTSYS 2D(TWODANT)	No	1.04434
DOORS 3D(TORT)	Not needed	0.96961
DANTSYS 3D(THREEDANT)	Not needed	0.97012

Other uncertainties

Additional information concerning uncertainties in predicting k_∞ can be derived from Refs. [187] and [188], the latter as related to the validation of the SCALE-4 criticality safety software. Assembling all the information, the apparent uncertainty value in calculated k_∞ seems to be about 3-4%. This is an

uncertainty range that could be obtained when using available calculational capabilities in an approach consistent with normal, independent BE practice. However, it is realised that such an uncertainty range is far too large to be able to make any firm statement about the actual core state. Within the uncertainty range the core could be in any state from subcritical to superprompt critical, and consequently other means are needed to increase the precision in the calculations to make the result useful. A commonly applied approach used for core-following calculations and core-monitoring systems is to use some kind of adaptive strategy to modify or correct calculated values to match specific core measured data. When adequately adapted to a measured specific core state the prediction of associated "off-state" conditions will thus include a BE extrapolation from the adapted state and will provide much higher precision in calculated values. The errors in calculated k_∞ (or k_{eff}) using such an approach will usually be of the order of a few hundred pcm.

2.13 Recommendations

In summary, in the analysis of PWR transient simulations with non-symmetric feedback effects the use of 3-D T-H models is recommended. When developing a core boundary conditions model the Cartesian geometry option provides a better spatial resolution of the power distribution and feedback effects. Further, it is expected to develop a coupling procedure between the 3-D Cartesian geometry T-H vessel model and 3-D cylindrical T-H vessel model when performing more complex system transient simulation with 3-D kinetics.

Future efforts in BWR coupled code calculations should be directed towards developing rules for choosing an optimal number of T-H channels, which accounts for the nature of the transient phenomena, initial power distribution and assembly geometry. Such efforts should be combined with the development of a BWR model with a "free" mass flow boundary condition where, according to the number of channels, the code has the opportunity to redistribute the mass flows depending on the channel power.

Uncertainties in coupled-code input databases reflect in the uncertainties of output results. Uncertainties are also originated by the individual coupled-code models and equations as well as by the adopted numerical solution schemes and by the manner in which coupling is undertaken. The approach described in Section 2.6.1 inherently addresses all the sources of uncertainty. An effort has been made within the present context to quantify the needed precision (Section 2.5). It is recommended to accord proper emphasis both to needed precision and to expected uncertainty when applying or developing new methods in the area of coupled 3-D neutron kinetics/thermal-hydraulics.

Chapter 3

FUEL

3.1 Overview of reactors and fuel types (background)

As the active part of a nuclear reactor, fuel is readily distinguishable from the other components of a reactor. It is within fuel that the nuclei of certain elements of high atomic mass, such as ^{235}U or ^{239}Pu, undergo fission, which causes energy to be released. It is the consumable part of a reactor, and this has several consequences. From an economic point of view, it is important to decrease fuel consumption and therefore to renew the fuel as little as possible by allowing it to remain in a reactor for longer periods. During the life of any given reactor, the fuel characteristics can be improved for higher efficiency, as long as they remain compatible with the operating conditions imposed by the type of reactor in question [95].

The fission reactions generate in the fuel radioactive elements such as fission products and actinides. The concept of a "clean reactor", generally chosen by those concerned, requires the provision of a gas-tight barrier around the fuel to contain the dispersion of these elements; this barrier is called the cladding. Under normal operating conditions and in case of incident, the rate of leaks (sometimes called cladding ruptures) of this first barrier must remain extremely low. Under accidental operating conditions, fuel plays an essential role, being the source of most of the radioactive elements likely to be dispersed and conditioning their dispersion by its behaviour.

Fission reactions occurring in the fuel, the fuel assembly materials, the fuel itself, the cladding material and the structural materials suffer the most severe damage, caused particularly by the neutrons. How the materials making up the fuel assembly perform under irradiation is thus one of the essential factors of fuel assembly behaviour in a reactor, along with resistance to temperature and corrosion.

A nuclear reactor essentially includes a core based on fuel that generally contains the heavy fissile elements (except in fast neutron reactors), a moderator that slows down the neutrons and a liquid or gas coolant that removes the heat produced in the fuel. The fissile elements are essentially ^{235}U, ^{233}U, ^{239}Pu and other plutonium isotopes. Other natural elements, called fertile elements, are interesting in that they can, when bombarded with neutrons, produce fissile materials: thus ^{238}U gives ^{239}Pu, and ^{232}Th gives ^{233}U.

The above-mentioned fissile elements cannot all be found in nature. Natural uranium is mostly made up of ^{238}U, with only about 0.71% of ^{235}U, but isotopic enrichment techniques can increase its ^{235}U content. Natural thorium is the ^{232}Th isotope. Plutonium and ^{233}U can only be obtained through irradiation of fertile isotopes. The various fissile and fertile elements do not behave in the same way, depending on the neutron energy. In the energy band of thermal neutrons, the neutron balance is more favourable with plutonium than with uranium. The plutonium formed in the reactor is always composed of a series of isotopes (essentially ^{238}Pu to ^{242}Pu), the 239 isotope being preponderant. In thermal reactors, only the odd plutonium isotopes are fissile.

In all uranium reactors, neutrons are absorbed by ^{238}U in parallel with the fission reactions, producing ^{239}Pu. But in thermal reactors, the quantity of ^{238}U which changes into ^{239}Pu is insufficient to make up for the ^{235}U consumed by fission.

3.1.1 Types of reactor concepts

The main types of power reactors developed up to the present can be listed as follows:

- Light water reactors (LWR), in which water is used both as coolant and moderator:
  - Pressurised water reactors (PWR), among which it is usual to distinguish those designed by the ex-USSR, the VVER (initials of the Russian name), located in the countries of Eastern Europe and Finland.
  - Boiling water reactors (BWR).
- Heavy water reactors (HWR), using heavy water as moderator, of which the most widely used system uses heavy water under pressure as coolant (PHWR, where P stands for pressurised).
- Graphite-moderated and gas-cooled reactors, with three different types, in increasing exit temperature order:
  - Natural uranium gas-graphite (NUGG) reactors, called MAGNOX in the United Kingdom (gas: CO_2).
  - Advanced gas-cooled reactors (AGR) (gas: CO_2).
  - High-temperature reactors (HTR) (gas: helium).
- Graphite-moderated and light boiling water-cooled reactors: RBMK (initials of the Russian name), regrettably famous for the accident of Chernobyl (1986).
- Fast neutron reactors (FR), or liquid metal fast reactors (LMFR), which are sodium-cooled.

These various types of reactors have had very unequal developments, the choices and developments made in the USA (PWR and BWR) having had a strong impact on the rest of the world. At the end of 2001, light water reactors represented 89% of the total net installed nuclear power generating capacity world-wide, with 73.7% for the PWR, and 26.2% for BWR. Thus, the present report refers in particular to these LWR.

3.1.2 Fuel elements materials

The choice of fuel materials and fuel design is closely linked to the type of reactor in which the fuel will be used, even though, for a given reactor, one can envisage relatively different fuels. The system of the given reactor will impose the level of stress to which the fuel will be subjected: temperature, coolant pressure, neutron flux, etc. The main selection criteria for the various components of the fuel assembly are:

- *Fuel material*:

  – Sufficient geometric stability during operation, given the temperature and irradiation conditions (swelling induced by fission products).

  – Satisfactory thermal properties during operation, in order to avoid core meltdown.

  – Acceptable chemical compatibility with the cladding, so as to avoid altering its properties.

  – Density in heavy fissile atoms. This property, while generally not entailing rejection of a fuel material, conditions neutron balance, hence reactivity, and fuel depletion by irradiation.

  – Sufficient chemical compatibility with the coolant, so that either a fuel element with a leak can be left in a reactor, or there is enough time to shut the reactor down and unload the defective fuel before the defect has severe consequences for the reactor (particle dispersion following cladding failure).

  – Compatibility with the fuel cycle steps. Economically acceptable fabrication costs (there is generally no technical impossibility), reprocessing ability (dissolution as complete as possible by nitric acid in the case of the PUREX process).

  The fuel material should then have the following characteristics:

  – A high thermal conductivity is desirable so that a high power density (*i.e*. high thermal power per unit core volume) and high specific power (*i.e*. high thermal power per unit fuel mass) can be attained without excessive fuel temperature gradients. For a cylindrical fuel rod (or pin), a high thermal conductivity permits a high heat rate, without the central temperature approaching the melting point of the material.

  – The fuel material should be resistant to radiation damage that can lead to dimensional changes, *e.g*. by swelling, cracking or creep. Physical properties, *e.g*. thermal conductivity, and mechanical properties, *e.g*. strength and ductility, should not be greatly affected by irradiation.

  – Chemical stability, particularly with respect to the coolant, is desirable, so that there would be little (or no) interaction in the result of a cladding failure.

  – The material should have a high melting point, and below the melting point there should be no phase transformations, which would be accompanied by density and other changes.

  – The physical and mechanical properties of the material should permit economical fabrication.

  – The fuel material should have a low coefficient of expansion.

  – The concentration of fissile (and fertile) atoms in the material should be high; other atoms with large neutron absorption cross-sections should be absent.

- *Cladding*:
  - Mechanical properties adapted to the imposed operating conditions (*e.g*. resistance to the internal pressure of fission gases released outside the fuel).
  - Satisfactory chemical compatibility with the coolant.
  - Compatibility with the fuel.
  - Low neutron capture. This property is vital if one wants to use a natural uranium fuel (HWR, NUGG) and it conditions fuel enrichment in the case of other thermal reactors. It is of lesser importance in the case of FR because of the low cross-sections in the neutron energy range, but its contents of some elements with elevated cross-sections are limited, even for FR.
  - Sufficient resistance to irradiation effects (embrittlement, swelling, etc.), especially if the fast neutron flux is high.
- *Assembly structures*:
  - Good mechanical strength of the assembly structures under normal and accidental operating conditions (*e.g*. earthquake), in order to guarantee circulation of the coolant, lack of assembly handling difficulties, etc.
  - Compatibility with the coolant.
  - Resistance to irradiation effects.

Fuel

Incompatibility with water eliminates, for all water-cooled reactors, the following materials: uranium or alloyed U-Pu, carbide and nitride. Therefore, the oxide fuel, essentially UO_2, is that which is the most widely used throughout the world and for which the largest experience is available.

Oxide, which is highly compatible with water, reacts with sodium, but the kinetics of the reaction allows enough time to extract a defective assembly from the core of the reactor, which permits the use of oxide in FR. Metal alloys, carbide and nitride do not react with sodium.

Uranium dioxide, a ceramic that is the most common fuel material in commercial power reactors, has the advantages of high-temperature stability and adequate resistance to radiation. It also has a high melting point (2 865°C). In addition, uranium dioxide is chemically inert to attack by hot water. It is this property that makes it attractive for use in water-cooled reactors, where the consequences of a cladding failure could be catastrophic if the fuel material reacted readily with the water at the existing high temperature. Another beneficial property of uranium dioxide is its ability to retain a large proportion of the fission gases provided the temperature does not exceed about 1 000°C. The major disadvantage of uranium dioxide as a fuel material is its low thermal conductivity, although this is partially offset by the fact that very high temperatures are permissible in the centre of the fuel element. Another disadvantage of ceramic fuels as compared to metal fuels is their inability to provide negative reactivity feedback by axial expansion.

The choice of natural uranium, made by some countries (*e.g.* Canada, France and the United Kingdom for their first reactors), limits the choice of fuel materials (and of cladding) due to neutronic considerations.

In a graphite reactor – graphite being a moderator of average efficiency – the use of metallic uranium (dense in heavy atoms) is necessary. Heavy water, which is a good moderator, allows the use of uranium oxide.

Plutonium fuels have not been widely used up to now, for various reasons. The only reactors in which they are necessary, for neutron reasons, are fast neutron reactors (even though these reactors can operate with enriched uranium), which are not widespread today.

The recycling of plutonium, which consists of replacing ^{235}U fuel by plutonium, exists only in a few countries, including France, because, on the one hand, only a small proportion of spent fuel is reprocessed in the world and, on the other hand, the use of plutonium for fuel fabrication is more difficult than uranium.

Cladding

Neutron considerations are fundamental for natural uranium reactors, the choices being Mg-Zr for NUGG, and zircaloy for HWR. They are less necessary for light water reactors, but should be taken into consideration on the economic level. For these reactors the replacement of the initially used stainless steel by a zirconium alloy has made it possible to lower fuel enrichment.

The operating temperature is an essential factor for reactors in which the temperature reaches or exceeds 700°C (AGR, FR); the use of stainless steel or a ferronickel alloy is necessary so as to obtain adequate mechanical characteristics. For high-temperature reactors, in which the external temperature exceeds 1 000°C, metallic materials are being replaced by refractory materials such as pyrolytic carbon.

The fuel element, rod or pin, is principally made up of the cladding containing the fuel pellets or bars and is closed by two welded end plugs, resulting in a gas-tight assembly. In the top part of the rod (or pin), there is generally a spring that maintains the fuel column in place and creates a gap (plenum) for fission gas expansion and fuel elongation. If the volume of fission gases released is very high (FR), a large gap at the bottom of the pin is also left.

The fuel assembly design, as far as the number, diameter and arrangement of fuel elements is concerned, is mainly guided by thermal, hydraulic and neutronic considerations, of which we provide some examples below. For a given power per unit length to be evacuated (linear power density in W/cm), the temperature at the centre of the fuel increases with its diameter, which leads to a fractioning of the fuel into several elements of small diameters so as to avoid reaching, at the centre of the fuel, a temperature which would be incompatible with its properties.

Another limit is constituted by the maximum surface heat flux (in W/cm^2) that the coolant is capable of extracting. For a given linear power density released by a fuel element, the surface heat flux decreases when the exchange surface increases, therefore, when the diameter increases. The fuel assembly is made up of a certain number of fuel elements of which the arrangement varies according to different considerations, in particular thermal-hydraulics:

- Square lattice: Western PWR & BWR.
- Hexagonal lattices: FR & VVER.
- Circular section: HWR, AGR & RBMK.

To assemble the fuel elements and guarantee their spacing over the whole length of the fuel assembly, different types of structural pieces are used:

- End grids (one or two).
- Intermediate grids.

Assembly (PWR)

Pressurised water reactor (PWR) fuel is made of either enriched uranium oxide, UO_2, or mixed uranium and plutonium oxide, $(U\text{-}Pu)O_2$. An assembly only includes one type of fuel. This type of plutonium-based fuel is generally called mixed-oxide (MOX) fuel. The fissile material content is lower than 5% in ^{235}U for uranium fuel, and can be higher than 5% in plutonium for MOX fuel (with above 58% Pu^{239} and 11% Pu^{241}).

The rod is closed under helium at a pressure equal to or higher than 25 bars cold, which allows partly counterbalancing the effect of external coolant pressure on the cladding.

The operating conditions for the cladding and assembly structures include: a coolant pressure of 155 bars, average coolant temperature between 286°C at entry and 323°C at exit for the 900 MWe reactors (288°C and 325°C for the 1 300 MWe reactors) and a maximum external cladding temperature of 350°C. These operating conditions lead to significant corrosion of the cladding on its external surface, with the formation of a zirconia layer of which the thickness increases with the stay time and a hydrogen pick up of the cladding. Oxide fuel operates at an average linear density power of 170-175 W/cm. Because of the relatively low cladding temperature, oxide operates at a centreline temperature which is much lower than 1 850°C (value at the hot spot under normal operation), which leads to low fuel restructuring and low release of fission gases.

The low thermal conductivity, which decreases further as the temperature is raised at least up to about 1 700°C, is important because it places a limit upon the maximum permissible heat rate without melting occurring in the interior of a fuel rod. The variation of the thermal conductivity with temperature of sintered, un-irradiated uranium dioxide as fabricated is based on the results of several different studies. However, it should be emphasised that the thermal conductivity of uranium dioxide is strongly dependent on the method of production. Consequently, tabulations and plots found in the literature must be used with caution. Irradiation at moderate temperatures is accompanied by a decrease in the thermal conductivity. However, there is an annealing effect at high temperatures such that the change in thermal conductivity is probably small in an operating fuel element. Detailed uranium dioxide properties are available in the MATPRO database.

An important stress is that which is imposed by the power variations of the reactor, an increase in power resulting in mechanical interaction between the fuel pellets and the cladding, occurring on a cladding weakened by the effects of irradiation.

3.1.3 Fuel cycle types

A number of variations of the fuel cycle exist, depending on the type of reactor to be fuelled and on the disposition of the spent fuel discharged from the reactor. Presently, a version of the once-through cycle is used in the United States and spent fuel is being stored indefinitely at the reactor site. In this process, spent fuel is treated as waste, and provisions must eventually be made for safe handling, packaging and transfer of the spent fuel to a permanent waste repository assumed to be a federal facility. No reprocessing and no recovery of fissile materials are performed in this cycle.

In the closed cycle the spent fuel is reprocessed to allow recovery of the uranium only, while the high-level waste with the plutonium and higher transuranic elements are treated as waste. The uranium is shipped back to the enrichment plant to raise its enrichment from about 0.8 to 3% or more, which is suitable for reuse as LWR fuel. The wastes require proper treatment, packaging and shipment to a permanent repository. Here, in addition to uranium, plutonium is also recovered. Since plutonium is a fissile material, it can be used as fuel. Plutonium oxide mixed with uranium oxide forms the so-called mixed-oxide (MOX) fuel that can be recycled in LWRs. Mixed-oxide fuel has been irradiated in test assemblies in a number of commercial reactors in the United States and overseas to demonstrate that it can be used successfully and without undue difficulty as LWR fuel. However, the recycling of plutonium has not become a commercial reality in the United States due to a number of impediments and restrictions. A keener interest in plutonium recycling has been evinced in Japan and Germany. In Japan, the main motivation is to enhance the country's energy independence, while in the German point of view it significantly simplifies the disposal of high-level wastes.

3.2 Effects on fuel behaviour (background)

During its lifetime in the core, a clad ceramic fuel rod has a substantial amount of fission products produced within it, and it is exposed to severe environmental conditions. Under such circumstances, it is not surprising that various physical changes occur, the control of which has been the subject of development efforts for the past few decades. Remedies have been found for most problems that have limited performance in LWR such that the failure rate in today's designs is well below 0.03%.

During irradiation, the clad tends to creep down onto the pellet, forming an elliptical cross-section under the action of coolant system pressure. Densification, which was a problem in the past, has been eliminated by fabrication improvements and the use of a high-initial-density fuel. Fission gases, which are released by a combination of processes, increase the rod internal pressure, but also degrade the thermal conductivity of the clad-pellet gas gap.

A major change during irradiation is radial cracking as a result of the thermal stresses of the pellet and some relocation of the cracked segments. The edges of the cracked portions tend to apply stress to local regions of the surrounding cladding, resulting in vulnerability to so-called pellet-clad interaction (PCI) effects. These effects are primarily a result of the attack by fission product iodine on the zircaloy, leading to stress corrosion cracking. The problem has been largely remedied by reduced power change rates and improved pellet design. Several stresses of various origin also affect the fuel behaviour:

- *Temperature effects*. Fuel is subjected to a high temperature that increases from the periphery to the centre. Separately from these direct effects, temperature governs the fuel behaviour, *i.e.* variation of mechanical properties, chemical reactions between materials, etc.

- *Irradiation effects*. Irradiation, a consequence of the fission phenomenon, has effects other than that of heat release:

- Fission products, solid or gaseous, are created within the fuel. Their distribution is different in a thermal reactor and in a fast neutron reactor, and depends on whether the fissile material is ^{235}U or plutonium.

- Fission products either remain within the fuel and produce effects such as swelling and modification of the physical and physico-chemical properties of fuel, or they can be released, creating a gaseous pressure within the cladding. They can also deposit themselves on the cladding, causing corrosion.

- Irradiation, and in particular the fast neutron flux, modifies the mechanical properties and the geometry of the metallic materials of the assembly: hardening, ductility loss, swelling (steels), growth (zircaloy) and irradiation creep.

- *Mechanical phenomena*. These phenomena concern either one of the components of the assembly, or two or more components that interact:

  - The high thermal gradient in the fuel, associated with a low thermal conductivity (oxide), can cause its cracking.

  - Cladding is subjected to primary stresses (external pressure of the coolant in PWR, internal pressure of the fission gases) and secondary stresses, resulting from the temperature.

  - There can be mechanical interaction between fuel and cladding at constant power or in case of power variation.

  - The assembly structures are subjected to stresses of different types: hydraulic thrust, hydraulic or mechanical vibration, mechanical interaction.

- *Chemical and physico-chemical phenomena*. Without being exhaustive, we can mention:

  - The fuel modification under temperature and irradiation effects: redistribution of the U and Pu components by diffusion, formation of plutonium and fission products, evolution of the O/(U+Pu) ratio in the oxide.

  - The reaction between cladding and coolant fluid: oxidation and hydrogen pick-up of zircaloy in PWR.

  - The possibility of a chemical reaction between fuel and cladding (PCI), which can be activated by some fission products.

- *Interaction between the different phenomena*. One of the difficulties in the study of fuel, and especially of the fuel element, is due to the interaction of a great number of the phenomena that have just been described.

- *Variations in time and space*. Like other industrial products, nuclear fuel has operating conditions and characteristics that vary with time and locally from one point to another. In a nuclear reactor, the neutron flux (and thus fuel power density) is not uniform, but decreases when one moves from the centre of the core to its outside boundaries. Thus, flux varies in a fuel assembly, which takes up all the height of the core and has a certain thickness compared to the radius of the latter. Moreover, fuel operates for several years, during which it is subjected to slow variations, such as the power loss resulting from fuel depletion by fission or the faster power variations caused by reactor load changes and especially by fast shutdown (in case of an operating incident).

- *Burn-up*. The stay time of fuel in a reactor, which determines its burn-up, in other words the consumption of fissile atoms, is an important factor in fuel behaviour, which generally deteriorates as residence time increases. The in-reactor residence time of fuel is limited by neutron or technological considerations. It is generally expressed by the term "burn-up". Burn-up is the total energy released during the life of fuel per unit of mass, of heavy metal (U or U+Pu). It is normally expressed in MWd/t. The fuel assembly must then meet a certain number of requirements:

  – Fuel elements must remain gas-tight during their life and the leaks which occur during operation must concern only a small number of them and/or not be very serious in order to avoid primary circuit contamination and reactor shutdown in order to extract the defective assemblies. Thus, in PWR, a leak rate of some 10^{-5} per cycle for the rods can be tolerated, which corresponds at most to a few defective rods per annual reactor cycle, the causes of the defects being largely outside the fuel.

  – Fuel elements and assemblies must have a limited geometric strain, to avoid deteriorating cooling conditions, hindering operation of reactivity control systems (absorber materials), and hindering or endangering fuel loading and unloading operations.

  – The behaviour of the fuel assembly in case of reactor accident, and its consequences on the evolution of the accident and on reactor safety, must be taken into account.

  – Fuel must be able to reach the highest possible burn-up, to lower cycle cost.

  – The choices made, especially concerning the materials, must lead to fuel cycle operations which are industrially feasible and economically profitable.

An essential characteristic of fuel studies is the difficulty of simulating irradiation effects. Their study requires in-reactor tests. As a good knowledge of how to accelerate time in an in-reactor fuel test without changing its behaviour has not yet been acquired, an irradiation test often takes a long time. If test preparation time (elaboration of components, fabrication) and the time required for post-irradiation examinations are added, it can take up to seven years or more between the launching of an irradiation experiment and its conclusion.

3.2.1 Temperature effects

Fuel modifications resulting solely from temperature occur rapidly. In PWR rods, major changes occur much more slowly as these changes, even if still governed by temperature, are mainly irradiation or fission effects. The axial power profile, and therefore the centreline temperature, is more or less smooth, only undergoing a local decrease coincident with grid plates.

3.2.1.1 Geometric effects of temperature

- *Thermal expansion*. The temperature rise in the fuel element results in thermal expansions which are not of the same value in the fuel as in the cladding because the temperatures and thermal expansion coefficients are different. These differential thermal expansions thus lead to a reduced fuel-cladding gap and affect in return the temperature of the fuel.

- *Fuel cracking*. The radial temperature gradient in the fuel induces internal stresses since the centre tends to expand more than the periphery. At the end of the first power rise, the pellets are therefore systematically cracked. Cross-sections of PWR pellets generally display about

ten cracks. Their orientation is predominantly radial, but transverse cracks (perpendicular to the cylindrical axis) also occur, as do circumferential cracks (generally closed when hot), after a few thermal cycles. Under the effect of vibration, the oxide fragments resulting from this cracking shift in relation to one another: this is a relocation mechanism that leads to a slight increase in average pellet diameter.

- *Thermoelastic strain*. The oxide pellets have a finite length (10-14 mm) and a plane strain approximation is no longer valid in the vicinity of the top and bottom of the pellet sides, as the axial stress becomes zero on these sides. Thermoelastic calculations show that under the effect of thermal stresses, the initially orthocylindrical pellet tends towards an hourglass shape, with convex surfaces on the top and bottom. Thus, the displacement of the external radius attains a maximum value at the pellet edges. This additional deformation, although slight, can nevertheless have detrimental consequences on cladding strength during power variations as the cladding then becomes the site of a stress concentration coinciding with inter-pellets.

3.2.1.2 Restructuring

- *Formation of columnar grains*. The higher the temperature, the faster and more extensive the changes in fuel microstructure, *i.e*. the morphology of the grains and fuel porosity. On the cold wall of the pore, the oxide condenses in a virtually single crystal configuration. When moving towards the centre of the pellet, the lenticular pores destroy the initial structure of the fuel and leave behind very elongated grains (1-3 mm in length by a few ten μm in width) called columnar or "basalt" grains. These grains appear very clearly in metallographs, since the grain boundaries are marked by a string of small bubbles released on the periphery of the lenticular pores during their migration.

- *Grain growth*. Post-irradiation examination has revealed a visible increase in grain size in the hottest central part of certain PWR fuels. This grain growth is the result of the displacement of the boundaries that tends to make smaller grains disappear to the benefit of larger ones. From a thermodynamic point of view, the reduction of energy linked to surface tension of the boundaries leads to this increase in size. This mechanism also occurs, of course, out-of-core, as soon as the temperature is high enough. The grain growth rate is a function of the displacement velocity of the grain boundaries, a velocity that itself is governed by the mobility of the pores which are trapped on these boundaries.

- *Gap closing*. The diametrical oxide-cladding gap under hot conditions, of the order of 120 μm (PWR) at the very beginning of life, decreases until it disappears altogether. In PWR rods, gap closing initially occurs through the relocation of oxide fragments. The gap is subsequently reduced, mainly through creep of the zircaloy cladding under external pressure. The gap is completely closed after about 15-20 GWd/t.

3.2.2 Irradiation effects

The irradiation itself, *i.e*. the neutron bombardment to which the material is subjected and above all the fission product recoil in the fission spikes, generates an extremely high number of point defects in the fuel which are all out of proportion to those in thermal agitation. The fluorite structure of the oxide fuel has proven to be particularly well adapted to withstanding such heavy damage, but certain properties will nevertheless be modified. Most importantly, thermally activated phenomena such as diffusion and creep can, under irradiation, continue to play a role at temperatures too low to be operative out-of-reactor.

Fission of the uranium and plutonium atoms introduces a great number of foreign atoms into the materials, some of which are rare gases. The behaviour of these fission gases will be discussed since it is closely linked to the irradiation effects. Moreover, it appears that at a high burn-up, when a great quantity of gas has been created, irradiation can bring about important changes in the microstructure at a temperature so low as to preclude explanation by thermally activated phenomena. Such an evolution has been observed, in particular, on the very edge of PWR pellets in what has been termed the "rim effect".

Table 5. Effect of fission products on the chemistry of oxide fuel [112]

Phenomena	Result
1. Large number of fission products produced.	1. The tendency to form or not form oxides controls oxygen level in fuel. High oxygen levels lead to cladding defects. Some chemical species such as iodine can attack cladding directly.
2. One uranium atom replaced by two fission products.	2. In LWR fuels, typical burn-up is 3%, so end-of-life fuel will contain about 6 at.% fission products. Swelling in fuel can produce internal stresses and mechanical contact with cladding.
3. A large fraction of fission products are noble gases (xenon and krypton).	3. Noble gases are not retained in the fuel matrix, but escape into the internal space within the cladding. This increases the internal pressure of the cladding. These gases also are poorer thermal conductors than He (the gas filled in the plenum during fuel fabrication), so that the fuel operates at a higher temperature.
4. Non-volatile fission products have different physical properties than UO_2.	4. Thermal conductivity of fuel decreases, internal temperatures increase. Melting point of fuel changes. Metallic inclusions form, sometimes leading to cracking. Fission products migrate up or down the temperature gradient existing during normal operation. Changes in grain size occur.

3.2.2.1 Diffusion

In UO_2 and $(U,Pu)O_2$ fuels, as in all fluorite-type oxides, the thermally activated diffusion of the oxygen anion is much faster than that of the metallic ion, and its diffusion rate increases with deviation from stoichiometric composition. The self-diffusion of the U and Pu cations occurs much more slowly. Therefore this cation diffusion controls the different mechanisms such as creep, sintering densification or grain growth.

In the reactor, the diffusion mechanisms of uranium and plutonium are not greatly affected at high temperatures, but below 1 000°C, an athermal diffusion mechanism appears which is dependent only on the fission density. This diffusion under irradiation operates due to the point defects created in the

fission spikes. Consequently, mechanisms such as densification or creep may intervene in the reactor under temperatures at which they are totally inoperative out-of-reactor. In an intermediate temperature range, ranging from 900-1 300°C, diffusion is both thermally activated and accelerated by irradiation.

In PWR fuel, only dishing provides a free space in which the fuel can creep; it is primarily during power ramps that these mechanisms play a significant role.

3.2.2.2 Fission gas behaviour

Fission gas formation

The release of the gaseous fission products krypton and xenon from uranium dioxide during irradiation has been studied for many years. A quantitative understanding of gas release has evolved slowly because several mechanisms for describing the movement of the gas are involved and also because a detailed operating history of the fuel rod was usually not clearly documented, thus introducing experimental uncertainties. Fuel temperature is the principal determinant of gas release. The small amount (< 3%) of gas released during normal operating is knocked out to the fuel pellet's free surface. As fuel temperatures exceed 1 725 K (2 592°F), the migration of gas bubbles can be significant, and releases approaching 100% can be observed for molten fuel. Burn-up has no discernible effect on gas release below 15 000 MWd/t. Above this burn-up, gas release is enhanced, particularly above 30 000 MWd/t. The knowledge of the inventory of short-lived (half-life < 10 days) isotopes in the fuel rod void volume is important form the standpoint of calculating the radiological consequences of accidents. Calculations of the time delay these isotopes experience in migrating to the gap should be based on operating history.

Mechanistic models based on the growth and migration of intergranular bubbles are applicable in describing gas release during steady-state and transient conditions; in mechanistic model calculations, however, they are often time-consuming. In their place, semi-empirical correlations based on available operating data and post-irradiation measurements of gas release are used in evaluations for application. Fission gas release at a high temperature (1 725 K) and high burn-up (30 000 MWd/t) has been measured and the models have been incorporated in computer codes. Fission product transport and aerosol removal models have also been developed.

Non-gaseous fission products are of interest not only because of their contribution to the radiological consequences of accidents, but also in some cases (notably those of iodine and caesium), because they may attack the cladding chemically and thus make it more susceptible to breaching. Although the migration mechanisms for iodine, caesium and the less-volatile fission products are not well characterised, it is known that essentially all of them are retained in the fuel pellet during normal operation, as studied at ORNL.

The generation of solid and gaseous fission products causes the uranium dioxide matrix to expand, and this expansion must be allowed for high burn-up. The volume expansion due to fuel swelling is accommodated by fabricating the pellets to less-than-theoretical density and by providing additional width for the pellet-cladding gap. Under normal irradiation conditions, fuel swelling is not particularly important, and nominal values of 0.3 to 1.0% $\Delta V/V$ per 1% burn-up are used, depending on the fuel temperature. Because fuel swelling accompanies gas release, most of the mechanisms proposed to describe gas release include a provision for describing the accompanying swelling. A thorough study of densification has shown that fuel densifies because of the annihilation of small (<1 μm diameter) pores by fission fragments.

The power decay of a LWR is a function of the time after scram and the time of operation before scram. For safety analysis the fuel rod is assumed to have been operated for a long time. The gaseous fission products are primarily rare gases:

- Xenon in the isotopic forms ^{129}Xe, ^{131}Xe, ^{132}Xe, ^{134}Xe, and ^{136}Xe.
- Krypton ^{83}Kr, ^{84}Kr, ^{85}Kr, and ^{86}Kr.
- Helium created by a few ternary fissions, neutron capture by oxygen and the α decay of some isotopes such as ^{238}Pu, ^{241}Am or ^{242}Cm.

The fission yield of these different gases depends on the following the neutron flux spectrum (thermal or fast), the nature of the fissile atom (U or Pu), its isotopic composition and the burn-up. In PWR, the ^{135}Xe, with its very high capture cross-section in the thermal domain, transmutes for the most part into ^{136}Xe before having time to decay into caesium. The gross yield is thus increased: the entire amount of stable gases created in a PWR is of the order of 0.31 at./fission but evolves during irradiation due to the growing number of Pu fissions.

The gases thus formed represent considerable quantities. In PWR fuel irradiated to 60 GWd/t, more than 1.5 cm^3 STP of gas per gram of oxide are occluded. Introducing practically insoluble gases into the crystal lattice has consequences on:

- Fuel swelling (*i.e.* the volume increase linked to fission) which, in turn, at the beginning of life, plays a role in closing the oxide-cladding gap (and thus in the temperatures) and at higher burn-up affects the oxide-cladding mechanical interaction, particularly during power transients.
- Release of these gases into the plenum, which conditions the pressure in the fuel element.
- Some properties of the oxide, in particular the thermal conductivity, with the gas bubbles playing a role similar to that of the pores.

The behaviour of these gases is governed by both athermal phenomena (linked to fission) and diffusion mechanisms linked to the temperature.

Athermal mechanisms

As the recoil distance of the fission fragments is in the vicinity of 8 μm, gas atoms emitted near the surface can directly escape from the fuel. Escaping by recoil, the atoms draw some of the atoms contained in the fission spike towards the exterior: this is termed “knock-out”.

These recoil and knock-out mechanisms play a dominant role in fission gas release at low temperatures, especially in the UO_2 fuel of PWR which, up to 45 GWd/t, has a very low release rate ($\leq$ 1%). The fraction of gas released by knockout depends on the surface/volume ratio and increases with the quantity of gas in solution, and therefore with burn-up.

The insolubility of fission gases in the fuel and diffusion under irradiation make the migration of gas atoms possible even at low temperatures. In PWR fuel, beyond 20 GWd/t, observations made on fractographs show progressive gas segregation in the grain boundary planes; the intersection off several planes leads to the appearance of tiny channels with triple boundaries through which a slow fission gas flux succeeds in escaping from the fuel.

3.2.3 Chemical and physico-chemical phenomena

3.2.3.1 Pellet and clad interaction

The fuel rod failure mechanisms of PCI may be divided into two categories: chemical and mechanical. The chemical failure mechanism is believed to originate from stress corrosion cracking (SCC) caused by aggressive iodine. Even though CsI is a stable compound, elemental iodine can still exist in several ways. As the oxygen activity of the fuel increases, the formation of Cs-U-O compounds is increasingly favoured, possibly liberating the iodine. Another source of elemental iodine is gamma radiolysis of CsI. Iodine causes SCC at temperatures lower than 850°F and reduces the clad ductility. However, it does not produce SCC in zircaloy above 850°F. Specimens damaged by iodine-SCC always exhibit intergranular cracking. There seems to be a threshold linear power density for iodine-SCC clad failures. The threshold for fresh fuel rods is about 13.7 kW/ft, and the threshold decreases as the burn-up increases.

The mechanical failure mechanism is believed to originate from an excessive local stress that breaks the embrittled clad. An interlayer formed from Cs-U-O-Zr tends to bond the pellet to clad and make it easier for radial cracks to propagate from the pellet into the clad during a power spike. Sometimes both failure mechanisms may be combined, because the effective threshold stress of the iodine SCC clad is only about half that of the yield point of the fresh clad (if the stress is maintained for a significant period).

3.2.3.2 Clad deformation and corrosion at high burn-up

Clad deformation under long irradiation and oxide thickness due to water-side corrosion are the two concerns, besides PCI, for preventing LWR fuel rod from having very high burn-up. Exxon has measured clad elongation and diameter creep-down and found that the rod growth and relaxation of spacer fingers do not over-limit at burn-up of up to 50 000 MWd/t in PWR and 40 000 MWd/t in BWR. KWU reported that PWR fuel rods of up to 50 000 MWd/t of rod average burn-up exhibit the consistent trends of rod elongation and diameter creep-down. The continued trend of diameter creep-down at high burn-up indicates both the good dimensional stability of the UO_2 pellets and that the clad is still free standing at a burn-up of 50 000 MWd/t.

B&W stated that the uniform waterside corrosion and its secondary effect of hydrogen pickup will not limit the routine operation of current-design PWR fuel up to burn-up of 50 000 MWd/t. KWU reported that at an oxide thickness of 70 μm, 250 ppm of hydrogen is the typical concentration found in the cladding around 50 000 MWd/t. At and beyond this hydrogen concentration, precipitation of zirconium hydrides has to be considered.

A study of the effect of coolant chemistry on in-core and build-up on PWR and BWR has indicated that for PWR, a high pH operation such as the Westinghouse boron-lithium trade-off curve in combination with hydrogen overpressure greater than about 25 cc (STP) per kilogram of water are effective in preventing crud build-up on the fuel. For BWR, maintaining oxygen at an optimum level and eliminating impurities in the feed water should result in minimising core crud deposits.

3.3 Thermo-physical properties of materials for LWRs

The Co-ordinated Research Programme (CRP) on Thermo-physical Properties Database for Light and Heavy Water Reactor Materials [108] was organised in 1997 in the framework of the IAEA International Working Group on Advanced Technologies for Water-cooled Reactors (IWGATWR).

(The database on reactor materials is incorporated into the existing THERSYST database system established at Stuttgart University in Germany. This database can be obtained through special request addressed to the Stuttgart University.) The objective of the CRP has been to collect and systematise a thermo-physical properties database for light and heavy water reactor materials under normal, transient and accident conditions. The materials properties considered include those needed for light and heavy water reactor operational and safety assessments. The materials have been grouped within the following categories:

- Nuclear fuels.
- Cladding materials.
- Absorber materials.
- Structural materials.
- Coolants.
- Gases.

The thermo-physical properties included in the database are:

- Thermal conductivity.
- Thermal diffusivity.
- Specific heat.
- Enthalpy.
- Heat of melting.
- Coefficient of thermal expansion (linear for solids, volume coefficient for fluids).
- Emittance.
- Density (and porosity, as a parameter defining sintered materials).
- Equation of state.

The data concerning thermal conductivity, thermal diffusivity, coefficient of thermal expansion, and emittance of solid materials were collected from room temperature to their melting points. The specific heat, enthalpy, and density for the same category of materials are also important and were collected from room temperature to a temperature exceeding their melting temperatures by approximately 100 K.

Recommended data for the thermo-physical properties of nuclear materials have been published in the MATPRO publications. The last issue of MATPRO data, in the SCDAP/RELAP5/MOD2 code manual from 1990, contains descriptions of material properties subroutines available in that database. The adequacy of the available data on the appropriate physical and chemical properties of some nuclear materials has been reviewed in the report EUR-12404 (1989) published by the Commission of European Communities. A variety of other recommendations have also been made with regard to the thermal conductivity and specific heat capacity of fuels.

3.4 Fuel failure mechanisms

Water reactor fuel continues to perform reliably in power reactors around the world. However, fuel failures from knows mechanisms still occur, occasionally with a significant impact on plant operation, and the current average fuel rod failure rates of around 10^{-5} are still high compared to the "zero failure" goal, which in today's understanding should correspond to a failure rate near 10^{-6}. Improving fuel reliability beyond current levels will be even more challenging for countries involved with programmes to further increase fuel discharge burn-up. A good understanding of fuel performance is essential for identifying the root causes of failures and for defining remedies at the design, manufacturing and operational levels.

The IAEA review has two major aims [109]. The first addresses the above technical background with the aim of updating and supplementing the earlier IAEA publication of 1979. The second aim of this study is to provide a combined presentation of the world-wide experience in this field so as to promote an exchange of information and future co-operation. The reactors covered by this study are Western-type boiling and pressurised light water reactors (BWR, PWR), and Soviet-type pressurised light water reactors (VVER). The acronym LWR refers collectively to the three types, BWR, PWR and VVER.

Recent surveys on fuel failures in general or those related to regional experience have been the subjects of several papers. In a comparison of the situations in 1979 and today, two factors are noteworthy. First, the fuel rod failure rates in LWR have been significantly reduced, on average by approximately one order of magnitude from the range above 10^{-4} to levels near 10^{-5}, *i.e.* a few rods per 100 000 rods in operation. Second, it is interesting to note that a majority of the mechanisms of earlier fuel failures are still active, mostly in combination with new root causes and contributing factors. Table 6 provides a brief list of the observed primary failure mechanisms.

Table 6. Observed primary failure mechanisms for nuclear fuel

Fuel rod failures	
Manufacturing defects	In clad, end plug or weld
Hydriding	By moisture or other contamination in pellets/rods
PCI/SCC	By high power rams, or assisted by clad/pellet imperfections
Corrosion	With large variety of different root causes and contributing factors
Dryout[a]	Only one case of overheating by excessive channel bow (BWR)
Clad collapse[b]	By axial gaps in the fuel column due to fuel densification (PWR)
Grid-rod fretting	With a large variety of different root causes and contributing factors
Debris fretting	From metallic debris circulating in the coolant
Rod bow[b]	From several root causes, can lead to exceeding design limits, but has not caused fuel rod failures except in one early vent of excessive bow
Baffle jetting	By cross-flow from defective core baffle joints (PWR)
Damage to the assembly structure[c]	
Assembly bow	From several root causes, can lead to handling damage or other problems
Other deformation[b]	By Zry growth/differential growth leading to structural misfit
Fretting wear	From a large variety of phenomena with different root causes
Zry hydriding[a]	Only one case of excessive hydrogen take-up in guide tubes (PWR)

[a] Isolated event.
[b] Earlier occurrences, no noticeable problems during the last ten years.
[c] With few exceptions no leaking rods.

With regard to fuel rod failures, only clad collapsing (PWR) and failures by excessive rod bow or differential length growth have practically disappeared, as adequate design and manufacturing solutions were found. Primary hydriding by moisture in the fuel, which had been a major source of failure in the early days not only in BWR and PWR but also in VVER has been essentially eliminated. These and other manufacturing related failures are low in absolute numbers, but with current low failure levels still constitute a substantial percentage. Important current issues as regards fuel performance include corrosion by itself or in combination with crud deposits in LWR, pellet-clad interaction/stress-corrosion cracking (PCI/SCC) in BWR, grid-rod fretting in PWR. In spite of all the efforts to find adequate remedies, there seem to be several new aspects and problems that continue to challenge the industry. Failures by baffle jetting (PWR) temporarily increased during the 1980s, but have now been reduced to near zero. Debris fretting has continued at a substantial level. A new experience since 1989 has been the frequent observation of severely degraded fuel rods, particularly in the form of long axial cracks with unusually high activity release, in BWR fuel.

In the field of assembly damage, effects from length growth still play a role, and bow phenomena have caused new problems. Handling damage on PWR fuel is often related to assembly bow with the consequence of spacer damage during loading or off-loading. A variety of incidents with fretting wear have been reported. Experience with these and other observed unexpected failure causes has made it clear that concerns about assembly damage are as of a similar importance today as fuel rod failures, at least for LWR fuel.

The most significant development since the mid-1980s for LWR fuel has been a continuous increase in average discharge burn-up to about 45 MWd/kgU, with further increases being planned. Numerous modifications in fuel designs and materials have been made to adapt fuel performance to higher burn-up goals or to improve neutron economy, and simultaneously to reduce the failure risk.

In BWR plants the earlier change from 7 × 7 fuel (14.3 mm rod diameter) to 8 × 8 fuel (with 12.25-12.5 mm rod diameter and a correspondingly lower average linear heat generation rate) in the 1970s was not sufficient to prevent PCI failures or PCI-related operating restrictions under the goals of increasing burn-up and higher power peaking factors. As remedies, General Electric (GE) introduced the Zr liner (barrier) cladding for the 8 × 8 fuel which was later adopted by most other fuel vendors. Siemens developed and introduced 9 × 9 reload fuel (10.7-11 mm rod diameter). For both 8 × 8 and 9 × 9 fuel, reactivity optimisation led to fuel versions with different numbers of water rods, and eventually to the 8 × 8 water cross design of ABB, called SVEA64, and the 9 × 9 ATRIUM fuel of Siemens with a central square water channel. In the meantime, both versions have also been introduced with a 10 × 10 fuel rod matrix (around 10 mm rod diameter), and GE has also recently presented 9 × 9 and 10 × 10 fuel designs. Most 8 × 8 and part of the 9 × 9 and 10 × 10 fuel use cladding with a Zr liner.

The PWR plants can be divided into two groups: (i) previous plant designs using the original fuel rod diameters in the range 10.7-11.2 mm, comprising all 14 × 14 and 15 × 15 fuel, and 16 × 16 fuel in Siemens plants; and (ii) later plant designs using smaller rods diameters in the range 9.1-9.8 mm, comprising 16 × 16 fuel in Combustion Engineering (CE) and Westinghouse plants, all 17 × 17 fuel, and 18 × 18 fuel in Siemens plants. Cladding with a Zr liner is not used commercially in PWR.

Many modified PWR fuel designs and product names (*e.g.* AFA, OFA, VANTAGE 5, FOCUS, HTP, mostly applied independently of the fuel matrices) have been introduced. Common features of these new fuel types are: (i) the use of advanced Zry spacer grids, (ii) some type of debris catcher to prevent debris fretting failures and (iii) cladding materials with improved corrosion resistance. Although most of the cladding material in operating fuel is still of the Zry-4 type within the ASTM

specification, the trend is to leave this range. New alloys have been introduced, in particular DUPLEX cladding with an outer layer of a corrosion-resistant alloy by Siemens, and ZIRLO cladding (Zr1 Sn1 Nb basis) by Westinghouse. Up to now, these new cladding types have not played a role in fuel failures.

The VVER plants can be divided into the original version VVER-440 with channelled fuel assemblies and 126 fuel rods, and the VVER-1000 series in operation since the mid-1980s with un-channelled fuel (one exception) and 312 fuel rods, both of which have a hexagonal rod matrix and honeycomb type spacer grids. Fuel rods with 9.1 mm diameter, Zr1Nb cladding, and annular pellets are used in both types. Additional important differences from Western PWR are a potassium-ammonia water chemistry, and the reactivity control in the VVER-440 by special fuel assemblies containing boron steel tubes in the upper part.

In addition to the introduction of spacer grids of ZrNb alloy in place of stainless steel (since 1987 in VVER-440 and now in VVER-1000), recent developments in the VVER fuel area comprise the use of a Russian ZrNbSnFe alloy with higher resistance to irradiation-induced growth, creep and corrosion for guide tubes, and also for fuel rod cladding in applications with extended residence time (5-6 years). For the VVER-1000 the introduction of dismountable assemblies and the optimisation of cap and control rod design are also under way.

3.4.1 Mechanisms and root causes of fuel failure

Ten mechanisms for fuel rod failures are identified and discussed below; assembly bow and other damage to the assembly (mostly without leaking rods) are also addressed.

- *Manufacturing defects*. Manufacturing defects others than those leading to primary internal hydriding (which historically is treated separately) have been identified. The major types of defects are end plug stringers, and several types of end plug weld deficiencies.

- *Primary hydriding*. Fuel failure by local internal hydriding is also known as sunburst failure in reference to its metallographic appearance. In the 1960s the sources of hydrogen were mainly residual amounts of moisture or organic contamination in the fuel pellets/rods. Secondary hydriding is formed after ingress of steam into the rods.

- *Pellet-clad interaction*. Pellet-clad interaction (PCI) has been a frequent cause of fuel failure for BWR, and sometimes VVER fuel but has been rare for PWR. PCI failure occurs as a result of a rapid power increase (power ramp), typically by the movement of the neighbouring control rod. PCI fuel failure has been reduced remarkably, mainly as a result of the use of operating guidelines and changes in fuel design. Failures at power ramp below the assumed PCI failure limit have been reported as a result of cladding defects or pellet chipping.

- *Corrosion*. In PWR, corrosion is uniform on the cladding surface, and excessive uniform corrosion leading to clad failure is very rare under normal operating conditions. Such failures were due either to abnormally high heat flux exceeding heat flux/burn-up corrosion limits or to water chemistry problems leading to excessive crud deposits. In BWR nodular corrosion is the dominating corrosion mechanism, and crud-induced localised corrosion (CILC) was one of the major causes of fuel failure in the 1980s. This CILC mechanism is rather complex, but copper in the coolant plays an important role in the formation of heat-insulating crud. In BWR and VVER, high contents of impurities such as carbon or degraded water chemistry in the coolant also resulted in fuel failure. An extended discussion concerning the influence of crud formation is provided in Section 4.1, in relation to high burn-up fuel.

- *Dry-out*. Dry-out of fuel rods has been reported only once from a BWR. The root cause of the failure was identified as excessive channel bow, which caused large local power peaking in the fuel rods.

- *Cladding collapse*. Cladding collapse due to densification of the fuel pellets forming axial gaps in the pellet column resulted in fuel failure in the early 1970s in many PWRs. This type of failure has been completely eliminated through the use of pellets with moderate densification and pre-pressurisation of the rods.

- *Grid-rod fretting*. Grid-rod fretting has become a frequent mechanism of fuel failure for PWR in the reporting period. The main root causes of the failures have been identified as insufficient fuel rod support in the assembly due to improper design and/or fabrication, fuel rod vibration due to fluid elastic instability by cross-flow in the assembly, and flow-induced assembly and rod vibration.

- *Debris fretting*. Debris fretting has been a common mechanism of fuel failure in all types of power reactors. Various types of debris circulating in the coolant, mainly machining chips of the core structure, protrude through the lower tie plate and either damage the lower part of the rod or are trapped further up in the grids and cause through-wall fretting of the cladding.

- *Baffle jetting*. Baffle jetting resulted in fuel failure in many PWRs. The root cause of the failure is the improper joining of the baffle plates that surround the core. The failure became rare as a result of the use of various remedies, *e.g.* a change in the coolant flow behind the baffle plate, which reduces differential pressure across the plates.

- *Assembly damage*. Assembly bow may result in PWR fuel rod failures after severe spacer damage, but this is rarely observed. The major root causes are high radial flux/power gradient or excess spring load on the skeleton of the assembly. In a few cases assembly bow caused delay of control rod insertion as a result of increased friction between the guide tube and the control rod. A more frequent consequence of assembly bow is mechanical damage of assemblies, especially grids, during handling.

3.4.2 Fuel failure prevention in plant operation

Fuel failures can greatly affect plant operating activities, and there are operating limits due to fuel failure. Equally, there exist recommendations for operating policies and practices that can be implemented so as to prevent fuel failures and to minimise their effects or propagation.

Coolant and off-gas activity

All plants must operate within their technical specifications for failed fuel as defined by the limit on coolant or off-gas activity. These technical specifications are imposed by the regulatory body. The allowable coolant or off-gas activity during normal operation can be different from plant to plant and from country to country: 1.0 $\mu Ci/cm^3$ (dose equivalent ^{131}I) is a typical coolant activity limit in the USA, but half this value is sometimes used in Europe. BWRs have similar limits on off-gas activity.

For VVER reactors, the operational failure limit of fuel rods with defects of the gas-leak type is 0.2% and in the case of direct contact between fuel and coolant it is 0.02%. The total iodine isotope activity of the primary circuit would then correspond to 1.5×10^{-2} Ci/kg for the VVER-1000. For the

VVER-440 the specific activity of non-gaseous fission products at this point would reach 1×10^{-4} Ci/kg. Such levels of coolant activity have never been reached or observed.

These limitations on the specific activity of the reactor coolant or off-gas minimise personnel exposure and ensure that the resulting doses at the site boundary will not exceed an appropriately small fraction of dose guideline values following a reactor accident.

The iodine-spiking phenomenon after plant transients has received particular attention in safety evaluations due to its potential to increase the radiological consequences of postulated accidents. Therefore, a limit to the amount of iodine activity allowed in the reactor coolant after some plant transients is specified in many LWR. In addition, some LWR plants are not authorised to start-up with failed fuel. They must identify, locate and remove failed fuel before re-start. Most utilities have no requirements to inspect or remove failed fuel, as the major control is on the coolant or off-gas activity.

These activity limits for current licensing are well below the design limits of the plant systems in which the radwaste circuits are designed to accommodate 1% of fuel rods failures.

Guidelines for power changes and load following operation

For LWRs, one of the most important fuel performance aspects of power changes and load following operation is PCI in the fuel rods. Indeed, power changes are directly accompanied by dimensional changes of the fuel and cladding in both directions. This effect is larger in the fuel because of the larger temperature variation as compared to the cladding. Thus, with an increasing linear heat generation rate the diametral pellet-to-clad gap may close and pellet-clad mechanical interaction may develop. Under such conditions PCI failures may result because of cladding stresses, if such ramps are not limited to acceptable levels. If the ramp rate is limited, the fuel rod may adapt to a higher linear heat generation rate level by creep and relaxation of the fuel and cladding. This mechanism, which takes some hours to a few days, is called “conditioning”, and leads to a new steady-state condition at a higher power level. The conditioning power level is defined as the rod power at a typical reference stress (corresponding to the equilibrium between pellet swelling and clad creep). The kinetics depend on rod design and on power history.

The need for continuous PCI surveillance is much more pronounced in BWRs than in PWRs. One important feature of PWRs is the possibility to operate the core at constant load without deeply inserted control rods, as burn-up compensation is done by boron control. Fast load changes can be performed by temporarily inserting one or several groups of control rods, called D or grey banks, without noticeable local power perturbation. Moreover, the most recent plants are equipped with a sophisticated or even an automatic control system for power distribution using direct input from in-core detectors. They can then operate with a very low power spike, and there are few restriction on load following operation except for starting up after refuelling. Recent experience shows that no PCI failure has ever been confirmed in a PWR fuel of modern design.

BWRs are more subject to the PCI problem than PWRs. Indeed, most of the time they must operate with deeply inserted control blades used for burn-up compensation. The movement of control blades induces more distortions in the power distribution of adjacent fuel rods and necessitates the use of operating rules to reduce the risk during start-up after refuelling or after control rod sequence exchange and on the control rod withdrawal speed in the high power region when the fuel is not pre-conditioned. Today, these rules are less important due to the use of remedies such as Zr liner fuel in BWRs.

Guidelines for prevention of severe degradation

Fission product release from failed fuel and severe degradation can be minimised by reducing the power level of the failed rods. In BWRs, it is often possible to locate the region or regions of the core that contain failed fuel employing the flux tilting method. Once those regions have been identified, it is possible to reduce the power of the fuel assemblies in those areas by selective placement of control blades. This practice is mainly applied to a detected leaking Zr liner or other sensitive fuel as early as possible in order to prevent severe degradation.

A set of guidelines or recommendations has been formulated by the EPRI to prevent the formation of secondary defects, and to limit the consequences of degradation should a secondary failure occur. The guidelines recommend: (a) close monitoring of primary failures using the key indicators, (b) prompt identification of the core location containing the failures through flux tilting and (c) local power suppression. GE has also issued similar guidelines. To prevent further fuel degradation, additional limits on normal operational ramp rates when failed fuel is present are also imposed by some utilities based on their own experience. For example, a French utility stops load following if the coolant activity reaches the surveillance limit value (0.12 μCi/cm^3 equivalent ^{131}I). In an extreme case, plant derating or early shutdown may be advisable in order to mitigate the effects of extensive degradation and loss of fuel. The effectiveness and impacts of these various mitigating actions on the subsequent degradation of failed barrier and non-barrier BWR rods are under discussion (see also Section 4.1.1).

Water chemistry controls

Effective control of water chemistry in the primary system is crucial for maintaining good fuel performance. Because of the possibility of intrusions from connected systems such as the spent fuel pool, control of water chemistry in these connected systems is equally important.

The primary water chemistry concern for fuel performance is the potential for corrosion-related cladding failures and associated excessive hydrogen pickup with resultant cladding embrittlement. Operating experience shows that the likelihood of excessive cladding corrosion depends greatly on reactor water chemistry conditions. For example, CILC fuel failures have occurred in BWR plants with high concentrations of copper in the feed water and/or chemical transients. Other chemistry intrusions during operation can similarly increase the chances of failures, especially if existing cladding and water chemistry conditions are conducive to corrosion.

Corrosion-related cladding failures have affected BWRs much more than PWRs. Recent experience has shown, however, that at high burn-up, PWR cladding corrosion can exceed its design limits, especially when the fuel is utilised under relatively high duty conditions and at high water temperatures. The boundaries of acceptable regimes of water chemistry, cladding materials, operating temperature and heat flux have not yet been fully defined except for specific local applications. However, EPRI, together with utility and industry specialists, has developed a set of water chemistry guidelines. These guidelines take into account the current state of knowledge as concerns how water chemistry affects the entire system, including the fuel. Water chemistry specifications are also provided by most nuclear steam supply system vendors and fuel suppliers.

Moreover, several water chemistry changes such as elevated lithium concentrations in PWRs, hydrogen water chemistry in BWRs and zinc injection in both BWRs and PWRs, have recently been introduced or are being considered to optimise light water reactor plant performance through a reduction of radiation fields and minimisation of irradiation-assisted stress corrosion cracking (IASCC) or

intergranular stress corrosion cracking (IGSCC) of plant components. These changes have potential or known implications for fuel performance and need to be monitored to provide information on whether or not these water chemistry changes exert significant effects on fuel performance.

Particular features of water chemistry control in VVER reactors should be mentioned. In order to limit free oxygen and maintain optimum pH in the primary system, VVER reactors operate with the water coolant alkalised by a mixture of ammonia and potassium hydroxide. Limitation of free oxygen produced by radiolysis decomposition of water is achieved by an equilibrium shift in the radiolysis reaction through the addition of hydrogen to the primary coolant. In VVER reactors, hydrogen is directly obtained in the primary coolant through radiation decomposition of ammonia. Under irradiation, ammonia dissociates with the formation of hydrogen and nitrogen. Excess hydrogen (30-60 mL/kg) is provided for suppression of coolant radiolysis, as a result of which the oxygen content is kept below 5 μg/kg. The alkalised mixture of potassium hydroxide and ammonia also provides the narrow range of pH which ensures low material corrosion. The alkali concentration is co-ordinated with the boric acid content. Recently, a new water chemistry control with continuous hydrazine hydrate ($N_2H_4 \cdot H_2O$) dosing of the coolant has been developed to replace the standard ammonia-boron-potassium regime. At reactor power operation hydrazine is quickly decomposed into N_2, H_2 and NH_3.

Long-term operational experience without deviation of water chemistry control has not revealed any case of fuel failure due to zirconium alloy corrosion. Oxide layers on fuel cladding irradiated at a burn-up of 45-49 MWd/kgU are usually less than 3-5 μm thick (additional discussion can be found in Section 4.1.1). The internal hydrogen content of irradiated fuel cladding is about 0.008%. However, experience has shown that violation of water chemistry control by intrusions into the primary circuit of organics can affect fuel behaviour and induce leakage of some fuel elements as a result of mechanisms such as accelerated corrosion, friction corrosion and nodular corrosion. Fretting by intrusion of metal debris may add to these effects.

Fuel loading/unloading practices

Interference between PWR fuel assemblies during loading and unloading operations has resulted in hang-ups between spacer grids that damaged the grids and at times the fuel rods. The causes of the interference have included spacers prone to hang-up, bowed fuel assemblies and handling practices.

Whereas BWR channel bow is no longer expected to be a significant fuel performance problem, a problem far less understood is PWR bow. The major consequences of PWR bow and twist are difficulties in positioning the fuel in the core. As remedies, some utilities and vendors have developed special tools to provide help during handling. These tools assist in positioning the bowed and twisted fuel assembly in the core and correct occasional misalignment of the bottom nozzle assembly with respect to the lower internals fuel alignment pins. Appropriate actions have also been taken to improve handling practices and procedures. Fuel handling activities must be performed by well trained and experienced personnel. Moreover, all fuel vendors have improved the spacer design to be less prone to hang-up, primarily by chamfering the corners.

Most LWR use load control during fuel handling, to monitor for indications of hang-up and to ensure that the load limit does nor exceed the pre-assigned value.

Current practice for handling, storage and disposal of failed fuel

Some utilities (France, Sweden) do not have specific conditions for the handling and storage of leaking fuel. Leaking fuel assemblies are stored in the spent fuel pool without special precaution.

In Japanese utilities, leaking fuel assemblies are contained in leak-tight containers and kept in the cooling pond of the plant.

For VVER, current practice is to store failed fuel assemblies after discharge in special containers. Transportation of failed fuel assemblies should also be carried out in these containers, although this lowers the transportation cask capacity and increases storage and transportation costs.

3.5 Fuel performance modelling

3.5.1 Important issues

The first action of the Task Force of the Nuclear Science Committee Activities [96] in the field of fuel behaviour was to identify topics and potential authors to review the then-current state of understanding, and to identify priority areas where further work was required. This was accomplished and a report addressing the following topics was issued [97]:

- *Thermal performance*. The thermal conductivity of LWR fuel has been studied extensively. Clearly, local measurements at different burn-up levels and temperatures are needed in order to better determine the influence of the accumulation of fission products and changes in stoichiometry. All details of the degradation of the local thermal conductivity require better experimental support which must be accomplished through a better theoretical understanding. The thermal conductivity of the rim structure is unknown and needs to be investigated. Local measurements of irradiated fuel are planned at the Institute for Transuranium Elements. All investigations should be extended to include gadolinia-doped fuel. The surface morphology and composition of LWR fuel and cladding at high burn-up should be investigated. The gap conductance at high burn-up requires further clarification, as does the thermal conductivity of zirconium oxide.

- *Fission gas release*. The advanced software developed for advanced chemistry by *ab initio* computations could be used to compute the chemical state of the xenon atom in the UO_2 matrix in various interstitial, substitutional or single- or multi-vacancy sites. The knowledge of the energy of each configuration will allow a better description of the precipitation kinetics of the fission gas in the irradiated fuel.

- *Fission product swelling*. The distinction between inexorable solid fission product swelling which is predominantly a function of burn-up and fission product accumulation, and gaseous swelling which is also dependent on high power operation must be made. It is considered that although no further data are required for solid fission product swelling and that a simple correlation is all that is necessary, further data are required on specific aspects of fission gas swelling. Discussion has concentrated on intergranular swelling, as this is the major contributor to dimensional changes, and although a useful database is available to develop and validate models, additional data are desirable, especially for application to new fuel products. There is however, a second-order contribution to fuel swelling from intragranular porosity, which can be significant under certain circumstances. Until now little attention has focused on this contribution, but as intergranular swelling better understood and quantified, so it will become necessary to direct attention toward the smaller but more numerous intragranular bubble population and its contribution towards pellet dimensional changes.

- *Stress corrosion cracking*. The estimation of the stress (or stress intensity) sustained by the cladding and its time dependence are extremely complex calculations that require further development. The chemical aspects of the process are poorly understood and a concentration

of efforts on theoretical and experimental studies would be most beneficial. More experimental work on the identification of the transgranular crack propagation mechanisms is also needed. The incorporation of solutions to the problem has greatly reduced the frequency of failures, rendering the economic incentives for continued research in this field less evident. However, the development of physico-chemical models for the prediction of operational thresholds is not possible within the current understanding. The assessment of future limits to performance requires an improved understanding of the mechanism.

- *Water chemistry*.
  - Water chemistry practice:
    - ⇒ To minimise activity transport, clad and out-of-core corrosion, it is recommended to use a modified Li-B water chemistry with a pH as close as possible to 7.2 in PWR reactors, and to use a co-ordinated K-B water chemistry with a pH_T of 7.0-7.1 in VVER reactors.
    - ⇒ Evaluation of alternative pH controlling agents, especially potassium hydroxide for PWR application.
    - ⇒ A further study of the influence of zinc on the activity transport is needed.
    - ⇒ Evaluation of the behaviour of zircaloy-4 in VVER water chemistry under normal operation and accident conditions, including the influence of the oxygen scavenger used on corrosion and hydriding (influence of nitrogen and ammonia).
    - ⇒ It is recommended to continue the comparative study of ammonia/hydrazine as an oxygen scavenger.
  - Cladding corrosion:
    - ⇒ More observations on cladding corrosion from power reactors and loops in MTR reactors are needed and an effort must be made to identify the specific influence of each parameter (temperature, fabrication route, annealing temperature, tin content, alkali concentration) on corrosion.
    - ⇒ Special attention should be paid to the in-core assessment of irradiation parameters (linear rate, temperature).
  - Corrosion modelling:
    - ⇒ The effect of radiation and energy deposition on the dissolution and deposition of oxide and hydroxide should be further studied.
    - ⇒ More mechanistic models of corrosion must be developed, starting from the observed kinetics of corrosion on well-characterised cladding.
  - On-line monitoring of water chemistry:
    - ⇒ Further development of the on-line monitoring of water chemistry is needed with appropriate sensors and the correlated modelling.

- *Hydrogen in cladding*. The extension of a fuel pin lifetime is not only of economic interest; it is beneficial for the utilisation of materials and also reduces the amount of radioactive waste. The irradiation of fuel pins up to a high burn-up is only possible if the soundness of the cladding can be monitored. In particular, the presence of high hydrogen concentrations can limit the cladding integrity. Therefore, measurement techniques are needed to detect hydrogen in fuel pin cladding. However, information concerning non-destructive methods to measure hydrogen concentrations in metals is very scarce. Neutron radiography appears promising. Research on hydrogen measurement in metals using non-destructive techniques should be encouraged.

- *Failed fuel*. Experimental and modelling activities in the area of detection of degradation processes should aim at the following results:

  – Identification of relevant processes and related available data. When specific data are needed, quality tests should be performed.

  – Review of computer models which already incorporate algorithms for failed fuel performance.

  – Predictability of selected models against actual data.

  – Connection between modelling of failed fuel behaviour and fuel failure characterisation based on water radiochemical fingerprints.

  – Recommendations on model upgrading, *i.e*. processes to be included and relevant data sets.

- *Spent fuel*. For almost all present issues practical solutions have been found. However, for the storage of high burn-up fuel and plutonium/uranium mixed fuel under wet or dry storage conditions, mechanical data such as tensile properties, fracture toughness, creep strength, etc., of the corresponding spent fuel must be obtained because of the property change in the cladding due to irradiation, oxidation and hydriding. During dry storage of spent fuel in an inert atmosphere, creep deformation is considered to be the critical degradation mechanism of spent fuel. On the other hand, for the dry storage method in an air-containing atmosphere, oxidation of UO_2 and the subsequent deformation of fuel rods due to volume expansion becomes a critical factor as concerns fuel integrity of defective rods.

  As already pointed out, the oxidation of irradiated UO_2 is different from that of un-irradiated UO_2, and oxidation data or irradiated UO_2 below 200°C are needed to evaluate the allowable storage temperature of the defected fuel rod during dry storage.

- *Quality assurance*. The process of verification ensures that the final model, calculation route or code performs the calculation as defined in the functional specification. At the highest level of quality assurance this entails a line-by-line check that the physics, mathematics and coding are free from error. In most fuel performance codes used for safety analysis this requires a check by persons independent of the original developers. Although fuel in nuclear reactors has proven to be highly reliable in its performance and safety, reactor operation has often been supported by rather generous bounding operating conditions. In the future the requirements will be more onerous. The economic requirement to increase efficiency means that fuel performance must be calculated accurately on a best-estimate basis. To do this requires good fuel performance computer codes validated by high quality data.

3.5.2 Identification of available experimental data

The second report commissioned by the task force and issued by the NEA was a review of existing data that could be made available to fulfil the aim of improving code performance. The report concentrated primarily on data produced in the Joint Programme carried out by the Halden Reactor Project, Norway [98].

Conditions in the Halden reactor are particularly well suited to the study of fuel performance. The boiling conditions ensure a constant coolant temperature, and hence a well-defined boundary condition from which to assess thermal performance from measurements of centreline fuel temperatures. Also, the low system pressure of 32 bar and low fast flux ensures negligible clad creep down, thus removing one parameter from through-life assessments of fuel dimensions and temperature. When more prototypic conditions are required, however, dedicated in-pile loops are available to simulate the thermal-hydraulic conditions of temperature and pressure as well as neutron flux spectrum for PWRs, BWRs and most recently, advanced gas-cooled reactors (AGCRs) as operated in the UK. The report outlined some of the experiments that have been performed in the Halden reactor and the most important data that they have provided, which are available for use in fuel performance studies. As to be expected from a project that has many years of experience and data production, several reviews of individual topics have already been written. This present report made extensive use of these with the aim of demonstrating the extent of the information available collated in a form that is most useful for the development of fuel performance codes and their validation.

The data can be divided into a number of categories depending on the use to be made of them. In this respect, the data are not of universal interest. The simplest division is into three broad categories:

1) Data useful for model development and validation, *e.g.* radial flux depression, fuel creep, fuel densification and swelling and clad creep down. These are the unsung needs of the code developer, not often apparent in code predictions but essential to obtain a good description if reliable predictions are to be obtained. Very often these data require special measuring techniques and non-prototypic rig designs.

2) Data of direct relevance to licensing requirements, *e.g.* fuel temperatures, stored heat, fission product release and rod internal pressure, waterside corrosion. Such data are of particular use for validation purposes.

3) Data for fuel development and optimisation, *e.g.* performance of fuel variants and new cladding materials, effect of changes in fuel design. These data are of most interest to fuel vendors in developing and supporting new products.

Within these categories, the report discussed data under the following phenomenological headings:

- Radial flux depression.
- Thermal performance.
- Fuel densification and swelling.
- UO_2 grain growth.
- Fission product release.
- Clad properties.

- Pellet-clad mechanical interaction (PCMI).
- Integral behaviour.
- High burn-up effects.

The report reviewed experiments that addressed single effects, *i.e*. where single parameters were isolated for study, (fuel centre temperature as a function of fuel pellet-to-clad gap), and experiments which addressed integral behaviour, where several effects were studied simultaneously, (fuel temperature, fuel and clad axial extension and rod internal pressure as a function of power and burn-up). In addition to Halden Project data, the report briefly reviewed data from certain Studsvik ramp tests and from the three Risø fission gas release projects. These had already been shown to be compatible with Halden experiments, particularly in the areas of PCI/SCC failure and PIE of ramp-tested fuel.

Despite the comprehensive nature of the data available as outlined in the report, it was clear that there were a number of areas where further experiments were necessary. With the move to higher discharge burn-up, it is necessary to extend the data to encompass the extremes of burn-up and power expected in commercial reactors. This implied a progressive extension of well qualified data in excess of 70 MWd/kgUO_2. New effects were being discovered at these levels of burn-up and further data were required on such topics as: the rim effect, further definition of the effect of burn-up on fuel thermal conductivity, clad corrosion and hydriding and clad mechanical properties. Although there were data on temperature changes during reactor scrams, for transient analysis there was a need for data on the evolution of temperatures during rapid power changes. There were (and still are) few data on this last topic and there is clearly a benefit to be claimed in reactivity faults, for example, to exploit the lag between power increase and the consequent increase in temperature.

The report supported the task force initiative to assemble an International Fuel Performance Experiments (IFPE) database, and recommended the inclusions of experimental data identified in the report from all three international programmes.

The database is restricted to thermal reactor fuel performance, principally with standard product zircaloy-clad UO_2 fuel, although the addition of advanced products with fuel and clad variants is not ruled out. Recent additions to the database include MOX fuel, (U,Gd)O_2 and defect fuel. Data include normal and off-normal behaviour, but not accident conditions entailing melting of fuel and clad resulting in loss of geometry. Of particular interest to fuel modellers are data on: fuel temperatures, fission gas release (FGR), clad deformation (*e.g*. creep-down, ridging) and mechanical interactions. In addition to direct measurement of these properties, every effort is made to include PIE information on the distribution of: grain size, porosity, Electron Probe Micro Analysis (EPMA) and X-ray Fluorescence (XRF) measurements on caesium, xenon, other fission products and actinides.

Emphasis has been placed on including well-qualified data that illustrate specific aspects of fuel performance. For example, cases are included which specifically address the effect of gap size and release of fission gas on fuel-to-clad heat transfer. Also in the context of thermal performance, the effect of burn-up on UO_2 thermal conductivity has been addressed. This is illustrated by cases where fuel temperatures have been measured throughout prolonged irradiation and at high burn-up where sections of fuel have been re-fabricated with newly inserted thermocouples. Regarding fission gas release, data are included for normal operation and for cases of power ramping at different levels of burn-up for fuel supplied by several different fuel vendors. In the case of power ramps, the data include cases where in-pile pressure measurements show the kinetics of release and the effect of slow axial gas transport due to closed fuel-to-clad gaps. Supplementing these in-pile studies, data sets of out-of-pile annealing studies measuring FGR under well-defined conditions of temperature and time are also included.

To date, data sets of about 502 rods/samples from various sources encompassing PWR, BWR, PHWR and VVER reactor systems have been included, as shown in Table 7.

Table 7. Fuel behaviour experiments in the public domain IFPE database (status March 2003)
http://www.nea.fr/html/science/fuel/ifpelst.html

Experiment	Cases
Halden irradiated IFA-432	5 rods
Halden irradiated IFA-429	7 rods
Halden irradiated IFA-562.1	12 rods
Halden irradiated IFA-533.2	1 rod
Halden irradiated IFA-535.5 &.6	4 rods
The Third Risø Fission Gas Release Project	16 rods
The Risø Transient Fission Gas Release Project	15 rods
The SOFIT VVER Fuel Irradiation Programme	12 rods
The High Burn-up Effects Programme	81 rods
VVER rods from Kola-3	32 rods
Rods from the TRIBULATION programme	19 rods
Studsvik INTER-RAMP BWR Project	20 rods
Studsvik OVER-RAMP PWR Project	39 rods
Studsvik SUPER-RAMP PWR Sub-programme	28 rods
Studsvik SUPER-RAMP BWR Sub-programme	16 rods
Studsvik DEMO-RAMP I BWR	5 rods
Studsvik DEMO-RAMP II BWR	8 rods
Studsvik TRANS-RAMP-I BWR	5 rods
Studsvik TRANS-RAMP-II PWR	6 rods
Studsvik TRANS-RAMP-IV BWR	7 rods
REGATE FGR and cladding diameter during and after a transient at Bu ≈ 47 MWd/kg	1 rod
CEA/EDF/FRAMATOME Contact 1 & 2	3 rods
AEAT-IMC NFB 8 and 34	22 samples
CEA/EDF/FRAMATOME PWR and OSIRIS ramped fuel rods	4 rods
CENG defect fuel experiments	8 rods
CANDU elements irradiated in NRU	36 rods
Siemens PWR rods irradiated in GINNA	17 rodlets
CEA failed PWR rods irradiated in SILOE: EDITH-MOX 01	1 rod
CNEA six power ramp irradiations with (PHWR) MOX fuels	5 rods
BN GAIN (U,Gd)O_2 fuel	4 rods
INR Pitesti – RO-89 and RO-51 CANDU fuel type	2 rods
HRP IFA-597.3 rods 7, 8 and 9 (cladding degradation, FCT, FGR at Bu ≈ 60 MWd/kgUO_2	3 rods
HRP IFA-534.14 rods 18 and 19 (EOL FGR and pressure, grains size of 22 and 8.5 micrometers and Bu ≈ 52 MWd/kgUO_2	2 rods
BR-3 High Burn-up Fuel Rod Hot Cell Program (DOE/ET 34073-1, Vol. 1 & 2)	5 rods
IFE/OECD/HRP FUMEX-I Cases 1-6	6 rods
IMC(UK) swelling data from ramping CAGR UO_2 fuel in the Halden Reactor	13 rods
NRU MT-4 and MT6A LOCA simulation tests	33 rods
Total	**503 cases**

3.5.3 Thermal performance

An international workshop on Thermal Performance of High Burn-up LWR Fuel was held on 3-6 March 1998 at CEA Cadarache [99], co-organised by the OECD NEA in co-operation with the IAEA and hosted by the Département d'Études des Combustibles (DEC). Relevant findings from this workshop are summarised hereafter.

Fuel thermal conductivity

- *Fuel thermal conductivity correlations*. The initial thermal conductivity correlations are well established for almost all fuel oxides that are loaded in commercial reactors. The influence of parameters such as temperature, stochiometry, plutonium content and gadolinium content are relatively well known. Some models are able to account for all these parameters simultaneously.

- *MOX fuels*. The non-homogeneity of MOX fuel can be accounted for using mathematical homogenisation techniques. However, even for high Pu content the fuel thermal conductivity is close to the uranium oxide fuel conductivity, providing O′M close to 2000. Participants seem to agree on a degradation of 4-5% per 10% Pu. However, it was shown that a deviation from stochiometry has a stronger effect.

- *The burn-up effect*. The burn-up effect on fuel thermal conductivity has been assessed up to 80 MWd/KgU, thanks to in-pile centreline temperature measurements and out-of-pile thermal diffusivity measurements. There is some agreement between these two methods.

- *Cp variation with burn-up*. Analysing shutdown temperature records in the Halden reactor, a slight increase of the Cp with burn-up is likely to occur. Nevertheless, the discussion outlined that the Cp variation with burn-up could be neglected. The experimental data expected in the near future will certainly allow verifying this assumption.

- *Heat transfer in the rim*. The rim thermal conductivity evolution is not yet clearly known. Thermal degradation due to the onset of numerous micrometer porosities could be balanced by the cleaning of the matrix subsequent to this porosity build-up. In order to investigate the net effect of the rim structure, samples irradiated to high burn-up and temperatures lower than 800 K are required. Other questions are still open concerning the rim fission gas release and the rim volume variation during the porosity build-up.

- *Further needs*. A lack of data is identified regarding the burn-up degradation at temperatures higher than 1 800 K. A decrease of the conductivity improvement due to the electronic heat transport is likely to occur with burn-up. This effect was already observed when increasing the gadolinium content.

Gap conductance

- *Pellet fragmentation and relocation*. The stochastic nature of this phenomenon prohibits analytical modelling of gap conductance. Reliance must be placed on benchmarking models against in-pile data. There is no general consensus as to a definitive formulation for gap conductance. Fortunately, a large database exists and providing this is employed, there are limited difficulties in formulating an adequate gap conductance model which correctly reflects the effects of gap dimension, fill gas composition and pressure.

- *Surface roughness*. In principle this should be an important contributor to gap conductance through its inhibiting heat flow effect. In practice, at both the beginning of line and at high burn-up, there appears to be a little effect on heat transfer between the fuel pellet and the cladding.

- *Formation of inner clad oxide layer*. At high burn-up, when the fuel and clad have been in intimate contact for some time, an inner oxide layer is formed, 6-10 microns thick. It has been shown that this has a complex structure, which can include zirconium oxide, uranium and caesium, depending on the heat rating and burn-up. It is supposed that its contribution to gap heat transfer is small and if anything, beneficial, as it would tend to eliminate effects due to surface roughness and misaligned pellet fragments.

- *Closed gap conductance*. There is evidence to suggest that under these conditions, heat transfer is good and substantially independent of the fill gas composition and pressure, since it corresponds to a solid bound between fuel and cladding. There is some debate as to whether or not the conductance depends on interfacial pressure.

3.5.4 Fission gas release

A workshop on fission gas release was held at CEA Cadarache, 26-29 September 2000, organised and hosted under the same arrangement as before [100]. The objective of the workshop was to emphasise more recent developments, from both the experimental and modelling points of view. The areas covered by the seminar included: diffusion coefficient of rare gases including helium, properties of bubbles, the effect of irradiation on re-solution and diffusion, FGR as a function of operating conditions, modelling and code validation. Relevant findings from this workshop are summarised hereafter.

Fission gas behaviour is a leading parameter in the overall fuel rod performance at high burn-up. A sharp increase in fuel temperature due to thermal feedback, cladding loading due to high temperature fuel swelling or an end-of-life fuel rod pressure increase are just some of the many possible consequences that may be ascribed to the behaviour of inert gases. For these reasons, the subject has been dealt with since the first steps of the nuclear industry and many basic data have become available over the years. However, there are still areas which require further investigation.

The need to understand and anticipate the way fission gases behave continues to justify the implementation of increasingly sophisticated experimental techniques (both in and out-of-pile). Their results, particularly over the past ten years, have called for more mechanistic modelling to confirm interpretations, specify and estimate physical interactions and extrapolate calculations to different operating conditions. It should be noted that in recent years the implementation of complex numerical schemes or atomistic simulations is being improved due to extended computer capacity.

Feedback from experience

It was concluded that an enhancement of fission gas release at high burn-up (>50 MWd/kg) occurs both in steady-state operation and in transient overpower, but that there is no accepted phenomenon to explain this. One consequence of this was that the well established Halden 1% FGR criterion relating fuel centreline temperature to burn-up overestimated the onset temperature at these levels of burn-up. That is, the temperature for the onset of release at high burn-up was *lower* than predicted by this criterion. It has been observed that high burn-up fuel contains a region of restructured fuel microstructure close to the pellet periphery, the so-called “rim” structure. It is tempting to use this

as a reason for the enhanced release, but a direct correlation can not be made. Indeed, a measure of the ratio of released krypton and xenon isotopes implied that their origin was the hot central regions of the fuel and not the cold plutonium-rich restructured region in the pellet rim. The implication of this observation was that the restructured rim served mainly to increase the thermal resistivity of the fuel, thus increasing fuel temperatures.

A discussion of this dilemma continued in the second session on *Basic Mechanisms*. Investigations showed that this rim structure consisted of a refinement of the original ~10 micron diameter grains into ~0.1 micron diameter grains and the introduction of a micron-sized population of bubbles which could account for a swelling up to ~10 vol.%. In addition, the fission gas concentration in the matrix fell to a low level. The impression of most workers was that the shortfall in fission gas resided in the bubbles and had not been released from the fuel, however the exact distribution of gas remained uncertain. The fission gas release from the rim was not more than 15-20%, showing a high retention capacity for such a restructured material. The mechanism of rim formation was not clear; one suggestion was that the build-up of irradiation damage caused the grain refinement and that this was followed by the collection of gas into the porosity. Alternatively, it has been postulated that the porosity was the first to form and that the sub-micron grains were nucleated from the pore surfaces. It remains a matter of debate whether this rim restructuring is beneficial or detrimental.

As a digression from fission gas, it was clear that helium generation in long term storage of high burn-up fuel can pose a significant problem, in particular for high burn-up MOX. Further data are required on low temperature helium diffusion coefficients.

Analytical experiments

The session began with two presentations describing a novel method of determining the disposition of gas between the matrix and the grain boundaries. Such studies complement those performed with X-ray Fluorescence (XRF) and EPMA and provide vital information for modellers. The techniques still need refining, particularly regarding the effect of small intragranular bubbles on the results, but promise an evaluation of the grain boundary capacity for gas prior to and during interlinkage. As mentioned previously, Halden has obtained data from high burn-up fuel which suggests that the temperature for the onset of FGR is lower than previously expected. It is clear that further data are required to substantiate this observation. In addition, there is a need to obtain further data on MOX fuel to compare it with UO_2 fuel performance under identical conditions.

The phenomenon of stable fission gas release is now qualitatively well understood, and this has been achieved with the additional help of studies on the release of the short-lived radioactive species. The dominant processes are the single gas atom diffusion through the grains to grain boundaries and the interlinkage of porosity allowing escape into the rod free volume. In addition, several other processes occur in parallel including intragranular bubble formation and irradiation-induced resolution. There also exists the possibility of release by other processes, including grain boundary sweeping and bubble migration. Although it is possible to qualitatively predict the effect of parameters and design variables such as grain size, power and ramp conditions on release, there is less confidence in quantitative predictions. For this reason there is still a need for well-qualified data to refine existing calculation methods, in particular the threshold for release in the burn-up range above ~30 MWd/kgUO_2.

Enhanced release at high burn-up can cause the rod internal pressure to exceed the coolant pressure, the effect of which requires attention. So far, experimental data suggests that the gap does not re-open by clad creep-out and positive feedback does not occur. However, the data are sparse and further experiments are necessary.

Industrial modelling and software packages

It was made clear that empirical modelling can be very valuable, but is limited in applicability and is essentially only valid within the confines of parameters and irradiation conditions covered in the database on which it is developed. Modellers were also cautioned about employing multiple mechanistic models and expecting to obtain good predictions by using appropriate fitting parameters. There is a case for independent assessment of mechanistic models and their supporting data before consideration for inclusion within fuel performance codes. The requirement for further data comparing UO_2 and MOX behaviour was re-affirmed in a paper by Struzik (CEA) which showed that there was a significant difference in behaviour in ramp test above 30 MWd/kg. Below 30 MWd/kg the differences in behaviour could be explained in terms of the radial power profile but at higher burn-up FGR and swelling in MOX was greater than expected.

A very detailed (mechanistic) fission gas release model is incorporated in the SPHERE-3 fuel code, which treats sphere-pac fuel. The model is based on several classical concepts and has been discussed in detail with experts; it should thus be considered as a model representing the state of the art. However, verification has just begun and the numerous parameters will be very difficult to adjust to the many different situations.

The Russian START-3 model is a combination of mechanistic and empirical approaches. The formation of this structure near the rim has an impact on the temperature level in the fuel and is responsible for the enhanced fission gas release observed at high burn-up. The release from the outer zones, in which more Pu is fissioned, is consistent with measured Xe-to-Kr ratios.

3.5.5 Pellet-clad interaction

Pellet-cladding mechanical interaction (PCMI)

Two contrary mechanisms lead to a mechanical interaction between pellet and cladding, namely, cladding creep-down and fuel swelling. Once the fuel-clad gap has closed, after two to three cycles, the compressive stress experienced by the cladding due to the system pressure is reversed to a tensile stress induced by continued fuel swelling. From this point, the fuel swelling is the main factor contributing to radial and axial constraints on the cladding. Enhanced clad strain is observed in the region of the pellet ends, where ridging is observed caused by the “wheat sheaf” shape adopted by the underlying cracked pellet due to the influence of the large radial temperature gradient. However, clad strain is reduced in the case of a compliant and dished fuel pellet. In these cases, clad deformation is reduced as fuel swelling and thermal expansion is accommodated by dish filling. This requires remnant volume to accommodate the expanding pellet and a relatively rapid irradiation creep rate of the fuel material. At high burn-ups, it is possible that fuel swelling could exhaust the remnant volume offered by pellet dishing; in this event, and in the absence of other effects, it may be expected that clad deformation would again accelerate, thus increasing the propensity of clad failure.

Pellet-cladding chemical interaction (PCCI)

After the fuel-clad gap has been closed for a period of time, it has been observed that a chemical bond forms between the internally oxidised cladding and the fuel. The composition can be basically described as a mixed Zr-U (Pu) oxide, containing up to 3-4 w/o Cs according to EMPA results. The beneficial aspect of this is that the thermal conductivity of the fuel-clad interface is improved over that of the original gas gap between the two components. This in turn leads to stabilised fuel temperatures

and a reduction in thermal feedback effects caused by fission gas release. The implication for PCMI depends largely on the mechanical properties of this bonding layer. For strong mechanical bonding, a detrimental aspect is that it can lead to strain concentration in the cladding ligaments situated immediately adjacent to pellet cracks. In the event of pellet expansion in an over-power transient, strain is concentrated in these ligaments and premature failure can occur through ductility exhaustion, particularly in the vicinity of the pellet ends. For weak bonding and soft mechanical properties, the bonding layer can act as a lubricant, thus minimising stress and strain concentrations in the cladding. Therefore a full understanding of this bonding layer is necessary to predict the likely outcome of fuel swelling and pellet expansion in transients. It is possible that the properties of the bonding layer are determined by its composition and structure, and this in turn could be a function of the irradiation history by way of temperature and fission product release and migration.

High burn-up fuel restructuring

At a pellet average burn-up of ≥60 MWd/kg, the local burn-up within ~100 μm of the pellet surface is increased by a factor 2 or 3 depending on the flux spectrum of the reactor. At the same time and in the same location, ceramography of discharged fuel has shown the presence of a large population of pores some 0.5-1 μm in diameter and a refinement of the original UO_2 grain size from typically 10 μm to 0.1-0.3 μm diameter. This small grain-sized re-crystallised structure is best observed by Scanning Electron Microscopy of a fractured specimen where the surface morphology takes on a distinctive cauliflower-like appearance. Because of its location at the pellet surface, this has become known as the rim effect. This is a misnomer, however, and the phenomena should properly be referred to as High Burn-up Structure or HBS. Observations have shown that the rim has mechanical properties different from those of the original pellet. In particular, it appears to be more resistant to crack propagation and deforms more easily under an applied stress. Like the bonding layer described before, the properties of this rim will have an important influence on PCMI at high burn-up. With the reported properties, in this case, it should provide an alleviation of PCMI under normal behaviour and during conditions of operational transients. However, there is a suspicion that its properties may change during rapid transients leading to enhanced PCMI, thus contributing to clad failure and fuel dispersion during RIA. This issue is the subject of substantial R&D programmes throughout the world using pulse reactors to generate the fast transients proposed as the event initiators.

Stress corrosion cracking

Initial research identified iodine as the most probable active species for stress corrosion cracking (SCC). Subsequent observations indicated that this type of failure was generic to zirconium alloy clad fuel that was subjected to significant power increases. Today, it is grouped with other types of pellet-clad interaction (PCI) failure mechanisms observed to occur in zirconium alloy fuel cladding.

Power changes are inevitable during the operation of nuclear power plants; hence, the possibility of a large number of fuel failures ensured a large allocation of resources to better understand and solve this problem. Cures were attempted based on the characteristics learned about the SCC process in zirconium alloys. Three types of solutions were widely applied: internal coatings (graphite or siloxane), barrier cladding (pure zirconium) and, equally important, a restriction on the reactor power changes and refuelling schedules. The incorporation of these solutions greatly reduced the frequency of SCC failures. Today, the number of SCC failures is well below the number of failures due to coolant debris.

In the event of a primary failure and ingress of coolant into the fuel rod, secondary failures may occur due to excessive local clad hydriding and additional clad stress due to fuel oxidation. A scenario

has been envisaged where the formation of a secondary failure results in a progressive deterioration of the cladding, leading to extended axial cracks along the length of the fuel rod. Such cracks have been observed in operating commercial BWRs.

Current manufacturing remedies to avoid failure by PCMI

Cladding without the liner is manufactured to achieve an optimised combination of grain texture and grain size, which improves resistance to pellet-to-clad interaction (PCI). Cladding with pure zirconium on the inner surface provides additional protection against PCI. Iron enhancement of the liner precludes the risk of excessive activity release in the unlikely event of cladding tube failure. Special low-temperature annealing processes used during manufacturing increase the resistance to both nodular and uniform corrosion.

Rods with niobia- or chromia-doped fuel pellets and pellets doped with different alumino-silicates, the so-called soft pellets, have been manufactured and supplied as a possible PCI remedy fuel. It can withstand considerably larger power ramps without failure than is the case for standard un-doped fuel. Enhanced creep of the doped fuel into large voids associated with controlled fabrication porosity as well as into cracks and pellet dimples (dishes) was confirmed to be the mechanism responsible for the improvement. These references show that the presence of additives to standard fuel can affect the swelling and creep properties. Thus, to proceed with modelling of these and other variants, *e.g*. gadolinia-doped fuel and MOX fuel, requires further dedicated experiments and modifications to the established principles of fuel property models.

3.5.6 Models for fuel behaviour simulation

Fuel behaviour codes analyse the thermal, mechanical and internal gas responses of fuel rod components with the goal of predicting rod condition and integrity. Modelling of thermal behaviour during normal and transient conditions includes surface heat transfer, the heat transfer across the fuel-to-cladding gap, thermal conductivity of fuel and cladding, power generation distribution in the fuel, and solution of the conduction equation.

3.5.6.1 Steady-state codes

FRAPCON-2 is a steady-state fuel rod behaviour code developed jointly by PNL and INEL for the NRC [111]. This code combines the previous codes FRAP-S and GAPCON. The FRAPCON-2 code calculates steady-state thermal and mechanical behaviour of light water reactor fuel rods under long-term irradiation conditions. It is a modular code containing sub-codes that model fuel temperature taking into consideration fuel cracking and relocation, fuel and cladding deformation (including elastic and plastic cladding deformation and creep), and rod internal pressure (including fission gas release effects). The materials property correlations used in FRAPCON-2 appear to be very adequate for modelling steady-state fuel rod thermal and pressure responses. The modelling of fuel centreline temperature was adequate above burn-up of 15 000 MWd/t. Uncertainty is increased at lower burn-up. The total code uncertainty for predicting the rod internal pressures was about ±23%, including data, input and correlation uncertainties.

3.5.6.2 Transient codes

A transient fuel code should be able to calculate the temperature increases and the accompanying time- and temperature-dependent processes expected during postulated occurrences such as LOCA,

power-cooling-mismatch accidents, and reactivity-initiated accidents, as well as processes occurring during normal operation. The code should also be general enough to treat expected asymmetries and all of the phenomena occurring, up to and including fuel melt. The FRAP-T6 code calculates fuel and cladding temperatures, cladding strain and ballooning, and internal gas pressure. The code contains several sub-codes. The FRACAS-II sub-code includes models need to calculate cladding stresses. The PARAGRASS sub-code calculates fission-product inventory. A MATPRO model called CESIOD calculates the release of caesium and iodine from irradiated fuel. A SCC model developed by EPRI was also incorporated in FRAP-T6 to calculate crack propagation, taking into account the irradiation hardening of the cladding in evaluation of the pellet-cladding mechanical interactions (PCI). The FRAP-T6 code was assessed for the fuel rod behaviour during over-power transient. The results of the assessment are as follows:

- The FRAIL-6 rod failure criteria are not realistic for modelling over-power ramp failure tests.
- FRACAS-II is the most appropriate option for simulating rod failure due to PCI for both PWR and BWR rod geometries.
- Both above models tend to under-predict failure probability for low powers and over-predict probability for high powers.
- The FASTGRASS sub-code calculates more realistic gas release fractions when it is used in conjunction with the FRACAS-II rod deformation model.
- FASTGRASS calculates more accurate gas release fraction for the burn-up greater than 15 000 MWd/t, and it over-predicts the gas release at lower burn-ups.

The FRAP-T6 code was also assessed using two Halden fuel rod experiments (IFA-508 and IFA-512) and two power burst facility tests (OPTRAN 1-1 and OPTRAN 1-2). The results of the assessment indicate that FRAP-T6 accurately calculates cladding elongation during an ATWS event and also accurately calculates the maximum cladding hoop strain during PCI.

3.5.6.3 Code comparison exercise

Today, there are several new fuel designs. Some are extensions of the current Generation II LWR, but some are more innovative and as such are classified under the generic Generation IV designs. Common features of these new designs include passive safety, high thermodynamic efficiency and proliferation-resistant fuel. Before entering full-scale commercial operation, these will require extensive qualification both in their design and in the materials used in their construction and operation. Based on the success of the Committee on Improvements of Models used for Fuel Behaviour Simulation (FUMEX-1) and its Code Comparison Exercise, the IAEA has agreed to launch an initiate project, FUMEX-2. The exercise was useful in demonstrating the strong points of the codes as well as highlighting deficiencies where improvements were necessary. As a consequence, most of the codes underwent some development during this programme. It was also apparent that many of the codes have been developed on a limited database, and that the FUMEX-1 cases provided a valuable addition. Developments pointed out, however, the limited knowledge that has been gained in the extended burn-up range (above 50 MWd/kg). Burn-up extension corresponds to a general trend in the field of fuel management, and reliable prediction of fuel behaviour at high burn-up constitutes a basic demand for safe and economic operation of nuclear fuel. This was the basis for launching FUMEX-2, which will run from December 2002 to 2006. Central to the project are selected cases in the IFPE database. This will help promote the use of the database while simultaneously generating feedback and peer review from users, thus assisting the quality assurance of the data sets within the database.

3.5.6.4 Fission gas release codes

The last fission gas models developed were presented in the Fission Gas Behaviour in LWR seminars [99,100], of which a summary is included here.

The GRSWEL module for fission gas (FG) behaviour prediction is a part of the full-scale fuel rod (FR) calculation code START-3 (Russian Federation) which incorporates the interrelated treatments of the FR mechanical and thermal physical behaviour with a view toward the investigation, justification and licensing of VVER-type fuel under normal, steady-state and transient (moderate) operation conditions. The START-3 code deals with FR accident-free performance and thus incorporates a treatment of stable fission gas, neglecting the presence of unstable gases. The following factors of the fission gas influence on the FR behaviour are taken into account:

- Deterioration of fuel rod mechanical characteristics because of additional fuel stack volumetric instability (fission gas swelling) and fuel rod internal pressure increase (fission gas release).

- Deterioration of fuel rod thermal-physical characteristics because of fuel porosity development and dilution of initial filling gas (He, as a rule) by FG products (Xe and Kr).

The original FG behaviour model used by the START-3 code is based on the solution of a two-stage diffusion problem for fission gas in UO_2 polycrystalline fuel. In this case, the fission gas release kinetics is determined by:

- Diffusive flow of FG mono-atoms to grain boundaries and subsequent quasi-diffusive percolation of the intergranular gas to fuel-free surface.

- Gas release by the thermal direct recoil and knock-out mechanisms.

- Fuel strain induced by fission products including:

  – Accumulation of solid products in fuel matrix.

  – Content of gas mono-atoms in fuel matrix.

  – Presence of gas-filled intragranular and intergranular bubbles in the fuel, under the assumption that the intragranular bubble is a small solid sphere of volume corresponding to the number of gas atoms inside.

The model enables the interrelated analysis of the different level physical process in the fuel, from micro-structural behaviour to macro-process, as applied to a wide range of fuel conditions. The physical part of the model has a flexible arrangement, allowing the capability of parametrical research and comparative analysis with different physical approaches. The structural arrangement of the model allows for further modelling development and facilitates its integration with the full-scale code. The structural isolation of the mathematical part of the model has allowed for experimental providing and parametrical optimisation of the ODE solver satisfactorily efficient for the applications within the stand-alone research programme module. At present, the model provides the application the capability of more adequate analysis of the FG behaviour under transient conditions, including RIA-type.

A computer code (TETO) was developed in the National Institute of Nuclear Research (Mexico), to carry out thermal-mechanical analysis and fission gas release in fuel rod elements of the BWR type. This program was especially designed for use in the simulations made with the Fuel Management

System (FMS) from Scandpower. Using experimental correlations, this code models the phenomena of swelling, fission gas release and fracture for fuel pellets and cladding that can occur during irradiation cycles. This code differs from other programs in that it uses a simplified model to obtain the temperature profile along the cooling channel with the supposition that there exists a two-phase flow. This profile is used to determine the radial temperature distribution. The code calculates the axial and radial temperature distributions along the fuel rod at half the distance of the pellet's length; in other words, there are as many axial points as pellets. The program also models the experimental correlation for swelling and fission gas releases and performs a thermal-elastic analysis for fuel pellets and cladding.

A new mechanistic code (RTOP) intended to predict fission product behaviour in polycrystalline UO_2 fuel under normal and accident conditions is being developed at TRINITI (Russia). The current version of the RTOP code models integral behaviour of pins with UO_2 fuel in water reactors. The code predictions of central temperature and internal pressure in the pin are in good agreement with available VVER experimental data. The code consistently takes into account the whole set of elementary physical processes affecting FP release from the fuel. The validation of separate process models was successfully performed. The validation of each model included:

- Testing of different models and choosing a model that does not qualitatively contradict the broadest set of experimental data.
- Optimisation of the model parameters against experiments with large sets of homogeneous data.
- Comparison of the model prediction with other available experiments.

New models of fuel oxidation through steam and grain growth under irradiation were developed and successfully validated. The inclusion of these models into the code allows achieving a consistent description of a broad set of integral experiments on FP release. Sensitivity studies of the gas release under isothermal irradiation conditions using different models of intergranular bubbles' behaviour have been performed. It was shown that only the model based on the production of bubbles by fission tracks and resolution of small bubbles as a whole is in agreement with the experimental data. A new model in which the "concentration barrier" appears due to the irradiation-induced resolution of grain face bubbles has been implemented in the code. The code correctly describes the conditions of formation of open intergranular porosity and the beginning of enhanced gaseous FP release over a wide range of fuel burn-up and heat generation rates. RTOP modelling of the fuel behaviour under RIA and power transient conditions qualitatively agrees with available experimental data. The validation of the models is being undertaken.

FRAMATOME has developed a fission gas release model that takes into account the important physical phenomena. In an industrial framework, the model must also be efficient, and in such a context it is kept as simple as possible. The fission gas release (FGR) model is included in COPERNIC, the FRAMATOME advanced fuel rod performance code. COPERNIC accurately predicts steady-state and transient fuel performance at extended burn-up. The code is based on the TRANSURANUS code that provides fast, accurate and numerically stable solutions. The FRAMATOME FGR model is also fast: it calculates the fission gas release fraction of an entire fuel rod history in about one second on a workstation. This is most important for anticipated statistical studies that require the analysis of a full fuel rod core. COPERNIC is validated on a large database obtained from many French and international programmes. The qualification range extends to 67, 55, 53 GWd/tM for UO_2-Gd_2O_3 and MOX fuels, respectively.

The COPERNIC thermal model was upgraded as recent high and ultra-high burn-up data became available. The FGR model had to be upgraded, as FGR strongly depends on fuel temperature. Recent

MOX data also made it possible to take into account the type of MOX fuel microstructure in the FGR model. Numerical algorithms to solve intragranular diffusion of fission gas have been analysed at the Institute for Transuranium Elements (Karlsruhe). Two were found to be superior: the URGAS algorithm based on reasonable physical assumptions, and the mathematically elegant FORMAS algorithm.

The URGAS and the new FORMAS algorithms have been incorporated into the TRANSURANUS code and have been tested extensively. In general, the difference between the two is insignificant. The URGAS algorithm requires slightly more computational time, while the FORMAS algorithm requires more storage which leads to additional read and write operations. Both effects compensate each other. Both algorithms are simple, fast, without numerical problems, insensitive to time step lengths and well balanced over the entire range of fission gas release.

Under steady-state conditions, the apparently higher fractional release in MOX fuels is interpreted with the METEOR fuel performance code from CEA (France) as a consequence of their lower thermal conductivity and the higher linear heat rates to which MOX fuel rods are subjected. Although more fundamental diffusion properties are needed, the apparently greater swelling of MOX fuel rods at higher linear heat rates can be ascribed to enhanced diffusion properties.

Under steady-state irradiation conditions, the differences observed in fission gas release values between MOX MIMAS AUC fuels and UO_2 fuels can be attributed to differing pellet temperature profiles due to the different linear heat rates MOX fuel rods generate and different fuel conductivities. The heterogeneous fuel microstructure causes a high proportion of fission gases to remain in grain boundary bubbles in a majority of medium and large Pu-rich clusters that have undergone rim-type fuel restructuring. Models developed to describe homogeneous UO_2 fuels can therefore easily be adapted to predict integral release fractions in MOX fuel rods. At higher temperatures, however, these models are at pains to describe the greater fuel swelling observed in MOX fuels. This could be an indication of these fuels' enhanced diffusion properties, although little quantitative data are available.

So as to further our understanding of fuel behaviour in this field, it therefore appears necessary to generate more data relative to basic fuel diffusion properties on the one hand, and on the other to develop models that have a use for these data and are capable of describing the local micro-structural changes observed. Such models could also be useful in so far as they provide information concerning the location and state of the fission gases, which is relevant to the modelling of accidental conditions or when models are used to extrapolate fuel behaviour to higher burn-up or heat rates.

Following Siemens' considerations, in high burn-up fuel the cold pellet rim shows a new fuel structure with small grains and xenon (Xe) loss in the fuel matrix. X-ray fluorescence studies of the rim region indicated that most of the Xe is still retained within this structure. With increasing burn-up this structure expands towards the pellet interior. Beside normal grains this grain subdivision was also seen in the inner zone of an annular pellet irradiated at moderate temperatures, particularly at higher burn-ups. The same type of structure was also observed in the plutonium-rich particles of MOX fuel in the inner regions of the pellet but with an increased grain size. Furthermore, an increased release of fission gases, which mainly come from the inner regions of the pellet despite falling fuel temperatures, is found for standard LWR fuel irradiated to high burn-up.

Other basic fuel properties, as for example fuel thermal conductivity, are dramatically influenced by burn-up. It is obvious that new FGR mechanisms have to be added to the standard diffusion theory to be able to describe these high burn-up fission gas release phenomena as well as the corresponding radial FGR profiles. Extending the standard diffusion model by generalised fission gas saturation effects in the fuel matrix enables the modelling of these new features. Moreover, the model extensions lay the basis for an accurate description of FGR enhancement at high burn-up up to very high burn-up near 100 MWd/kgU.

The extended saturation concept proves to be a mighty candidate to describe FG release at very high burn-up. It does not claim to be a new transport mechanism for the fission gases, but in some way adds mechanisms controlling the diffusion processes and therefore the effective diffusion coefficients. It should also be kept in mind that the standard diffusion model remains an effective approach for summarising the generation and resolution of the fission gas in intragranular bubbles. A change in the behaviour of these intragranular bubbles (for example a change in the resolution behaviour) would therefore necessitate a change in the effective diffusion coefficients.

The extended saturation concept offers an easy means of describing the overall behaviour. The Lassmann formula used in the concept contains an implicit time dependence (the release is connected to burn-up), which is proportional to time. Of course this approach might be weak in describing releases for very short times (seconds), where the rate of mass transport is important and a more mechanistic model is necessary, but the concept could be used in such a mechanistic model as a trigger.

From a mechanistic point of view it is necessary to understand the reasons for the observed FG behaviour on a more or less microscopic scale. It is also necessary to determine if the primitive "phase diagram" spanned by the extended saturation approach, which up to now has depended only on local burn-up and temperature, is complete or not. Nevertheless the extended saturation concept seems to be a powerful tool to describe this phenomenon using an overall macroscopic approach added to standard diffusion modelling for FG release.

3.6 Safety limits

3.6.1 PWR fuel behaviour in design basis accident conditions

A considerable world-wide effort has been expended in the experimental study and modelling of PWR fuel behaviour in accident conditions. The substantial amount of information now available allows a mature view to be formulated as to the likely response of fuel to a loss-of-coolant accident in which the emergency core cooling systems function as designed. The Committee on the Safety of Nuclear Installations (CSNI) prepared a state-of-the-art report on the behaviour of PWR fuel in a loss of coolant accident. This report is based on a survey of PWR fuel behaviour in loss-of-coolant accidents published in April 1982. It has now been considerably extended and updated to include a substantial amount of recently published information from many countries [101].

Although a major loss of coolant from a pressurised water reactor would lead to shutdown by loss of moderator, even if the control rods were not inserted, fission product decay heat generated in the fuel would raise its temperature in the absence of water coolant. The emergency core cooling system is designed to re-flood the core, but while this was happening the fuel would undergo a temperature excursion. This might be severe enough to oxidise the fuel cladding, while the combination of high temperature and stress in the cladding might cause it to distend. The fuel cladding could therefore become embrittled, or it might deform and, by closing subchannels between rods, impede the rise of the ECCS water through the core, making the temperature transient more severe. In the range of stresses and temperatures which may be produced in accidents, strains in the range 30-90% can be produced.

The behaviour of cladding in a temperature transient is strongly influenced by the temperature distribution spatially. This distribution is in turn dependent on heat transfer mechanisms at the surfaces of the cladding. A meaningful experimental simulation must therefore accurately reproduce these mechanisms. This implies the use of realistically heated fuel rod simulators, realistic conditions of surface heat transfer, and the use of multi-rod assemblies to reproduce the heat transfer conditions in the subchannels between rods. Co-planar deformation with strains up to and including those leading to

mechanical interaction between fuel rods have been demonstrated experimentally. No experiment realistically simulating a design basis LOCA, *i.e*. one with a multi-rod array and simulated re-flood cooling, has produced deformations which would inhibit quenching.

3.6.2 Safety activities on fuel behaviour

Under the auspices of the Committee on the Safety of Nuclear Installations (CSNI) a report has been issued reviewing the status of safety-related research activities in member countries [102]. This report suggested that members of a Special Experts Group on Fuel Safety Margins (SEGFSM) compile ongoing and planned fuel safety research in NEA member states with the aim of providing CSNI an overview on related R&D international programmes and projects, along with the identification of current and future needs and priorities. The main issues for the current generation of reactors are those of high burn-up performance under normal operations, LOCA and RIA conditions; the main goal for the industry is to consolidate the safety issues to bring all countries up to a licensed discharge burn-up of ~60 MWd/kg and possibly 65 MWd/kg. The principal issues requiring attention can be broken down as follows:

- *Normal operation:*
  - Fission gas release and rod over-pressure.
  - Properties of the High Burn-up Structure (HBS) at the pellet rim, its effect on thermal performance and fission gas release.
  - Cladding oxidation, hydriding and embrittlement.
- *Loss of coolant accidents (LOCA):*
  - The possibility of fuel slumping into the ballooned region; the effect of fuel-clad bonding at high burn-up.
  - Increase of pressure in the ballooned region due to fission gas release from slumped fuel.
  - Response of irradiation hardened and hydride embrittled cladding.
  - Review of the 17% Equivalent Clad Reacted (ECR) criterion.
- *Reactivity-initiated accidents (RIA):*
  - Pellet-clad mechanical interaction (PCMI) loading mechanism(s) on the cladding, the effect of the HBS at the pellet rim.
  - Effect of HBS on fuel dispersal.
  - Response of embrittled cladding to transient PCMI.

In addition to these, for those countries that load both MOX and UO_2 fuelled assemblies, there is a requirement to bring the MOX database to the same level as that for UO_2 fuel with the aim of treating MOX indistinguishably from that of UO_2 as far as safety is concerned.

3.7 Innovative fuels

Plutonium and minor actinide recycling in thermal and fast reactors is being studied in many countries with the aim of maintaining and developing fuel cycle options which can be adjusted to changing demands and constraints. The challenge is to move towards an economically and socially sustainable nuclear energy system based on advanced reactors – advanced water-cooled reactors, fast reactors and perhaps accelerator-based, hybrid reactors – and new types of fuel cycles which help to minimise waste arising. In this context, topics of interest are: the multiple recycling of plutonium in thermal reactors, enhanced consumption of surplus plutonium in thermal and fast reactors, reduction of the uranium demand of thermal reactors to stretch the fissile material resources, transmutation of minor actinides to extract fission energy and reduce the quantity and toxicity of the actinide waste, etc.

A variety of light water and fast reactors using different fuels are capable of fully incorporating plutonium into their fuel cycles; options range from "concentration" (plutonium without uranium) to "dilution" which requires the presence of slightly enriched uranium. A number of PWR concepts that use uranium-free plutonium fuel include APA, while the CAPRA programme established a concept necessitating a high plutonium concentration in fast reactors to counterbalance the absorption of minor actinides. Plutonium utilisation in LWRs can also be enhanced through the use of highly moderated 100% MOX cores with moderation ratios ranging from 4 to 6 for PWRs, and from 6 to 7 for BWRs. The recycling of reprocessed uranium in LWRs, an essential element in closing the fuel cycle, was considered a relevant issue because it contains minor actinides, and requires treatment like other transuranic elements. Fuel fabrication that makes use of recycled uranium must also be competitive with conventional fuel cycles, and utilities must act to facilitate this process through careful consideration of technological solutions.

MOX fuel breeding for PWR and BWR aims at effective resource utilisation, and is based on current PWR and BWR technologies. Innovative PWR concepts such as tight hexagonal lattices were presented in a breeding PWR case study in Japan whereby the breeding ratio is 1.1 with a D_2O moderated heterogeneous core design with fertile zones. Two innovative BWR concepts using tight lattice configurations were also discussed. The first concerned a resource-renewable BWR (RBWR) which operates using mixed-oxide fuel within an epithermal spectrum and displays a breeding ratio of 1.0, while the other case involved a breeding BWR (BBWR) with a fast neutron spectrum and a breeding ratio >1. However, the presence of rare-earth elements in the fuel cycle may deteriorate core characteristics such as the breeding ratio. A negative void reactivity effect can be achieved with the presence of the cavity can in the streaming channel structure; furthermore, the reactor has the potential to transmute minor actinides.

KAERI is currently developing a concept to increase uranium resource utilisation in CANDU reactors. DUPIC (Direct Use of Spent PWR Fuel in CANDU reactors) fuel technology uses spent PWR fuel (35 GWd/t) that can be directly fabricated into a reusable fuel for CANDU reactors (additional 15 GWd/t). Fuel characteristics are markedly different from standard CANDU fuel types. International co-operation has already been established through the IAEA and an experimental programme is underway. This research aims at achieving competitive costs.

JAERI is involved in the design of several innovative MOX-fuelled PWRs and BWRs, with an ambitious goal to achieve 100 GWd/t burn-up and three-year cycle length with a water-cooled full MOX core. Proposed designs feature moderation ratios of 2.6 and a Pu content of 12% for PWRs, and moderation ratios of 2.0 and a Pu content of 16% for BWRs, respectively; these values are feasible from the perspective of reactor physics parameters.

A more fundamental approach is being investigated at IRI, which seeks to establish fuel temperature coefficients (FTC) for several fuel types from MOX fuel to uranium-free inert matrix fuel, two of which included reactor-grade and weapons-grade plutonium. All fuels, including those containing weapons-grade plutonium, have negative FTC.

Zero-power facilities for reactor physics analyses are needed for the validation of data and codes. The LR-0 facility (NRI Rez, Czech Republic), for example, is suited for a simulation of a VVER-1000 and VVER-440 with a hexagonal lattice configuration, as well as for conducting basic neutron physics experiments. A weapons-grade MOX programme was proposed for VVER-1000.

The PROTEUS facility in Switzerland has developed a three-year LWR experimental programme using real fuel assemblies with some generic research and development aspects. The programme is supported by Swiss utilities and is being conducted in two experimental phases for BWRs and PWRs.

Three conclusions can be drawn from the 1998 NEA Workshop on Advanced Reactors with Innovative Fuels [103] regarding the various fuel technologies and reactor design issues discussed above:

- Fuel performance improvements can occur by enhancing MOX fuel burn-up and re-using spent fuel, as exemplified by the DUPIC and URT concepts. Such improvements in the fuel cycle will also act to reduce costs.

- There exist a wide range of options in terms of consumption and breeding using plutonium in LWRs and FRs. The implementation of such options is strongly linked to the time scale considered. Research and development concerning various plutonium utilisation routes are thus justified.

- There are several specific issues concerning present and future research and development. Current facilities – which include irradiation facilities, zero power reactors, hot laboratories and nuclear data management centres – operate under strong restrictions. Thus, often research and development needs that arise cannot be adequately addressed. It is therefore important to maintain and develop R&D "tools", and to define the role of international organisations within this context as that of co-ordinating, fostering and providing guidance. So as to achieve this objective in the short term, it is necessary to create a comprehensive survey report that acts to clarify the needs, develop strategies and gain the support of all partners.

3.7.1 Uranium-free reactors

Numerous fuel cycle systems for uranium-free reactors have been proposed, a summary of which is provided in Table 8. For the purpose of this summary, four types of fuels considered in current uranium-free reactor programmes are outlined. These fuels are being developed with four principal objectives in mind: plutonium burning capacity, reduction of radiotoxicity and actinide transmutation, optimal use of natural resources, and improved safety.

Promising reactor physics characteristics have been achieved for ZrO_2-based solid solution inert-matrix fuel (IMF) assemblies. Although fabrication technology is only available on a laboratory scale, 100% (homogeneous) IMF cores have been shown to reduce plutonium as effectively as for MOX fuels without requiring any further reprocessing treatment (once-through). The (low) thermal conductivity of this fuel type is one of the major uncertainties for its application.

Table 8. Fuel cycle systems for uranium-free reactors

Materials	Additives	Assembly	Core loading	Reactor	Strategy
Y-SZR	Er_2O_3	Homogeneous	Partial	BWR	Recycling
$MgAl_2O_4$	Gd_2O_3	Heterogeneous	Full	CANDU	Once-through
SiC	ThO_2			LWR	
CeO_2	UO_2			FNR	
THO_2	^{11}B				
Metals					

Table 9. Uranium-free fuel types and materials

Uranium-free reactor fuel type	Materials
SS-IMF	(Zr, Y, Pu, X) O_2
CERCER	(Zr, Y, Pu, X) O_2 in spinel or MgO
CERMET	(Zr, Y, Pu, X) O_2 in metal
Thoria	(Th, Pu) O_2

Although not really inert, thoria-based fuels (TD) show good Pu burning capability for some LWRs and Na-cooled FRs. The technology for thoria-based fuels is partly available from experience from the past. Thoria-based fuel is also of great relevance from the point of view of resources.

Two other types of inert-matrix fuels are being studied. Research concerning the combination of CERamic fuel and a METallic matrix (CERMET) for PWR, based on zirconia and a conducting metal, is mainly theoretical and little experimental work has been carried out. Materials composing the fuel have not yet been adequately defined, and burn-up studies and accident research, which offer good potential for CERMETs, are to be initiated. Much experimental work is being undertaken on CERamic matrix and CERamic fuel (CERCER), mainly for "once-through" burning of plutonium in LWR. The fuel concepts for CERCER fuel are converging in the sense that the $MgAl_2O_4$ (spinel) is foreseen as matrix and plutonium (or americium) dissolved in stabilised zirconia as fuel. Issues to be addressed in R&D for CERCER include resistance to irradiation, reactor-initiated accidents (RIA) and increases in thermal activity.

Three main conclusions can be drawn: no common strategy for uranium-free fuels is emerging, materials issues are poorly addressed and licensing procedures for new fuels may take from 15 to 20 years to complete.

3.7.2 Other reactors

Reactors with non-oxide fuels

The advantages of the use, research and development of non-oxide fuels lies in their: a) passively safe response to anticipated transients without scram (ATWS), b) high linear pin power and high thermal conductivity, c) excellent neutron economy, d) effective use of neutron for plutonium and/or minor actinide burning (high heavy metal density), e) the large proliferation resistance of these fuels is illustrated in remote reprocessing and re-fabrication and the fact that non-oxide fuels are associated with MA and FP by the pyrochemical process.

The following findings with regard to current programmes incorporating non-oxide fuels into reactor fuel cycles were presented:

- Tests on metallic fuel in fast reactors have yielded a very high burn-up capability in excess of 20 at.%.

- Examination of core performance of the nitride fuel fast reactor (LMFBR) was presented together with the pyrochemical process, which has the possibility of recovering the radiotoxic ^{14}C and the expensive ^{15}N.

- Studies on large plutonium consumption in fast reactors within the context of the CAPRA programme revealed that pure PuN fuel dissolves properly during PUREX reprocessing operations, with a high Pu burning rate and dynamic performance of PuN core.

- The KALIMER liquid metal reactor design contains a uranium-metallic-fuelled core with a power of 390 MWt.

- In a comparative study of dynamic behaviour of a nitride-fuelled LMR core and an oxide core, the unprotected loss of flow (ULOF) event displayed a larger Doppler feedback effect when necessary and a smaller effect for nitride cores in unfavourable conditions.

- In a study of the thermal decomposition behaviour of UN and ($U_{0.8}$ $Pu_{0.2}$) pellets, the initial thermal decomposition temperatures of UN and MN pellets was found to be at least 1 800°C, in various atmospheres. In the higher temperature range, thermal decomposition occurred with vaporisation of metal.

- Molten salt reactor technology in Russia was reviewed and evaluated, including aspects of fuel technology, container materials, components and fuel clean-up.

- Experimental work is being carried out in the Czech Republic on liquid fuel concepts, which have several advantages over traditional solid nuclear fuels. New reactor systems using liquid fuels provide for nuclear incineration of spent fuel from conventional reactors and a clean energy source.

Principal issues on advanced reactors with innovative fuels regarding plutonium utilisation, uranium resources and waste management strategy

- Enhancing UO_2 and MOX fuel utilisation in current LWR to reduce costs.

- Reducing separated plutonium stocks by means of evolutionary and innovative concepts [*e.g*. highly-moderated MOX-loaded LWRs, inert-matrix fuels (IMF)].

- Preserving fissile inventories as an energy resource for the future (*e.g*. tight hexagonal PWR lattices, thorium fuels).

- Minimising waste by effectively burning MAs and transmuting long-lived FPs.

- Ensuring energy security for the long term.

Principal issues on advanced reactors with innovative fuels regarding reactor and fuel technology

- Enhanced safety and proliferation resistance.
- Simplified fuel cycles.
- Material problems of non-oxide fuels for plutonium burning and transmutation.
- Long licensing procedures for new fuels to be taken into account.

In the 2001 NEA Workshop on Advanced Reactors with Innovative Fuels [104], the main conclusion was that a new generation of reactor designs are being developed that are intended to meet the requirements of the 21st century. In the short term, the most important requirement is to overcome the relative non-competitiveness of current reactor designs in the deregulated market. For this purpose, evolutionary light water reactor (LWR) designs have been maturing and are being actively promoted. They are specifically designed to be less expensive to build and operate than the previous generation of LWR, are genuinely competitive with alternative forms of generation and also establish higher levels of safety. A new generation of modular, small-to-medium (100-300 MWe/module), integral design water-cooled reactors are under development. They are designed to be competitive with nuclear and non-nuclear power plants, to have significantly enhanced safety, to be proliferation resistant and to reduce the amount of radioactive waste produced. A different approach to improve competitiveness is the re-emergence of high-temperature reactors (HTR) using gas turbine technology so as to provide higher thermal efficiencies, low construction and operating costs, inherent safety characteristics and low proliferation risk.

In the longer term, assuming that the current stagnation in the market is successfully overcome, other requirements related to long-term sustainability will emerge. Important amongst these will be the need to minimise the environmental burden passed on to future generations (or at least to ensure that the cost to future generations is in balance with the benefits to the current generation), the need to establish sustainability of fuel and the need to minimise stocks of separated plutonium at the minimum possible working level and to limit accessibility to plutonium. In this context, the most interesting advanced reactors are: reactors consuming excess plutonium, advanced LWRs, HTRs, fast spectrum reactors, subcritical systems, minor actinide systems and radical innovative systems.

While new reactor designs currently available or under development promise to achieve significant improvements in total generating cost such that they can be competitive in deregulated markets, there are nevertheless some difficult obstacles to overcome, in particular the need for a stable regulatory environment in which potential investors can be certain that the regulatory process will not change during the course of construction and also the need for the regulatory processes to be consistent in different countries. A further point is the need for the environmental discharge requirements to be driven by rational cost/benefit approaches and not by demanding near-zero discharges that have no justification. For sustainable advanced reactors and fuel cycle systems which are intended to stabilise the accumulation of plutonium and/or minor actinides, getting the economics right will be a considerable challenge. It seems likely that any strategy which is primarily designed to achieve significant benefits in terms of waste reduction, reduced radiotoxicity per GWe, etc., will be economically disadvantaged compared with minimum-cost-generation strategies. De-regulated markets are not presently set up to deal with anything other than simple cost-minimisation as a driver and therefore a major barrier to overcome in deregulated markets will be the need to establish mechanisms whereby the non-tangible benefits of advanced fuel cycles can be fully recognised.

High-temperature gas reactors

Theoretical fuel cycle studies for the pebble bed modular reactor (PBMR) have led to the development of a design for B_4C burnable poison particles that might be used in a batch refuelling scheme for PBMR and which explores the effects of self-shielding as a function of particle diameter and ^{10}B enrichment, and demonstrates the flexibility of the PBMR for utilising different fuels, including U-Th, U-Pu and Th-Pu.

Innovative fuels

Inert-matrix fuels, specifically zirconia-plutonia, zirconium nitride, cerium-plutonium oxide and rock-like fuels are innovative fuels. The design of (U-Pu) N fuel for the RBEC lead-bismuth fast reactor and minor actinide target fuels should also be considered as such.

Evolutionary and modular water reactors

New reactor concepts include small modular PWR, an upgraded VVER-440, a simplified BWR, a simplified PWR, a PWR with supercritical coolant state and reduced moderation LWR designed to increase the plutonium breeding ratio. Novel fuel concepts include a PWR using HTGR particle fuel, a PWR partially loaded with inert-matrix fuel, and the use of thorium fuel in LWRs. The research emphasis is on enhanced safety and improved utilisation of plutonium.

Fast spectrum reactors

A simplified sodium-cooled fast reactor which eliminates the intermediate circuit through the use of novel high-integrity steam generators is proposed, as are a Pb-Bi-cooled fast reactor and a gas-cooled fast reactor. A novel concept compatible with a very long life core is the candle strategy, where only a small axial section of the core undergoes fissions and the fissioning region automatically propagates axially at a rate of a few cm per year. The same concept could apply to a thermal system as well. The emphasis is on fast reactors that are economically competitive with the current generation of LWR and the evolutionary LWR derived from them.

Molten salt reactors

This type of reactor is designed for both attractive fissile fuel utilisation and incinerating minor actinides. A thorium-fuelled molten salt subcritical system intended for primary energy generation with low radiotoxic burdens is also proposed.

Accelerator-driven systems

A molten cascade molten salt subcritical system uses a supercritical central core surrounded by a subcritical region where the bulk of the minor actinide transmutation takes place. The supercritical central zone acts to amplify the source neutrons and reduces the current requirements of the accelerator beam. A subcritical molten salt system for minor actinide transmutation is also proposed.

Miscellaneous themes

An interesting concept features a core which is only just subcritical and which uses an accelerator beam to simulate the effect of delayed neutrons. This system has the advantage of being able to load a large fraction of minor actinides using a coupling to the accelerator current to mimic the effect of an extra delayed neutron group. In this way, many of the difficulties of more conventional subcritical systems (such as demanding beam requirements and rapid spatial variations of flux) are avoided. The objectives of advanced concepts are usually concerned with areas such as safety, proliferation resistance, environmental impact/radiotoxic burden, strategic and so on.

- Safety:
  - Enhanced safety.
  - Improved reliability.
  - Inherent safety (*e.g.* passive systems).
  - Advanced control and monitoring systems.
  - Plant simplification.
  - Improved ISI and maintenance.
  - Reduced worker dose.
  - Reduced consequences of severe accidents.
- Proliferation resistance:
  - Proliferation-resistant fuel cycles.
  - Fissile material accounting.
  - Assured inspection processes (easy accountability and inspection).
  - IAEA requirements.
- On environmental impact:
  - Improved fuel utilisation.
  - Reduction in wastes.
  - No increase in natural environmental burden.
  - Decommissioning.

There is a clear agreement on the need to establish meaningful and useful metrics, *i.e.* what measures should be adopted to ensure that utility requirements are met, but a recognition that in most areas they are very difficult to define. For example, there is no easy measure to assess whether one

system is more proliferation-resistant than another. There is a need to develop scales to measure such issues. The economics of different systems is the only area where clear quantitative metrics exist and utilities' decisions are understandably dominated by this aspect. In spite of the difficulties of making progress in this area, it is important enough that it should not be neglected. There may be benefits in attempting to generate suitable metrics even if they are not perfect, as the process may give rise to important new questions and generate new perspectives. There may be benefits to be gained from other fields, such as environmental protection, where there is a need for analogous metrics.

Among the objectives of initiatives such as Generation IV is sustainability. The sustainability of nuclear energy should addresses the following main requirements:

- Uranium resources need to be saved.
- Known resources: 4.3 Mt (NEA-1997) combined with consumption of 70 kt/year equates to 60 years of supply.
- Nuclear waste production should be minimised with an adequate management of spent nuclear fuel. But until now no country has implemented a permanent solution such as partitioning and transmutation and/or geological disposal.
- Enhanced safety.
- Enhanced resistance to proliferation risks.
- Economic competitiveness, which needs to be reinforced.

The assets and limits of LWRs for sustainable development include:

- A mature technology with an irreplaceable experience.
- Convincing results on economy, safety and reliability.

For the immediate future, *e.g.* the new generation of PWR (EPR) with high levels of burn-up (65 GWd/t), important issues include:

- Plutonium control.
- Waste volume reduction.
- The non-optimum use of resources – only 1% of initial U is used (even with reprocessing) in LWRs.

Sustainability in the context of a future equilibrium system is an important issue as concerns humankind. After a certain period of transition, it will certainly become viable. Once-through fuel cycles cannot be accepted for the future equilibrium system, but should be acceptable in the interim. This depends on the burn-up strategy and reprocessing R&D. For higher burn-up such as Pu burner, the once-through option may be acceptable. For higher fissile content in the spent fuel, the reprocessing option may be better. Temporarily, the interim storage option may be attractive. The questions of safety and proliferation resistance are the most urgent. The question of reducing the radiotoxic burden is less so.

Chapter 4

ADVANCED FUEL

4.1 High burn-up fuel

As more demanding operating conditions and new fuel designs are introduced, there is an increased regulatory focus on the fuel area, particularly as concerns high burn-up issues in general and the search for lower RIA and LOCA criteria. Utilities are interested in burn-up extension, which will improve fuel cycle economics and operation flexibility that produce:

- Increasing discharge burn-up and long cycle length.
- Increased fuel peaking and enrichment (4% in BWRs, 4.4% in PWRs).
- Plant up-rates (stretch power ~ 7%, extended power ~ 20%).
- Elevated pH and lithium in primary coolant.
- Fuel design changes and introduction of new materials.

In order to reduce the regulatory burden, the issues for the EPRI [107] in the new Robust Fuel Programme are:

- Providing a draft of the licensing framework for the industry to achieve high burn-up goal:
  - 75 GWd/t for PWRs, 70 GWd/t for BWRs (rod average).
  - Streamlining the licensing process.
  - Submission of a topical to the Nuclear Regulatory Commission (NRC) in 2003.
- Developing new RIA criteria and submitting the RIA topical to the NRC:
  - Radial average fuel enthalpy is 170 cal/gr < 36 GWd/t, 125 cal/gr < 80 GWd/t.
  - For burn-up extension and advanced alloys.
  - Can be met by 3-D methodology.
  - RIA tests on advanced alloys will determine the extent of future work.

- Working closely with the NRC to develop technology for new LOCA criteria for high burn-up fuel:
  - NRC rule-making initiative on 10 CFR 50.46
  - Proper tests need to be performed to ensure LOCA criteria for high burn-up fuel are not unduly conservative (Zr-4, Zr-2, M5, and Zirlo).

To ensure margins under high duty conditions the issues are:

- For PWRs:
  - Advanced alloys (Zirlo, M5) have better corrosion performance than Zr-4; margin confirmations are required for representative materials and high duty conditions.
- For BWRs:
  - Corrosion performance is excellent with pre-noble metal clad (NMCA). Surveillance showed increased cladding corrosion and spallation for some plants implementing NMCA. Programmes are in place to determine the impact of NMCA on fuel cladding corrosion.
  - GNF cladding and hardware at 57 and 70 GWd/t with and without NMCA P5 and P6.
  - Channel deformation limits fuel assembly life (monitoring and coupon irradiation planned).
  - Positive ramp test results of low-concentration additive fuel (an alternative to barrier fuel as a PCI remedy).

To provide the technology required to increase burn-up to the target level (70 GWd/t), the goal is to control the axial-offset asymmetry and the crud deposition:

- Interim remedies are available (UT cleaning, EPRI Axial Offset Asymmetry, AOA, guidelines and fuel designs).
- New solutions are being investigated/developed such as:
  - EBA, elevated pH and Zn injection.
  - AOA model BOA.
- Margins for BWR cladding are reduced as a result of NMCA, poolside/hot cell exams and in-reactor tests are performed and planned to quantify the impact and investigate mitigation measures.

To resolve existing operation and reliability problems the issues are the water-chemistry-related NMCA for BWR and PWR chemistry options (EBA, elevated pH):

- PWR fuel reliability remains steady with no major incidences. The main cause of failure is still grid-rod fretting.

- Many BWR units experienced fuel failures in 2001/2002:
  - Primary failure causes need to be confirmed; PCI, debris and corrosion-related failures appear to be the major causes.
  - Important to understand the failure causes to avoid recurrence at other plants.
  - Accurate and timely sharing of fuel failure information.
  - Use of the FRED database (web-based).
  - Need to identify the root causes of the failure so as to prevent recurrence, including the least failure root cause investigations.

4.1.1 Fouling and crud formation influence

The relevance of the fouling or crud formation upon the surface of fuel pins and its influence upon the RIA has already been mentioned in the present report (Chapter 3, Sections 3.4 and 3.7, see also above under Section 4.1). However, recent elements suggested the utility of a section devoted to this subject [167].

Fouling and/or corrosion of fuel elements is significant and ubiquitous among light water nuclear power reactors. This fouling and/or corrosion increases the severity of RIA. Such a phenomenon is a heat transfer barrier. The heat transfer barrier inhibits heat transfer from the fuel to the water and thus increases the severity of the RIA. This also leads to a substantial increase in the steady-state operating temperature of the fuel at the initiation of the RIA, which is another factor leading to increased severity.

The fuel damage limits that are supposed to ensure a coolable core are 280 cal/g peak fuel enthalpy (NRC Regulatory Guide 1.77) for the reactivity accidents and 17% cladding oxidation and 2 200°F peak cladding temperature for the loss-of-coolant accidents (10 CFR 50.46).

Recent experiments show that cladding failure accompanied by fuel dispersal (loss of geometry) could occur at fuel enthalpies below 100 cal/g for high-burn-up fuel. This is far below the current regulatory criterion. Further, the failures were occurring as a result of a brittle mechanical fracture mechanism rather than the high-temperature process seen in the original studies on fresh fuel, from which the current criterion was derived. In addition, different cladding alloys may behave in a completely different manner depending on their ductility. To complicate matters, the industry (here making reference to the US) is now using three distinctly different PWR cladding alloys and two different BWR cladding types, all of which may have different mechanical properties in their highly irradiated state.

In extreme cases, fuel rods in commercial reactors have accumulated nearly 17% cladding oxidation during normal operation. The extent to which this reduces the amount of oxidation that can be tolerated during the accident is not known, and thus the NRC is currently taking the conservative position that the sum of transient and steady-state oxidation should be limited to 17%. Even if the oxidation and peak cladding temperature embrittlement criteria of 10 CFR 50.46 can be shown to be adequate at high burn-up for all cladding types, it is likely that the evaluation models for oxidation, ballooning and rupture will be affected.

Fortunately, design-basis accidents are unlikely and current analyses generally contain conservative margins. Therefore, in its high-burn-up programme plan, the NRC concluded that there was time to resolve these issues with long-range research programmes (3-5 years). To this end, we engaged in a

number of formal agreements to gain access to international programmes and we initiated some of our own work. A list of current NRC research activities on high-burn-up fuel can be found in Ref. [167]. Related information can also be found in Ref. [169] and at Internet sites http://www.et.anl.gov/aghcf and http://www.nrc.gov/RES/FRAPCON3.

4.1.1.1 Operational experience with fouling

Fuel performance problems have occurred with both pressurised water reactors and boiling water reactors, albeit with different timelines and differences related to core and fuel designs.

PWRs, many of which shifted to higher initial fuel enrichment levels (4.5% and higher) in the mid-1990s, have experienced varying degrees of axial offset anomaly (AOA), or a downward shift of the reactor core power profile, as a result of a build-up of corrosion-product deposits commonly known as crud on fuel surfaces that, in turn, is caused by increased fuel duty. EPRI has successfully demonstrated at two PWR plants an ultrasonic method for removing crud deposits to mitigate AOA. Although occurrences of AOA persist, its frequency and severity have diminished significantly from recent trends. Grid-rod fretting – the metal spacers that separate individual rods in fuel assemblies – continues to be the main root cause of PWR fuel failures.

For BWRs, the principal industry concern today is the relatively large increase in the number of reported fuel failures beginning in 2002, after more than a decade of steadily decreasing failure rates. Over a 17-month period from January 2002 to May 2003, 19 BWRs reported fuel failures and 10 were operating with failed fuel in June 2003. At some BWRs, excessive bowing of the fuel channels can increase control blade insertion times. The industry is investigating a number of open technical issues posed by the BWR fuel failures. Although nuclear plants are designed to operate with some failed fuel, plant owners pursue a constant operating goal of keeping personnel exposure to radiation as low as is reasonably achievable.

For both reactor types, the role of new water chemistry regimes introduced to lower in-plant radiation exposures to plant personnel or to support extended plant operation are being assessed with respect to fuel performance. For PWRs, these regimes include elevated coolant pH using lithium and zinc injection and for BWRs include the addition of noble metal chemicals and zinc.

4.1.1.2 Industry response to the fouling issue

EPRI's Robust Fuel Programme (RFP) is playing an important technical support role in the nuclear power industry's response to recent fuel performance problems, as already mentioned in this report.

The programme is currently directed toward developing ultrasonic cleaning technology (UT) for BWR fuel, modifying the technology successfully used for PWR. Once tests and evaluation to address BWR-specific issues are completed, UT technology for BWR applications is expected to be available in early 2004.

Removing the corrosion products before reloading the fuel can reduce the risk of AOA in the subsequent fuel cycle, and the lowered corrosion product deposits will reduce the amount of activated material that would otherwise contribute to personnel radiation exposure [168]. The EPRI-patented method has been used successfully at Callaway and at the South Texas Project Unit 2 PWR plants.

The core at the Callaway NPP remained free of AOA throughout the fuel cycle for the first time in eight subsequent cycles after one fuel cycle in which all reload fuel was ultrasonically cleaned.

It is feasible to consider the elimination of a 4°F average core temperature reduction imposed earlier as a precaution to minimise AOA (each degree of recovered core temperature restores approximately 4.5 MW of generating capacity over a fuel cycle).

4.1.1.3 The Paks event

In a May 2003 report to the Chairman of the Hungarian AEC, the extensive fouling of the Paks units is candidly discussed. There is no description of the thermal resistance of the fouling or the amount of zircaloy corrosion. However, the fouling (magnetite) has been extensive. Quoting his remarks, "...magnetite deposits in the fuel assembles increased and the cooling water flow rate decreased. Consequently the power of Units 1-3 had to be decreased."

Chemical cleaning of fuel elements in batches of seven elements has become routine. In 2002, FRAMATOME-ANP expanded the cleaning process to 30-element batches.

On 10 April 2003, while the assemblies were being cleaned for Unit 2, severe damage occurred to an entire batch. The state of the fuel prior to the accident has not been disclosed. But as this data including the extent of fouling become available, it is likely that analysis will yield further insights on the impact of fouling on severe accidents.

4.2 Use of plutonium

The plutonium and uranium in spent fuel can be utilised if it is recycled. The spent fuel is reprocessed; that is, the plutonium and uranium are chemically extracted from the fuel. The plutonium, in the form of PuO_2, is then mixed with UO_2, fabricated into what is called mixed-oxide fuel, and returned to the reactor. The residual, slightly enriched uranium produced in the reprocessing plant is converted to UF_6 for re-enrichment. It is estimated that the adoption of a uranium-plutonium recycle would reduce the cumulative U_3O_8 requirements of LWR by about 40% over the 30-year lifetimes of these reactors. Nevertheless, it is still not clear whether the additional costs of reprocessing and mixed-oxide fuel fabrication can in fact render uranium-plutonium recycling an economically attractive fuel option. However, economics notwithstanding, it is reasonable for some nations such as Japan to adopt recycling in an effort to reduce their dependence on foreign uranium suppliers and so ensure their independence. After studies conducted on the technical, industrial and economic aspects of plutonium recycling in PWR, Electricité de France decided to recycle, in some reactors, the plutonium and uranium obtained from reprocessing. The consequence of this recycling is that in some reactors, assemblies of MOX type are used, in other words assemblies in which the fuel pellets are obtained by sintering of depleted uranium oxide, which is used as a fertile support, and of fissile plutonium oxide.

The authorisation to reload plutonium fuel is presently restricted in France to 30% of the core, *i.e.* 16 MOX assemblies out of a total of 52 which make up the yearly reloading for a 900 MWe reactor core; since 1995, these units reloaded with MOX fuel have been authorised to operate in load follow.

The average plutonium content of a MOX assembly is close to 5%, equivalent to ^{235}U enrichment of 3.25% in a UO_2 fuel. This varies according to the isotopic composition of the plutonium used in oxide fabrication. The average content of 5.3% corresponds to the isotopic quality of the plutonium emerging from the reprocessing facility in the 1990s:

^{238}Pu: 1.83%	^{240}Pu: 22.50%	^{242}Pu: 5.60%
^{239}Pu: 57.93%	^{241}Pu: 11.06%	^{241}Am: 1.08%

The juxtaposition of assemblies only containing uranium and of MOX assemblies caused the neutron flux in the periphery of the latter to increase. To avoid this local power excess, the plutonium content varies in the assembly: there are three areas in which the plutonium contents increase from the periphery to the centre. One of the characteristics of this type of assembly is the presence of plutonium-rich agglomerates in a matrix of low plutonium content, which has several drawbacks:

- They create local fission density peaks, which are likely to increase fission gas release.
- They can reduce fuel solubility during reprocessing.

For both uranium and plutonium, the increase in burn-up is manifested by a decrease in fissile isotopes (^{235}U, odd plutonium isotopes), as can be seen from Table 10.

Table 10. Isotopic composition of uranium after irradiation (in % by weight) 900 MW PWR fuel three years after unloading

Burn-up	^{232}U	^{234}U	^{235}U	^{236}U	^{238}U
33 GWd/t, 3.25% initial ^{235}U	$\approx 10^{-7}$	0.020	0.86	0.43	98.7
60 GWd/t, 4.95% initial ^{235}U	$\approx 10^{-7}$	0.024	0.83	0.75	98.4

On the other hand, PuO_2 is not a mixture of oxides. As the plutonium burns, the oxygen, which is very reactive, has nowhere to go except to "attack" the fuel cladding. To overcome this phenomenon, when plutonium is to be used as a reactor fuel it is mixed with uranium oxide. Such mixing mitigates the effects of oxygen on plutonium fuel performance and fuel pin lifetime. The oxygen ratio in mixed plutonium-uranium oxide fuels increases during operation; if the initial oxygen/metal ratio were not adjusted to hypostoichiometric ratios (1.93-1.97), then excess oxygen once again could cause cladding problems. Low stoichiometric ratios are achieved by adjusting the plutonium concentration in the fuel and controlling conditions during fuel manufacturing to reduce oxygen concentrations. Low oxygen levels are also necessary to mitigate fuel migration, *e.g.* the tendency of plutonium to migrate toward higher temperature regions. Plutonium redistribution is not a problem when the oxygen levels are kept low. Otherwise, hot spots in the fuel could develop as the plutonium migrated to the centre of the fuel rod.

Table 11. Isotopic composition of plutonium (in % by weight) 900 MW PWR fuel three years after unloading

Burn-up	^{238}Pu	^{239}Pu	^{240}Pu	^{241}Pu	^{242}Pu
33 GWd/t	1.7	57.2	22.8	12.2	6.0
60 GWd/t	3.9	49.5	24.8	12.9	8.9

4.2.1 Physics of plutonium recycling

The recycling of plutonium in LWR has for quite some time been seen as an important interim step prior to the large-scale introduction of fast reactors; several countries have, in fact, been using MOX fuel in PWRs on a commercial scale for many years. Now that fast reactors are no longer expected to be introduced for some time, the need to manage existing plutonium stocks puts even more emphasis on LWR MOX. Even though there is sufficient experience of MOX in PWRs to be assured of satisfactory performance under existing conditions, the situation is not static and it is very important to address future requirements.

There are two main trends which should be addressed. First, discharge burn-ups continue to steadily increase. Second, the fissile quality of the plutonium is generally becoming poorer. The decline in fissile quality is partly a consequence of the higher burn-ups, but another major consideration is the effect of recycling MOX fuel itself. Multiple recycle scenarios cause a significant decline in fissile quality in each recycle generation. One result of this is that the initial plutonium content of MOX fuel is considerably increased in each recycle generation; this poses a considerable challenge to current nuclear design codes and the associated nuclear data libraries.

The OECD Working Group on the Physics of Plutonium Recycling (WPPR) has addressed the issue of multiple plutonium recycling in advanced PWRs [105]. The earlier benchmark work identified major discrepancies between the various nuclear design codes and nuclear data libraries, specifically differences of up to 4%Δk in reactivities. A portion of the range of discrepancy was explained because some of the codes did not apply self-shielding to the resonance treatment of the higher plutonium isotopes; with the large concentration of ^{242}Pu specified in the benchmark, self-shielding in this nuclide was very important. Nevertheless the remaining discrepancy was considered sufficiently large that further work would clearly be necessary before the multiple recycle scenario envisaged in the specification could be implemented.

A shortcoming of the initial benchmark was that the cases examined included only one that corresponds to today's situation (with plutonium of good isotopic quality), and one which might arise after many generations of MOX recycle (with extremely poor isotopic quality). Analysis of the intermediate steps was missing, and therefore there was no possibility of determining precisely when the nuclear codes and data libraries would start to lose their applicability. Accordingly, CEA suggested a benchmark in which five consecutive generations of multiple recycle in a PWR would be followed. In the specification of the benchmark, attempts were made to render the scenario as realistic as possible, taking into account details such as the length of time between recycle generations (including the time delays in pond storage, MOX fabrication, etc.) and the diffusion effect when MOX and UO_2 assemblies are co-reprocessed.

Multiple recycle scenarios therefore appear to be practicable and feasible in conventional PWRs, at least in the near term. Questions arising from a possible positive void coefficient would almost certainly preclude recycle beyond the second generation and even possibly even in the second generation in this particular scenario.

For the longer term, the (highly-moderated) HM PWR concept shows some merit. However, the principal advantage, that of needing a lower initial plutonium content with the same dilution ratio, is largely eroded in later recycle generations; in spite of the much improved moderation, the HM PWR degrades the plutonium isotopic quality more rapidly than the STD PWR, to a large extent negating the benefit of the softer spectrum. The HM PWR case also seems to present more difficulties for present nuclear data libraries and codes, as evidenced by the larger number of discrepant results seen in the HM PWR benchmark. Therefore, even the HM PWR is of questionable practicability with respect to the later recycle generations.

The discharge burn-up of MOX fuel, and indeed its overall performance, is essentially the same as that of UO_2 fuel. Thus the MOX fuel currently being irradiated in PWRs is typically intended to be discharged at burn-ups of 40-45 MWd/t. The initial plutonium content needed to achieve such burn-ups varies depending on the precise source of the plutonium, but is typically in the range 7-8 w/o total plutonium, expressed as an average over the whole assembly. The experience of MOX utilisation in PWRs has been positive, and there are no outstanding operational or safety issues to be resolved. The situation is not static, however, and such issues will have to be addressed in the near future as the background conditions change.

The fundamental changes are that discharge burn-ups continue on an upward trend, while a need is also arising to recycle the plutonium from discharged MOX assemblies. Both these changes will manifest themselves through a decrease in the isotopic quality of the plutonium that is available for recycle. For thermal reactors the even isotopes of plutonium (238, 240 and 242) do not contribute significantly to fissions. The ratio (^{239}Pu + ^{241}Pu)/total plutonium) is thus denoted the fissile fraction of the plutonium and is a measure of plutonium quality for thermal reactor MOX. The problem is that plutonium quality decreases as the discharge burn-up increases and decreases yet further following recycle of the plutonium recovered from MOX. Combined with the self-evident need to increase plutonium content to reach higher burn-ups, it will be necessary to significantly increase the total plutonium content of the MOX fuel.

Compared to conventional UO_2 fuel, MOX fuel is already significantly different from a neutronic point of view, there being a much smaller thermal flux for a given rating. This is due to the combined effects of the higher fission and absorption cross-sections of ^{239}Pu and ^{241}Pu compared with ^{235}U, exacerbated by the significant absorption of the ^{240}Pu and the ^{242}Pu. The difference in spectrum affects the core performance because the control, reactivity coefficient and transient behaviours are all altered. Increasing the total plutonium content beyond present levels further exaggerates all of these effects. Ultimately, the deterioration in parameters such as control rod reactivity worth, boron reactivity worth and moderator void and temperature coefficients may become a barrier to further utilisation of MOX in PWRs, at least in conventional lattices. Therefore, the question to be asked is: At what precise point will such considerations present a barrier? It is equally important to determine whether present nuclear data libraries and nuclear codes agree as to when this point occurs.

Multiple recycle scenarios presently form a very important topic for MOX recycle in LWR. With the prospects for large-scale deployment of fast reactors having receded in recent years, MOX is becoming more significant as a means of utilising plutonium stocks that were originally intended to start fast reactor cycles. The existence of surplus ex-weapons plutonium and establishing a means for its consumption or disposal has, at the same time, added further urgency and importance. The question of how many times plutonium recovered from MOX assemblies can be re-used in PWRs is important strategically and logistically. Strategically, it is important because it affects the energy potential that is available from plutonium. Logistically it determines whether there will be a need to store or dispose of MOX assemblies and/or plutonium at some future point if indefinite recycle does not prove practical.

Each recycle generation involves irradiation of MOX fuel (lasting typically four to five years), followed by pond cooling (typically five years), then by reprocessing and re-fabrication as MOX (taking a further two years). Thus each generation of multiple recycle will last at least 11 years. Multiple recycle scenarios therefore extend over very long periods measured in decades. It is clear that over such extended time scales there will be ample opportunity for major changes in world energy requirements and strategies. It may well be the case that the scenario considered here is overtaken by events well before even the first or second generations of recycle are completed. Nevertheless, it is important to analyse such scenarios, just to be sure that they are practical technically, strategically and logistically, and to establish their impact on environmental and safety considerations.

The rationale behind including a highly-moderated PWR lattice is that theoretically, such a lattice may demonstrate technical advantages in multiple recycle scenarios. The idea would be to dedicate a small number of new PWRs exclusively to MOX usage. With no need to accommodate UO_2 fuel, the reactor designer could then choose to optimise the moderator/fuel volume ratio for plutonium. It turns out that the optimum occurs at moderator/fuel volume ratio of about 3.5, compared with 2.0 for uranium fuel in a standard lattice. This could be achieved by preserving the fuel rod design and dimensions and simply increasing the rod-to-rod pitch. The reactor core would be marginally larger in its radial

dimensions, but otherwise the reactor design and the associated equipment would be much as for a conventional PWR. The key physics issues are those of:

- *The variation of k_∞ with burn-up for the MOX infinite lattice calculations with burn-up during each recycle generation*. It is important for nuclear designers to be able to predict the k_∞ behaviour with a good degree of confidence if cycle length predictions are to be accurate enough for a utility's requirements.

- *The behaviour of reactivity coefficients with recycle generation*. Reactivity coefficients such as boron, fuel temperature (Doppler), moderator temperature and moderator void are key parameters that will largely determine the practicability of multiple recycle. Determining precisely at what point any of these coefficients would become unacceptable is outside the scope of this study, as it necessarily requires a core-wide spatial analysis. Nevertheless, establishing the underlying trends with the number of recycle generations is a valuable first step.

- *The calculation of the isotopic evolution in each recycle generation.* Particularly as regards plutonium, burn-up calculations will determine the dependence of initial plutonium content on recycle generation. In turn, the initial plutonium content has major impacts on fuel fabrication, reprocessing and fuel thermo-mechanical and physics behaviour.

- *The comparison of the highly-moderated MOX lattice with a standard MOX lattice*. To test, in particular, whether such lattices would be advantageous in a multiple recycle scenario.

4.2.2 Weapons-grade plutonium

In order to understand the potential connection between fuels in commercial reactors and weapons proliferation, a discussion of materials is necessary. Materials suitable for nuclear explosive devices are commonly ^{235}U or ^{239}Pu; ^{233}U can also be used. ^{233}U extracted from short irradiation of thorium is suitable for small weapons such as tactical nuclear warheads or priming devices for hydrogen bombs.

The quality of the material is very important for the construction of an explosive device [112]. Uranium used for this purpose is typically more than 90% enriched in ^{235}U. Since ^{235}U undergoes fast fission, it can contribute to the fission process. Lower enrichment material can be used, but it becomes progressively more difficult to achieve a sustained multiplication factor higher than prompt critical. With lower enrichment, the critical mass of ^{235}U increases sharply. The increase is not as great in the case of ^{239}Pu. Plutonium seems, at first glance, an easier means of creating an explosive device. However, plutonium presents other difficulties: (1) it is a harder material than uranium to machine and to shape into a bomb, and (2) it requires a difficult implosion technique for detonation, while the simpler gun concept can be used with ^{235}U. Hence, the first ^{235}U bomb was used without testing, while the first ^{239}Pu bomb had to be tested first.

The lowest fissile content for the construction of a nuclear weapon is in the range of 10-20%. The figure 20% has been, somewhat arbitrarily, adopted for ^{235}U as a threshold by international organisations. Materials having an enrichment of about 20% are called Special Nuclear Materials (SNM) and are subject to special treatment. Since proliferation concerns were heightened, an effort was mounted to reduce to below 20% the fissile content of a number of experimental reactors, which were previously designed to operate with highly-enriched uranium. Similarly, the quality of plutonium affects the ease of construction and the efficiency of a plutonium bomb. The undesirable isotopes are ^{238}Pu, ^{240}Pu and ^{241}Pu, which build up with irradiation. ^{238}Pu, with its particularly high heating effect due to alpha

decay, raises the temperature of the metal, and causes a metallurgical phase transition that hampers the explosion of the device. ^{240}Pu causes two problems: first it dilutes the fissile ^{239}Pu; second, it is a strong source of spontaneous fission neutrons, making for a much less efficient and less predictable device. The third contaminant, ^{241}Pu, even though a superior fissile isotope, presents yet another problem. It decays, by beta decay, to americium with a half-life of 14.5 yr, which in turn decays by alpha emission with a half-life of 433 yr. Therefore, both ^{241}Pu and ^{238}Pu affect the "shelf life" of a weapon because of the heat and helium gas released in the decay. Since plutonium is a relatively weak and brittle material, the alpha decay of contaminants leads to rapid deterioration of the weapon and hence to the need for periodic replacement.

The fuel used in LWRs is enriched to 3-4%, an amount unsuitable for explosive devices. It is, of course, easier to reach higher enrichments starting from 3 or 4% than when starting from natural uranium (0.71%). The main concern for LWRs is rooted in the production of plutonium contained in spent fuel. The annual spent fuel discharge from a 1 000 MWe reactor contains an amount of the order of 200 kg plutonium.

Because of the high burn-up to which the fuel is typically exposed in a reactor, higher isotopes build up which degrade the plutonium for weapons purposes. But proliferation must be considered in the context of the entire fuel cycle. In this respect, the single most important item in the cycle is the existence of a reprocessing and re-fabrication facility wherein plutonium (and fissile uranium) are separated from fission products and re-fabricated for recycle in the reactor. It seems prudent to attempt to separate the reactor from its fuel cycle. While the exportation of reactor technology could be relatively unrestrained, the transfer of fuel cycle technology needs to be strictly regulated to render the fuel cycle proliferation resistant.

The United States and Russian Federation have declared significant quantities of weapons-grade (WG) plutonium to be surplus to their defence needs. Under a mutual agreement, both countries are working towards a plan for the final disposition of the material, with one option being the conversion of the material to mixed-oxide (MOX) fuel for nuclear reactors. The current agreement calls for the disposition of approximately 34 tonnes of WG plutonium by each country over the next 25 years. The experience with MOX fuel in these two countries is relatively small compared with that accumulated in European countries and Japan. For this reason an international experts group has been established at the OECD/NEA to facilitate the sharing of existing information and experience in the physics and fuel behaviour of MOX fuel as it relates to the disposition of weapons-grade plutonium. The experts group deals with the status and trends of reactor physics, fuel performance and fuel cycle issues related to the disposition of weapons-grade plutonium as mixed-oxide fuel.

In Russia the WG MOX fuel will be used in both fast (BN-600) and light water reactors (VVER-1000). Recent work in Russia has focused on the certification of the calculation codes and the design of MOX fuel assemblies and core configurations. The experts group has performed several benchmarking efforts to aid in the code certification process by providing experimental data and by sponsoring benchmarking exercises that provide useful verification of the Russian calculation methods. The VVER-1000 MOX Assembly Computational Benchmark [106] is one such benchmarking activity performed by the experts group. While the Russian codes and data have been certified for LEU-based fuel, the certification for MOX fuel is required because of the essential differences between reactors fuelled with MOX:

- Reduced worth of the control rods, boric acid and burnable poisons.
- Reduced effective fraction of delayed neutrons.

- Reduced moderator temperature reactivity coefficient at the end of fuel cycle.
- Increased pin power peaking factor at the boundary between MOX and UOX FA which makes it necessary to use fuel rods with different contents of plutonium in the fuel assembly.
- Increased quantity of fission neutrons.
- Increased neutron flux sensitivity to local changes of moderator/fuel ratio.

Chapter 5

OPERATOR TRAINING

Items originally intended to be addressed in this chapter include (items are taken from Table 1):

- *Simulator*. Needs for 3-D representations of the actual core configuration in actual NPP. Need to qualify simulators by coupled 3-D techniques.
- *Control room*. How can control room be improved based on application of 3-D coupled techniques? Suggestions to be provided.
- *EOP* that can be improved by the use of 3-D coupled techniques. Recommended analyses.
- *Operator*. Need to qualify operators in relation to 3-D neutron kinetics. Essential information to be given to operators that is connected with the subjects of present report/activity.

Notwithstanding the effort made, almost no information was found in relation to the second and fourth items listed, namely the connection between 3-D coupled neutron kinetics/thermal-hydraulics techniques and the concerned item. In and of itself, this constitutes a conclusion and is at the basis of the recommendations for future activities.

5.1 Simulators

Generally, the simulators are drawn up as full-scope simulators. Advanced thermal-hydraulic system codes coupled with 3-D neutronic models with different levels of simplification (due to the simulator requirements) are used for transients modelling.

A very important element of operator education is training on full-scale simulators, which are replicas of plant control rooms. Operators are trained in the simulators to operate the nuclear power plants in a safe and economical manner. The training includes both normal operation and all types of plant disturbances. Simulator courses comprise basic training and retraining as well as operational leadership and maintenance. The simulator computer replicates the actual plant processes using real-time mathematical models.

Simulator courses in Sweden include normal operation, abnormal operation and emergency operation. Normal operation includes training to start-up and shutdown the nuclear power plant according to operator procedures. Abnormal operation includes training to operate the plant according to abnormal operation procedures. Emergency operation includes training to shut down the nuclear power plant according to emergency operating procedure.

Requirements on simulator capability to model plant as realistically as possibly have increased in recent years. Development of more advanced and realistic simulators has to great extent been facilitated by the development of faster computers. An important reason for upgrading reactor models has been the necessity to consider various operational aspects as well as the risk of unforeseen incidents due to

new fuel designs. For example, introduction of part-long fuel rods in Forsmark 1 nuclear power plant has led to re-evaluation of the simulator's capacity to provide an adequate operator education. A recent inventory of modern educational requirements for the Forsmark 1 simulator has shown that the following issues should be handled by the new simulator:

- Local criticality.
- Stability.
- Injection of cold water into the core.
- Blockage of fuel element entrance.
- Loss of one or more main recirculation pumps.
- Power changes due to movement of one or more neighbouring control rods.
- Positive temperature coefficient during heat-up due to part-long fuel rods.

Proper treatment of the above issues requires the use of coupled multi-dimensional computer codes. Forsmark 1 has decided to upgrade its simulator using the coupled 3-D neutron kinetics code SIMULATE S3R with thermal-hydraulic code RELAP5. Input data to SIMULATE S3R is taken directly from CASMO/SIMULATE. The new simulator provides better training through greater accuracy.

5.1.1 Simulator of VVER-440 Dukovany NPP

There are two full-scope simulators at Dukovany NPP, the first being the full-scale display multi-functional simulator developed by Siemens AG Belgatom, CorysTESS and NPP Dukovany; it has been in operation since 1999. The second was developed by ORGREZ SC a.s. Brno, GSE Systems Inc. (USA), REGULA Praha a.s. and Silicon Graphics Computer Systems (computing system of simulator). This simulator is connected to a true replica of the Dukovany NPP main control room. The replica accurately represents the control room layout and plant design in all areas and is used to support initial and periodical training of shift operations staff. The full-sized main control room simulator (MCR) has been in use since January 2001.

5.1.2 Full-scope simulator of VVER-1000 in Temelín NPP

The full-scope simulator of the Temelín NPP is a mathematical model of the power plant, programmed on the Silicon Graphics computers and connected to a true replica of the Temelín NPP main control room. The general supplier is ORGREZ SC a.s. Brno. The simulator has been in operation since 2000. Basic information concerning the full-scope simulator VVER-1000 is provided below.

The simulator is used for preparation of operational control personnel for Temelín NPP and the verification of I&C system algorithms according to the power plant design and operating procedures (among other things).

The following main parts constitute the simulator: the control room, which is a true replica of the main control room (including all instrumentation) at Unit 1 of Temelín NPP, input and output system with a capacity of 16 000 signals used as a link between the instrumentation of the control room and the computer system of the simulator. The computer system of the simulator is based on multiprocessor computers using the Silicon Graphics' Challenge series.

Capabilities include simulation in real time with a possibility to slow down, stop or proceed in steps; acceleration is possible for certain processes. The fidelity of simulation meets the highest level of world standards of similar equipment in use.

The scope of simulation includes all normal operational conditions, abnormal conditions and selected emergency conditions.

The level of complexity of the simulator can be evaluated by considering that 3 600 actuators (valves, engines, switches, etc.), 6 500 sensors and 500 000 variables are part of the system and that approximately ten thousand failures can be simulated.

5.2 Control room

This subject was included in the plan of the CRISSUE-S prepared for the kick-off meeting. A limited amount of information was found in relation to the control room issue and the application of coupled neutron kinetics/thermal-hydraulic techniques. Some information can be found in Sections 5.1 and 5.3.

5.3 Emergency operating procedures

5.3.1 Background information and objectives

Emergency operating procedures (EOP) are essential for maintaining fundamental safety functions and preventing core damage during both design basis accidents (DBA) and beyond design basis accidents (BDBA) in a nuclear power plant. Many NPP are currently improving their EOP. The level of implementation in different NPPs is however very different, varying from the preparatory phase up to fully implemented and validated set of procedures. The use of international experience can therefore be helpful for the development and implementation of EOP in individual NPPs as well as for their independent review [55].

At present EOP are also implemented in operator training and in full-scope simulators in NPPs equipped with VVER reactors. A brief description of full-scope simulators for Dukovany NPP (VVER-440) and Temelín NPP (VVER-1000) has been presented.

5.3.2 EOP role in operator training

In an overall training programme it is obvious that only a limited amount of time can be dedicated to the EOP. Therefore, it is very important that the procedures be written in a user-friendly way. Even then there is a need for training that should be provided in two phases: initial theoretical training, and continuous re-training. The programme would be greatly plant specific and would have to meet overall plant training practices and general regulatory requirements. However, it is worth providing some indications as to the priorities that should be reflected in the training programme as well offering some illustrative examples.

Ref. [56] discusses the development of a sophisticated training programme realised by Paks NPP in collaboration with WESE as from 1988. The basic goal of the training programme was to provide operators with adequate knowledge of the plant response during emergency situations so as to achieve a better understanding of EOP strategies. The content of the training included:

- *Thermal-hydraulic phenomena*. Heat transfer, natural circulation, mixing in the reactor pressure vessel (RPV), pressurised thermal shock (PTS), use of main loop isolation valves (MLIV) during emergencies.

- *Loss-of-coolant accident (LOCA)*. Classification of LOCA, core dry-out and flooding during LOCA, loop seal effect, demonstration of LOCA of different sizes.

- *Steam generator tube rupture (SGTR)*. Classification and features, possible post-SGTR cool-down techniques, major operator actions during SGTR, demonstration of SGTRs of different size.

- *Secondary breaks*. Review and classification of secondary breaks, major operator actions, demonstration of different sizes of secondary breaks

Initial theoretical training should mainly include explanations of the overall logic of the EOP package, rules of usage, major strategies, etc. It is recommended that adequate training material be prepared in advance for the operators for two reasons: at this stage there are usually no other training materials available, and EOP documentation is quite extensive and provides too much information for the operators to digest. Experience shows that the operators are not able, without previous knowledge, to use the background documentation and other EOP support documents for individual study. The training material should include discussion and explanation of all topics and concepts that are new to the operators.

If the plant developed a new, sophisticated EOP package the highest priority is to explain the concepts of symptom-based guidance, scenario independence, function/state orientation, safety functions (critical safety functions), etc., which are in conflict with what the operators were used to. Another high-priority item is a description of strategies and their physical background. It has been experienced that the operators have not been adequately aware of or accustomed to applying basic physical concepts that underlie some basic strategies, like subcooling, mass and energy equilibrium during SI safety injection cool-down, etc.

Possible re-training ideally should be mainly of the hands-on type with transients being trained on the simulator. It should also include some theoretical study that reflects the hypothetical problems that could be encountered during the practical training. The focus and high priority should be placed on the following aspects and scenarios, including:

- Rules of usage.

- Most probable accidents (for instance it is of good practice to train the operators of PWRs and VVERs in dealing with steam generator tube ruptures).

- Accidents with a high probability of radioactive releases.

- Accidents – or a sequence of steps – that may be time-critical.

5.3.3 Implementation of EOP in the control room

The implementation of EOP is the milestone of the entire project, the final objective of the EOP development programme and the real moment at which plant safety is greatly improved. If the validation and training could be performed on a full-scope simulator that is a replica of the control room a number

of feedback cases could certainly be provided on the real use and implementation of the procedures. All necessary adjustments could be made from this feedback and the operator should feel comfortable with his new situation.

Other such implementation optimisation items may be needed or desired and will strongly depend upon the control room design. Response-time items and crew-efficiency items are a couple of the non-technical aspects of the EOP that are usually good candidates to be given a specific look with respect to the control room implementation optimisation. An indicative list (not complete) is given below:

- Careful review of the control room staff and distribution of roles.
- Distribution of control room staff EOP documents (one per operator or only one for the supervisor).
- Careful review of the control room communication standards.
- Implementation rules for the monitoring of specific safety functions.
- Rules of usage for the continuous diagnostic.
- Implementation of checklist, detailed action list provided in attachments, etc.
- Identification of time-consuming actions and proper sequencing of such actions.
- Field actions (communication with the control room, availability of necessary documentation to the field operators, ability to synchronise control room actions with field actions whenever necessary).
- Participation of instructors.

It should be noted that implementation of symptom-based EOP (symptoms are defined as direct/ unambiguous pieces of information of measurable plant parameters that can be made available to the operator in the control room) may involve plant modifications necessary for the realisation of strategies or leading to improvement of the plant response to specific events based on information gained throughout the EOP development project. An example of plant modifications undertaken due to EOP implementation in a VVER 440/V-213 NPP Dukovany include [57]:

- Hardware modifications:
  - Installation of power operated relief valve (PORV).
  - Modification (increasing of head pressure) of the auxiliary feed water pump.
  - Decreasing the hydro-accumulator pressure to 3.5 MPa and change in operational status of the isolation valves to be energised.
  - Installation of the hydrogen recombiners in containment.
  - Sump protection against clogging.

- Improvement of control of PRZ safety valve.
- Installation of the reactor pressure vessel head venting.
- Replacement of emergency feed water piping.
- Realisation of connection between reactor coolant pump (RCP) room and the containment.

- I&C (instrumentation and control) modifications:
  - Measurement of level in the containment.
  - Extension of pressure measurement in the containment.
  - Modification of the Engineered Safety Features Actuation System (ESFAS) signal – "Main steam header rupture".
  - Extension of the core exit temperature measurement to 1 000°C.
  - Realisation of the automatic switch of the suction of safety injection (SI) pump.

- Planned modifications related to the EOP:
  - Reactor protection system – new signals and hardware upgrading.
  - ESFAS upgrading.
  - Enabling of ESFAS reset?
  - Exchange of ionisation chambers.
  - Simplification of the Automatic Load sequencer.
  - Installation of the Safety Parameter Display System (SPDS) and the Post-accident Monitoring System (PAMS).
  - Provision for connection of fire water into SG.
  - Establishment of Technical Support Centre.
  - Installation of steam dump to atmosphere on steam lines.

5.4 Operator

This issue was included in the plan of the CRISSUE-S prepared for the kick-off meeting. A limited amount of information was found in relation to this subject and the application of coupled neutron kinetics/thermal-hydraulic techniques. However, some information, namely operator qualification and tools to achieve the operator qualification, is discussed in Section 5.1 above.

Chapter 6

REGULATORY REQUIREMENTS

6.1 Background

The subjects addressed in this chapter include (items taken from Table 1):

- *The ATWS issue*. Lists of recommended ATWS analyses and requested calculation assumptions.
- *The prescribed reactivity accident analysis low power (hot, cold)*. Hypotheses requested for the CR ejection analysis in the FSAR.
- *Acceptance criteria*. Typical list of checked quantities and threshold values acceptable to various regulatory authorities (as much as possible).
- *BWR stability*.

These issues were selected during the CRISSUE-S kick-off meeting and provide an idea of the current status of the interaction between the regulatory requirements and the coupled 3-D neutron kinetics/thermal-hydraulic techniques.

6.2 The ATWS issue

Anticipated transients without scram (ATWS) are anticipated operational occurrences followed by the failure of one reactor scram function. Available transient analyses of ATWS events indicate that VVER reactors, like PWRs, have a tendency to shut themselves down if the inherent nuclear feedback is sufficiently negative. Various control and limitation functions of the VVER plants also provide a degree of defence against ATWS. In the following sections the essential conclusions valid for VVER ATWS analyses are summarised [58].

6.2.1 Safety rules and practices for ATWS in different countries

6.2.1.1 Bulgaria

The list of initiating events to be analysed for plant licensing is defined in Annex 3 of Order No. 5 of the “Law on the Use of Atomic Energy for Peaceful Purposes”. This list does not include ATWS. In addition, there is no direct requirement to consider ATWS events in the relevant Russian regulations applicable to VVER reactors.

6.2.1.2 Czech Republic

In the Czech Republic, consideration of the ATWS-related accidents is not required by the regulations as part of the Safety Analysis Report (SAR). Nevertheless, they were included into the

Temelín NPP SAR prepared by Westinghouse, in compliance with the US regulatory requirements of the NUREG-0800 Standard Review Plan. A similar scope for ATWS calculations is recommended by the International Atomic Energy Agency (IAEA) and the European Nuclear Assistance Consortium (ENAC).

Following these recommendations, the Nuclear Research Institute (NRI) at Rez has provided ATWS calculations for VVER-440/213 NPPs, especially with regard to:

- Loss of steam generator feed water.
- Loss of flow.

ATWS analyses have also been performed for VVER-1000 plants using the RELAP5 computer code. The following accidents in particular were taken into account:

- Loss of flow.
- Inadvertent opening of the pressuriser safety valves.
- Inadvertent opening of steam dump valves to atmosphere.
- Leakage from the pressuriser upper part.

According to previous US practice, the ATWS-related calculations should consider the following limiting values: fuel damage limits are not exceeded during ATWS events, reactor coolant pressure boundary limits are not exceeded during ATWS events.

6.2.1.3 Finland

The position of the Finnish Regulatory Authority STUK on ATWS requirements is presented in the Guides YVL 2.2. and YVL 2.4. The former concerns transient and accident analyses and the latter concerns overpressure protection.

The basic approach is to consider ATWS events as design basic events. Therefore, the general assumptions and acceptance criteria for postulated accidents are also applied to ATWS events. This implies conservative assumptions as pertains to uncertainties of various parameters and system characteristics. As a rule, safety systems are assumed to operate in their minimum design configuration.

6.2.1.4 Hungary

In the original design there was no requirement to carry out analysis of ATWS events as part of the SAR. Therefore, the first ATWS analysis was performed in 1993 only in the framework of the AGNES project for the Paks NPP Unit 3. According to the new regulations issued in 1997 there are regulatory requirements for ATWS events, stipulating that “the design basis shall also incorporate those anticipated operational occurrences which can be derived from the assumption that one of the safety protection functions will not work”.

The ATWS events have to be analysed whenever the frequency of the initiating event together with that of failure of any of the safety protection functions is higher than 10^{-5}/reactor-year. These requirements have also been applied for the Periodic Safety Review of Paks NPP Units 1-2, which was completed in 1996. Numerical criteria for fuel elements as well as for primary and secondary circuit pressures have been established for ATWS analysis.

Best-estimate calculations using the SMATRA code (developed by VTT, Finland) have been performed for the following initiating events: inadvertent withdrawal of a control assembly group, loss of feed water, loss of off-site power, trip of both turbines and inadvertent closure of the main steam isolation valve. It was stated that over the course of the ATWS events analysed, no violation of safety criteria occurred. It was further stated that neither the cladding temperature nor the pressures exceed values allowed by the regulations.

6.2.1.5 Russian Federation

The ATWS concept is not mentioned in Russian regulations, and ATWS events are not included in the list of initiating events recommended by the Russian Safety Authority Gosatomnadzor of concern in the VVER design. In other words, Gosatomnadzor does not bring up the deterministic requirement on the necessity of ATWS consideration. The Russian safety rules indicate the safety goals which a reactor designer should try to attain: core melt frequency less than 10^{-5}/reactor-years and excessive radioactivity release frequency, requiring the evacuation of the population, less than 10^{7}/reactor-years. Therefore, all the initiating events which could contribute essentially to these values must be included in the beyond design basis accident (BDBA) list to be agreed upon with Gosatomnadzor and analysed.

However, reactor scram (AZ) failure is not included in the lists of BDBA agreed upon with Gosatomnadzor for the Balakovo, Kalinin and Novovoronezh NPPs. The main reason for this fact is the low probability of reactor scram failure. Nevertheless, ATWS scenarios for VVER-1000 reactors have been under detailed investigation in Russia since the early 1980s. The first studies were carried out in response to scientific interest or because of the development of the reactor designs for potential foreign customers.

6.2.1.6 Slovakia

ATWS-related analysis was not originally considered within the framework of SARs until 1994. Starting with the major gradual upgrading of Bohunice NPP Units 1 and 2, both of which are equipped with VVER-440/230 reactors, ATWS analyses were required by the Nuclear Regulatory Authority of the Slovak Republic to be included in the SAR for plant modifications. The general regulatory requirement on accident analysis incorporating ATWS events was also issued in 1996. This requirement regarding conditions for ATWS analysis is consistent with the IAEA Guidelines.

The acceptance criteria for ATWS events were selected as for postulated accident conditions, with the exception of increased values for limitation of pressure both in the primary and secondary circuits. Further restrictions were prescribed in 1997 under the preparatory phase of the SAR for the Mochovce NPP. Conditions for long-term stable cooling of the reactor core are required if a departure from the nuclear boiling ratio (DNBR) limit is exceeded. Calculations were performed using realistic values of initial steady-state parameters for RELAP5 and DYN3D best-estimate codes. Except for the blocking of all control rods, all safety-related equipment was assumed operable.

6.2.1.7 Sweden

There are not any specific ATWS rules in effect in Sweden. The reason is that the probability for ATWS was considered to be very low because of the possibility to insert control rods by electrical motors in addition to fast hydraulic insertion. The Swedish BWRs also have a manual boron system. The primary objective of the boron system is to keep the system subcritical in case several adjacent control rods cannot be fully inserted.

The electrical control rod insertion system and the boron system do not fulfil all requirements that exist on safety systems and new regulations are being discussed. The final proposal will probably be that all anticipated transients during plant lifetime should be analysed with respect to failure to scram. The success criteria will be that of the design basis accidents, *i.e*. fuel melting, cladding temperature and oxidation, and integrity of the pressure boundary.

6.2.1.8 Ukraine

According to the Ukrainian Law "On the Use of Nuclear Power and Radiation Safety" all power units should have obtained their operating licences before the year 2000. A new regulatory document: "The Requirements for Contents of Safety Analysis Report" was introduced in Ukraine in 1996. One of the sections of the SAR deals with ATWS analysis.

The list of accidents and ATWS events must be approved by the Nuclear Regulatory Administration. In accordance with regulatory requirements, the utilities have to perform ATWS analyses and must define the probabilities of the transients. Depending on the probability of ATWS events, two cases are to be evaluated.

If ATWS events have not been considered in the original design, but have a high probability of occurrence, then they should be assessed according to DBA requirements. Based on the results of the assessment, procedures or system and component modifications should be implemented (*e.g*. replacement of pressuriser safety valves using a "feed and bleed" procedure). If ATWS events have not been considered in the original design, but have a low probability of occurrence ($<10^{-4}$/reactor-year) they can be analysed with less conservative assumption or best-estimate methods. ATWS events with rather low probability ($<10^{-5}$/reactor-year) are not to be considered in the design, but may be studied from an accident management point of view.

6.2.2 Guidance for performing ATWS analyses

This section is devoted to providing guidance for performing specific ATWS analyses for VVER plants using computer codes and IAEA guidance [58]. This guidance reflects international practice. It is more focused on VVER-1000 reactors, but also provides guidance for ATWS events in VVER-440 reactors taking into consideration the differences in reactor type.

6.2.2.1 Initiating events

Definitions of ATWS can be found in a new regulatory document which are currently in force (US 10 CFR, German RSK guidelines, IAEA Guide 50-SG-D11, French guidelines). According to these definitions, an ATWS event is an anticipated operational occurrence followed by the failure of the reactor scram function. Therefore, only the events which are expected once or several times during the life of the nuclear power unit must be considered as ATWS initiators. Such events are included in the list of VVER-1000 design basis events under the designation "violations of normal conditions of operation", which is considered to be equivalent to the Western designation "anticipated operational occurrences".

For standard VVER-1000/320 NPPs, the conditions to be considered as potential ATWS transient initiators are listed below based on the recommendations set out in Ref. [59]:

- Reactivity accidents:
  - Inadvertent withdrawal of a control rod group during start-up.
  - Inadvertent withdrawal of a control rod group during power operation.
  - Control rod malfunction, including:
    - ⇒ Drop of one CR.
    - ⇒ Static misalignment of one CR in a group.
  - Decrease of the boron concentration in the reactor coolant due to chemical and volume control system malfunction.
- Loss of flow transients:
  - Single and multiple MCP trips.
- Increase of coolant mass inventory in primary circuit:
  - Inadvertent actuation of ECCS during power operation.
  - Chemical and volume control system malfunction that increases reactor coolant inventory.
  - Feed water system malfunction that decrease feed water temperature.
  - Feed water system malfunctions that increase feed water flow rate.
  - Secondary pressure regulator malfunctions that increase steam flow rate.
  - Inadvertent opening of one steam generator safety or relief valve or turbine bypass valve.
  - Control system malfunction that decreases steam flow rate.
  - Loss of external electric load.
  - Turbine stop valve closure.
  - Main steam isolation valve closure.
  - Loss of condenser vacuum.
  - Main feed water pump trips.
  - Loss of on-site and off-site power to the station.

From the above list, only events such as turbine trip that are normally terminated by reactor scram (AZ) should be considered as potential candidates for the list of ATWS to be analysed. The reactor protection system design for VVER-1000 plants has been developed with a view to reducing or limiting the reactor power and thereby avoiding an unnecessary reactor scram. There are four levels of reactor protection related to power reduction:

- *Preliminary protection of the second level (PZ-2 in the design documentation) AZ4.* The function of PZ-2 is to stop the control rod group withdrawal to prevent a reactor power increase above the values allowed by the technical specifications.

- *Preliminary protection of the first level (PZ-1) AZ3*. The function of PZ-1 is to insert the control rod groups (beginning with the "working" control group) with the normal velocity of 2 cm/s to decrease the reactor power until the actuation signal disappears.

- *Accelerated off-loading of the unit (URB) AZ2 20 cm/s*. The function of URB is to decrease reactor power rapidly by means of pre-selected control rod group dropping (the power decrease upon the current worth of the pre-selected group). Further decreasing of the reactor power (if needed) up to the allowed level is performed by the PZ-1 operation.

- *Emergency protection (AZ) which is the reactor trip portion of the protection system AZ1*. The function of AZ is to decrease reactor power rapidly down to residual heat by means of the simultaneous dropping of all control rod groups, thereby bringing the core to subcriticality.

When considering the above list of occurrences and protection signals to detect incidents leading to reactor scram, it should be kept in mind that an ATWS event belongs to a category of events which should be handled differently from the design basis accident (DBA) approach. In particular, with the exception of those systems which are affected by the initiating event itself or as a consequence thereof, all systems may be assumed to function as designed. Therefore, assumptions concerning the operability of PZ and URB systems must be based on the scram failure modes assumed for a given ATWS analysis. Some failure modes may preclude the operation of PZ or/and URB (*e.g*. if mechanical sticking of control rods is assumed as the reason for scram failure, URB must be assumed inoperable). Clearly, with this approach, the list of ATWS events to be analysed will to some extent be plant specific, as certain PZ/URB set points and/or signals may vary from plant to plant.

Nevertheless, to simplify the work of plant specific ATWS analysis, and especially for the purposes of generic ATWS analysis, one may assume inoperability of all functions related to the insertion of the control rods into the core. Taking this approach, it is recommended that the ATWS events listed below be analysed for VVER-1000 nuclear power plants:

- Uncontrolled withdrawal of a control rod group during start-up or power operation.

- Loss of main feed water flow.

- Loss of on-site and off-site power to the station.

- Loss of condenser vacuum.

- Turbine trip.

- Loss of electrical load.

- Closure of main steam isolation valves.

- Inadvertent opening of one steam generator safety or relief valve or turbine bypass valve.

6.2.2.2 Assumptions in the analysis

According to Western practice, ATWS events belong to the beyond design basis accident (BDBA) category and can therefore be analysed with best-estimate methods. The same approach should be applied to VVER-1000 reactors. However, if the work performed in a particular country results in a relatively high probability of scram failure, the application of the best-estimate method should be limited accordingly.

Initial conditions

Initial conditions (measured or calculated) should be chosen at their most probable values, without uncertainties and errors, and based on their operating range in the foreseen initial state. The initial conditions should be consistent at least for full-load initial state. Of course, beginning of cycle (BOC) or end of cycle (EOC) should be chosen correspondingly when penalising for the considered event. Important parameters (reactivity coefficients, peaking factors, etc.) should correspond to the neutronic calculations without uncertainty and calculation errors. Equilibrium xenon at full power and xenon-free at low power should be assumed when calculating reactivity coefficients.

Operability of systems

Operability of systems should be considered in a realistic way. Proper modelling of all control and safety systems that affect the accident should be included. No failures, no artificial delay in the actuation signals, no conservative protection system set points, no penalising value in the resulting effect should be considered in the analyses.

Non-safety systems or equipment may be considered and modelled in the analyses if they are designed to withstand accident conditions. This covers particularly all the control devices, even when favourable consequences are foreseen. However, careful attention should be paid to the control system actuating a control rod group (temperature or power control rod group) as long as a clear understanding of independence between scram actuating signal and control actuation has not been established. In such a case, bearing in mind the common mode failure (CMF) concept, it is recommended not to model the control function as a means of mitigating the consequences of ATWS events.

Further applicable assumptions are as follows:

- The single failure assumption need not be considered, nor simultaneous repair work postulated.
- Loss of off-site power (LOOP) should not be considered unless it is a direct consequence of the initiating event itself.
- If the accident is affected by the phenomena that cannot be modelled properly (*e.g.* due to the lack of the experimental data) an approach should be selected which derives conservative results.

Operator intervention

Provided there is a clear and reliable indication for diagnosis in the framework of ATWS events, the time for operator intervention may be assumed to be (at a minimum) 10 minutes if the action can

be initiated from the control room, when the action corresponds to the respective operating procedure and the operator has been adequately trained in its use. For other action, this time margin should be realistically evaluated.

6.2.3 Acceptance criteria

In general, ATWS acceptance criteria are comparable to the criteria for the postulated accidents and address primary system integrity, fuel cooling capability, shutdown reactivity and off-site radiological consequences. In particular:

- International practice accepts less restrictive reactor coolant system (RCS) pressure limits for ATWS. ATWS limits are generally based on allowable stress limits for ASME Service Level C or 135% of design pressure (for VVER-1000 reactors, this is also the primary circuit hydro test pressure).

- Fuel cooling capability should be demonstrated, *i.e.* core damage and calculated changes in core geometry do not prevent long-term core cooling. However, there is no international consensus as regards acceptance criteria.

- The analysis of ATWS events should demonstrate that a safe and stable shutdown of the reactor is achieved. Common international practice is to accept a subcriticality of 1% as an adequate indication of reactor shutdown.

- For radiological assessment, a generally accepted approach is to assume that fuel cladding failure (leakage) occurs for all fuel rods having a potential for boiling crisis, *e.g.* having a DNBR less than the value that gives 95% probability at 95% confidence level that DNB does not occur. Less conservative approaches have not been found necessary to demonstrate that site boundary limits for postulated accidents are not violated.

6.3 The BWR stability issue

The stability of BWR reactor systems has been a concern from the inception of this reactor type, and extensive experimental and theoretical studies have been performed to design a stable fuel and core configuration. The requirement of stability is expressed in the general design criteria for nuclear power plants as outlined here: “The reactor core and associated coolant, control and protection systems shall be designed to assure that power oscillations which can result in conditions exceeding specified acceptable fuel design limits are not possible or can be reliably and readily detected and suppressed”.

The problem seemed to be resolved for a long period of time, as no oscillation occurrence was experienced in BWRs for several years. Since then a number of fuel and core design changes have taken place and the power densities of the core have increased. Indications appeared in the late 80s that instability may still be a problem. Instability events had been observed in TVO-1 and Forsmark 1 (1987) and later also in LaSalle (1988). Subsequently, authorities in all countries required a review of the stability features of their BWRs. All authorities include analyses in the safety analysis reports. Authorities in some countries required changes in the procedures and plant safety systems. In other countries recommendations were made. In many cases the stability question is an integral part of the reload analyses using advanced methodology. Such technology is not generally used and in many cases only engineering judgement is available. For other reactors possible exclusion regions are identified by measurements as a part of the start-up procedure.

Authorities have also emphasised the importance of training the operators to handle instabilities. One problem with this is that the computer programs' full-scope simulators can not truly simulate an instance of instability, a state of affairs which also calls for development of improved simulation methods for operator training.

The major safety concerns associated with instability are the cooling of the fuel and cladding integrity. A further safety concern is large undetected reactivity insertions taking place (for instance) during regional oscillations. In cases where the two halves of the core oscillate are in opposite phase, the oscillation may not always show up in the APRM signal, which is used by the reactor protection system. It has also been observed that severe un-damped oscillations may occur as a result of other kinds of transients such as feed water transients. Also of importance is the case during which external disturbances occur at or near the resonance frequency of the core.

Modern technology in the control room may also render instability detection more difficult. At one Swedish plant digital instrumentation had been introduced, which prevented detection of instability although the amplitudes were large. Dedicated stability monitors are thus used in many cases to provide the operators with a warning when unstable areas are approached.

For the long term, modifications of the protection systems are under consideration in many countries. Such modifications should ensure that the reactor instrumentation and protection system can reliably protect the core against all kinds of instability without being wrongly activated under other circumstances.

6.4 The reactivity accident issue and the events to be considered

A description of the methodology used when analysing control rod ejection belonging to the group of reactivity-initiated accidents is given. A first example focuses on the methodology used by Westinghouse for rod ejection analysis in Temelín NPP. A second example describes the methodology used by Vuje-Trnava (Slovakia) for control rod ejection analysis in Bohunice NPP. Within this framework, the essential conclusions valid for VVER control rod ejection analysis, taken from the IAEA guidelines [59], are accounted for and described.

Table 12 provides a list of the events for which analysis is required by the Czech regulatory authorities and by US NRC RG 1.70 [65,66]. Event classification is included, and reference is made to the acceptance criteria listed in Table 13 (see Section 6.4.3.3).

6.4.1 Spectrum of rod ejection accidents for the Temelín NPP (VVER-1000)

6.4.1.1 Event description

The rod ejection accident is defined as an assumed failure of a control rod mechanism pressure housing such that the reactor coolant system pressure would eject the control rod and drive shaft to the fully withdrawn position. The consequence of this mechanical failure is a rapid reactivity insertion with an adverse core power distribution.

If such an event were to occur, a fuel rod thermal transient which could cause DNB may take place, engendering limited fuel damage. The amount of fuel damage that can result will be governed mainly by the worth of the ejected rod and the power distribution attained with the remaining control rod pattern. The transient is terminated by the Doppler reactivity effect of the increased fuel temperature

Table 12. List of reactivity accident events, classification and specification of acceptance criteria used for Dukovany and Temelín NPPs

Event	Classification		Acceptance criteria*	
	Decree No. 2 [59,64]	ANS-51.1/ N18.2 1973 [67]	Dukovany NPP	Temelín NPP
Uncontrolled control rod assembly bank withdrawal from a subcritical or low start-up conditions	Abnormal	Condition II	(1,2a,2b,3)	(1,2c)
Uncontrolled control rod assembly bank withdrawal at power	Abnormal	Condition II	(1,2a,2b,3,4a, 4b)	(1,2c,4c,4d)
Control rod assembly malfunction a) Dropped rod b) Single rod (assembly/cluster) withdrawal at power	Abnormal	Condition II Condition III	(1,2a,2b,3,4a, 4b)	(1,2c,4c,4d) (7)
Start-up of an inactive reactor coolant loop at an incorrect temperature	Abnormal	Condition II	(1,2a,2b,3,4a, 4b)	(1,2c,4c,4d)
Chemical and volume control system malfunction that results in a decrease in boron concentration in the reactor coolant	Abnormal	Condition II	(1,2a,2b,3,4a, 4b,11)	(1,2c,4c,4d, 11)
Inadvertent loading of a fuel assembly into an improper position		Condition III		
Spectrum of control rod ejection accidents	Accident	Condition IV	(5,6,9,15)	(5,6,8,9,10, 15)
Spectrum of steam system piping failures	Accident	Condition III & IV	(1,12,13,14, 15)	(1,2c,4c,4d, 15)

* See Table 13 in Section 6.4.3.3.

and by the reactor trip actuated by neutron high flux signals, before conditions are reached that can result in damage to the reactor coolant pressure boundary, or sufficiently disturb the core, its support structures or other reactor pressure vessel internals such that the capability to cool the core is impaired significantly.

Features of the Temelín design preclude the possibility of a rod ejection accident, or limit the consequences of the event if it were to occur. These include a thorough quality control programme during assembly, and a nuclear design which lessens the potential ejected worth of the control rods.

Conservatively, the nuclear design analysis assumes that the rods are positioned at the rod insertion limits as the precondition for the accident. The single rod resulting in the largest reactivity worth and total peaking factor is assumed to be an ejected rod. Since the resulting transient is very rapid, the Doppler and moderator feedback from the precondition case is frozen when the worth and total peaking factor following the rod ejection is determined. The resulting worth and peaking factors for the worst ejected rod are verified to be below the bounding values assumed in the transient analysis. The ability to maintain a subcritical core subsequent to a rod ejection assuming an adjacent rod remains stuck out of the core in addition to the ejected rod is also verified.

6.4.1.2 Acceptance criteria

The rod ejection event is classified as a postulated accident. Postulated accidents are of such low frequency (<10^{-2}/year) that they are not really expected to occur, though they are considered in the design. Acceptance criteria include:

- Average fuel pellet enthalpy at the spot shall remain below 200 cal/g for un-irradiated fuel and for irradiated fuel. This criterion ensures that core coolability is maintained.

- Average clad temperature at the hot spot shall not exceed 1 649°C and zirconium-water reaction less than 16% by weight (mg of reacted Zr per volume). This ensures that clad melting and embrittlement are avoided.

- Peak reactor coolant pressure shall remain at a value lower than the value which could cause stress to exceed the faulted condition stress limits. This ensures that the structural of the reactor coolant boundary is not threatened.

- Fuel melting limited to less than 10% of the fuel volume at the hot spot, even if the average fuel pellet enthalpy is below the limits of the first item in this list. This ensures that fuel dispersal in the coolant will not occur.

6.4.1.3 Initial conditions

The rod ejection event is analysed to bound operation from zero to full power. However, if shutdown margin requirements are met, the ejection of a rod during hot shutdown would not insert sufficient reactivity to attain criticality, as the shutdown margin requirements are determined assuming that the most reactive rod is fully withdrawn. In cold shutdown and refuelling conditions, ejection is impossible, because the RCS is depressurised. This event is analysed in eight cases to bound the entire fuel cycle and operating conditions expected. These cases are as follows:

- Beginning of cycle, zero power, two-loop operation.

- End of cycle, zero power, two-loop operation.

- Beginning of cycle, full power, four-loop operation.

- End of cycle, full power, four-loop operation.

- Beginning of cycle, full power, three-loop operation.

- End of cycle, full power, three-loop operation.

- Beginning of cycle, full power, two-loop operation.

- End of cycle, full power, two-loop operation.

In the zero-power TWINKLE calculations [60] (see also Section 6.4.1.5), a power level lower than expected for critical, zero-power conditions is assumed. This corresponds to a flux level of 10^{-9} of nominal rated full power. This initial power level minimises the Doppler reactivity feedback. In the

full-power TWINKLE calculations, a nominal core power corresponding to four-, three- and two-loop operation is assumed (100%, 67%, 50%). These initial power level values maximise the time until the power range high neutron flux (high setting) set-point is reached.

In the zero-power FACTRAN calculations [61] (see also Section 6.4.1.5), a flux level of 0.001 of nominal is assumed. In the full-power FACTRAN calculation, a maximum core heat flux corresponding to four-, three- and two-loop operation is assumed (104%, 70%, 52%). These initial core heat flux values maximise the initial fuel and clad temperatures.

Since the magnitude of the power peak reached during the initial part of the transient for any given ejected rod worth is strongly dependent on the Doppler coefficient, a conservatively low (least negative) value is used. A Doppler defect value of 0.8% $\Delta k/k$ is assumed in the initialisation of analysis. A Doppler weighting factor is then applied to the overly conservative one-dimensional calculated Doppler feedback to account for the expected increase in feedback as a result of the skewed power distribution that would occur after the control rod is ejected.

Calculation of the effective delayed neutron fraction (β_{eff}) typically yields a value no less than 0.75% at beginning of life and 0.44% at end of life. The accident is sensitive to β_{eff} if the ejected rod worth is equal to or greater than β_{eff} as in zero-power transients. In order to allow for future cycles, pessimistic estimates of β_{eff} of 0.55% at beginning of cycle and 0.44% at end of cycle were used in the analysis.

For the zero-power cases, two main coolant pumps are assumed to be in operation, which is the minimum number of pumps required. For the full-power cases, four, three and two main coolant pumps are assumed in operation.

6.4.1.4 Availability and functioning of systems and components

The primary reactor protection system (PRPS) mitigates the consequences of these events. Reactor trips can be generated by any of the following protection functions of the PRPS:

- Source range high neutron flux.
- Source range high flux rate.
- Wide range high neutron flux.
- Wide range flux rate.
- Power range high neutron flux (low setting).
- Power range high neutron flux (high setting).
- Power range high neutron flux rate.

For the zero power case, a 10% increase in the nominal power range high neutron flux (low setting) reactor trip set-point is assumed. Thus, a set-point of 35% of the nominal rated full power is assumed.

For the full-power cases, 9%, 6% and 5% increase in the nominal power range high neutron flux (high setting) reactor trip set-point for four-, three- and two-loop operation, respectively, are assumed. Thus, set-points of 118%, 80% and 62% of nominal rated full power are assumed for the four-, three- and two-loop operation cases.

The time delay after the reactor trip set-point is reached and before the rods start to fall is assumed to be 0.9 seconds. After the release of the rods, a rod drop time to dashpot of 3.5 seconds is assumed.

Trip reactivity insertion is simulated by dropping the appropriate rod worth into the core from the full-out position. This is conservative, since some control banks will actually be partially inserted in the core. The trip of these banks would provide a more rapid rate of negative reactivity addition than assumed in the analysis.

Reactor control and limitation systems are assumed to function only if their operation results in more severe transient conditions. No control or limitation system is assumed to function in the rod ejection event because the transient is faster than the expected effects of control or limitation system operation.

The most limiting single failure for this event is assumed to be failure of one division of the PRPS. The protection function is then carried out by the two remaining divisions of the PRPS. No single active failure will prevent operation of the PRPS.

6.4.1.5 Computer codes used for the analysis

The TWINKLE [60] and FACTRAN [61] codes are used to perform the rod ejection analyses. The following is a brief description of the codes.

TWINKLE is a neutron kinetics code which solves the multi-dimensional, two-group transient diffusion equations using a finite-difference technique. It is used to predict the kinetic behaviour of a reactor for transients. The code contains a detailed six-region fuel-clad-coolant transient heat transfer model at each spatial point for calculating Doppler and moderator feedback effects. The code handles up to 2 000 spatial points in one-, two- or three-dimensional rectangular geometries (it has also been adopted for hexagonal geometry) and performs its own steady-state initialisation. Aside from basic cross-section data and thermal-hydraulic parameters, the code accepts as input basic driving functions such as inlet temperature, pressure, flow, boron concentration, control rod motion and others to produce output of nuclear power as a function of time.

The FACTRAN code calculates the transient temperature distribution in a cross-section of a metal clad, uranium dioxide fuel rod and the transient heat flux at the surface of the clad, using as input the nuclear power and the time-dependent coolant parameters (pressure, flow, temperature and density). FACTRAN uses a fuel model containing a sufficiently large number of radial space increments to adequately model even very fast transients. The code also uses material properties that are functions of temperature and has the capability to perform fuel-to-clad gap heat transfer calculation. Two sets of transient equations representing an energy balance and the heat conduction for each node are solved simultaneously. The solution to these equations consists of the heat fluxes and temperatures at the end of each time step. Additionally, the code can perform the necessary calculations to deal with post-DNB transients: film boiling heat transfer correlations, the zircaloy-water reaction and partial melting of the materials.

For the rod ejection analysis, the nuclear power input is a time-dependent parameter obtained from TWINKLE: the input parameters for pressure, flow, temperature and density are maintained at a constant conservative value to produce a limiting calculation.

6.4.2 Spectrum of rod ejection accidents for Bohunice V-2 (VVER-440/v-213)

6.4.2.1 Event description

The rod ejection accident is defined as an assumed failure of a control rod mechanism pressure housing such that the reactor coolant system pressure would eject the control rod and drive shaft to the fully withdrawn position. The consequence of this mechanical failure is a rapid reactivity insertion with an adverse core power distribution.

If this event were to take place, a fuel rod thermal transient which could cause DNB may occur, along with limited fuel damage. The amount of fuel damage that can result from such an accident will be governed principally by the worth of the ejected rod and the power distribution attained with the remaining control rod pattern. The transient is terminated by the Doppler reactivity effect of the increased fuel temperature and by the reactor trip actuated by neutron high flux signals, before conditions are reached that can result in damage to the reactor coolant pressure boundary, or sufficiently disturb the core, its support structures or other reactor pressure vessel internals such that the capability to cool the core is significantly impaired.

Features in the VVER-440/213 design preclude the possibility of a rod ejection accident, or limit the consequences of the event if it were to occur. Besides the fact that the control rod mechanism pressure housing is sufficiently dimensioned, there is a hydraulic stop that prevents a rod ejection when a pressure difference of 0.05 to 0.1 MPa on the hydraulic stop occurs.

The consequences of this accident are limited by the presence of control rod insertion limits and the limited reactivity worth of the individual control rods. The control rod insertion limits, which vary as a function of power level, are present to limit the reactivity worth of the rod inserted in the core when the core is critical. In addition to ensuring that an adequate shutdown margin is available throughout the cycle at all power levels, the rod insertion limits also constrain the amount of reactivity associated with the ejection of a control rod as well as the resulting core peaking factors following the ejection.

After the control rod mechanism pressure housing rupture and failure of the hydraulic stop, the affected rod would be ejected from the core to the uppermost position. The velocity of the ejected rod depends on the pressure difference and the control rod mechanism hydraulic characteristics. The analyses conservatively assume that the rods are positioned at the rod insertion limits as the precondition for the accident. The single rod resulting in the largest reactivity worth is assumed to be ejected rod.

A sudden ejection of a control rod during power operation could create high peaking factors in the core and cause the reactor coolant temperature to rapidly increase. If either of these conditions is excessive, a localised hotspot may be created which could result in fuel melting. In addition, the increase in core power and resultant increase in fuel temperatures expected during a rod ejection could challenge the fuel cladding integrity. Cladding temperature is a concern, particularly at zero power, because of the reduction in the forced reactor coolant flow associated with fewer reactor coolant pumps in operation.

6.4.2.2 Acceptance criteria

A control rod ejection accident is classified as a postulated accident that is of such low frequency that is not expected to occur, but is considered in the reactor design to demonstrate the ability of the safety systems to prevent excessive fuel damage and to prove compliance with the requirement of radiation protection of the population. The criteria for the rod ejection accident are as follows:

1) There shall be no prompt rupture of the fuel rods. This criterion is met when:

   – The radially-averaged fuel enthalpy does not exceed 840 kJ/kg for irradiated and 963 kJ/kg for fresh fuel at any axial location in a rod.

   – Fuel melting does not exceed 10% of the fuel pellet volume at any axial location in a rod.

   – Fuel rod cladding temperature does not exceed 1 480°C.

2) Pressure in the reactor coolant and main steam systems shall be maintained below 110% of design pressure.

3) Calculated doses shall be below the limits for postulated accidents, assuming an event generated iodine spike and equilibrium iodine concentration for continued full power operation, and taking into consideration actual primary and secondary coolant activity.

6.4.2.3 Initial conditions

The rod ejection event is analysed to bound operation from zero to full power. In accordance with requirements outlined in the guide for neutron and thermal-hydraulic analysis [62] the following cases are analysed:

- Beginning of the cycle, zero reactor power, sixth control rod bank at the bottom position.
- End of the cycle, zero reactor power, sixth control rod bank at the bottom position.
- Beginning of the cycle, reactor power 2.0% N_{nom}, sixth control rod bank 0.5 m above the bottom position.
- End of the cycle, reactor power 2.0% N_{nom}, sixth control rod bank 0.5 m above the bottom position.
- Beginning of the cycle, full reactor power, sixth control rod bank 1.25 m above the bottom position.
- End of the cycle, full reactor power, sixth control rod bank 1.25 m above the bottom position.

In the zero-power cases a reactor power of 0.001% of the nominal reactor power is assumed. In full-power cases a reactor power of 102.0% of the nominal reactor power is assumed. In all cases the position of control rod banks 1 to 5 is assumed to be completely withdrawn from the core. In the first and second cases the initial position of the ejected rod was bottom position, which results in the maximisation of reactivity released and bounds uncertainty of the rod position in the critical conditions.

Taking into account pressure difference, weights and cross-sectional areas of the control rod and the driving mechanism and neglecting hydraulic and friction losses of the rod being ejected, the rod ejection time would be 0.67 s. In the analyses the complete control rod ejection time was conservatively assumed to be 0.1 s.

The velocity of functioning control rods was assumed to be 0.02 m/sec for the rod insertion and 0.2 m/sec for the rod drop in the core. In the case of a reactor trip a delay of 1.6 seconds after the trip point is reached was assumed. The choice of such a conservative insertion rate means that over two seconds after the trip point is reached passes before significant shutdown reactivity is inserted into the core. Such conservatism is particularly important for full power accidents.

In all cases the values for the prompt neutron lifetime, the decay constant λ, and the effective ratio of delayed neutrons β_{eff}, were used as recommended for BOC and EOC [63].

6.4.2.4 Availability and functioning of systems and components

The reactor protection system (RPS) mitigates the consequences of this event. Reactor trips can be generated by high neutron flux or high neutron flux rate signals.

All cases were analysed without the reactor trip, the most adverse case (full power) was then recalculated, taking into account reactor trip due to high neutron flux (110% of N_{nom}). The trip signals due to high neutron flux rate were not considered. Since the high neutron flux rate reactor trip set-points are reached before the high neutron flux reactor trip set-points, this is a conservative assumption. In that case, a time delay of 1.6 seconds after the trip set-point is reached and before the rods start to fall is assumed.

Trip reactivity insertion is simulated by dropping the appropriate rod worth into the core from the full-out position. This is a conservative assumption, since some control banks will actually be partially inserted in the core. The trip of these banks would provide a more rapid rate of negative reactivity addition than assumed in the analyses.

Reactor control and limitation systems are assumed to function only if their operation results in more severe transient conditions. No control or limitation system is assumed to function during the rod ejection event because the transient is faster than the expected effects of control or limitation system operation.

6.4.2.5 Computer codes used for the analysis

The computer code DYN3D is used to perform the rod ejection analyses. A summary description can be found in Section 2.2.3; see also Refs. [51,52].

6.4.3 Acceptance criteria

6.4.3.1 Definition of basic terms

Former Czechoslovak Atomic Energy Commission has issued a basic document [64] dealing with NPP safety. General safety requirements and definitions or explanations of key safety-related technical

terms are contained in this document. The most important terms necessary for correct interpretation of the core design basic requirements are as follows:

- *Normal operation*. Includes all planned operations and occurrences specific to normal conditions of the plant, with operation limits and conditions (technical specifications) for its safe operation being fulfilled. Such operations include start-up, steady-state operation and shutdown of the reactor, increasing or decreasing of its power, partial or full loading, maintenance, repairs and refuelling.

- *Abnormal operation*. Includes unplanned conditions, operations and events, though occurrence can be expected during plant operation. These include (emergency) reactor trip, unexpected loading decrease, turbine trip and loss of power to the station. Such operational conditions must not lead to fuel rod damage or to the violation of the reactor coolant system integrity. After termination of these events or after elimination of the causes and consequences the station is capable of returning to normal operation.

- *Accident conditions*. Includes all events caused by failure or damage of the building structures, process systems or equipment which could occur by external influence or personal errors that adversely affect safe operation of the plant and lead to the violation of the operational limits and conditions and can cause failure of the fuel rods.

- *Limiting damage of the fuel rods*. Represents the largest admissible number of the fuel rods failed and the extent of their damage in the core during the design basic accident.

- *Limiting parameters of the fuel rods*. The maximum parameters of the fuel rods and the extent of their damage that must not be exceeded during normal and abnormal operation.

6.4.3.2 General design requirements

In accordance with these definitions the following general design requirements (criteria) for the reactor core are established in Decree No. 2 [64]. First, the reactor core design and related control and protection systems must assure with sufficient margin that during normal and abnormal operation the prescribed limiting parameters of the fuel rods are not exceeded. Further, during accident conditions:

- The reactivity excess is not released.

- The reactor can be tripped safely.

- The core is coolable for a sufficiently long period.

- The limiting damage of the fuel rods is not exceeded.

Based on Decree No. 2 [64], the instructions (or guidelines) [65] for reactivity-initiated accidents analyses have been elaborated, and contain more detailed recommendations, a list of events that has to be analysed and basic acceptance criteria. The significant items for the evaluation of the consequences of an accident were determined in Ref. [65]:

- *Fuel rod failure criteria*. The fuel is assumed to fail if the heat flux equals or exceeds the value corresponding to the onset of the transition from nucleate to film boiling or the radial average fuel enthalpy reaches or exceeds at any axial locations in any fuel rod the maximum value determined for normal and abnormal conditions (*e.g*. 710 kJ/kg).

- *Limiting parameters of the fuel rods*. The limiting parameters of the fuel rods are not exceeded if the heat flux does not reach the value corresponding to the onset of the transition from nucleate to film boiling and the maximum fuel temperature (*i.e*. the fuel centreline temperature in the peak linear power location) does not reach the fuel melting point.

Safety analyses for Dukovany NPP (VVER-440) have been performed basically in accordance with the requirements given in Refs. [64,65]. This is not the case for the Temelín NPP (VVER-1000) where it was decided, independently on an extent of changes in the original Russian design, to follow RG 1.70 [66] as concerns the content of the safety report. The acceptance criteria used here correspond to US practice and acceptability as determined by the US NRC. The basis is the classification of plant conditions into four categories dependent upon the expected frequency of the events occurrence and potential radiological consequences to the public [67]:

Condition I	Normal operation and operation transients.
Condition II	Incidents of moderate frequency (occurrence during the lifetime of a particular plant).
Condition III	Infrequent faults (occurrence during the lifetime of a particular plant).
Condition IV	Limiting faults (no occurrence is expected – postulated as the limiting design case).

In addition to this classification, a specific guide for control rod ejection cases has been applied for Temelín analysis [68]. Despite the different classification of the events and the different approaches applied by different organisations in the analyses, there are no significant contradictions in the safety evaluations of Dukovany in comparison with Temelín.

In recent years Decree No. 2 [64] was replaced by Decree No. 195/1999 [64b] issued by the State Office for Nuclear Safety (SONS). The basic terms used in the former document are slightly modified therein. Nevertheless, the spirit of the two documents is much the same.

6.4.3.3 List of acceptance criteria for the evaluation of reactivity accident results

The acceptance criteria for process variables and system parameters for NPP Dukovany are given in Table 13, as derived from Refs. [59,65,69-71].

Table 13. List of acceptance criteria for reactivity accident analysis

(1)*	No boiling crisis in the core (calculated with probability higher than 95% with a 95% confidence level). By ensuring that the minimum departure from nucleate boiling ratio (DNBR) remains above the limit value the fuel cladding integrity will be maintained. The actual DNBR limit value is dependent on the DNB methodology and correlation employed.
(2)	No fuel melting. The melting point is 2 840°C for fresh fuel and 2 670°C for burnout fuel. For Temelín NPP the peak central temperature at peak linear power for prevention of centreline melt is 2 593°C.
(3)	Radially-averaged fuel enthalpy in any point of the core lower than 710 kJ/kg (fuel rod failure criterion for normal and abnormal operation).
(4)	The preservation of the reactor coolant system and the main steam system integrity by maintaining pressure at or below 110% of the design pressure values for these pressure boundaries. For Dukovany NPP, primary pressure does not exceed maximum value given by limits and conditions for safe operation (present value 13.8 MPa). Also, there is no direct steam relief from the secondary circuit to the atmosphere (applicable pressure 5.2 MPa). For Temelín NPP, primary pressure for safety analyses is 19.4 MPa, and the secondary pressure limit for safety analyses is 8.69 MPa.
(5)	Maximum reactor pressure during any portion of the assumed transient will be less than the value that will cause stresses to exceed the emergency condition stress limits as defined in Section III of the ASME Boiler and Pressure Vessel Code (non-acceptable stresses).
(6)	Radially-averaged fuel enthalpy in any point of the core lower than 840 kJ/kg (acceptable fuel damage from the point of view of long-term coolability of the fuel rods).
(7)	The number of fuel rods experiencing DNBR should be less than 5% of the total fuel rods in the core.
(8)	Peak cladding average temperature lower than 1 649°C.
(9)	Fuel melt in hot pellet lower than 10%.
(10)	Zirconium-water reaction lower than 16% (by weight).
(11)	Sufficient time for operator actions (30 minutes during refuelling, 15 minutes for other operational conditions).
(12)	Pressure and temperature in the primary circuit should be kept within acceptable limits established with regard to brittle as well as ductile fracture.
(13)	Reactor core should not be re-critical due to rapid cooling down of the primary circuit. Reactor subcriticality should also be assured during long-term cooling.
(14)	Maximum pressure, temperature and differential pressure should not exceed design values with sufficient margins.
(15)	Dose equivalents for the most endangered individuals should be less than 0.25 Sv for the whole body, 1.5 Sv for the thyroid in adults, 0.75 Sv for the thyroid in children [71].

* Parentheses used for ID in Table 12.

Chapter 7

CONCLUSIONS

The present chapter consists of four main sections. Section 7.1 connects the performed activity with the goals of the CRISSUE-S project as identified in the research proposal and includes the benefits expected by the EC. Section 7.2 summarises the main content of the report. Innovations and findings are discussed in the Section 7.3, and recommendations for the future activities constitute Section 7.4.

7.1 Framework

A full understanding of neutron kinetics/thermal-hydraulics coupling as well as the evaluation of NPP behaviour should a transient that affects the coupling occur, constitutes a relevant problem in LWR technology since the core integrity is challenged. Actions aiming at controlling the fission power should a RIA occur, *i.e*. limiting the flow rate injected by emergency systems, may conflict with the vital requirement in nuclear reactor safety to keep the core cooled. This provides a notion of the importance of the problem dealt with in the present research framework.

Subjects requested in the EC research bid that have been part of the CRISSUE-S proposal are identified by the headings below and comments are provided at the completion of the research activity.

Competing techniques

The resulting scenarios can be predicted by coupled system thermal-hydraulics and 3-D neutron kinetics codes solving the diffusion equations separately developed and qualified by the nuclear industry and associated research institutions over the last twenty years. Alternative techniques available within the thermal-hydraulics and the neutron physics domains include the adoption of computational fluid dynamics, subchannel codes, Monte Carlo and neutron transport codes. All of these have a level of maturity not suitable for immediate application in the industry. Attention has thus focused on the present report addressing coupled system thermal-hydraulics and 3-D neutron kinetics techniques.

Emphasis has been placed on limitations whose understanding is not only relevant for the estimation of the actual safety margins of the NPP, but also constitute a driving force for the introduction of advanced (competing) techniques based on the aforementioned tools.

The limitations and the drawbacks discussed in the report apply to the best available techniques in the concerned areas. The approach pursued did not aim at identifying or characterising the best tool in each area, rather at establishing a consistent and integrated methodology acceptable for the industry, the utilities, the regulators and the research organisations.

Advancement of the state of the art

The establishment of an agreed methodology covering all the considered topics for the evaluation of RIA consequences constitutes an advancement of the present state of the art. Progress has also been achieved in relation to:

- Recommendations useful to utilities and regulators.
- Characterisation of drawbacks of the techniques.
- Identification of areas for application of the techniques, including characterisation of precision targets.
- The availability of qualified tools (*e.g*. nodalisations).
- The availability of databases.

Originality and innovation of the work

Luckily, in the field of nuclear reactor safety technology, nothing is fully original. The originality, as well as the innovation is basically the same as that discussed in the previous section. The exploitation in this area of sophisticated computer tools and of current computer capabilities also constitutes an innovation. In more general terms, innovations are constituted by:

- Co-operation between industry, utilities, regulators and research organisations (of private and public nature) focused on a unique topic of relevance to nuclear reactor safety and operation.
- Consideration of data and methodologies qualification; this is achieved by examining measured NPP planned and unplanned transient events.
- Co-operation between EU countries and the US.

Integration with planned or ongoing international programmes

The CRISSUE-S project constitutes a self-standing activity that, among the other things, coagulates the findings of several years of development as regards the application of coupled 3-D neutron kinetics/ thermal-hydraulics techniques within the nuclear technology domain. This does not imply the end of research activities in the area or the recognition of low importance of further developments. It is worthwhile to distinguish hereafter among international ongoing or envisaged activities within the CRISSUE-S area of interest:

- NEA/NSC has recently proposed a benchmark based on NUPEC BWR Full-size Bundle Test (BFSB). The planned project aims at a detailed investigation of the bundle/pin (subchannel) thermal-hydraulics that is relevant for a more precise calculation of the neutron feedback, including the derivation of 3-D neutron kinetics cross-sections.
- NEA/NSC and NEA/CSNI are supporting the VVER-1000 Coolant Transient (CT) Benchmark. This may be seen as the natural continuation of the TMI-1 MSLB and of the Peach Bottom BWR TT Benchmarks. As in the case of the BWR TT, experimental data are available, from the Kozloduy VVER-1000 Unit 6 NPP, for comparison with calculations and the analysis of an extreme transient is planned.

- IAEA has launched a CRP entitled “Assessment of the Interface Between Neutronic, Thermal-Hydraulic, Structural and Radiological Aspects in Accident Analysis”. The objectives for such an activity are to verify IAEA guidance for accident analysis in light of the novel techniques available and to increase the quality and harmonise accident analysis in member states. Within the same framework, IAEA hosted a Technical Meeting in Vienna (Nov. 2003) dealing with coupled techniques. The conclusions of the CRISSUE-S project have been presented.

- The VALCO project, one of the EC-funded project in the 5th Framework Programme, has been in many respects complementary to the CRISSUE-S project and has provided a number of feedbacks. A lower level of co-operation was established with the NACUSP project. Within the EC domain, the NURESIM proposal, currently under design, can be mentioned as its focus is the coupled 3-D neutron kinetics/thermal-hydraulics domain. It aims at establishing a common informatics platform among the partner institutions in this area.

7.2 Summary

The present document constitutes the second report in a series of three issued within the CRISSUE-S framework. The first report deals with the required input database for the analyses and includes the identification of NPP transients useful for the qualification of coupled techniques. The third report deals with recommendations, mainly to the industry and to the regulators, which are the outcome of the entire project.

The description of the modelling and of the related capabilities in the areas of thermal-hydraulics, 3-D neutron kinetics and nuclear fuel constituted the main topic for the present report, together with the required numerical techniques. Emphasis has also been placed on transients measured in nuclear power plants, to connected aspects of the technology (*e.g*. the simulator) and to the presentation of the licensing/regulatory point of view. Finally, a database of results has been created and is described in Annex I.

Thermal-hydraulics

System thermal-hydraulics codes based upon six partial differential balance equations, mass momentum and energy per each of the two phases, and solved in the 1-D geometry constitute the state of the art. Specific techniques are available to construct equivalent (fictitious) 3-D nodalisations for the core or the vessel regions as needed. Errors in the predictions mostly originate through incomplete knowledge of the constitutive relationships that determine the evolution of the two-phase mixture, *e.g*. the prediction of transient flow regimes in complex geometries like those characterising the reactor pressure vessels. Approximate numerical solution methods aggravate such a problem but do not become the main cause for uncertainty in the predictions.

The acceptability of the results is not dissociable from the quality assurance process and with the rigor in developing and qualifying input decks or nodalisations.

Models belonging to the structure of existing codes, whose quality is critical as regards the acceptability of the code prediction, are identified (*e.g*. dynamic subcooled void formation) and are distinguished (Section 2.9) from models that cannot be considered within the capabilities of current computational tools (*e.g*. pressure wave propagation phenomena inside vessels).

The expertise in transient thermal-hydraulics, with main reference to accident analysis for light water reactors, and the knowledge of current licensing needs in the area, led to a proposal for a number of accidents to be considered for calculation within the regulatory framework, as better detailed under Section 7.3.

Neutron kinetics

In neutron kinetics the fundamental structure of the models is consistent with the physics of the phenomena involved. Even though approximate diffusion equations are typically adopted in the available industrial computational tools, reference solutions exist that are obtained with more sophisticated techniques including Monte Carlo and deterministic neutron transport methods. These solutions are used to benchmark the results from diffusion equations.

Consequently, the problem of uncertainty evaluation is more manageable and the numerical solution methods play a greater role in the accuracy of results than is the case in thermal-hydraulics.

The consistent and efficient cross-section history and instantaneous dependencies modelling, along with the correct definition of the assembly discontinuity factors (ADF) and accounting for core environment effects, constitute the primary challenges affronting neutron kinetics. The main limitation comes from the approximations embedded into the neutron cross-section generation and modelling, linked with the traditional two-energy group approach and the use of homogenisation techniques on both the pin cell and assembly levels. These approximations allow performing coupled 3-D kinetics/ thermal-hydraulic calculations in reasonable CPU time and are in principal the consequence of the available computer power.

Fuel

In physical terms nuclear fuel constitutes the subject of investigation of coupled neutron kinetics/ thermal-hydraulic calculation. In actuality, fuel is considered as a sort of boundary condition for these calculations. This is further discussed in Section 7.3.

A wide range of phenomena connected with nuclear fuel burning in nuclear reactors has been reviewed, ranging from matrix restructuring to fission gas diffusion to corrosion, to the various chemical and physical aspects of the interaction between clad and pellet. Mechanisms for fuel failure have been considered in this context. The potential influence of crud formation upon RIA has been stressed.

Emphasis has been placed in the report on high burn-up and to uranium-plutonium fuel (MOX). In both cases a number of elements that play an insignificant role with fresh UO_2 fuel may become important as regards the prediction of phenomena of interest.

Operator training

The operator role may be relevant in cases of reactivity accident in NPPs. It is worthwhile to reiterate that possible operator actions, if necessary, may be beneficial in the direction opposite to that requested in cases where loss of flow or loss of coolant accident occurs. For instance, stopping of the recirculation pumps and preventing cold water from reaching the core are typical actions needed following RIA-ATWS. Within the present project it was not possible to assess whether adequate qualification of the operator for dealing with such situations is available from the industry.

Attention in the report is focused on simulator, control room and especially emergency operating procedures. The interaction of these subjects with the coupled 3-D neutron kinetics/thermal-hydraulic calculations is mentioned. The topic has not been addressed as thoroughly as would appear necessary because this (*i.e*. the interaction between simulator, control room, operator qualification and coupled 3-D neutron kinetics techniques) does not appear to be part of the current technological practice.

Regulatory position

Attention is focused toward the regulatory approach pursued by various countries in the area of NPP accidents where neutron physics is relevant. Specifically, a non-systematic review of regulations in force and of performed licensing calculations is presented. Acceptance criteria and guidelines for conducting the analyses are discussed. The overall picture demonstrates that a large amount of attention is devoted to transients involving neutron physics, but little or no importance is conferred upon the capabilities of the coupled 3-D neutron kinetics/thermal-hydraulic techniques.

Database of results

A database of results has been gathered within the framework of the CRISSUE-S project. This complements the input database that constitutes the main content of the first CRISSUE-S report [170]. The database of results constitutes Annex I of the present report and includes results of transient coupled 3-D neutron kinetics/thermal-hydraulic calculations performed to predict transient scenarios in BWR, PWR, VVER-440 and VVER-1000 NPPs. The cases considered are part of the ensemble of transients recommended for safety analyses as detailed in Sections 1.1 to 1.3 (see also Section 7.3).

7.3 Main findings

The links existing among a number of subjects (*e.g*. derivation of neutron cross-section, BWR stability, numerical solution methods, fuel modelling) that have been treated separately in the recent past have been made evident. This may be seen as the first finding of the activity, and streamlines the need to pursue an interdisciplinary approach in the future for the concerned subjects.

Capabilities of 3-D thermal-hydraulic computational tools

Codes are considered here that allow the 3-D porous media modelling approach (*i.e*. those codes that do not have the capability to predict the local turbulence and associated phenomena like the velocity or temperature profile inside a cross-section). The conclusion is that these codes are available and ready to be used but their qualification level is not acceptable.

List of transients in relation to which analysis is recommended

The prediction of NPP scenarios is the ultimate goal of coupled neutron kinetics/thermal-hydraulics techniques. The optimal exploitation of such techniques, however, implies streamlining their use and developing recommendations for the accomplishment of this task. Transients have thus been selected within the present framework whose analysis is recommended by coupled techniques. The distinction has been made between BWR, PWR and VVER (Sections 1.2 to 1.4), and only the PWR-related list of transients is proposed hereafter. This includes:

- MSLB.
- LOFW-ATWS.
- CR ejection.
- LBLOCA-DBA.
- Incorrect connection (start-up) of an inactive (idle) loop.
- MSLB-ATWS.
- SBLOCA-ATWS.

Identifiying thresholds of acceptability

Answering the question, "How good is good enough?" constitutes an enormous task that cannot be resolved once and for ever. The progress of science continually advances the acceptability of any technological product, including the results of code applications to nuclear reactor safety. However, an attempt has been made (Section 2.5) to fix acceptable targets for calculation precision, distinguishing between (acceptable) quantity and time errors. The considered values provide a notion of the current capabilities of computational tools, provided qualification methods are adopted. Four examples of acceptability thresholds taken from more than a dozen considered in Section 2.5 are reported below:

- For pressure pulses characterised by FWHM < 0.1 s the acceptable error is 10% nominal pressure.
- For core power pulses characterised by FWHM < 0.1 s the acceptable error is 100% nominal power or 300% initial power, which ever is smaller.
- For core power pulses characterised by FWHM ≥ 0.1 s, the acceptable threshold error is 20% nominal power or 100% initial power, which ever is smaller.
- The acceptable time error that can be associated with the prediction of time of occurrence of pressure or core pulse is 100% of the best-estimate value.

The acceptability of neutron kinetics calculations shall be consistent with discrepancies in the application of state-of-the-art codes to reference problems (see Section 2.12). Errors in predicting k_{eff} (or k_{∞}) can be expected to be of the order of 3-4% without adaptation to measurements of actual core states. However, the common practice is to apply some kind of adaptive strategy to modify or correct calculated values to match specific core measured data. With such an adaptation the prediction of corresponding off-state conditions will provide greater precision, and the errors in calculated k_{∞} (or k_{eff}) will usually be of the order of a few hundred pcm, which can be viewed as acceptable.

Relevance of the role of fuel

The minor role of the fuel within the coupled neutron kinetics/thermal-hydraulic environment was noted. Actually, transient modelling of fuel performance must become the third ring of an ideally unbroken chain including the two other disciplines. Changes of fuel geometric and physical properties

are expected during RIA and must be properly accounted for in the modelling. For instance, in case of local power increase fuel fragmentation and release of fission gases may have an effect upon neutron kinetic cross-section as well as upon the thermal properties of the gap and of the fuel itself. The feedback in terms of neutron power and of power transmitted to the coolant might be non-negligible. No approach currently deals with this phenomenon.

Uncertainty

Due to numerous reasons discussed in the report, the results from coupled 3-D neutron kinetics/ thermal-hydraulic calculations are not precise. Therefore, uncertainty must be connected with any prediction. Two main findings emerge from the performed activity. The first is related to the demonstration that the Internal Assessment of Uncertainty method, based upon the interpolation of the detected accuracy, is applicable for coupled techniques even though relevant resources are necessary to develop a suitable error database. The second is linked to the identification of the main sources of uncertainty. These can be summarised as follows:

- Subcooled HTC, namely in transient conditions characterised by a large time derivative for the produced power.
- Pressure wave propagation inside the complex vessel geometry when a single phase of the two-phase fluid is present.
- Effect of (prompt) radiolysis upon neutron cross-section following fast transients.
- Effect of direct energy release to the coolant following a fast transient.
- Detailed specifications concerning mechanical components such as valves and control rods. The function valve net cross-sectional flow area versus time during opening or closure events is irrelevant for the majority of thermal-hydraulic transients, but may become important when neutron kinetics feedback is computed. Analogously, the velocity as a function of time during a control rod ejections transient is relevant (*i.e.* not only the total ejection time).
- Parameters connected with fuel must be calculated during reactivity accident transient allowing proper feedback (*e.g.* neutron kinetic cross-section and thermal parameters such as gap thickness and conductivity should be calculated as a function of time and provide suitable feedback for the power evaluation).

Uncertainty sources connected with the selected neutron kinetics parameters are mentioned in Section 2.12. Examples include rod worth, fraction of delayed neutron and Doppler coefficients, and are typically defined with uncertainties given by ±10%, ±5% and ±20%, respectively.

Licensing status

The main finding is that great attention is paid by regulatory bodies toward issues like control rod ejection and ultimate fuel resistance. However, the importance of the use of coupled 3-D neutron kinetics/thermal-hydraulic techniques is not recognised. Making reference to the ATWS issue, the survey of the regulatory position in eight countries brings to light the following additional main findings:

- ATWS analyses are mandatory (*i.e*. foreseen in the licensing process) in a small number of countries compared with the number of countries that were taken into consideration. However, generic safety analyses are performed in almost all countries to address the issue.

- The attention toward coupled 3-D neutron kinetics/thermal-hydraulic techniques from the regulatory bodies is insignificant in almost all cases.

Created database

The database of results presented in Annex I gives an idea of the transient behaviour of selected NPP in cases when neutron kinetics/thermal-hydraulic coupling is relevant and constitutes a reference for those code users engaged in similar analyses.

7.4 New frontier

The new frontier for research or recommendations for future development can be derived from the analyses performed and, more specifically, from the items summarised in this chapter. A clear-cut list of recommendations would be:

- Systematic qualification of the various steps of the process of the application of coupled neutron kinetics/thermal-hydraulic techniques is needed, including the adoption of available tools and procedures.

- Full consideration shall be given to the identified sources of uncertainties (section above).

- It must be clear that results obtained by 0-D neutron kinetics coupled with thermal-hydraulics are not necessarily conservative. This observation must provide the impulse for the extended application of coupled 3-D neutron kinetics/thermal-hydraulic techniques in the nuclear safety domain.

- The integration of nuclear-fuel-related models into neutron kinetics/thermal-hydraulics coupling is needed. This also includes the chemistry, with main reference to the processes of crud formation and release.

- The industry and the regulatory bodies should become fully aware of the capabilities (and the limitations) of the concerned techniques. It is expected that regulatory bodies consider the list of transients in LWR whose analysis is recommended by coupled techniques: BWR stability, ATWS and those transients characterised by asymmetric core behaviour are the most important. On the industry side, operators should be made aware of transients that are calculated by 3-D coupled neutron/thermal-hydraulic techniques and simulators, control rooms and EOP should benefit from the experience gained through the application of such techniques.

REFERENCES

[1] International Atomic Energy Agency (IAEA), *Accident Analysis for Nuclear Power Plants*, IAEA Safety Report Series, No. 23, Vienna (2002).

[2] European Community (EC), *CRISSUE-S Project – Database for 3-D Coupled Neutronics/Thermal-hydraulics Analyses, WP1 Report* (2004).

[3] United States Nuclear Regulatory Commission (US NRC), *Standard Review Plan*, NUREG-0800, Washington DC (1980).

[4] Organisation for Economic Co-operation and Development (OECD), *Fuel Safety Criteria Technical Review – Results of OECD/CSNI/PWG2 Task Force on Fuel Safety Criteria*, NEA/CSNI/R(99)25, Paris, France, July (2000).

[5] Commisariat à l'Énergie Atomique (CEA), *The Nuclear Fuel of Pressurized Water Reactors and Fast Reactors, Design and Behavior*, H. Bailly, D. Menessier, C. Prunier, eds., ISBN CEA 2-7272-0198-2 (1999).

[6] OECD Nuclear Energy Agency (OECD/NEA), "An Analysis of Principal Nuclear Issues: Probabilistic Safety Assessment: An Analytical Tool for Assessing Nuclear Safety", *NEA Issue Brief No. 8*, Paris, France, January (1992).

[7] IAEA, "Accident Analysis for Nuclear Power Plants, Guideline for PWR and WWER", *IAEA Safety Report Series*, to be issued, Vienna (2003).

[8] IAEA, "Accident Analysis for Nuclear Power Plants, Guideline for BWR", *IAEA Safety Report Series*, to be issued, Vienna (2003).

[9] D'Auria, F., W. Ambrosini, T. Anegawa, J. Blomstrand, J. In De Betou, S. Langenbuch, T. Lefvert, K. Valtonen, *State-of-the-Art Report on Boiling Water Reactor Stability (SOAR on BWR)*, F. D'Auria (ed.), OECD/CSNI Report OECD/GD(97)13, Paris, France, January 1997.

[10] Hotta, A., "Development and Verification of a BWR Core Simulation System for Space and Time Dependent Coupled Phenomena", PhD Thesis, Tokyo Institute of Technology, Tokyo, Japan, March 2001.

[11] Hotta, A., M. Homna, H. Ninokatta, Y. Matsui, "BWR Regional Instability Analysis by Trac/BF1-Entrée-1: Application to Density-wave Oscillation", *J. Nuclear Technology*, Vol. 135, July 2001.

[12] Ivanov, K., T. Beam, A. Baratta, A. Irani and N. Trikouros, *PWR MSLB Benchmark Volume 1: Final Specifications*, NEA/NSC/DOC(99)8, Paris, France, April 1999.

[13] Solis, J., K. Ivanov and B. Sarikaya, *Boiling Water Reactor Turbine Trip (TT) Benchmark – Volume I, Final Specifications*, OECD/NEA Report NEA/NSC/DOC(2001)1, Paris, France, June 2001.

[14] Ivanov, B. and K. Ivanov, *Neutron Kinetics Core Specifications for WWER-1000 Coolant Transient Benchmark*, OECD/NEA Starter Meeting for the WWER-1000 Coolant Transient Benchmark, Rossendorf, Germany, 28-30 May 2002.

[15] D'Auria, F., N. Debrecin, G.M. Galassi and S. Galeazzi, "Application of RELAP5/MOD3 to the Evaluation of Loss of Feed-water in Test Facilities and in Nuclear Plants", *J. Nuclear Engineering & Design*, Vol. 141, No. 3, pp. 409-428 (1993).

[16] Bovalini, R., F. D'Auria, A. De Varti, P. Maugeri and M. Mazzini, "Analysis of Counterpart Tests Performed in BWR Experimental Simulators", *J. Nuclear Technology*, Vol. 97, No. 1 (1992).

[17] Tarantino, M., F. D'Auria and G.M. Galassi, "Simulation of a Large Break LOCA on WWER-1000 NPP by Relap5/mod3.2 Code", *ANS/HPS Student Conference*, Texas A&M University, College Park, TX, USA, 29-31 March 2001.

[18] D'Auria, F., G.M. Galassi, A. Spadoni and Y. Hassan, "Application of the Relap5-3D© to Phase 1 and 3 of the OECD/CSNI/NSC PWR MSLB Benchmark Related to TMI-1", *ASME/JSME Int. Conf. on Nuclear Engineering (ICONE-9)*, Nice, France, 8-12 April 2001.

[19] Bousbia Salah, A. and F. D'Auria, "Analysis of the Peach Bottom 2 BWR Turbine Trip Experiment by Relap5/3.2 Code", 57th Conference Italian Thermotechnic Association (ATI), Pisa, Italy, 17-20 September 2002.

[20] Groundev, P. and M. Pavlova, *Relap5/mod3.2 Investigation of Exercise 1 of a WWER-1000 Benchmark*, OECD/NEA Starter Meeting for the WWER-1000 Coolant Transient Benchmark, Rossendorf, Germany, 28-30 May 2002.

[21] Maggini, F., R. Mirò, J. Vedovi and F. D'Auria, *BWR Stability Analysis by Relap5/Parcs: Validation Against OECD/NEA Ringhals 1 Stability Benchmark*, Submitted at ICAPP Conference, Cordoba, Spain, 4-7 May 2003.

[22a] Asaka, H., V.G. Zimin, T. Iguchi and Y. Anoda, "Coupling of the Thermal-hydraulic Code TRAC with 3-D Neutron Kinetics Code SKETCH-N", *OECD/CSNI Workshop on Advanced Thermal-hydraulic and Neutronic Codes: Current and Future Applications Summary and Conclusions*, NEA/CSNI/R(2001), Barcelona, Spain, 10-13 April 2000.

[22b] Jurković I., D. Grgić and N. Debrecin, *Core-wide DNBR Calculation for NPP Krško MSLB*, Int. Conf. on Nuclear Energy in Central Europe, Bled, Slovenia, 11-14 September 2000.

[22c] D'Auria, A., Nigro Lo, G. Saiu and A. Spadoni, *MSLB Coupled 3-D Neutronics/ Thermal-hydraulic Analysis of a Large PWR Using RELAP5-3D*, Int. Conf. on Nuclear Energy in Central Europe, Nuclear Society of Slovenia (2001).

[22d] Bovalini, R., F. D'Auria, G.M. Galassi, A. Spadoni and Y. Hassan, "TMI-1 MSLB Coupled 3-D Neutronics/Thermal-hydraulics Analysis: Application of Relap5-3d and Comparison with Different Codes", *2001 RELAP5 International Users Seminar*, Sun Valley, Idaho, 5-7 Sept. 2001.

[22e] Todorova, N. and K. Ivanov, "PWR REA Sensitivity Analysis of TRAC-PF1/NEM Coupling Schemes", *9th International Conference on Nuclear Engineering*, Nice, France, 8-12 April 2001.

[22f] Sánchez, A.M., G. Verdú and A. Gómez, "Coupled 3-D Neutronic/Thermal-hydraulic Codes Applied to Peach Bottom Unit-2", to be identified.

[22g] Hegyi, G., A. Keresztúri and I. Trosztel, "Study of the Asymmetric Steam Line Break Problem by the Coupled Code System KIKO3D/ATHLET", *Proc. of the 10th Symposium of AER*, Moscow, Russia, 18-22 October 2000, Budapest: KFKI AEKI (2000).

[22h] Langenbuch, S., K. Velkov, S. Kliem, U. Rohde, M. Lizorkin, G. Hegyi and A. Kereszturi, *Development of Coupled Systems of 3-D Neutronics and Fluid-dynamic System Codes and Their Application for Safety Analysis*, GRS report to be identified.

[22i] Aounallah, Y. and P. Coddington, "VIPRE-02 Sub-channel Validation Against NUPEC BWR Void Fraction Data", *J. Nuclear Technology*, Vol. 128-2, (1999).

[22j] Kuehnel, K., K.D. Richter, G. Drescher and I. Endrizzi, "High Local Power Densities Permissible at Siemens Pressurized Water Reactors", *J. Nuclear Technology*, Vol. 137-2 (2002).

[22k] Rohde, U., I. Elkin and V. Kalinenko, "Analysis of a Boron Dilution Accident for WWER-440 Combining the Use of the Codes DYN3D and SiTap", *Nuclear Engineering and Development*, Vol. 170, 1-7 (1997).

[22l] Holmes, B.J., G.R. Kimber, J.N. Lillington and M.R. Parkes, "RELAP5-PANTHER Coupled Code Transient Analysis", *OECD/CSNI Workshop on Advanced Thermal-hydraulic and Neutronic Codes: Current and Future Applications Summary and Conclusions*, NEA/CSNI/R(2001), Barcelona, Spain, 10-13 April 2000.

[22m] Schoels, H. and Yu.M. Nikitin, *TACIS R2.30/94 Project Transient Analysis for RBMK Reactors*, TACIS PROJECT R8.01/97.

[22n] Feltus, M. and K. Labowski, "PWR Anticipated Transients without SCRAM Analyses Using PVM-Coupled RETRAN and STAR 3D Kinetics Codes", to be identified.

[22o] Broeders, C., V. Sanchez-Espinoza and A. Travleev, *Development and First Results of Coupled Neutronic and Thermo-hydraulic Calculations for the High Performance LWR*, 5th EC Framework Programme, to be identified.

[22p] Kliem, S., "Analysis and Calculation of an Accident with Delayed Scram on NPP Greifswald Using the Coupled Code DYN3D/ATHLET", *Proc. of the 7th Symposium of AER*, Hörnitz, Germany, September 1997.

[22q] Ivanov, K., T. Beam, A. Baratta, A. Irani and N. Trikouros, "Multidimensional TMI-1 Main Steam Line Break Analysis Methodology Using TRAC-PF/NEM", *J. Nuclear Technology*, Vol. 133-2 (2001).

[22r] Riverola, J., T. Núñez and J. Vicente, *Realistic and Conservative Rod Ejection Simulation in a PWR Core at HZP, EOC with Coupled PARCS and RELAP Codes*, ENUSA Industrias Avanzadas, S.A Santiago Rusiñol 12, 28040 Madrid, Spain.

[22s] OECD/NEA, "OECD/NRC BWR Benchmark 5rd Workshop", *OECD/NEA Proceedings*, to be identified.

[22t] Hadek, J. and J. Macek, *Calculation of the Drop of One Turbine to House Load Level Experiment on Loviisa-1 NPP with Coupled Codes , DYN3D/ATHLET –Final Results*, Phare Program/Safety Related Research Project SRR1/95, NRI/SRR195/LOVI1.4.

[22u] Hadek, J., "Final Results of the 5th Three-dimensional Dynamic AER Benchmark Problem Calculations", *Proceedings of the 9th AER Symposium on WWER Reactor Physics and Reactor Safety*, Hotel Repiská, Slovakia, 4-8 October 1999.

[22v] Hadek, J., P. Kral and J. Macek, "Interim Results of the 6th Three-dimensional AER Dynamic Benchmark Problem Calculation. Solution of Problem with DYN3D and RELAP5-3D© Codes", *Proceedings of the 11th AER Symposium on WWER Reactor Physics and Reactor Safety*, Csopak, Hungary, 24-28 September 2001.

[22w] Macek, J., R. Meca and J. Hadek, *Thermal-hydraulic Analyses of 2MSL Break for Safety Case 28m, Temelin NPP*, Report ÚJV, ÚJV Z 876 T.

[22x] Aragones, J.M., C. Ahnert, O. Cabellos, N. García-Herranz and V. Aragonés-Ahnert, "Methods and Results for the MSLB NEA Benchmark Using SIMTRAN and RELAP-5", Submitted to *Nuclear Technology* (July 2001), ISSN: 0029-5639.

[23] Edenius, M., K. Ekberg, B.H. Forssen and D.G. Knott, *A Fuel Assembly Burn-up Program User's Manual*, STUDSVIK/SOA-95/01 (1995).

[24] USNRC, *Relap5/Mod3.2 Code Manual*, NUREG/CR-5535, INEL-95/0174, August 1995.

[25] RELAP5-3D© Code Development Team, *RELAP5-3D© Code Manual*, INEEL-EXT-98-0083 – Rev. 1.2, May 2000.

[26] Bestion, D. and G. Geffraye, "The CATHARE Code", in *Operational Practice of Nuclear Power Plants of University of Budapest*, CEA Report DTP/SMTHL/LMDS/EM/2001-063, Grenoble, France, April 2002.

[27a] Schnurr, N.M., R.G. Steinke, V. Martinez and J.W. Spore, *TRAC-PF1/MOD2 Code Manual*, NUREG/CR-5673, LA-12031-m, Vol. 2, R4, July 1992.

[27b] Thurgood, M.J., *et al*., *Cobra/TRAC: A Thermal-hydraulic Code for Transient Analysis of Nuclear Reactor Vessel and Primary Coolant System*, NUREG/CR 2046, PNL 4385 (Pacific Northwest Laboratory), March 1983.

[28] Uhle, J. and B. Aktas, "USNRC Code Consolidation and Development Program", *Proceedings OECD/CSNI Workshop on Advanced Thermal-hydraulic and Neutronic Codes*, Barcelona, Spain, April 2000.

[29] US NRC, *TRAC-BF1/MOD1 Code Manual*, NUREG/CR-4356, L1485, Vol. 1.

[30a] Bandini, R., *A Three-dimensional Transient Neutronics Routine for the TRAC-PF1 Reactor Thermal-hydraulic Computer Code*, PhD Thesis, The Pennsylvania State University (1990).

[30b] Ivanov, K., *et al*., "Nodal Kinetic Model Upgrade in The Penn State Coupled TRAC/NEM Codes", *Annl. Nucl. Ener*., 26, 1205 (1999).

[31] Turinsky, P.J., *et al*., *NESTLE: A Few-group Neutron Diffusion Equation Solver Utilizing the Nodal Expansion Method for Eigenvalue, Adjoint, Fixed-source Steady State and Transient Problems*, EGG-NRE-11406, Idaho National Engineering Laboratory, June 1994.

[32a] Joo, H.G., D.A. Barber, G. Jiang and T.J. Downar, *PARCS: A Multidimensional Two-group Reactor Kinetic Code Based on the Non-linear Analytical Nodal Method*, University of Purdue Report PU/NE-98-26 (1998).

[32b] Barber, D.A., T.J. Downar and W. Wang, *Final Completion Report for the Coupled Relap5/ Parcs Code*, University of Purdue Report PU/NE-98-31 (1998).

[33] Langenbuch, S., *QUABBOX/CUBBOX-HYCA, Ein Dreidimensionales Kernmodell mit parallelen Kühlkanälen für Leichtwasser-reaktoren*, GRS-A-926, Garching, Germany (1984).

[34] Langenbuch, S., *et al*., "Investigation of Modeling Aspects for Coupled Code Application in Safety Analysis", *Proc. of the Int. Conf. on Mathematics, Computation, Reactor Physics and Environmental Analysis (M&C 2001)*, Salt Lake City, Utah, USA, September 2001.

[35] Ivanov, K. and A. Baratta, "Coupling Methodologies for Best Estimate Safety Analysis", *Proc. of the Int. Conf. on Mathematics, Computation, Reactor Physics and Environmental Analysis (M&C'99)*, Madrid, Spain, 27-30 September 1999, Vol. 1, pp. 493-502.

[36] Langenbuch, S., *et al*., "Interface Requirements to Couple Thermal-hydraulic Codes to 3-D Neutronic Codes", OECD/CSNI Workshop on Transient Thermal-hydraulic and Neutronics Codes Requirements, Annapolis, MD, USA, Nov. 1996.

[37] Grundmann, U., *et al*., "Coupling of the Thermo-hydraulic Code ATHLET with the Neutron Kinetic Core Model Dyn3d", *Proc. of the Int. Conf. on Mathematics and Computations, Reactor Physics and Environmental Analysis (M&C'95)*, Portland, OR, USA 30 April-5 May 1995, Vol. 1, pp. 257-263.

[38] Todorova, N. and K. Ivanov, *PWR REA Studies Using Different Coupling Options of TRAC-PF1/NEM*, ANS TANSAO 82, 240-242 (2000).

[39] Edenius, M. and B. Forssen, *CASMO-3, A Fuel Assembly Burn-up Program, Users Manual*, STUDSVIK/NFA-89/3.

[40] Stamm'ler, R., *HELIOS-1.6 Methods*, Studsvik Scandpower, April 2000.

[41] Watson, J., K. Ivanov, *et al*., *Cross-section Generation Methodology for Three-dimensional Transient Reactor Simulations*, ANS TANSAO 77, p. 175 (1998).

[42] Watson, J. and K. Ivanov, "Improved Cross-section Modeling Methodology for Coupled Three-dimensional Transient Calculations", *Annals of Nuclear Energy*, 29, 937-966 (2002).

[43] The Pennsylvania State University (PSU), *Algorithm 600: ACM-TRANS. MATH Software*, Vol. 9, No. 2, pp. 258-259 (1983).

[44] Ewing, R.E., R.D. Lazarov, J.E. Pasciak and P.S. Vassilevski, "Domain Decomposition Type Iterative Techniques for Parabolic Problems on Locally Refined Grids", *SIAM J. Numer. Anal*., 30(6), 1537-1557 (1993).

[45] Georgiev, A., S. Margenov, P.S. Vassilevski and L. Zikatanov, "Robust Block Size Reduction Block ILU Solver for 3-D Problems of Geomechanics", Proceedings of *HIPERGEOS'96*, Beklema, The Netherlands, September 1996.

[46] Xu, J., "Iterative Methods by Space Decomposition and Subspace Correction", *SIAM Review*, 34, pp. 581-613 (1992).

[47] Xu, J. and L. Zikatanov, *The Method of Alternating Projections and the Method of Subspace Corrections in Hilbert Space*, PSU Technical Report AM223, CCMA 2000.

[48] Dryja, M. and O. Widlund, *Multilevel Additive Methods for Elliptic Finite Element Problems, Parallel Algorithms for Partial Differential Equations*, Kiel (1990), pp. 58-69 Vieweg, Braunschweig (1991).

[49] Lerchl, G. and H. Austregesilo, *ATHLET Mod 1.2 Cycle A – User's Manual*, Gesellschaft für Anlagen- und Reaktorsicherheit (GRS) mbH, GRS-P-1, Vol. 1, October 1998.

[50] Austregesilo, H. and T. Voggenberger, *The General Control Simulation Module GCSM Within the ATHLET Code*, Gesellschaft für Anlagen- und Reaktorsicherheit (GRS) mbH, GRS-A-1660, April 1990.

[51] Grundmann, U. and U. Rohde, *Dyn3d/M2 – A Code for Calculation of Reactivity Transients in Cores with Hexagonal Geometry*, Research Center Rossendorf Inc., FZR 93-01, Reprint of Report ZfK-690, January 1993.

[52] Grundmann, U., S. Mittag and U. Rohde, *Dyn3d2000/M1 for the Calculation of Reactivity Initiated Transients in LWR with Hexagonal and Quadratic Fuel Elements – Code Manual and Input Data Description for Release*, 3rd Edition, Research Center Rossendorf Inc., Sept. 2001.

[53] Grundmann, U., D. Lucas, S. Mittag and U. Rohde, *The Further Development and Verification of a Three-dimensional Nuclear Model for WWER Reactors and Its Coupling with the Plant Transient Code ATHLET*, Research Center Rossendorf Inc., FZR-84, April 1995 (in German).

[54] Grundmann, U., S. Kliem, D. Lucas and U. Rohde, "Coupling of the Thermo-hydraulic Code ATHLET with the 3-D Neutron Kinetic Core Model Dyn3d", *Proceedings of the 6th AER Symposium on WWER Reactor Physics and Safety*, Kirkkonummi, Finland (1996).

[55] Misak, J., *Draft Report Presented at IAEA Technical Meeting to Develop a Guidance Document of the Development and Review of Emergency Operating Procedure*, IAEA Vienna, Austria, 25 May-1 June 2002.

[56] WANO-MC, *Workshop on Emergency Operating Instructions: Validation, Inculcation of EOI and Personnel Training*, EOP Training at Paks NPP, Nuclear Technology Training Section, Paks NPP, Hungary, 10-14 December 2001.

[57] Trnka, M. and E. Hoffman, "Plant Modification and New Analyses – Dukovany NPP", *WANO-MC Workshop on Emergency Operating Instructions: Validation, Inculcation of EOI and Personnel Training*, Paks NPP, Hungary, 10-14 December 2001.

[58] IAEA, *Anticipated Transients Without Scram for WWER Reactors*, A Publication of the Extra-budgetary Programme on the Safety of WWER and RBMK Nuclear Power Plants, IAEA-EBP-WWER-12, Vienna, Austria, December 1999.

[59] IAEA, *Guidelines for Accident Analysis of WWER NPP*, IAEA-EBP-WWER-01, Vienna, Austria, December 1995.

[60] Risher, D.H. and R.F. Barry, *TWINKLE – A Multi-dimensional Neutron Kinetics Computer Code*, WCAP-7979-P-A (proprietary), WCAP-8028-A (non-proprietary) (1975).

[61] Hargrov, H.G., *FACTRAN – A Fortran IV Code for Thermal Transients in UO_2 Fuel Rod*, WCAP-7908-A (non-proprietary) (1984).

[62] Czechoslovak Atomic Energy Commission (CAEC), *Guide for Neutron and Thermal-hydraulic Analyses and Reactivity-induced Analyses*, ISSN 0139-777X, No. 1 (1986).

[63] Korínek, J., *et al*., *Database for Accident Analyses of EBO V-2 NPP*, VUJE, Trnava, April 1994.

[64a] CAEC, *Decree No.2 of the Czechoslovak Atomic Energy Commission on Nuclear Safety Assurance During Designing, Approving and Performing of the Structures with Nuclear Energy Equipment*, CAEC Report, 27 October 27 1978 (in Czech).

[64b] CAEC, *Decree of the State Office for Nuclear Safety (Czech Republic) No. 195/1999 Coll. on Basic Design Criteria for Nuclear Installations with Respect to Nuclear Safety Radiation Protection and Emergency Preparedness*, CAEC Report (1999) (in Czech).

[65] CAEC, *Instruction for Performing of the Neutronic-physical and Thermal-hydraulic Safety Analyses of the Reactivity Initiated Occurrences*, Bezpecnost jadernych zarizeni (Safety of Nuclear Equipments), No. 1, (1986) (in Czech).

[66] US NRC, *Standard Format and Content of Safety Analysis Reports for Nuclear Power Plants*, US NRC RG 1.70, Rev.3.

[67] *Nuclear Safety Criteria for the Design of Stationary Pressurized Water Reactors*, ANS-51.1/N18.2-1973.

[68] US AEC, *Assumption Used for Evaluating a Control Rod Ejection Accident for Pressurized Water Reactor Plants*, US AEC RG 1.77.

[69] Tinka, I., "Assumptions and Acceptance Criteria for Analyzing Reactivity Related Transients and Accidents in Czech Republic", *5th Symposium of Atomic Energy Research*, Dobogoko, Hungary, 16-19 October 1995.

[70] Hadek, J., "Information on Acceptance Criteria for Reactivity Initiated Accidents in Czech Republic", *Meeting of Working Group D on WWER Reactor Safety Analysis*, Research Center Rossendorf, Germany, 4-6 May 1994.

[71] CAEC, *Decree No. 4 of the Czechoslovak Atomic Energy Commission on General Criteria for Nuclear Safety Assurance on Placement of Structures with Nuclear Energy Equipment*, 31 March 1979 (in Czech).

[72] D'Auria, F., K. Fischer, B. Mavko and A. Sartmandjiev (lead authors), *Validation of Accident and Safety Analysis Methodology*, IAEA Report CRP/J.020.03, Vienna, Austria , June 2001.

[73] Aksan, N., F. D'Auria, H. Glaeser, R. Pochard, C. Richards and A. Sjoberg, *A Separate Effects Test Matrix for Thermal-hydraulic Code Validation: Phenomena Characterization and Selection of Facilities and Tests*, Vols. I and II, OECD/CSNI Report OCDE/GD(94)82, Paris, France (1993).

[74] Annunziato, A., H. Glaeser, J.N. Lillington, P. Marsili, C. Renault and A. Sjoberg, *CSNI Code Validation Matrix of Thermal-hydraulic Codes for LWR LOCA and Transients*, OECD/CSNI Report No. 132, Rev. 1, Paris, France, July 1996.

[75] D'Auria, F. and G.M. Galassi, "Code Validation and Uncertainties in System Thermal-hydraulics", *J. Progress in Nuclear Energy*, Vol. 33, Nos. 1 & 2, pp. 175-216 (1998).

[76] Aksan, S.N., F. D'Auria and H. Staedtke, "User Effects on the Thermal-hydraulic Transient System Codes Calculations", *J. Nuclear Engineering & Design*, Vol. 145, Nos. 1 & 2 (1993), also OECD Status Report NEA/CSNI R(94)35, Paris, France, January 1995.

[77] Ashley, R., M. El-Shanawany, F. Eltawila and F. D'Auria, *Good Practices for User Effect Reduction*, OECD/CSNI Report NEA/CSNI/R(98)22, Paris, France, November 1998.

[78] Bonuccelli, M., F. D'Auria, N. Debrecin and G.M. Galassi, "A Methodology for the Qualification of Thermal-hydraulic Code Nodalisations", *Proc. of NURETH-6 Conference*, Grenoble, France, 5-8 October 1993.

[79] D'Auria, F., M. Frogheri and W. Giannotti, *Relap5/mod3.2 Post Test Analysis and Accuracy Quantification of SPES Test SP-SB-03*, US NRC NUREG/IA-0154, Washington, USA, Feb. 1999.

[80] D'Auria, F., M. Frogheri and W. Giannotti, *Relap5/mod3.2 Post Test Analysis and Accuracy Quantification of LOBI Test BL-44*, US NRC NUREG/IA-0153, Washington, USA, Feb. 1999.

[81] D'Auria, F., N. Debrecin and G.M. Galassi, "Outline of the Uncertainty Methodology Based on Accuracy Extrapolation", *J. Nuclear Technology*, Vol. 109, No. 1, pp. 21-38 (1995).

[82] Ambrosiani, W., R. Bovalini and F. D'Auria, "Evaluation of Accuracy of Thermal-hydraulic Codes Calculations", *J. Energia Nucleare*, Vol. 7, No. 2 (1990).

[83] Kunz, R.F., G.F. Kasmala, J.H. Mahaffy and C.J. Murray, "On the Automated Assessment of Nuclear Reactor System Code Accuracy", *J. Nuclear Engineering and Design*, Vol. 211, Nos. 2 & 3 (2002).

[84] Mavko, B., A. Prosek and F. D'Auria, "Determination of Code Accuracy in Predicting Small Break LOCA Experiments", *J. Nuclear Technology*, Vol. 120, pp. 1-18 (1997).

[85] D'Auria, F., E. Chojnacki, H. Glaeser, C. Lage and T. Wickett, "Overview of Uncertainty Issues and Methodologies", *OECD/CSNI Seminar on Best-estimate Methods in Thermal-hydraulic Analyses*, Ankara, Turkey, 29 June-1 July 1998.

[86] D'Auria, F. and W. Giannotti, "Development of Code with Capability of Internal Assessment of Uncertainty", *J. Nuclear Technology*, Vol. 131, No. 1, pp. 159-196 (2000).

[87] Watson, J. and K. Ivanov, "Improved Cross-section Modeling Methodology for Coupled Three-Dimensional Transient Calculations", *Annals of Nuclear Energy*, 29, pp. 937-966 (2002).

[88] Diamond, D.J., "Multidimensional Reactor Kinetics Modeling", *Proc. of the OECD/CSNI Workshop on Transient Thermal-hydraulic and Neutronics Codes*, NEA/CSNI/R(97)4.

[89] IAEA, *Thermophysical Properties of Materials for Water Cooled Reactors*, IAEA TECDOC 949, Vienna, Austria, June 1997.

[90] OECD/CSNI (Parsons, P.D., *et al*.), *PWR Fuel Behavior in Design Basis Accident Conditions: The Deformation, Oxidation and Embrittlement of PWR Fuel Cladding in a Loss-of-coolant Accident – A State-of-the-art Report*, CSNI Report 129, Paris, France, December 1986.

[91] Yegorova, L., F. Schmitz and J. Papin, *Mechanical Behavior of Fuel Element During RIA Transients*, Kurchatov and IPSN joint paper (1999) (conference in Paris).

[92] FRAMATOME-ANP, *Safety Aspects of Advanced Fuel Assemblies Under Intense Discussion*, Siemens – Service&Fuel 2/1998.

[93] Hache, G. and H.M. Chung, *The History of LOCA Embrittlement Criteria* (2000).

[94] IAEA, *Review of Fuel Failures in Water Cooled Reactors*, Technical Report Series No. 388, Vienna, Austria (1998).

[95] Bailly, H., D. Menessier and C. Premier, *The Nuclear Fuel of Pressurized Water Reactors and Fast Reactors, Design and behavior*, TEC&DOC (1999), ISBN: CEA-2-7272-0198-2.

[96] Sartori, E., J.A. Turnbull, *Status of the Nuclear Science Committee Activities in the Field of Fuel Behaviour*, NEA/OECD, January 2003.

[97] OECD Task Force, *Scientific Issues in Fuel Behaviour*, OECD Document, ISBN 92-64-14420-X, January 1995.

[98] Turnbull, J.A., *Review of Nuclear Fuel Experimental Data, Fuel Behaviour Data Available from IFE-OECD Halden Project for Development and Validation of Computer Codes*, OECD Document, ISBN 92-64-14422-6January 1995.

[99] *Proceedings of the Workshop on Thermal Performance of High Burn-up LWR Fuel*, Cadarache, France, 3-6 March 1998, 389 pages, OECD/NEA Proceedings, ISBN 92-64-16957-1 (1999).

[100] *Proceedings of the Workshop on Fission Gas Behaviour in Water Reactor Fuels*, Cadarache, France, 26-29 September 2000, 564 pages, OECD/NEA Proceedings, ISBN 92-64-19715-X (2001).

[101] *PWR Fuel Behavior in Design Basis Accident Conditions*, OECD/CSNI Report, CSNI No. 129 (1986).

[102] *Fuel Safety Research in NEA Member States, A Compilation of Member Contributions*, OECD/NEA Report, February 2002.

[103] *Proceedings of the Workshop on Advanced Reactors With Innovative Fuels (ARWIF'98)*, Villigen, Switzerland, 21-23 October 1998, OECD/NEA Proceedings, ISBN 92-64-17386-2 (1999).

[104] *Proceedings of the Workshop on Advanced Reactors With Innovative Fuels (ARWIF'01)*, Chester, United Kingdom, 22-24 October 2001, OECD/NEA Proceedings, ISBN 92-64-19847-4 (2002).

[105] *Physics of Plutonium Recycling. Vol. VI: Multiple Plutonium Recycling in Advanced PWR*, OECD Report, ISBN 92-64-19957-8 (2002).

[106] *A VVER-1000 LEU and MOX Assembly Computational Benchmark*, OECD/NEA Report NEA/NSC/DOC (2002)10, ISBN 92-64-19891-0 (2002).

[107] Yang, R., *Robust Fuel Program*, EPRI, Madrid UNESA presentation (2002).

[108] *Thermophysical Properties of Materials for Water-cooled Reactors*, IAEA Report IAEA-TECDOC-949 (1997).

[109] *Review of Fuel Failures in Water-cooled Reactors*, IAEA Tec. Report Series No. 388 (1998).

[110] Glasstone, S. and A. Sesonske, *Nuclear Reactor Engineering*, Chapman & Hall (1994).

[111] Tong, L.S., *Principles of Design Improvement for Light Water Reactors*, Hemisphere Pub. Co (1988).

[112] Rahn, F.J., *et al*., *A Guide to Nuclear Power Technology*, Krieger Pub. Co (1992).

[113] Panayotov, D., U. Bredolt and P. Jerfsten, "POLCA-T – Consistent BWR Core and Systems Modelling", *ANS/AESJ/ENS Int. Conf. Top Fuel 2003*, Paper 410, Würzburg, Germany, 16-19 March 2003.

[114] Lindahl, S-Ö. and E. Müller, "Status of ABB Atom's Core Simulator POLCA", *Int. Conf. PHYSOR'96*, Mito, Japan, 16-20 September 1996.

[115] Wijkström, H., "ABB Atom's New Code for 3-D Static and Transient Analysis", *Proceedings of the German Nuclear Society Workshop on Thermal and Fluid Dynamics, Reactor Physics and Computing Methods*, Rossendorf, Germany, 31 January-1 February 2000.

[116] Panayotov, D., "OECD/NRC BWR Turbine Trip Benchmark: Simulation by POLCA-T Code", *PHYSOR2002 International Conference on the New Frontiers of Nuclear Technology: Reactor Physics, Safety and High-performance Computing*, Track H-2, Paper 3C-02, Seoul, Korea, 7-10 October 2002.

[117] Chao, Y.A., "Coarse Mesh Finite Difference Methods and Applications", *Proc. ANS Int. Top. Meeting on Advances in Reactor Physics and Mathematics and Computation into the Next Millenium (PHYSOR 2000)*, Pittsburh PA, USA, 7-12 May 2000.

[118] García-Herranz, N., O. Cabellos, J.M. Aragonés and C. Ahnert, "Analytic Coarse Mesh Finite Difference Method Generalized for Heterogeneous Multidimensional Two-group Diffusion Calculations", *Nuclear Science and Engineering*, 144, 1-13 (2003).

[119] Finnemann, H., H. Bennewitz and M.R. Wagner, "Interface Current Techniques for Multidimendional Reactor Calculations", *Atomkernenergie*, 30, 123-128 (1977).

[120] Smith, K.S., "An Analytic Nodal Method for Solving the Two-group, Multidimensional, Static and Transient Neutron Diffusion Equations", *Prog. Nucl. Energy*, 17, 271 (1979).

[121] Smith, K.S. and J.T. Cronin, *SIMULATE-3 Methodology*, STUDSVIK/SOA-9202, Studsvik (1992).

[122] Eisenhart, L.D., *ARROTA-01, Advanced Rapid Reactor Operational Transient Analysis*, EPRI Code Manual, Project 1936-6, Electric Power Research Institute (1993).

[123] Liu, Y.S., *et al*., *ANC – A Westinghouse Advanced Nodal Computer Code*, WCAP-10966-NP-A, Westinghouse Electric Corporation (1985).

[124] Turinsky, P., *NESTLE: A Few-group Neutron Diffusion Equation Solver*, Electric Power Research Center, North Carolina State University (1994).

[125] Downar, T.J., H.G. Joo and G. Jiang, "A Hybrid ANM/NEM Interface Current Technique for the Nonlinear Nodal Calculation", *Proc. Joint. Int. Conf. Mathematical Methods and Supercomputing for Nuclear Applications*, Saratoga Springs, New York, 5-9 October 1997, Vol. 1, 124, American Nuclear Society (1997).

[126] Finnemann. H., F. Bennewitz and M.R. Wagner, "Interface Current Techniques for Multidimensional Reactor Calculations", *Atomkernenergie*, 30, 123, (1977).

[127] Lee, H.C. and C.H. Kim, "Unified Formulation for Nodal Expansion Method and Analytic Nodal Method Solutions to Two-group Diffusion Equations", *Nuclear Science and Engineering*, 138, 192-204 (2001).

[128] Lee, H.C. and C.H. Kim, "Unified Nodal Method Formulation for Analytic Function Expansion Nodal Method Solution to Two-group Diffusion", *Nuclear Science and Engineering*, 140, 137-151 (2002).

[129] Cho, N.Z. and J.M. Noh, "Analytical Function Expansion Nodal Method for Hexagonal Geometry", *Nuclear Science and Engineering*, 121, 245 (1995).

[130] Noh, J.M. and N.Z. Cho, "A New Approach of Analytic Basis Functions Expansion to Neutron Diffusion Nodal Calculation", *Nuclear Science and Engineering*, 116, 165 (1994).

[131] Cho, N.Z. and J.M. Noh, "Hybrid of AFEN and PEN Methods for Multigroup Diffusion Nodal Calculation", *Trans. Am. Nucl. Soc*., 73, 438 (1995).

[132] Cho, J.Y. and H. Kim, "Higher Order Polynomial Expansion Nodal Method for Hexagonal Core Neutronics Analysis", *Annals Nuclear Energy*, 25, 1021-1031 (1998).

[133] Hebert, A., "Development of the Nodal Collocation Method for Solving the Neutron Diffusion Equation", *Annals Nuclear Energy*, 14, 527-541 (1987).

[134] Miró, R., D. Ginestar, G. Verdú and G. Hennig, "A Nodal Modal Method for the Neutron Diffusion Equation. Application to BWR Instabilities Analysis", *Ann. Nucl. Energy*, 29, pp. 1171-1194 (2002).

[135] Verdú, G., D. Ginestar, V. Vidal and J.L. Muñoz-Cobo, "3-D λ-modes of the Neutron Diffusion Equation", *Ann. Nucl. Energy*, 21, 7, pp. 404-421 (1994).

[136] Langenbuch, S., W. Maurer and W. Werner, "Coarse-mesh Flux-expansion Method for the Analysis of Space-time Effects in Large Light Water Reactor Cores", *Nuclear Science and Engineering*, 63, 437-456 (1997).

[137] Grundmann, U. and F. Hollstein, "A Two-dimensional Intranodal Flux Expansion Method for Hexagonal Geometry", *Nuclear Science and Engineering*, 133, 201-212 (1999).

[138] Verdú, G., R. Miró, D. Ginestar and V. Vidal, "The Implicit Restarted Arnoldi Method, an Efficient Alternative to Solve the Neutron Diffusion Equation", *Annals of Nuclear Energy*, 26, 579-593 (1999).

[139] Hennart, J.P., E.M. Malambu, E.H. Mund and E. Del Valle, "Efficient Higher Order Nodal Finite Element Formulations for Neutron Multigroup Diffusion Equations", *Nuclear Science and Engineering*, 124, 97-110 (1996).

[140] Hébert, A., "Application of the Hermite Method to Finite Element Reactor Calculations", *Nuclear Science and Engineering*, 91, 34-58 (1985).

[141] Aragonés, J.M., J.M. Martínez-Val and M.R. Corella, "Core State Models for Fuel Management of Equilibrium and Transition Cycles in Pressurized Water Reactors", *Nuclear Technology*, 34-3, 398-411 (1977).

[142] Velarde, G., C. Ahnert and J.M. Aragonés, "Analysis of the Eigenvalue Equations in k, λ, γ and α Applied to Fast and Thermal Neutron Systems", *Nuclear Science and Engineering*, 66-3, 284-294 (1978).

[143] Aragonés, J.M., "Detailed Calculations in Energy and Space of Effective Neutron Resonance Cross-sections", *Nuclear Science and Engineering*, 68-3, 281-298 (1978).

[144] Ahnert, C. and J.M. Aragonés, "Fuel Management and Core Designs Code Systems for PWR Neutronic Calculations", *Nuclear Technology*, 69, 350-367 (1984).

[145] Ahnert, C. and J.M. Aragonés, "A Coupled Fine/Coarse-mesh Few Group Diffusion Method", *Trans. Am. Nucl. Soc.*, 47, 414 (1984).

[146] Ahnert, C. and J.M. Aragonés, "Finite Difference Formulation for Coarse-mesh Few-group Diffusion Calculations", *Trans. Am. Nucl. Soc.*, 50, 281-282 (1985).

[147] Aragonés, J.M. and C. Ahnert, "Linear-discontinuous Finite-difference Formulation for Synthetic Coarse-mesh Few-group Diffusion Calculations", *Nuclear Science & Engineering*, 94, 309-322 (1986).

[148] Ahnert, C., J.M. Aragonés, A. Crespo, A. Labay, J.R. León and A.I. Alvarez, "Validation of the PWR Core Analysis System SEANAP with Measurements", *Nuclear Science & Engineering*, 100, 305-313 (1988).

[149] Crespo, A., C. Ahnert and J.M. Aragonés, "Pin Power and Burn-up Calculation by the SEANAP PWR Core Analysis System Comparison with Measurements and Benchmarks and Applications to Detailed Core Reload Optimization", *1988 International Reactor Physics Conference*, American Nuclear Society, Jackson Hole, WY, USA, ISBN 0-89448-141-X, Vol. 2, pp. 65-74, Sept. 1998.

[150] Aragonés, J.M. and C. Ahnert, "Reactivity Effects of Fission Product Decay in PWRs", *Trans. Am. Nucl. Soc*., 57, 311 (1988).

[151] Aragonés, J.M., C. Ahnert, A. Crespo and J.R. León, "Isotopic Depletion of Soluble Boron in a PWR", *Trans. Am. Nucl. Soc*., 57, 314 (1988).

[152] Ahnert, C., J.M. Aragonés and A. Crespo, "Advances in the PWR Analysis System SEANAP", *In-Core Fuel Management Practices*, IAEA, IAEA-TECDOC-567, ISSN: 1011-4289, Vienna, Austria (1990).

[153] Martínez-Val, J.M., J.M. Aragonés, E. Mínguez, J.M. Perlado and G. Velarde, "An Analysis of the Physical Causes of the Chernobyl Accident", *Nuclear Technology*, 90, 371-388 (1990).

[154] Merino, F., C. Ahnert and J.M. Aragonés, "Development and Validation of the 3-D PWR Core Dynamics SIMTRAN Code", *Mathematical Methods and Supercomputing in Nuclear Applications*, Kernforschungzentrum Karlsruhe, H. Kusters, E. Stein, W. Werner (eds.), ISBN 3-923704-11-9, Vol. 1, pp. 646-657, Germany (1993).

[155] Aragonés, J.M. and C. Ahnert, "Computational Methods and Implementation of the 3-D PWR Core Dynamics SIMTRAN Code for On-line Surveillance and Prediction", *Mathematics and Computations, Reactor Physics and Environmental Analysis*, L. Briggs (ed.), American Nuclear Society, Portland, OR, USA, ISBN 0-89448-198-3, Vol. I, pp. 237-246 (1995).

[156] Ahnert, C., J.M. Aragonés and F. Merino, "In-core Fuel Management Code Package Validation for PWRs", *In-core Fuel Management Codes Validation*, IAEA, IAEA-TECDOC-815, ISSN 1011-5295, Vienna (1995).

[157] Aragonés, J.M., C. Ahnert, D. Cano and N. García-Herranz, "Planning of Operational Manoeuvres with the 3-D PWR Core Dynamics SIMTRAN On-line Code", *Proceedings of the International Conference on Reactor Physics (PHYSOR 96)*, Mito, Ibaraki, Japan, Vol. 4, pp. K-9-17 (Sept. 1996).

[158] Cabellos, O., C. Ahnert and J.M. Aragonés, "Generalized Effects in Two-group Cross-sections and Discontinuity Factors for PWRs", *Proceedings of the International Conference on Reactor Physics (PHYSOR 96)*, Mito, Ibaraki, Japan, Vol. 1, pp. B-82-91 (Sept. 1996).

[159] Aragonés, J.M., C. Ahnert and O. Cabellos, "Methods and Performance of the Three-dimensional Pressurized Water Reactor Core Dynamics SIMTRAN On-line Code", *Nuclear Science and Engineering*, 124(1), 111-124 (1996).

[160] Aragonés, J.M., C. Ahnert C. and V. Aragonés, "Coupled 3-D Neutronic/Thermal-hydraulic Analysis of Transients in PWR Cores", *Mathematical Methods and Supercomputing for Nuclear Applications*, F. Brown (ed.), American Nuclear Society, Saratoga Springs, NY, USA, ISBN 0-89448-619-5, Vol. 2, pp. 1380-1390 (October 1997).

[161] Ahnert, C., J.M. Aragonés, O. Cabellos and N. García-Herránz, "Continuous Validation and Development for Extended Applications of the SEANAP Integrated 3-D PWR Core Analysis System", *Mathematics and Computation, Reactor Physics and Environmental Analysis in Nuclear Applications*, J.M. Aragonés (ed.), Senda Editorial, Madrid, ISBN 84-699-0942-8, Vol. 1, pp. 710-719 (Septmeber 1999).

[162] Cabellos. O., J.M. Aragonés and C. Ahnert, "Generalized Effects in Two-group Cross-sections and Discontinuity Factors in the DELFOS Code for PWR Cores", *Mathematics and Computation, Reactor Physics and Environmental Analysis in Nuclear Applications*, J.M. Aragones (ed.), Senda Editorial, Madrid, ISBN 84-699-0942-8, Vol. 1, pp. 700-709 (September 1999).

[163] García-Herránz, N., J.M. Aragonés, O. Cabellos and C. Ahnert, "Dependence of the Nodal Homogenized Two-group Cross-sections on Intranodal Flux-Spectrum, Burn-up and History", *Mathematics and Computation, Reactor Physics and Environmental Analysis in Nuclear Applications*, J.M. Aragonés (ed.), Senda Editorial, Madrid, ISBN 84-699-0942-8, Vol. 1, pp. 127-138 (September 1999).

[164] Aragonés, J.M., C. Ahnert, O. Cabellos, N. García-Herranz and V. Aragonés-Ahnert, "Methods and Results for the MSLB NEA Benchmark Using SIMTRAN and RELAP-5", *Trans. Am. Nucl. Soc*., 84, 23, Milwaukee (June 2001).

[165] García-Herranz, N., J.M. Aragonés, O. Cabellos and C. Ahnert, "Analytic Coarse Mesh Finite Difference Method for Heterogeneous Multi-dimensional Two-group Diffusion Calculations", *J. Nuclear Science and Engineering*, 144, 23-35 (2003).

[166] García-Herranz, N., O. Cabellos, J.M. Aragonés and C. Ahnert, "Performance of the Analytic Coarse Mesh Finite Difference Method with Heterogeneous Nodes", *Proceedings of the International Reactor Physics Conference (PHYSOR 2002)*, Seoul, Korea (October 2002).

[167] Leyse, R.H., Personal communication to F. D'Auria, West Yellowstone, USA, August 2003 and letter of September 2003.

[168] Frattini, P.L., "Axial Offset Anomaly: Coupling PWR Primary Chemistry with Core Design", *J. Nuclear Energy*, 40, No. 2, 123-135 (2001).

[169] US NRC, NUREG-CP0/168, Washington (October 1999).

[170] CRISSUE-S Partners, *CRISSUE-S WP-1-Report, Neutronics/Thermal-hydraulics Coupling in LWR Technology: Data Requirements and Databases Needed for Transient Simulations and Qualifications (DATABASE)*, ISBN 92-64-02083-7, OECD (2004).

[171] CRISSUE-S Partners, *CRISSUE-S WP3-Report, Neutronics/Thermal-hydraulics Coupling in LWR Technology: Achievements and Recommendations Report (FINARES)*, ISBN 92-64-02085-3, OECD (2004).

[172] Petruzzi, A., F. D'Auria and K. Ivanov, "A Novel Methodology of Internal Assessment of Uncertainty for Coupled Three-dimensional Neutronics/Thermal-hydraulics System Codes", *NURETH-10 Int. Conf.*, Seoul, S. Korea, 5-11 October 2003.

[173] Solis, J., K. Ivanov and B. Sarikaya, *BWR Turbine Trip (TT) Benchmark. Volume 1: Final Specifications*, NEA/NSC/DOC(2001)1, June 2001.

[174] Kliem, S., "Information on Neutron-kinetic Library Uncertainty Estimation – Appendix. Information on Working Group Activities' from 3rd Symposium of AER, Budapest 1993", Personal communication to F. D'Auria, letter FZR, 18 February 2003.

[175] Langenbuch, S., *The Specific Objectives of the Validation of Coupled Thermo-hydraulics/3-D Neutron Kinetics Codes*, Technical Report GRS/SRR195/Val2.0, Phare Program (1999).

[176] Leppanen, J., "Cross-section Library Based Discrepancies in MCNP Criticality Calculations", *Int. Conf. Nuclear Energy for New Europe*, Portoroz, Slovenia, 8-11 September 2003.

[177] Le Pallec, J.C., E. Studer, E. Royer, "PWR Rod Ejection Accident: Uncertainty Analysis on a High Burn-up Core Configuration", *Int. Conf. on Supercomputing in Nuclear Applications (SNA 2003)*, Paris, France, 22-24 September 2003.

[178] Bideaud, A., I. Kodeli, V. Mastrangelo and E. Sartori, "Validation of a Multi-dimensional Deterministic Nuclear Data Sensitivity and Uncertainty Code System: An Application Needing Supercomputing", *Int. Conf. on Supercomputing in Nuclear Applications (SNA 2003)*, Paris, France, 22-24 September 2003.

[179] Danilin, S., S. Nikonov and M. Lizorkin, "The New Solution of the AER Sixth Dynamic Benchmark Problem with ATHLET/BIPR8", *AER Meeting*, Moscow, Russia, 21-22 May 2002.

[180] Nikonov. S., A. Kotsarev, M. Lizorkin and G. Lerchl, "3-D Modelling of Coolant Characteristics Distribution in the Reactor Pressure Vessel by Coupled Computer Codes ATHLET/BIPR8KN", *Int. Conference on Supercomputing in Nuclear Applications (SNA 2003)*, Paris, France, 22-24 September 2003.

[181] Loubiere, S., *et al*., "APOLLO 2 Twelve Years Later", *Conf. Reactor Physics and Environment Analysis in Nuclear Applications*, Madrid, Spain, September 1999.

[182] Lautard, J.J., *et al*., "CRONOS2: A Modular Computational System for Neutronic Core Calculations", *IAEA Specialists Meeting on Advanced Calculational Methods for Power Reactors*, Cadarache, France, September 1990.

[183] Toumi, *et al*., "FLICA4: A 3-D Two-phase Flow Computer Code with Advanced Numerical Methods for Nuclear Applications", *J. Nuclear Engineering and Design*, Vol. 200 (2000).

[184] Rhoades, W.A., *et al*., *DORS3.2, One-, Two- Three-dimensional Discrete Ordinates Neutron/ Photon Transport Code System*, Radiation Safety Information Computational Center, Oak Ridge National Laboratory, CCC-650 (1998).

[185] Alcouffe, R.E., R.S. Baker, F.W. Brinkley, D.R. Marr, R.D. O'Dell and W.F. Walters, *DANTSYS 3.0 – A Diffusion-accelerated Neutron Particle Transport System*, LA-12969-M, Los Alamos National Laboratory, June 1995.

[186] OECD/NEA, *Benchmark on the VENUS-2 MOX Core Measurement*, NEA/NSC/DOC(2000)7, Paris, France (2000).

[187] Misu, St., H.D. Kiehlmann, H. Spierling and F. Wehle, "The Comprehensive Methodology for Challenging BWR Fuel Assembly and Core Design Used at FRAMATOME ANP", *Int. Conf. PHYSOR 2002*, Seoul, Korea, October 2002.

[188] Emmett, M.B. and W.C. Jordan, *Guide to Verification and Validation of the SCALE-4 Criticality Safety Software*, Oak Ridge National Laboratory, NUREG/CR-6483, ORNL/TM-12834, Oak Ridge, TN, USA, November 1996.

[189] Santopadre, F., Letter to F. D'Auria, November 2003.

[190] Laletin, N.I. and A.A. Kovalishin, "Analysis of Neutron Physical Part of Accident-related Codes, Proposals for Improvement", *3rd Scientific Technical Conference on Assurance of Safety of NPP with WWER*, Podolsk, Russia, 26-30 May 2003.

[191] Pretel, C., F. Reventós, L. Batet, "Qualifying, Validating and Documenting a Thermal-hydraulic Code Input Deck", *Proc. of the OECD/CSNI Workshop on Advanced Thermal-hydraulic and Neutronic Codes: Current and Future Applications*, Barcelona, Spain, 10-13 April 2000, NEA/CSNI/R(2001).

[192] Reventós, F. and C. Llopis, "Benefits of Using Integral Plant Models in Utilities: Availability and Safety Issues", *Proc. of the OECD/CSNI Workshop on Advanced Thermal-hydraulic and Neutronic Codes: Current and Future Applications*, Barcelona, Spain, 10-13 April 2000, NEA/CSNI/R(2001).

LIST OF ABBREVIATIONS

A

ABB	Asea Brown Boveri
ABWR	Advanced Boiling Water Reactor
ACC	Accumulator
ACMFD	Analytical Coarse Mesh Finite Difference Method
ADF	Assembly discontinuity factor
AEC	*See* US AEC
AFENM	Analytical Function Expansion Nodal Method
AGCR	Advanced Gas-Cooled Reactors
AGR	Advanced Gas Reactor
AHTLM	Adaptive High-order Table Look-up Method
ANAV-UP	Asociación Nuclear Ascó-Vandellòs, Technical University of Catalonia
ANM	Analytic Nodal Method
ANS	American Nuclear Society
AOA	Axial offset asymmetry (guidelines)
APA	Advanced plutonium assembly
APRM	Average power range monitor
AP-1000	Advanced PWR (1 000 MWe)
ASME	American Society of Mechanical Engineering
ASTM	American Society of Testing and Materials
ATHLET	Analysis of Thermal-hydraulics of Leaks (*code*)
ATWS	Anticipated transient without scram
AZ	*Russian acronym for scram*

B

BDBA	Beyond design basis accident
BE	Best-estimate
BFSB	BWR full size bundle test
BiLU	Blockwise incomplete, or biconjugated lower upper (*numerics pre-conditioner*)
BOA	Boron-induced offset anomaly
BOC	Beginning of (fuel) cycle (*into the reactor core*)
BOP	Balance of plant
BP	Burnable poison
BPLU	Border Profiled Lower Upper Matrix Solver (*numerical method*)
BU	Burn-up
BWR	Boiling water reactor
BWRS	BWR stability
BWRTT	Boiling water reactor turbine trip (*see also* TT)
B&W	Babcock & Wilcox

C

CAEC	Czechoslovak Atomic Energy Commission
CANDU	Canadian Deuterium Uranium
CDF	Corner discontinuity factor
CEA	Commissariat à l'Énergie Atomique
CERCER	Ceramic matrix and ceramic fuel
CERMET	Ceramic fuel and metallic matrix
CFD	Computational fluid-dynamics
CFR	Code of Federal Regulation (*US NRC*)
CHF	Critical heat flux
CIAU	Code with capability of internal assessment of uncertainty
CILC	Crud-induced localised corrosion
CL	Cold leg
CMF	Common mode failure
CMFD	Coarse mesh finite difference
CPM	Collision Probability Method
CPU	Central process unit
CR	Control rod
CRGT	Control rod guide tubes
CRHFT	Core region at high (centreline) fuel temperature
CRHST	Core region at high (fuel rod) surface temperature
CRP	Co-ordinated research project
CRISSUE-S	Critical Issues in Nuclear Reactor Technology: A State-of-the-art Report
CSAU	Code Scaling, Applicability and Uncertainty (*US NRC uncertainty method*)
CSC	Cross-section code
CSNI	Committee on the Safety of Nuclear Installations
CT	Coolant transient
CVCS	Chemical and volume control system

D

DBA	Design basis accident
DC	Downcomer (*of RPV*)
DEC	Département d'Études des Combustibles (*CEA Cadarache*)
DF	Discontinuity factor
DNB	Departure from nucleate boiling
DNBR	DNB ratio
DO	Dry-out
DOE	Department of Energy (*US*)
DR	Decay ratio
DUPIC	Direct use of spent PWR fuel in CANDU reactors
DW	Density wave (*originated*)

E

EBA	Enriched boron addition
ECCS	Emergency core cooling system
ENAC	European Nuclear Assistance Consortium
EOC	End of cycle
EOP	Emergency operating procedure
EP	External (recirculation) pump (*BWR*)
EPMA	Electron probe micro analysis

EPRI	Electric Power Research Institute
ES	Eigenvalue separation
ESFAS	Engineered Safety Features Actuation System
EU	European Union

F

FA	Fuel assembly
FEBE	Forward-Euler, Backward-Euler (*ATHLET module*)
FGR	Fission gas release
FMS	Fuel management system
FSAR	Final safety analysis report
FP	Full power or fission product
FR	Fast (neutron) reactor
FTC	Fuel temperature coefficient
FW	Feed water
FWHM	Full width (of the concerned peak) at half maximum
FZR	Forschungszentrum Rossendorf (*near Dresden, Germany*)

G

GCSM	Transients General Control Simulation Module (*ATHLET module*)
GE	General Electrics
GI	General interface
GMRES	Generalised minimal residual algorithm
GRS	Gesellschaft fuer Anlagen- und Reaktorsicherheit (*also ID for uncertainty method*)

H

HCO	Heat Conduction Objects (*ATHLET module*)
HECU	Heat Transfer and Heat Conduction (*ATHLET module*)
HFP	Hot full power
HL	Hot leg
HOSG	Horizontal (tubes) steam generator
HPIS	High pressure injection system
HPLWR	High-performance LWR
HT	Heat transfer
HTA	Heat transfer area
HTC	Heat transfer coefficient
HTGR	High-Temperature Gas Reactor
HTR	High-Temperature Reactor
HWR	Heavy Water Reactor
HZP	Hot zero power

I

IAEA	International Atomic Energy Agency
IASCC	Irradiation-assisted stress corrosion cracking
ICE	A numerical solution method
ID	Identification
IET	Integral Effect Test (*facility*)
IFPE	International Fuel Performance Experiment
IGSCC	Intergranular stress corrosion cracking
IMF	Inert-matrix fuel
IP	Internal (recirculation) pump (*BWR*)

IRI	Interfaculty Reactor Institute (*Delft University, The Netherlands*)
ITF	Integral test facility
IWGATWR	IAEA Int. Working Group on Advanced Technologies for Water-cooled Reactors
J	
JP	Jet pump (*BWR*)
K	
KAERI	Korean Atomic Energy Research Institute
KKL	Leibstadt NPP
KTH	Kungl. Tekniska Högskolan
KWU	KraftWerk Union
L	
LBLOCA	Large break loss of coolant accident
LMFR	Liquid-metal fast reactor
LOCA	Loss of coolant accident
LOFW	Loss of feedwater
LOOP	Loss of off-site power
LPRM	Local power range monitor
LPIS	Low pressure injection system
LWR	Light water reactor
M	
MCP	Main coolant pump
MFT	Maximum fuel (centreline) temperature
MIT	Massachusetts Institute of Technology
MLIV	Main loop isolation valves
MOX	Mixed U-Pu oxide nuclear fuel
MPI	Multi-processor interaction
MSIV	Main steam isolation valve
MSLB	Main steam line break
MTU	Metric tons of uranium
MWD	Megawatt-day
N	
NACUSP	Natural circulation and stability performance of BWRs
NC	Natural circulation
NCM	Nodal Collocation Method
NCTH	Nuclear coupled thermal-hydraulics
NEA	Nuclear Energy Agency
NEM	Nodal Expansion Method
NEUKIN	Neutron Kinetics (*ATHLET module*)
NK	Neutron kinetics
NKC	Neutron kinetics code
NMCA	Noble metal chemical application, or noble metal clad assembly
NPP	Nuclear power plant
NRC	Nuclear Regulatory Commission (*US*)
NRI	Nuclear Research Institute (*Czech Republic*)
NSC	Nuclear Science Committee
NUGG	Natural Uranium Gas-Graphite
NUPEC	Nuclear Power Engineering Test Center

O

OECD	Organisation for Economic Co-operation and Development
ODE	Ordinary differential equations
O′M	Oxygen-to-metal (*ratio*)
ORNL	Oak Ridge National Laboratory
OTSG	Once-through steam generator

P

PAMS	Post-accident monitoring system
PBMR	Pebble bed modular reactor
PCCI	Pellet-cladding chemical interaction
PCI	Pellet-clad interaction
PCMI	Pellet-clad mechanical interaction
PCT	Peak cladding temperature
PDE	Partial differential equations
PEN	Polynomial Expansion Nodal (*method*)
PF	Peak factors (*for linear power of fuel pins*)
PHWR	Pressurised HWR
PIE	Post-irradiation examination
PORV	Pilot-operated relief valve
PRZ	Pressuriser
PRPS	Primary reactor protection system
PSA	Probabilistic safety assessment
PSU	Pennsylvania State University
PVM	Parallel virtual machine
PWR	Pressurised water reactor
PZ-1	First protection level (*Russian acronym*)
PZ-2	Second protection level (*Russian acronym*)

Q

QA	Quality assessment
QC	Quality control

R

RBMK	Boiling water cooled/graphite moderated (*Russian reactor*)
RCCA	Rod cluster control assembly
RCS	Reactor coolant system
REA	Rod ejection accident
REAC	Reactivity accidents (*ATWS, RIA, BWRS, boron-dilution, low power*)
RFP	Robust Fuel Program (*EPRI*)
RG	Regulatory guide
RHS	Right-hand side
RIA	Reactivity-initiated (or induced) accident
RIT	Royal Institute of Technology (*see also KTH*)
RPS	Reactor protection system
RPV	Reactor pressure vessel
RSK	Licensing guidelines (*Germany*)
R&D	Research and development

S

SAPR	Semi-analytical Perturbation Reconstruction (*numerical module*)
SAR	Safety analysis report
SBLOCA	Small break loss of coolant accident
SCC	Stress corrosion cracking
SEGFSM	Special Experts Group on Fuel Safety Margins
SET	Separate Effect Test (*facility*)
SG	Steam generator
SGTR	Steam generator tube rupture
SI	Safety injection
SIT	Safety injection tanks (*used as synonymous of ACC*)
SKI	Statens Kärnkraftinspektion (*Swedish Nuclear Power Inspectorate*)
SL	Steam line
SOAR	State-of-the-art report
SONS	State Office for Nuclear Safety (*Czech Republic*)
SOR	Successive Over-relaxation (*numerical method*)
SPDS	Safety parameter display system
SRV	Steam relief valve
STP	Standard temperature and pressure
SYS-TH	System thermal-hydraulics

T

TAMU	Texas A&M University
TD	Thoria-based fuels
TFD	Thermo-fluid-dynamics (*ATHLET module*)
TFO	Thermo-fluid-dynamic Object (*ATHLET module*)
T-H	Thermal-hydraulics
THSC	Thermal-hydraulics System Code
TIN	Transverse integrated nodal
TIP	Traversing in-core probe
TMI-1	Three Mile Island Unit 1
TPEN	Triangle-based Polynomial Expansion Method
TT	Turbine trip (*in BWR*)
TTEF	Total thermal energy released to the fluid (*during the calculated transient*)

U

UMAE	Uncertainty method based on accuracy extrapolation
UP	Upper plenum
UPISA	University of Pisa
UPTF	Upper plenum test facility
URB	Accelerated off-loading of the unit (*Russian acronym*)
UT	Ultrasonic (cleaning) technology
UTSG	U-tubes steam generator
US	*See* USA
USA	United States of America
US AEC	US Atomic Energy Commission
UVA	University of Valencia

V

VALCO	Validation of coupled neutronics/thermal-hydraulics codes for WWER reactors
VUJE	Nuclear Power Plant Research Institute (*Trnava, Slovak Republic*)
VVER	*See* WWER

W

WANO	World Association of Nuclear Operators
WESE	Westinghouse Energy Systems Europe
WG	Weapons grade
WWER	Water-cooled Water-moderated Energy Reactor

X

XRF	X-ray fluorescence
XS	Xenon samarium

Additional abbreviations

0-D	Zero-dimensional (point model)
1-D	One-dimensional
2-D	Two-dimensional
3-D	Three-dimensional

Appendix A

AN INSIGHT INTO THE BWR STABILITY ISSUE

A-1 Detailed review of nuclear coupled thermal-hydraulics stabilities in BWR

A-1.1 An overview of main definitions and current issues

Before a review of the current approaches to analyse nuclear coupled thermal-hydraulics (NCTH), two features of NCTH instabilities in BWR are mentioned here. First, BWR can experience in-phase (core wide) or out-of-phase (regional) oscillations. Second, some NCTH instabilities in reactor cores have resulted in stable, finite amplitude oscillations [A4-A6], while others lead to increasing amplitude oscillations until scram [A7,A8]. While in-phase and out-of-phase oscillations can be distinguished by linear analyses using a detailed model of the core, the analysis of the second phenomenon necessarily requires the set of non-linear equations either integrated numerically or studied using bifurcation techniques. In general there have been three approaches to analyse nuclear coupled thermal-hydraulics in BWRs:

1) Time domain numerical simulations using large-scale, high-fidelity codes such as RAMONA, TRAB-BWR, TRACG, RETRAN, TOSDYN-2, RELAP/PANBOX and others discussed in Refs. [A1,A9-A19].

2) Frequency domain analyses using codes such as LAPUR, NUFREQ-NP, MATSTAB, STAIF [A6,A20-A23], etc., or using low-dimensional models [A24-A28].

3) Bifurcation analyses usually carried out with low-dimensional models that are obtained after reducing the set of governing partial differential equations (PDE) to a set of ordinary differential equations (ODE) [A24,A29-33]. In addition, experiments have been conducted in BWRs to develop a database for code verification purposes [A4,A34,A35].

Large-scale, time domain numerical integration

One disadvantage of large codes is that parametric studies with such codes, though generally reliable, are prohibitively expensive and time consuming, leading to a generally limited use by reactor operators. For example, recent oscillations in Oskarshamn-3 were supposed to have resulted from the "control rod sequence used and the power distribution created as a result" [A8]. Analyses using large-scale system codes of every power distribution resulting from the myriad of control rod movements to identify those that might lead to instabilities, would have been an expensive and time consuming proposition. Another task for which the large-scale time domain codes are not ideally suited is the identification of conditions under which a system predicted to be stable for small perturbations would become unstable if a large perturbation were applied. Such conditions are important to identify because they occur in parameter regions predicted to be stable by (conventional) stability analysis. These codes are however, fairly adequate to simulate an incident *after* it has occurred, and have been researchers' workhorse to simulate instability events in BWRs [A8,A9,A11,A13].

Frequency domain codes

Frequency domain (linear) analyses are carried out either using simple low-dimensional models like LAPUR (few ODE) or using the complete set of PDE as in the NUFREQ [A22] series of codes. Frequency domain codes can be used to efficiently carry out parametric studies and sensitivity analyses to study the impact of modelling and simplifications on the stability boundaries. Karve, *et al*. [A36] compared the stability boundary obtained using a linear profile for liquid enthalpy and for two-phase quality (linear-linear) with that obtained using a quadratic profile for both quantities, and showed that the linear-linear combination actually leads to significantly more conservative SB than the latter. Karve, Rizwan-uddin and Dorning used the frequency domain approach to study the stability of a low-dimensional model of BWR [A25-A27]. Van Bragt and van der Hagen have also used the frequency domain approach, and analysed the stability of a natural circulation BWR using a low-dimensional model consisting of a set of ODE [A28]. Linear studies that use the frequency domain approach do not, however, provide any information about the nature of bifurcation (see the following subsection) as the SB is crossed. Nor can they be used for bifurcation's sensitivity on models used, and on approximations made in arriving at the low-dimensional set of ODE.

Bifurcation analysis (numerical and/or analytical)

The third bifurcation approach treats the mathematical model as a dynamical system [A37-A41]. Further information is gained from a bifurcation analysis that is not available from a stability analysis. For example, one can learn if a system predicted to be stable by the linear (frequency domain) analysis would become unstable if a sufficiently large perturbation were applied.

Mathematically, there are two possibilities: the resulting oscillations grow and then saturate at some finite amplitude, or they continue to grow. While the former (supercritical Hopf bifurcation) occurs when operating close to the stability boundary on the unstable side of it, the latter (subcritical Hopf bifurcation) occurs when operating near, but on the stable side, of the stability boundary [A37-A41]. Hence, due to ever-present finite amplitude noise, the region near the stability boundary even on the stable side is not safe when the bifurcation is subcritical. BWR plant data from known instability events and controlled experiments suggest the possibility of supercritical Hopf bifurcation in some cases and subcritical Hopf bifurcation in others [A4-A8]. Unfortunately, conditions that lead to one or the other are not yet well understood.

The seminal bifurcation study of BWR dynamics by March-Leuba, Cacuci and Perez [A29,A30] was carried out entirely numerically. Similar studies on stability of two-phase flow in heated channels (without neutronics) have also been carried out [A42 and A43]. Such numerical studies, being very time consuming, are restricted to small regions in parameter space. The seminal work on analytical bifurcation analysis of two-phase flow stability without neutronics [employing the homogeneous equilibrium model (HEM)], was by Achard, Drew and Lahey [A44]. This study was later extended by Rizwan-uddin and Dorning [A45], who analysed uniformly and non-uniformly heated channels using the drift flux model to represent the two-phase flow. For nuclear coupled thermal-hydraulic instabilities, this approach has been used by Muñoz-Cobo and Verdu [A31], Tsuji, *et al*. [A24] and by Van Bragt, Rizwan-uddin and van der Hagen [A32]. The drawback of the full, analytical Linstedt-Poincaré analysis like that performed by Muñoz-Cobo and Verdu [A31] is that the algebraic complexity increases rapidly with the number of equations. Using a computer code called BIFOR2 [A46], Tsuji, *et al*. [A24] demonstrated that the bifurcation, under certain conditions, is subcritical. A successor to BIFOR2 called BIFDD was used by Rizwan-uddin for xenon oscillations [A47] and by van Bragt, Rizwan-uddin and van der Hagen for bifurcation analysis of nuclear coupled thermal-hydraulics in natural circulation BWR [A32].

A-1.2 Analyses of specific events

There have been several attempts made to analyse specific instability events that took place at operating power plants or those observed at NPPs under controlled conditions. These vary in nature from data analysis using autoregressive models to analyses using large-scale numerical integration codes. The titles of the following references are fairly descriptive of the tasks concerned [A57-A62].

A-1.3 What is missing?

Another BWR (Oskarshamn-3) experienced an oscillation-cum-scram in February 1998 [A8]. A review of the possible causes suggested that the oscillations resulted from the "control rod sequence used and the power distribution created as a result" [A8]. In today's BWRs, detailed analysis is not required to test the system stability for the large number of power distributions that result due to control rod movements. A possible reason for this state of affairs is that the system codes are very labour intensive, while low-dimensional codes are too qualitative to be of much help for practitioners. In other words, the gap between low-dimensional models (appropriate for semi-analytical dynamical system treatment) and models used in system codes has been very large. This has led to a disconnect between the two approaches with little or no advantage of the semi-analytical approaches becoming available to the user of system codes. This gap must be shortened by quasi-quantitative models that possess all the advantages of the low-dimensional models. [A quasi-quantitative model, for our purpose, is one which predicts roughly the same behaviour as that predicted by a system code but possibly for a slightly (10-20%) different set of parameter values than those used in the system code.] These models can be used to efficiently identify those scenarios (even if only qualitatively) that are susceptible to NCTH instabilities. These scenarios can then be selectively analysed using quantitative system codes.

A-2 Detailed simulations of BWR stability incidents using nuclear coupled thermal-hydraulics codes

A-2.1 Introduction

Several instability events have been observed in BWR plants, including both inadvertent events and those induced intentionally as experiments. Such instabilities were identified as periodic oscillations of the neutron flux via instrumentation readings. Essentially, neutronic power signals from local power range monitors (LPRM) and average power range monitors (APRM) have been used to detect and study the power oscillations. A wide review of reported instability events can be found in [A63]. Attention is concentrated here on what are known as neutronic/thermal-hydraulic instabilities [A64], where a strong non-linear coupling exists between the neutronic and thermal-hydraulic processes via the void feedback reactivity. Mainly two kinds of neutronic/thermal-hydraulic instabilities in BWR plants have been described, the core-wide (in-phase) oscillations, where the whole core behaves as one entity, oscillating the power of all the fuel bundles together, and the regional (out-of-phase) oscillations, where half of the core behaves out-of-phase from the other half. That is, when the power rises in one half of the core, it is reduced in the other half so that the average power remains essentially constant. These two kinds of oscillations have occurred either separately or overlapped in the same event.

Though there are features unique to each instability event, certain common characteristics for all these events exist, such as: All events have arisen under low-flow conditions (30-40% of the rated coolant mass flow) and power levels of about 40-70% of the nominal power. Further, the radial and axial power shapes affect the instability. A strongly bottom-peaked axial power shape makes the core more unstable and a radially-increasing power shape (bowl shape) makes the core susceptible to excite

out-of-phase oscillations. Frequencies in all observed oscillations happen to be over a range of 0.3 to 0.6 Hz, which is correlated with the steam bubble velocity in a hydraulic channel (the concentration wave propagation velocity).

A great deal of work has been devoted to explaining the physical mechanisms underlying the neutronic/thermal-hydraulic instabilities in BWRs [A65-A71]. In this context, reduced-order models have been proposed to explain the neutronic oscillations. Some of these models are based on an expansion of the neutron flux in terms of spatial modes, which are solutions of the static neutron diffusion equation, the so-called λ-modes [A72]. Instead of the λ-modes we can also use the Inhour or ω-modes defined by Henry [A73]. The expansion in terms of the λ-modes results in a system of coupled ordinary differential equations for the fundamental and first modes, and this system of equations can be partially decoupled assuming that the generation time matrix is diagonal dominant ($\Lambda_{mn} << \Lambda_{mm}$, $m \neq n$, with m and n denoting the mode number). This is a reasonable assumption from the physical point of view [A68]. Therefore, we will use the λ-modes expansion.

Using a modes expansion model, the in-phase oscillations are associated with the amplitude of the fundamental mode, and the out-of-phase oscillations are related to the contributions of the first subcritical modes (for a critical reactor the higher modes are subcritical ones). But the detailed mechanism by which the reactor core under unstable conditions develops an in-phase oscillation, an out-of-phase oscillation, or both, remains an enigma [A74-A76]. With the aim to better understand the instability development process, we have studied the stability behaviour of different operational points of the nuclear power plant (NPP) Leibstadt (Cycle7 and Cycle 10) with the Studsvik-Scandpower system code RAMONA3-12 (for the theoretical background of this code see Ref. [A77]). At one of the operational points studied a limit cycle corresponding to an in-phase oscillation is developed (Cycle 10), and for the other ones the limit cycle obtained corresponds to out-of-phase oscillations (Cycle7) [A78]. With the RAMONA code it is possible to obtain detailed information regarding the state of the reactor for each integration time step. In this way, were obtained for each time step the power distribution and the nuclear cross-sections for each of the 648×27 NPP Leibstadt (KKL) core nodes (without reflector) with a volume of $15.24 \times 15.24 \times 15.24$ cm^3 and. From these values were calculated the different mode feedback reactivities versus time using the λ-modes of the stationary configuration of the reactor, expecting that the time behaviour of the mode reactivities could be used as an indicator for the oscillation type in an unstable reactor state.

A-2.2 NPP Leibstadt stability tests

In September 1990 a stability test was conducted at the NPP Leibstadt, addressing among other issues the qualification of the KKL core stability monitoring system [A79,A80]. The test was performed during Cycle 7 reactor start-up. The KKL core in Cycle 7 contained only 8×8 fuel assemblies supplied by General Electric, apart from 4 SVEA-64 fuel assemblies supplied by ABB Atom [A79].

To test the ability of the monitoring system to cope with demanding operational situations, the power oscillations were deliberately transformed from the in-phase mode into the out-of-phase mode, by changing some control rod positions [A79,A80]. The control rod movements had a large impact on the spatial power distribution and it will be demonstrate that, for a spatial power distribution characterised axially by a relatively strong bottom peak and radially by a higher (in comparison to the central) peripheral power level (the so-called bowl shape), out-of-phase oscillations should be expected if the core is in an unstable dynamical state.

The search for the instability threshold began by raising the power through the withdrawal of the control rod banks 40 and 38 (Table A-1).

Table A-1. Control rod configuration for signal recording 4 (rec4)

KKL c7, rec4: Different control rod configuration for signal recording 4 (rec4) One notch = 7.62 cm										
Control rod position notches (absorber rods of control rod bank 36...45 are xy notches withdrawn)										
CR bank / Time	36	37	38	39	40	41	42	43	44	45
23:20	*48*	*48*	*10*	*48*	*12*	*0*	*24*	*48*	*42*	*42*
23:32	*48*	*48*	*10*	*48*	*14*	*0*	*24*	*48*	*42*	*42*
23:37	*48*	*48*	*12*	*48*	*14*	*0*	*24*	*48*	*42*	*42*
23:38	*48*	*48*	*14*	*48*	*14*	*0*	*24*	*48*	*42*	*42*
23:39	*48*	*48*	*0*	*48*	*14*	*0*	*24*	*48*	*42*	*42*
23:41	*48*	*48*	*0*	*48*	*0*	*0*	*24*	*48*	*42*	*42*
23:53	*48*	*48*	*10*	*48*	*0*	*0*	*24*	*48*	*42*	*42*

The control rod positions are shown also in Figure A-1, where we have represented the number of notches withdrawn for each control rod (48 means that the control rod is completely out, 0 means that the control rod is completely in). This signal recording yielded non-stationary LPRM signals (a typical LPRM signal is shown in Figure A-2). In this figure, we see that after 660 s (23:38 h) an unstable oscillation started. From the phase shift analysis of two opposite LPRM signals we learn that this oscillation is out-of-phase (Figure A-3). At ~740 s (~ 23:39 h) the maximal oscillation amplitude was reached and the oscillation was suppressed by decreasing the power. The power history is demonstrated in Figure 2.4. At 23.27 h the reactor power was about 58%. The search for the instability threshold in Record 4 began by raising the power by withdrawing the control rod banks 40 (withdrawn from node 12 at 23:20 h to node 14 at 23:32 h) and 38 (withdrawn from node 10 at 23:32 h to node 14 at 23:38 h) [A80], see Table A-1 and Figure A-4. At 23:38 h a power level of about 61% was reached and in the experiment an unstable out-of-phase oscillation started (Figure A-2). To supress the power oscillation the control rod bank 38 began to be inserted, and it was fully inserted at 23:39 h (power level about 60%). But the core configuration at 23:39 h was unstable and had a strong tendency to oscillate in an out-of-phase mode. Then control rod bank 40 was also fully inserted and the oscillations were suppressed. At 23:41 h record 4 was terminated.

From the phase shift in Figure A-3 we conclude that the core configuration at 23:39 h had a tendency to excite out-of-phase oscillations. RAMONA simulations for times 23:27 h (with data for 23:32 h), 23:38 h and 23:39 h were carried out with the core configurations provided in Table 2.1.

A-2.2.1 Calculation of the mode feedback reactivities

First of all, the stability behaviour of the Leibstadt reactor was analysed using RAMONA3-12. The following operational point data were used [A80] (Figure A-2):

Case A	23:27 h: 58.0% thermal power, 36.7% mass flow rate
Case B	23:38 h: 61.0% thermal power, 36.7% mass flow rate
Case C	23:39 h: 60.5% thermal power, 36.7% mass flow rate

Figure A-1. Different control rod positions (at 23:27 h, 23:38 h and 23:39 h)

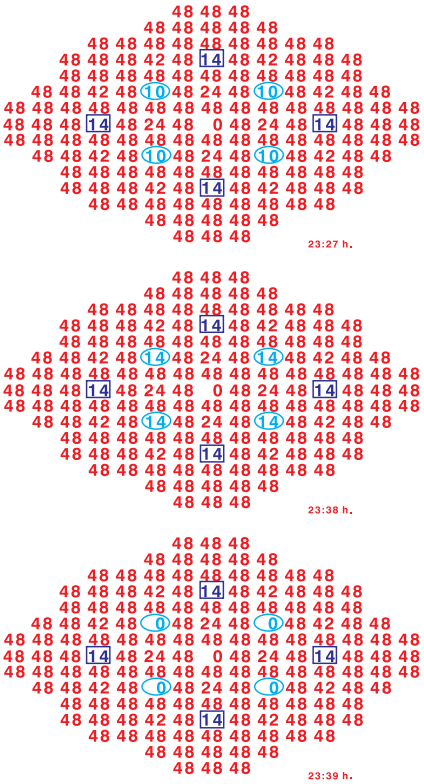

Figure A-2. Measured LPRM (19:4) signal and power spectral density

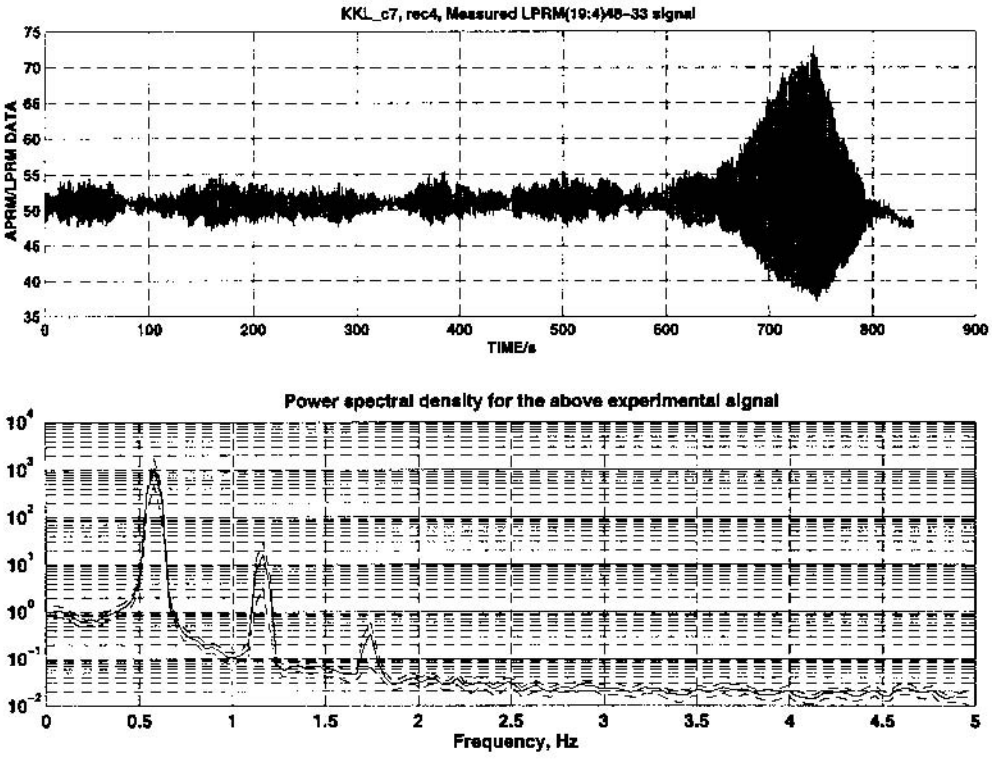

Figure A-3. Phase shift between two LPRM signals. A 180° phase shift is recognisable at the natural frequency of 0.58 Hz.

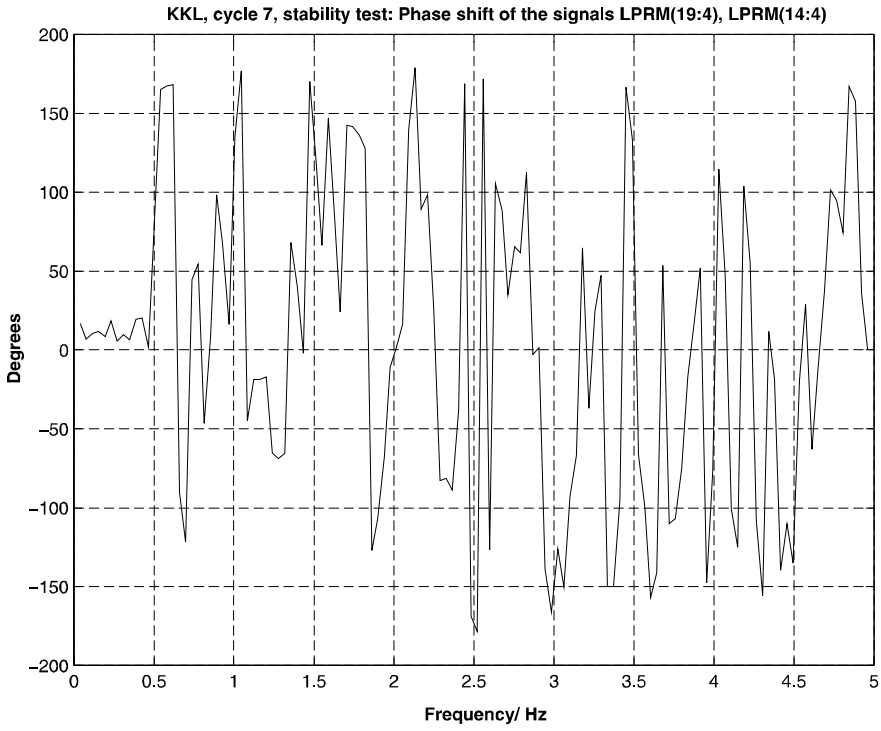

Figure A-4. Experimental power history

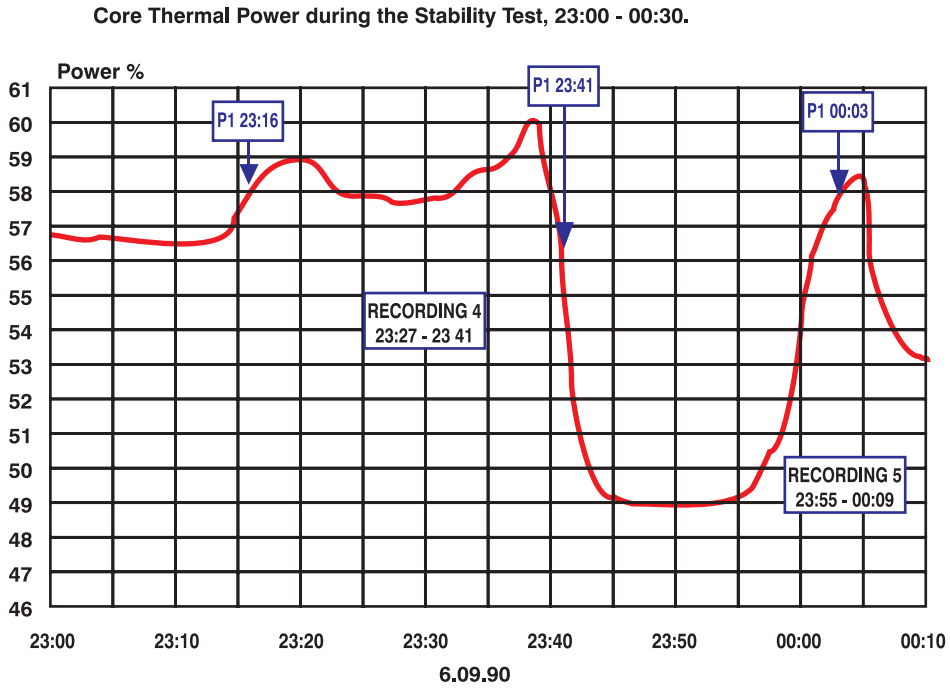

For a comparison of results an unstable in-phase operational point for KKL, Cycle 10 (designated Case D), and a stable operational point for the same cycle (designated Case E) were also analysed. The LPRM locations are presented in Figure A-5. For all these cases computed the spatial indices for the power distributions R, RL and the axial peaking proposed in Ref. [A67] were calculated. The results obtained are presented in Table A-2.

Figure A-5. LPRM locations

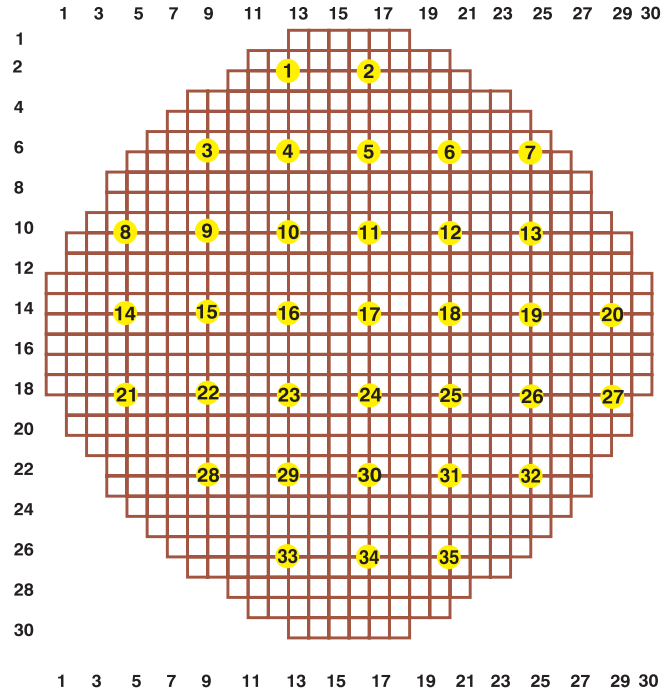

Table A-2. Spatial indices, R, RL, axial peaking factors

Case	R	RL	Axial peaking (at node)
Case A	*1.0734*	*0.9976*	*1.605 (4)*
Case B	*1.0747*	*0.9933*	*1.546 (4)*
Case C	*1.0622*	*1.0152*	*1.750 (4)*
Case D	*1.0918*	*0.9802*	*1.545 (4)*
Case E	*1.0887*	*0.9771*	*1.356 (4)*

Cases A and B of Cycle 7 seem to be stable points (see Figure A-6). The oscillation amplitude is very small and quite irregular, and it seems to be a numerical fluctuation. The RL values are slightly lower than 1.0 (flat radial power distribution) and the axial peaking values are lower than those obtained for the Case C value (Table A-2). Case C is clearly unstable (Figure A-6), and the core oscillates in an out-of-phase mode (Figure A-7). The RL value for this case is larger than 1.0 (RL = 1.0152, Table A-2), meaning that the radial power distribution is bowl-shaped (higher at the periphery). In Figure 2.7 the core symmetry line that divides the core into the two halves has been drawn, both halves having power oscillations with a phase shift of about 180°. The symmetry line orientation is time-dependent [A79]. At a given point in time the predicted orientation of the symmetry line can thus be different from the measured one.

Figure A-6. LPRM signals for Case A (23:27 h) and Case C (23:39 h)

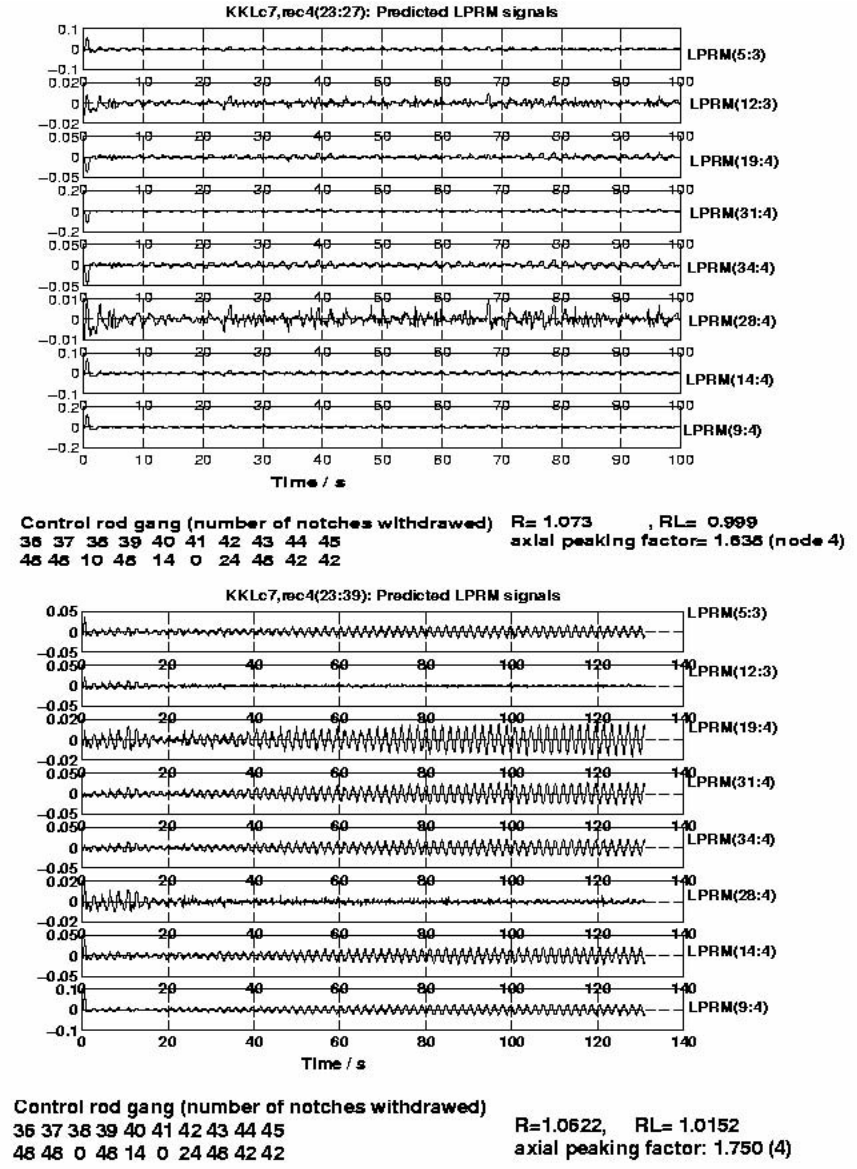

Furthermore, the modal feedback reactivities were calculated for Cases A, B, C, D and E using the VALKIN code. Figures 2.8 through 2.12 show the (dynamical) mode feedback reactivities evolution, $\rho_{00}^{F}(t)$ and $\rho_{01}^{F}(t)$, for the cases analysed. It should be noted, however, that for the feedback reactivity $\rho_{11}^{F}(t)$ we observe a similar behaviour to that of $\rho_{00}^{F}(t)$, while the reactivity $\rho_{10}^{F}(t)$ behaves similarly to $\rho_{01}^{F}(t)$. In Cases A and B the mode coupling is weak and the fundamental mode reactivity is dominant. In Case C, the coupling reactivities become clearly dominant (Figure 2.10). Figure 2.11 represents the feedback reactivities for Case D. This behaviour is definitively different from the out-of-phase case. The feedback cross-terms $\rho_{10}^{F}(t)$ and $\rho_{01}^{F}(t)$ are no longer the dominant terms. Also, the reactivity curves of Case E show a non-dominant coupling reactivity (Figure 2.12). Cases C and D clearly show fully developed out-of-phase and in-phase oscillations, respectively [A81].

Figure A-7. Out-of-phase oscillation, Case C

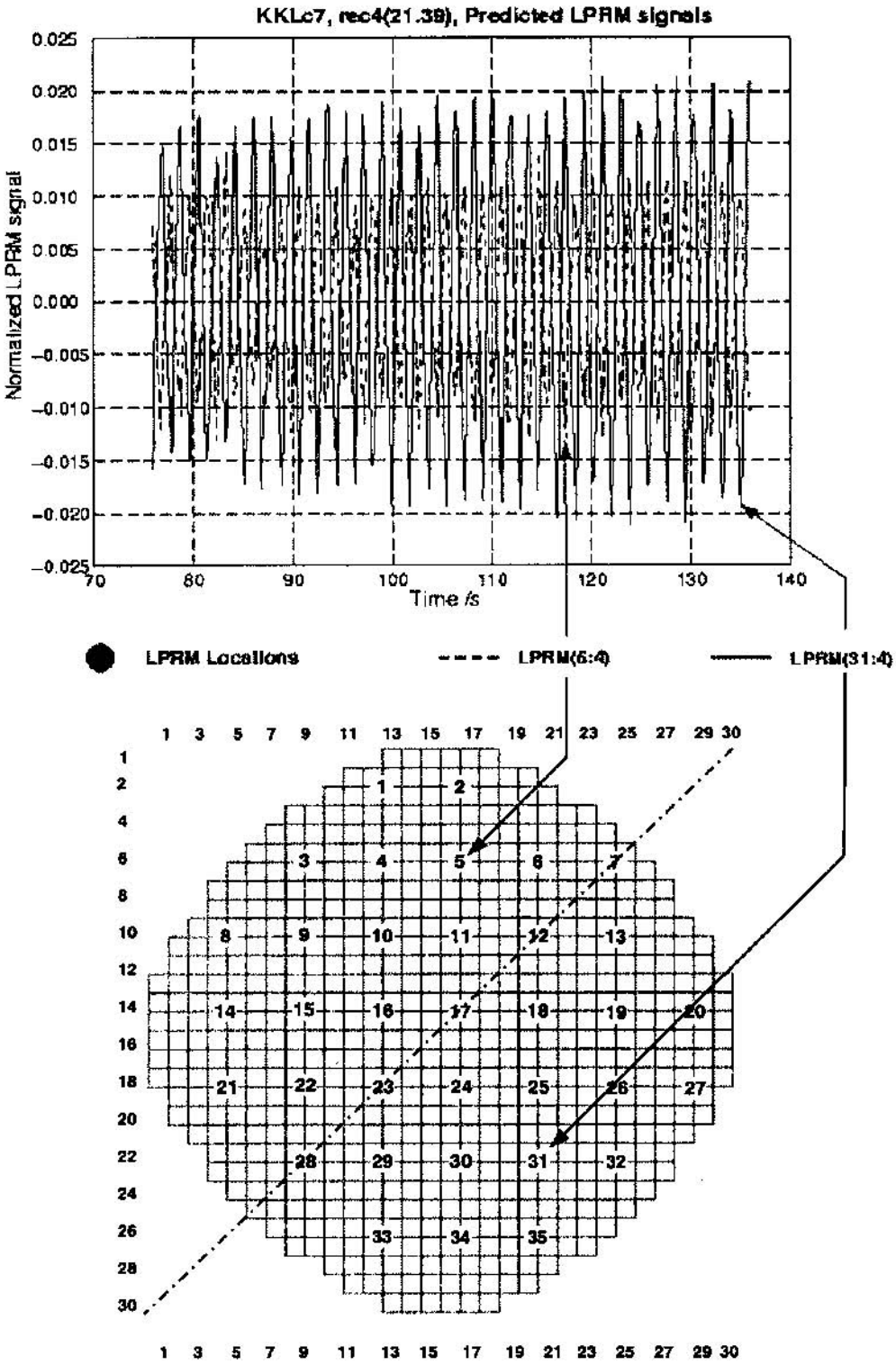

From Figures A-8 to A-12 we can conclude that in an out-of-phase state the mode coupling reactivity is a characteristic indicator.

Figure A-8. Case A (stable): Mode feedback reactivities (fundamental and first mode)

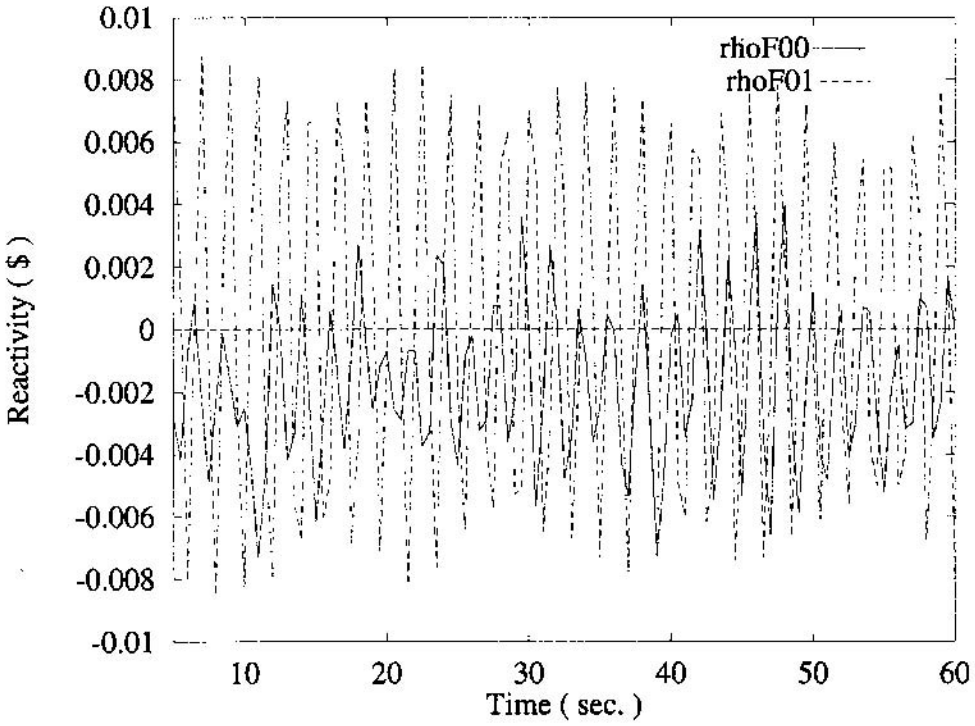

Figure A-9. Case B (stable): Mode feedback reactivities (fundamental and first mode)

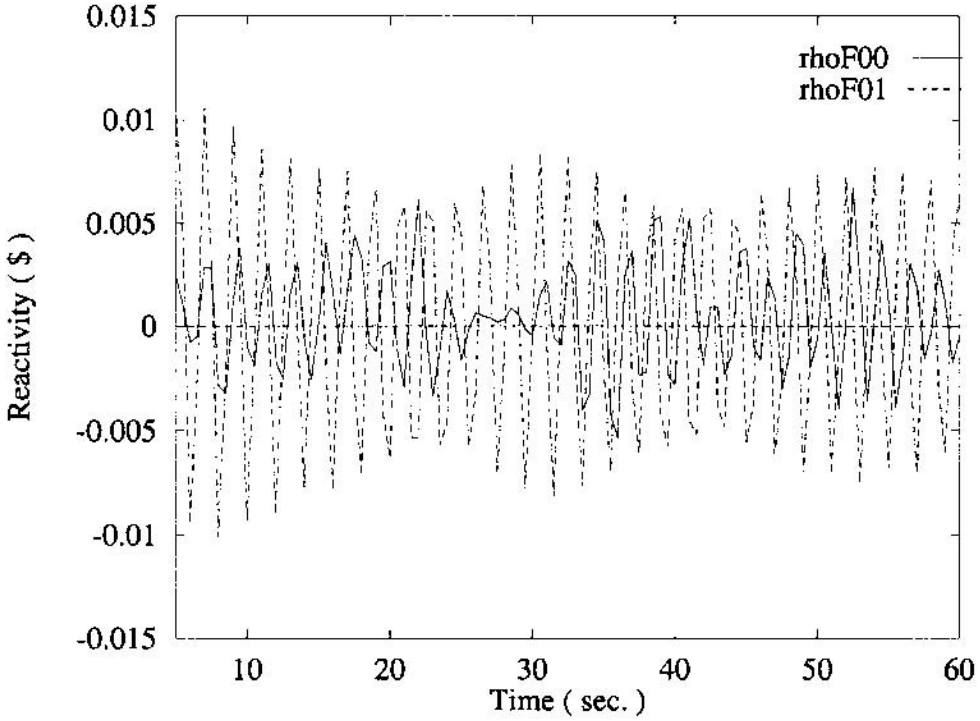

Figure A-10. Case C (out-of-phase): Mode feedback reactivities (fundamental and first mode)

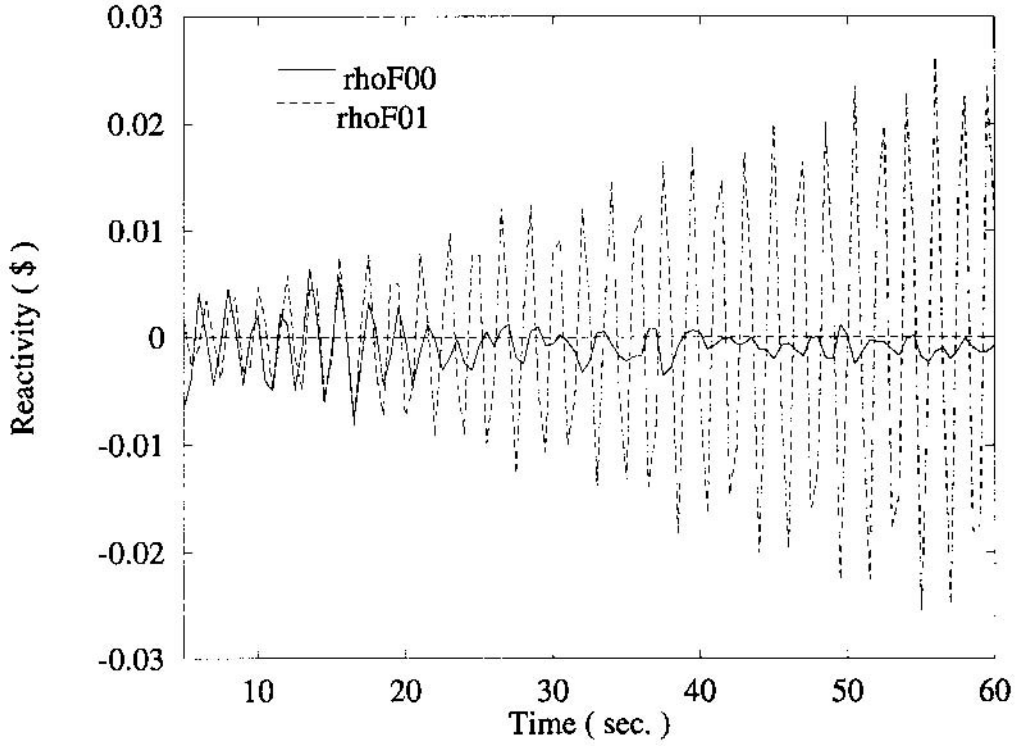

Figure A-11. Case D (in-phase): Mode feedback reactivities (fundamental and first mode)

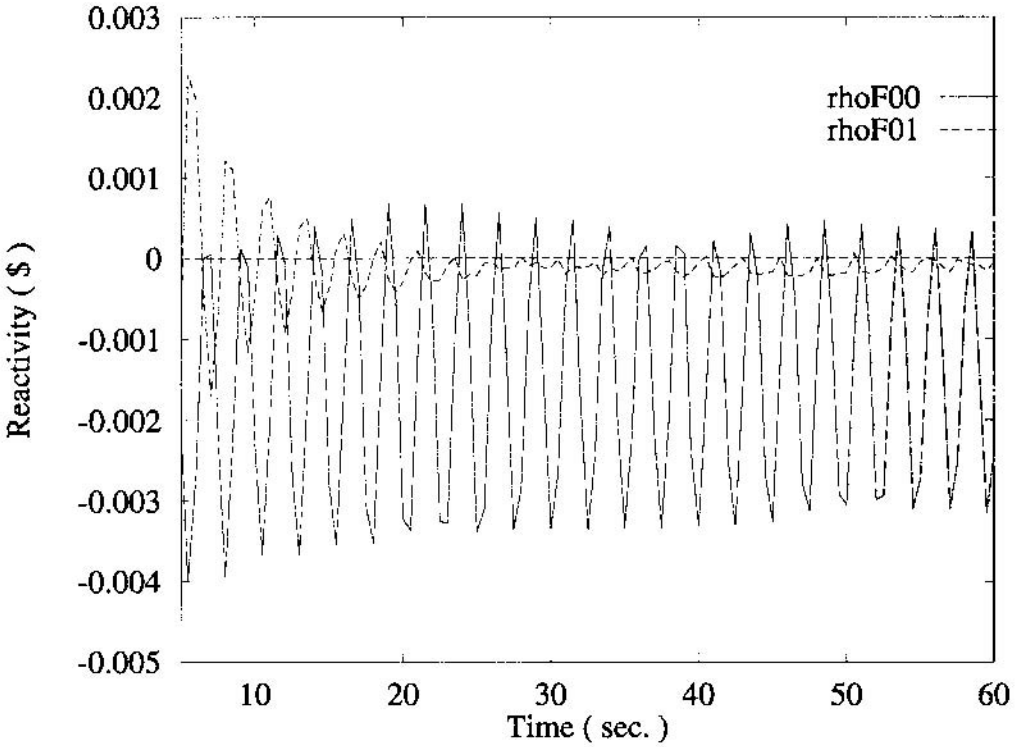

Figure A-12. Case E (stable): Mode feedback reactivities (fundamental and first mode)

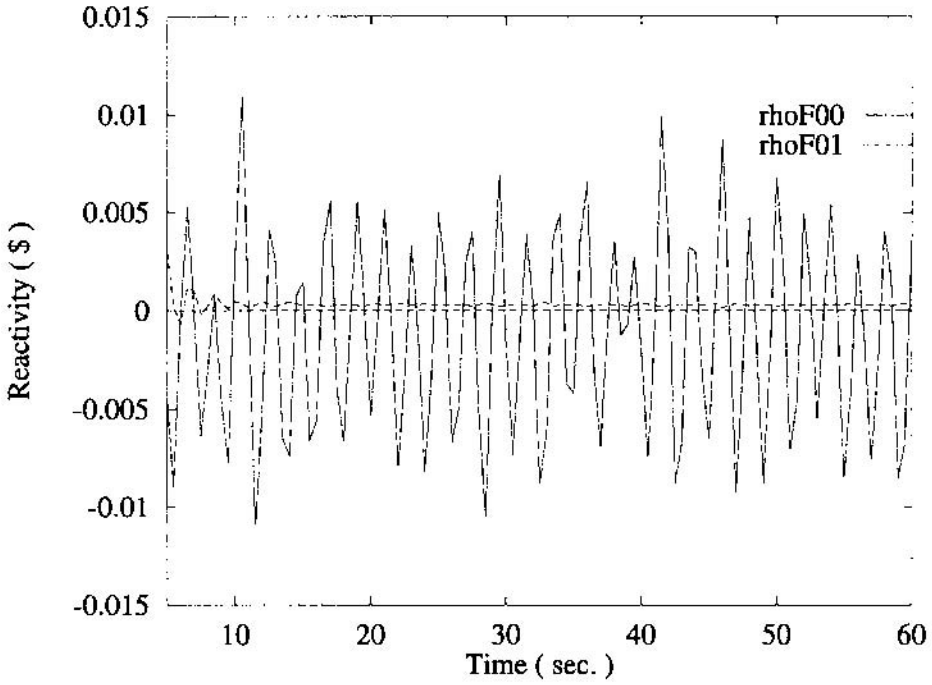

Finally, we compare the eigenvalue separation for the different modes calculated for the different cases. The data in Table A-3 demonstrate that the eigenvalue separation gets its smallest value (~5.7 mK ≅ 1$) for the regional oscillation Case C, but the eigenvalues separation values obtained for Cases A and B are not so different. Nevertheless, for Cases D and E, the differences are larger. We can conclude that the eigenvalue separation is a very sensitive parameter, which only provides relative information about the stability conditions of the reactor core and the kind of oscillation developed in unstable conditions.

Table A-3. Eigenvalue separation, ES = (λ_0-λ_m = k_{eff0}-k_{effm})

Eigenvalue separation			
Case	λ_0-λ_1	λ_0-λ_2	λ_0-λ_3
Case A	5.872×10^{-3}	5.891×10^{-3}	7.179×10^{-3}
Case B	6.083×10^{-3}	6.104×10^{-3}	7.039×10^{-3}
Case C	5.709×10^{-3}	5.732×10^{-3}	8.259×10^{-3}
Case D	6.661×10^{-3}	6.902×10^{-3}	8.281×10^{-3}
Case E	7.285×10^{-3}	7.504×10^{-3}	9.126×10^{-3}

A-2.2.2 Decomposition of the LPRM signals

It will now be attempted to complement the results presented above for the power modal decomposition by considering the information provided by the simulation of the LPRM signals by RAMONA [A78].

The LPRM are positioned between axial and lateral planes corresponding to the reactor discretisation (nodes). The spatial location of the LPRM across in the core is indicated in Figure A-5.

For each cell, (*i*,*j*,*k*), of the reactor core discretisation, local harmonic power modes are considered:

$$P_{n,i,j,k} = \alpha\left(\sum_{f1i,j,k} \phi_{1,ijk,n} + \sum_{f2i,j,k} \phi_{2,ijk,n}\right)$$

For a given LPRM, *l*, in the axial level k_l, we define the *n*-th modal power contribution to the LPRM as:

$$LP_{n,l,k_l} = \sum_{i,j,k} P_{n,i,j,k_l}$$

where *i*,*j* sum over the adjacent nodes to LPRM *l*, as shown in Figure A-13, and *k* sums over the two axial planes containing the LPRM.

Figure A-13. Adjacent nodes to LPRM *l*

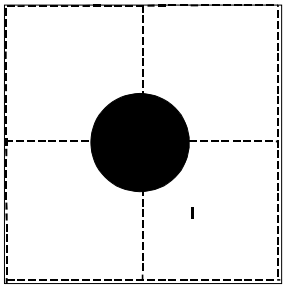

Now, it is supposed that the LPRM signals can be expressed as:

$$LPRM_{l,k_l}(t) = \sum_{n} a_n^{k_l}(t) LP_{n,l,k_l} \tag{A-1}$$

The fast adjoint modes are used to construct a weighting factor to obtain the power amplitudes, $a_n(t)$. For each LPRM, (l,k_l), is defined:

$$W_{n,l,k_l} = \sum_{i,j,k} \phi^{+}_{1,ijk,n} \tag{A-2}$$

where $\phi^{+}_{1,ijk,n}$ is the average fast *n*-th mode in cell (*i*,*j*,*k*), and *i*, *j* and *k* sum over the adjacent nodes to LPRM *l*.

Supposing that the experimental signals $LPRM_{l,k_l}(t)$ are modelled by Eq. (A-1), and using the weights (A-2), for each axial level, k_l, the following system of linear equations is constructed:

$$\sum_{l} LPRM_{l,k_l}(t) W_{m,l.k_l} = \sum_{l} \sum_{n=1}^{N} a_n^{k_l}(t) LP_{n,l,k_l} W_{m,l,k_l} \tag{A-3}$$

where *m = 0,...,N*, *N* being the number of considered modes for the power decomposition. Calculating the dominant lambda modes for the steady-state configurations corresponding to the analysed cases, we have found, consecutively, the fundamental mode, two azimuthal modes and an axial mode [A82]. For a given axial level k_l we can not obtain information about the axial mode. The number of modes considered is three, the fundamental, ϕ_0, and two azimuthal modes, ϕ_1 and ϕ_2.

For the analysis of Cases C and D, the first axial level of LPRM has been considered. The results obtained for the amplitudes $a_0(t)$, $a_1(t)$ and $a_2(t)$ are shown in Figures A-14 and A-15. The same results for the out-of-phase Case C are shown in Figures A-16 and A-17.

Figure A-14. $a_0(t)$ amplitude for Case D (LPRM decomposition)

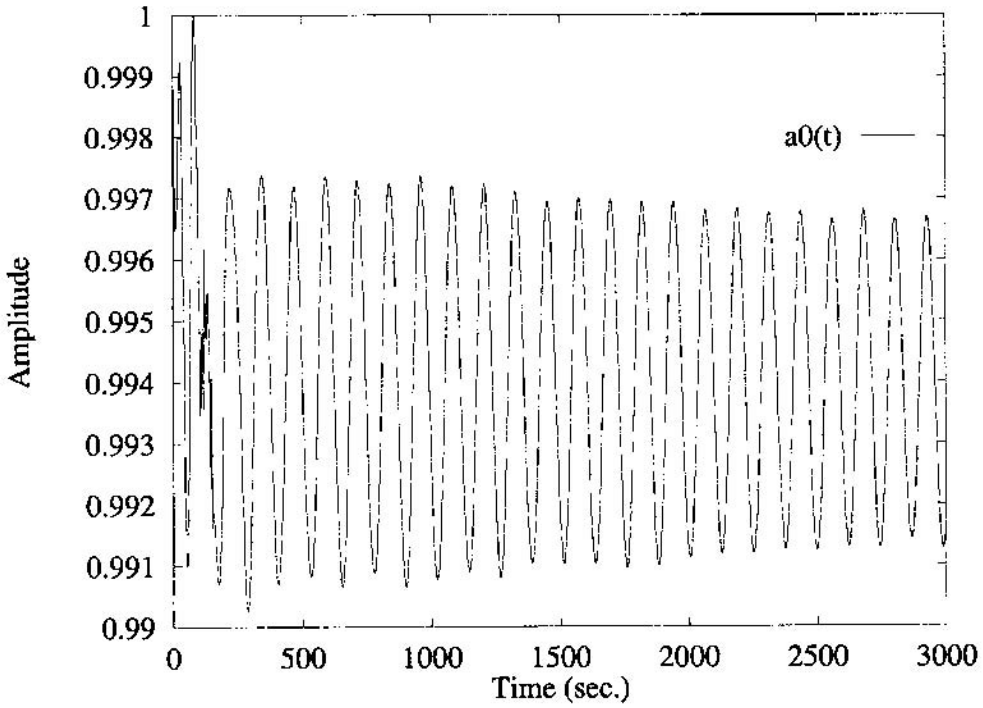

Figure A-15. $a_1(t)$ amplitude for Case D (LPRM decomposition)

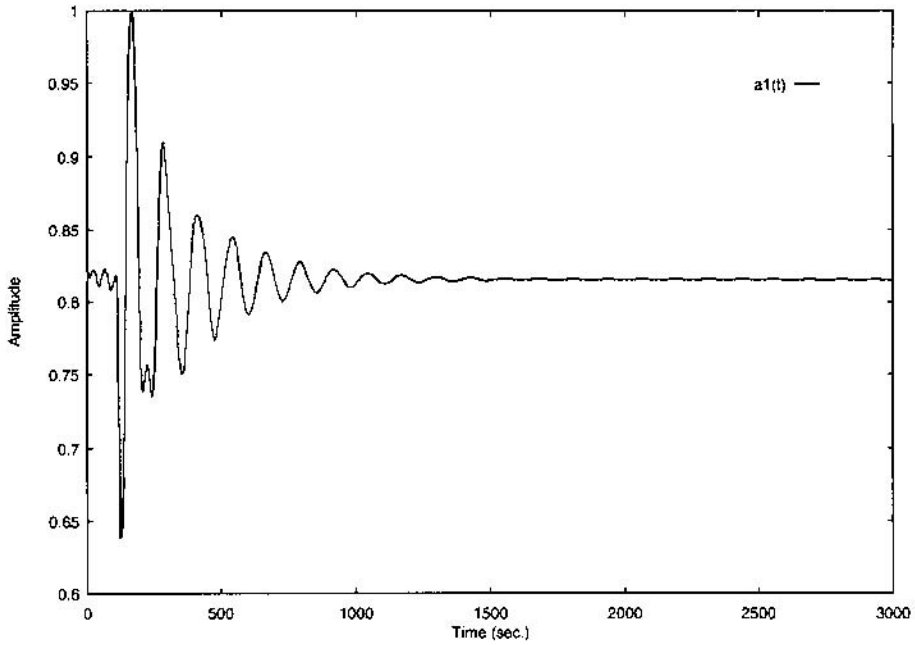

Figure A-16. $a_0(t)$ amplitude for Case C (LPRM decomposition)

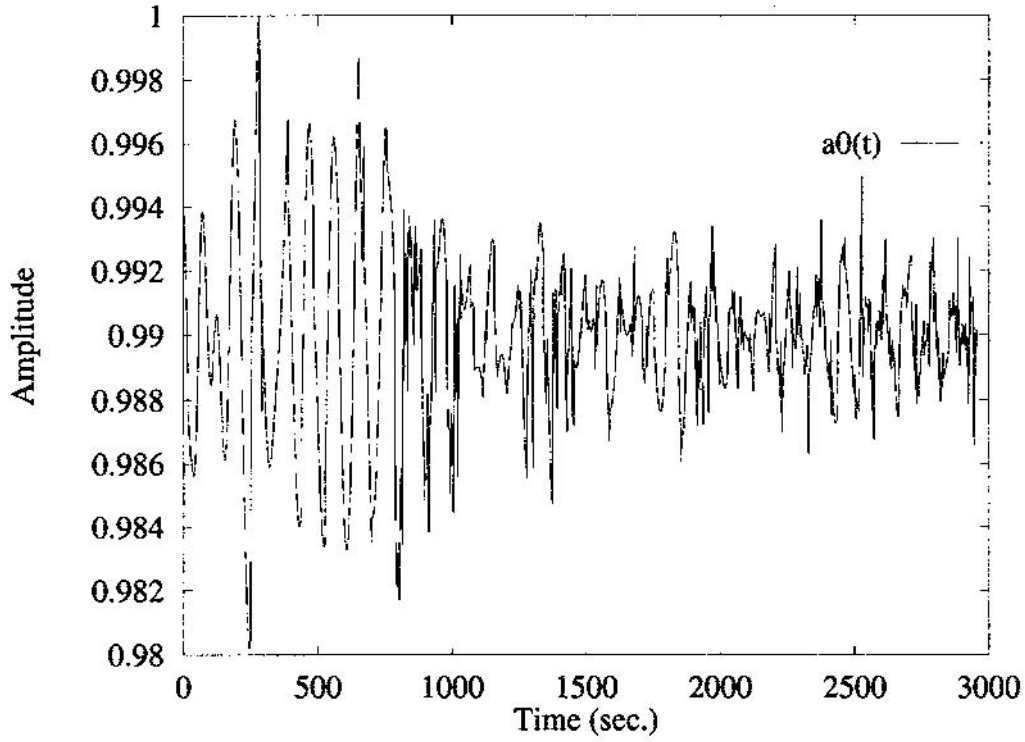

Figure A-17. $a_1(t)$ amplitude for Case C (LPRM decomposition)

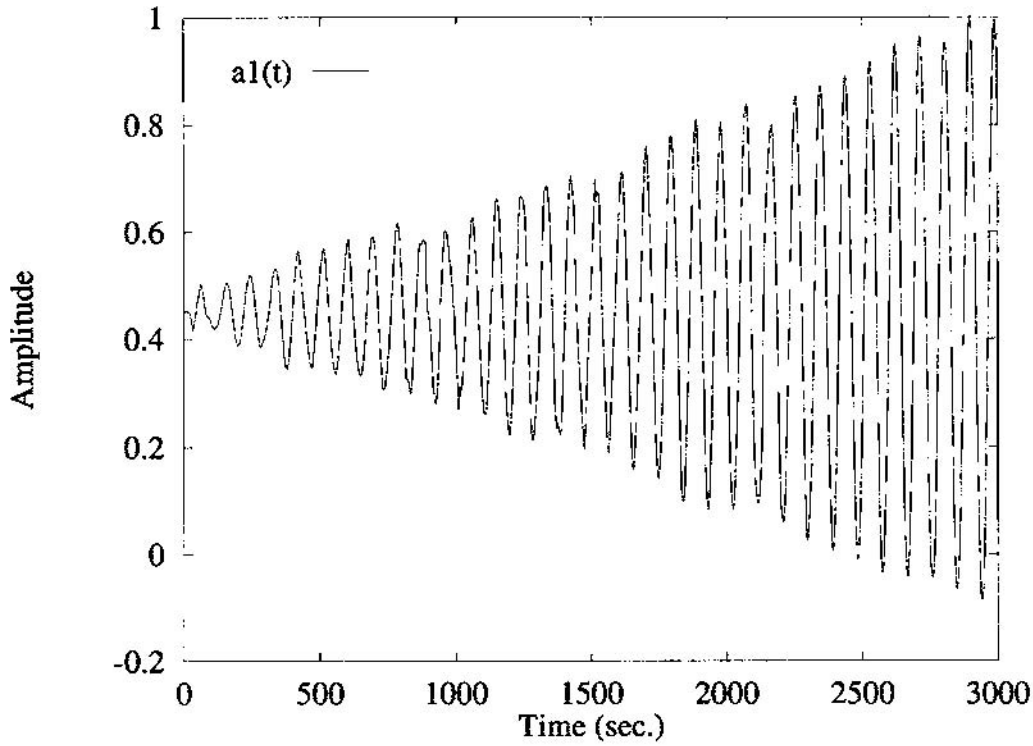

It is observed from the figures that it is possible to obtain the same qualitative information by simply considering the signals from one of the axial levels of LPRM as is obtained from the detailed nodal analysis, where it is necessary to know the power distribution for all the reactor nodes at each time step.

A-2.3 Ringhals benchmark case analysis

The focus is particularly on Case 9 (Case G) of Cycle 14, which corresponds to a configuration with 72.6% of the nominal power of the reactor and a core mass flow of 3 694 kg/s [A83]. In the benchmark exercise it was stated that this case corresponds to an unstable situation of the reactor with a fully developed out-of-phase oscillation (DR = 0.99) together with a more stable in-phase oscillation (DR = 0.8). Both took place at 0.5 Hz.

The Ringhals 1 reactor core has been discretised in 27 axial planes of 14.72 cm length, 25 of which correspond to the fuel and one plane at the top and another at the bottom that correspond to the reflector. Each axial plane has been also discretised in 15.275 × 15.275 cm cells distributed as shown in Figure A-18. The cells corresponding to the reflector have also been taken into account.

Figure A-18. LPRM disposition in an axial plane for Ringhals 1 reactor

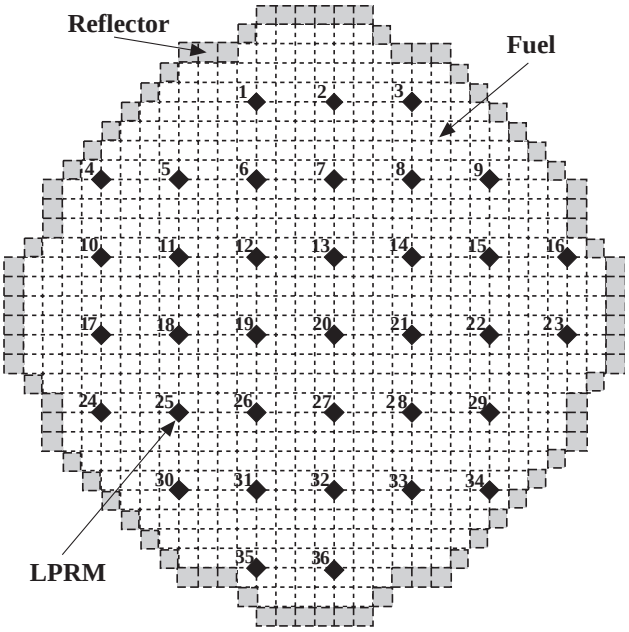

The first five dominant modes for this initial reactor core configuration have been calculated. The values of the eigenvalues obtained are given in Table A-4.

Table A-4. Eigenvalues of Ringhals reactor

1.0023	0.9955	0.9940	0.9913	0.9849

The local power profiles associated with the corresponding eigenmodes are represented schematically in Figures A-19 to A-23.

Figure A-19. Power profile for the first mode (fundamental mode, radial)

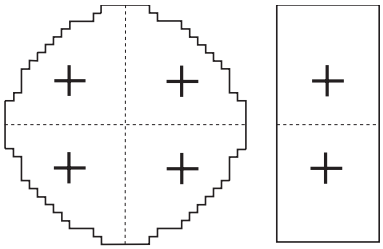

Figure A-20. Power profile for the second mode (first azimuthal mode)

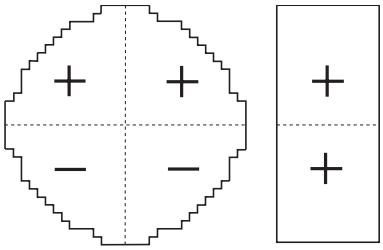

Figure A-21. Power profile for the third mode (second azimuthal mode)

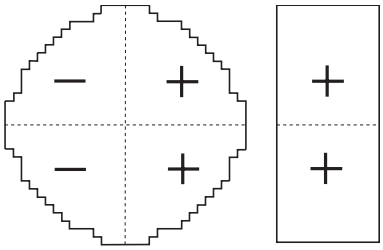

Figure A-22. Power profile for the fourth mode (axial mode)

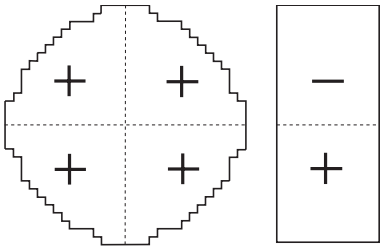

Figure A-23. Power profile for the fifth mode (third azimuthal mode)

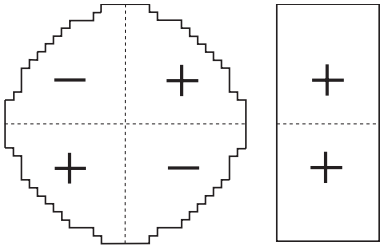

In each representation, the figure on the left shows the sign structure of the relative power map for a generic reactor plane, and the figure on the right gives the sign structure of the axial level, obtaining the signs of the power map multiplying the signs of the plane and the axial level. To simplify the representation the sign structure has been shown to be spatially symmetric, although this is only approximate, as can be observed in Figure A-24, where the relative power map corresponding to the axial plane number 11 of the second mode is represented.

Figure A-24. Power map for the first azimuthal mode, axial plane 11

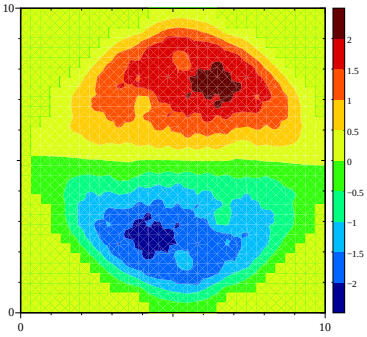

With the data provided for the benchmark exercise, a plant model has been set up for Ringhals 1.

The solution of the transient with the modal method was obtained using the first five dominant modes. The power evolution of the transient is compared using a standard 3-D thermal-hydraulic code and the modal code in Figure A-25.

Figure A-25. Power evolution calculated with 3-D/T-H code and with the modal method

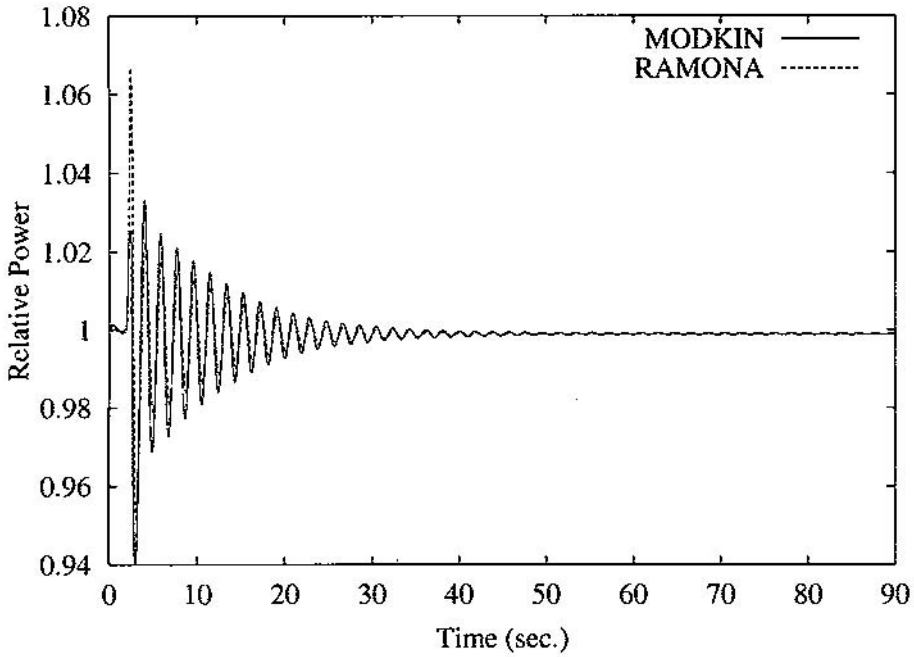

We observe that there is a good agreement between the results provided by both codes.

In Figure A-26, the evolution of the amplitude associated with the fundamental mode, $n_1(t)$, is shown. Figure A-27 shows the evolution associated with the first azimuthal mode amplitude, $n_2(t)$, and Figure A-28 shows the evolution of the amplitude associated with the second azimuthal mode, $n_3(t)$.

It can be concluded from the curves that this case corresponds to an instability event where the in-phase oscillation, associated with the fundamental mode, is damped, but an out-of-phase oscillation related with the first and second azimuthal modes is developed. the amplitude of the first azimuthal mode is 10 times larger than the one associated with the second azimuthal mode.

Figure A-26. Evolution of the amplitude associated with the fundamental mode

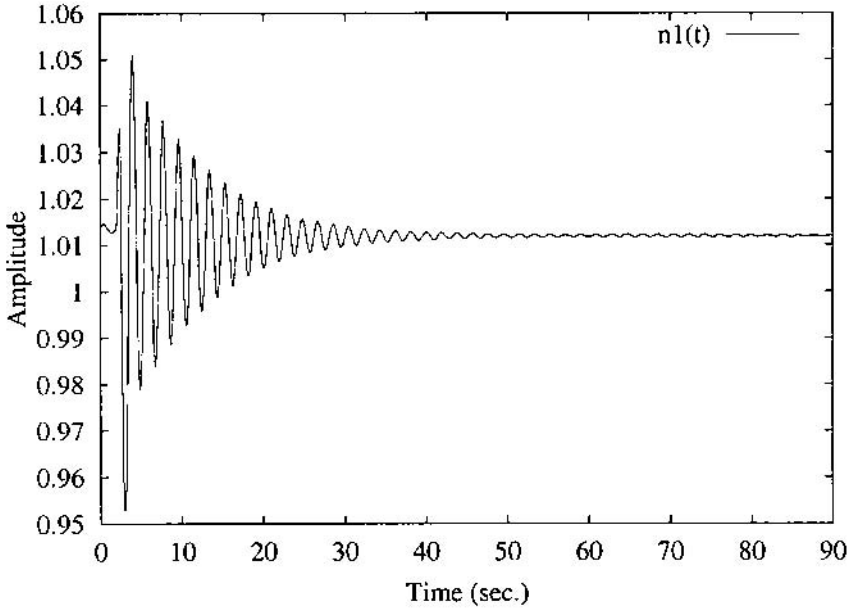

Figure A-27. Amplitude evolution associated with the first azimuthal mode

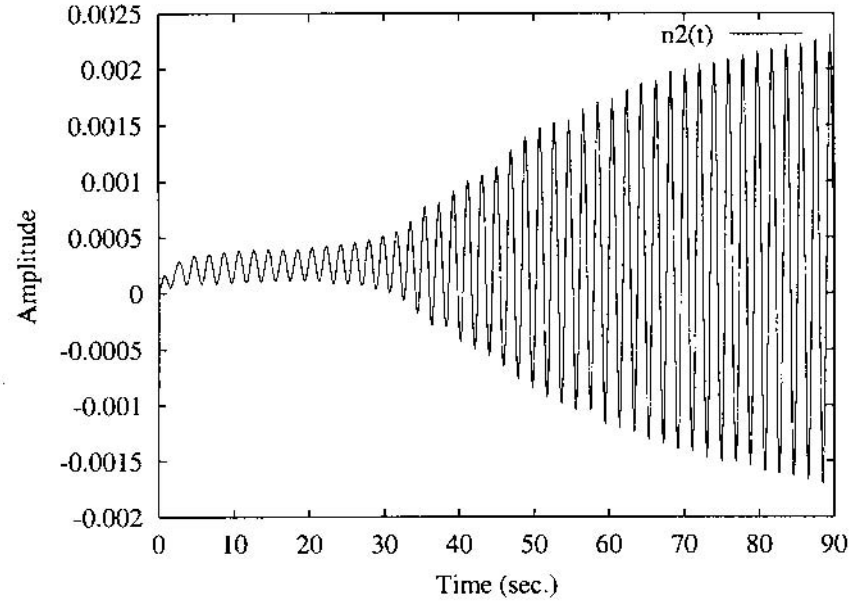

Figure A-28. Evolution of the amplitude associated with the second azimuthal mode

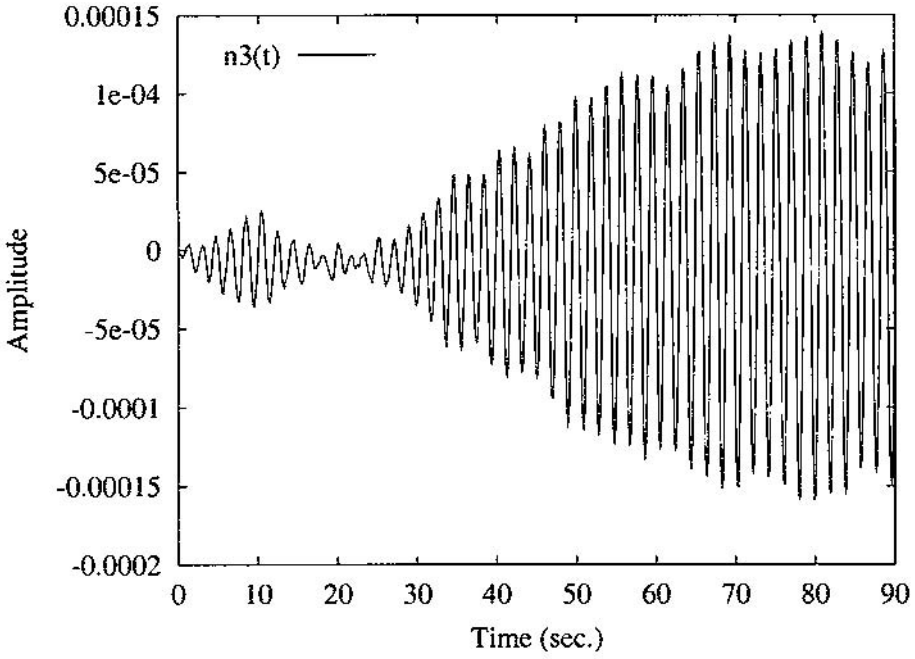

REFERENCES

[A1] March-Leuba, J. and J.M. Rey, "Coupled Thermo-hydraulic-Neutronic Instabilities in Boiling Water Nuclear Reactors: A Review of the State of the Art", *Nucl. Eng. Des*., 145, 99 (1993).

[A2] *Proceedings of the International Workshop on Boiling Water Reactor Stability*, sponsored by the Nuclear Energy Agency of the Organisation for Economic Co-operation and Development, OECD/NEA, CSNI Report 178, Brookhaven, NY, October 1990.

[A3] Rizwan-uddin, "A Two-phase Density-wave Oscillations and Nuclear-coupled Two-phase Thermal Hydraulic Instabilities: A Review", *Proc. of the 1st ISHMT-ASME Heat and Mass Transfer Conference*, Bombay, India, 5-7 January 1994, pp. 511-520.

[A4] Bergdahl, B.G., F. Reisch, R. Oguma, J. Lorenzen and F. Akerhielm, "BWR Stability Investigation at Forsmark-1", *Ann. Nucl. Energy*, 16, No. 10, 509-520 (1989).

[A5] Gialdi, E., S. Grifoni, C. Parmeggiani and C. Tricoli, "A Core Stability in Operating BWR: Operational Experience", *Progress in Nuclear Energy*, 15, 447-459 (1985).

[A6] Farawila, Y.M., D.W. Pruitt and P.E. Smith, "Analysis of the Laguna Verde Instability Event", *Proc. ANS National Heat Transfer Conf*., HTC-Vol. 9, pp. 198-202, American. Nuclear Society, La Grange Park, IL (1996).

[A7] Cheng, H.S., J.G. Guppy, A.N. Mallen and W. Wulff, "Simulations of the Recent LaSalle-2 Incident with BNL Plant Analyzer", *Trans. Amer. Nucl. Soc*., 57, 385 (1988). See also, *A Reactor Scram on High Average Power Range Monitor Flux Level Due to Personnel Valving Error*, LER 88-003-00, Commonwealth Edison Company (7 April 1988).

[A8] Kruners, M., *Analysis of Instability Event in Oskarshamn-3, Feb. 8, 1998, with Simulate-3K*, SKI Report, 98:42, ISSN 1104-1374, December 1998.

[A9] Wulff, W., H.S. Cheng, A.N. Mallen and U.S. Rohatgi, *BWR Stability Analysis with the BNL Engineering Plant Analyzer*, BNL-NUREG-52312 (1992).

[A10] Wulff, W., *Description and Assessment of RAMONA-3B MOD0 Cycle 4: A Computer Code with Three-dimensional Neutron Kinetics for BWR System Transients*, NUREG/CR-3664 (1984).

[A11] Giust, F.D. and L. Moberg, *RAMONA Stability Analysis on Ringhals-1, Phase 1: Model Qualification*, TR1/42.83.06, ScandPower (1991). See also Grandi, G.M. and F.D. Giust, *RAMONA Stability Analysis on Ringhals-1, Phase 2: Predictive Calculations*, TR2/42.83.06, ScandPower (1991).

[A12] Hotta, A., H. Ninokata and A. Baratta, "Development of Three-dimensional Kinetic Code ENTREE Coupled with TRAC-BF1", *Proc. Nuclear Reactor Thermal Hydraulics Conference, NURETH-9*, CD, American Nuclear Society (1999).

[A13] Valtonnen, K., "RAMONA-3B and TRAB Assessment Using Oscillation Data from TVO-I", *Proc. Int. Workshop on BWR Stability*, OECD/NEA, CSNI Report 178, 205-231 (1990).

[A14] Shaug, J.C., J.G.M. Andersen and J.K. Garrett, "TRACG Analysis of BWR Plant Stability Data", *Proc. Int. Workshop on BWR Stability*, OECD/NEA CSNI Report 178, 55 (1990).

[A15] Araya, F., M. Hirano, K. Yoshida, K. Matsumoto, M. Yokobayashi and A. Kohsaka, "Summary of RETRAN Calculations on LaSalle 2 Neutron Flux Oscillation Event Performed at JAERI", *Proc. Int. Workshop on BWR Stability*, OECD/NEA CSNI Report 178, 370 (1990).

[A16] Takigawa, Y., Y. Takeuchi, S. Tsunoyama, S. Ebata, K.C. Chan and C. Tricoli, "Coarso Limit Cycle Oscillation Analysis With Three-dimensional Transient Code TOSDYN-2", *Nucl. Technol.*, 79, 210 (1987).

[A17] Takeuchi, Y., Y. Takigawa, S. Tsunoyama and A. Kojima, "Analysis of Selected Rod Insertion Test in BWR Plant with Three-dimensional Transient Code TOSDYN-2", *J. Nucl. Sci. Tech*., 28, 3, 199-207 (1991).

[A18] Jackson, C.J., D.G. Cacuci and H. Finnemann, "Dimensionally Adaptive Neutron Kinetics for Multidimensional Reactor Safety Transients, Part I: New Features of RELAP5/PANBOX", *Nucl. Sci. Eng*., 131, 143 (1999). See also "Part II: Dimensionally Adaptive Switching Algorithms", *Nucl. Sci. Eng*., 131, 164 (1999).

[A19] Barber, D., R. Miller, H. Joo, T. Downar, W. Wang, V. Mousseau and D. Ebert, "Coupled 3-D Reactor Kinetics and Thermal Hydraulic Code Activities at the US Nuclear Regulatory Commission", *Proc. M&C'99 International Conference on Mathematics and Computation, Reactor Physics and Environmental Analysis in Nuclear Applications*, Madrid, Spain, 27-30 September 1999, pp. 311-320.

[A20] Otaduy, P. and J. March-Leuba, *LAPUR User's Guide*, NUREG/CR-5421 (1989). See also March-Leuba, J. and P. Otaduy, *Comparison of BWR Stability Measurements with Calculations Using the Code LAPUR-IV*, NUREG/CR-2998, ORNL/TM-8546, ORNL, January 1993.

[A21] March-Leuba, J. and E.D. Blakeman, "Mechanism for Out-of-phase Power Instabilities in Boiling Water Reactors", *Nucl. Sci. Eng*., 107, 173 (1991).

[A22] Peng, S.J., M.Z. Podowski, R.T. Lahey and M. Becker, "NUFREQ-NP: A Computer Code for the Stability Analysis of Boiling Water Nuclear Reactors", *Nucl. Sci. Eng*., 88, 404-411 (1984).

[A23] Hanggi, P., T. Smed and P. Lansaker, "MATSTAB, A Fast Frequency Domain Based Code to Predict Boiling Water Reactor Stability Using a Detailed Three-dimensional Model", *Proc. Nuclear Reactor Thermal Hydraulics Conference, NURETH-9*, CD, American Nuclear Society (1999).

[A24] Tsuji, M., K. Nishio and M. Narita, "Stability Analysis of BWRs Using Bifurcation Theory", *J. Nuc. Sci. and Tech*., 30, 11, 1107-1119 (1993).

[A25] Karve, A.A., Rizwan-uddin and J.J. Dorning, "Stability Analysis of BWR Nuclear-coupled Thermal-hydraulics Using a Simple Model", *Proc. Nuclear Reactor Thermal-Hydraulics Conference, NURETH-7*, Saratoga Springs, New York, 10-15 September 1995, Vol. 4, 2677, NUREG/CP-0142 (1995). See also Karve, A.A., Rizwan-uddin and J.J. Dorning, "Stability Analysis of Nuclear-coupled Thermal-hydraulics in a BWR Using a Simple Model", *Nuclear Engineering & Design*, 177, No. 1-3, 155-177 (1997).

[A26] Karve, A.A., Rizwan-uddin and J.J. Dorning, "Stability Boundaries of BWRs in Operating Parameter Space and in the Power-Flow Plane", *Trans. Am. Nucl. Soc*., 75, 392-394 (1996).

[A27] Karve, A.A., Rizwan-uddin and J.J. Dorning, "Out of Phase Power Oscillations in Boiling Water Reactors", *Proc. of the Joint Int. Conf. on Mathematical Methods and Supercomputing* Saratoga Springs, NY, 5-9 October 1997, Vol. 2, pp. 1633-1647, American Nuclear Society, La Grange Park, IL (1997).

[A28] Van Bragt, D.D.B. and T.H.J.J. van der Hagen, "Stability of Natural Circulation Boiling Water Reactors, Part I: Description Stability Model and Theoretical Analysis in Terms of Dimensionless Groups", *Nucl. Technol.*, 121, 40 (1998). See also Van Bragt, D.D.B. and T.H.J.J. van der Hagen, "Stability of Natural Circulation Boiling Water Reactors, Part II: Parametric Study of Coupled Neutronic/Thermo-hydraulic Stability, *Nucl. Technol.*, 121, 52 (1998).

[A29] March-Leuba, J., D.G. Cacuci and R.B. Perez, "Nonlinear Dynamics and Stability of Boiling Water Reactors, Part I: Qualitative Analysis", *Nucl. Sci. Eng*., 93, 111-123 (1986).

[A30] March-Leuba, J., D.G. Cacuci and R.B. Perez, "Nonlinear Dynamics and Stability of Boiling Water Reactors, Part II: Quantitative Analysis", *Nucl. Sci. Eng*., 93, 124-136 (1986).

[A31] Muñoz-Cobo, J.L. and G. Verdú, "Application of Hopf Bifurcation Theory and Variational Methods to the Study of Limit Cycles in Boiling Water Reactors", *Ann. Nucl. Energy*, 18, No. 5, 269 (1991).

[A32] Van Bragt, D.D.B., Rizwan-uddin and T.H.J.J. van der Hagen, **"**Nonlinear Analysis of a Natural Circulation Boiling Water Reactor", *Nucl. Sci. Eng.*, 131, 23-44 (1999).

[A33] Van Bragt, D.D.B., Rizwan-uddin and T.H.J.J. van der Hagen, **"**Effect of Void Distribution Parameter and Axial Power Profile on BWR Bifurcation Characteristics", *Nucl. Sci. Eng.*, 134, 227-235 (2000).

[A34] Pollmann, E., J. Schulze and D. Kreuter, "Stability Measurements in the German Nuclear Power Plant Wuergassen During Cycle 14", *Nucl. Technol.*, 108, 350 (1994).

[A35] van der Hagen, T.H.J.J., D.D.B. Van Bragt, F.J. Van Der Kaa, D. Killian, W.H.M. Nissen, A.J.C. Stekelenburg and J.A.A. Wouters, "Exploring the Dodeward Type-I and Type-II Stability; From Start-up to Shutdown, from Stable to Unstable", *Ann. Nucl. Energy*, 24, 8, 659 (1997).

[A36] Karve, A.A., Rizwan-uddin and J.J. Dorning, "On Spatial Approximations for Liquid Enthalpy and Two-phase Quality During Density-wave Oscillations", *Trans. Am. Nucl. Soc*., 71, 533-535 (1994).

[A37] Hale, J.K. and H. Kocak, *Dynamics and Bifurcations*, Springer-Verlag, New York (1991).

[A38] Hassard, B.D., N.D. Kazarinoff and Y.H. Wan, *Theory and Applications of Hopf Bifurcation*, Cambridge University Press, New York (1981).

[A39] Guckenheimer, J. and P. Holmes, *Nonlinear Oscillations, Dynamical Systems and Bifurcations of Vector Fields*, Springer-Verlag (1983).

[A40] Wiggins, S., *Introduction to Applied Nonlinear Dynamical Systems and Chaos*, Springer-Verlag (1990).

[A41] Nayfeh, A.H. and B. Balachandran, *Applied Nonlinear Dynamics: Analytical, Computational, and Experimental Methods*, John Wiley (1995).

[A42] Clausse, A. and R.T. Lahey, "The Analysis of Periodic and Strange Attractors During Density-wave Oscillations in Boiling Flows", *Chaos, Solitons and Fractals*, 1, 2, 167-178 (1991).

[A43] Takenaka, N., R.T. Lahey and M.Z. Podowski, "The Analysis of Chaotic Density-wave Oscillations", *Trans. Am. Nucl. Soc*., 63, 197-198 (1991).

[A44] Achard, J-L., D.A. Drew and R. Lahey, "The Analysis of Nonlinear Density-wave Oscillations in Boiling Channels", *J. Fluid Mech*., 155, 213-232 (1985).

[A45] Rizwan-uddin and J.J. Dorning, "Some Nonlinear Dynamics of a Heated Channel", *Nucl. Eng. Des*., 93, 1-14 (1986). See also Rizwan-uddin and J.J. Dorning, "Nonlinear Stability Analysis of Density-wave Oscillations in Nonuniformly Heated Channels", *Trans. Am. Nucl. Soc*., 54, p. 172 (1987).

[A46] Hassard, B.D., "Numerical Evaluation of Hopf Bifurcation Formulas", *Dynamics of Nonlinear Systems*, Chapter 9, V. Hlavacek, ed., Gordon and Breach (1986).

[A47] Hennig, D., "A Study on Boiling Water Reactor Behavior", *Nuclear Tech.*, 126, 10-31 (1999).

[A48] Miro, R., D. Ginestar, D. Hennig and G. Verdu, "On the Regional Oscillation Phenomenon in BWRs", *Progress in Nuclear Energy*, 36, 2, 189-229 (2000).

[A49] Verdu, G., D. Ginestar, V. Vidal and R. Miro, "Modal Decomposition Method for BWR Stability Analysis", *J. Nucl. Sci. and Tech*., 35, 8, 538-546 (1998)

[A50] Dokhane, A., D. Hennig, Rizwan-uddin, R. Chawla, "A Parametric Study of Heated Channels with Two-phase Flow Using Bifurcation Analysis", *Trans. Amer. Nucl. Soc*., 86 (2002).

[A51] Quan Zhou and Rizwan-uddin, "Bifurcation Analysis of Nuclear-coupled Thermal-hydraulics of BWRs Using BIFDD", *Trans. Amer. Nucl. Soc*., 86 (2002).

[A52] Quan Zhou and Rizwan-uddin, "Impact of Modeling Assumptions on Stability and Bifurcation Analyses of BWRs", *Trans. Amer. Nucl. Soc*., 86 (2002).

[A53] Quan Zhou and Rizwan-uddin, **"**Bifurcation Analysis of Nuclear-coupled Dynamics of BWRs Using BIFDD", *Proc. Int. Conf on Nuclear Engineering (ICONE-10)*, Arlington, VA, 14-18 April 2002.

[A54] Dokhane, A., D. Hennig, R. Chawla and Rizwan-uddin, "Stability and Bifurcation Analyses of Two-phase Flow Using a Drift Flux Model and Bifurcation Code BIFDD", *Proc. Int. Conf. on Nuclear Engineering (ICONE-10)*, Arlington, VA, 14-18 April 2002.

[A55] Quan Zhou and Rizwan-uddin, "Bifurcation Analysis of Nuclear-coupled Dynamics of BWRs Using BIFDD", *Proc. Int. Conference on New Frontiers of Nuclear Technology Reactor Physics, Safety and High-performance Computing (PHYSOR-2002)*, Seoul, Korea, 7-10 October 2002.

[A56] Dokhane, A., D. Hennig, Rizwan-uddin and R. Chawla, "Bifurcation Analysis of Density-wave Oscillations Using a Drift Flux Model", *Proc. Int. Conference on New Frontiers of Nuclear Technology Reactor Physics, Safety and High-performance Computing (PHYSOR-2002)*, Seoul, Korea, 7-10 October 2002.

[A57] Pereira, C., G. Verdu, J-L. Munoz-Cobo and R. Sanchis, "BWR Stability from Dynamic Reconstruction and Autoregressive Model Analysis: Application to Cofrentes Nuclear Power Plant", *Progress in Nuclear Energy*, 27, 1, 51-68 (1992).

[A58] Analytis, G.Th., D. Hennig and J.K-H. Karlsson, "The Physical Mechanism of Core-wide and Local Instabilities at the Forsmark-1 BWR", *Nuclear Engineering and Design*, 205, 91-105 (2001).

[A59] Gialdi, E., S. Grifoni, C. Parmeggiani and C. Tricoli, "Core Stability in Operating BWR: Operational Experience", *Progress in Nuclear Energy*, 15, 447-459 (1985).

[A60] Farawila, Y.M., D.W. Pruitt and P.E. Smith, "Analysis of Laguna Verde Instability Event", *Proc. of ANS National Heat Transfer Conf.*, HTC-Vol. 9, 198-202, ANS (1996).

[A61] Bergdahl, B.G., F. Reisch, R. Oguma, J. Lorenzen and F. Akerhielm, "BWR Stability Investigation at Forsmark 1", *Ann. Nucl. Energy*, 16, 10, 509-520 (1989).

[A62] Araya, F., K. Yoshida, M. Hirano and Y. Yabushita, "Analysis of a Neutron Flux Oscillation Event at LaSalle-2", *Nucl. Tech*., 93, 82-91 (1991).

[A63] D'Auria, F., *State-of-the-art Report on Boiling Water Reactor Stability*, OECD/NEA (1996).

[A64] March-Leuba, J. and J.M. Rey, "Thermo-hydraulic/Neutronic Instabilities in Boiling Water Reactors: A Review of the State of the Art", *Nuclear Engineering and Design*, 145, 97-111 (1993).

[A65] March-Leuba, J., D.G. Cacuci and R.B. Pérez, "Nonlinear Dynamics and Stability of Boiling Water Reactors, Part 1: Qualitative Analysis", *Nucl. Sci. Eng*., 93, 111-123 (1986).

[A66] March-Leuba, J. and E.D. Blakeman, "A Mechanism for Out-of-phase Power Instabilities in Boiling Water Reactors", *Nucl. Sci. Eng*., 107, 173-179 (1991).

[A67] Takeuchi, Y., Y. Takigawa, and H. Uematsu, "A Study on Boiling Water Reactor Regional Stability from the Viewpoint of Higher Harmonics", *Nuclear Technology*, 106, 300-314 (1994).

[A68] Muñoz-Cobo, J.L., R.B. Pérez, D. Ginestar, A. Escrivá, and G. Verdú, "Nonlinear Analysis of Out of Phase Oscillations in Boiling Water Reactors", *Ann. Nucl. Energy*, 23, 16, 1301-1335 (1996).

[A69] Turso, J.A., J. March-Leuba and R.M. Edwards, "A Modal-based Reduced-order Model of BWR Out-of-phase Instabilities", *Ann. Nucl. Energy*, 24, 12, 921-934 (1997).

[A70] Karve, A.A., Rizwan-uddin and J.J. Dorning, "Out-of-phase Oscillations at BWRs", *Proc. Joint Int. Conference on Mathematical Methods and Supercomputing for Nuclear Applications*, Saratoga Springs, NY, 1633-1647 (1997).

[A71] Hennig, D., "A Study of Boiling Water Reactor Stability Behaviour", *Nuclear Technology*, 125, pp. 10-31 (1999).

[A72] Stacey Jr., W.M., *Space-time Nuclear Reactor Kinetics*, Academic Press, New York (1969).

[A73] Henry, A.F., "The Application of the Inhour Modes to the Description of on Nonseparable Reactor Transients", *Nucl. Sci. Eng*., 20, 338-351 (1964).

[A74] Miró, R., D. Ginestar, D. Hennig and G. Verdú, "On the Regional Oscillation Phenomenon in BWRs", *Progress in Nuclear Energy*, 36, 2, 189-229 (2000).

[A75] Miró, R., D. Ginestar, G. Verdú and D. Hennig, "A Nodal Modal Method for the Neutron Diffusion Equation. Application to BWR Instabilities Analysis", *Ann. of Nucl. Energy*, 29, 10, 1171-1194 (2002).

[A76] Ginestar, D., R. Miró, G. Verdú and D. Hennig, "A Transient Modal Analysis of a BWR Instability Event", *Journal of Nuclear Science and Technology*, 39, 5, 554-563 (2002).

[A77] Wulff, W., H.S. Cheng, D.J. Diamond and M. Khatib-Rhabar, *A Description and Assessment of RAMONA-3B Mod.0 Cycle 4: A Computer Code with Three-dimensional Neutron Kinetic for BWR System Transients*, NUREG/CR-3664, BNL-NUREG-51746 (1984). See also *RAMONA-3, User's Manual*, Scandpower.

[A78] Hennig, D., *Stability Analysis KKL (Part 2)*, PSI Technical Report, TM-41-98-39 (1998) (in German).

[A79] Blomstrand, J., *The KKL Core Stability Test, Conducted in September 1990*, ABB-Report, BR91-245 (1992).

[A80] Wiktor, C.G., *KKL Cycle 7 Stability Test – Core Simulation Input Data*, KKL Report BET/97/111 (1997).

[A81] Ikeda, H. and A. Hotta, "Development of a Time-domain 3-D Core Analysis Code and its Application to Space-dependent BWR Stability Analysis", *Proc. Joint International Conference on Mathematical Methods and Supercomputing for Nuclear Applications* (Vol. 2, 1624), Saratoga Springs, NY, 5-9 October 1997.

[A82] Verdú, G., D. Ginestar, V. Vidal and J.L. Muñoz-Cobo, "3-D Lambda-modes of the Neutron Diffusion Equation", *Ann. Nucl. Energy*, 21, 405-421 (1994).

[A83] Lefvert, T., *Ringhals 1 Stability Benchmark*, NEA/NSC/DOC(96)22 (1996).

Annex I, Part I

OUTLINE OF THE DATABASE OF RESULTS FOR COUPLED 3-D NEUTRON KINETICS/THERMAL-HYDRAULICS CALCULATIONS

A. Bousbia Salah[1], F. D'Auria[1], G. Galassi[1], W. Giannotti[1], K. Ivanov[2], A. Lo Nigro[1], F. Maggini[1,3], R. Mirò[3], C. Parisi[1,2], A. Spadoni[1,4], J. Vedovi[1,2], S. Kliem[5], A. Cuadra[6]
[1]UPISA, [2]PSU, [3]UVA, [4]TAMU, [5]FRZ, [6]ASCO & University of Barcelona

Introductory remarks

The aim of the current annex is to provide an overview of the database performed for typical NPPs using coupled 3-D neutron kinetics/thermal-hydraulic calculations. The adopted format describing each calculation, including figures and tables, is as follows:

1. NPP type and simulated transient. This section includes a short description and two tables:
   - Main boundary and initial conditions (initial core power, core inlet flow rate and temperature, SG pressure, etc.).
   - Imposed sequence of main events (break occurrence or initial failure, actual scram signal, isolation of MSIV or of FW line, MCP trip, etc.).
2. Resulting sequence of main events and description of the transient scenario. This section includes one table and "main parameters" figures:
   - The table reports the list of resulting events (*e.g.* time and value of peak power and FWHM, time of scram, end of the calculation, etc.).
   - The figures typically show total core power, reactivity, pressure and fuel temperatures.
3. Significant results. The main results and findings from the analysis are summarised in a few statements.

Calculation results and related notes are added in relation to the energy released to the fuel during the most relevant among the considered transients.

Table I-1. Overview of performed analyses: Considered transients are those identified in Sections 1.2 to 1.4 of WP2

ID	Transient type	Reactor type – analyses ID and status		
		PWR case identity	BWR case identity	VVER case identity
I	MSLB	Case 1-PWR: TMI [X] Case 2-PWR: ASCO [X]	–	Case 1-VVER:VVER-1000 [X] Case 2-VVER: VVER-440 [X]
II	LOFW-ATWS	Case 3-PWR: TMI [X]	–	Case 3-VVER: VVER-1000 [X] Case 4-VVER: VVER-440 *
III	CR ejection	Case 4-PWR: TMI [X]	Case 3-BWR: PB2 [X] Case 4-BWR: PB2 CR bank ejection [X]	Case 5a-VVER: VVER-1000 [X] Case 5b-VVER: VVER-1000 CR bank ejection [X] Case 6-VVER: VVER-440 *
IV	LBLOCA-DBA	Case 5-PWR: TMI [X]	Case 9-BWR: PB2 [Y]	Case 7-VVER: VVER-1000 [Y] Case 8-VVER: VVER-440 *
V	Incorrect insertion of an inactive loop	Case 6-PWR: TMI [X]	–	Case 9-VVER: VVER-1000 [Y] Case 10-VVER: VVER-440 *
VI	MSLB-ATWS	Case 7-PWR: TMI [X]	–	Case 11-VVER: VVER-1000 [X] Case 12 -VVER: VVER-440 *
VII	SBLOCA-ATWS	Case 8-PWR: TMI [X]	–	Case 13-VVER: VVER-1000 SBLOCA [X] Case 14-VVER: VVER-440 *
VIII	Turbine trip	–	Case 1-BWR: PB2 [X]	–
IX	Turbine trip-ATWS	–	Case 2-BWR: PB2 [X]	–
X	FW temperature increase	–	Case 5-BWR: PB2 [X]	–
XI	MCP flow rate increase	–	Case 6-BWR: PB2 [X]	–
XII	MCP flow rate increase-ATWS	–	Case 7-BWR: PB2 [X]	–
XIII	BWR stability	–	Case 8-BWR: PB2 [X]	–
IVX	BWR stability-ATWS	–	Case 9-BWR: PB2 *	–

[X] Analysis performed and documented.
[Y] Analysis performed and not documented.
– Analysis not applicable or not considered.
* Analysis not performed.

I.1 PWR NPPs

The reference NPPs are the TMI-1 (B&W), equipped with two OTSG and ASCO unit 2 (W).

PWR Table 1. Cases analysed

Case ID	Transient	Event	Code used	Scram/ ATWS
PWR-1	MSLB (TMI-1)	Double-ended guillotine break of one SL	RELAP-3D	Scram
PWR-2	MSLB (ASCO)	Double-ended guillotine break of one SL	RELAP5/PARCS	Scram
PWR-3	LOFW (TMI-1)	Trip of the feed water pumps	RELAP-3D	ATWS
PWR-4	CR-EXP (TMI-1)	Completely inserted control ejection	RELAP-3D	Scram
PWR-5	LBLOCA-DBA (TMI-1)	Double-ended guillotine break of HL	RELAP5/PARCS	Scram
PWR-6	LOOP-BW (TMI-1)	De-borated water injection in one loop	RELAP-3D	Scram
PWR-7	MSLB (TMI-1)	Double-ended guillotine break of one SL	RELAP-3D RELAP5/PARCS	ATWS
PWR-8	SBLOCA (TMI-1)	Break in the cold leg of 2% of flow area	RELAP-3D	ATWS

I.1.1 TMI-1 – MSLB

The main operating conditions of TMI-1 are summarised in Table I.1.1 below.

Table I.1.1. Relevant initial conditions for nominal operation of the TMI-1 plant

Quantity	Units	Design value	Code value
Core power	MWt	2 772	2 772
CL temperature & subcooling	K/K	563.76 (51.30)	565.9 (49.16)
HL temperature & subcooling	K/K	591.43 (23.63)	593.8 (21.26)
Lower plenum pressure	MPa	15.36	15.26
Outlet plenum pressure	MPa	15.17	15.13
RCS pressure	MPa	14.96	14.96
Total RCS flow rate	kg/s	17 602.2	17 482
Core flow rate	kg/s	16 052.4	15 951
Feed water flow per OTSG	kg/s	761.59	761.7
OTSG outlet pressure	MPa	6.41	6.44

The transient is modelled using RELAP5-3D©/NESTLE. In order to emphasise the severity of the accidental scenario the "modified" cross-section, generated for a hypothetical return to power scenario, has been adopted. On the other hand the trip of the main coolant pumps has been disabled, and any boron effect has been taken into account. The mechanical failure of the feed water regulating valve in broken SG in an open position is assumed.

Due to the asymmetric cooling of the core an appropriate nodalisation involving 3-D neutronics coupled with a thermal-hydraulic multi-channel core model is deemed suitable to represent the behaviour of the spatial core power release and the time evolution of the parameters relevant for the neutronic feedback. The entire plant has been modelled with a detailed nodalisation; thermal-hydraulically the vessel has been modelled with 18 parallel channels, four DC pipes and four LP regions. From the neutron kinetics point of view, the core is modelled with 26 axial slabs, a radial lattice of 17 × 17 and a set of 438 cross-section compositions.

Case 1 – PWR: Table 1. Imposed sequence of main events

Event description	Time(s)
Breaks open	0.0
Reactor trip	6.9
MCP trip	Not occurring
Turbine valve closure (start-end)	7.9-11.9
High pressure injection start	46.4
Transient end	100.0

The MSLB is supposed to originate through the double-ended guillotine break of one SL. The fast depressurisation of one SG causes the primary water cooling, as soon as a plug of cold water reaches the core inlet, a positive insertion of reactivity due to the moderator neutronic feedback produces core power release. The initial power excursion is terminated by scram at about 10 s after accident initiation. However following scram (see also hypothesis below), due to one stuck withdrawn CR in a critical position of the core, return to power occurs at about 60 s. This is not a re-criticality accident and is phenomenologically controlled by delayed neutron groups.

The second power peak damps down without any active system intervention when a number of generated neutrons physically decays to zero. In the DC and LP regions a partial mixing between "cold" water coming from the loop affected by the broken SG and the "hot" water of the intact loop takes place. A non-uniform distribution of moderator temperature in the core section enhances localised positive insertion of reactivity showing that the side of the core connected with the broken loop is characterised by lower moderator temperatures and higher relative power peak.

In the following figures the main parameters governing the transient have been plotted: power, liquid and steam temperature in LP and UP, SG mass inventory, mass flow rate at the break, primary and secondary pressure, 3-D view of moderator temperature and relative power at second power peak instant in the core.

Case 1 – PWR – Figures

Figure 1. Core power

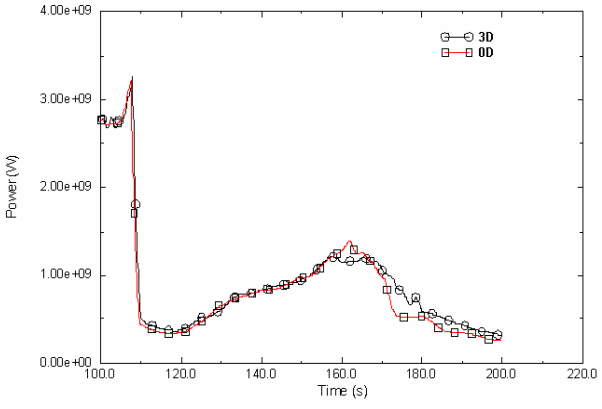

Figure 2. Mass inventory

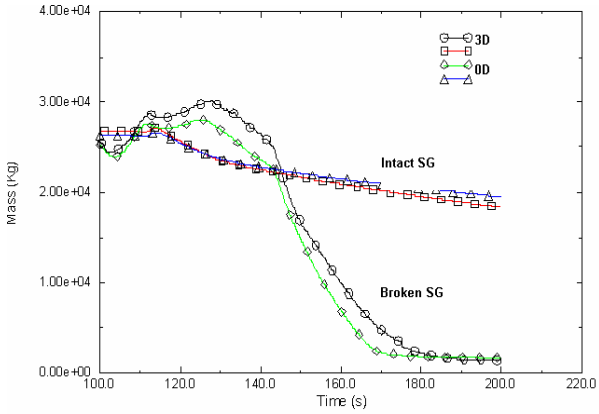

Figure 3. Liquid and steam temperatures in LP and UP

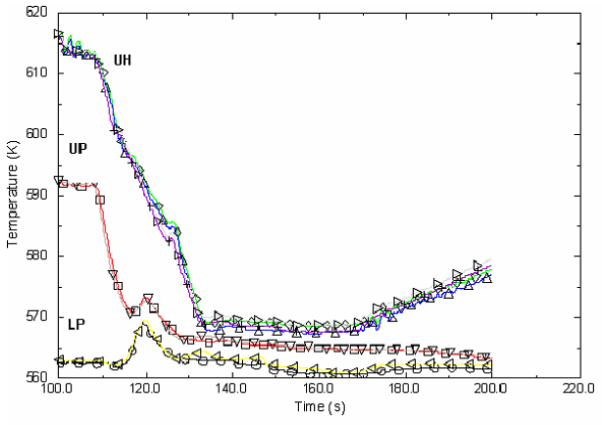

Figure 4. Mass flow rate at break

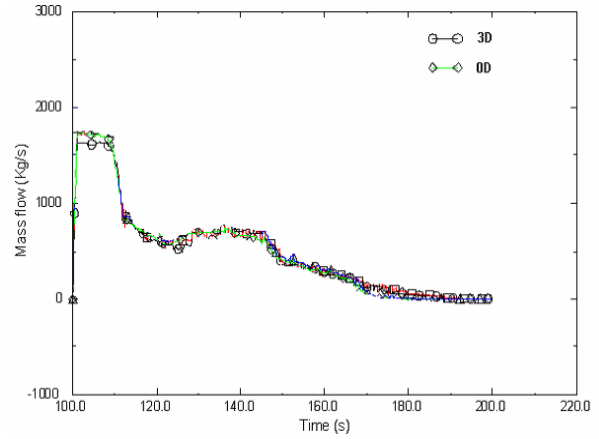

Figure 5. Primary pressure in PRZ, UP and core

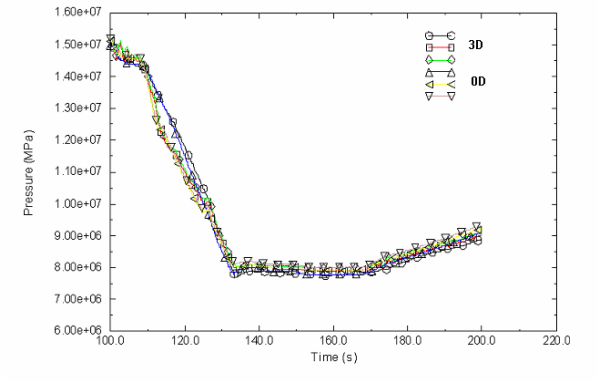

Figure 6. Secondary pressure in SG1 and SG2

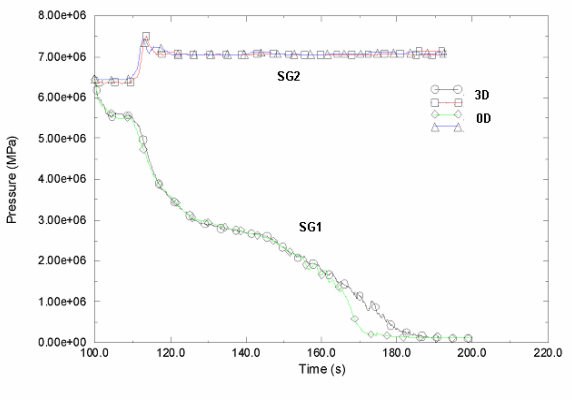

Figure 7. Moderator temperature at second power peak

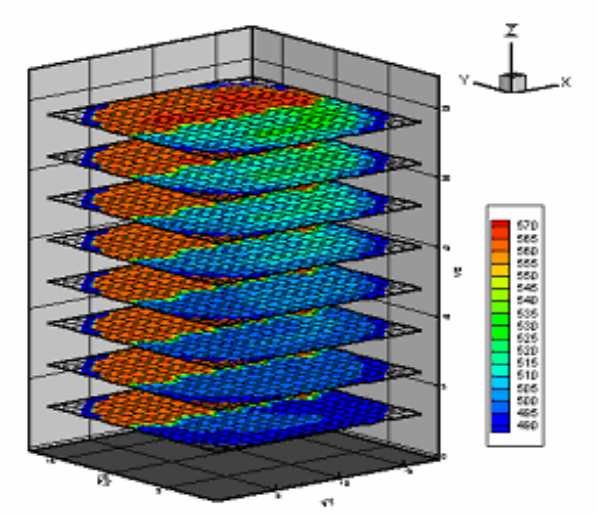

Figure 8. TMI-MSLB – Relative power distribution at second power peak

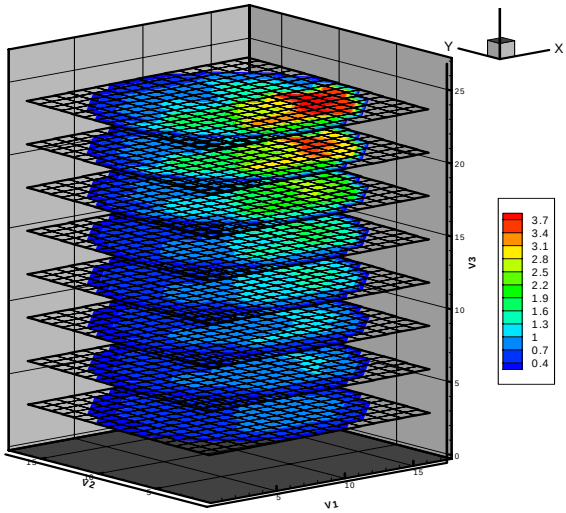

I.1.2 ASCO – MSLB

The ASCO NPP has been in operation since 1983. The analyses were performed using the thermal-hydraulic system code RELAP5 in which a three-dimensional vessel is modelled. The core is divided into 21 heated channels subdivided into 24 axial nodes. On the other hand, the neutronic model considers 27 types of fuel elements, also subdivided into 24 axial meshes.

The transient is modelled using RELAP5/PARCS. The main results of the considered transient are shown in Figure 1 for the 3-D peak power and Figure 2 for the reactivity evolution. The calculations showed no return to power.

Case 2 – PWR: Table 1. Imposed sequence of main events

Event description	Time(s)
Breaks open	0.0
Transient end	100.0

Case 2 – PWR – Figures

Figure 1. Power distribution during the peak

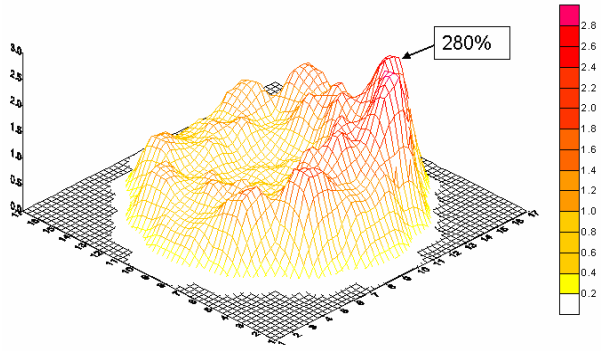

Figure 2. Total reactivity evolution during the transient

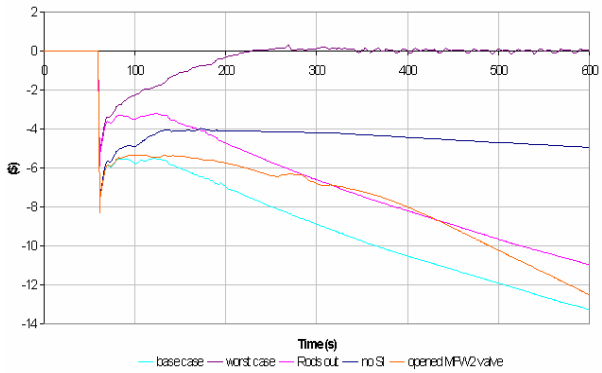

I.1.3 TMI-1 – LOFW-ATWS

The accidental scenario envisaged is supposed to originate though the trip of both the FW pumps and the failure of the CR insertion mechanism. The capability of the SG to remove the power produced in the core is limited by the loss of FW pumps. The following increase of the moderator temperature at the core inlet introduces negative reactivity due to the neutronic moderator temperature feedback. The power in the core decreases at about 20 s after the accident, and the primary pressure reaches the PORV opening limits. The surface temperature of the hottest rod in the core, however, is kept below 335°C. Even if a release of primary inventory through the PORV occurs and the CR insertion is blocked the reactor tends to gradually switch off.

The nodalisation adopted for the analysis is directly derived from the MSLB analysis case, though few modifications have been introduced. The thermal-hydraulic model of the core is constituted by 19 parallel channels; the central core assembly has been represented with a channel and active heat structure. The neutronic nodalisation of the core is the same 3-D mesh adopted for the previous MSLB case (17 × 17 × 26 with 438 compositions). The coupling schema between thermal-hydraulic and neutronic nodalisation takes into account the introduction of the central core assembly element.

In the following figures the main parameters governing the transient have been plotted: core power, liquid temperature in HL and CL, primary and secondary pressure, fuel temperature, pressuriser level, PORV mass flow rate and core inlet mass flow rate.

Case 3 – PWR: Table 1. Imposed sequence of main events

Event description	Time(s)
Trip of both the FW pumps	0.0
Reactor trip	Not occurring
MCP trip	Not occurring
Transient end	100.0

Case 3 – PWR – Figures

Figure 1. LOFW-ATWS – core power

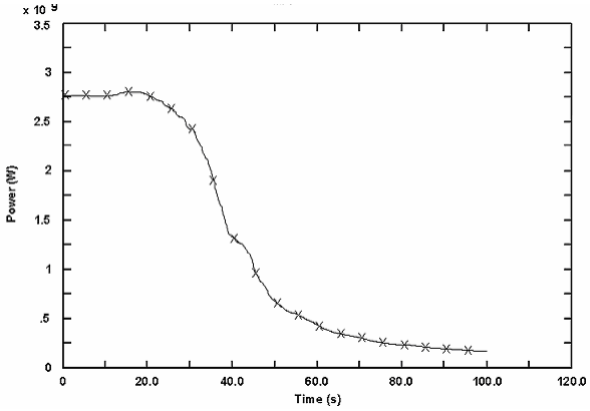

Figure 2. LOFW-ATWS – liquid temperature in HLs and CLs

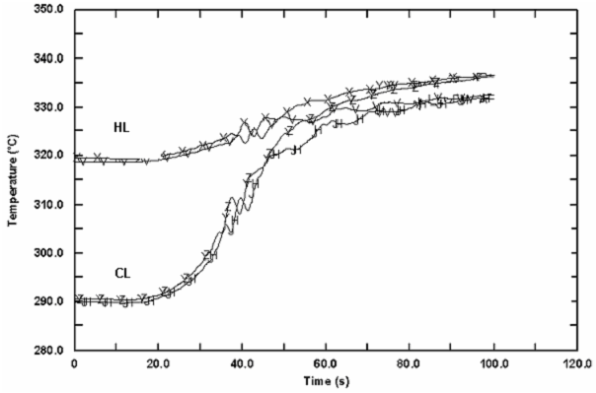

Figure 3. LOFW-ATWS – primary pressure

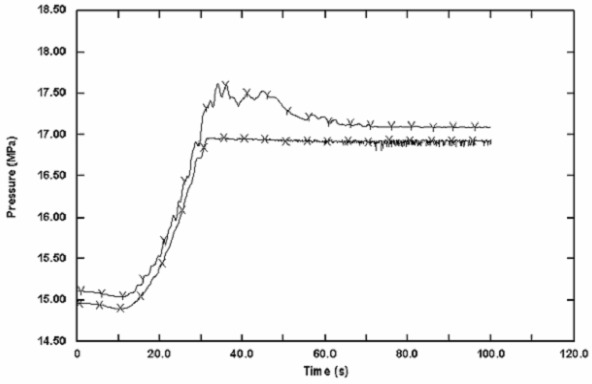

Figure 4. LOFW-ATWS – secondary pressure

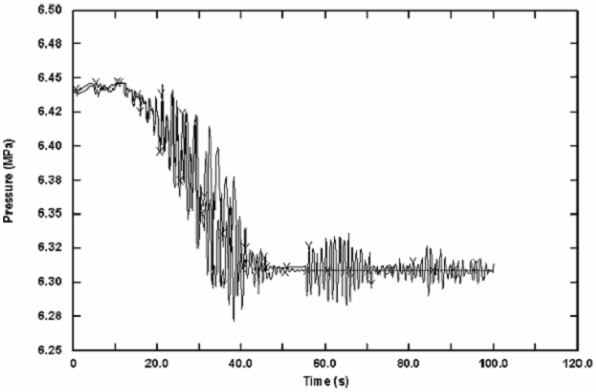

Figure 5. LOFW-ATWS – core clad temperature at different axial positions

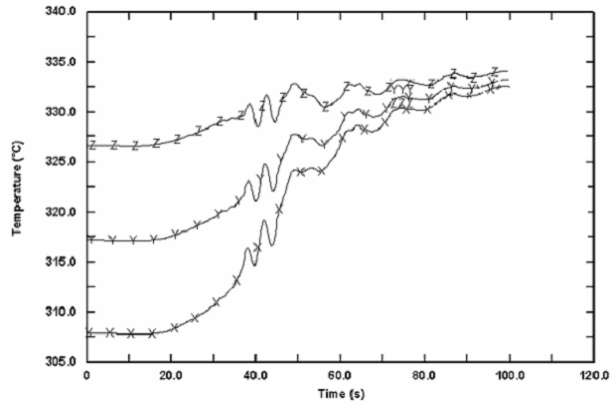

Figure 6. LOFW-ATWS – pressuriser level

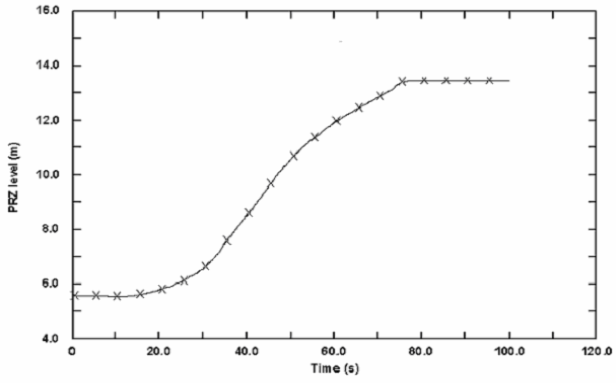

Figure 7. LOFW-ATWS – PORV mass flow rate

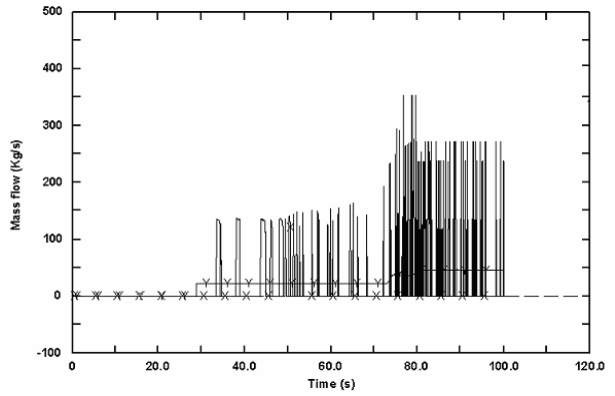

Figure 8. LOFW-ATWS – core inlet mass flow rate

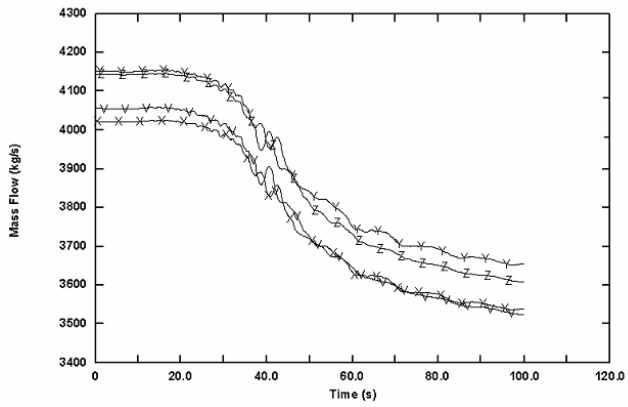

I.1.4 TMI-1 – CR-EXP

The accidental scenario envisaged is supposed to originate by sudden ejection of one CR. The reactor is at the EOC and most of the CR are practically all out; the expulsed CR is located in the central region of the core and has been withdrawn from 90 to 100% of its path. The ejection of the CR has local effects, but it influences the total reactor power. A power peak is caused in the first instants of the transient and without any action the reactor tends to find a new stationary condition. Locally the temperature of the channel where the CR moves rises, as does the fuel temperature in the upper part. However, the liquid temperature in the loop and core inlet have small variations less than 1°C and the pressuriser level decreases a few centimetres.

The analysis has been carried out into two steps. In the first step, the steady-state condition has been obtained using the steady-state option of the RELAP5-3D and in the second step the re-start calculation with the transient option enabled has been run. The 3-D neutronic/thermal-hydraulic coupling was enabled during both steps. The nodalisation adopted for the analysis is directly derived from the LOFW analysis case. The thermal-hydraulic model of the core is constituted by 19 parallel channels; the central core assembly has been represented with a channel and active heat structure. The neutronic

nodalisation of the core is the same 3-D mesh adopted for the previous MSLB case (17 × 17 × 26 with 438 compositions). The coupling schema between thermal-hydraulic and neutronic nodalisation takes into account the introduction of the central core assembly element.

In the following figures the main parameters governing the transient have been plotted: the core power, clad temperature pressure evolution in the pressuriser, UH, SG1 and SG2, fuel temperature at different elevations, pressuriser level, coolant mass flow rate in HL and CL, and finally the core inlet temperature evolution.

Case 4 – PWR: Table 1. Imposed sequence of main events

Event description	Time(s)
CR ejection form 90% to 100%	0.0-0.1
Transient end	100.0

Case 4 – PWR – Figures

Figure 1. Core power

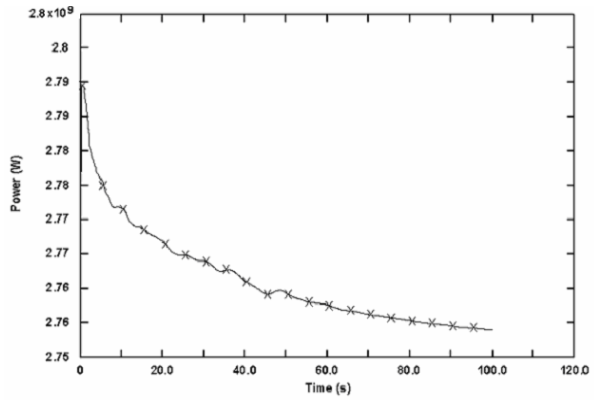

Figure 2. Three axial fuel surface temperatures in central heat structure

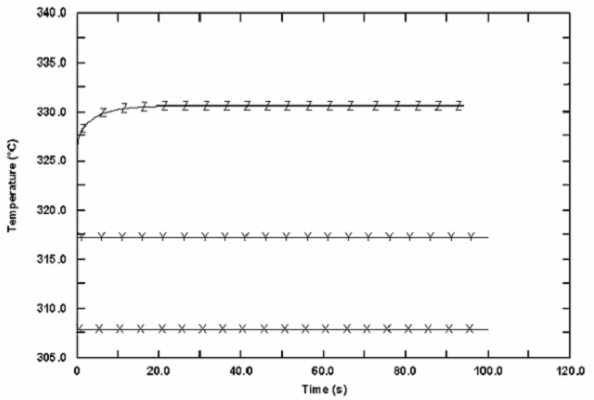

Figure 3. Pressure in pressuriser and UH

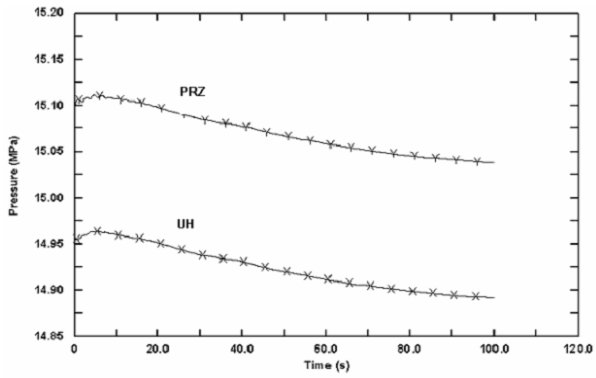

Figure 4. Pressure in SG1 and SG2

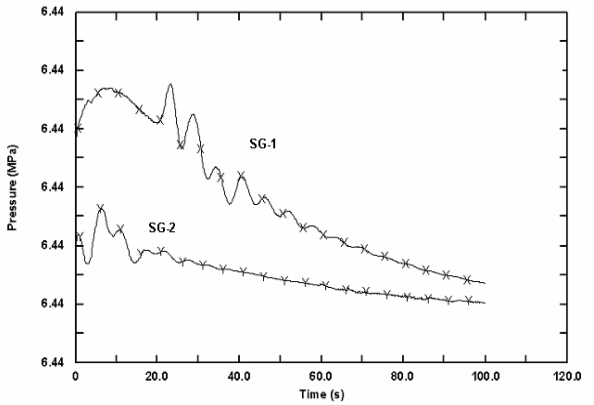

Figure 5. Fuel centreline temperature at three elevations

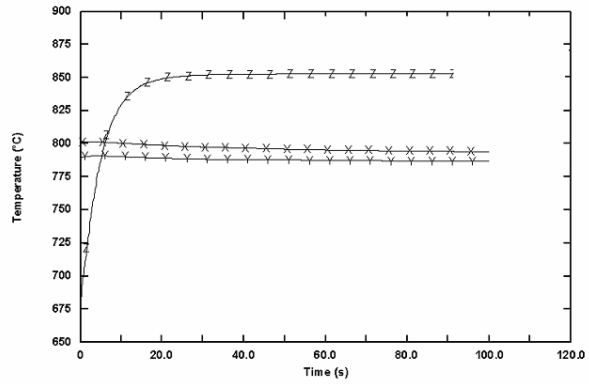

Figure 6. Pressuriser level

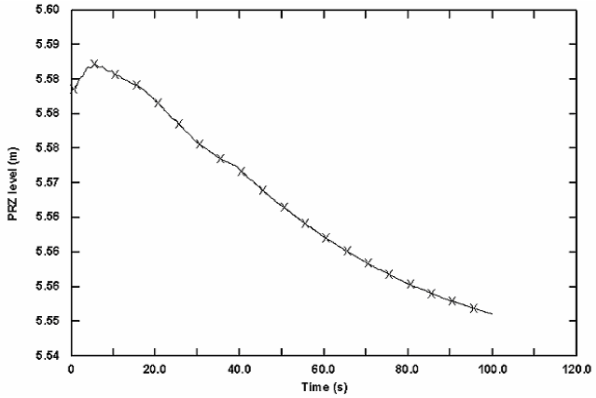

Figure 7. Mass flow in HLs and CLs

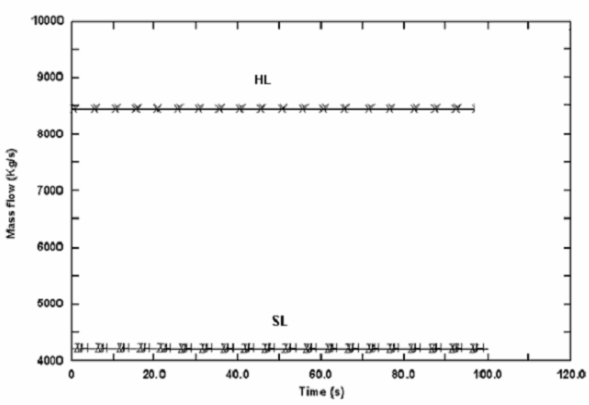

Figure 8. Moderator temperature at core inlet

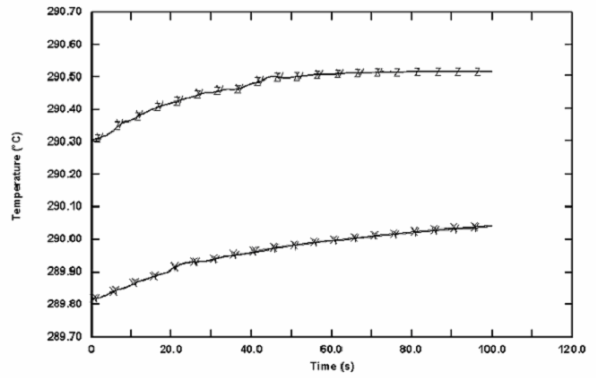

I.1.5 TMI-1 – LBLOCA-DBA – RELAP5/PARCS

A suitable qualified set of nuclear cross-sections for each individual fuel element, as well as corresponding values of relevant parameters (namely Doppler and moderator coefficients) for 0-D neutron kinetics were available in the case of the TMI-1. This suggested to adopt this database (*i.e.* thermal-hydraulic nodalisation and set of 3-D neutron kinetics cross-section) for performing comparative calculations between results from the RELAP5 stand-alone code and results from the coupled RELAP5-PARCS code. The same thermal-hydraulic nodalisation was adopted in the two cases and a one-by-one fuel element nodalisation was adopted as input for the 3-D neutron kinetics, including 24 axial subdivisions (this ends up being about 24 × 200 ≈ 4 800 fuel nodes).

Case 5 – PWR: Table 2. Imposed sequence of main events

Event description	Time(s)
Breaks open	0.0
Transient end	25.0

Relevant results are given in Figures 1-4. The upper plenum pressure and the total reactor power are reported (Figures 1 and 2) to show that the thermal-hydraulic evolution of the transient is the same from the two calculations. Differences in the pressure curves (Figure 1) mostly originate from differences

in the total power trends (Figure 2). Differences in power trend curves can originate other than through the feedback coefficient, by the burn-up level and by the decay power production that is derived from different sources (no attempt was made to homogenise the related databases). The comparison between time trends in Figure 3 constitutes the main target of the investigation: it is shown that predicted blow-down PCT can be lower in the case of the coupled thermal-hydraulics/3-D neutron kinetics for an amount larger than 300 K. The variation of the axial profile for linear power during the transient can be seen from Figure 4 when a coupled thermal-hydraulics/3-D neutron kinetics calculation is performed. The same axial profile remains unchanged when 0-D neutron kinetics analysis is performed. This is one of the explanations for the lower PCT in the case of the coupled calculation. Definitely, blow-down PCT is about 300 K lower when 3-D neutron kinetics is considered instead of 0-D neutron kinetics. Re-flood PCT is also expected to be lower when 3-D neutron kinetics modelling is adopted, but its value is largely affected by the ECCS configuration and response time; it is thus difficult to generalise the result from a single calculation and its evaluation was excluded from the present investigation.

Case 5 – PWR – Figures

Figure 1. Upper plenum pressure

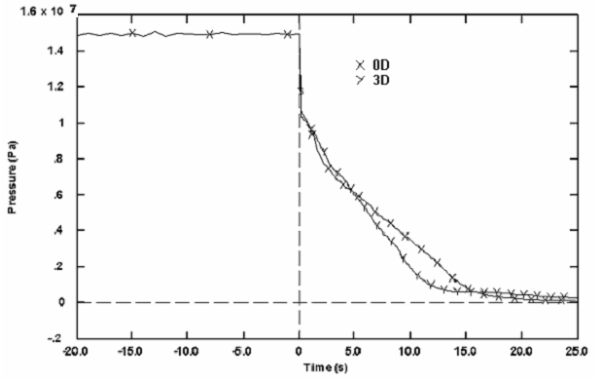

Figure 2. Total core power

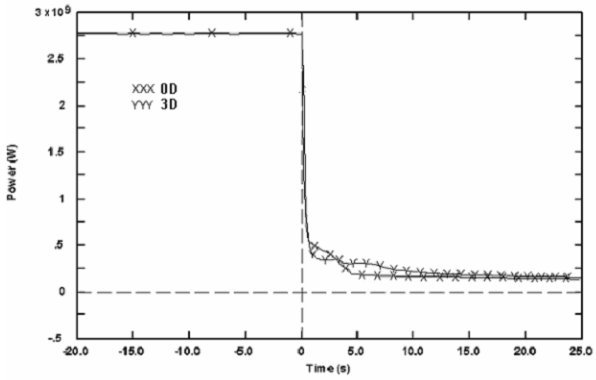

Figure 3. Rod surface temperature at the PCT location

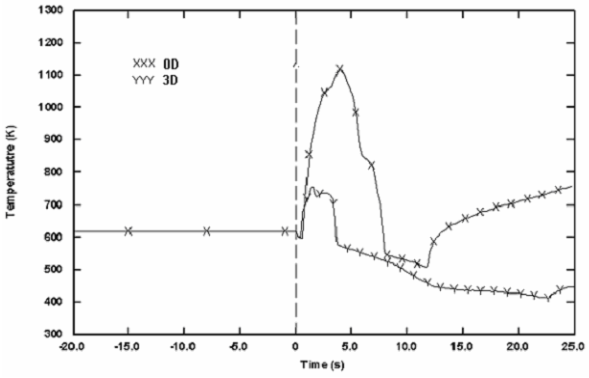

Figure 4. SS axial power distribution

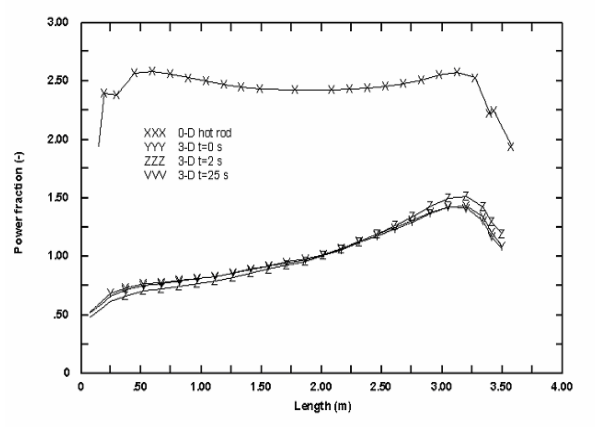

I.1.6 TMI-1 – LOOP-BW

The accidental scenario envisaged is supposed to originate through the inadvertent injection of de-borated water in one loop or the presence of a low boron concentration in the loop seal following a

SBLOCA. The plug of de-borated water moves into the core when natural circulation resumes in the loop. Depending on the boron concentration of the primary system at the moment of the accident stronger effects on power control are expected.

For this purpose two main cases have been considered. In the first case the reactor is supposed to be at EOC and the primary circuit is filled with a boron concentration of about 5 ppm; in the second case the boron concentration is supposed to be 950 ppm.

First case: 5 ppm – 800 kg/s

In the first case (5 ppm) a continuous injection of de-borated water is imposed in one loop. The scenario shows that the power increase due to the de-borated water moving into the core inlet reaches the value to start the scam. The trip of the MCP, the FW and the insertion of CR lead the reactor in safety conditions. The primary and secondary pressures remain constant after the first 20 seconds as do the pressuriser level and the loop temperatures. The boron concentration at core inlet decreases to 0 ppm in the four regions representing the LP.

The time trends of the primary pressure, secondary pressure, core power, pressuriser level and boron concentration at the core inlet have been plotted in the figures below.

Second case

In the second case a boron concentration of about 950 ppm has been supposed uniformly present in the primary inventory. Two sensitivity analyses have been envisaged. De-borated water has been continuously injected in one loop with two flow rates in order to determine in connection with the amount of “clean” water which are the effects.

The first sensitivity case is characterised by the injection of about 8 000 kg/s of de-borated water in one loop. In the second sensitivity case 800 kg/s of de-borated water are continuously injected.

- *950 ppm – 8 000 kg/s de-borated water*. In less than three seconds the heat structures of the core reaches the melting point. As soon as the de-borated water moves into the core inlet at about 2.5 s, in the half side of the core connected with the incriminated loop the power suddenly rises. The scram signal starts but the calculation stops due to high heat structure temperature. The plots of core power, fuel temperature and boron concentration at core inlet are represented hereafter.

- *950 ppm – 800 kg/s*. In this transient, the boron concentration at inlet core starts to decrease slowly; after five seconds the boron concentration in the core is such that an excursion in core power production occurs. The power peak leads to the scram signal. The pumps trip and the SGs are isolated. The insertion of negative reactivity due to the increasing moderator inlet core temperature together with the insertion of positive reactivity due to the boron dilution in the core contribute with the CR insertion to mitigate power production for 150 seconds. Then, when the boon concentration decreases below 700 ppm the power rises again, oscillating, and as consequence the primary and secondary pressures increase. Core power, boron concentration, core inlet temperature are represented in the figures below.

The nodalisation adopted for the analysis is directly derived from the LOFW analysis case. The thermal-hydraulic model of the core is constituted by 19 parallel channels, and the central core assembly has been represented with a channel and active heat structure. The neutronic nodalisation of the core is

the same 3-D mesh adopted for the previous MSLB case (17 × 17 × 26, 438 compositions). The coupling schema between thermal-hydraulic and neutronic nodalisation takes into account the introduction of the central core assembly element.

In the following figures the main parameters governing the transient have been plotted for both boron concentrations: power, boron concentration, primary and secondary pressure, and for only the 950 ppm case the rod surface temperatures, and temperature at core inlet.

Case 6 – PWR – Figures

Figure 1. 5 ppm core power

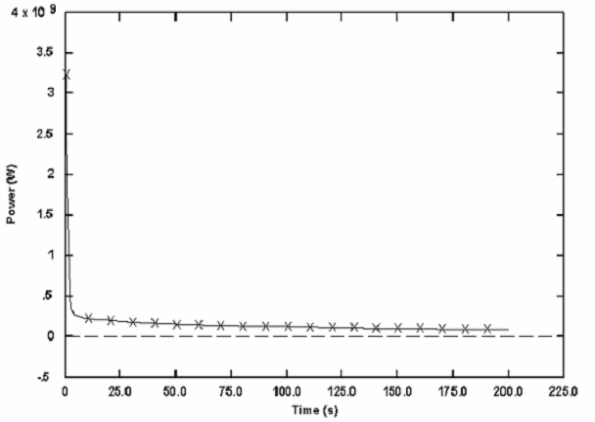

Figure 2. 5 ppm – boron concentration in core inlet

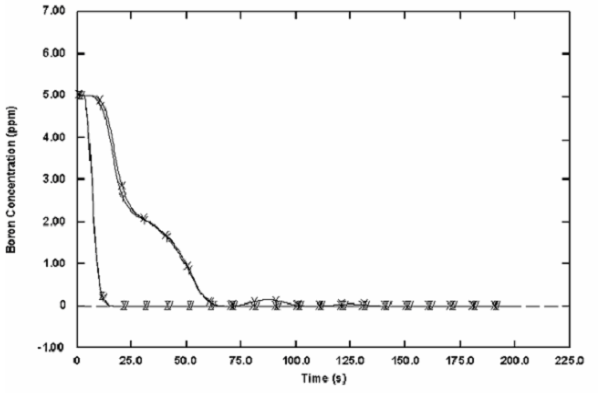

Figure 3. 5 ppm – primary pressure

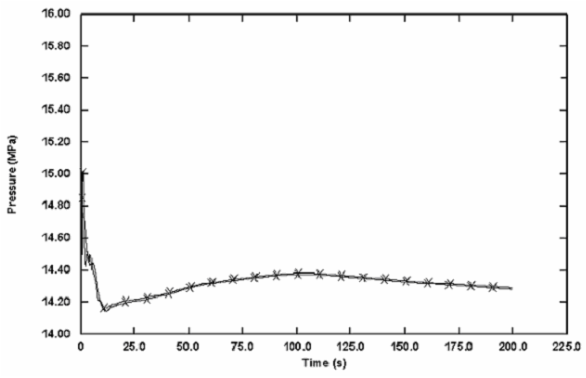

Figure 4. 5 ppm – secondary pressure

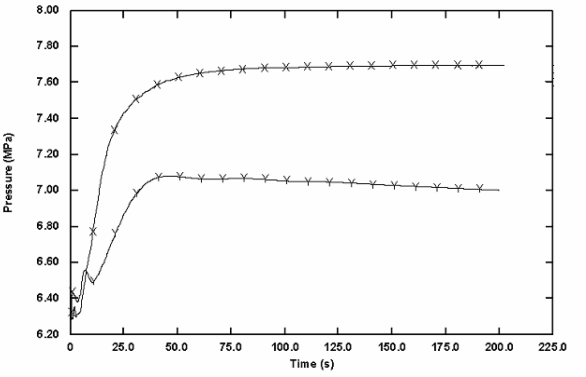

Figure 5. 950 ppm – 1 – core power

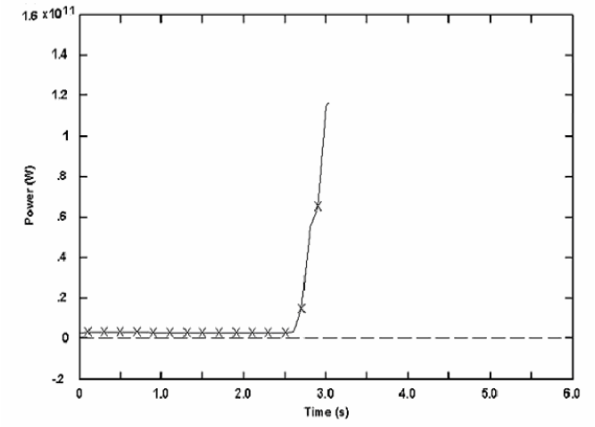

Figure 6. 950 ppm – 1 – boron concentration at core inlet

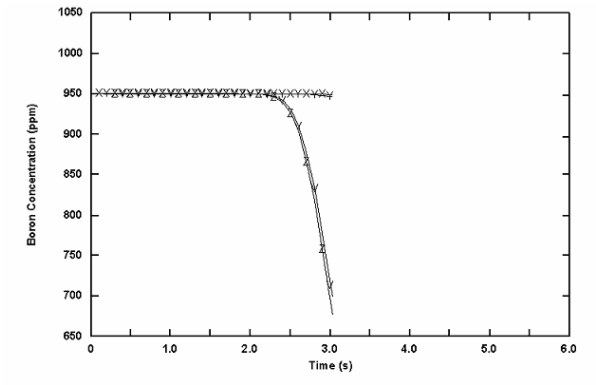

Figure 7. 950 ppm – 2 – primary pressure

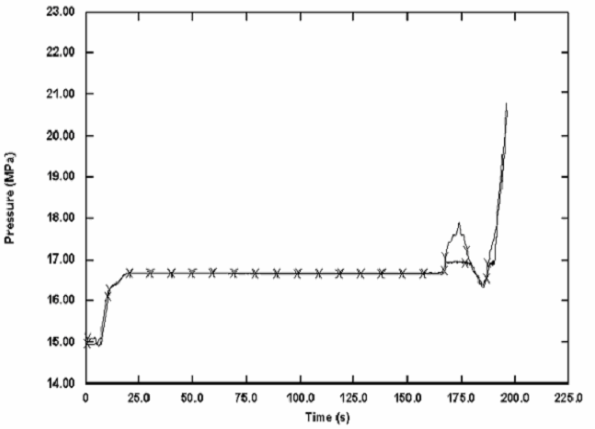

Figure 8. 950 ppm – 2 – secondary pressure

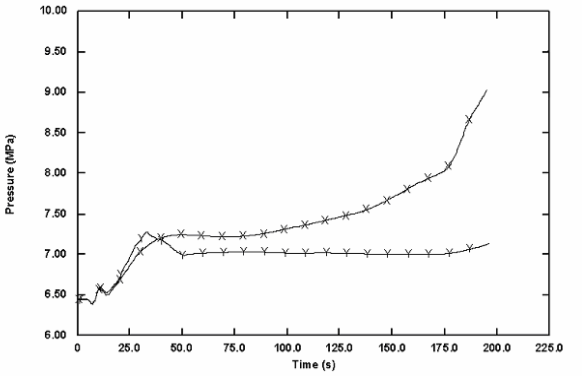

Figure 9. 950 ppm – 2 – core power

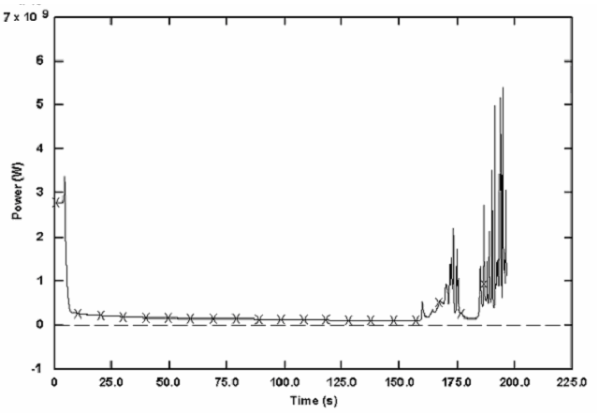

Figure 10. 950 ppm – 2 – boron concentration at core inlet

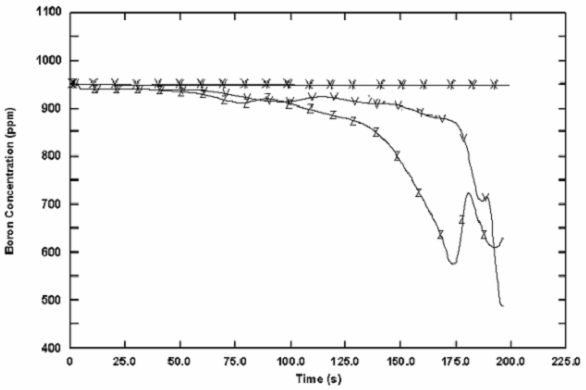

Figure 11. 950 ppm – 1 – three axial fuel temperatures

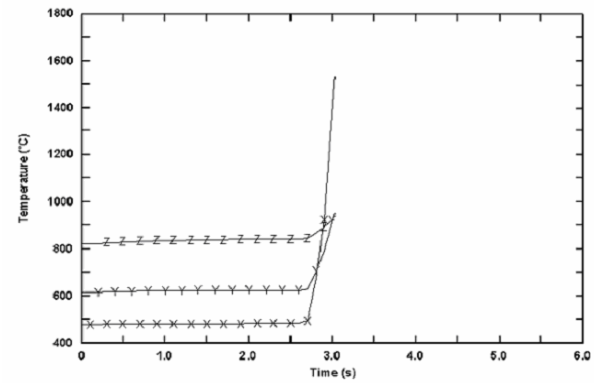

Figure 12. 950 ppm – 2 – core inlet temperature

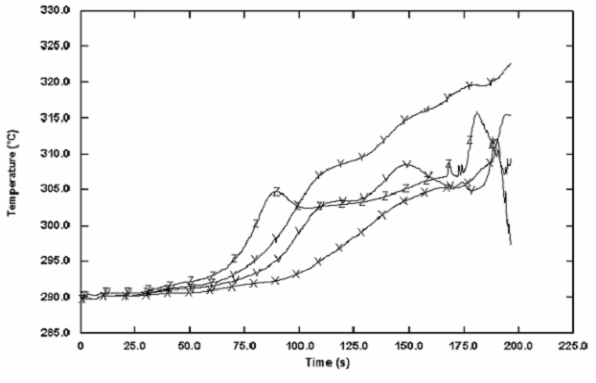

I.1.7 TMI-1 – MSLB-ATWS

The accident analysed is a main steam line break with ATWS (see MSLB case); it is supposed to originate through a double-ended guillotine break of one SL. The same boundary conditions adopted in the MSLB case have been applied and assumptions on operational characteristics of the pressuriser valves, of the valves installed on the steam lines and of the main coolant pumps have been taken.

The total power produced in the core never exceeds 140% of the nominal value. When the primary pressure reaches the set point of pressuriser the safety valve opens at about 60 s into the transient. At the same time the coolant temperature at the core inlet starts to increase, causing core power decrease. The asymmetric cooling of the core starts at about 15 s. In the region of the core affected by the broken loop, the moderator temperature decreases between 15-20 s and the neutronic feedback increases the power by the order of 140%, causing a second power peak. The amount of energy dissipated by the broken SG during the considered transient is larger then the energy dissipated by the intact steam generator. This is a consequence of the flow rate assumed for the feed water.

The main parameters governing the transient have been plotted in the following figures: core power, temperature at core inlet, primary and secondary pressure, liquid temperature in HL and CL, SG exchanged power, pressuriser level mass inventory, and FW imposed flow rate.

Case 7 – PWR: Table 1. Imposed sequence of main events

Event description	Time(s)
Breaks open	0.0
Reactor trip	Not occurring
MCP trip	Not occurring
Turbine valve closure (start-end)	7.9-11.9
High pressure injection start	46.4
Transient end	70.0

Case 7 – PWR – Figures

Figure 1. Core power

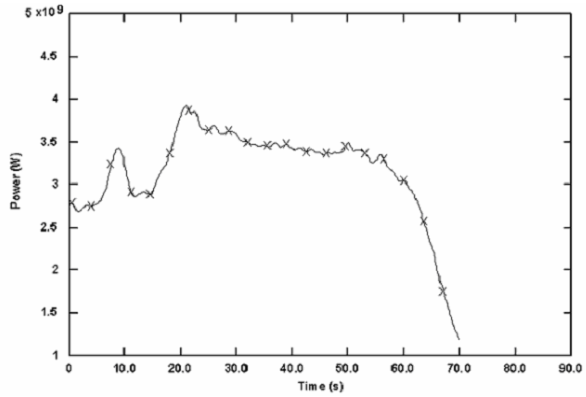

Figure 2. Moderator temperature at core inlet

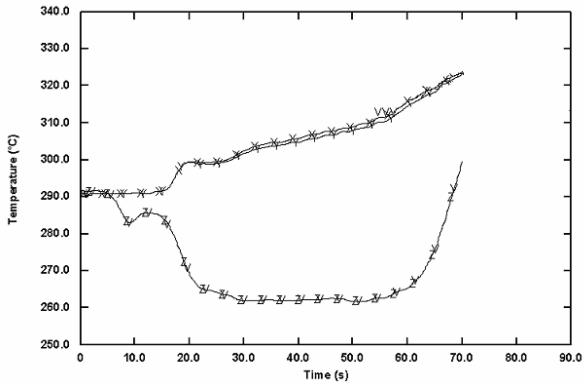

Figure 3. Pressure in pressuriser and UH

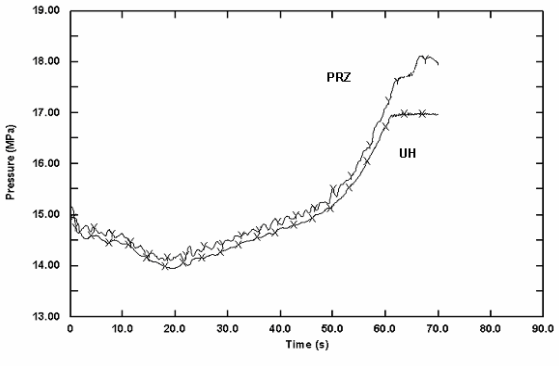

Figure 4. Pressure in SG1 and SG2

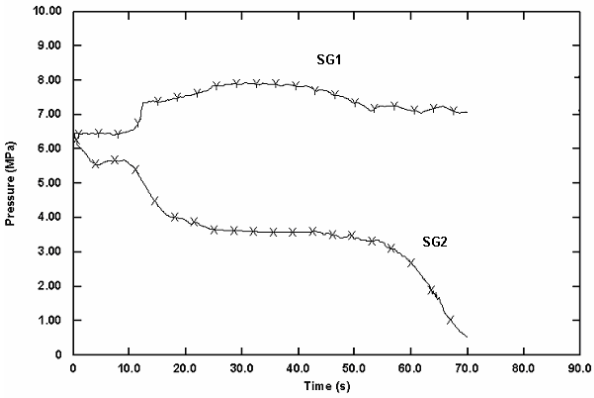

Figure 5. Liquid temperatures in HLs and CLs

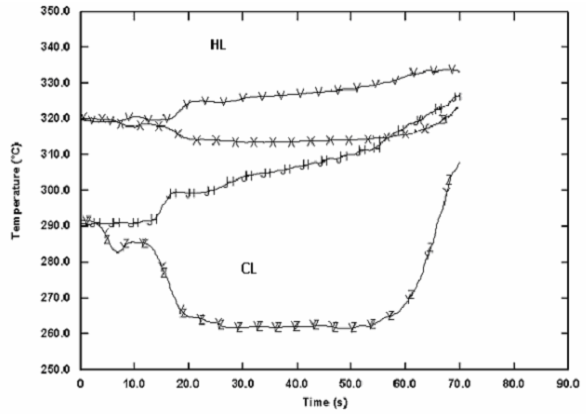

Figure 6. SGs exchanged power

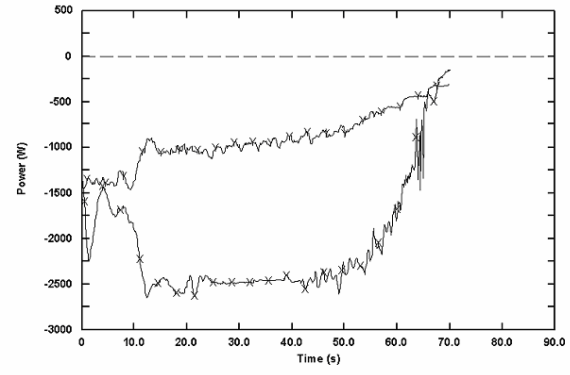

Figure 7. PRZ level

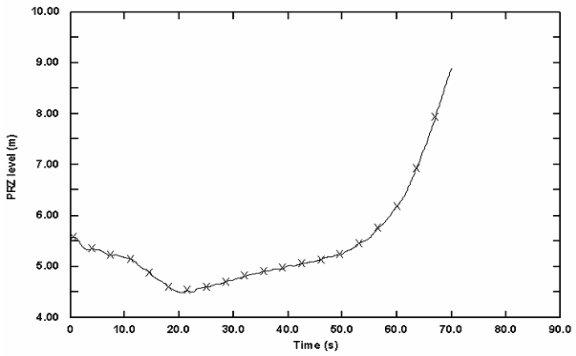

Figure 8. Feed water imposed flow rate

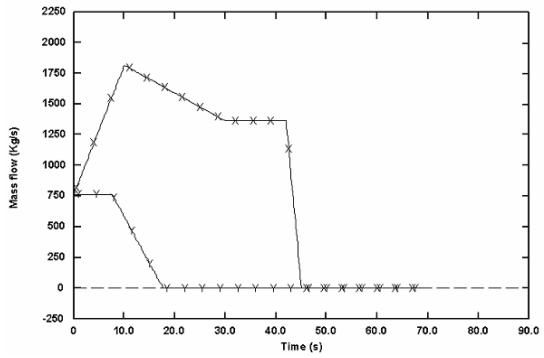

I.1.8 TMI-1 – SBLOCA-ATWS

The accidental scenario envisaged originates through a small break in the cold leg of 2% of flow area; the failure of the CR insertion mechanism is supposed to occur and all the injection systems HPIS, LPIS and ACC are supplied with de-borated water.

The fast depressurisation of the primary system carries the reactor to the scram condition, the FW pumps and the MCP stop and the pressure at the beginning rises. The SGs pressure rises until the opening of the safety relief valves and the heat removed by the two isolated SG decreases in about 100 s. In 100 s the power decreases due to the rise of the moderator temperature at the core inlet. Then the primary pressure continues to slow down, leading to the HPIS injection at 300 s. The mass flow rate through the break progressively reduces but the injection capability of the HPIS is not sufficient to recover the pressuriser level. The de-borated water injected after 300 s does not have a significant effect on the total power production in the core, and due to the decreasing temperature at the core inlet the neutronic moderator feedback does not have an immediate effect on the reactor power. Since the vessel model of the core is composed by four separated parallel paths the behaviour of the channels differs. Any mixing effect has been taken into account in the DC and LP regions. Due to the representation of the vessel volume with four parallel DC, connected with four LP and 19 core channels, strong spatial effects are enhanced. In fact, the nodalisation adopted for the analysis is directlt derived from the MSLB analysis case, though a few modifications have been introduced. The thermal-hydraulic model of the core is constituted by 19 parallel channels, the central core assembly has been represented with a channel and an active heat structure. The neutronic nodalisation of the core covers the same 3-D mesh adopted for the previous MSLB case (17 × 17 × 26 with 438 compositions). The coupling schema between thermal-hydraulic and neutronic nodalisation takes into account the introduction of the central core assembly element.

In the figures below the main parameters governing the transient have been plotted: core power, power exchanged in SG, primary and secondary pressure, pressuriser level, mass flow at break HPIS injection, and the coolant core inlet temperature.

Case 8 – PWR: Table 1. Imposed sequence of main events

Event description	Time(s)
Cold leg break open	0.0
Reactor trip	Not occurring
High pressure injection start	300.0
Transient end	600.0

Case 8 – PWR – Figures

Figure 1. Core power

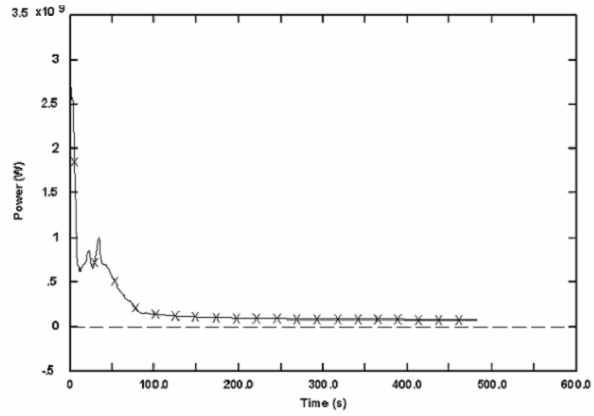

Figure 2. Power exchanged in SGs

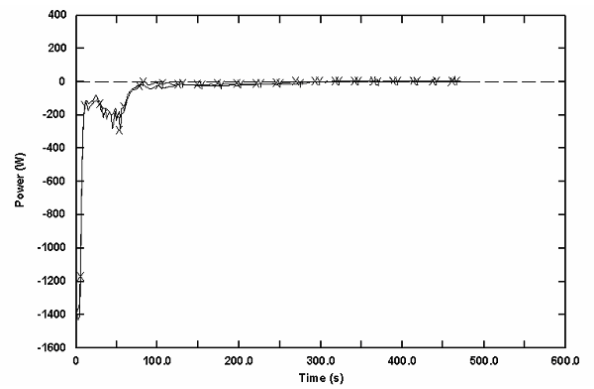

Figure 3. Pressure in pressuriser and UH

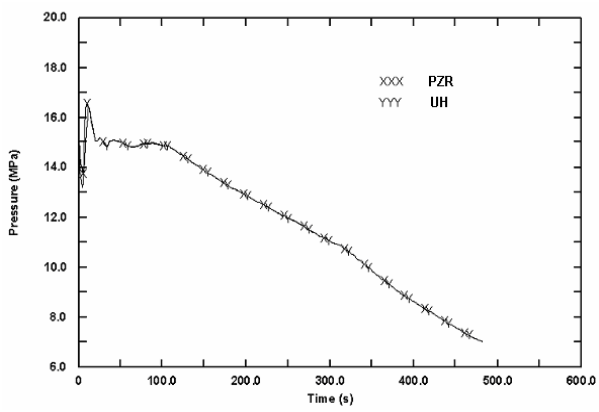

Figure 4. Pressure in SG1 and SG2

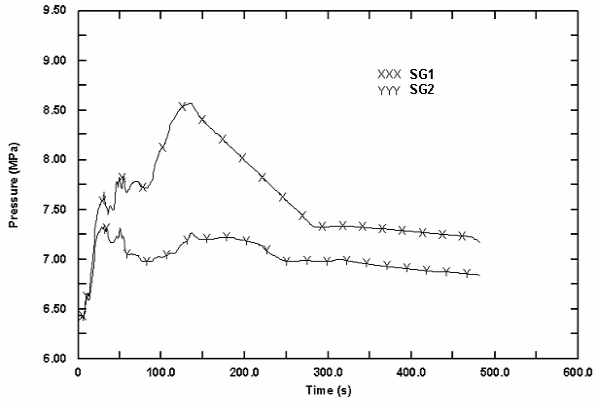

Figure 5. Pressuriser level

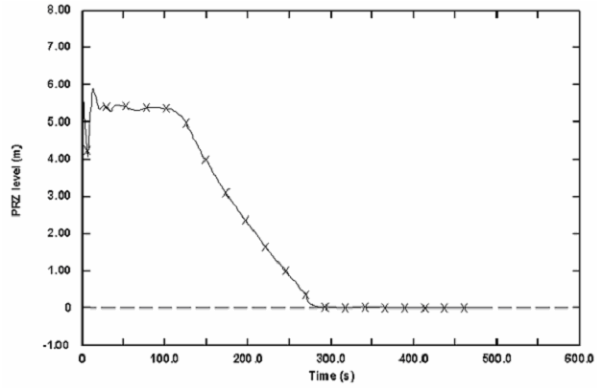

Figure 6. Mass flow at break

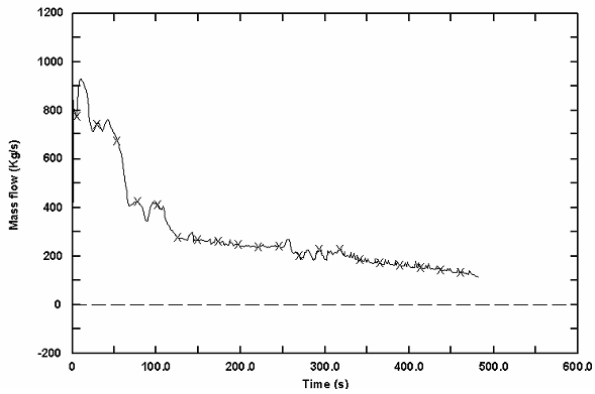

Figure 7. HPIS injection

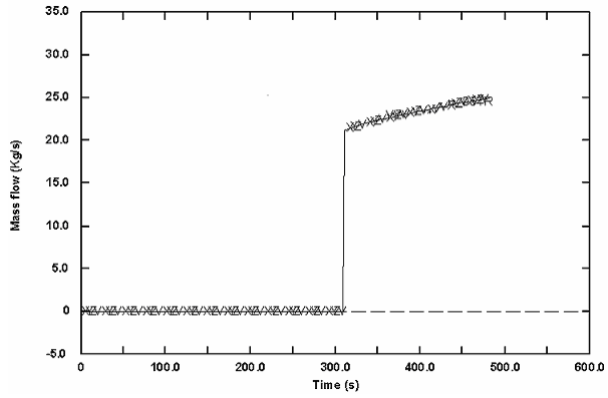

Figure 8. Moderator temperature at core inlet

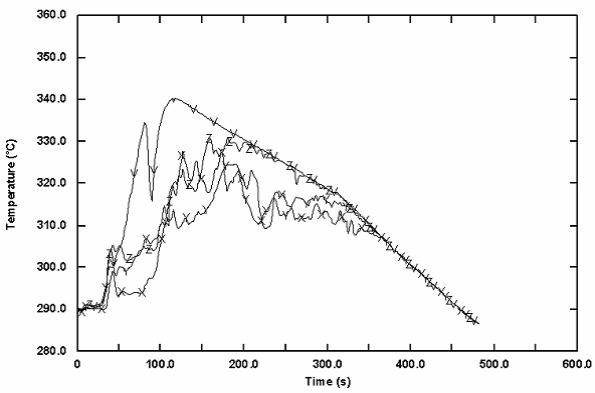

I.2 BWR NPP

In this framework, Peach Bottom (GE) NPP was taken to represent the BWRs. Several relevant transients are chosen and classified according to the nature of the induced reactivity. Two categories of REAC are considered in this framework. The first one is related to cases where reactivity addition to the system is caused by thermal-hydraulic feedback effects. These cases are generally characterised by uniform reparation of the phenomena into the core. The second category is a positive reactivity insertion into the core caused by control rod ejection. The insertion in this case could be either uniform or asymmetric in space. Along with these categories, ATWS conditions are also examined; they must be considered as a "bounding condition" in safety analysis.

The main operating conditions of PB2 are summarised in Table 1, and the scram characteristics adopted for the entire calculation case are outlined in Table 2 and the subsequent tables.

BWR: Table 1. Main PB2 TT2 initial conditions

Item	Value
Core thermal power, MWt	2 030.0 (61.9% of nominal value)
Feed water flow, kg/s	980.26
Reactor pressure, Pa	6.79847
Total core flow, kg/s	10 445.0
Core inlet subcooling, J/kg	48 005.3
Feed water temperature, K	442.31

BWR: Table 2. PB2 scram characteristics

Scram set-point, % rated	95
Time delay prior to rod motion, ms	120
CR time insertion, s	0.75

BWR: Table 3. Boundary conditions of the leading event

Case ID	Transient	Event	Code used	Scram/ATWS
BWR-1	Turbine trip without bypass opening	Turbine stop valve closed BPV	RELAP5/PARCS	Scram
BWR-2	Turbine trip	Turbine stop valve closed BPV opening	RELAP5/PARCS	ATWS
BWR-3	Single control rod ejection	Completely inserted rod ejection	RELAP5/PARCS	Scram
BWR-4	Control rod bank ejection	Completely inserted control rod bank ejection	RELAP5/PARCS	Scram
BWR-5	Feed water failure	Feed water temperature decrease by 100 K	RELAP5/PARCS	ATWS
BWR-6	Pump overflow	Mass flow rate increases by 30%	RELAP5/PARCS	Scram
BWR-7	Pump overflow	Mass flow rate increases by 30%	RELAP5/PARCS	ATWS
BWR-8	Stability issue	–	RELAP5/PARCS RELAP-3D	ATWS

BWR: Table 4. Main results of the considered cases

Case ID	Maximum amount of inserted reactivity $	Peak power (%) nominal power
BWR-1	0.90	441.0
BWR-2	0.82	393.0
BWR-3	0.56	224.0
BWR-4	1.72	25 668.0
BWR-5	0.043	76.0
BWR-6	0.43	108.0
BWR-7	0.41	112.0
BWR-8	–	–

I.2.1 PB2 – turbine trip without condenser bypass available

Turbine trip constitutes a relatively frequent event for BWR operation. A positive pressure wave propagates from the turbine isolation valve to the vessel and reaches the core from the top (*e.g.* across the steam separator and dryer) and from the bottom (*e.g.* across the downcomer and the lower plenum). Void collapse causes positive reactivity insertion and power excursion is typically stopped by scram occurrence. Opening the condenser bypass valves makes the effect of the pressure wave amplitude milder, but this effect is neglected in the proposed scenario.

The turbine trip without steam bypass opening results are illustrated along with the turbine trip case in order to emphasise the role of the steam bypass under such conditions. As can be seen from Figure 1, the peak power difference between the two cases is relatively important – about 50% higher. In fact the positive reactivity induced (Figure 2) is larger in this case close to the super prompt critical situation. The amount of inserted reactivity is higher due to a longer effect in time of the pressure wave in the absence of BPV opening (see Figure 3). According to Figure 4 the energy released into the fuel is far from causing any damage to the core integrity. Figures 5 and 6 show the core mean void and the core inlet temperature evolution, respectively.

Case 1 – BWR: Table 1 – Imposed sequence of main events

Event description	Time(s)
Turbine stop valve close	0.096
Reactor trip	0.73
Transient end	5.0

Case 1 – BWR – Figures

Figure 1. Core power

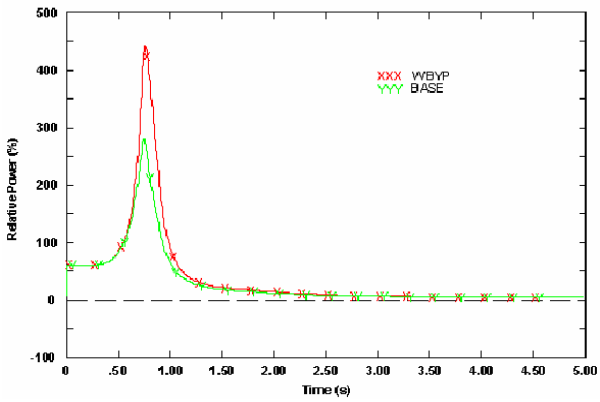

Figure 2. Core reactivity

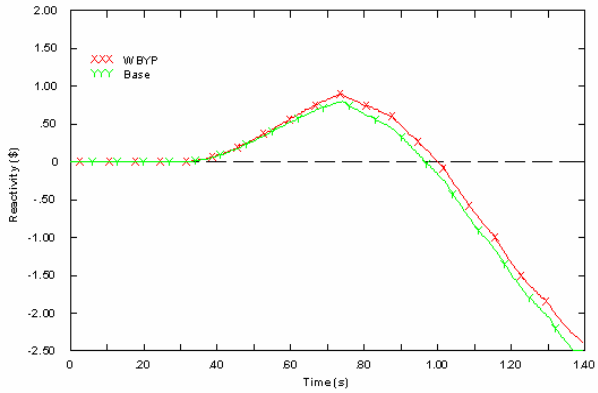

Figure 3. Core pressure

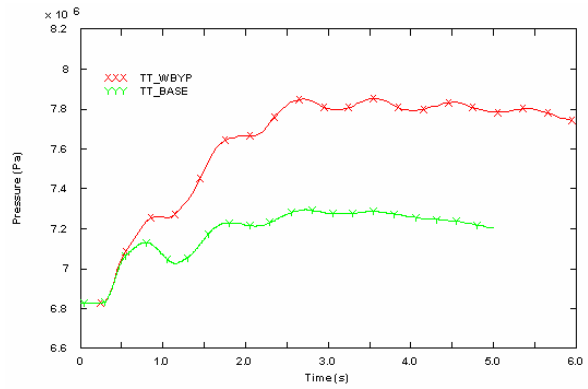

Figure 4. Clad temperature

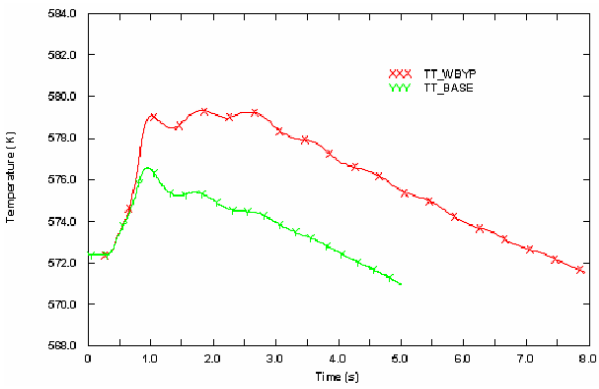

Figure 5. Core mean void

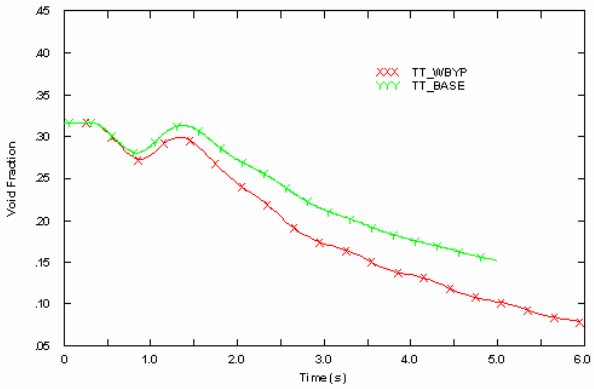

Figure 6. Core inlet mass flow

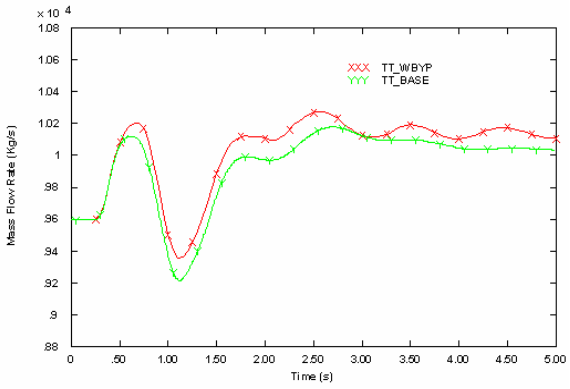

I.2.2 PB2 – turbine trip without scram

Turbine trip without scram constitutes a relatively severe event until the amount of void collapse is larger and consequently larger positive reactivity is inserted. Opening the condenser bypass valves makes the effect of the pressure wave amplitude milder, though this effect is negligible in the proposed scenario.

As can be seen in Figure 1, the peak power is relatively large – 395% of its nominal value. In fact the positive reactivity induced (Figure 2) is larger and close to a super prompt critical situation. The higher amount of inserted reactivity is due to a longer void collapsing effect caused by a continuous pressure rise (see Figure 3). According to Figure 4 the energy released into the fuel is too low to cause any damage to the core integrity.

Case 2 – BWR: Table 1. Imposed sequence of main events

Event description	Time(s)
Turbine stop valve open-close	0.0-0.096
Reactor trip	Not occurring
Steam bypass valve open	0.06
Transient end	5.0

Case 2 – BWR – Figures

Figure 1. Core power

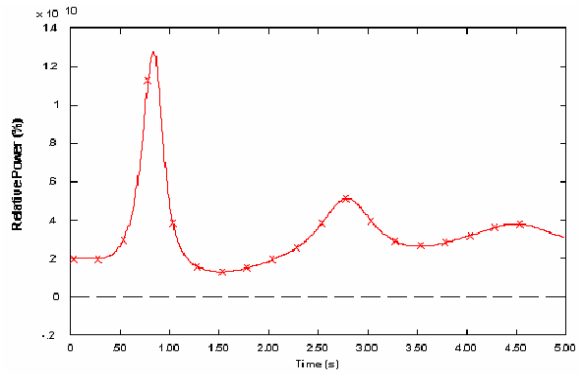

Figure 2. Turbine trip without scram: core reactivity

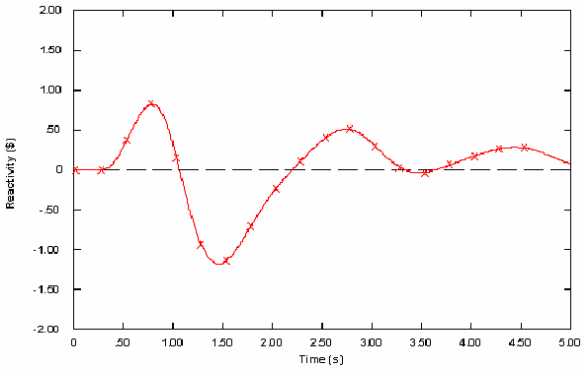

Figure 3. Core pressure

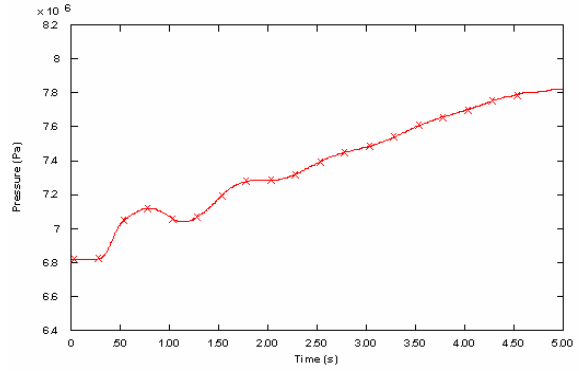

Figure 4. Turbine trip without scram: clad temperature

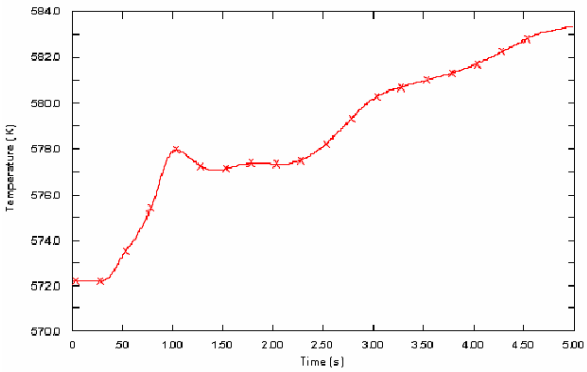

I.2.3 PB2 – single control rod ejection

A regional reactivity increase is expected following single control rod ejection. This test emphasises local effects, which justifies the application of the 3-D coupled techniques. A single peripheral control rod is considered in this case, initially completely inserted, and withdrawn after a period of 0.1 s.

The transient was modelled using 36 heated channels (instead of 33) to take into account the local asymmetric effect into the core. This constitutes only a first approach, since the model requires more local channel representation to take into account all the interactions between the channels' geometrical asymmetries.

Case 3 – BWR: Table 1. Imposed sequence of main events

Event description	Time(s)
Single control rod ejection	1.0-1.1
Reactor trip	1.19
Transient end	5.0

The obtained results are illustrated in the figures below. As can be seen in Figure 1, the power peak reaches 224% of its nominal value. The inserted reactivity due to the control rod ejection is shown in Figure 2. It is noted that the amount of inserted reactivity is less than one dollar, hence the mechanisms are governed by the super-delayed critical behaviour. The power rise is halted by control rod drop (see Figure 3). The power rise in this case is narrow, and consequently the energy released to the fuel is low. The thermal-hydraulic parameters' response to such a transient is weak (Figure 4) for the pressure and for the clad temperature (Figure 5). Figure 6 shows the core mean void, and Figure 7 the core inlet flow rate which is strongly affected by the core void evolution.

Case 3 – BWR – Figures

Figure 1. Location of the ejected control rod bank

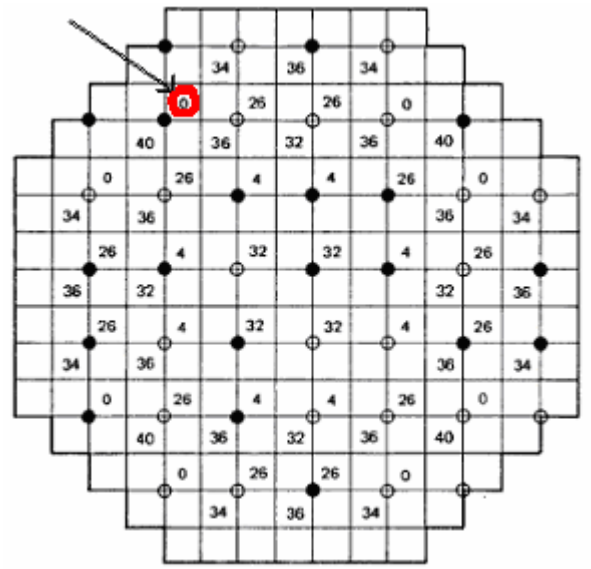

Figure 2. Core reactivity

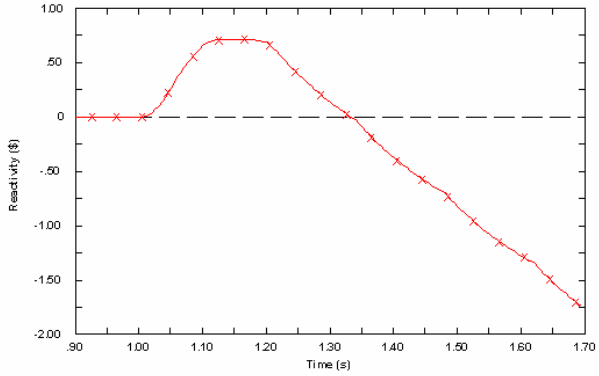

Figure 3. Core power

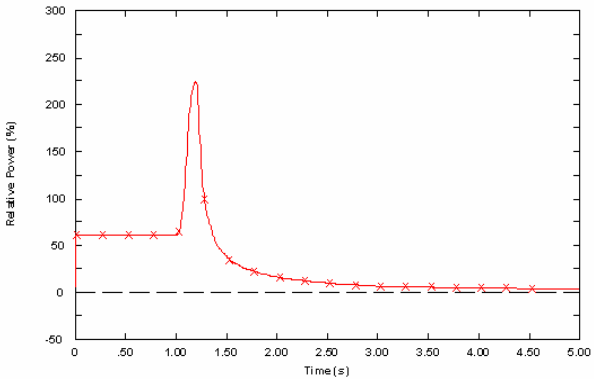

Figure 4. Core pressure

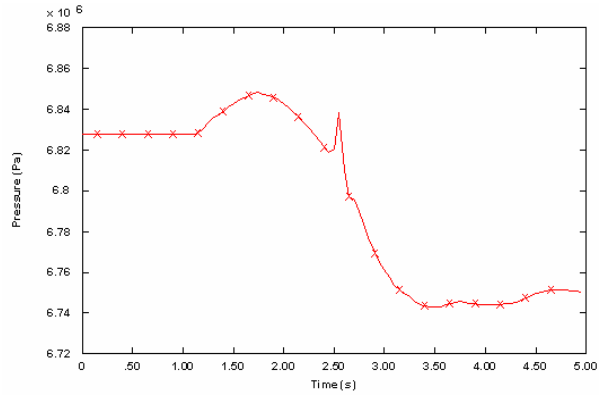

Figure 5. Clad temperature

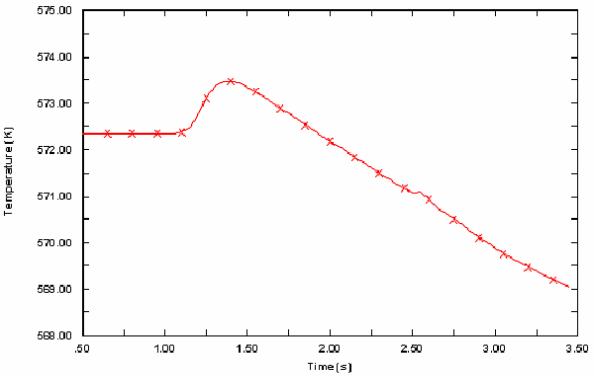

Figure 6. Core mean void

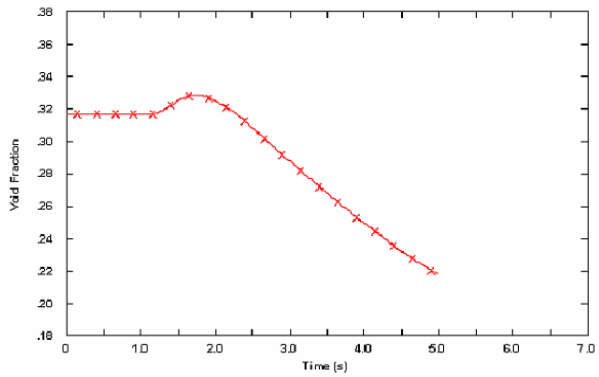

Figure 7. Core inlet flow

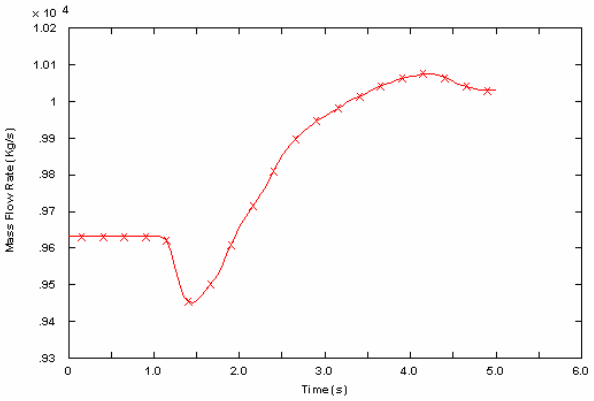

I.2.4 PB2 – control rod bank ejection

An extreme protected case is considered here. All the completely inserted control rods (eight) as shown in Figure 1 are withdrawn within a time span of 0.1 s. This will introduce a large amount of positive reactivity into the core and leads to a super prompt critical power excursion. The transient was modelled using 33 heated channels due to the symmetric position of the control rod bank in the core. The obtained results are illustrated in the figures below. A large peak power of about 25 000% of the nominal value is reached (Figure 2). This very large pulse is reached in a very short time, about 0.1 s. The amount of inserted reactivity in this case is large and exceeds one dollar (Figure 3). Hence, the dynamic of the neutronics is governed by a super-prompt critical trend. Only the Doppler feedback effect acts to slow down the power excursion. Figure 4 shows the core pressure evolution, Figure 5 shows the core mass flow rate which exhibits a strong decrease due to a large void formation in the core. In this case, as can be seen in Figures 6 and 7, the clad temperature and the amount of void go to a higher value, and the energy released to the fuel is sufficient to cause dry-out of the fuel element.

Case 4 – BWR: Table 1. Imposed sequence of main events

Event description	Time(s)
Control rod bank ejection	1.0-1.1
Reactor trip	1.14
Transient end	5.0

Case 4 – BWR – Figures

Figure 1. Location of the ejected control rod bank

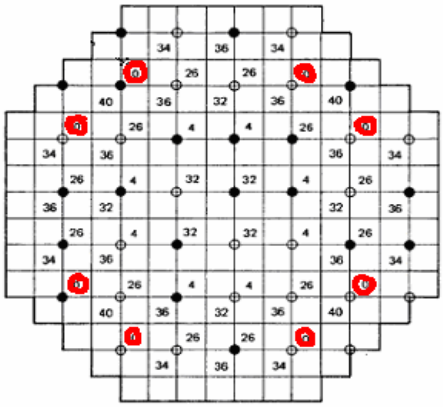

Figure 2. Core power

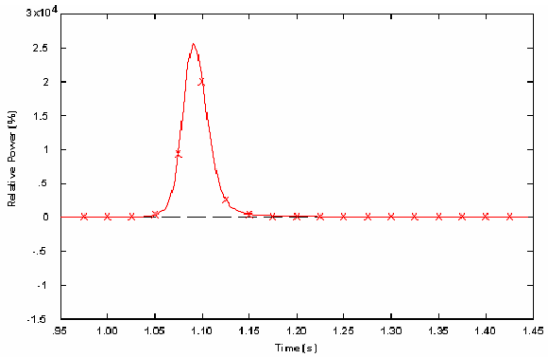

Figure 3. Core reactivity

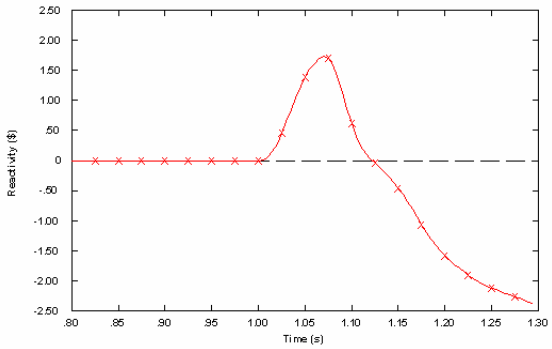

Figure 4. Core pressure

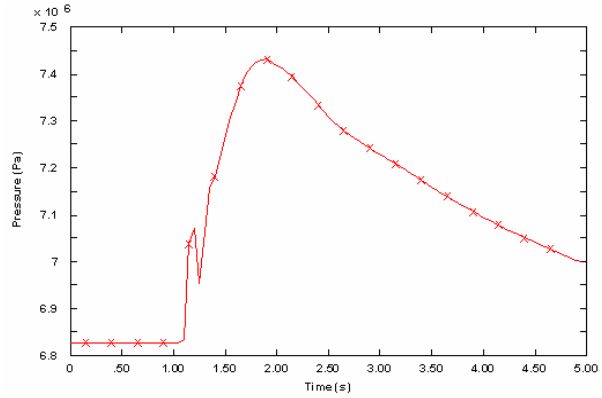

Figure 5. Clad temperature

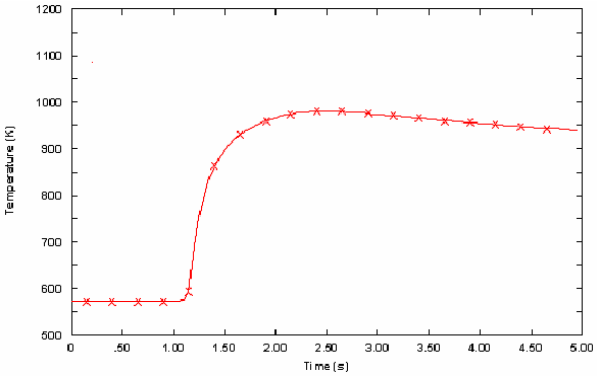

Figure 6. Core mass flow rate

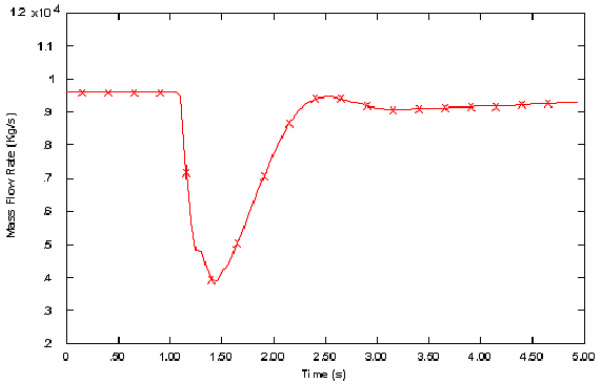

Figure 7. Core mean void

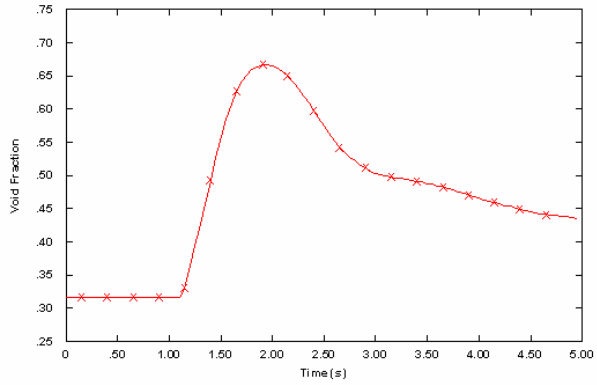

I.2.5 PB2 – FW temperature decrease

Malfunction of FW pre-heaters (*e.g.* sudden depressurisation in one pre-heater on the heating side) and of FW pumps may cause a FW temperature decrease that results in colder water at the core inlet. This creates the potential for reduction of the steam occupied volume in the core and consequently the fission power increase. In the current case it is supposed a decrease of the feed water temperature of 100 K over a time span of 100 s.

Due to the fact that the temperature at the core inlet zone is uniformly distributed, the 33 heated channels model is used. The transient is governed by the core inlet temperature evolution as shown in Figure 5, which follows the decrease of the feed water temperature. Due to the mixing effect at the core lower plenum, however, the inlet temperature decreases only by 8 (K). The core power response is shown in Figure 1. After 60 s, a steady power increase can be noted, due to a constant decrease of inlet temperature (Figure 4), and the power trend begins to oscillate. A short time afterwards the oscillations are sustained but the trend drifts toward a steady level of about 73% of its nominal value. The power oscillations are due to the insertion mode of the reactivity which is governed by the coolant void feedback effects (Figures 2 and 3). Consequently, all the related thermal-hydraulic parameters oscillate, which can be seen for the core mass flow (Figure 5) and for the core pressure (Figure 6).

Case 5 – BWR: Table 1. Imposed sequence of main events

Event description	Time(s)
Feed water temperature decrease by 100 K	0.0-100.0
Reactor trip	No scram
Transient end	200.0

Case 5 – BWR – Figures

Figure 1. Core power

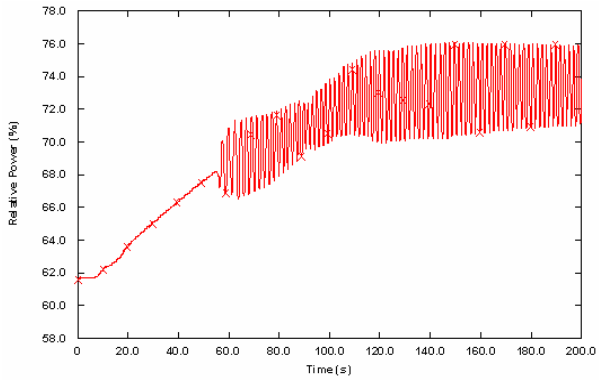

Figure 2. Core reactivity

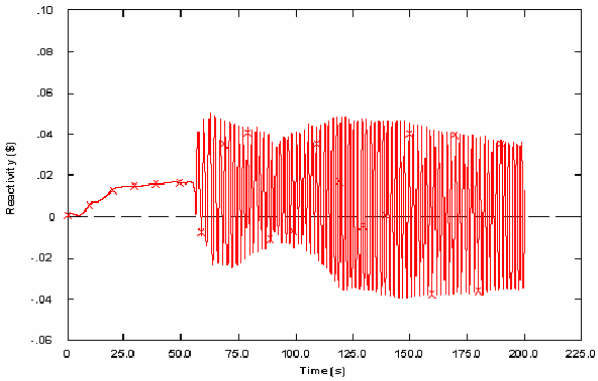

Figure 3. Core mean void

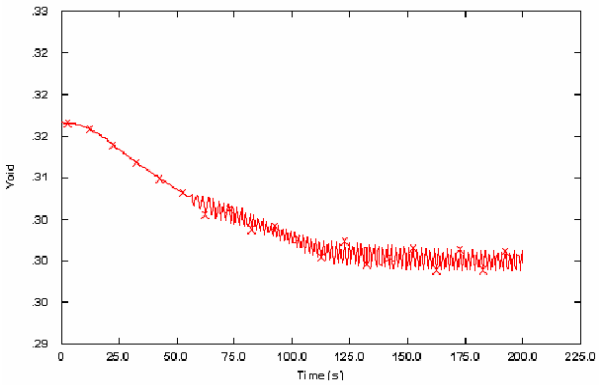

Figure 4. Core inlet temperature

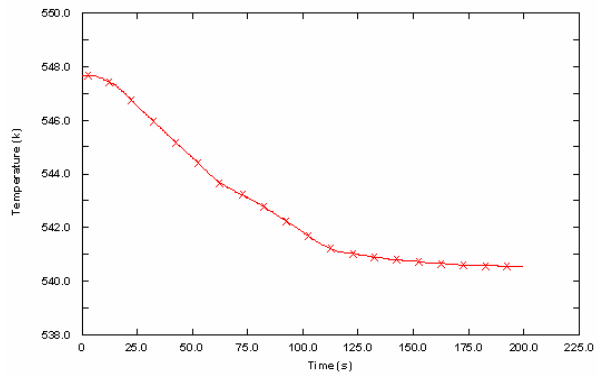

Figure 5. Core mass flow rate

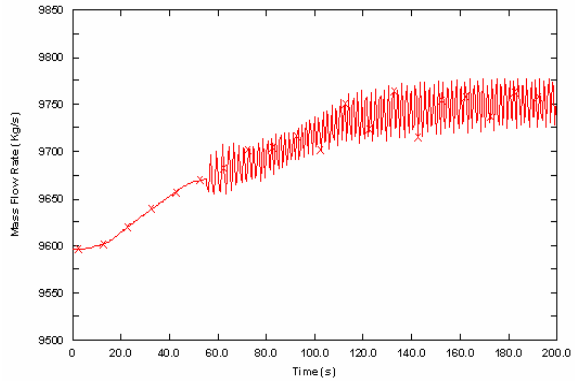

Figure 6. Core inlet temperature

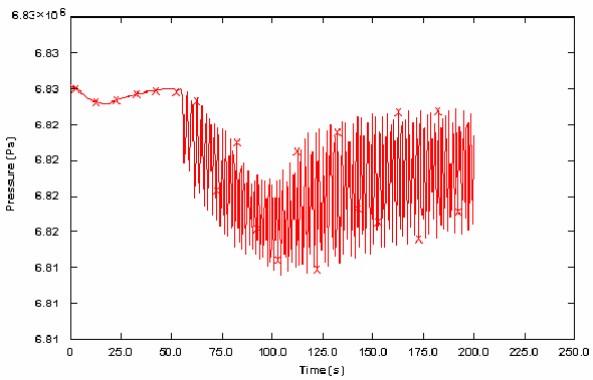

I.2.6 PB2 – main coolant pump flow rate increase

Core flow rate increase may be caused by malfunction of valves installed in the MCP lines or by a spurious signal controlling the pump speed. Two cases are considered, with and without scram. The transient is governed by an increase of the main pump flow rate by about 30% within a time span of 100 s. This will alter the core void distribution and, due to the inherent negative feedback of the core, a positive reactivity is inserted into system and a power excursion should take place.

This transient belongs to a category governed by thermal-hydraulic feedback, which inserts a positive reactivity into the core. In this case 33 heated channels for RELAP5 are used. The power response to such transients is shown in Figure 1. It is interesting to see that in this case the peak power difference between the protected and unprotected case are not so different; the peak power for the first case is 108% and for the second is 112% – only a 4% difference. In Figure 2 the difference between the inherent reactivity response of the system can be seen, which leads to a self-power-limiting behaviour during the ATWS case, and in the second case (with scram) the reactivity rise is stopped by the drop of the control rods.

The thermal-hydraulic response during the unprotected case is strong enough to maintain a power level similar to the initial state; the power level is maintained at 67% of its nominal value.

Both of the considered transients are governed by the inlet core mass flow rate evolution as shown in Figure 3. The inlet core coolant temperature, the clad temperature and the core mean void responses are plotted in Figures 4, 5 and 6, respectively.

Case 6, 7 – BWR: Table 1. Imposed sequence of main events

Event description	Time(s)
MCP flow rate increased by 30%	0.0-100.0
Reactor trip	No scram (Case 6) ATWS (Case 7)
Transient end	200.0

Case 6, 7 – BWR – Figures

Figure 1. Core power

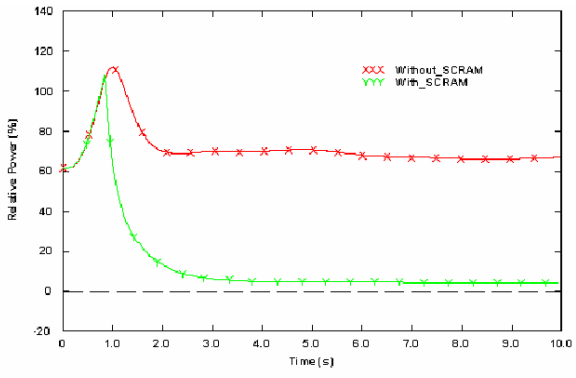

Figure 2. Core reactivity

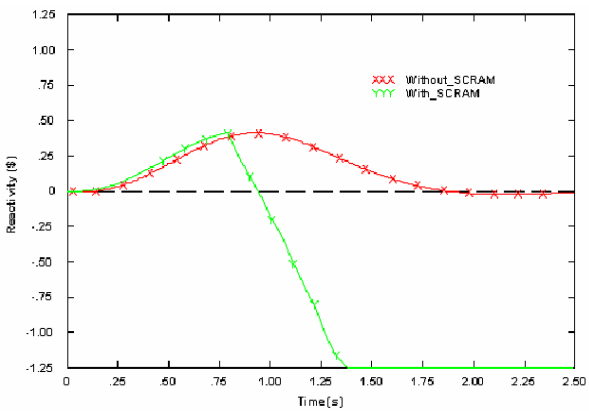

Figure 3. Core mass flow rate

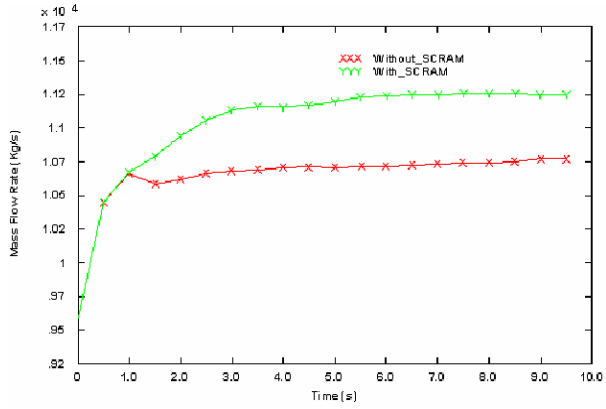

Figure 4. Coolant temperature

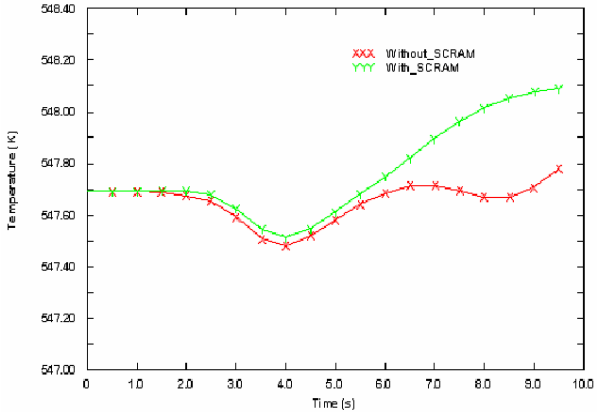

Figure 5. Clad temperature

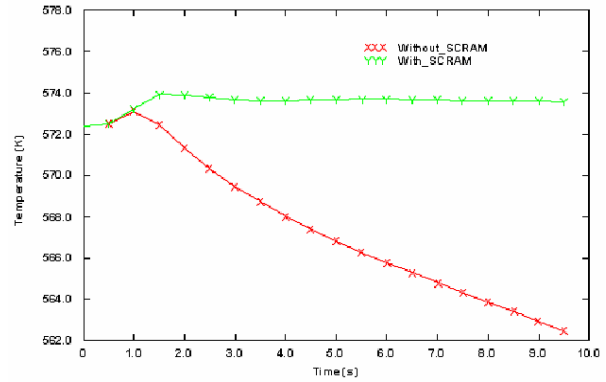

Figure 6. Core mean void

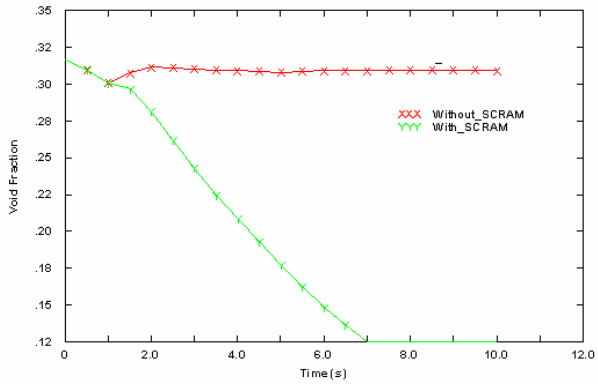

I.2.7 PB2 – stability issue (MCP trip) – RELAP5

The purpose of this work is to analyse the reactor's behaviour under instable conditions. According to the core power to flow map, a BWR plant may operate under instable conditions at approximately 30% of nominal flow and 50% of nominal power.

The transient analysis has been developed in two steps:

- The first step consists in performing the calculation using RELAP5 without any kinetics calculation (the reactor power was imposed in time).

- In the second step, coupled (3-D neutron kinetics/thermal-hydraulic) code calculations have been carried out.

To allow the identification of differences between the calculation methods, the results have been compared with results obtained for the same accident using the coupled code RELAP5-3D©/NESTLE (same T-H nodalisation with ¼ 3-D neutronic core symmetry).

In order to simulate the reactor behaviour under instable conditions the following assumptions have been made:

- Both main coolant pumps have been tripped in 20 seconds (due to the pump's stop, a natural circulation regime is established in the vessel).

- The feed water flow has been reduced to 30% of its nominal flow (760 kg/s).

For the RELAP5/PARCS code the plant has been modelled with a detailed nodalisation of the entire plant. The thermal-hydraulic core representation is constituted with 33 parallel heated channels; the 3-D core mesh is composed of 764 nodes, with a large cross-section set including 435 compositions.

For the RELAP5-3D©/NESTLE code the following considerations are adopted:

- The steady-state condition is reached using the steady-state option of the code where the 3-D neutronic/T-H coupling is enabled.

- The transient calculation starts at 100 seconds, the main coolant pumps are stopped in 20 seconds and the feed water decreased to 45% of its nominal value.

From the first calculation (RELAP5), irregular oscillating flows at core inlet were observed from approximately 1 600 seconds to 3 000 seconds. After that, the flow's oscillations become very low with a stable decreasing trend. In the coupled calculation the reactor's behaviour is unstable after about 70 seconds. After 250 seconds, the flow's oscillations become regular.

In the figures below (Figures 1 to 8), a comparison between the three calculated trends of core inlet flow are shown. The last three figures emphasise the zones of major oscillation. Figure 7 outlines the exit void fraction history during the transient in four central channels. The last figure (Figure 8) gives an overview of the 3-D relative power distribution for the time of maximum power peak.

Case 8 – BWR: Table 1. Imposed sequence of main events

Event description	Time(s)
Main coolant pumps tripped	0.0
Feed water flow rate reduced by	70%
Rector trip	Not occurring
Transient end	3 000.0

Case 8 – BWR – Figures

Figure 1. RELAP5 base case, mass flow rate at core inlet

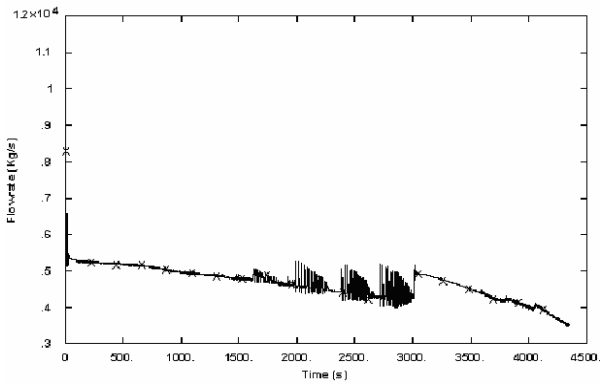

Figure 2. RELAP5/PARCS, mass flow rate at core inlet

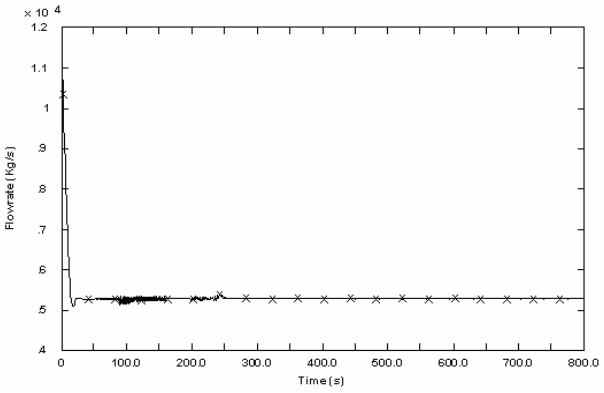

Figure 3. RELAP5-3D©/NESTLE, mass flow rate at core inlet

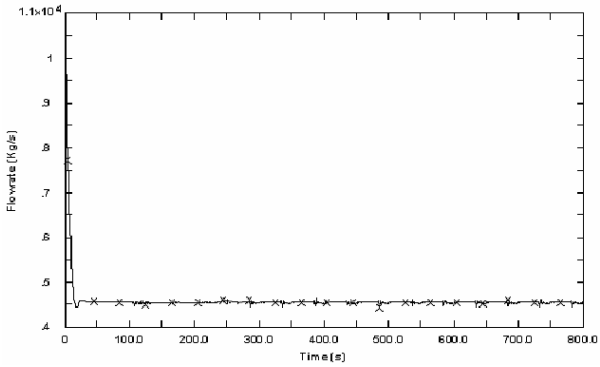

Figure 4. RELAP5 base case, mass flow rate at core inlet

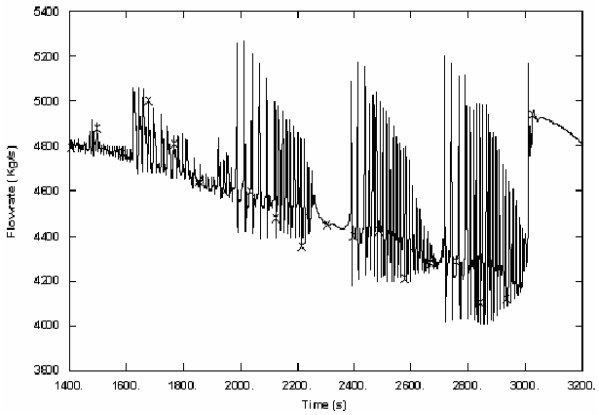

Figure 5. RELAP5/PARCS, mass flow rate at core inlet

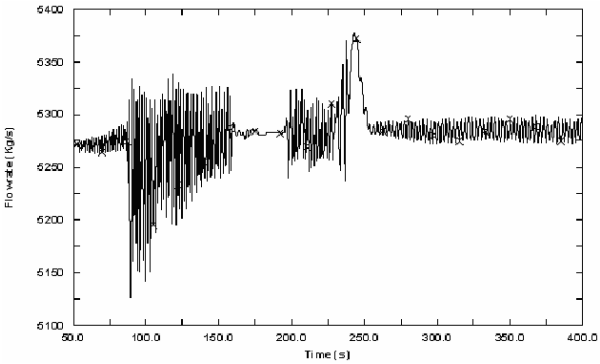

Figure 6. RELAP5/PARCS, void fraction at core outlet

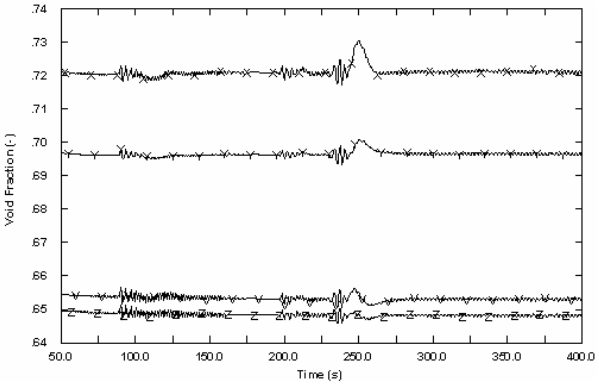

Figure 7. RELAP5-3D©/NESTLE, mass flow rate at core inlet

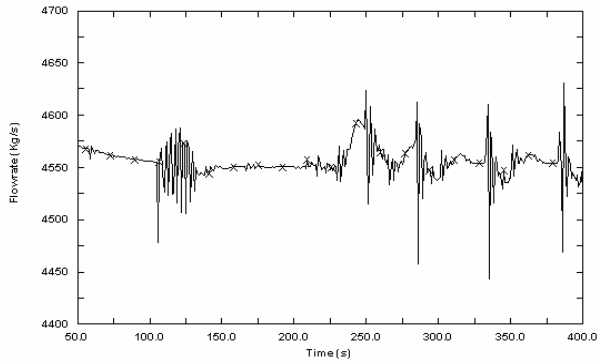

Figure 8. Average radial power distribution (at the time of the maximum peak)

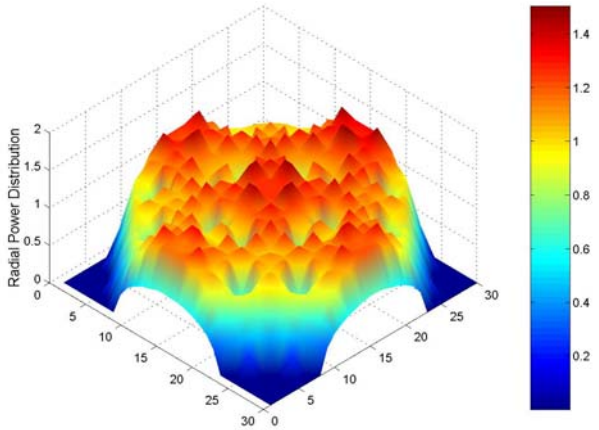

I.3 VVER NPP

Two VVER NPPs are considered in the current framework, namely the VVER-1000 and the VVER-440.

VVER: Table 1. Cases analysed

Case ID	Transient	Event	Code used	Scram/ ATWS
VVER-1	MSLB VVER-1000	Double-ended break of the main SL	RELAP5/PARCS	Scram
VVER-2	MSLB VVER-440	Double-ended break of the main SL	DYN3D/ATHLET	Scram
VVER-3	LOFW VVER-1000	Trip of the feed water pumps	RELAP-3D	ATWS
VVER-4	CR ejection VVER-1000	Completely inserted control rod is ejected	RELAP5/PARCS	Scram
VVER-5	CR bank ejection VVER-1000	Completely inserted control rod bank is ejected	RELAP5/PARCS	Scram
VVER-6	MSLB VVER-1000	Double-ended break of the main SL	RELAP5/PARCS	ATWS
VVER-7	SBLOCA VVER-1000	SBLOCA that occurs in cold leg no. 4	RELAP-3D RELAP5/PARCS	ATWS

I.3.1 VVER-1000 MSLB

The reference nuclear power plant considered in the analysis is a “generic” VVER-1000, equipped with four HSG. Some relevant operating conditions are summarised hereafter.

Table 2. Nominal conditions at steady state

No	Quantity	Unit	Design
1	Primary circuit balance	MWth	3 000
2	Secondary circuit balance	MWth	750
3	PRZ pressure	MPa	15.7
4	SG pressure	MPa	6.3
5	Core inlet temperature	K	562
6	SG inlet plenum temperature	K	593
7	SG outlet plenum temperature	K	559
8	SG feed water temperature	K	493
9	Core pressure losses	MPa	0.142
10	PS total loop coolant flow rate	kg/s	18 250
11	SG feed water mass flow rate	kg/s	**408**
12	PRZ liquid level	m	8.45
13	SG SS level	m	2.55
14	SG stem mass flow rate	kg/s	**408**

The transient analysed is a main steam line break (MSLB), which is simulated by a double-ended break (DEB) in the steam line (SL) of loop no. 1 before the SG 1-4 common collector. The transient is performed at 100% of nominal rated power. The fast depressurisation of one SG causes the primary water cooling. A core power release occurs when the plug of cold water reaches the core inlet, because a positive insertion of reactivity is due to the moderator neutronic feedback.

In the downcomer (DC) and lower plenum (LP) regions a partial mixing between “cold” water coming from the loop affected by the broken SG and the “hot” water of the intact loops takes place.

The half of the core connected with the broken loop is characterised by lower moderator temperatures and higher relative power peak, producing a localised positive insertion of reactivity.

Scram occurs 35 s after the beginning of the transient for a low-level signal in the SG secondary side and not for high neutron flux signal.

A nodalisation involving 3-D kinetics coupled with a thermal-hydraulic multi-channel core model is considered suitable to represent the behaviour of the spatial core power release and the time evolution of the parameters relevant for the neutronic feedback. The nodalisation developed includes the modelling of all four loops, four HSG and emergency core cooling system (ECCS); the core is modelled using 28 thermal-hydraulic channels (and related heat structures). In addition, one channel simulates the bypass.

The 3-D neutronic core was modelled in hexagonal geometry with nine rings (including the radial reflector region) and 20 axial planes; two additional planes are also included to model the upper and lower reflectors. The set of cross-sections used was that provided for the VVER-1000 Cooling Transient (CT-1) benchmark, related to the Kozloduy NPP Unit 6: they consist of 283 un-rodded compositions and 110 rodded compositions, and they are provided in tabular format as a function of the fuel temperature and moderator density. PARCS could not yet read such a tabular format, so the cross-sections were modified to be in a “partial linear format” (polynomial) readable by PARCS. The two-group diffusion equation is solved using the Triangular Polynomial Expansion Method (TPEN).

In the figures below the main parameters governing the transient the were plotted: core and SG exchanged power, PS mass inventory and SG SS coolant mass, break mass flow rate, pressuriser and UP pressure, hot leg temperatures, cold leg temperatures and clad surface temperatures of element 108 (hot channel) at the various planes.

Case 1 – VVER: Table 1. Imposed sequence of main events

Event description	Time(s)
Breaks open	0.0
Reactor trip	Not occurring
MCP trip	Not occurring
Turbine valve closure (start-end)	7.9-11.9
High pressure injection start	46.4
Transient end	70.0

Case 1 – VVER – Figures

Figure 1. Core and SG exchanged power

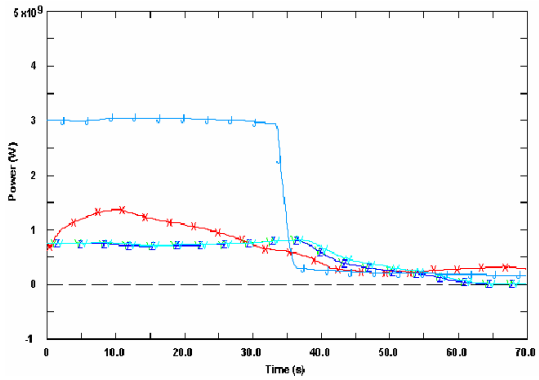

Figure 2. PS mass inventory and SG SS coolant mass

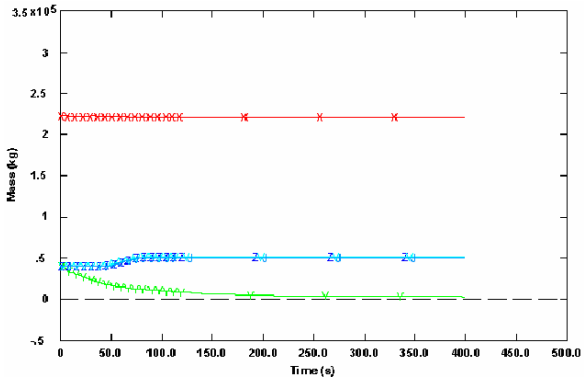

Figure 3. Break mass flow rate

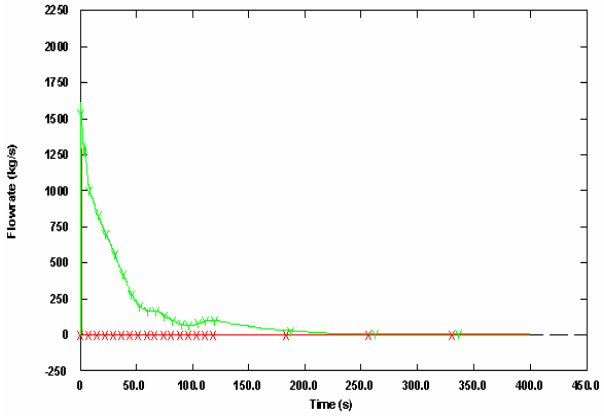

Figure 4. Pressuriser and UP pressure

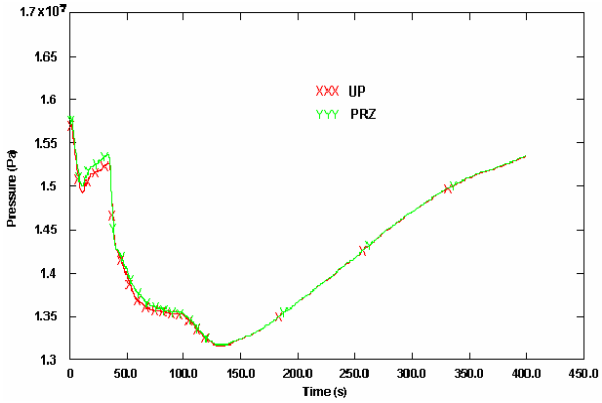

Figure 5. Hot leg temperatures

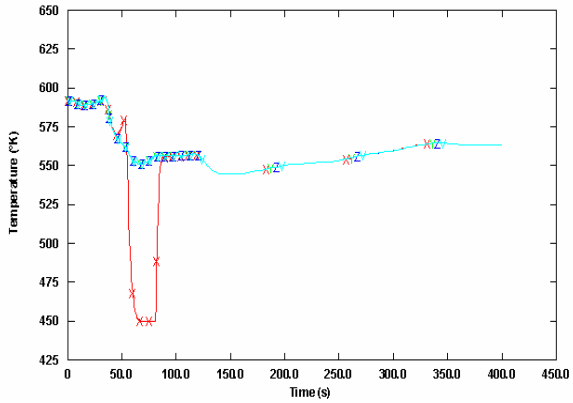

Figure 6. Cold leg temperatures

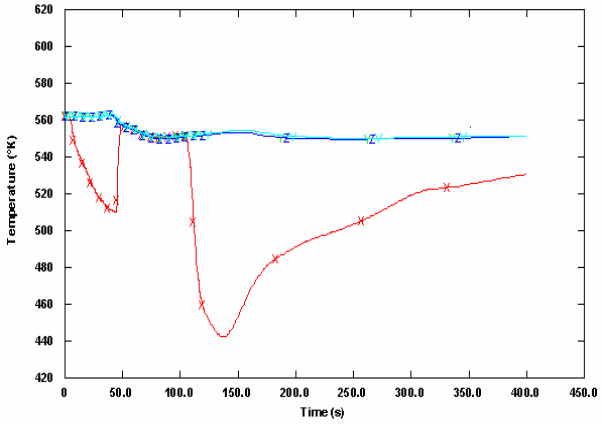

Figure 7. Axial clad temperature

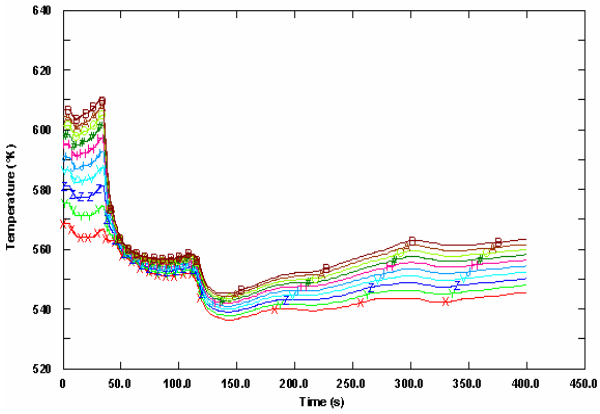

I.3.2 VVER-440/213 – MSLB

The VVER-440 is a six-loop 1 375 MWth pressurised water reactor with horizontal steam generators and two turbines. The MSLB is postulated as a double-ended break (DEB) of the main steam line (MSL) downstream from the steam generator (SG) in front of the steam isolation valve (SIV) at hot zero power under end of cycle conditions. The MSLB accident was modelled according to the following scenario.

Case 2 – VVER: Table 1. Imposed sequence of main events

Event description	Time(s)
Breaks open	0.0
Critical rate of pressure decreases 0.05 MPa/s	1.3
SIV closure (start-end)	6.3-12.3
Transient end	500.0

The closing of the SIV causes the shutdown of the MCP in the corresponding loop. Closing of more then three SIVs causes the reactor scram. All withdrawn control rod groups are immediately inserted into the core, the most efficient control rod excepted, which is assumed to be stuck in the fully withdrawn position. During the transient the primary pressure reaches the actuation point of the high pressure injection system (HPIS). In the calculations presented here the failure of the HPIS is postulated to aggravate the accident.

On the secondary side the MSCOL and the intact SGs were isolated from the leak by closing all SIVs. Then, continuing pressure decrease is only occurring in the leaking SG (Figure 2). The secondary side temperature of the broken loop decreases together with the pressure along the saturation line. This temperature decrease leads to an increasing heat flux from the primary to the secondary side (Figure 4) and causes a temperature decrease in the corresponding primary loop of about 100 K (Figure 3). Due to this temperature decrease the core inlet temperature decreases as well, from 260°C to 216°C, at the end of the investigated time interval (500 s after the break). This temperature drop leads to a positive reactivity insertion into the core. To study the influence of lower plenum coolant mixing assumptions, three calculations were performed. The first calculation implies ideal mixing in the lower plenum. In the second calculation the coolant mixing was treated by means of the VVER-440 mixing model included in the DYN3D code. In the third calculation coolant mixing in the lower plenum was completely inhibited. Each loop was connected to a particular sector of the core. The temperature distribution obtained with the mixing model is demonstrated in Figure 5. For conservative assumptions, the stuck control rod was supposed to be situated in the same sector of the core. Thus, the superposition of effects of overcooling and stuck rod causes a strongly asymmetric neutron flux and power distribution. Due to these effects, the positive reactivity insertion caused by the coolant temperature decrease compensates the scram reactivity in the calculation with the mixing model and in the calculation without mixing. Re-criticality of the shut-down reactor is reached in these two cases (Figure 7). At that time the cold leg temperature is at minimum, later the positive reactivity insertion is stopped and the power level is stabilised by Doppler feedback (Figure 8).

Case 2 – VVER – Figures

Figure 1. Leak mass flow rate

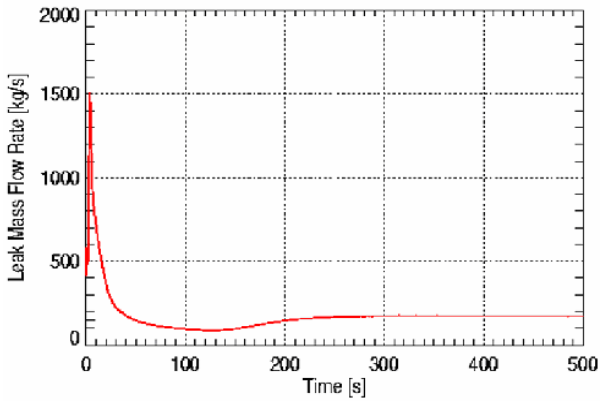

Figure 2. Secondary side pressure

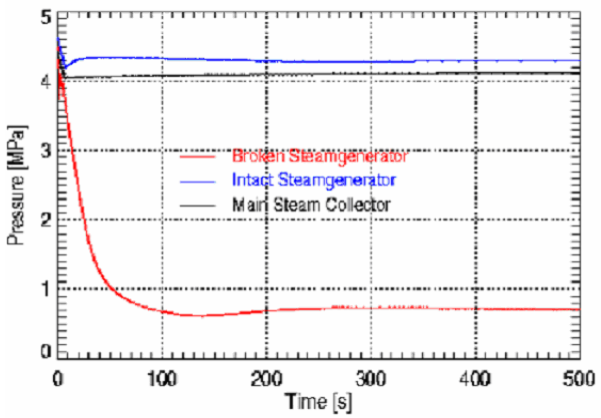

Figure 3. Coolant temperature (primary side)

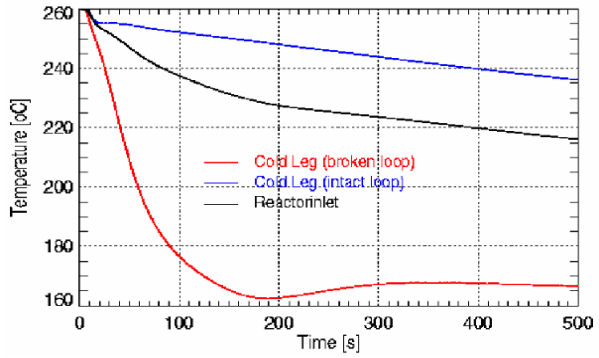

Figure 4. Heat transfer in the steam generators

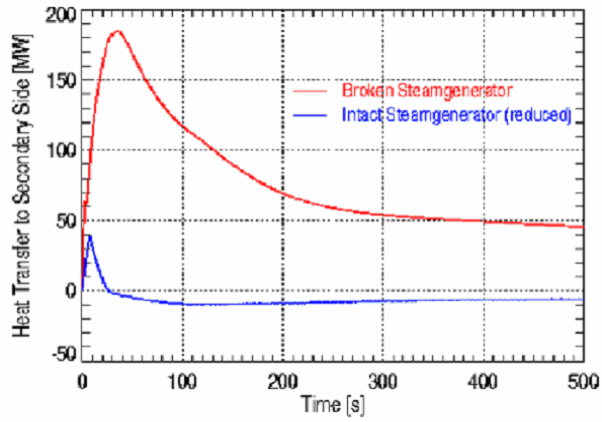

Figure 5. Core inlet temperature distribution (mixing model)

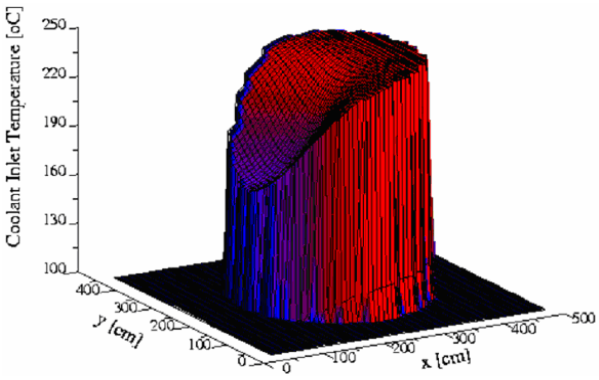

Figure 6. Mass flow rates in primary circuit loops

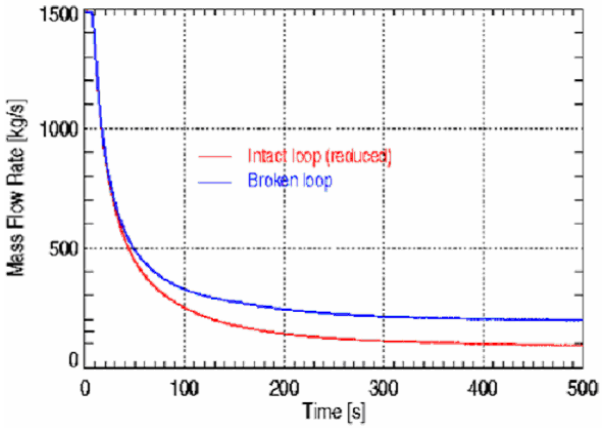

Figure 7. Reactivity dependence on coolant mixing option

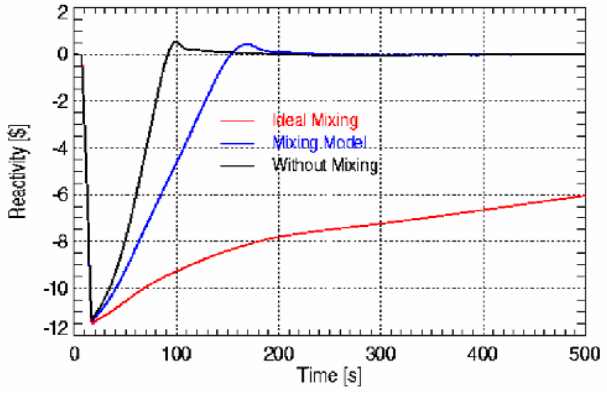

Figure 8. Core power dependence on coolant mixing option

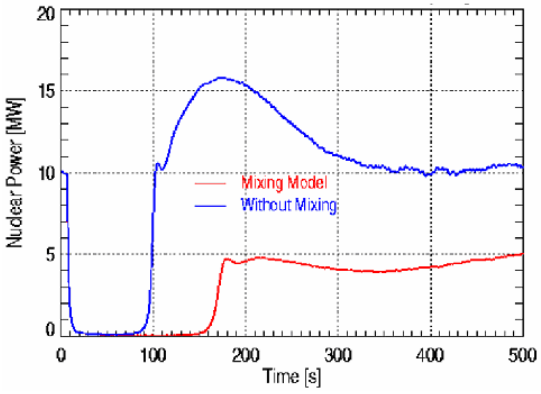

I.3.3 VVER-1000 – LOFW

The reference nuclear power plant considered in the analysis is a generic VVER-1000 as specified in Section I.3.1: the 3-D kinetics/thermal-hydraulics model adopted to perform the analysis is also the same as described therein. The transient analysed is a LOFW-ATWS using RELAP5/PARCS; it is supposed to originate from the trip of all the feed water (FW) pumps in correspondence of scram failure. The capability of the SG to remove the power produced in the core is limited by the loss of FW pumps. The following increase of the moderator temperature at the core inlet introduces negative reactivity due to the neutronic moderator temperature feedback. The accident occurs when the power is at 1 005 of nominal rated power and it decreases at about 50 s after the beginning of the transient. The maximum cladding temperature of the hottest rod in the core reaches 400°C.

In the following figures the main parameters governing the transient have been plotted: core power, power exchanged in all the SGs, pressuriser (PRZ) and upper plenum (UP) pressures, PRZ level, steam line (SLs) pressures, HSG pressures, liquid temperature in all the CL, liquid temperature at UP and lower plenum (LP), cladding temperature in hottest channel.

Case 3 – VVER: Table 1. Imposed sequence of main events

Event description	Time(s)
Trip of all the FW pumps	0.0
Reactor trip	Not occurring
MCP trip	Not occurring
Transient end	140.0

Case 3 – VVER – Figures

Figure 1. LOFW-ATWS – core power and SG exchanged power

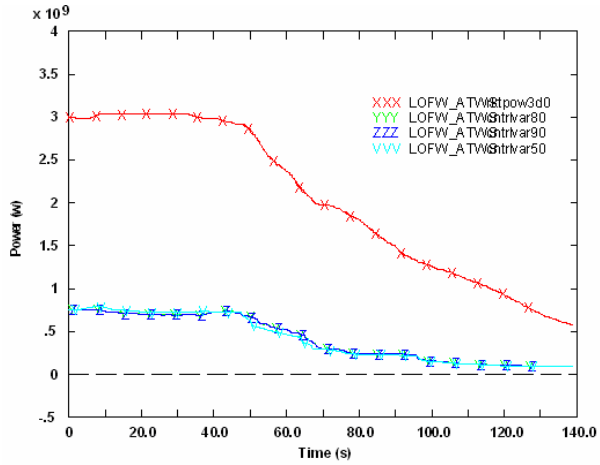

Figure 2. LOFW-ATWS – liquid temperature at LP and UP

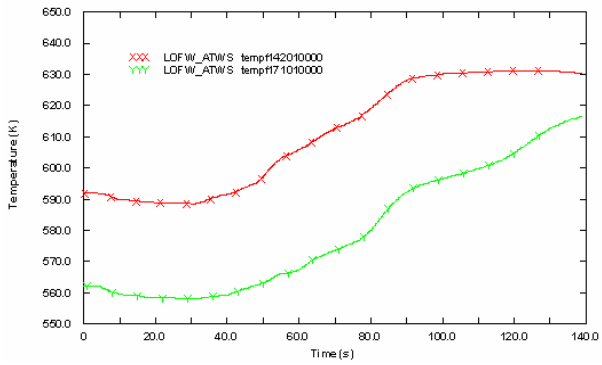

Figure 3. LOFW-ATWS – pressuriser level

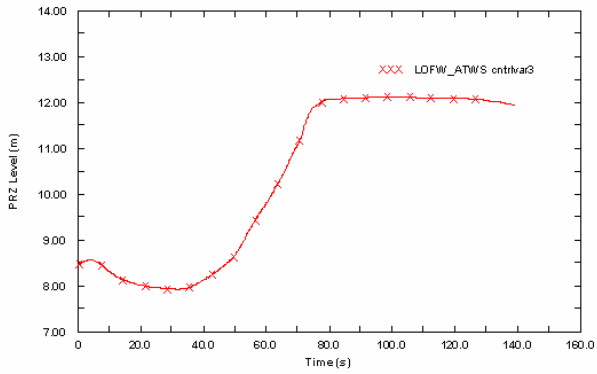

Figure 4. LOFW-ATWS – mass flow rate into the steam lines

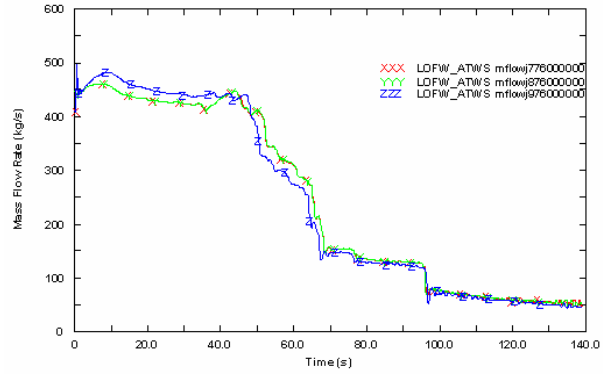

Figure 5. LOFW-ATWS – cladding temperature at different axial positions

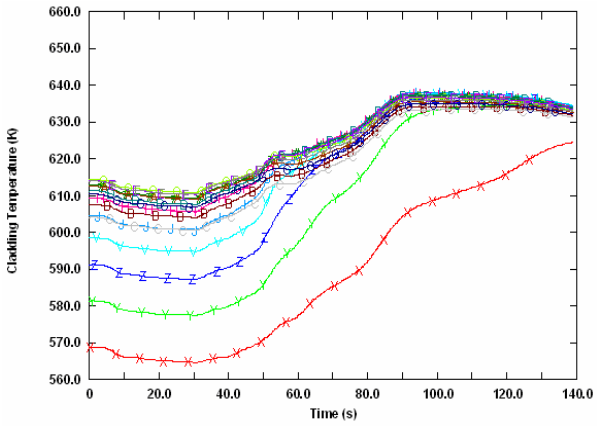

Figure 6. LOFW-ATWS – pressures into the HSGs

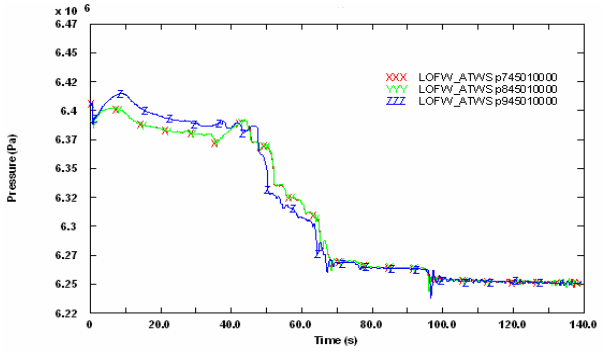

Figure 7. LOFW-ATWS – liquid temperature in CLs

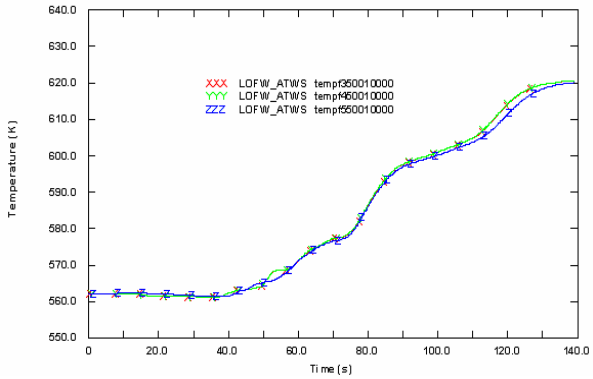

I.3.4 VVER-1000 – CR ejection

The reference nuclear power plant considered in the analysis is a generic VVER-1000 as specified in Section I.3.1: the 3-D kinetics/thermal-hydraulics model adopted to perform the analysis is also the same as described therein.

The accidental scenario envisioned is supposed to originate from the sudden ejection of one control rod (CR). The control rod expulsed is that indicated in Figure 1. The 61 CAs, arranged into 10 groups, are full-length control rods except group no. 5, which consists of part-length control rods. The part-length control rods have neutron absorber only in the lower half; their purpose is to damp the Xe oscillations.

The reactor is at 100% of nominal rated power and only bank no. 10, used for regulating the power, is partially inserted. The CR expulsed belong to bank no. 6. The ejection of the CR has local effects, but it does influence the total reactor power. A power peak is caused but it is quite smooth, and it is reached after about 1 s of transient and without any action the reactor tends to find a new stationary condition. Locally the temperature of the channel where the CR moves rises and the fuel temperature in the upper part rises as well. However, the average core outlet liquid temperature has a variation of about 1°C, even less at the core inlet.

In the following figures the main parameters governing the transient have been plotted: the core and HSGs exchanged power, fuel and clad temperatures at different elevations for element 111 (*i.e.* where the CR is ejected), pressure evolution in the pressuriser, UP, temperatures in HL and CL, average core outlet temperature and reactivity.

Case 4 – VVER: Table 1. Imposed sequence of main events

Event description	Time(s)
One CR ejection of bank no. 6	0.0-0.1
Transient end	10.0

Case 4 – VVER – Figures

Figure 1. Position of all the CRs and of the CR ejected

Red = CR fully withdrawn, orange = CR bank no. 10 partially inserted

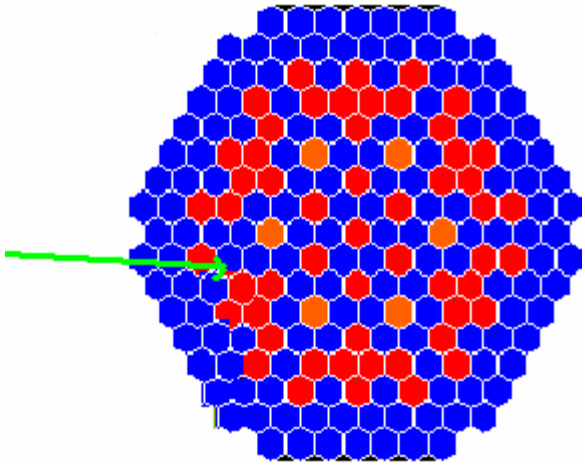

Figure 2. Core and HSGs exchanged power

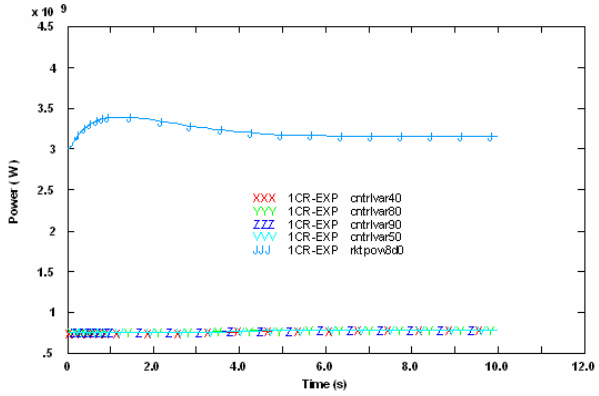

Figure 3. Pressuriser and UP pressures

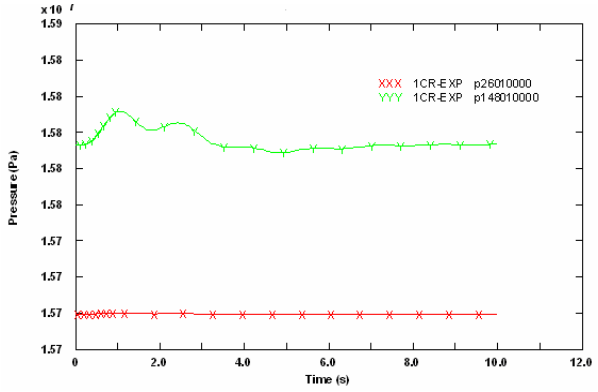

Figure 4. HL temperatures

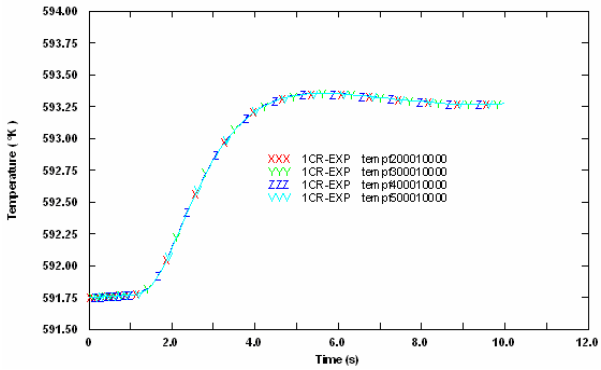

Figure 5. CL temperatures

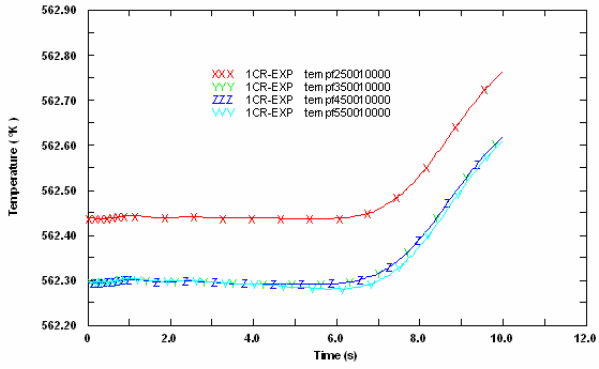

Figure 6. Average core outlet liquid temperature

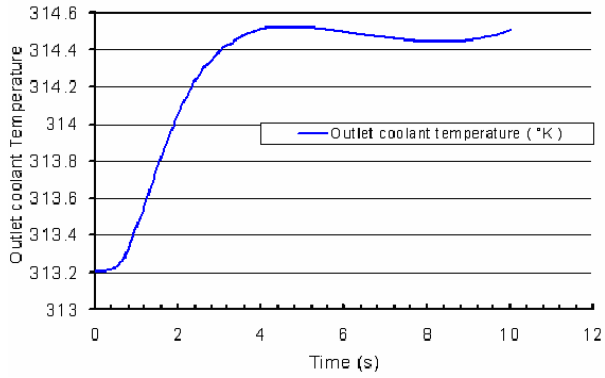

Figure 7. Reactivity

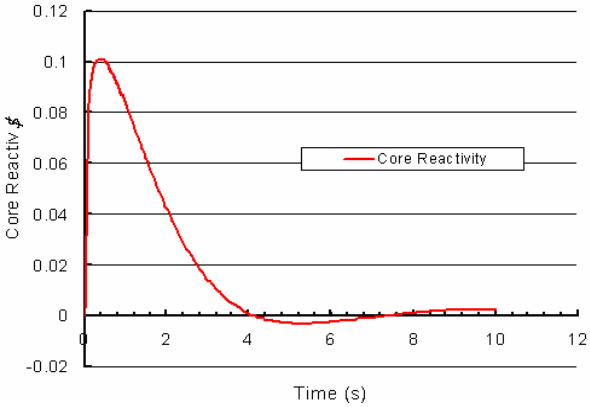

Figure 8. Clad temperatures at various axial planes

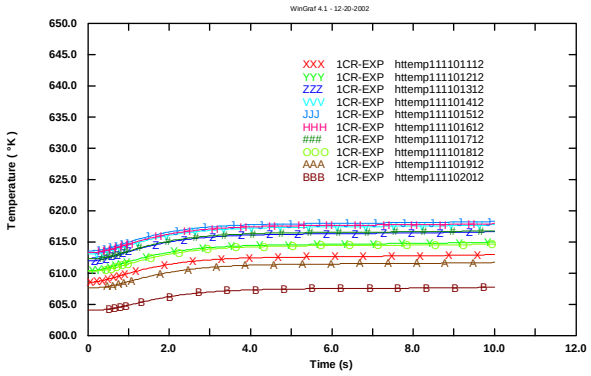

Figure 9. Fuel temperatures at various axial planes

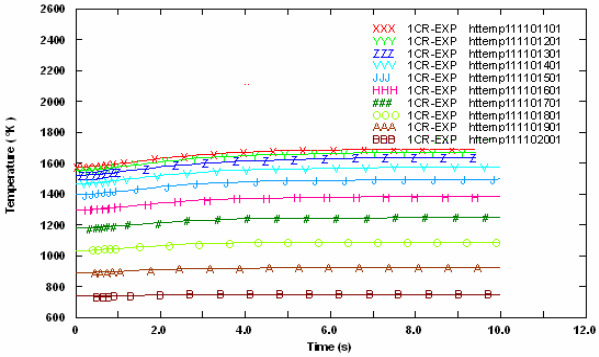

I.3.5 VVER-1000 – one CR bank ejection

The reference nuclear power plant considered in the analysis is a generic VVER-1000 as specified in Section I.3.1: the 3-D kinetics/thermal-hydraulics model adopted to perform the analysis is also the same as described therein.

The scenario considered here is the ejection of all six CRs of bank no. 10, when the reactor is at 100% of nominal rated power, and all the other CR are withdrawn. During steady state CR bank no. 10 is about 20% partially inserted into the core. The ejection occurs in 0.1 s. The position of CR bank no. 10 is indicated in Figure 1.

In the figures below the main parameters governing the transient have been plotted: the core and HSGs exchanged power, fuel and clad temperatures at different elevations for element 108 (*i.e.* the hottest channel), pressure evolution in the pressuriser and UP, the temperatures in HL and CL, core average fuel temperature and reactivity.

Case 5 – VVER: Table 1. Imposed sequence of main events

Event description	Time(s)
CR ejection of bank no. 10	0.0-0.1
Transient end	10.0

Case 5 – VVER – Figures

Figure 1. Position of all the CRs and of the ejected CR bank no. 10

Red = CR fully withdrawn

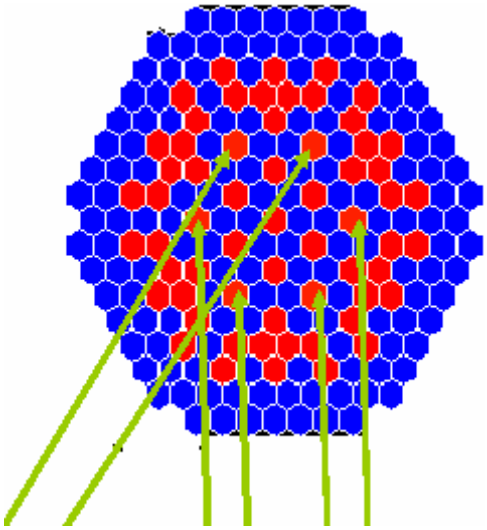

Figure 2. Core and HSGs exchanged power

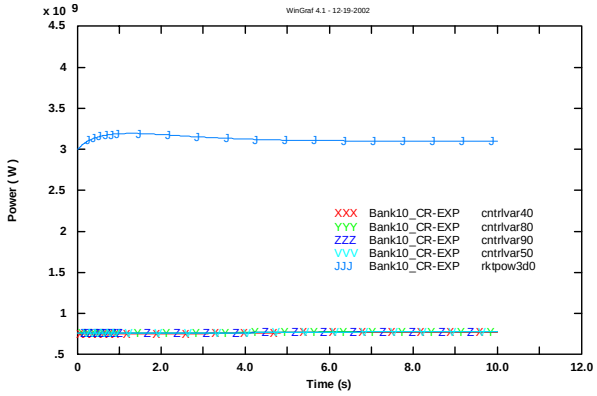

Figure 3. Pressuriser and UP pressures

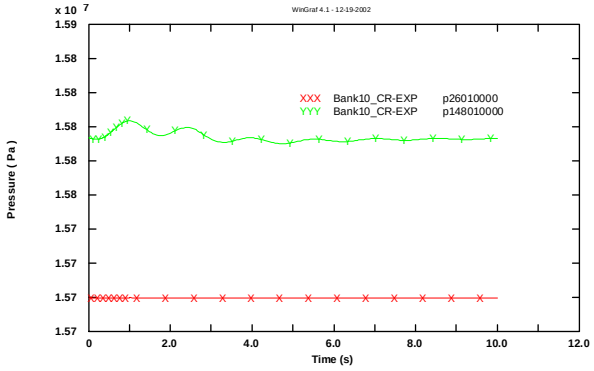

Figure 4. HL temperatures

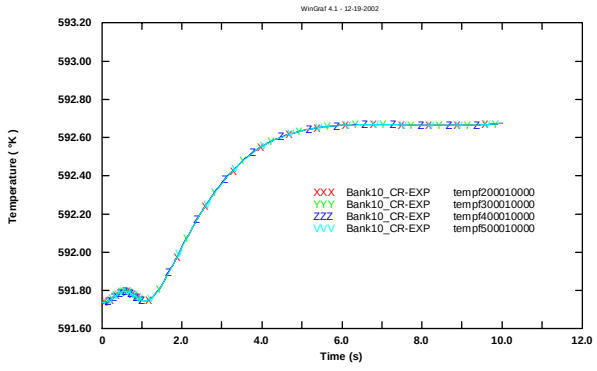

Figure 5. CL temperatures

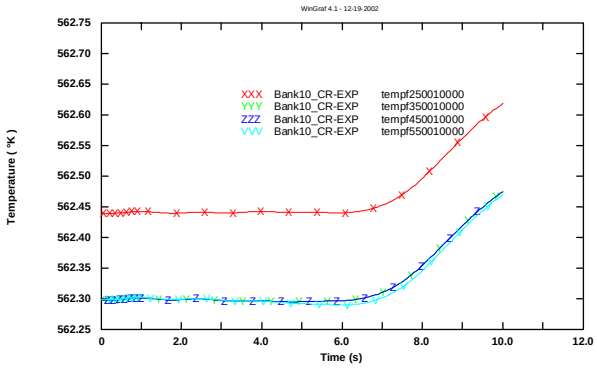

Figure 6. Core average fuel temperature

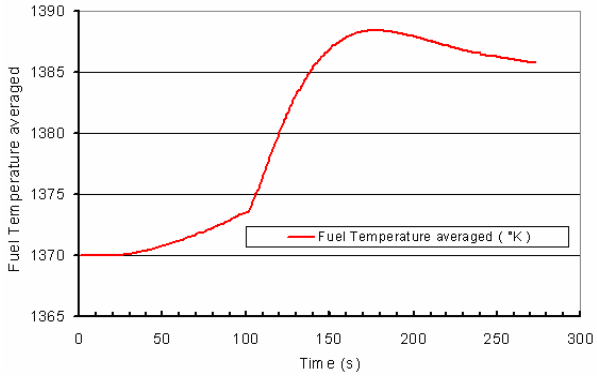

Figure 7. Reactivity

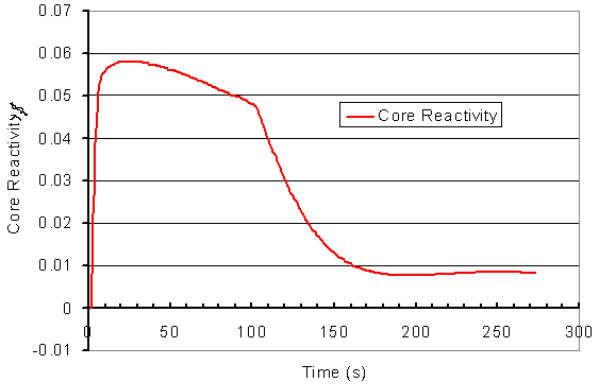

Figure 8. Clad temperatures at various axial planes

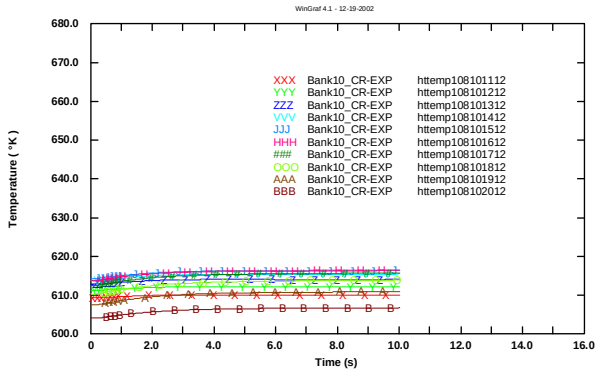

Figure 9. Fuel temperatures at various axial planes

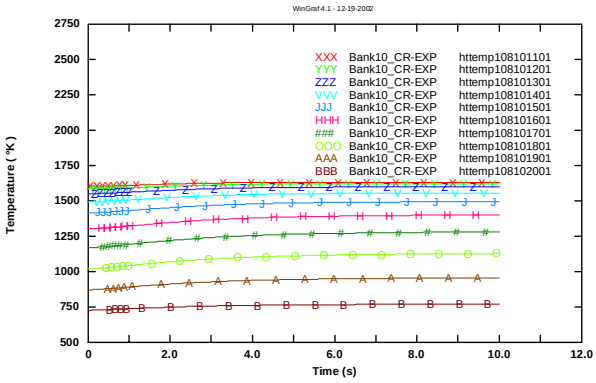

I.3.6 VVER-1000 – MSLB

The reference nuclear power plant considered in the analysis is a generic VVER-1000 as specified in Section I.3.1: the 3-D kinetics/thermal-hydraulics model adopted to perform the analysis is also the same as described therein. The transient analysed is also the same as that described in that section, with an additional scram failure.

Compared to the MSLB transient, in this case the power is not reduced by the scram, but after about 300 s decreases to about 50% of nominal value; this is due to the large decrease of the core inlet flow rate that occurs at that time, and also the temperature at LP increases and introduces negative reactivity, as well as for the Doppler because the fuel temperature is decreasing. The UP temperature increases by about 30°C between 300 s and 350 s of the transient. The maximum clad temperature maintains below 640 K.

In the figures below the main parameters governing the transient the were plotted: core and SG exchanged power, PS mass inventory and SG SS coolant mass, pressuriser and UP pressure, hot leg temperatures, cold leg temperatures and clad surface temperatures of element 108 (hot channel) at the various planes, UP and LP temperatures, core inlet flow rate, pressuriser and SGs collapsed level.

Case 6 – VVER: Table 1. Imposed sequence of main events

Event description	Time(s)
Breaks open	0.0
Reactor trip	Not occurring
MCP trip	Not occurring
Transient end	400.0 s

Case 6 – VVER – Figures

Figure 1. Pressuriser and UP pressures

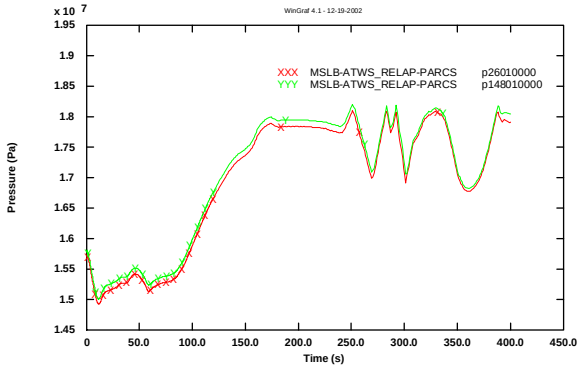

Figure 2. UP and HSGs pressures

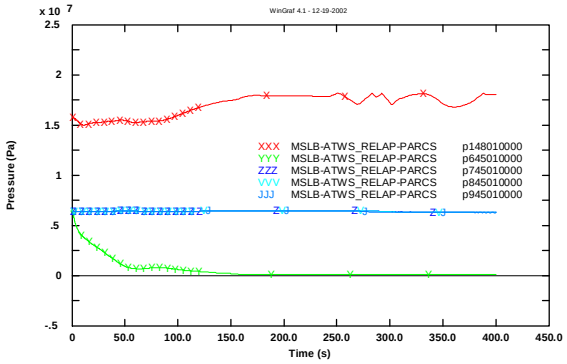

Figure 3. PS mass inventory and SG SS coolant mass

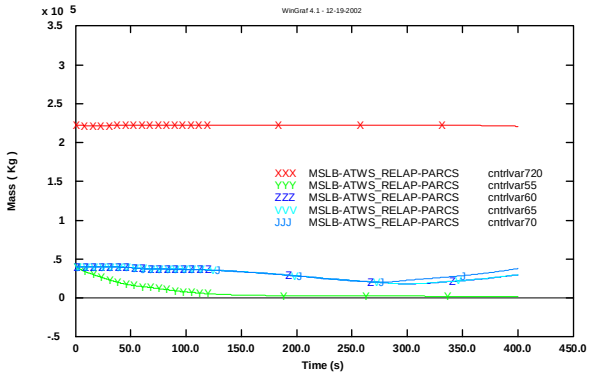

Figure 4. Pressuriser and SGs collapsed level

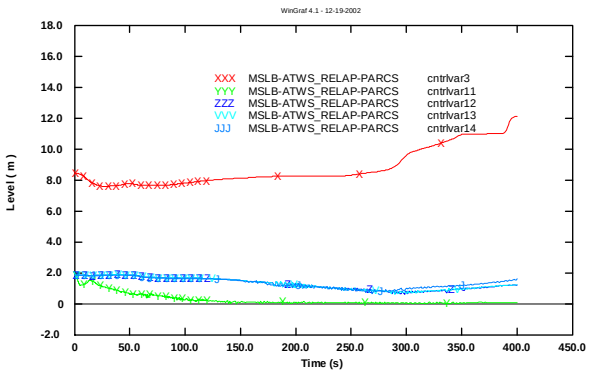

Figure 5. Core inlet flow rate

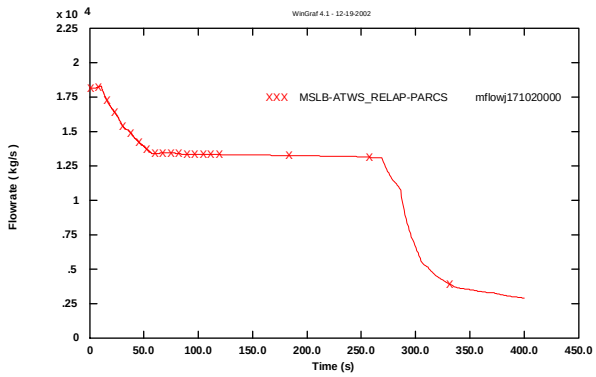

Figure 6. Core and SGs exchanged power

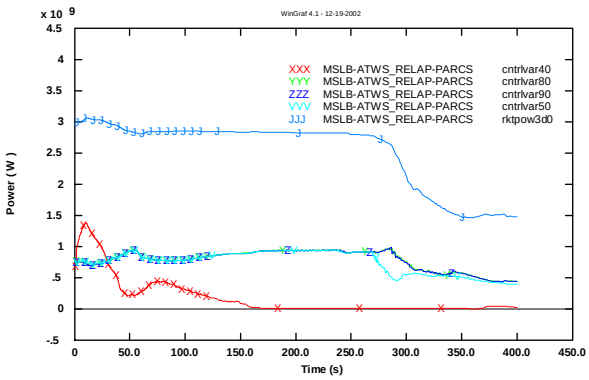

Figure 7. HL temperatures

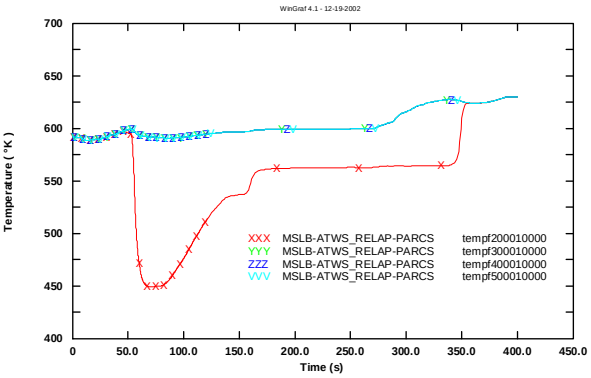

Figure 8. CL temperatures

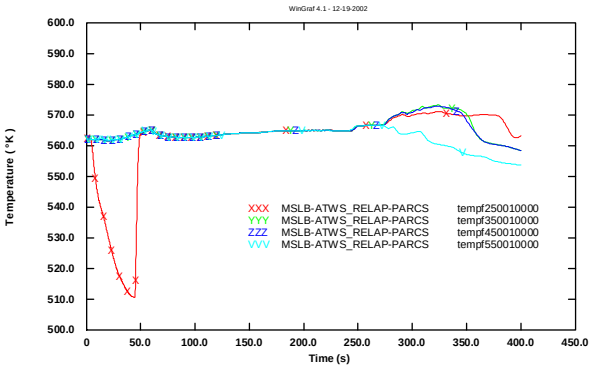

Figure 9. UP and LP temperatures

Figure 10. Clad temperature for element 108 at different axial planes (1-10)

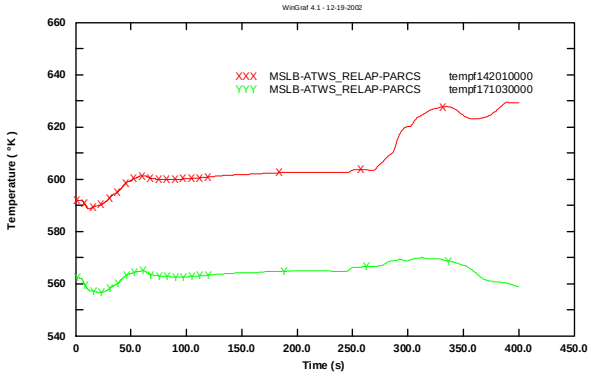

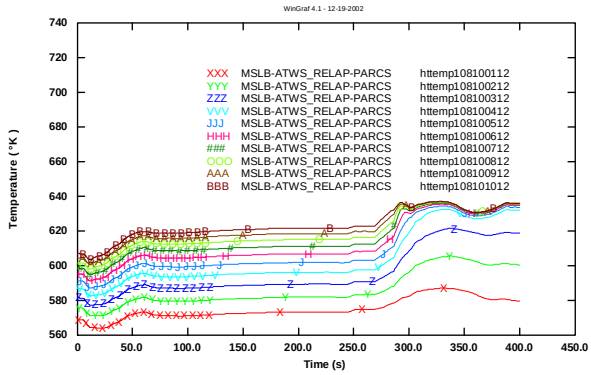

Figure 11. Clad temperature for element 108 at different axial planes (11-20)

Figure 12. Fuel temperature for element 108 at different axial planes (1-10)

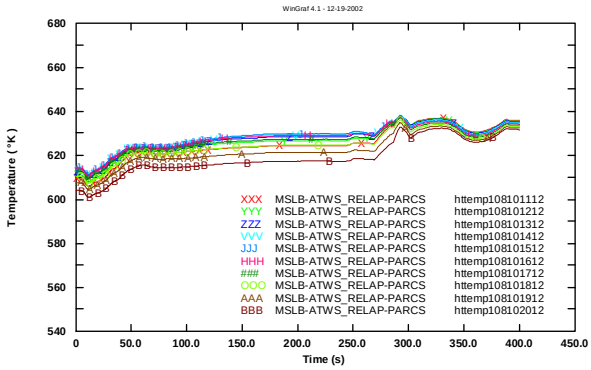

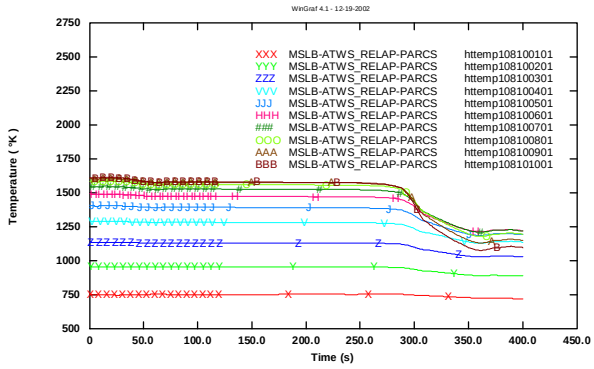

Figure 13. Fuel temperature for element 108 at different axial planes (11-20)

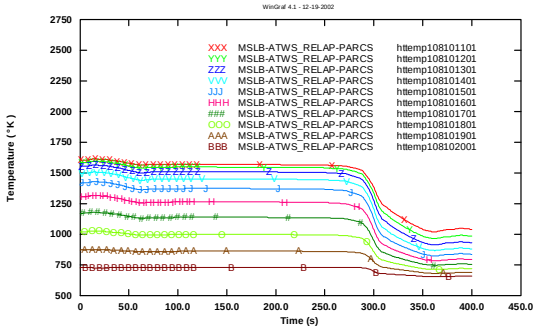

I.3.7 VVER-1000 – SBLOCA

The reference nuclear power plant considered in the analysis is a generic VVER-1000 as specified in Section I.3.1: the 3-D kinetics/thermal-hydraulics model adopted to perform the analysis is also the same as described therein.

The transient envisioned is a small break loss of coolant accident (SBLOCA) that occurs in cold leg no. 4 just before the connection to the DC of the reactor pressure vessel (RPV). The break simulated has a size that is 2% of the CL flow area.

Following the break a fast depressurisation occurs, the LP temperature slightly decreases whereas the power basically maintains constant. After 20 s the scram occurs for low level signal into the SGs. The cladding and fuel temperature are decreased suddenly after the scram occurs.

In the following figures the main parameters governing the transient have been plotted: core power, power exchanged in SG, primary and secondary pressure, pressuriser and SGs collapsed level, LP and UP temperatures, CL and HL temperatures, cladding and fuel temperatures for element 108.

Case 7 – VVER: Table 1. Imposed sequence of main events

Event description	Time(s)
Cold leg break open	0.0
Reactor trip	Not occurring
Transient end	500.0

Case 7 – VVER – Figures

Figure 1. Pressuriser and UP pressures

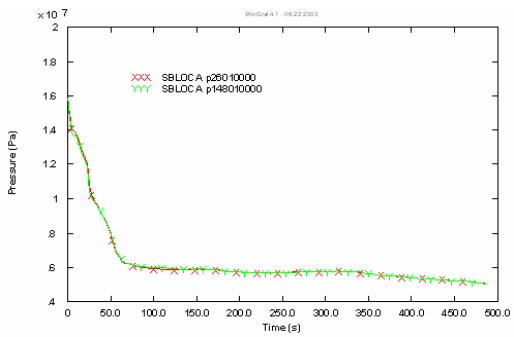

Figure 2. SGs pressures

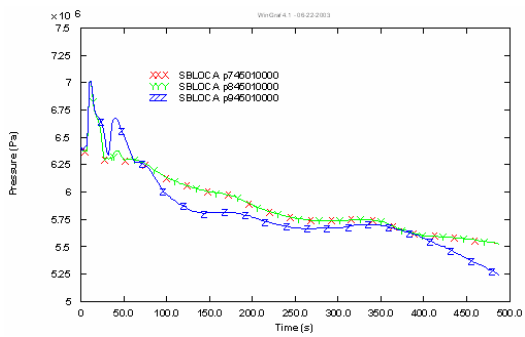

Figure 3. Core and SGs exchanged power

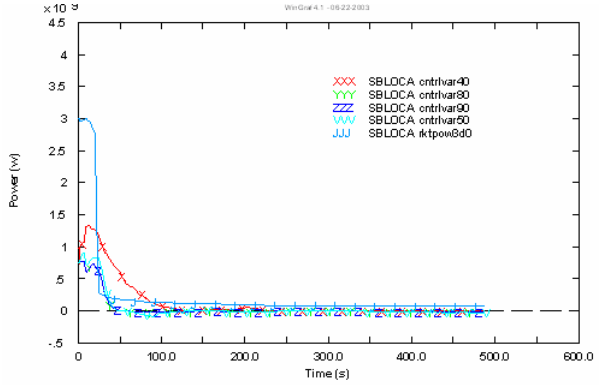

Figure 4. UP and LP temperatures

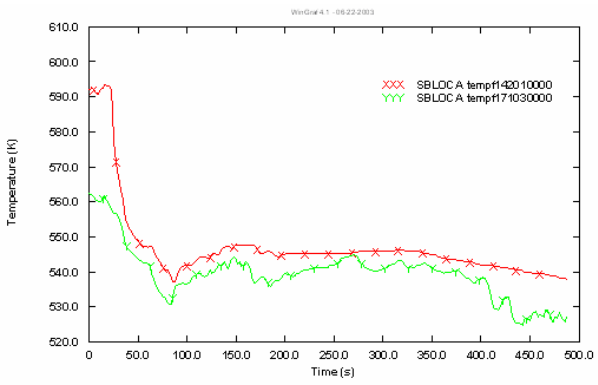

Figure 5. CL temperatures

Figure 6. HL temperatures

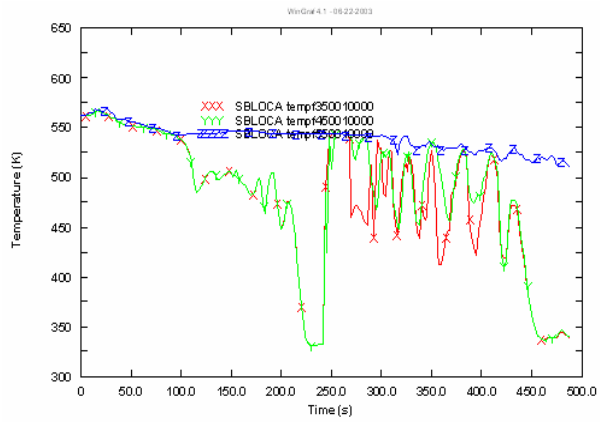

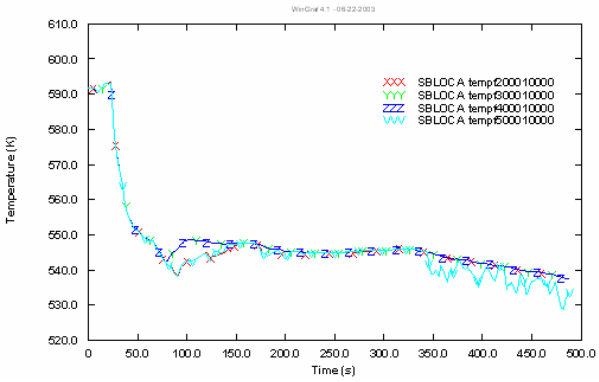

Figure 7. Clad temperature at different axial planes for element 108

Figure 8. Clad temperature at different axial planes for element 108

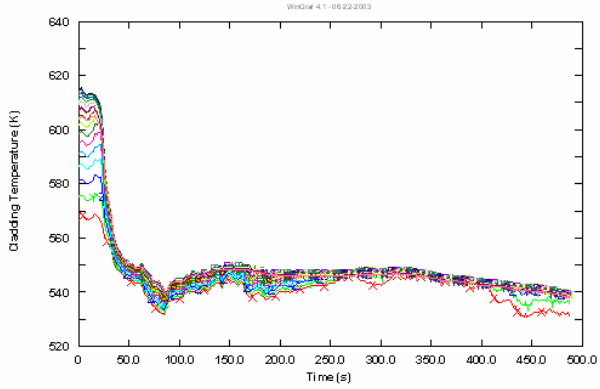

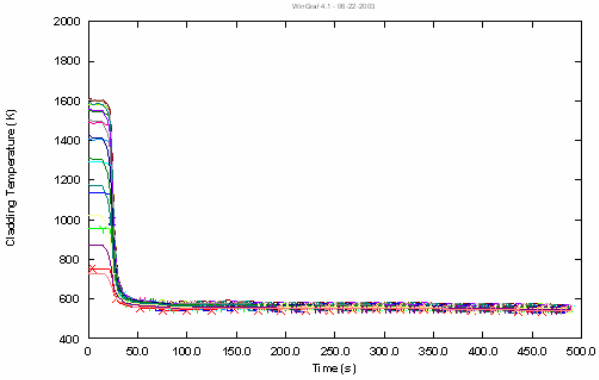

II Energy released to the fuel during REAC accidents

The aim is to evaluate the amount of energy released to the fuel during reactivity-initiated accidents using the results obtained from the analyses carried out by coupled 3-D neutronics/thermal-hydraulic codes. The most severe scenarios for the fuel have been selected (see table below).

NPP type	Type of transients	Max. peak enthalpy fuel (cal/g)	NPP	Codes
BWR	CR bank ejection (eight CR)	78	BWR Peach Bottom	RELAP5/mod 3.3 & PARCS
BWR	One CR ejection (four bundles model)	7.5		
BWR	Pump failure ATWS	3.6		
VVER	CR bank ejection (six CR)	1.2	Generic VVER-1000	
VVER	One CR ejection (multiple bundle model)	24.3		
VVER	MSLB ATWS	0.8		
PWR	MSLB ATWS	38.6	PWR TMI-1	RELAP5-3D© & NESTLE
PWR	De-borated water in loop seal	>120		

The analysis has been executed following the steps below:

- To derive the pin radially averaged temperature at various times.
- To select the heat structures “more severely” interested by the power excursion.
- To calculate the maximum value of enthalpy released into the fuel, multiplying the maximum temperature increase by the specific thermal capacity of the UO_2 (the average value in the interval for fresh fuel).

Predicted/reported values are below the threshold of 170 cal/g (710 kJ/kg), apart from the last case. Reference threshold values are (fresh fuel and non-embrittled clad):

- 170 cal/g for clad damage.
- 200 cal/g for fuel damage.
- Minimum experimental values for pin failures are as low as 30 cal/g (CABRI tests).

Figures

Figure 1. Radial fuel average temperature

BWR – CR bank ejection (8 CR) – RELAP5 & PARCS

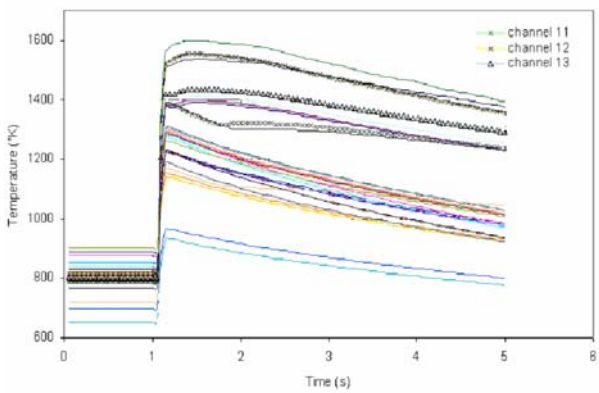

Figure 2. Radial averaged fuel temperature

BWR – one CR ejection (four-bundle model) – RELAP5 & PARCS

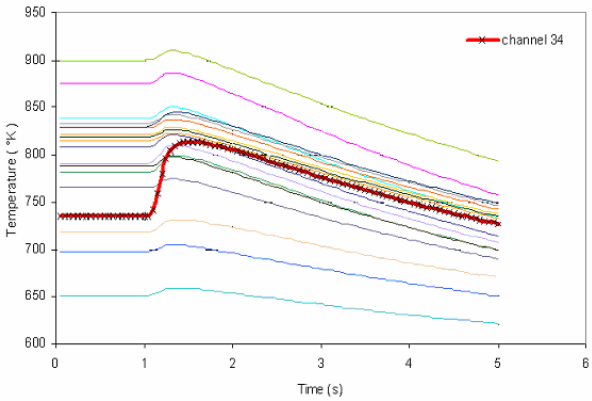

Figure 3. Radial averaged fuel temperature

BWR – pump failure ATWS – RELAP5 & PARCS

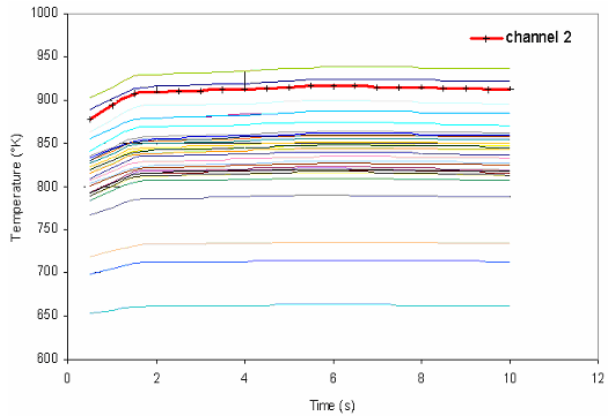

Figure 4. Radial averaged fuel temperature

Generic VVER – CR bank ejection (six CR) – RELAP5 & PARCS

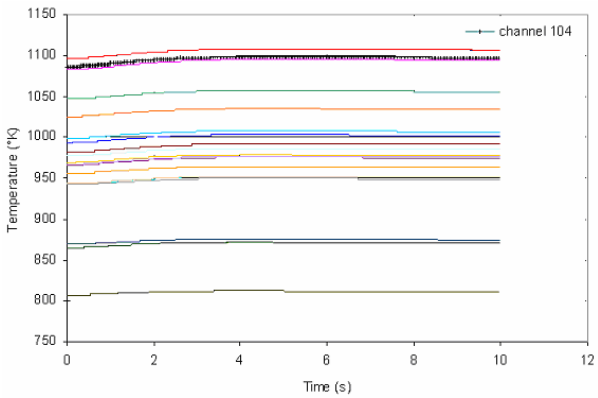

Figure 5. Radially averaged fuel temperature

Generic VVER– one CR ejection (multiple bundle model) – PARCS stand alone

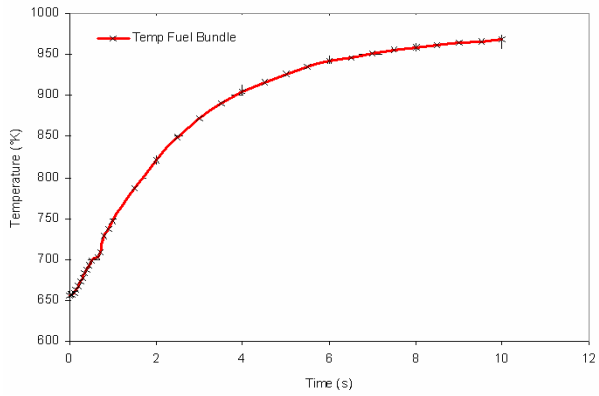

Figure 6. Radially averaged fuel temperature

Generic VVER – MSLB ATWS – RELAP5 & PARCS

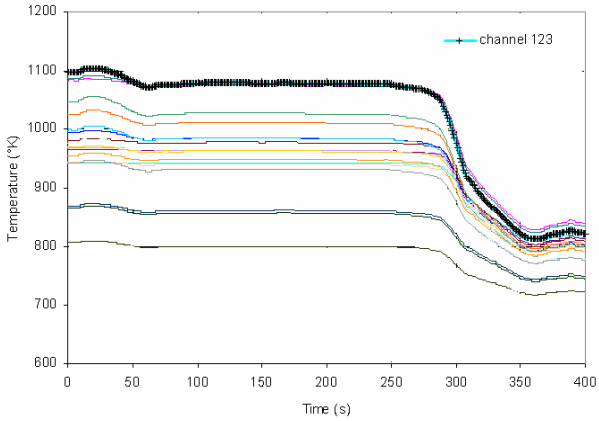

Figure 7. Radially averaged fuel temperature

PWR – MSLB ATWS – RELAP5-3D © & NESTLE

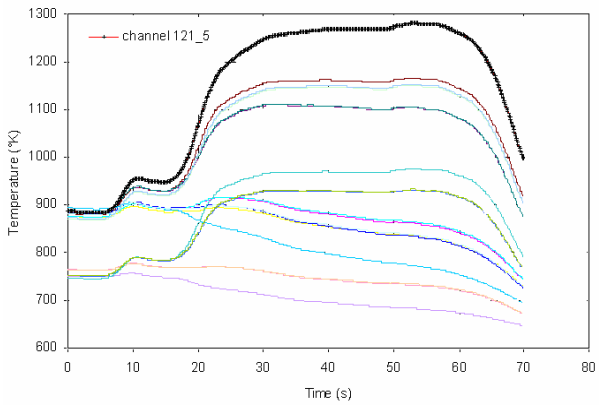

Figure 8. Radially averaged fuel temperature

PWR – de-borated water in loop seal – RELAP5-3D

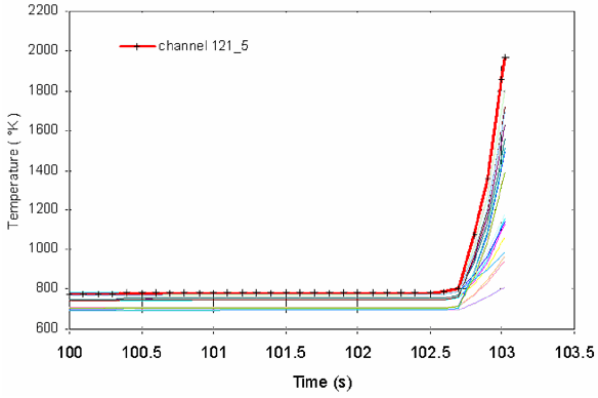

*Annex 1, Part II**

SOME DETAILED SIMULATIONS OF BWR STABILITY INCIDENTS USING NUCLEAR COUPLED THERMAL-HYDRAULICS CODES

Introduction

Several instability events have been observed in BWR plants. Some of them were inadvertent events and other ones were induced intentionally as experiments. These instabilities were identified as periodic oscillations of the neutron flux via instrumentation readings. Essentially, neutronic power signals from local power range monitors (LPRMs) and average power range monitors (APRMs) have been used to detect and study the power oscillations. A wide review of reported instability events can be found in Ref. [3]. We will concentrate our attention on what are known as neutronic/thermal-hydraulic instabilities [2], where a strong non-linear coupling exists between the neutronic and thermal-hydraulic processes via the void feedback reactivity. Mainly, two kinds of neutronic/thermal-hydraulic instabilities in BWR plants have been described, the core-wide (in-phase) oscillations, during which the whole core behaves as one, oscillating the power of all the fuel bundles together, and regional (out-of-phase) oscillations, where half of the core behaves out-of-phase from the other half. That is, when the power rises in one half of the core, it is reduced in the other half so that the average power remains essentially constant. These two kinds of oscillations occurred either separately or overlapped in the same event.

Though there are unique features in each instability event, there are certain common characteristics in all these events, such as the following: All events have arisen under low-flow conditions (30-40% of the rated coolant mass flow) and power levels of about 40-70% of the nominal power. Also, the radial and axial power shapes affect the instability. A strongly bottom-peaked axial power shape makes the core more unstable and a radially-increasing power shape (bowl shape) makes the core susceptible to excite out-of-phase oscillations. Frequencies in all observed oscillations happen to be in a range from 0.3-0.6 Hz, which is correlated with the steam bubble velocity in a hydraulic channel (the concentration wave propagation velocity).

A great deal of work has been devoted to explaining the physical mechanisms underlying the neutronic/thermal-hydraulic instabilities in BWRs [3-9]. In this way, reduced-order models have been proposed to explain the neutronic oscillations. Some of these models are based on an expansion of the neutron flux in terms of spatial modes, which are solutions of the static neutron diffusion equation, the so-called λ-modes [10]. Instead of the λ-modes we can also use the Inhour or ω-modes defined by Henry [11]. The expansion in terms of the λ-modes results in a system of coupled ordinary differential equations for the fundamental and first modes, and this system of equations can be partially decoupled assuming that the generation time matrix is diagonal dominant ($\Lambda_{mn} << \Lambda_{mm}$, $m \neq n$, m, n denoting the mode number). This is a reasonable assumption from the physical point of view [6]. Therefore, we will use the λ-modes expansion.

Using a modes expansion model, the in-phase oscillations are associated with the amplitude of the fundamental mode, and the out-of-phase oscillations are related to the contributions of the first

* Part II was omitted from the printed version of the publication, as it was not available at the time of printing.

subcritical modes (for a critical reactor the higher modes are subcritical ones). But it still remains as an open question to provide the detailed mechanism by which the reactor core under unstable conditions develops an in-phase oscillation, an out-of-phase oscillation or both [12-14].

With the aim of better understanding the instability development process, we studied the stability behaviour of different operational points of the nuclear power plant (NPP) Leibstadt (cycle 7 and cycle 10) with the Studsvik-Scandpower system code RAMONA3-12 (for the theoretical background of this code see Ref. [15]). At one of the operational points studied a limit cycle corresponding to an in-phase oscillation is developed (cycle 10), and for the others the limit cycle obtained corresponds to out-of-phase oscillations (cycle 7 [16]). With the RAMONA code it is possible to obtain detailed information regarding the state of the reactor for each integration time step. In this way, we obtained, for each time step, the power distribution and the nuclear cross-sections for each of the 648 × 27 NPP Leibstadt (KKL) core nodes (without reflector) with a volume of 15.24 × 15.24 × 15.24 cm^3 and from these values we calculated the different mode feedback reactivities versus time using the λ-modes of the stationary configuration of the reactor, expecting that the time behaviour of the mode reactivities can be used as an indicator for the oscillation type in an unstable reactor state.

We performed a similar analysis for Ringhals 1 NPP benchmark case analysis (cycle 14, case 9), which corresponds to a fully developed out-of-phase oscillation.

The coupled codes RELAP5/PARCS and TRAC-BF1/VALKIN were also used to study the unstable behaviour of the Peach Bottom Unit 2 BWR during the low-flow tests performed in this NPP in 1977. Point 3 (PT3) of these tests was chosen due to its position close to the stability boundary in the power/flow map.

NPP Leibstadt stability tests

In September 1990 a stability test was conducted at the NPP Leibstadt (KKL), addressing among other goals the qualification of the KKL core stability monitoring system [17,18]. The test was performed during cycle 7 reactor start-up. The KKL core in cycle 7 contained only 8 × 8 fuel assemblies supplied by General Electric, apart from four SVEA-64 fuel assemblies supplied by ABB Atom [17].

To test the ability of the monitoring system to cope with demanding operation situations, the power oscillations were deliberately transformed from the in-phase mode into the out-of-phase mode, by changing some control rod positions [17,18]. The control rod movements had a large impact on the spatial power distribution and we will demonstrate that, for a spatial power distribution characterised axially by a relatively strong bottom peak and radially by a higher peripheral (in comparison to the central) power level (the so-called bowl shape), we have to expect out-of-phase oscillations if the core is in an unstable dynamical state.

The search for the instability threshold began by raising the power by withdrawing control rod banks 40 and 38 (see Table 2.1).

The control rod positions are shown also in Figure 2.1, where we represented the number of notches withdrawn for each control rod (48 means that the control rod is completely out, 0 means that the control rod is completely in). This signal recording yielded non-stationary LPRM signals (a typical LPRM signal is shown in Figure 2.2). In this figure, we see that after 660 s of measurement time (23:38 h) an unstable oscillation started. From the phase shift analysis of two opposite LPRM signals we learn that this oscillation is out-of-phase (Figure 2.3). At ~740 s (~ 23:39 h) the maximal oscillation amplitude was reached and the oscillation was suppressed by decreasing the power. The power history

Table 2.1. Control rod configuration for signal recording 4 (rec4)

KKL c7, rec4: Different control rod configuration for signal recording 4 (rec4). 1 notch = 7.62 cm										
CR-bank / Time	Control rod position notches (absorber rods of control rod bank 36...45 are xy notches withdrawn)									
	36	**37**	**38**	**39**	**40**	**41**	**42**	**43**	**44**	**45**
23:20	*48*	*48*	*10*	*48*	*12*	*0*	*24*	*48*	*42*	*42*
23:32	*48*	*48*	*10*	*48*	*14*	*0*	*24*	*48*	*42*	*42*
23:37	*48*	*48*	*12*	*48*	*14*	*0*	*24*	*48*	*42*	*42*
23:38	*48*	*48*	*14*	*48*	*14*	*0*	*24*	*48*	*42*	*42*
23:39	*48*	*48*	*0*	*48*	*14*	*0*	*24*	*48*	*42*	*42*
23:41	*48*	*48*	*0*	*48*	*0*	*0*	*24*	*48*	*42*	*42*
23:53	*48*	*48*	*10*	*48*	*0*	*0*	*24*	*48*	*42*	*42*

Figure 2.1. Different control rod positions (at 23:27 h, 23:38 h and 23:39 h)

Figure 2.2. Measured LPRM (19:4) signal and power spectral density

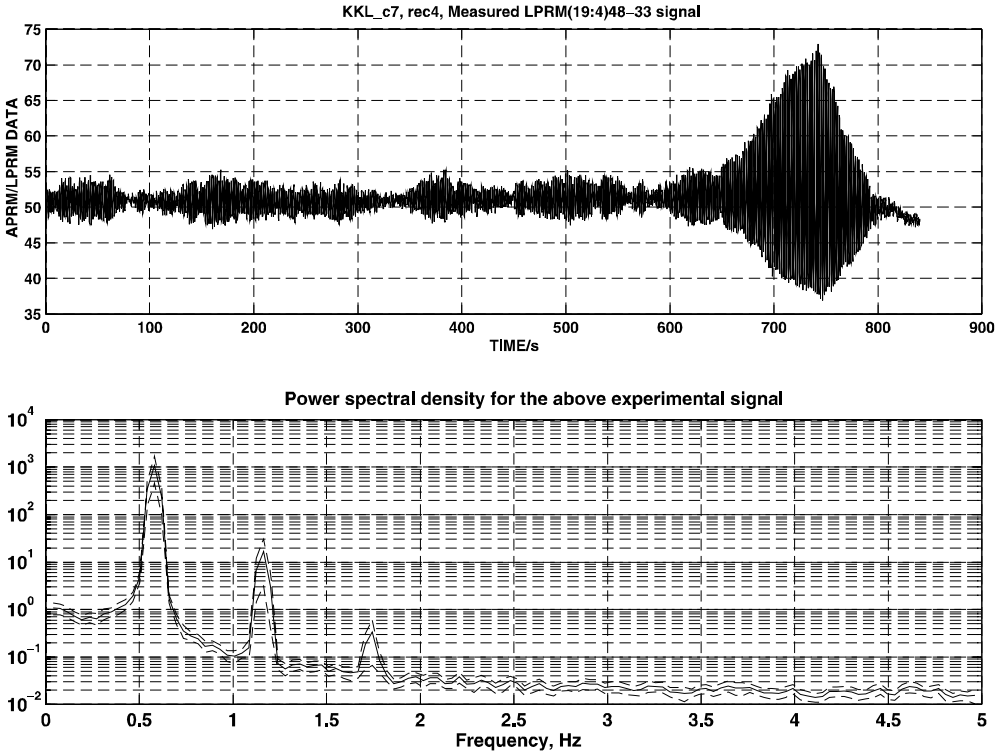

Figure 2.3. Phase shift between two LPRM signals. A 180° phase shift is recognisable at the natural frequency of 0.58 Hz.

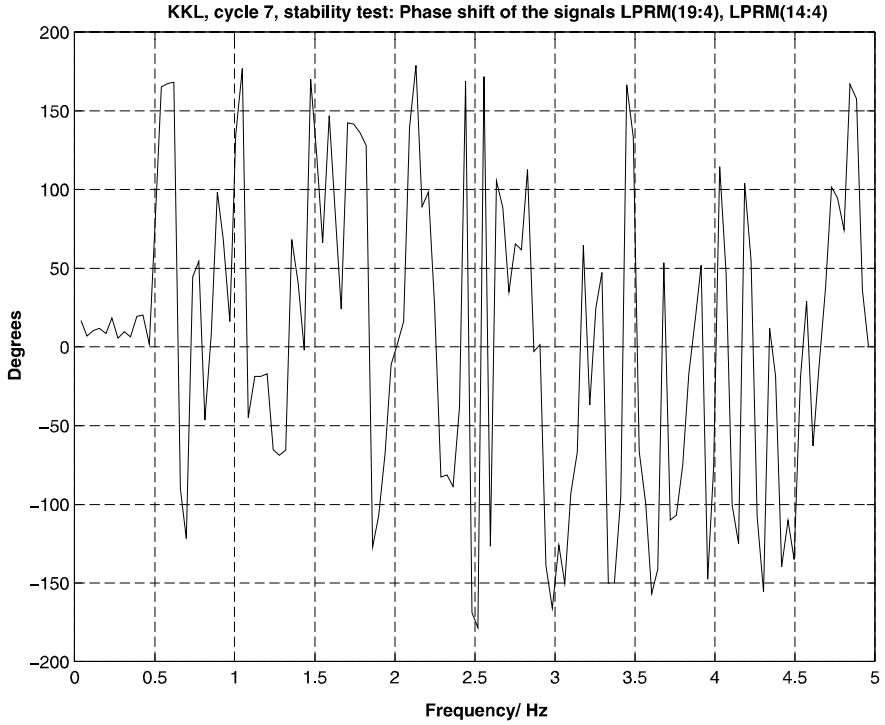

is demonstrated in Figure 2.4. At 23.27 h the reactor power was about 58%. The search for the instability threshold in record 4 began by raising the power, this by withdrawing control rod banks 40 (withdrawn from node 12 at 23:20 h to node 14 at 23:32 h) and 38 (withdrawn from node 10 at 23:32 h to node 14 at 23:38 h) [18]; see Table 2.1 and Figure 2.4. At 23:38 h a power level of about 61% was reached and in the experiment an unstable out-of-phase oscillation started (Figure 2.2). So as to suppressing the power oscillation control rod bank 38 began to be inserted; it was fully inserted at 23:39 h (power level about 60%). But the core configuration at 23:39 h was unstable, and it had a strong tendency to oscillate in an out-of-phase mode. Then control rod bank 40 was also fully inserted and the oscillations were suppressed. At 23:41 h record 4 was terminated.

Figure 2.4. Experimental power history

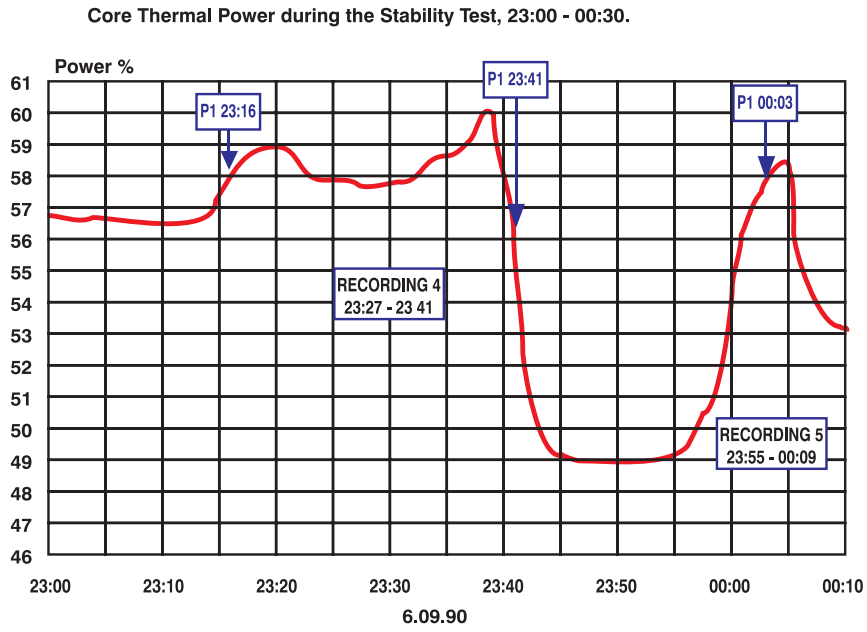

From the phase shift in Figure 2.3 we conclude that the core configuration at 23:39 h had a tendency to excite out-of-phase oscillations. We carried out RAMONA simulations for times 23:27 h (with data for 23:32 h), 23:38 h and 23:39 h with the core configurations given in Table 2.1.

Calculation of the mode feedback reactivities

First of all, we analysed the stability behaviour of the Leibstadt reactor using RAMONA3-12. We used the following operational point data (see Ref. [18], Figure 2.2):

Case A: 23:27 h: 58.0% thermal power, 36.7% mass flow rate
Case B: 23:38 h: 61.0% thermal power, 36.7% mass flow rate
Case C: 23:39 h: 60.5% thermal power, 36.7% mass flow rate

For results comparison we have also analysed an unstable in-phase operational point for KKL, cycle 10, called Case D, and a stable operational point for the same cycle, called Case E. The LPRM locations are presented in Figure 2.5. For all these cases we computed the spatial indices for the power distributions R, RL and the axial peaking proposed in Ref. [5]. The obtained results are presented in Table 2.2.

Figure 2.5. LPRM locations

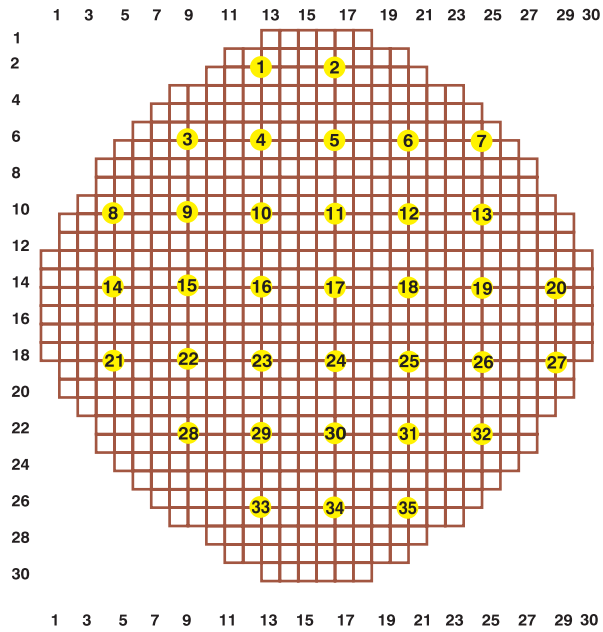

Table 2.2. Spatial indices, R, RL, axial peaking factors

Case	R	RL	Axial peaking (at node)
Case A	1.0734	0.9976	1.605 (4)
Case B	1.0747	0.9933	1.546 (4)
Case C	1.0622	1.0152	1.750 (4)
Case D	1.0918	0.9802	1.545 (4)
Case E	1.0887	0.9771	1.356 (4)

Cases A and B of cycle 7 seem to be stable points (see Figure 2.6). The oscillation amplitude is very small and quite irregular, and it seems to be a numerical fluctuation. The RL values are slightly lower than 1.0 (flat radial power distribution) and the axial peaking values are lower than obtained for Case C value (Table 2.2). Case C is clearly unstable (Figure 2.6), and the core oscillates in an out-of-phase mode (Figure 2.7). The RL value for this case is larger than 1.0 (RL = 1.0152, Table 2.2), which means that the radial power distribution is bowl-shaped (higher at the periphery). In Figure 2.7 we drew the core symmetry line which divides the core into two halves having power oscillations with a phase shift of about 180°. The symmetry line orientation is time dependent [17]. At a given time the predicted orientation of the symmetry line can thus be different from the measured one.

Furthermore, we calculated the modal feedback reactivities for Cases A, B, C, D and E using the VALKIN code.

Figures 2.8, 2.9, 2.10, 2.11 and 2.12 show the (dynamical) mode feedback reactivities evolution, $\rho_{00}^{F}(t)$ and $\rho_{01}^{F}(t)$, for the cases analysed. Nevertheless, it should be emphasised that for the feedback reactivity $\rho_{11}^{F}(t)$ we observe a similar behaviour to $\rho_{00}^{F}(t)$, while the reactivity $\rho_{10}^{F}(t)$ behaves similarly to $\rho_{01}^{F}(t)$. In Cases A and B the mode coupling is weak and the fundamental mode reactivity is dominant. In Case C, the coupling reactivities become clearly dominant (Figure 2.10). Figure 2.11

represents the feedback reactivities for Case D. This behaviour is definitively different from the out-of-phase case. The feedback cross-terms $\rho_{10}^{F}(t)$ and $\rho_{01}^{F}(t)$ are no more the dominant terms. Also, the reactivity curves of Case E show a non-dominant coupling reactivity (Figure 2.12). Clearly, Cases C and D show, respectively, fully developed out-of-phase and in-phase oscillations (see also Ref. [19]).

Figure 2.6. LPRM signals for Case A (23:27 h) and Case C (23:39 h).

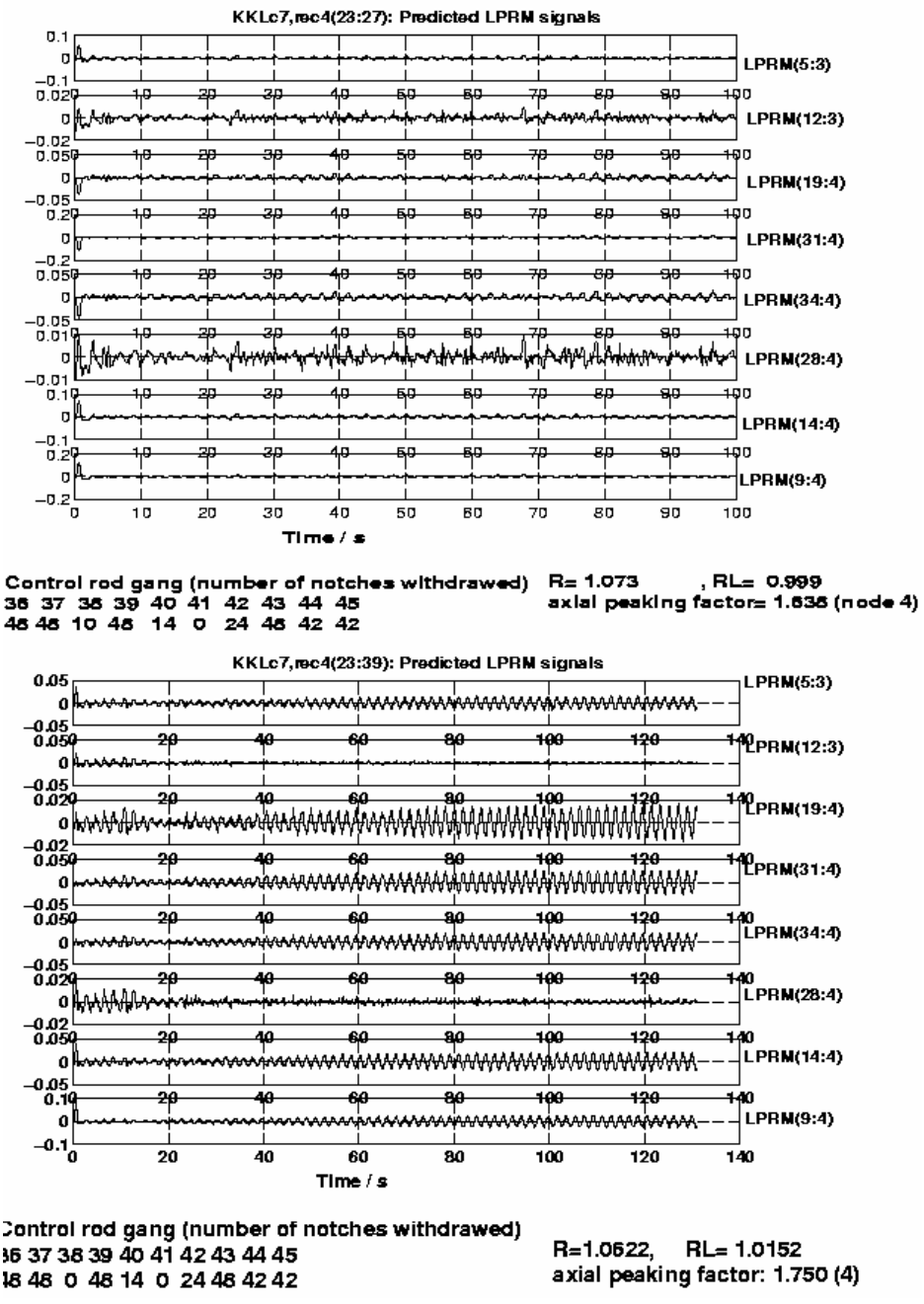

Figure 2.7. Out-of-phase oscillation, Case C

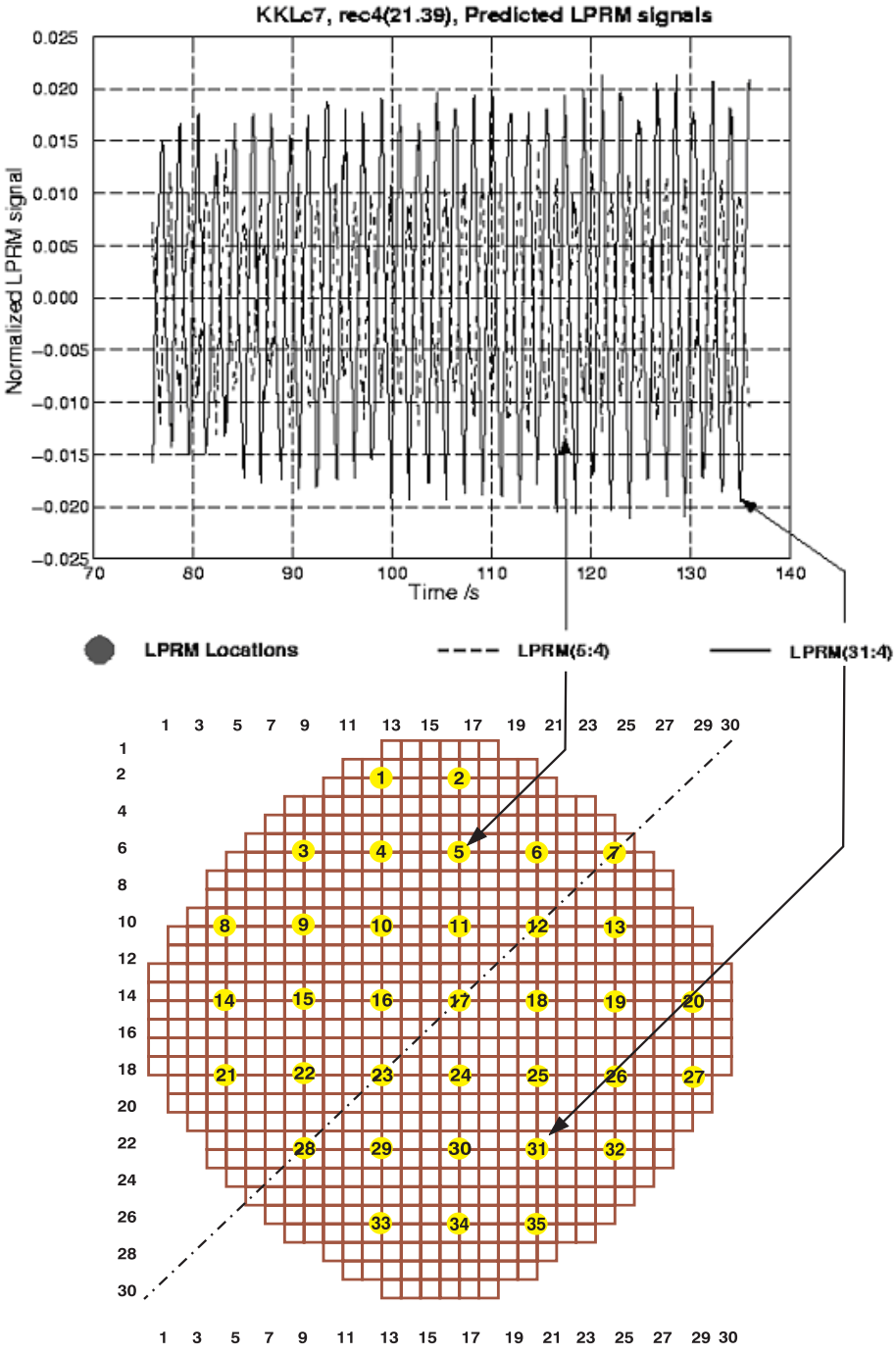

Figure 2.8. Case A (stable): Mode feedback reactivities (fundamental and first mode)

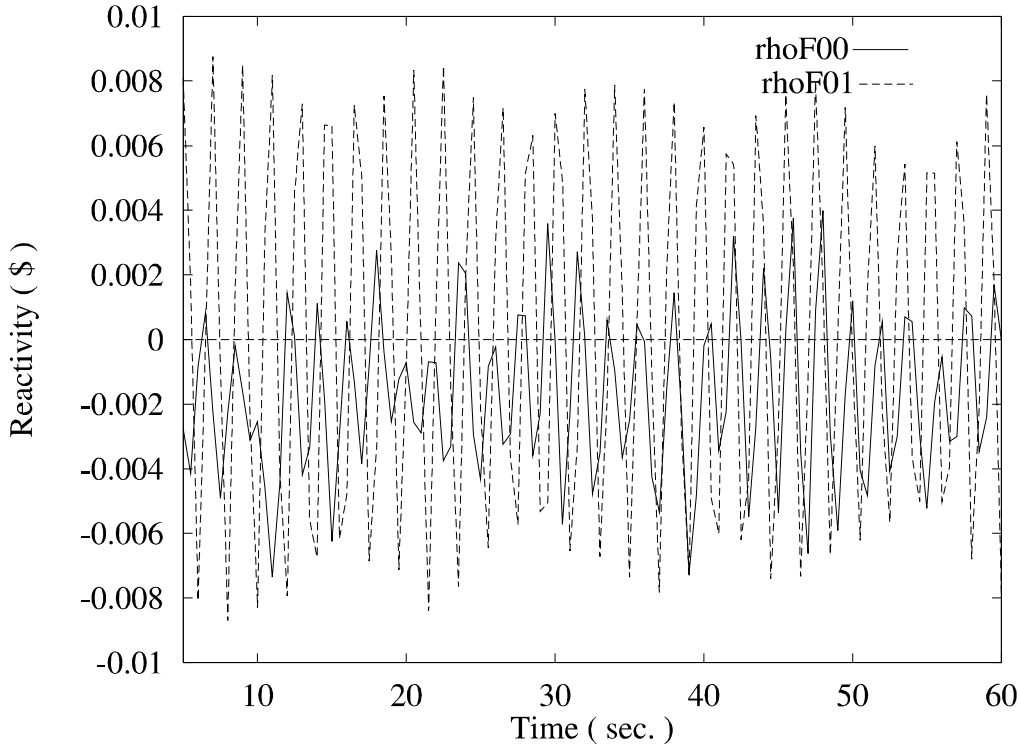

Figure 2.9. Case B (stable): Mode feedback reactivities (fundamental and first mode)

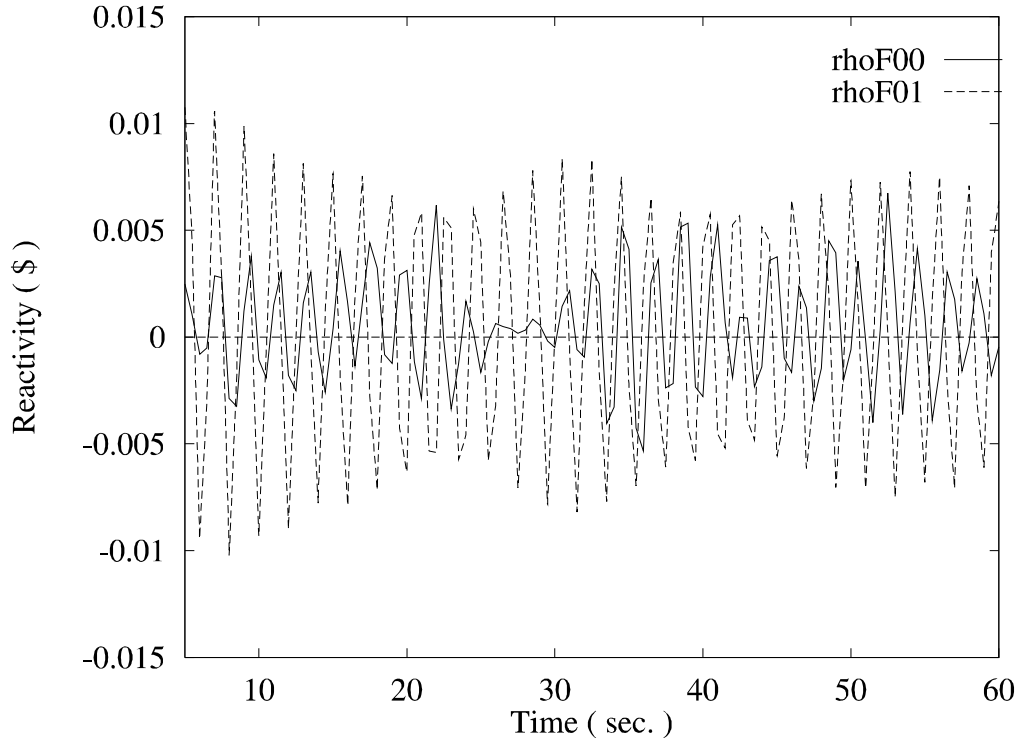

Figure 2.10. Case C (out-of-phase): Mode feedback reactivities (fundamental and first mode)

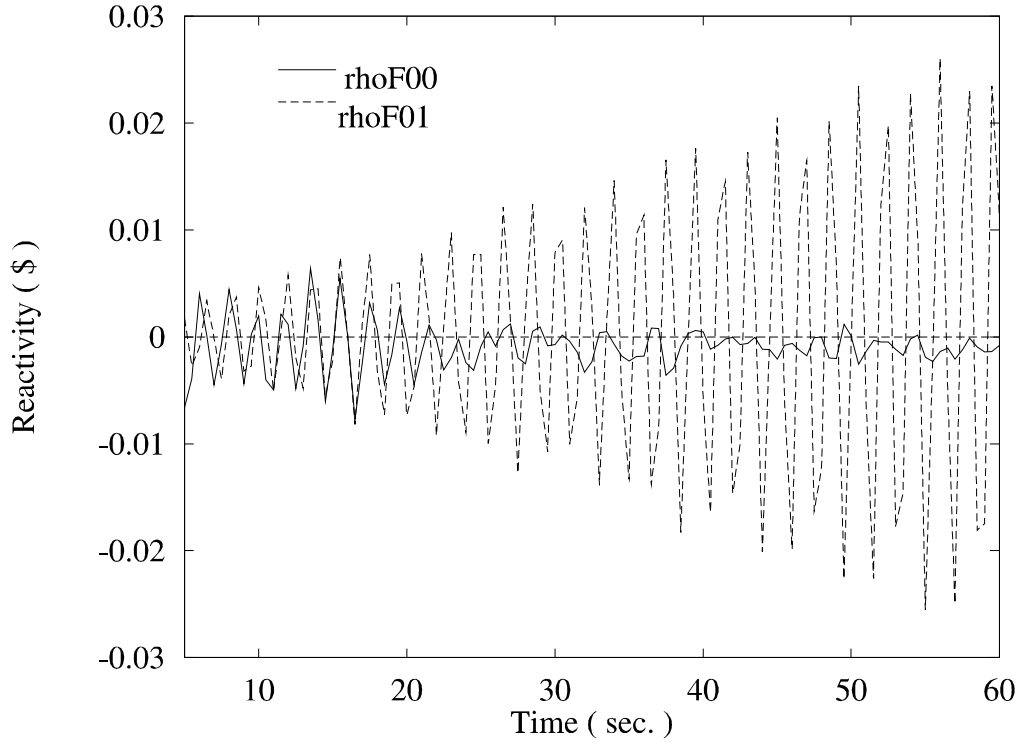

Figure 2.11. Case D (in-phase): Mode feedback reactivities (fundamental and first mode)

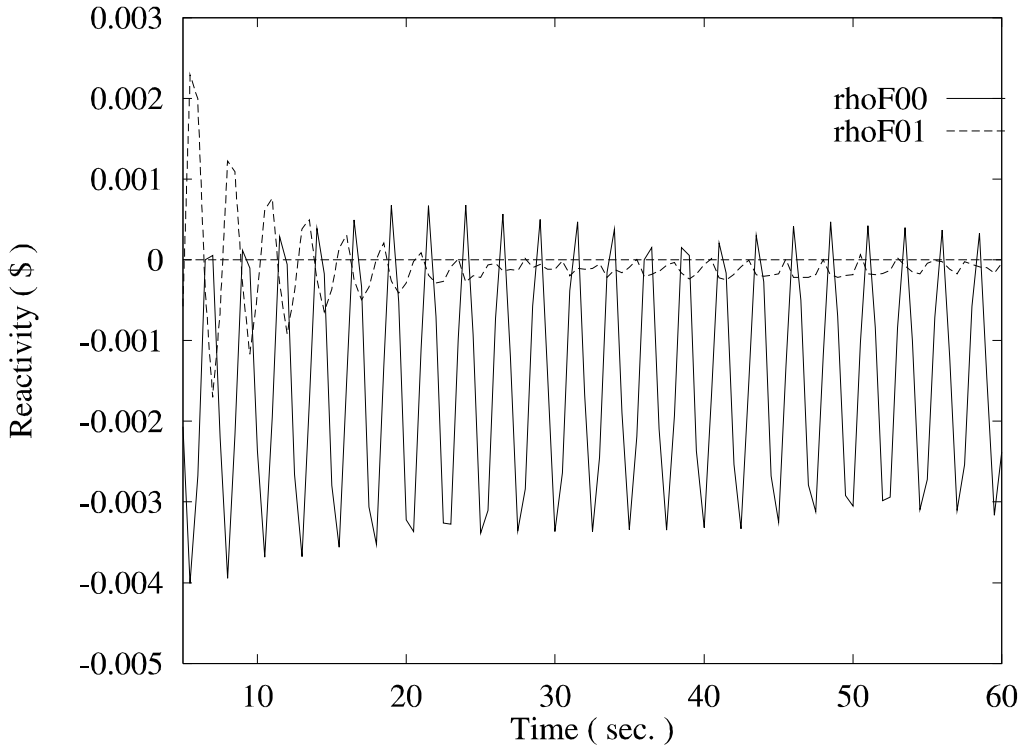

Figure 2.12. Case E (stable): Mode feedback reactivities (fundamental and first mode)

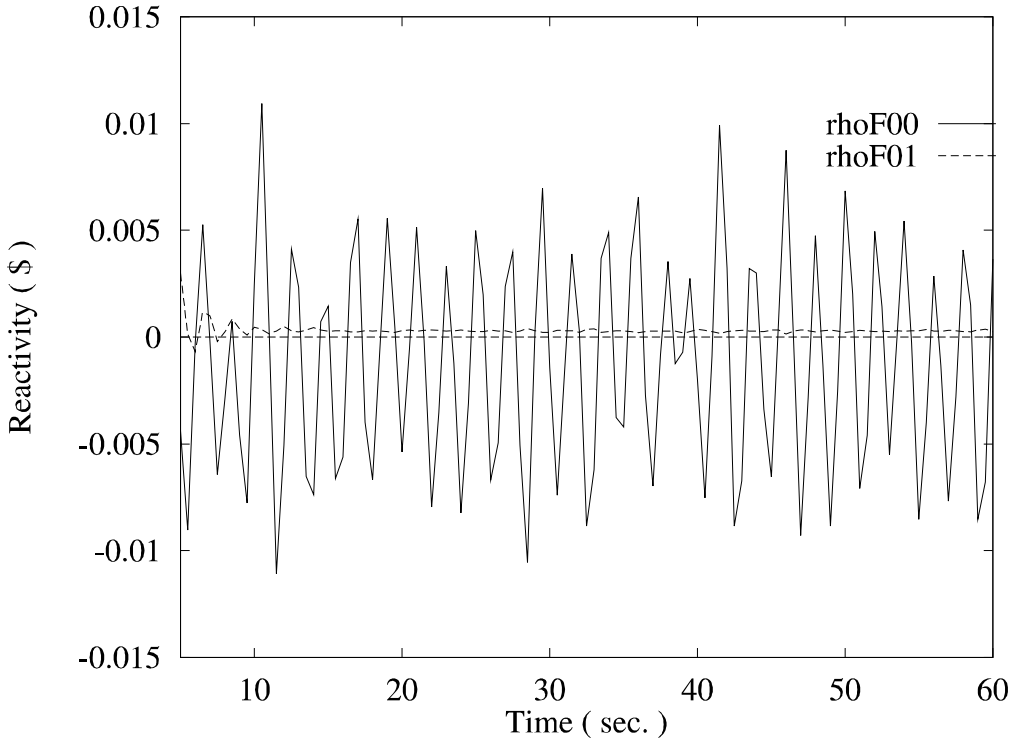

From Figures 2.8-2.12 we can conclude that in an out-of-phase state the mode coupling reactivity is a characteristic indicator.

Finally, we compare the eigenvalue separation for the different modes calculated for the different cases.

Table 2.3 demonstrates that the eigenvalue separation gets its smallest value (~5.7 mK ≅ 1$) for the regional oscillation Case C, but the eigenvalues separation values obtained for Cases A and B are not so different. Nevertheless, for Cases D and E, the differences are larger. We can conclude that the eigenvalue separation is a very sensitive parameter, which only provides relative information about the stability conditions of the reactor core and about the kind of oscillation developed in unstable conditions.

Table 2.3. Eigenvalue separation (ES = (λ_0-λ_m = k_{eff0}-k_{effm}))

Eigenvalue separation			
Case	**λ_0-λ_1**	**λ_0-λ_2**	**λ_0-λ_3**
Case A	5.872×10^{-3}	5.891×10^{-3}	7.179×10^{-3}
Case B	6.083×10^{-3}	6.104×10^{-3}	7.039×10^{-3}
Case C	5.709×10^{-3}	5.732×10^{-3}	8.259×10^{-3}
Case D	6.661×10^{-3}	6.902×10^{-3}	8.281×10^{-3}
Case E	7.285×10^{-3}	7.504×10^{-3}	9.126×10^{-3}

Decomposition of the LPRM signals

Now, we will try to complement the results presented above for the power modal decomposition by considering the information provided by the simulation of the LPRM signals by RAMONA [16].

The LPRMs are positioned between axial and lateral planes corresponding to the reactor discretisation (nodes). The spatial location of the LPRMs across in the core is indicated in Figure 2.5.

For each cell, (*i,j,k*), of the reactor core discretisation, we consider local harmonic power modes:

$$P_{n,i,j,k} = \alpha\left(\Sigma_{f1i,j,k}\phi_{1,ijk,n} + \Sigma_{f2i,j,k}\phi_{2,ijk,n}\right)$$

For a given LPRM, *l*, in the axial level k_l, we define the *n*-th modal power contribution to the LPRM as:

$$LP_{n,l,k_l} = \sum_{i,j,k} P_{n,i,j,k_l}$$

where *i,j* sum over the adjacent nodes to LPRM *l*, as shown in Figure 2.13, and *k* sums over the two axial planes containing the LPRM.

Figure 2.13. Adjacent nodes to LPRM *l*

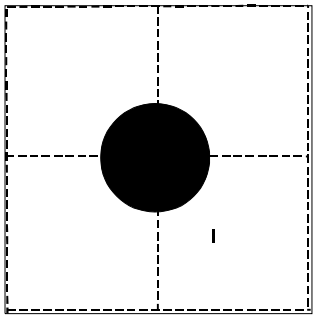

Now, we suppose that the LPRM signals can be expressed as:

$$LPRM_{l,k_l}(t) = \sum_{n} a_n^{k_l}(t) LP_{n,l,k_l} \tag{2.1}$$

We use the fast adjoint modes to construct a weighting factor to obtain the power amplitudes, $a_n(t)$. For each LPRM, (l,k_l), we define:

$$W_{n,l,k_l} = \sum_{i,j,k} \phi^{+}_{1,ijk,n} \tag{2.2}$$

where $\phi^{+}_{1,ijk,n}$ is the average fast *n*-th mode in cell (*i,j,k*), and *i*, *j* and *k* sum over the adjacent nodes to LPRM *l*.

Supposing that the experimental signals $LPRM_{l,k_l}(t)$ are modelled by Eq. (2.1), and using the weights (2.2) for each axial level, k_l, we construct the system of linear equations:

$$\sum_{l} LPRM_{l,k_l}(t) W_{m,l.k_l} = \sum_{l} \sum_{n=1}^{N} a_n^{k_l}(t) LP_{n,l,k_l} W_{m,l,k_l} \tag{2.3}$$

where $m = 0,...,N$, N being the number of considered modes for the power decomposition. Calculating the dominant λ modes for the steady-state configurations corresponding to the analysed cases, we have found, consecutively, the fundamental mode, two azimuthal modes and an axial mode [20]. For a given axial level k_l we cannot obtain information about the axial mode. The number of modes considered is three, the fundamental, ϕ_0, and two azimuthal modes, ϕ_1 and ϕ_2.

For the analysis of Cases C and D, we considered the first axial level of LPRMs. The results obtained for the amplitudes $a_0(t)$, $a_1(t)$ and $a_2(t)$ are shown in Figures 2.14 and 2.15. The same results for the out-of-phase Case C are shown in Figures 2.16 and 2.17.

We observe from the figures that it is possible to obtain the same qualitative information by simply considering the signals from one of the axial levels of LPRMs as is obtained from the detailed nodal analysis, where it is necessary to know the power distribution for all the reactor nodes at each time step.

Ringhals benchmark case analysis

Particularly, we considerer Case 9 (Case G) of Cycle 14, which corresponds to a configuration with 72.6% of the nominal power of the reactor and a core mass flow of 3 694 kg/s [21]. In the benchmark exercise it was stated that this case corresponded to an unstable situation of the reactor with an out-of-phase oscillation fully developed (DR = 0.99) together with a more stable in-phase oscillation (DR = 0.8). Both took place to 0.5 Hz.

Figure 2.14. $a_0(t)$ amplitude for Case D (LPRMs decomposition)

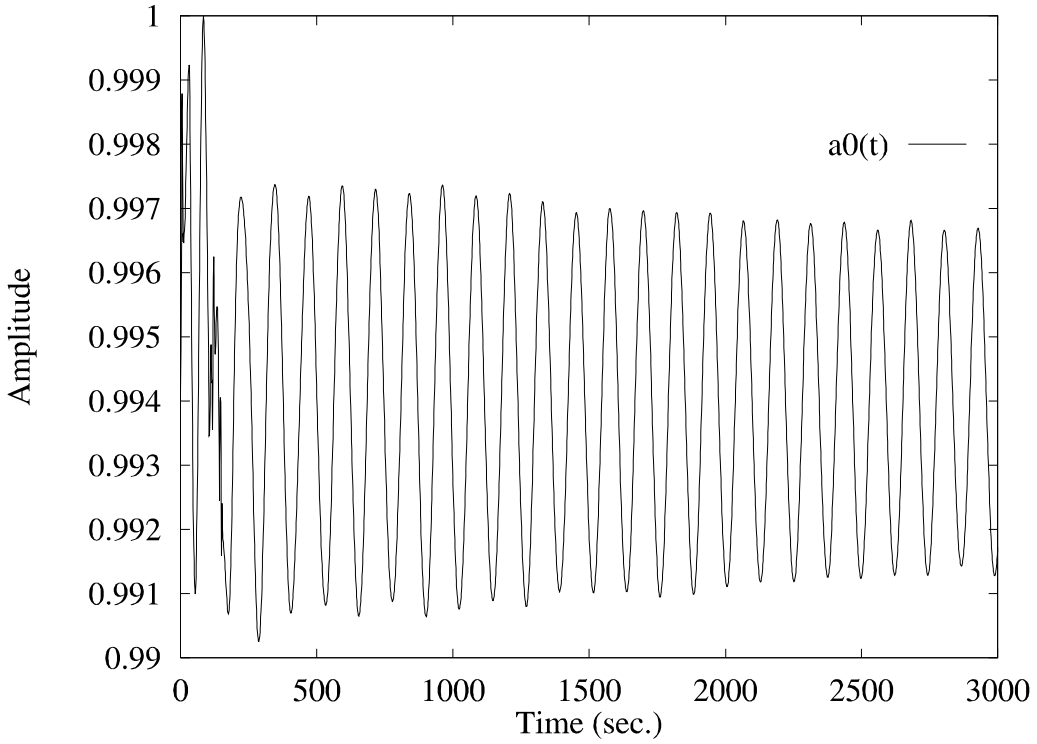

Figure 2.15. $a_1(t)$ amplitude for Case D (LPRMs decomposition)

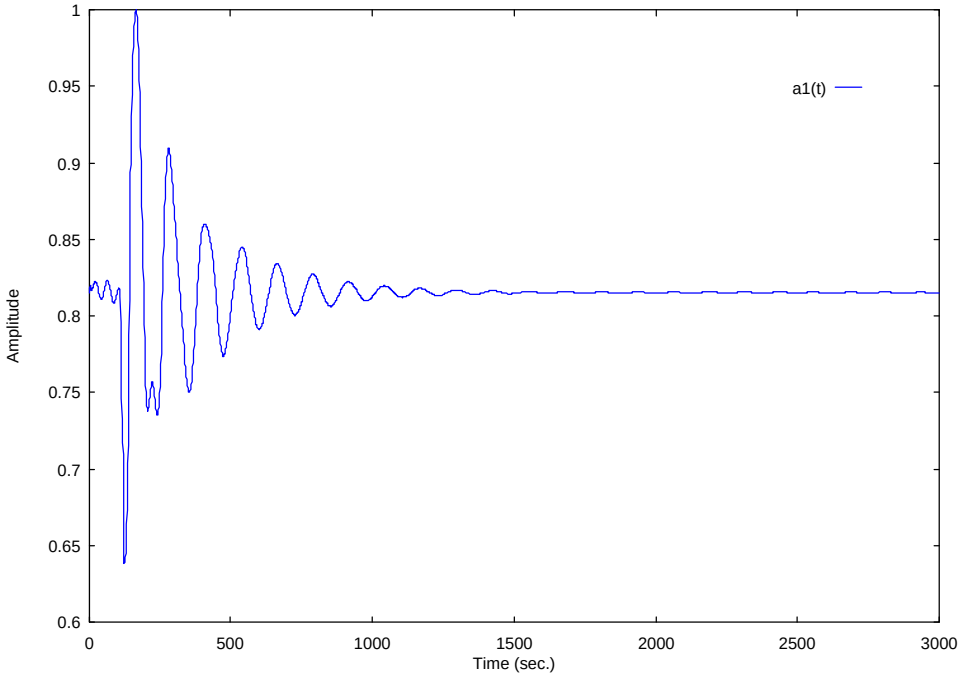

Figure 2.16. $a_0(t)$ amplitude for Case C (LPRMs decomposition)

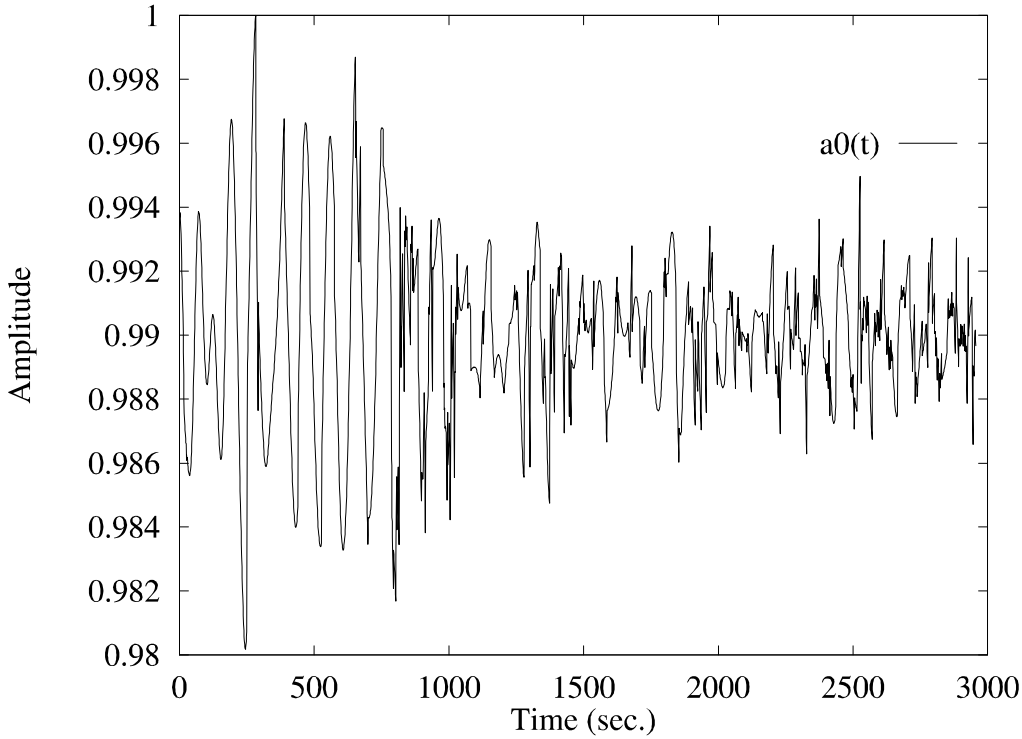

Figure 2.17. $a_1(t)$ amplitude for Case C (LPRMs decomposition)

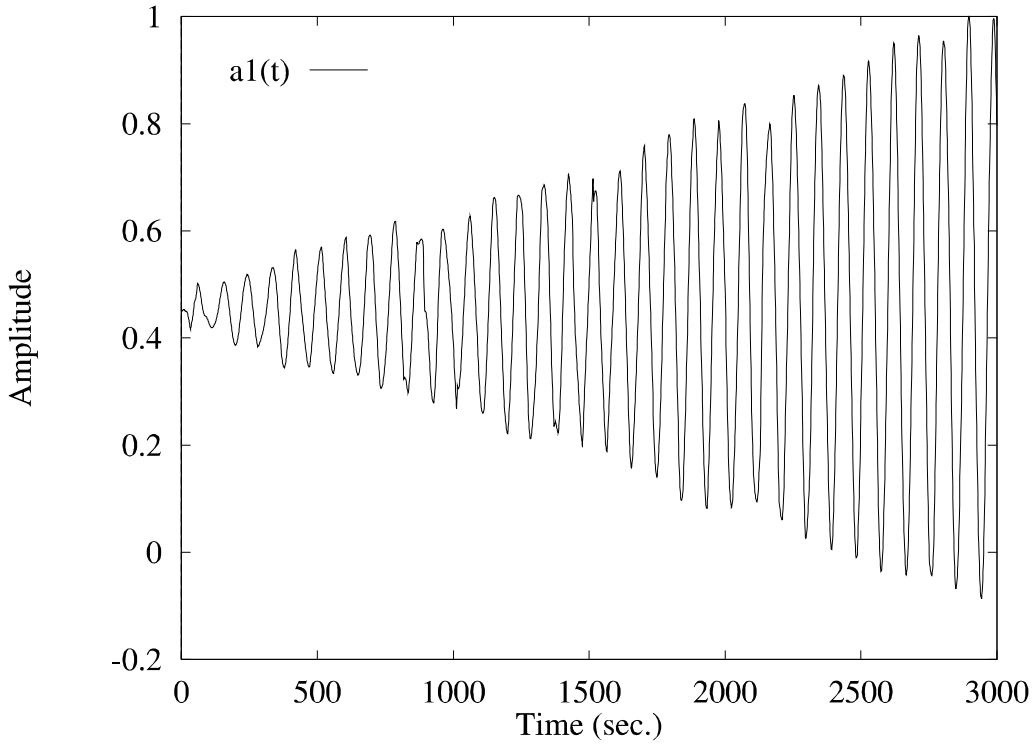

Ringhals 1 reactor core was discretised in 27 axial planes of 14.72 cm length, 25 corresponding to the fuel and one plane at the top and another at the bottom corresponding to the reflector. Each axial plane was also discretised in 15.275 × 15.275 cm cells distributed as shown in Figure 3.1. The cells corresponding to the reflector were also taken into account.

Figure 3.1. LPRMs disposition in an axial plane for Ringhals 1 reactor

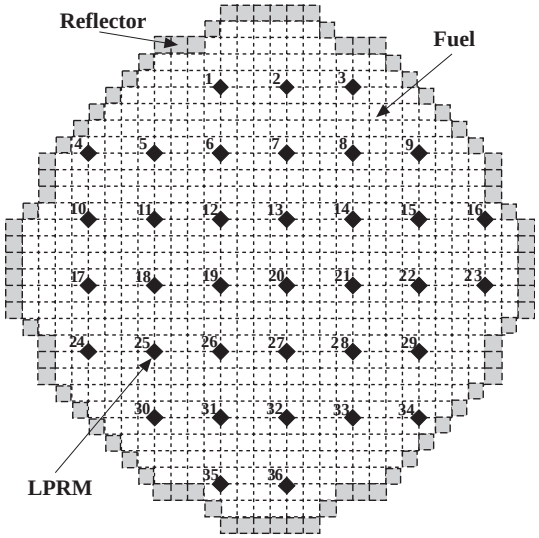

The first five dominant modes for this initial configuration of the reactor core were calculated. In Table 3.1, the values of the obtained eigenvalues are shown.

Table 3.1. Eigenvalues of Ringhals reactor

1.0023	0.9955	0.9940	0.9913	0.9849

The local power profiles associated with the corresponding eigenmodes are represented schematically in Figures 3.2, 3.3, 3.4 3.5 and 3.6.

Figure 3.2. Power profile for the first mode (fundamental mode, radial)

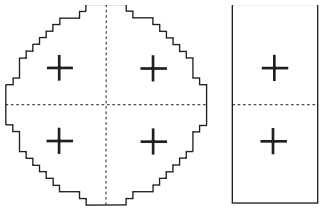

Figure 3.3. Power profile for the second mode (first azimuthal mode)

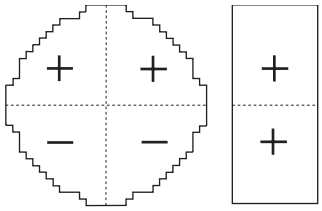

Figure 3.4. Power profile for the third mode (second azimuthal mode)

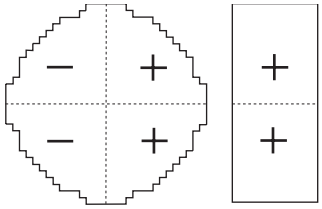

Figure 3.5. Power profile for the fourth mode (axial mode)

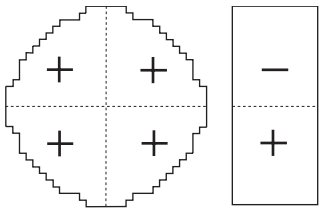

Figure 3.6. Power profile for the fifth mode (third azimuthal mode)

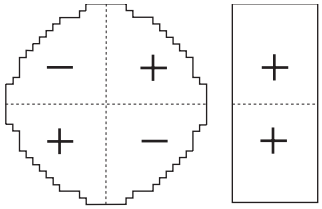

In each representation, the figure on the left shows the signs structure of the relative power map for a generic reactor plane, and the figure on the right gives the signs structure of the axial level, obtaining the signs of the power map multiplying the signs of the plane and the axial level. To simplify the representation the sign structure has been shown spatially symmetric, although this is only approximate, as can be observed in Figure 3.7, where the relative power map corresponding to the axial plane number 11 of the second mode is represented.

Figure 3.7. Power map for the first azimuthal mode. Axial plane 11.

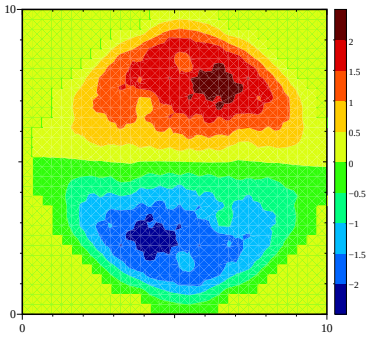

With the provided data for the benchmark exercise, a plant model has been set up for Ringhals 1.

The solution of the transient with the modal method has been obtained using the first five dominant modes. In Figure 3.8 we compare the power evolution for the transient using a standard 3-D thermal-hydraulic code and the modal code. We observe that there is a good agreement between the results provided by both codes.

Figure 3.8. Power evolution calculated with 3-D/TH code and with the modal method

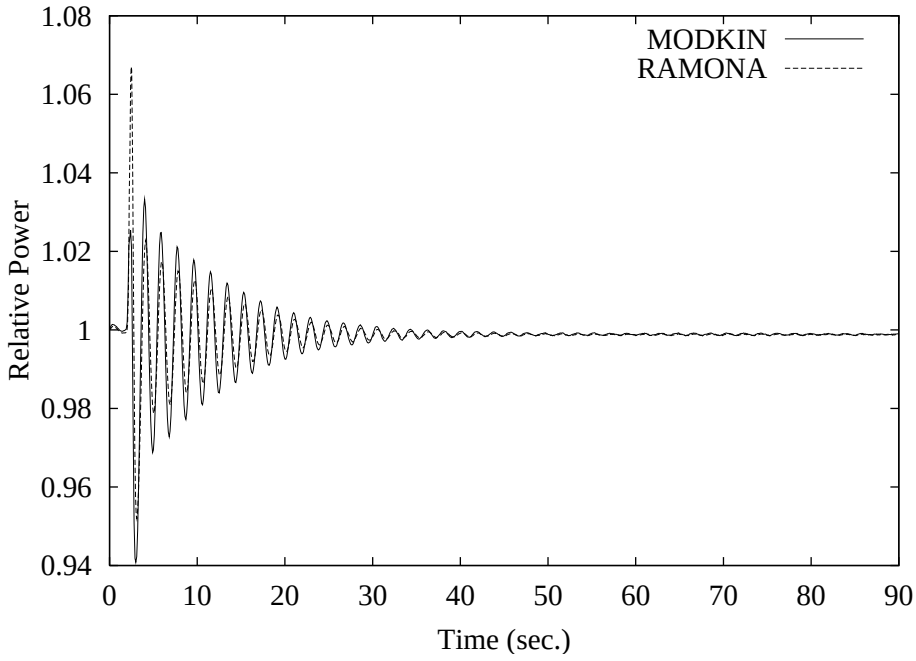

In Figure 3.9, we show the evolution of the amplitude associated with the fundamental mode, $n_1(t)$. In Figure 3.10, we show the evolution associated with the first azimuthal mode amplitude, $n_2(t)$, and in Figure 3.11, we show the evolution of the amplitude associated with the second azimuthal mode, $n_3(t)$.

Figure 3.9. Evolution of the amplitude associated with the fundamental mode

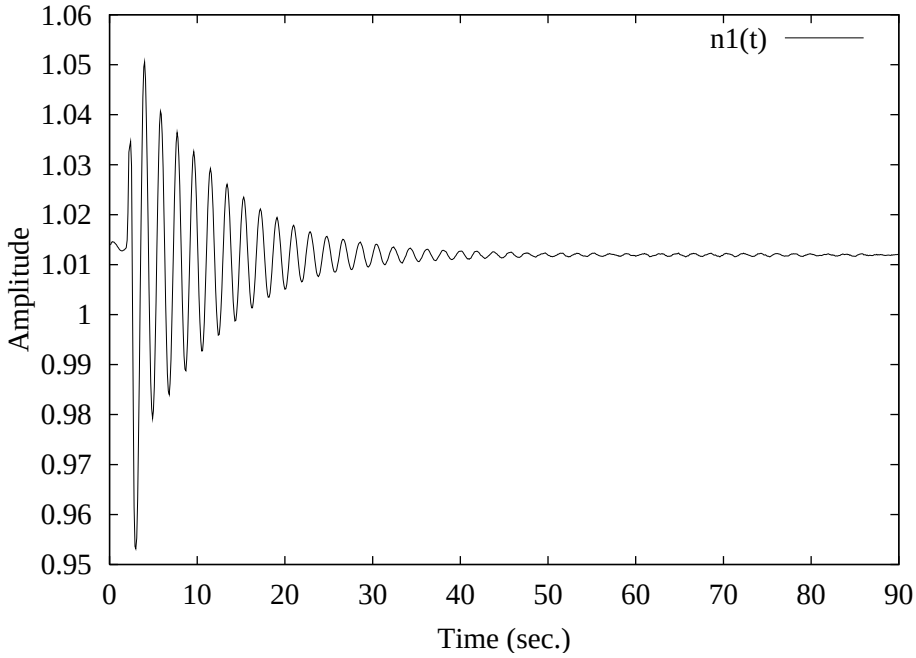

Figure 3.10. Amplitude evolution associated with the first azimuthal mode

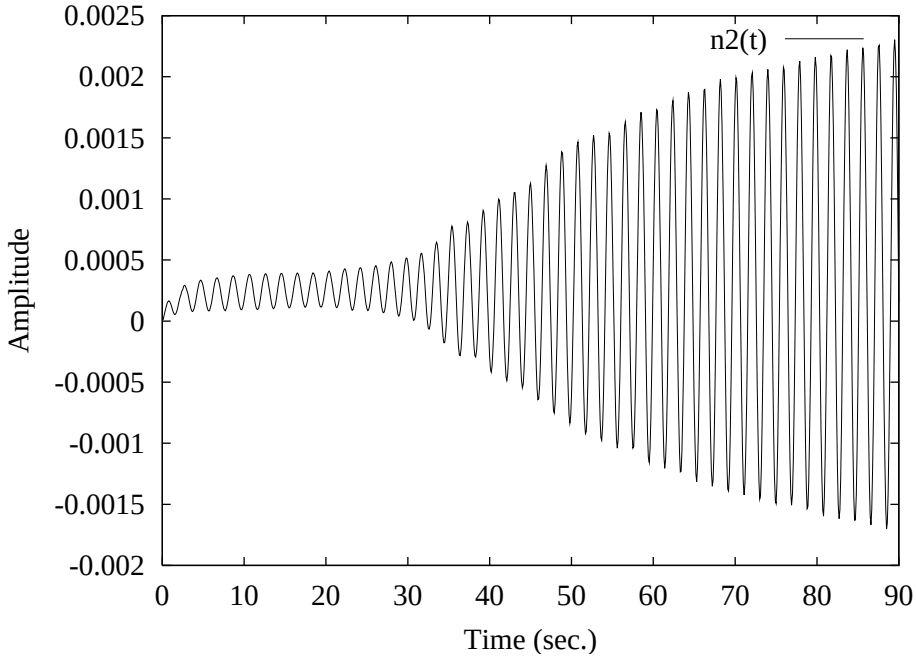

Figure 3.11. Evolution of the amplitude associated with the second azimuthal mode

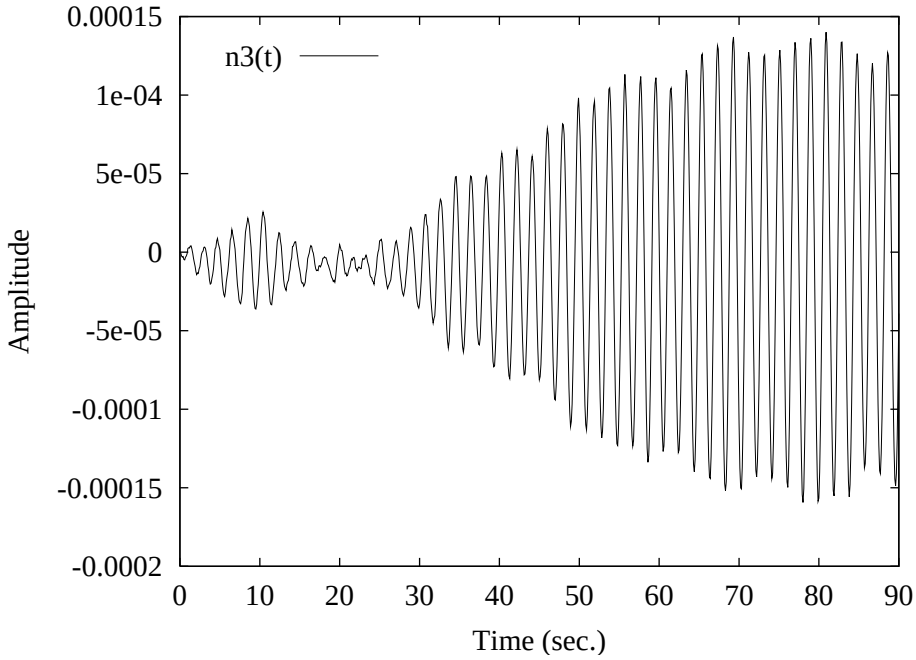

From the curves shown above, we can conclude that this case corresponds to an instability event where the in-phase oscillation, associated with the fundamental mode, is damped, but an out-of-phase oscillation related with the first and second azimuthal modes is developed, as the amplitude of the first azimuthal mode is 10 times larger than the one associated with the second azimuthal mode.

Peach Bottom 2 case analysis

To characterise the unstable behaviour of the Peach Bottom Unit 2 BWR, a number of perturbation analyses were performed: arrangements were made with the Philadelphia Electric Co. (PECo) to conduct a different series of low flow stability tests at Peach Bottom 2 during the first quarter of 1977.

The low flow stability tests were intended to measure the reactor core stability margins at the limiting conditions used in design and safety analysis, providing a one-to-one comparison to design calculations.

The selection of this reactor was based on its being a large BWR/4 which reached the end of its No. 2 reload fuel cycle early in 1977, with an accumulated average core exposure of 12.7 GWd/t.

Stability tests were conducted along the low-flow end of the rated power-flow line, and along the power-flow line corresponding to minimum recirculation pump speed. The actual reactor operating conditions at which the low-flow core stability testing was conducted are listed in Table 4.1 and shown in Figure 4.1 [22].

For the analysis performed in this study, at actual steady-state conditions, point 3 of these low flow stability tests was chosen, in such a way that the reactor state is close to the stability boundary in the power/flow map.

The core neutronic data used in all the calculations are specified in Ref. [23].

Table 4.1. Peach Bottom 2 end-of-cycle 2 tests. Actual low-flow stability test conditions.

Test number	Reactor power		Core flow rate		Core pressure[a]	Core inlet enthalpy
	(MWt)	(% rated)	(kg/s)	(% rated)	(MPa)	(kJ/kg)
PT1	1 995	60.6	6 753.6	51.3	6.89	1 184.61
PT2	1 702	51.7	5 657.4	42.0	6.84	1 187.78
PT3	1 948	59.2	5 216.4	38.0	6.93	1 184.61
PT4	1 434	43.5	5 203.8	38.0	6.89	1 183.83

[a] Based on process computer edit (P1), corrected for steam separator pressure drop.

Figure 4.1. Peach Bottom 2 low flow stability tests. Actual test conditions.

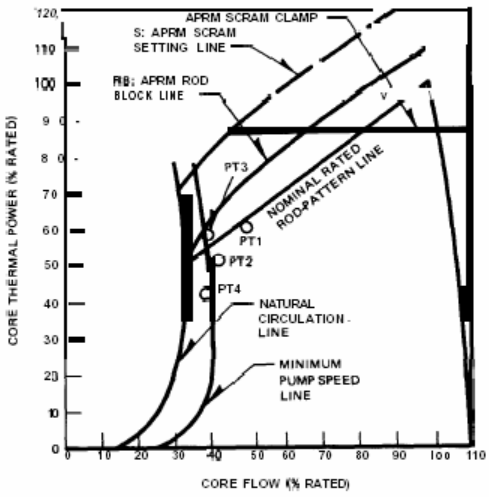

For all the calculations, the same detailed thermal-hydraulic nodalisation reproducing each geometrical zone of the plant was developed [24,25].

For the core, 33 thermal-hydraulic channels were modelled to represent the active part of the core and one channel for all bypasses. For the rest of the plant a coarse nodalisation was adopted so as to limit the computer resources required.

For the neutronic code, a nodalisation with a 3-D core mesh composed of 764 axial nodes was modelled. A large set of cross-section data including 435 compositions was adopted in the neutronic input deck [23].

With the aim of better understanding the instability development process, the stability response of this operational point to a steam line pressure disturbance (see Figure 4.2) was studied with the coupled codes TRAC-BF1/VALKIN and RELAP5Mod3.3/PARCS. With these codes it is possible to obtain detailed information regarding the state of the reactor for each time step.

Moreover, using nodal cross-sections obtained with RELAP5/PARCS, a modal decomposition with the VALKIN code [13,26] was performed, with the aim to compare the transient power evolution using a classic 3-D neutronic/thermal-hydraulic coupled code and a 3-D modal code. To characterise the studied transient as in-phase or out-of-phase and also to study the importance of different modes during the transients, the amplitudes of the different power modes were computed with VALKIN.

Finally, in order to observe the difference between the results obtained using different numbers of modes or different updating times, different transient calculations were carried out.

Figure 4.2. Steam line pressure perturbation

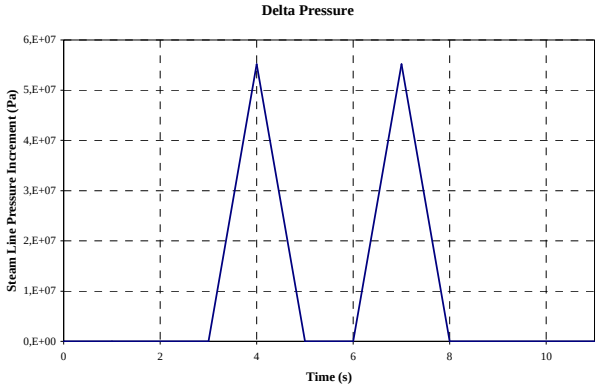

Steady-state results

The main parameters obtained in steady-state calculations and after-zero transient calculations were compared to make it sure that the stable conditions exist before the reactor perturbation.

The list of compared parameters covers reactor power and mass flow, core exit pressure, core inlet temperature, core inlet enthalpy, power peaking factor and core average axial power distribution [22]. Table 4.2 presents the reactor main parameters prior to its disturbance for the two calculations performed and their comparison with available measured data. Figure 4.3 compares the core average axial power distribution simulated with the codes, with the measured one.

Table 4.2. Reactor main parameters prior to its disturbance

Parameters, units	Measured	RELAP5/PARCS (33 channels)	TRAC-BF1/VALKIN (33 channels)
Core thermal power, MWt	1 948.0	1 949.0	1 949.0
Reactor flow, kg/s	5 216.40	5 216.332	5 212.6
Core inlet temperature, K	543.16	543.014	541
Core inlet enthalpy, J/kg	1.1846E6	1.1839E6	1.1741E6
Pressure at core outlet, Pa	7.0980E6	7.0979E6	7.035E6
Feedwater mass flow, kg/s	941.22	941.22	941.10

Figure 4.3. Comparison of RELAP5/PARCS and TRAC-BF1/VALKIN calculated core average axial power distributions with experimental test (process computer corrected)

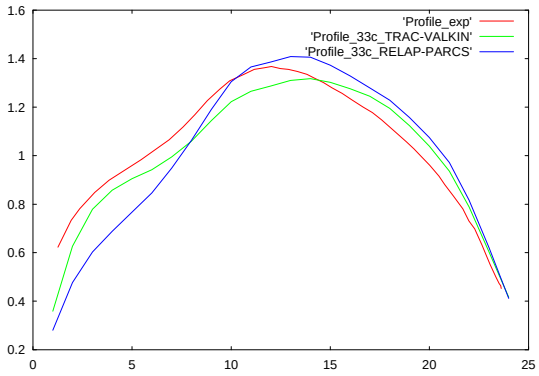

Spatial modes

The first three spatial modes were computed using the nuclear cross-sections provided by a RELAP5/PARCS simulation as an input for the VALKIN code. Figure 4.4 represents the obtained modes shapes.

Figure 4.4. Power profile of the first three λ modes for Peach Bottom2 LFST PT3

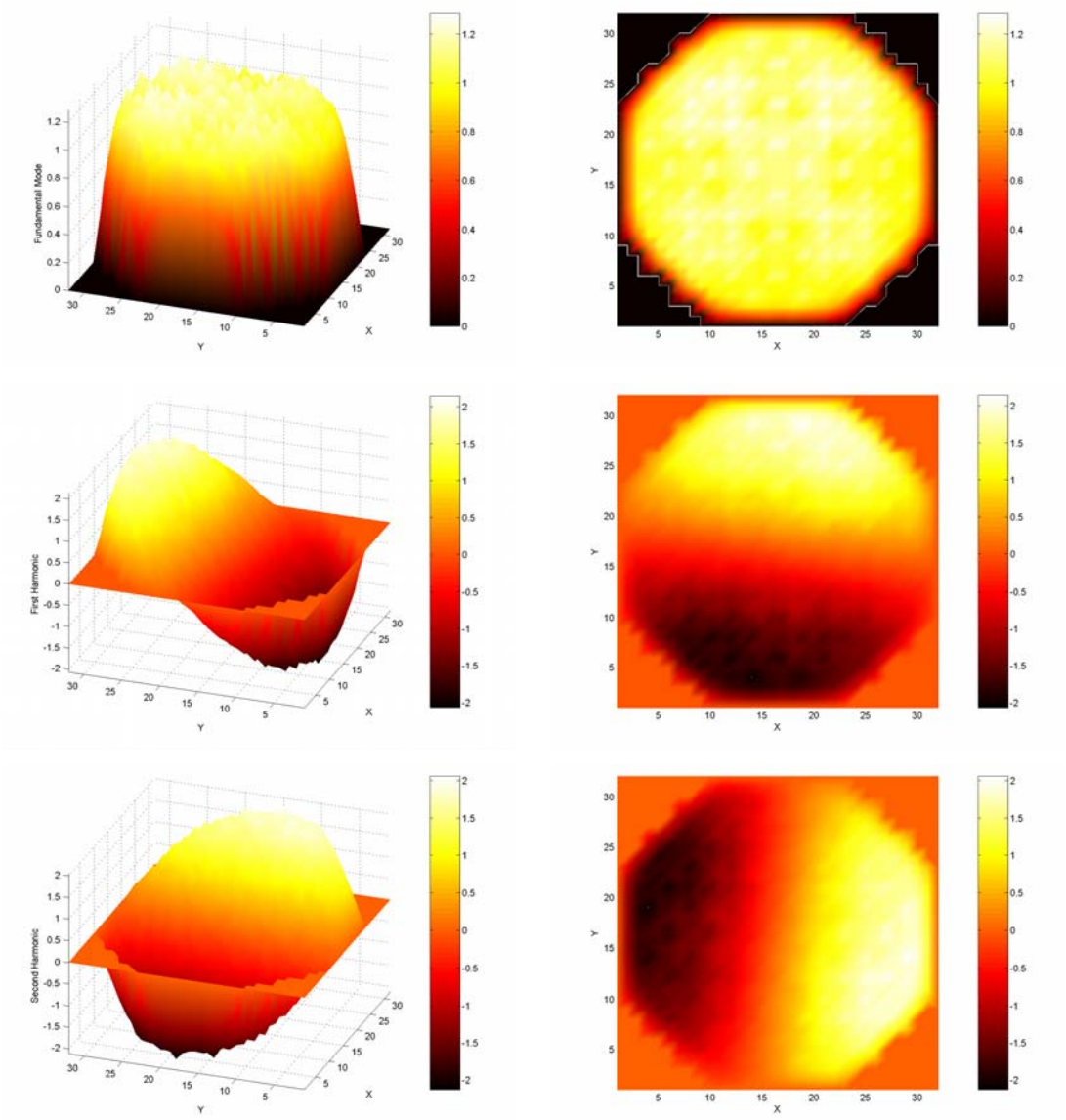

Transient results

Point PT3 was simulated with RELAP5/PARCS and the results compared with those obtained using the stand-alone neutronic code VALKIN.

With the coupled code TRAC-BF1/VALKIN two different calculations were performed, the first, Case 1, without updating the mode, and the second one, Case2, updating the mode each 1 second.

Table 4.3 presents the decay ratio and the natural reactor frequency that are usually used to characterise the instability phenomena.

Table 4.3. Time series analyses results

	DR	Freq.
Reference	0.331	0.430
TRAC/VALKIN Case 1	0.4172	0.3032
TRAC/VALKIN Case 2	0.4883	0.3097
RELAP5/PARCS	0.299	0.316

RELAP/PARCS results

With the nuclear cross-section provided by the transient calculation performed with RELAP5/ PARCS, different analyses with the VALKIN code were carried out.

The process of updating the modes considerably increases the accuracy of the solution obtained but is an expensive process from the computational point of view; it is thus necessary to find the equilibrium between the number of modes and its updating time to optimise the performance of the method. With VALKIN, we executed two transient calculations, with one and three modes, respectively, in order to analyse the influence of the number of modes in the results.

Figure 4.5 shows the power evolution calculated with one and three modes and the comparison with the one achieved with the RELAP5/PARCS calculation. It is possible to observe the good agreement among the results, so in order to reduce the CPU time but conserving the same accuracy we will continue the analysis using only one mode.

Figure 4.5. Comparison between the power evolution obtained with RELAP5/PARCS and the power evolution obtained using the VALKIN code with a different number of eigenvalues

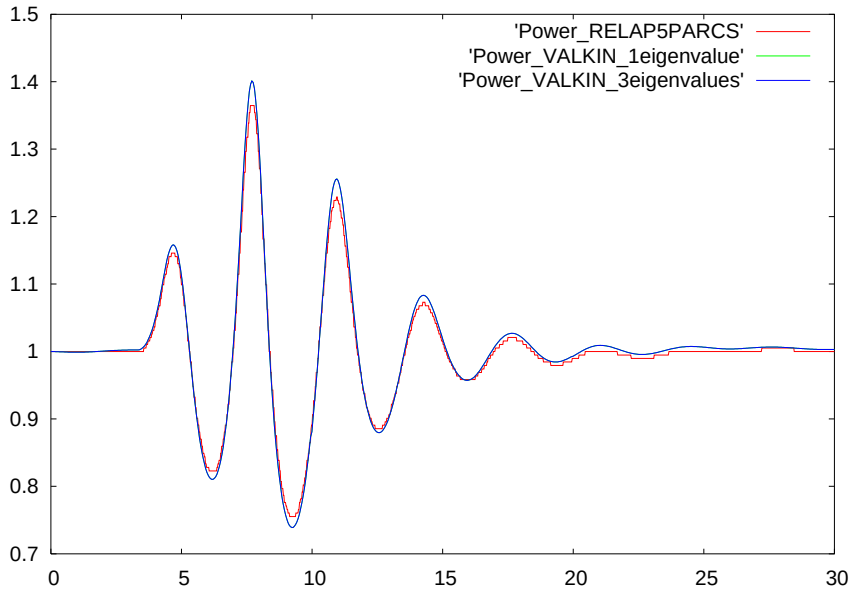

In Figure 4.6 we show a detail of the power evolution for the transient calculated using one mode. We compare the solution obtained without updating the modes and updating the modes every 0.956 sec and every 0.0956 sec with the solution obtained with RELAP5/PARCS taken as reference. We observe that the updating process increases the accuracy of the obtained solution.

Figure 4.6. Comparison between the power evolution obtained with RELAP5/PARCS and the power evolution obtained using VALKIN code with one eigenvalue and different updating times

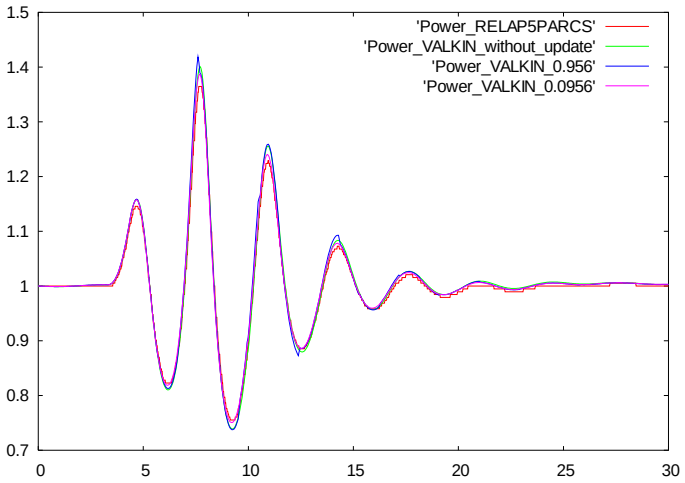

The main difference in the transient appears in the maximum power peak achieved during the transient. As has already been mentioned, the relative error decreases as the updating time decreases.

To characterise the studied transients as in-phase or out-of-phase and also to study the importance of different modes during the transients, we also calculated the time-dependent amplitudes, $n_l(t)$, of the fundamental mode and two harmonics, using an updating time of 0.956 seconds.

Figure 4.7 show the evolution of $n_0(t)$, $n_l(t)$ and $n_2(t)$ obtained with an updating time of 0.956 sec.

Figure 4.7. Power evolution with RELAP/PARCS and VALKIN, and amplitudes of the first three modes

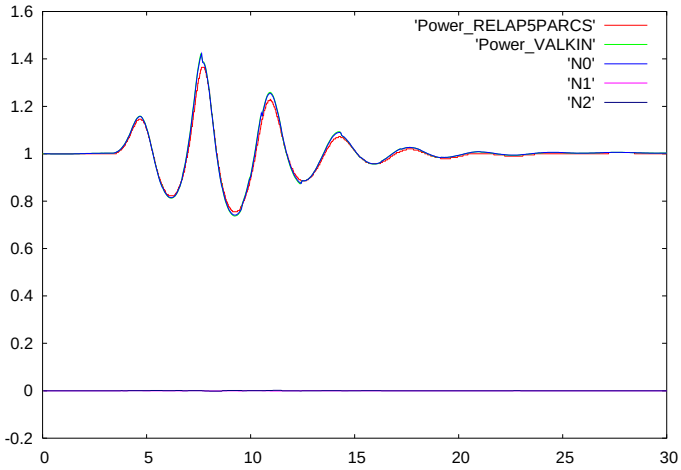

We observe that the amplitude $n_0(t)$ is clearly the dominant force during the oscillation, while $n_1(t)$ and $n_2(t)$are practically negligible.

TRAC/VALKIN results

Figure 4.8 presents the total power evolution along the transient obtained for the two cases.

Figure 4.8. Power evolution for Case 1 (no update) and Case 2 (update 1 s) with TRAC/VALKIN

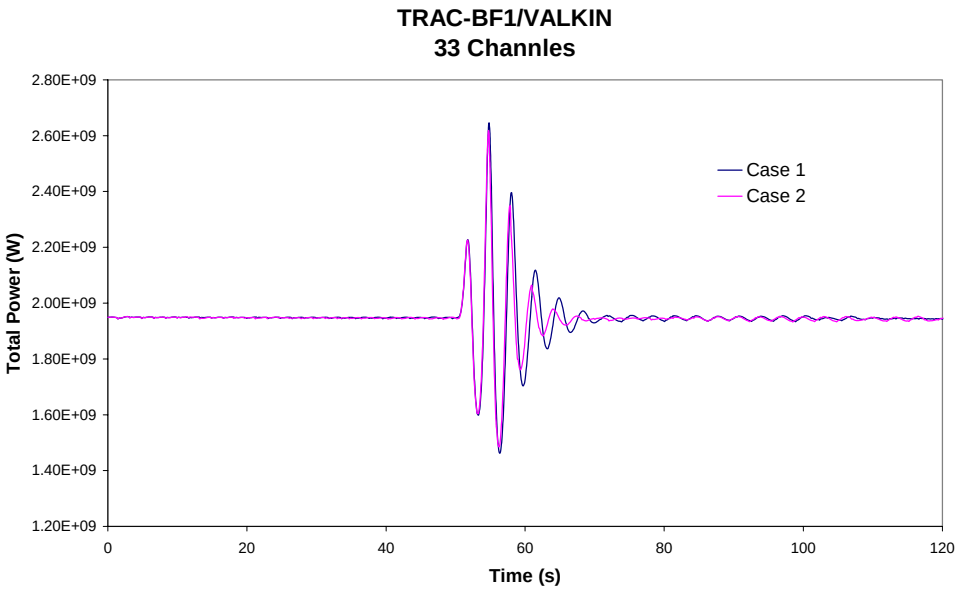

Figure 4.9 presents a detail of the end of this transient, where we can see the evolution of the oscillations. For Case 1, without updating, the oscillations are decreasing, but in Case 2 the oscillation has a constant amplitude of about 20 MW.

Figure 4.9. Detail of the residual oscillation at the end of the transient

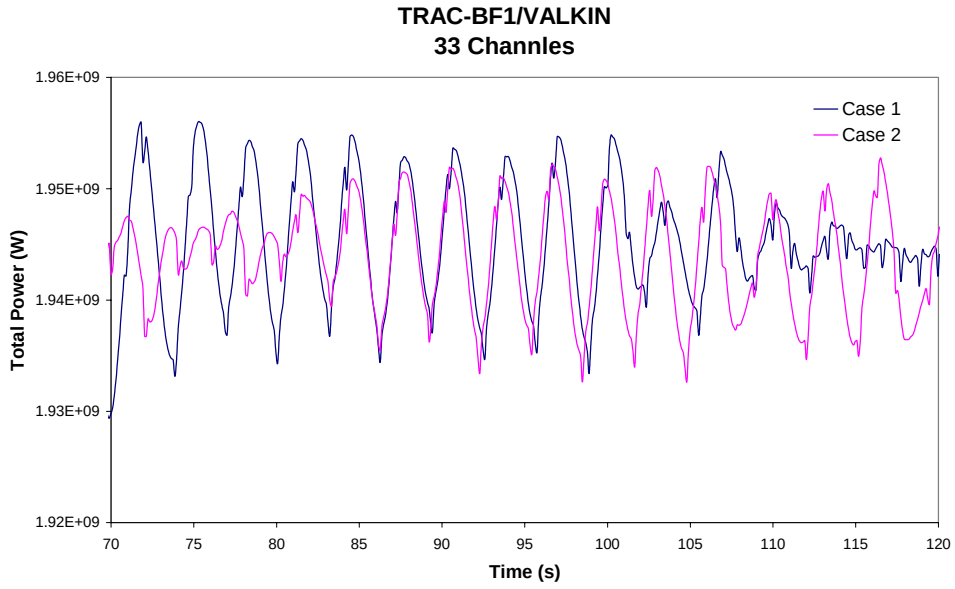

Comparison of results

Finally, Figure 4.10 compares the results obtained with RELAP5/PARCS and TRAC/VALKIN, using only one mode, without updating (Case 1) and updating the mode each second (Case 2). It shows a better agreement between RELAP/PARCS and TRAC/VALKIN with the updating strategy.

Figure 4.10. Comparison between RELAP/PARCS and TRAC/VALKIN with no update and with an updating time of 1 second

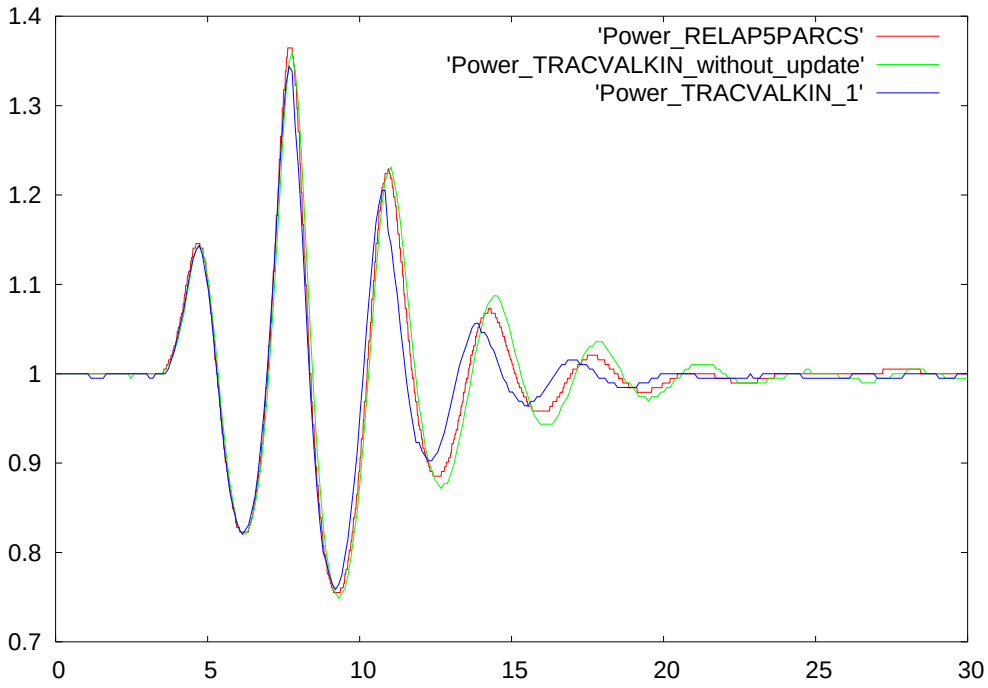

Conclusions

Point 3 of the low flow stability tests performed at Peach Bottom NPP is a nearly stable point at the end of the cycle 2 (this point is close to the stability boundary in the power/flow map, and besides, its axial power profile is not bottom-peaked).

Nevertheless, with the analysed cases the characteristics of in-phase instability can be recognised; for example, frequencies in all the oscillations produced in the analyses were from 0.3-0.4 Hz, *i.e.* in the typical frequency range of this kind of instability event.

Characteristics of the in-phase instability can be recognised using the coupled codes TRAC-BF1/ VALKIN and RELAP5/PARCS.

REFERENCES

[1] D'Auria, F., *et al*., *State-of-the-art Report on Boiling Water Reactor Stability*, OECD-NEA (1996).

[2] March-Leuba, J., J.M. Rey, "Thermohydraulic-Neutronic Instabilities in Boiling Water Reactors: A Review of the State of the Art", *Nuclear Engineering and Design*, 145, 97-111 (1993).

[3] March-Leuba, J., D.G. Cacuci, R.B. Pérez, "Nonlinear Dynamics and Stability of Boiling Water Reactors: Part 1-Qualitative Analysis", *Nuclear Science and Engineering*, 93, 111-123 (1986).

[4] March-Leuba, J., E.D. Blakeman, "A Mechanism for Out-of-phase Power Instabilities in Boiling Water Reactors", *Nuclear Science and Engineering*, 107, 173-179 (1991).

[5] Takeuchi, Y., Y. Takigawa, H. Uematsu, "A Study on Boiling Water Reactor Regional Stability from the Viewpoint of Higher Harmonics", *Nuclear Technology*, 106, 300-314 (1994).

[6] Muñoz-Cobo, J.L., R.B. Pérez, D. Ginestar, A. Escrivá, G. Verdú, "Nonlinear Analysis of Out of Phase Oscillations in Boiling Water Reactors", *Ann. Nucl. Energy*, 23, 16, 1301-1335 (1996).

[7] Turso, J.A., J. March-Leuba, R.M. Edwards, "A Modal-based Reduced-order Model of BWR Out-of-phase Instabilities", *Ann. Nucl. Energy*, 24, 12, 921-934 (1997).

[8] Karve, A.A., Rizwan-Uddin, J.J. Dorning, "Out-of-phase Oscillations at BWRs", *Proceedings of the Joint International Conference on Mathematical Methods and Supercomputing for Nuclear Applications*, Saratoga Springs, NY, 1633-1647 (1997).

[9] Hennig, D., "A Study of Boiling Water Reactor Stability Behaviour", *Nuclear Technology*, 125, pp. 10-31 (1999).

[10] Stacey, W.M., Jr., *Space-time Nuclear Reactor Kinetics*, Academic Press, New York (1969).

[11] Henry, A.F., "The Application of the Inhour Modes to the Description of on Nonseparable Reactor Transients", *Nucl. Sci. and Eng*., 20, 338-351 (1964).

[12] Miró, R., D. Ginestar, D. Hennig, G. Verdú, "On the Regional Oscillation Phenomenon in BWRs", *Progress in Nuclear Energy*, 36, 2, 189-229 (2000).

[13] Miró, R., D. Ginestar, G. Verdú, D. Hennig, "A Nodal Modal Method for the Neutron Diffusion Equation. Application to BWR Instabilities Analysis", *Ann. of Nucl. Energy*, 29, 10, 1171-1194 (2002).

[14] Ginestar, D., R. Miró, G. Verdú, D. Hennig, "A Transient Modal Analysis of a BWR Instability Event", *Journal of Nuclear Science and Technology*, 39, 5, 554-563 (2002).

[15] Wulff, W., H.S. Cheng, D.J. Diamond, M. Khatib-Rhabar, *A Description and Assessment of RAMONA-3B Mod.0 Cycle 4: A Computer Code with Three-dimensional Neutron Kinetic for BWR System Transients*, NUREG/CR-3664, BNL-NUREG-51746 (1984, 1993). See also: *RAMONA-3 User's Manual*, Scandpower.

[16] Hennig, D., *Stability Analysis KKL (Part 2)*, PSI Technical Report, TM-41-98-39 (in German) (1998).

[17] Blomstrand, J, *The KKL Core Stability Test*, Conducted in September 1990, ABB-Report, BR91-245 (1992).

[18] Wiktor, C.G., *KKL Cycle 7 Stability Test-core Simulation Input Data*, KKL Report BET/97/111 (1997).

[19] Ikeda, H., A. Hotta, "Development of a Time-domain 3-D Core Analysis Code and its Application to Space-dependent BWR Stability Analysis", *Proceedings of the Joint International Conference on Mathematical Methods and Supercomputing for Nuclear Applications* (Vol. 2, 1 624), Saratoga Springs, NY, 5-9 October 1997.

[20] Verdú, G., D. Ginestar, V. Vidal, J.L. Muñoz-Cobo, "3-D Lambda-modes of the Neutron Diffusion Equation", *Ann. Nucl. Energy*, 21, 405-421 (1994).

[21] Lefvert, T., *Ringhals 1 Stability Benchmark*, NEA/NSC/DOC(96)22 (1996).

[22] Carmichael, L.A., R.O. Niemi, *Transient and Stability Tests at Peach Bottom Atomic Power Station Unit 2 at End of Cycle 2*, EPRI Report NP-564 (1978).

[23] Ivanov, K., *et al*., *Boiling Water Reactor Turbine Trip (TT) Benchmark, Volume 1: Final Specifications*, NEA/NSC/DOC, 2001.

[24] Maggini, F., R. Miró, F. D'Auria, G. Verdú, D. Ginestar, "Peach Bottom Cycle 2 Stability Analysis Using RELAP5/PARCS", *International Conference Nuclear Energy for New Europe*, Ljubljana, Slovenia (2003).

[25] Sánchez, A.M., R. Miró, G. Verdú, D. Ginestar, "Test de Estabilidad en el Reactor Peach Bottom Unit 2 con el Código Acoplado TRAC-BF1/VALKIN", *29 Reunión Anual de la Sociedad Nuclear Española*, Zaragoza, Spain (2003).

[26] Verdú, G., R. Miró, D. Ginestar, V. Vidal, "Transients Modal Analysis using TRAC-BF1/ VALKIN", *PHYSOR 2002*, Seoul, Korea, 7-10 October 2002.

OECD PUBLICATIONS, 2 rue André-Pascal, 75775 PARIS CEDEX 16
Printed in France.